Resistance of Arabidopsis thaliana seeds exposed to monochromatic and simulated solar polychromatic UV radiation: Preparation for the EXPOSE space missions to the International Space Station (ISS)

Andreja Zalar

UNIVERSITÉ DE VERSAILLES SAINT-QUENTIN-EN-YVELINES

INRA

THÈSE DE DOCTORAT

DE L'UNIVERSITÉ DE VERSAILLES SAINT-QUENTIN-EN-YVELINES

Pour obtenir le titre :

DOCTEUR DE L'UNIVERSITÉ DE VERSAILLES SAINT-QUENTIN-EN-YVELINES

École doctorale GAO - Des génomes aux organismes

Présentée par :

Andreja ZALAR

Sujet de la thèse :

Résistance des graines d'*Arabidopsis thaliana* aux rayonnements UV monochromatiques et polychromatiques simulant la lumière solaire :
Préparation des expériences pour les missions spatiales EXPOSE menées à bord de la Station Spatiale Internationale (ISS)

Resistance of Arabidopsis thaliana seeds exposed to monochromatic and simulated solar polychromatic UV radiation:
Preparation for the EXPOSE space missions to the International Space Station (ISS)

Soutenue le 12 octobre 2010 devant le jury composé de :

M. Bernard MIGNOTTE (Professeur, Université de Versailles Saint-Quentin-en-Yvelines)	Président
M. Charles S. COCKELL (Professeur, Open University, Milton Keynes)	Rapporteur
Mme Julia BUITINK (Directeur de recherche, INRA Angers)	Rapporteur
M. Sydney LEACH (Directeur de recherche émérite, Observatoire de Paris-Meudon)	Examinateur
Mme Françoise CORBINEAU (Professeur, Université Pierre et Marie Curie, Paris 6)	Examinateur
M. David TEPFER (Directeur de recherche, INRA Versailles)	Directeur de Thèse

RÉSUMÉ

Les rayonnements UV ont une grande influence sur tous les systèmes biologiques connus et sont considérés comme un des obstacles majeurs à la dispersion de la vie. Dans l'espace, le spectre solaire complet comprend les rayonnements UV-A (315-365 nm), UV-B (280-315 nm), ainsi que les très énergétiques UV-C (200-280 nm) et VUV (<200 nm). Contrairement à aujourd'hui où la Terre est protégée des VUV et UV-C par la couche d'ozone situé dans la stratosphère, la vie sur Terre à ses débuts a probablement du faire face à ce rayonnement solaire nuisible hautement énergétique. Afin de comprendre la résistance de l'ADN face aux UV, nous avons étudié les propriétés d'absorption de l'ADN et de ses composants (nucléotides). Pour les organismes, un des moyens pour résister au rayonnement est la biosynthèse d'écrans UV. En mesurant, le spectre d'absorption VUV-UV, nous avons estimé les capacités de protection d'omniprésents écrans UV supposés (protéines, acides aminés, polyamines, tyramine et nucléotides dont ATP) et d'autres spécialisés issus d'organismes provenant de différents groupes phylogénétiques (acides aminés de type mycosporine (MAA), scytonemin, caroténoïdes, mélanines et flavonoïdes). Les flavonoïdes, composés phénoliques des plantes, apparaissent comme les protecteurs anti-UV les plus efficaces pour l'ADN. Ces flavonoïdes sont présents en grande concentration dans les graines de plantes. Ce rôle protecteur des flavonoïdes contre les UV a été confirmé par des expériences *in vivo* utilisant des graines d'*Arabidopsis thaliana*. Ces expériences ont permis de quantifier l'exceptionnelle résistance de ces graines au rayonnement monochromatique UV-C_{254} (jusqu'à 6 x 10^5 kJm^{-2}), et au rayonnement solaire simulé polychromatique $UV_{200-400}$ (1.5 x 10^5 kJm^{-2}) dans des conditions reproduisant le vide spatial et l'atmosphère de Mars simulée. Afin d'évaluer plus avant la résistance des graines au spectre solaire complet et de vérifier la plausibilité de la théorie de la panspermie, nous avons préparé des échantillons pour les deux missions spatiales EXPOSE menées à l'extérieur de la Station Spatiale Internationale (ISS).

Mots clés: Résistance aux UV, écrans UV, spectroscopie d'absorption VUV-UV, graines de plantes, flavonoïdes, esters sinapiques, espace, origine de la vie, Station Spatiale Internationale (ISS)

ABSTRACT

Ultraviolet (UV) radiation has a strong impact on all known biological systems and it is considered as one of the main limitation factors for dispersal of life on Earth and beyond. In space, the full solar spectrum can be encountered, including the UV-A (315-365 nm), the UV-B (280-315 nm), and highly energetic UV-C (200-280 nm) and the VUV (<200 nm). Neither VUV nor UV-C reaches the surface of the present-day Earth, thanks to filtration by the stratospheric ozone layer. However, life on the early Earth had probably to cope with damaging short-wavelength solar UV. In an effort to better understand the UV viability of DNA, we studied VUV-UV absorption properties of DNA and its components (nucleotides). One of the strategies for resisting UV radiation is a biosynthesis of UV screens. By measuring VUV-UV absorption spectra, we estimated the protection capacities for some ubiquitous potential UV screens (proteins, amino acids, polyamines, tyramine and nucleotides, including ATP), as well as specialized UV screens, isolated from phylogenetically distinct groups of organisms (mycosporine-like amino acids (MAA), scytonemin, carotenoids, melanins and flavonoids). Flavonoids, the phenolic compounds in plants, seemed the best suited to provide efficient UV screening protection to DNA. Flavonoids accumulate in high concentration in plant seeds. The UV protective role of flavonoids was demonstrated in experiments *in vivo*, using *Arabidopsis thaliana* seeds, which exhibited exceptionally high resistance to monochromatic UV-C_{254} (up to 6×10^5 kJm^{-2}), and simulated solar polychromatic $UV_{200-400}$ (1.5×10^5 kJm^{-2}) under simulated space vacuum and simulated Mars CO_2 atmosphere. In order to further evaluate the resistance of seeds to the full spectrum of solar light and to test the plausibility of panspermia theory, we prepared the experiments for space missions EXPOSE carried out on the exterior of the International Space Station (ISS).

Key words: UV resistance, UV screens, VUV-UV absorption spectroscopy, plant seeds, flavonoids, sinapate esters, space, origins of life, International Space Station (ISS)

AKNOWLEDGEMENTS

This work was performed mainly at the Laboratoire de Biologie de la Rhizosphère, PESSAC department, INRA Versailles. Some of the experimental parts of this thesis were performed using particular facilities: the synchrotron radiation source ASTRID at ISA, University of Aarhus (DK) and the Planetary and Space Simulation Facilities at DLR, Cologne (DE). The experiments were financially supported by the Centre National d'Etudes Spatiales (CNES) and the University of Aarhus (EC Integrated Activity on Synchrotron and Free Electron Laser Science, contract number R113-CT-2004-50608). Through the years of my work I have met a great number of people who contributed in many different ways to the realisation of this thesis. Here I would like to express my deepest gratitude to all these people that helped me on my way here.

In the first place I would like to acknowledge David Tepfer for giving me the opportunity to work in his laboratory, as well as for his supervision and advice during my thesis work.

I would also like to express my sincere gratitude to all the members of my thesis committee for their help, critical reading, evaluation and valuable advice and discussion. Particularly, I gratefully acknowledge Charles S. Cockell and Julia Buitink for their expertise and their precious time and patience in reviewing my voluminous thesis manuscript. I am also grateful to Françoise Corbineau for her attention and interest in my work, as well for stimulating discussion that helped me in shaping up some new ideas. I am much indebted to Bernard Mignotte for his kind understanding and thoughtful support.

I owe my deepest gratitude to Sydney Leach, whose kindness, as well as his rich scientific and life experiences have been invaluable to me. He provided me with many helpful suggestions and advices, and he kindly helped me with the proof-reading. I gratefully acknowledge his thoughtful support and personal encouragement during the course of my work, and particularly during the hard times that I encountered at the very end of my thesis.

Further, I would like to express collective and individual acknowledgments to all colleagues from INRA Versailles, and particularly PESSAC department, who helped me with their valuable expertise, kind assistance and friendly encouragement.
I wish to express my cordial appreciations to Christian Mougin, head of PESSAC department, for his understanding and kind support. I gratefully acknowledge Albert Kollmann for his

valuable contribution in HPLC analyses. I would like to thank him for giving me the opportunity to use his equipment, and for many interesting discussions that helped to extend my knowledge in analytical chemistry, particularly chromatography. I express a special acknowledgement to Lucien Kerhoas who performed LC-MS analyses, which improved the quality of this study. His precious expertise and work helped me to learn more about mass spectrometry. I would also like to thank Jacques Einhorn for his kind encouragement and always stimulating discussion about metabolomics, and particularly flavonoids.

Special thanks go to present and past members of the Laboratoire de Biologie de la Rhizosphère. I wish to thank Brigitte Message and Michèle Crespin for their kindness and helpful technical assistance. Many thanks to Salim Benabdelmoumène for his very efficient assistance with the bibliography. To Catherine Albertini and Éliane Caminade, special thanks for interesting discussions and their friendly encouragement. It is also pleasure to mention here my dear lab colleagues, PhD students and post-doctoral fellows: Moumita Bandyopadhyay, Kuntal Narayan Chaudhuri, Anna Kostrzak, Mayssa Al Jouda, Devendra Bellary Nagaraju and others, with whom I have shared interesting lab experiences and memorable moments of friendship.

Further, I would like also to thank several research groups that we have collaborated with.

It was my great pleasure to work at the University of Aarhus (DK), where I was always kindly welcomed by the ISA stuff. I particularly acknowledge Søren V. Hoffmann for his valuable contribution in VUV-UV absorption spectroscopy. I am thankful for helping me out with experiments at the UV1 beamline of the ASTRID synchrotron facility. I also warmly thank Nykola C. Jones for her efficient help in the storage ring experiments. Sincere thanks are extended to Finn Folkmann from the Department of Physics and Astronomy, University of Aarhus, for enabling my preliminary work on the effects of accelerated proton particles on plant seeds, using a 5 MeV van de Graff accelerator.

I would also like to thank to our collaborators at DLR, Cologne (DE) for performing simulated solar polychromatic UV exposure experiments. My thanks go in particularly to Elke Rabbow who co-ordinated EXPOSE preflight verification tests (EVT) and EXPOSE mission ground reference experiments.

Many thanks also to Pascale Ehrenfreund and the other members of her laboratory at the Leiden University (NL) for kind welcome and help during the final steps of sample preparation for the EXPOSE-R mission.

I would like also to express my gratitude to the members of the AMPlus group at LERMA, Observatoire de Paris-Meudon, and all kind people that I have met there for their warm welcome, interesting discussions and all encouragements during the last difficult steps of my thesis writing marathon.

Finally, where would I be without my family? My parents deserve a special mention for all their love and constant emotional and moral support in all matters of my life. Words fail to express my gratitude to my dearest sister Mirela and my beloved Louis for all their generous love, patience and support, shearing with me most of the ups and downs during my thesis work. They provided me with the constant encouragement and belief in what I have been doing. To them I dedicate this thesis.

TABLE OF CONTENTS:

Chapter 1 INTRODUCTION

Chapter 2 METHODS AND MATERIALS

Chapter 4 DISCUSSION I

PART II: TESTING UV RESISTANCE OF *Arabidopsis* SEEDS AND COMPARISON TO UV RESISTANCE OF *Bacillus subtilis* SPORES

Chapter 5 RESULTS II

LIST OF FIGURES:

LIST OF TABLES:

LIST OF ACRONYMS AND ABBREVIATIONS

A	Absorbance
ABA	Abscisic acid (type of phytohormones)
ACN	Acetonitrile
ANOVA	Analysis of variance (statistic test)
APF	Aminophenyl fluorescein (fluorescent probe for ROS detection)
ATP	Adenosine-5'-triphosphate
AU	Astronomical unit, it refers to the mean distance between the Earth and the Sun over one Earth orbit (1AU =149,597,870.7 km).
BBCH-scale	Biologische Bundesanstalt, Bundessortenamt and Chemical industry-scale, used to identify the phenological development stages in plants (sponsored by Bayer, BASF, Ciba-Geigy and Hoechst)
BER	Base excision repair (DNA repair mechanism)
BRs	Brassinosteroids (type of phytohormones)
BSA	Bovine serum albumin
3-BzOP	3-Benzoyloxypropyl glucosinolate (glucomalcomiin)
CAT	Catalase
CC	Pyrimidine dimer between two adjacent cytidine nucleic bases (type of DNA lesion)
CHS	Chalcone synthase, a key enzyme in biosynthesis of flavonoids
Col-0	Columbia ecotype of the plant *Arabidopsis thaliana*
CT	Pyrimidine dimer between two neighbouring cytidine and thymidine nucleic bases (type of DNA lesion)
CFU	Colony Forming Units
CIE	International Commission on Illumination
CNES	Centre National d'Etudes Spatiales (French government space agency)
CO_2	Carbon dioxide
CPDs	Cyclobutane pyrimidine dimers (type of DNA lesions)
D_2O	Deuterium oxide (heavy water)
DAI	Days after imbibition
DCFH-DA	2'-7' dichlorofluorescein diacetate (fluorescent probe for ROS detection)
dATP	Deoxyadenosine triphosphate nucleotide
dCTP	Deoxycytidine triphosphate nucleotide
dGTP	Deoxyguanosine triphosphate nucleotide
dTTP	Deoxythymidine triphosphate nucleotide
DLR	Deutsches Zentrum für Luft-und Raumfahrt (German aerospace center)
DNA	Deoxyribonucleic acid
DPA	Dipicolinic acid
ds break	DNA double strand break
ESA	European Space Agency
EuTEF	European Technology Exposure Facility
eV	electronvolt (~1.602×10^{-19} J)
EVA	Extravehicular Activity
EVT	Experiment Verification Tests
F_{10}	10% survival rate, equivalent for LD_{90} (see below)
$FADH^-$	Two-electron-reduced flavin adenine dinucleotide
fah1-2	Ferulate-5-hydroxilase nontransgenic mutant of the plant *Arabidopsis thaliana* (formerly named *sin1-2*)
Fe(II)	Ferrous iron
Fe(III)	Ferric iron
F5H	Ferulate-5-hydroxilase, a key enzyme in biosynthesis of sinapate esters
fw	Fresh weight
Ga	Giga annum (billion years)
GAs	Gibberellins (type of phyt hormones)
$G_{max\%}$	Maximal germination percentage (germination capacity)
G+C content	Total percentage of guanine and cytosine nucleic bases in DNA
GCR	Galactic Cosmic Radiation

GMOs Genetically modified organisms

HAI Hours after imbibition

HPF Hydroxyphenyl fluorescein (fluorescent probe for ROS detection)

HPLC High Performance Liquid Chromatography

HZE High charge (*z*) and Energy particles

ISA Institute for Storage Ring Facilities, University of Aarhus, Denmark

ISS International Space Station

ISTA International Seed Testing Association

I-Glu-Rha Isorhamnetin-glucoside-rhamnoside

IR Infrared radiation

I-Rha-Rha Isorhamnetin-di-rhamnoside

K-Glu-Rha Kaempferol-3-*O*-glucoside-7-*O*-rhamnoside

K-Rha Kaempferol-rhamnoside

K-Rha-Rha Kaempferol-3,7-di-*O*-rhamnoside

LB Luria-Bertani medium

LC-MS Liquid Chromatography coupled with Mass Spectrometry

LD_{90} Lethal dose that kills 90% of the population (cells, spores or individuals), equivalent for F_{10} (see above)

LD_{50} Lethal dose that kills 50% of the population (cells, spores or individuals)

LDEF Long Duration Expose Facility

LEA proteins Late embryogenesis abundant proteins

LEO Low Earth Orbit

Ler-0 Landsberg erecta ecotype of the plant *Arabidopsis thaliana*

LET Linear Energy Transfer

$[M]^+$ In mass spectrometry, molecular ions, detectable in positive ionization mode

MAAs Mycosporine-like amino acids

MeOH Methanol

MgF_2 window An optical filter made of magnesium fluoride

MGT Mean germination time

$[M+H]^+$ In mass spectrometry, protonated molecular ions, detectable in positive ionization mode

$[M+Na]^+$ In mass spectrometry, sodium adduct ions, detectable in positive ionization mode

$[M-H]^-$ In mass spectrometry, deprotonated molecular ions, detectable in negative ionization mode

monoA/G/T/C Mononucleotides containing one of the nucleic bases, adenine/guanine/thymine/cytosine

MS Mass Spectrometry

MS-MS Tandem Mass Spectrometry, involves multiple steps fragmentation and analysis of daughter ions

8-MSOO 8-Methylsulfinyloctyl glucosinolate (glucohirsutin)

3-MSOP 3-Methylsulfinylpropyl glucosinolate (glucoiberin)

8-MTO 8-Metylthiooctyl glucosinolate

Mw Molecular weight

m/z In mass spectrometry, mass (*m*)-to-charge (*z*) ratio of analyzed charged particles (ions)

NADH Nicotinamide adenine dinucleotide (reduced form)

NASA National Aeronautics and Space Administration

NER Nucleotide excision repair (DNA repair mechanism)

nptII Bacterial kanamycin resistance gene

O_2 Molecular oxygen

O_3 Ozone

OD Optical density

OD_{560} Optical density measured at 560 nm

oligoA_{20}/G_{20}/T_{20}/C_{20} Homooligonucleotides, the short tracts of single-stranded DNA composed of 20 identical nucleotides carrying one of the nucleic bases, adenine/guanine/thymine/cytosine

oligoA+oligoT Mixture of two complementary homooligonucleotides, oligoA_{20} and oligoT_{20} (see above)

oligoG+oligoC Mixture of two complementary homooligonucleotides, oligoG_{20} and oligoC_{20} (see above)

PAs Proanthocyanidins (also called condensed tannins)

PAL Present Atmospheric Level

PAR Photosynthetically Active Radiation (λ = 400-700 nm)

PCR Polymerase Chain Reaction, a technique in molecular biology to amplify a fragment of DNA

(6-4) photoproducts Pyrimidine (6-4) pyrimidinone dimers (type of DNA lesions)

POD Peroxidase

PR Photoreactivation (DNA repair mechanisms)

PS I and II Photosystem I and II, protein complexes involved in photosynthesis

Q-Glu Quercetin-3-*O*-glucoside

Q-Glu-Rha Quercetin-glucoside-rhamnoside

Q-Rha-Rha Quercetin-di-rhamnoside

Q-Rha Quercetin-3-*O*-rhamnoside (also called quercitrin)

rcf Relative centrifugal force

RFOs Raffinose family oligosaccharides (e.g. raffinose, stachylose, verbascose etc.)

RNA Ribonucleic acid

ROS Reactive oxygen species

RT In chromatography, retention time

SCR Solar Cosmic Radiation

Sinapoyl-Ch Sinapoylcholine

di-Sinapoyl-Glu di-Sinapoylglucose

Sinapoyl-Glu Sinapoylglucose

Sinapoyl-Me Methyl-containing sinapate ester

SOD Superoxide dismutase

SPs Spore photoproduct (type of DNA lesion)

SPEs Solar Particle Events

ss break DNA single strand break

SSM Schaeffer' Sporulation Medium

T% Transmittance

$T_{50\%}$ Time necessary for seeds reaching 50% of maximum germination (median of germination time course)

$T_{25\text{-}75\%}$ Time period for seeds reaching from 25% to 75% of maximum germination (measure for germination uniformity)

T-DNA Transfer DNA, used in *Agrobacterium*-mediated genetic transformation of plants

TC Pyrimidine dimer between two neighbouring thymidine and cytidine nucleic bases (type of DNA lesion)

TT Pyrimidine dimer between two adjacent thymidine nucleic bases (type of DNA lesion)

tt4-1 Transparent testa 4-1 nontransgenic mutant of the plant *Arabidopsis thaliana*

tt4-8 Transparent testa 4-8 transgenic mutant of the plant *Arabidopsis thaliana*

TZ test Tetrazolium (salt) test

u Unified atomic mass unit (synonym of atomic mass unit, amu)

UV Ultraviolet radiation

$UV_{200\text{-}400}$ Polychromatic ultraviolet radiation (λ = 200-400 nm)

UV-A Ultraviolet radiation (λ = 315 -365 nm)

$UV\text{-}A_{365}$ Monochromatic ultraviolet radiation (λ = 365 nm)

UV-B Ultraviolet radiation (λ = 280 -315 nm)

$UV\text{-}B_{312}$ Monochromatic ultraviolet radiation (λ = 312 nm)

UV-B+UV-A Ultraviolet light composed of ~ 8% $UV\text{-}B_{312}$ and ~ 2% $UV\text{-}A_{365}$ light

UV-C Ultraviolet radiation (λ = 200 -280 nm)

$UV\text{-}C_{254}$ Monochromatic ultraviolet radiation (λ = 254 nm)

UV-C+(UV-B+UV-A) Quasi-monochromatic UV-C light , composed of ~ 90% $UV\text{-}C_{254}$ and ~ 10% of combined $UV\text{-}B_{312}$+ $UV\text{-}A_{365}$ light (see above)

% (v/v) Percent volume per volume (volume percent)

UV-VIS spectrum In the present work, spectrum measured in the wavelength range 200-700 nm

VIS Visible light (λ = 390 -750 nm for human eye)

VUV Vacuum ultraviolet radiation (λ < 200 nm)

VUV-UV spectrum In the present work, spectrum measured in the wavelength range 125-340 nm

Ws-2 Wassilevskija ecotype of the plant *Arabidopsis thaliana*

% (w/v)	Weight in volume percentage
% (w/w)	Weight in weight percentage (mass percentage)
z	Charge of an ion
α	In statistics, the level of significance (critical *p*-value)
λ	Wavelength of electromagnetic radiation
λ_{min}	In spectroscopy, the wavelength of minimum absorbance
λ_{max}	In spectroscopy, the wavelength of maximum absorbance
ψ_w	Water potential

Chapter 1

INTRODUCTION

1. SCOPE AND OBJECTIVES OF THE THESIS

The space environment has been considered as extremely hostile to all forms of life. The chances for survival of an organism are determined by its ability to withstand the deleterious conditions of space, including highly energetic electromagnetic radiation (UV, X and γ radiation), cosmic rays, temperature extremes, high space vacuum and microgravity. The complete spectrum of solar UV radiation is known as one of the most deleterious factors of space environment due to its highly damaging effects on DNA (Horneck, 1993; Nicholson et al., 2000; Horneck et al., 2001). However, some organisms on Earth have developed strategies of survival in extreme conditions. Spore-forming bacteria, such as the bacterium *Bacillus subtilis*, are considered as extremely resistant life forms because of their ability to withstand various harsh physical and chemical conditions (Nicholson et al., 2000). Past research has therefore mainly focussed on bacterial spores as terrestrial models for biotic propagators of life in space (Bücker et al., 1974; Horneck et al., 1984a; Horneck, 1993; Horneck et al., 1995). Horneck et al. (1994) reported that a considerable percentage of *Bacillus subtilis* spores remained viable after nearly 6 years of exposure to space environment. However, without efficient UV-protective shield, bacterial spores were killed within a few seconds of exposure to open space (Horneck et al., 1984b; Horneck et al., 2001; Rettberg et al., 2002). Tepfer and Leach (2006) proposed that plant seeds should also be considered as model vehicles for the transfer of life through space. Seeds evolved on Earth to conserve the species and their genomes during prolonged periods of stress. Seed anatomy and chemistry are adapted to protect the embryo from harsh environmental conditions. Seeds are resistant to heat, extreme cold and desiccation. Some plant seeds have remained viable on Earth after more than 1200 years, and some seeds were capable of germinating even after 2000 years (Shen-Miller et al., 2002; Sallon et al., 2008).

The aim of the present work was to test the resistance of plant seeds to conditions encountered in space, particularly to highly deleterious UV radiation, and to prepare the samples, pre-flight experimental procedures and post-flight analysis for the EXPOSE space missions, supported by the European Space Agency (ESA). The EXPOSE/ SEEDS space experiments are carried out on the exterior of the International Space Station (ISS), where the samples (dry plant seeds, DNA and UV screening compounds) are exposed to conditions of open space environment, including highly energetic solar UV light for about 1.5 years.

The seeds of the *Arabidopsis thaliana* plant were chosen as an experimental model in our experiments due to several reasons. Above all, it is their remarkably small size (< 500 μm) that enabled the preparation of relatively large number of seeds per limited exposure surface of the

sample carriers used in EXPOSE experiments. Secondly, *Arabidopsis* plants have a short life cycle and high reproductive capacity, making feasible the study of the entire cycle of plant development and enabling production of large quantities of seeds in a relatively short time period. Due to its small genome that has been entirely sequenced, *Arabidopsis* represents a model plant in molecular biology and plant genetics, which enables the production of a large collection of mutants that lack one or more selected chemical compounds. Such mutant *Arabidopsis* seeds that lack UV screening compounds were used in our EXPOSE experiments. In addition, *Arabidopsis* seeds have been already used in previous space experiments studying microgravity, and particularly the effects of cosmic radiation (Kranz et al., 1990; Gartenbach et al., 1994; Zimmermann et al., 1996; Link et al., 2003). Yet, the full spectrum solar UV radiation and its impacts on plant seeds have received little attention in past space studies. In past few decades, several radiobiological experiments have been carried out in open space, where plant seeds were exposed only to cosmic radiation or in combination with space vacuum (**Annex A-1**). So far, only one study has been reported regarding a 13-day *in situ* exposure of *Arabidopsis* seeds to complete space conditions, including the full spectrum of solar UV light. Unfortunately, UV doses were not recorded during these experiments (Anikeeva et al., 1990). In the literature, even less attention was paid to the effects of highly energetic UV-C and VUV part of spectrum on plant seeds, since this part of the solar spectrum does not reach the surface of present-day Earth thanks to the stratospheric ozone layer. However, due to the high absorption of DNA in this part of the spectrum, VUV and UV-C are considered particularly damaging for all organisms. These highly energetic UV wavelengths can be encountered in space and extraterrestrial environments (e.g. Mars and Moon). In the early history of the Earth, highly energetic UV light was likely one of the most limiting factors for the life emergence and its evolution.

Following the general introduction chapter, which reviews the issues related to the EXPOSE experiments, astrobiology context of the origins of life, evolution and possibilities for its distribution, as well as those related to the structure, physiology and chemistry of plant seeds, this thesis is organized in two main parts: (1) the chemical basis of UV protection and (2) the biological study of UV resistance in *Arabidopsis* seeds.

The aim of the first part of this work was to provide better understanding of the chemical basis of UV resistance, which is attained through a UV screening strategy. Since DNA is a strong chromophore for UV light, we aimed to better understand the UV viability of DNA by studying the VUV-UV absorption spectra of DNA and its components (nucleotides). We attempted to determine whether the UV absorption characteristics of DNA depend on the overall base composition and its nucleotide sequence. The UV screens have the function of absorbing

the incident photons and dissipating their energy away from the DNA target, thus protecting DNA from damage. The screening effect should be maximal at wavelengths of maximal absorption. In this study we measured the VUV-UV absorption spectra of different putative and known specialized UV screens (mycosporine-like amino acids, scytonemin, β-carotene, melanin and flavonoids) that are specific for phylogenetically distinct groups of organisms. Comparing these absorption spectra to that of DNA, we evaluated the likely effectiveness of these natural substances to protect DNA from unfiltered solar UV light. In order to better understand a remarkably high UV resistance of plant seeds, which is elaborated in the second part of this thesis, we purified and identified the chemical substances that act as efficient UV screens in *Arabidopsis* seeds. We measured their UV absorption spectra using conventional and VUV-UV absorption spectroscopy, and we compared these spectra to that of DNA. Moreover, we identified a flavonoid compound, which is an abundant secondary metabolite in *Arabidopsis* seeds that likely provides the major screening protection against UV radiation.

The aim of the second part of this thesis was to simulate in the laboratory the conditions of the highly energetic UV radiation environment that is encountered in space and to study the resistance of *Arabidopsis thaliana* seeds exposed to these simulated conditions in order to predict their survivability after 1.5 years of space mission. In this regard, it was necessary to determine the upper limits for survival of *Arabidopsis thaliana* seeds exposed to monochromatic UV-C_{254} light, as well as simulated solar polychromatic $UV_{200\text{-}400}$ radiation, with fluences high enough to be compared to those after 1.5 years of mission in space. The UV response of *Arabidopsis* seeds was compared to that of *Bacillus subtilis* spores, which is used as an extremely resistant terrestrial model for studying the feasibility of interplanetary transfer of life. Besides germination as the first indicator for viability and seed damage, other biological endpoints induced by UV radiation were also studied during the course of plant development, from the early seedling stage up to the stage of mature plants. In order to determine *in vivo* the UV-protection capacity of the main plant UV screening compounds (flavonoids and sinapate esters), it was further necessary to study the resistance of mutant seeds that are deficient in these compounds. Since previous space and laboratory experiments indicated that the damaging effects of UV radiation may be increased by simultaneous exposure to space vacuum (Horneck et al., 1984b; Weber and Greenberg, 1985), it was further important to determine the resistance of *Arabidopsis* seeds exposed to the combined effects of simulated solar polychromatic $UV_{200\text{-}400}$ radiation and simulated space vacuum. Although the effects of other parameters of space environment were not a direct focus of this work, we have performed some preliminary simulation experiments on resistance of plant seeds exposed to extremely low and high temperatures, as well as accelerated proton particles, which represent a dominant component of cosmic radiation. A brief discussion on the effects of the other space parameters is included in the annex to this thesis.

2. EXPOSE: SPACE EXPERIMENT ONBOARD THE INTERNATIONAL SPACE STATION (ISS)

Space technology has developed particular means for transporting terrestrial organic and biological material beyond the protective cover of the Earth's atmosphere, thus providing a unique opportunity for studying their responses to conditions encountered in the space environment (see **Annex A-1**). Such studies aim to provide better understanding of processes and phenomena pertinent to astrobiology, such as the impact of UV radiation in the early evolution of life on Earth, the relevance of extraterrestrial organic matter to the emergence of life on Earth or any other planet, and the chances and limits for life to be transported from one planet to another (Horneck, 1999).

Derived from the earlier concepts of exposure facilities flown aboard the free flying carriers (e.g. ERA on EURECA and BIOPAN on Foton), the European Space Agency (ESA) has developed a new multi-user exposure facility, EXPOSE, designed to be attached to the exterior of the International Space Station (ISS), and supporting long-duration (1-1.5 years) exposure experiments under conditions of free space or selected space parameters (Horneck, 1999). The EXPOSE facility hosts astrobiology experiments prepared by scientists from various European and other research laboratories (**Table 1** and **Table 2**) (Rabbow et al., 2009). Among selected experiments, EXPOSE comprises different photochemical, photobiological and radiobiological studies, using biological samples as diverse as bacterial cells and spores, archaea, cyanobacteria, algae, fungi, lichens and plant seeds, as well as chemical samples, such as DNA, UV screening organic compounds, amino acids, polycyclic aromatic hydrocarbons (PAHs), and other organics of prebiotic relevance. The biology experiments use the full extraterrestrial spectrum of solar UV radiation and suitable cut-off filters to study the role of the ozone layer in protecting our biosphere, as well as the likelihood of resistant terrestrial life forms to survive in outer space. The latter has relevance to testing the feasibility of the panspermia hypothesis (see section **3.1.2**) and it provides basic data to planetary protection issues e.g. by determining the upper limits for survival of terrestrial life forms that might contaminate planetary bodies (e. g. Mars) as a result of human space exploration activity. To get better insight into the habitability of Mars, one set of samples has been assigned for exposure to simulated Martian conditions (extraterrestrial UV radiation and simulated Martian atmosphere and pressure), while flown in space. The chemical set of experiments is designed to reach a better understanding of the role of interstellar, cometary and planetary chemistry in the origin of life (Horneck et al., 2000; Rabbow et al., 2009).

The EXPOSE facility hardware is composed of three experiment trays, each one containing four square sample carriers, of which some are sealed, thus allowing the samples to be kept under selected atmosphere and pressure during space exposure experiments, while other sample carriers are vented via a venting system integrated in the tray, enabling the samples an access to the space vacuum. Each sample carrier is composed of at least two layers: one top sample holder for UV exposure of the samples and underneath one or two carriers that accommodated the dark control samples. The sample carriers contain a number of the samples cells, which depending on the type of experiment differ in their number and geometry. The sample cells were loaded with different biological and chemical samples, which were covered by optical windows (MgF_2 or quartz) and filters for wavelength selection and/ or attenuation of solar UV radiation. The EXPOSE facility is equipped with various sensors, including pressure sensors, six temperature sensors attached to the three trays, four broad band UV sensors (220-380 nm) located at the four corners of the facility and one passive radiation dosimeter for measuring ionizing radiation. In addition, the instruments integrated into the R3D compartment provide on-line data on UV-A, UV-B, UV-C and visible solar radiation, as well as ionizing radiation, measured by one active radiation dosimeter. The EXPOSE facility also accommodates an electronic unit for data acquisition, ground telemetry and telecommanding (Baglioni et al., 2007; Rabbow et al., 2009).

Parallel to the space flight experiments, there is another set of experiments, called the mission ground reference experiment, which runs in the Planetary and Space Simulation Facilities at the German Aerospace Center (DLR), Institute of Aerospace Medicine and Cologne (**Fig. 1**). For these ground experiments, identical biological and chemical samples were prepared in the same way as the samples for the space experiments, using the same EXPOSE hardware (carriers and trays). According to the data on solar UV radiation, temperature and vacuum, acquired in the space, the ground control samples are exposed to simulated space conditions at DLR (Horneck et al., 2000; Rabbow et al., 2009). Since the ionizing radiation in space has a very complex nature (for details see sections **3.2.1.1** and **3.2.2**), hence difficult to simulate in the laboratory, the ground experiments serve as a negative control for the effects of cosmic radiation on samples exposed in space (**Fig. 1**).

Two astrobiological experiments, EXPOSE-E and EXPOSE-R, using two separate EXPOSE facilities have been successfully prepared and launched to the ISS for exposure in LEO (Low Earth Orbit) up to 1.5 years. EXPOSE-E was installed as part of the European Technology Exposure Facility (EuTEF) on one of the external platforms of the European *Columbus* module of the ISS. EXPOSE-R that is currently running in space was installed on the external URM-D platform of the Russian *Zvezda* module of the ISS (**Fig. 2**).

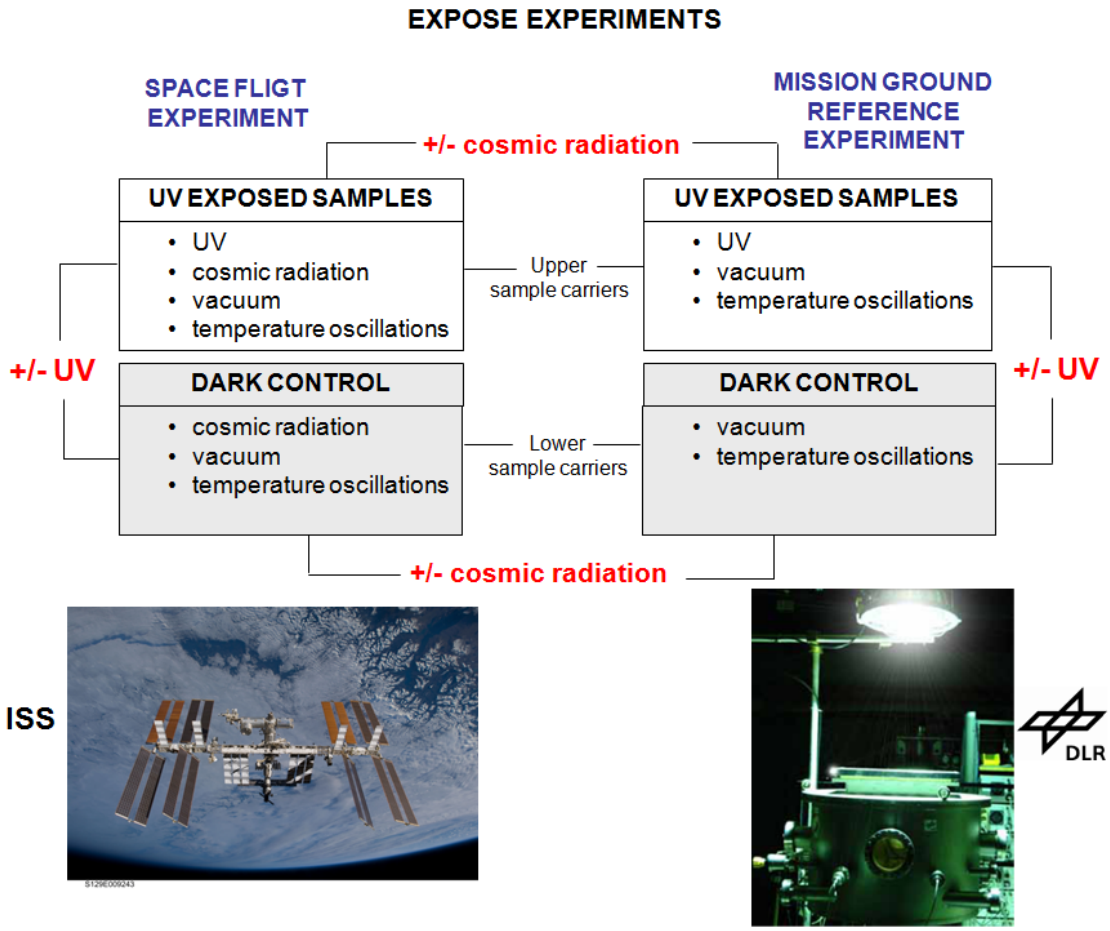

Fig. 1. Schematic representation of the experimental design for EXPOSE mission. Two sets of experiments were performed in parallel: the space flight experiment carried out at the ISS (Photo: NASA) and the mission ground reference experiment performed in the Planetary and Space Simulation Facilities at the German Aerospace Center (DLR), Institute of Aerospace Medicine, Cologne (Photo: DLR). The effects of four parameters of the space environment were studied: the solar polychromatic UV radiation, cosmic radiation, space vacuum and temperature oscillations. Samples were loaded in two stacked carriers; upper carrier contained the samples exposed to UV light, while samples in lower carrier were shaded from sunlight and served as a negative control for UV light (dark control). The samples from the mission ground reference experiment served as negative control for cosmic radiation.

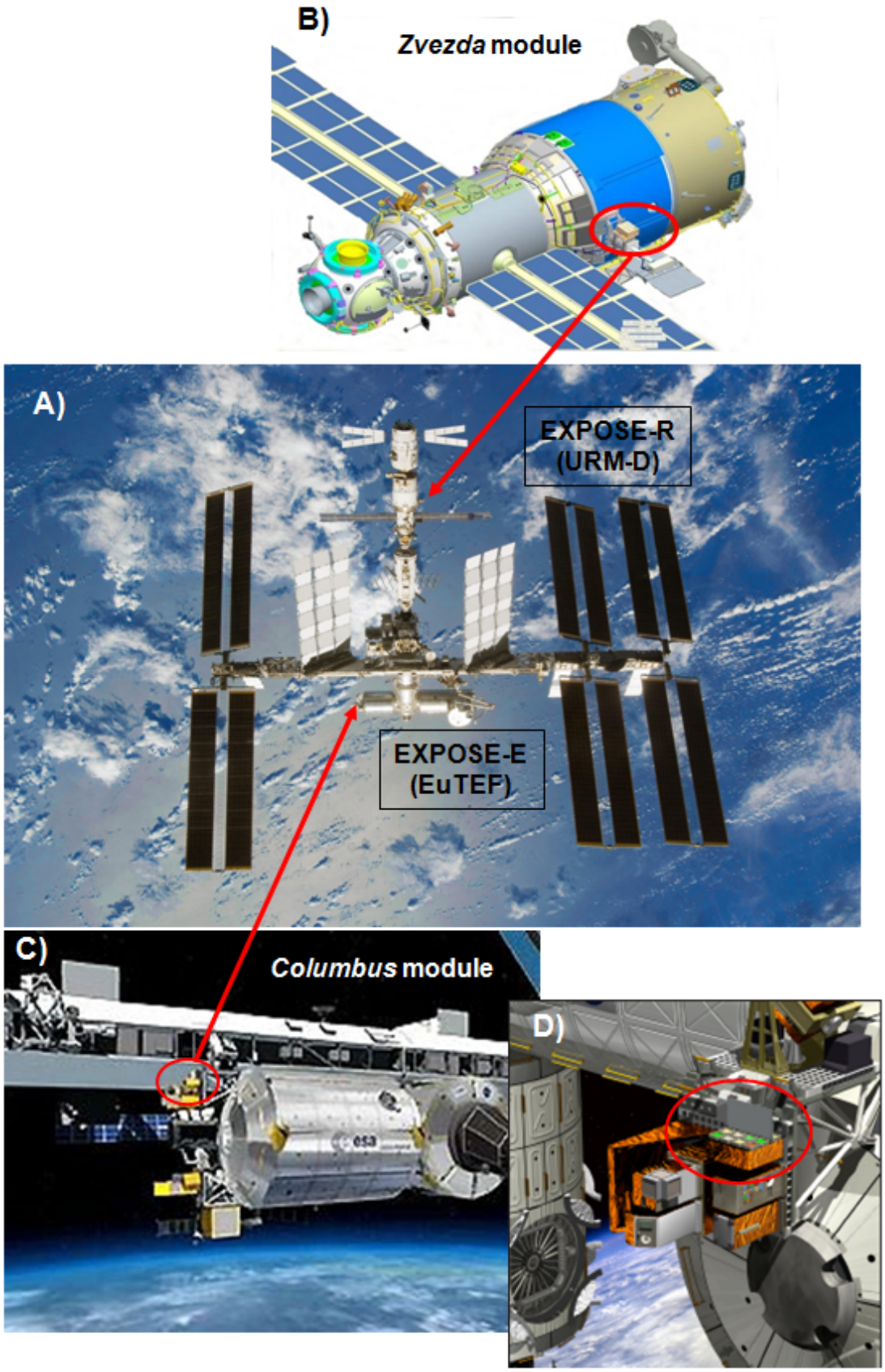

Fig. 2. The International Space Station (ISS) as seen in 2008 (Photo credits NASA) (A) and schematic representations of the Russian module Zvezda (Image: RSC Energia) (B) and European space laboratory Columbus (Photo: ESA) (C). Two astrobiological experiments carried out onboard the ISS: the EXPOSE-E was integrated into the EuTEF facility that was attached outside the ISS on the starboard cone of the Columbus module (C and close up view in D, Image: CNES) and EXSPOSE-R installed on the URM-D platform outside the Zvezda segment (B). The arrows show the places of attachment of the EuTEF and URM-D platforms, carrying the EXPOSE-E and EXPOSE-R facilities, respectively.

2.1. EXPOSE-E mission: SEEDS experiment

The selected EXPOSE-E experiments consist of five astrobiological experiments, which includes four biological experiments (ADAPT, PROTECT, LIFE and SEEDS) and one organic chemistry experiment (PROCESS). In addition, the experiments related to radiation dosimentry (R3D, DOSIS & DOBIES) are also included in the EXPOSE-E mission (**Table 1**) (Rabbow et al., 2009).

Table 1. List of experiments in the EXPOSE-E mission (adapted from Rabbow et al., 2009).

Experiment	Topic of research	Laboratory
ADAPT	To study molecular adaptation strategies of microorganisms to different space and planetary UV climate conditions	P. Rettberg et al. (DE)
PROTECT	To determine the resistance of spacecraft isolates to outer space for planetary protection purposes	G. Horneck et al. (DE)
LIFE	To study the resistance of lichens and lithic fungi to space conditions	S. Onofri et al. (IT)
SEEDS	To test plant seeds as a terrestrial model for panspermia vehicle and as a source of universal UV screens	D. Tepfer et al. (FR)
PROCESS	To study photochemical organic chemistry relevant to comets, meteorites, Mars and Titan	H. Cottin et al. (FR)
R3D	Active radiation dosimetry (VIS, UV-A, UV-B, UV-C ; LET spectra of cosmic radiation)	D-P. Häder et al. (DE)
DOSIS/ DOBIES	Passive radiation dosimetry at the sample sites	G. Reitz et al. (DE) F. Vanhavere et al. (BE)

Since the present work was in the context of the preparation of the SEEDS experiment for the EXPOSE-E mission, the design of SEEDS carriers and sample preparation, as well as the space mission protocol are briefly described here below.

The aim of the EXPOSE-E/ SEEDS experiment was to determine whether dry plant seeds are capable of surviving long periods under harsh conditions of the space environment, including high vacuum, full spectrum of solar UV radiation, cosmic radiation and temperature variations. The results will provide more information concerning the possibility for extreme forms of terrestrial life, such as plant seeds, to be transported from one planet to the other and for their survival in possible extraterrestrial environments e.g. Mars (Tepfer and Leach, 2006). In addition, these experiments aim to determine the chemical stability of known UV screening molecules after exposure to the high flux of the full spectrum of solar radiation. The SEEDS

experiment consisted of two sets of experiments: the flight experiments and the mission ground reference experiments. Each of these two sets comprised the UV exposed samples in the upper sample carrier and the dark control samples in the lower sample carrier (**Fig. 1** and **Fig. 3A**). The SEEDS experiment included 36 samples per each carrier (**Fig. 3B**), of which were two lines of *Nicotiana tabacum* (tobacco) seeds and six lines of *Arabidopsis thaliana* seeds, including mutants that lack UV-screening compounds (flavonoids and sinapate esters), as well as a mutant with increased seeds flavonoid content that was prepared in our laboratory (Chaudhuri et al., 2009`, see **Article 4** in chapter 9). Dry plant seeds were deposited in monolayers into small square cells (9.5 x 9.5 mm), each covered separately by a small MgF_2 window. Seed monolayers were sandwiched between small metal plates and MgF_2 windows and they were held in place by the pressure of springs placed beneath the metal plates (**Fig. 3C**). For details about the design of SEEDS sample cells and carriers see the technical drawings presented in **Annex B-1**, **B-2** and **B-3**. Beside dry seeds, the SEEDS experiment also included chemical samples, such as purified, naked DNA and known UV screening compounds (flavonoids, scytonemin and melanin), which were dried onto MgF_2 windows inside the sample cells **Fig. 3B**). No other cut-off or neutral density optical filter was used in the SEEDS experiment. All samples had free access to the space vacuum.

Loaded EXPOSE-E carriers were first integrated into experiment trays at the DLR. They were than transported to NASA's Kennedy Space Center (KSC) in Florida, USA. At the KSC, the EXPOSE-E facility was integrated into the EuTEF platform, which in addition to EXPOSE, also carried several other European experiment facilities (**Fig. 4**). On February 7, 2008, the Atlantis Space Shuttle (STS-122 mission) was successfully launched from KSC, carrying the EuTEF facility, together with the European space laboratory *Columbus* and the SOLAR facility to the ISS (**Fig. 5A** and **Fig. 5B**). Following the integration of the *Columbus* module to the ISS, EXPOSE-E was successfully installed during the third EVA (extravehicular activity) of the STS-122 mission on the starboard cone of *Columbus* and began to run on February 20, 2008 (**Fig. 5C**) (Rabbow et al., 2009). After 558 operative days, EXPOSE-E was retrieved, together with the whole EuTEF platform from *Columbus* module on September 2, 2009 and returned back to Earth by the Discovery Space Shuttle (STS-128 mission), which landed on September 12, 2009 at Edwards Air Force Base, California, USA. After the successful space mission, EXPOSE-E samples were returned to the research laboratories, where the sample analyses are currently in progress.

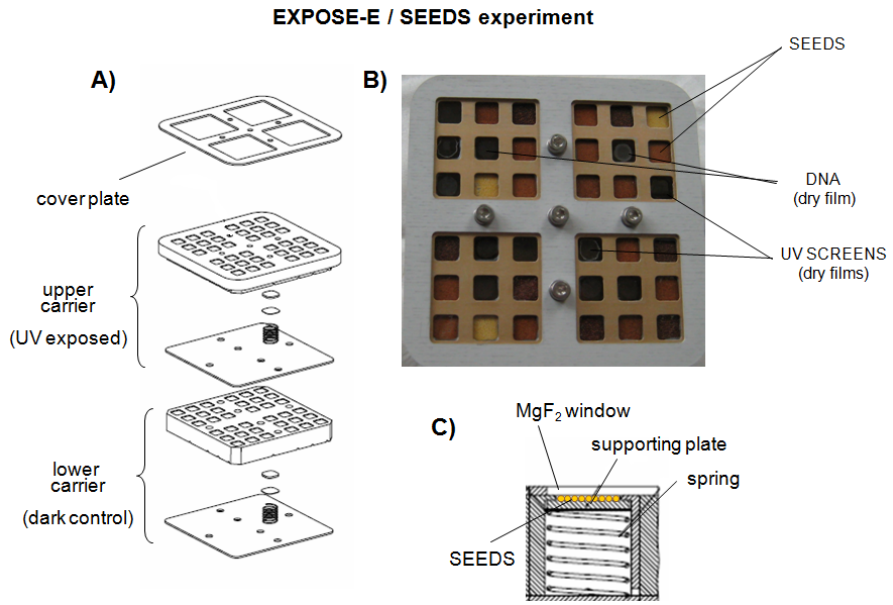

Fig. 3. Design of the EXPOSE-E/ SEEDS experiment. Drawing of the EXPOSE-E/ SEEDS sample carrier assembly (exploded view) (A). Loaded and assembled EXPOSE-E/ SEEDS sample carrier (top view) (Photo taken by Andreja Zalar) (B). Detail of a sample cell loaded with seeds (cross-section drawing) (extracted from technical drawings made by HTS AG., Wallisellen, CH) (C).

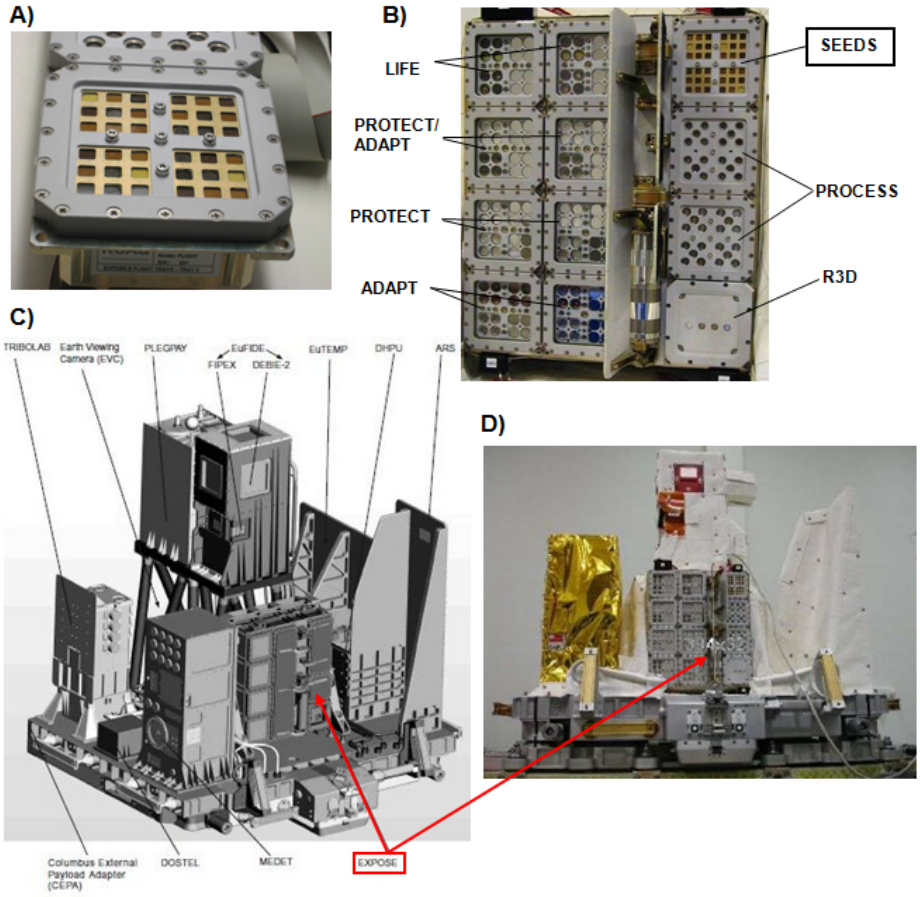

Fig. 4. Loaded SEEDS sample carrier integrated into the EXPOSE tray (Photo taken by Andreja Zalar) (A). The EXPOSE facility with installed sample carriers loaded with different biological and chemical samples used in EXPOSE-E experiments. The position of each experiment is here indicated and the SEEDS experiment is highlighted (Photo: ESA) (B). Drawing of the EuTEF platform with integrated different measuring instruments and experimental facilities, including the EXPOSE facility here indicated with the arrow (Image: ESA) (C). The EuTEF facility photographed at the Kennedy Space Center (NASA), Florida, USA, prior its loading in the space shuttle cargo bay. While other instruments are hidden behind the protective covers, the EXPOSE-E facility is here indicated with arrow (Photo: ESA) (D).

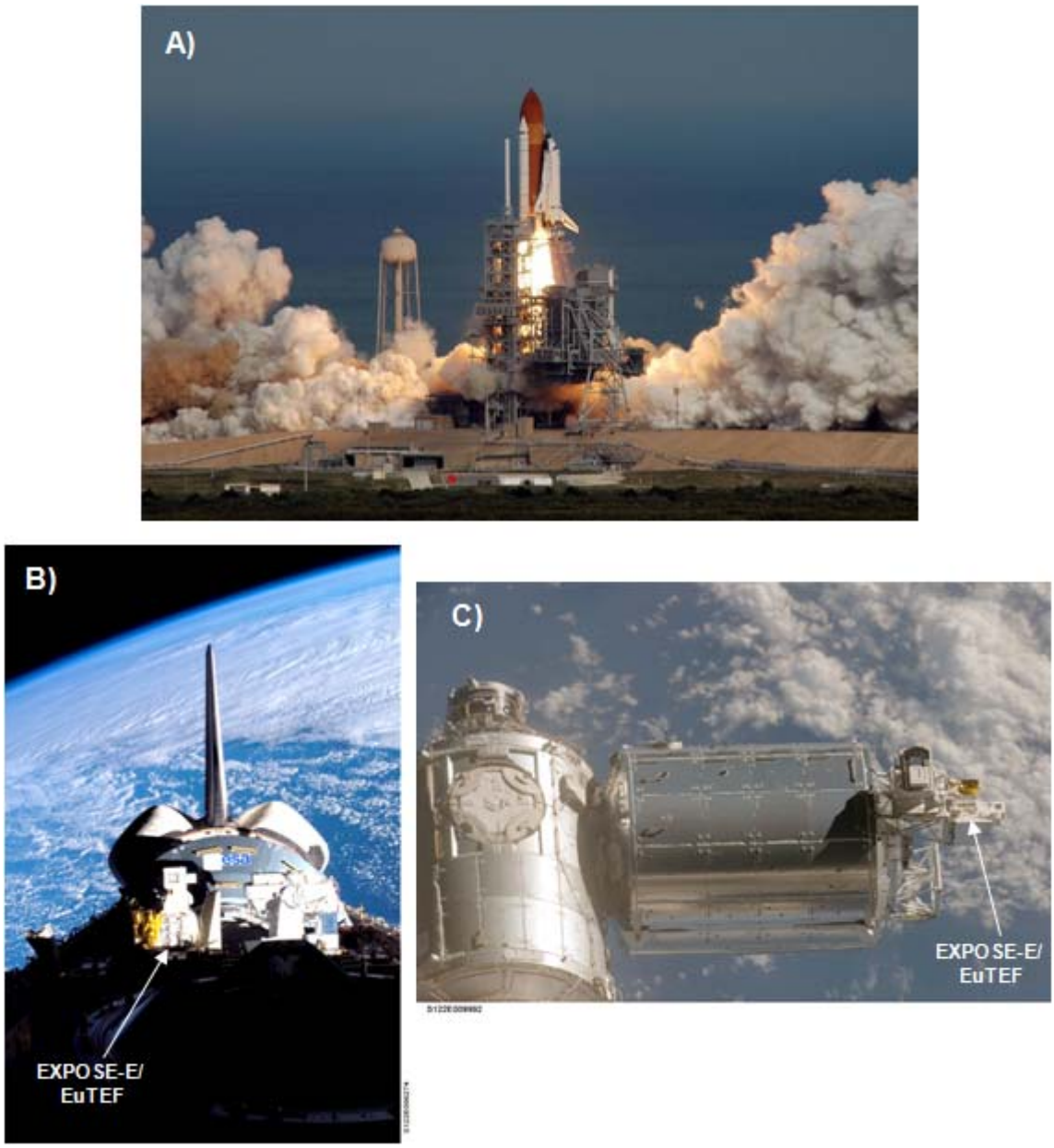

Fig. 5. Space shuttle Atlantis (mission STS-122) lifts off from Kennedy Space Center, Florida, USA on February 7, 2008 (Photo: NASA/ Jim Grossmann) (A). The EuTEF platform with integrated EXPOSE-E facility (marked with arrow) in the open cargo bay of Atlantis shuttle docked at the ISS. The EuTEF facility was delivered to the ISS together with the SOLAR facility (right to the EuTEF facility) and *Columbus* module (in the background) (Photo: NASA/ESA) (B). *Columbus* module installed to the ISS with attached EuTEF platform carrying the EXPOSE-E facility (marked with arrow) (Photo: NASA/ESA) (C).

2.2. EXPOSE-R mission: AMINO/ SEEDS experiment

The EXPOSE-R experiments consist of seven biological experiments (ROSE consortium 1-6 and SEEDS) and two organic chemistry experiments (AMINO and ORGANIC) (**Table 2**) (Rabbow et al., 2009). In addition, the EXPOSE-R project also includes several experiments proposed by Russian scientists (not presented here).

Besides EXPOSE-E, the aim of the present work was also to prepare the samples and post-flight analysis for the SEEDS experiment of the EXPOSE-R mission. Due to administrative reasons, the SEEDS experiment was integrated within the AMINO experimental group. Some details about AMINO/ SEEDS hardware design and sample preparation are given here below.

Table 2. List of EXPOSE-R experiments that are currently running on the ISS (modified from Rabbow et al., 2009)

Experiment	Topic of research	Laboratory
AMINO SEEDS	To study photochemical processing of amino acids in Earth orbit To test survival of plant seeds to extreme conditions encountered in space (UV, vacuum and cosmic radiation).	H. Cottin (A. Brack) et al. (FR)
ORGANIC	To study the evolution of organic matter in space	P. Ehrenfreund et al. (NL)
ROSE-1/ ENDO	To assess the impact of extraterrestrial UV radiation on microbial primary producers (algae, cyanobacteria)	C. Cockell et al. (UK)
ROSE-2/ OSMO	To asses the protective effects of osmophilic microorganisms enclosed within gypsum-halite crust	R. Mancinelli et al. (US)
ROSE-3/ SPORES R3D	To asses the protection of spores by meteorite material against space conditions: UV, vacuum and ionizing radiation/ Radiation dosimetry	G. Horneck et al. (DE)
ROSE-4/ PHOTO	To determine the photoproducts resulting from exposure of dry DNA samples or bacterial spores to solar UV radiation	J. Cadet et al. (FR)
ROSE-5/ SUBTIL	To determine the mutational spectra of *Bacillus subtilis* spores induced by space vacuum and/ or solar UV radiation	N. Munakata et al. (JP)
ROSE-8/ PUR	To determine the biologically effective dose of solar extraterrestrial UV radiation by biological dosimetry	G. Rontó et al. (HU)

The AMINO/ SEEDS experiment serves as a backup experiment for the EXPOSE-E/ SEEDS experiment, and it is performed to some extent under different local UV radiation environment, since it is placed on the opposite side of the ISS (**Fig. 2**). The EXPOSE-R/ SEEDS experiment shares hardware with ORGANIC experiment, occupying one quarter of the sample carrier (**Fig. 6** and **Fig. 7**).

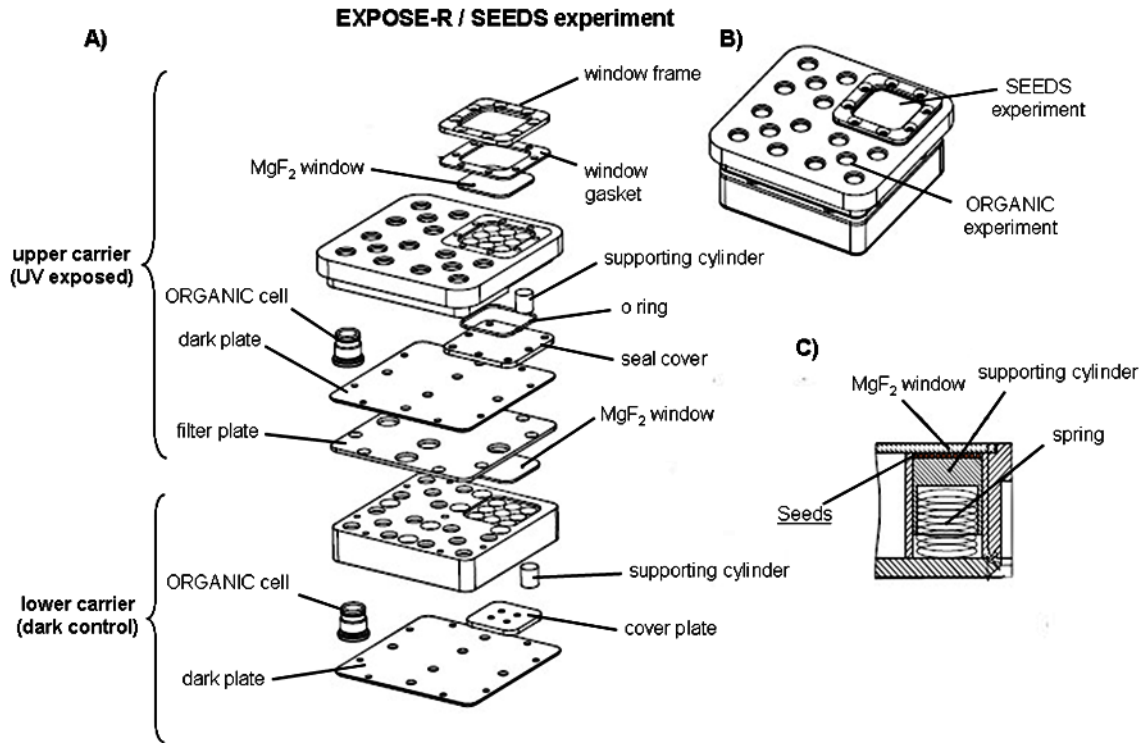

Fig. 6. Design of the SEEDS sample carrier for EXPOSE-R mission. Drawing of the ORGANIC/ SEEDS sample carrier assembly (exploded view) (A). Assembled ORGANIC/ SEEDS sample carrier (B). Detail of the SEEDS sample cell loaded with seeds (cross-section drawing) (C) (extracted from technical drawings made by HTS AG., Wallisellen, CH).

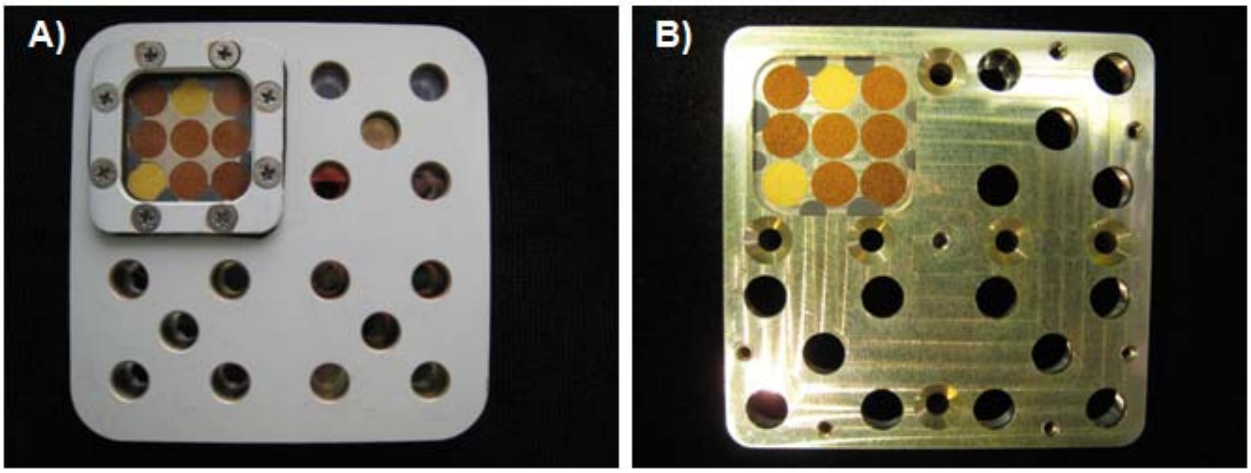

Fig. 7. Loaded ORGANIC/ SEEDS carriers for EXPOSE-R mission: upper (A) and lower (B) flight carrier (Photo taken by Andreja Zalar).

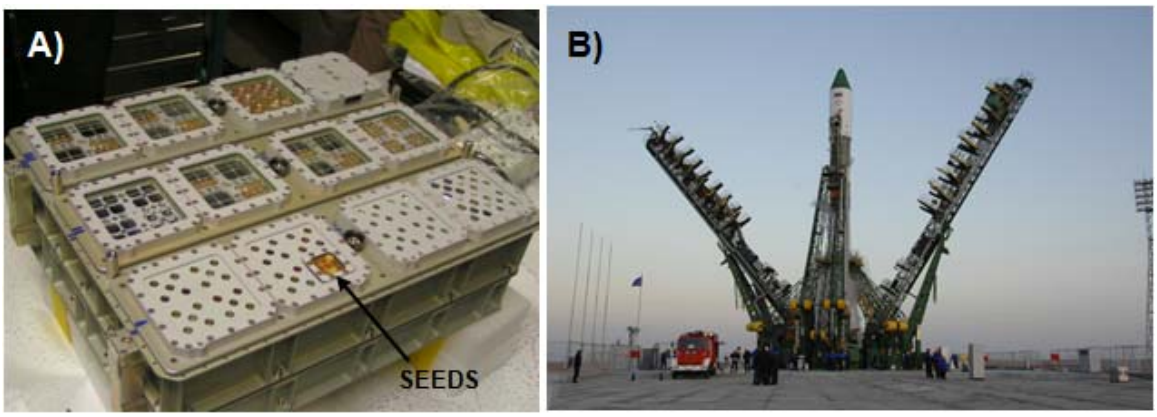

Fig. 8. Loaded sample carriers integrated into the EXPOSE-R facility. The EXPOSE-R/ SEEDS experiment is indicated with arrow (Photo: ESA) (A). Russian cargo vehicle Progress 31-P carrying EXPOSE-R facility prior its launch from Baikonour Cosmodrome in Kazakhstan on November 26, 2008 (Photo: S. P. Korolev RSC Energia) (B)

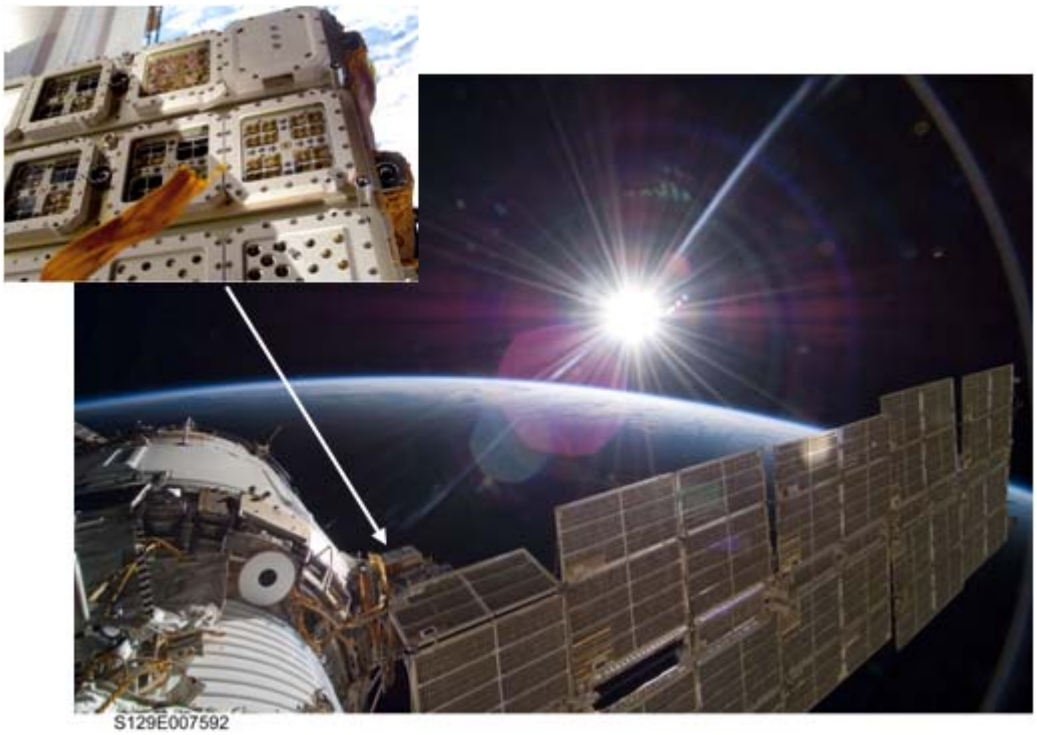

Fig. 9. The EXPOSE-R facility (see arrow) installed outside the Russian *Zvezda* module of the ISS. Inset: a close up view of the EXPOSE-R (Photo: ESA).

This experiment included 9 samples of *Arabidopsis thaliana* dry seeds per each sample carrier. Seed samples consisted of wild type seeds and mutant lines that lack UV screening compounds, flavonoids and sinapate esters. Samples were loaded into small rounded cells (∅ ≅ 8 mm), which differed in design from those used in the EXPOSE-E/ SEEDS experiment (**Fig. 6**). For details about the design of EXPOSE-R/ SEEDS sample cells and carriers see the technical drawings presented in **Annex B-4**. Dry seeds were deposited in monolayers, which were held in position by supporting cylinders and springs beneath. All 9 cells were covered by one bigger square MgF_2 window. Just as for EXPOSE-E, no cut-off or neutral density filters were used in the EXPOSE-R/ SEEDS experiment. All sample cells are vented, allowing access to the space vacuum. Similar to EXPOSE-E, EXPOSE-R/ SEEDS experiments consist of UV exposed (upper carrier) and dark control (lower carrier) sets of samples (**Fig. 6**). EXPOSE-R/ SEEDS is composed of three sets of experiments: the flight experiments, mission ground reference experiments, and additional laboratory control experiments. The latter includes the seed samples that are loaded in the same EXPOSE-R/ SEEDS hardware and stored in the laboratory in the dark under argon atmosphere during the whole space mission period.

Following the integration of loaded sample carriers, EXPOSE-R was launched on November 26, 2008 with a Russian unmanned Progress 31-P (M-01M) cargo vehicle from Baikonour Cosmodrome in Kazakhstan (**Fig. 8**). After docking with the ISS on November 30, 2008 EXPOSE-R was transferred from the Progress capsule into the Russian module *Zvezda*. During EVA on March 10, 2009, EXPOSE-R was installed on the URM-D platform outside the *Zvezda* segment of the ISS (**Fig. 9**), and one day later, the exposure experiments started. At the present, EXPOSE-R flight experiments, as well as Mission Ground Reference Experiments at DLR are still running. After about 1.5 years of mission, each of the three experiment trays will be removed from the EXPOSE-R core facility and returned to Earth on a Russian Soyuz spacecraft (Rabbow et al., 2009).

3. ASTROBIOLOGY: ORIGINS OF LIFE, EVOLUTION AND POSSIBILITIES FOR LIFE PROPAGATION

With the development of our means for extensive exploration of the solar system and beyond, astrobiology (also termed exobiology) has been established as a new scientific discipline. It comprises knowledge from diverse fields of research and technology, including biology, organic chemistry, astrophysics, geology, planetary science, paleontology, space technology and engineering etc. Astrobiology can be defined as "the study of the living universe" (Chyba and Hand, 2005). Its primary goal is to provide better understanding of the processes that have been involved in the origin, evolution and distribution of life on the Earth or elsewhere in the universe (Horneck and Brack, 1992; Horneck, 1995). Astrobiology includes the study of terrestrial biology, since the search for life elsewhere is influenced by our knowledge of life as we know it on the Earth, and on the other hand, studies on conditions in extraterrestrial environments may help us with ideas about possible conditions on early Earth, which influenced the origin and evolution of terrestrial life (Chyba and Hand, 2005).

3.1. The origins of life on Earth

The origin of life still remains a fundamental mystery that nearly every culture attempts to explain. Although it seems reasonable to discuss the term "life" prior its origin, to this date, there is no generally accepted definition of this word. Nevertheless, most scientists agree that the three main characteristics of living entities are metabolism, growth and reproduction. Life as we know it is based on the availability of liquid water and biogenic chemical elements (e. g. C, H, O, N, S, P), and it requires some usable source of energy. Water is considered one of the prerequisites for life due to its unique properties, such as the formation of hydrogen bonds, high polarity and high dielectric constant, which make water an ideal solvent, reactant and stabilizer of the complex three-dimensional molecular structures in all known living systems (Horneck, 1995; Brack, 1999; Chyba and Hand, 2005). Life as we know it is based on carbon as the principal biogenic element, which is incorporated into living systems by the use of energy, obtained either chemically or by capturing sunlight (Chyba and Hand, 2005). Despite our lack of scientific understanding of the origin of life, some points are almost certain; all known organisms depend on DNA to store their genetic information and they use a similar genetic code (Crick, 1981; Eigen et al., 1989). Therefore it seems reasonable to assume that all life forms on Earth came from a single source. Our knowledge about the timescale of the emergence of life on Earth is

constrained on the one hand end by the time of planetary formation in our solar system, and on the other hand by the available geological evidence of early life on Earth (Chyba and Hand, 2005).

The age of our solar system is about 4.56 Ga, and the Earth's crust probably formed as early as 4.42 Ga ago (Lehto, 2007). The geochemical signatures of history imprinted into zircon crystals indicate that liquid water may have existed on Earth 4.3-4.4 Ga ago (Mojzsis et al., 2001; Wilde et al., 2001). There is good evidence that life on Earth emerged as early as 3.5 Ga ago. Fossil records have revealed a remarkable diversity of ancient microflora existing at that time (Schopf and Packer, 1987; Schopf, 1993). The 3.5 Ga old cyanobacteria-like microfossils and stromatolites suggest an early existence of photosynthesis, which represents a remarkable metabolic sophistication for early life on the Earth (Awramik, 1992; Schopf, 1993; Garcia-Pichel, 1998; Des Marais, 2000). Moreover, the isotopic signatures of organic carbon brought indirect evidence that life on Earth might be as old as 3.8 Ga (Mojzsis et al., 1996). On the other hand, heavy cosmic bombardment with potentially sterilizing capacity is believed to have occurred until about 3.8-3.9 Ga ago (Sagan, 1974; Maher and Stevenson, 1988). This would mean that life had probably a very narrow "time window" to emerge and to evolve up to a well advanced cellular level, which seems paradoxical given the complexity of the job and the probability that the conditions on early Earth were inhospitable to life (Chyba and Hand, 2005).

In spite of the fact that much essential information is still missing, different theories have been proposed to explain the appearance of life on Earth. There are two principal approaches to the origin of life on Earth that are currently considered: the hypothesis of abiogenesis, which refers to *in situ* development of life through chemical evolution, starting from inanimate (inorganic) matter, and alternatively, the panspermia hypothesis that implies the introduction of life from outside the Earth (Crick, 1981; Burchell, 2010).

3.1.1. Abiogenesis

This hypothesis of chemical evolution on Earth is based on the so-called "primordial soup" theory. This scenario of prebiotic evolution was first speculated by Charles Darwin (1871), who suggested that the life may have begun in "some warm little pond, with all sorts of ammonia and phosphoric salts, lights, heat, electricity, etc. present, so that a protein compound was chemically formed ready to undergo still more complex changes, …". This theory of chemical stage of prebiotic evolution was further supported by Aleksander Oparin (1924), who considered the

synthesis of organic compounds in putatively reducing the Earth's primitive atmosphere and their accumulation in the primitive ocean. It was experimentally tested by Stanley Miller and Harold Urey (Miller, 1953; Miller and Urey, 1959), who synthesized complex organic compounds, including four naturally occurring proteinogenic amino acids, from a mixture of simple, hydrogen-rich molecules, such as methane, ammonia, hydrogen and water, exposed to an electric discharge. Since this historical experiment, other prebiotic precursors and seventeen natural amino acids have been obtained under simulated putative prebiotic conditions, using electric discharge, UV light or ionizing radiation as sources of energy (Dyson, 1985; Horneck and Brack, 1992; Kobayashi et al., 1998; Chyba and Hand, 2005). This has encouraged some optimistic extrapolations that further reactions would generate more complex compounds, such as proteins and nucleic acids, leading eventually to the emergence of life (Chyba and Hand, 2005). However, Miller-Urey's type of organic synthesis occurs only under reducing conditions in gas mixtures that contain significant amounts of hydrogen. Although the true composition of primitive Earth atmosphere remains unknown, recent geochemical and photochemical studies favoured the existence of early atmosphere in a neutral oxidation state that was probably dominated by carbon dioxide, rather then the existence of reducing atmosphere (Walker, 1985; Chyba and Sagan, 1992; Sagan and Chyba, 1997). Under such conditions, the production of amino acids appears to be very limited (Dyson, 1985; Horneck and Brack, 1992; Brack, 1999). The nucleotides, which are building blocks of nucleic acids composed of nucleic base, sugar and phosphate, are even more difficult to synthesize (Dyson, 1985). The most plausible way to synthesize a nucleic base was demonstrated by Joan Oró (1960). However, to go from a nucleic base to a complete and stereochemically well arranged nucleotide is an even more delicate matter. Furthermore, once formed, nucleotides are fairly unstable in solution, since they tend to hydrolyse back into their components (Dyson, 1985). In addition, the organic molecules presumably formed in primitive Earth's atmosphere are then supposed to rain down into the primitive oceans producing a dilute soup. In such an exceedingly dilute solution, the reaction rates would be minimal and complex chemical transformation needed for production of biologically important molecules would be hardly feasible. Seeking for the answer of this puzzle, it is proposed that evaporation of water from shallow lakes and ponds, as well as at the margins of the sea may have led to sufficient concentrations of organics for prebiotic chemistry to proceed. Alternatively, possible prebiotic chemical evolution in undersea black smokers has been also considered.

Due to serious constraints of prebiotic chemistry on Earth, recent studies have considered plausible the extraterrestrial origin of prebiotic chemicals. Recent evidence has revealed that

space is a vast laboratory where organic chemistry does occur (Horneck, 1995; Ehrenfreund, 1999; Ehrenfreund and Charnley, 2000). The evolution of potential precursors of life may have happened in space (Ehrenfreund et al., 2006). A large fraction of prebiotic organic molecules could have been brought to the Earth by the infall of meteorites, interplanetary dust particles (micrometeorites) and comets (Chyba and Sagan, 1992; Horneck and Brack, 1992; Maurette et al., 1995; Brack, 1999). A great flux of micrometeorites (3-6 x 10^5 kg $year^{-1}$) and meteorites (10^2 tons $year^{-1}$) reaches the surface of Earth each year. This infall of extraterrestrial material might be even more considerable during the period of heavy bombardment on Earth. (Chyba and Sagan, 1992; Maurette et al., 1995). The carbonaceous meteorites, such as the Murchison meteorite, usually contain up to 5% (w/w) of organic compounds (Horneck and Brack, 1992; Horneck, 1995; Brack, 1999). Recent evidences demonstrated a high molecular diversity of the Murchison meteorite, revealing tens of thousands of different molecular composition and likely millions of diverse structure (Schmitt-Kopplin et al., 1010). From the Murchison meteorite, 8 of the L-amino acids that naturally occur in proteins have been identified among more than 70 amino acids that were found in the mixture of both D- and L-enantiomers (Cronin and Pizzarello, 1983; Brack, 1999; Botta and Bada, 2002). In addition, some purine and pyrimidine bases of nucleic acids have been also identified in meteorites (Brack, 1999; Botta and Bada, 2002). Since there is evidence for intense meteorite bombardment more than 3.9 Ga ago, when the meteorite flux was enhanced by a factor of 10^4, meteorites may have been an important source of prebiotic organics on the primitive Earth (Horneck and Brack, 1992).

Regardless of the source of complex organic compounds on primitive Earth, the prebiotic synthesis of polymeric macromolecules (proteins and nucleic acids) remains a still unsolved challenge. Even less is known about the process of assembly of macromolecules into the first cell-like organized system, which requires at least boundary molecules (membrane lipids) that isolate the system from its environment, catalytic molecules that enable basic metabolic reactions (enzymes) and information molecules allowing the storage and the transfer of genetic information (nucleic acids) (Brack, 1999).

3.1.2. Panspermia

As recent paleogeochemical evidences left an extremely narrow “time window” for life to evolve from the simple molecular precursors to the level of a metabolically advanced photoautotrophic cell, and so far, contemporary research has failed to provide a satisfactory

explanation for abiogenesis on Earth, the alternative hypothesis of panspermia has been suggested. It proposes that life did not arise on Earth *de novo*, but rather came from elsewhere in the universe. Panspermia (from Greek: *pan* = all and *sperma* = seed) was put forward by the chemist Svente Arrhenius (1903), who postulated that "life seeds" could be dispersed in space by radiation pressure from the Sun, thereby seeding life from one planet to another or even between solar systems. Although it is difficult to prove whether panspermia has occurred in the history of the Earth, and whether interplanetary transfer of life through our solar system is plausible at all, the chances for the different steps of a hypothetical panspermia event to occur can be determined experimentally or by calculations (Horneck, 1995). The scenario of interplanetary transfer of life would involve the following three hypothetical steps: (1) the escape process, during which the organism will have to survive transfer from the planetary surface to high altitudes (e.g. ejection of organism caused by volcanic eruptions or giant impact events, such as meteorite, asteroid or comet collisions); (2) the interim state in space, during which the organism will have to survive interplanetary or interstellar transfer, being exposed for long time periods to the harsh conditions of open space (for details about detrimental factors of space environment see section **3.2**); (3) the entry process, during which the organism, being captured by the gravitational force of the hosting planet, will have to survive transit through the atmosphere and landing. In addition, an organism has to be capable of growing under the physical and chemical conditions encountered on the host planet (Horneck and Brack, 1992; Horneck, 1995; Nicholson et al., 2000; Cockell, 2008).

The panspermia hypothesis can be subdivided into distinct classes based on the scenario of the transport of the organisms through space (Secker et al., 1996). For instance, radiopanspermia, as one of the initial panspermia theories, refers to the transfer of a single exposed organism, which is small enough to be accelerated and propelled through space by solar radiation pressure (Arrhenius, 1903; Secker et al., 1996). Lithopanspermia refers to the interplanetary transfer of organisms embedded within meteorites (Mileikowsky et al., 2000; Bernardini et al., 2003; Cockell et al., 2007; Cockell, 2008; Horneck et al., 2008; Sancho et al., 2008; de la Torre et al., 2010). Cometary panspermia promotes the idea that microorganisms might be transported through space by comets, being in freeze-dried state until the time they find a favourable environment for their propagation (Hoyle and Wickramasinghe, 1999; Wickramasinghe, 2004; Wickramasinghe, 2010). Directed panspermia refers to the hypothesis that life can be disseminated through space deliberately by an intelligent civilization, such as human civilization (Crick and Orgel, 1973; Crick, 1981). Exospermia tests the plausibility of Earth's life to be propagated through space, for instance following the natural impact events that happened in the

history of Earth or by human current activities in space exploration (Tepfer and Leach, 2006; Zalar et al., 2007a; Zalar et al., 2007b; Tepfer, 2008).

Nevertheless, ever since its formulation, panspermia has been strongly criticized or even severely rejected, arguing that panspermia can not be experimentally tested, that it shunts aside the question of the origin of life, and that the living organisms will not survive long exposure to the hostile environment of space (Horneck, 1995; Nicholson et al., 2000; Horneck et al., 2001). However, several recent discoveries have led to reexamination of the plausibility of panspermia theory. Among others, these are: (1) the discovery of meteorites on the Earth, some of which are of Martian and some of lunar origin (Warren, 1994); (2) the detection of organic compounds, including amino acids and nucleic acid bases in Martian meteorites (for review see Botta and Bada, 2002); (3) the discovery, although still fairly controversial, of hints of past microbial life on Mars (e.g. putatively biogenic microstructures in ALH84001 meteorite and structures in Murchison and Orgueil meteorites that might resemble the terrestrial microfossils of cyanobacteria) (McKay et al., 1996; Hoover, 2007); (4) the probability of small particles and even boulder-sized rocks reaching escape velocities through the impact of a large meteorite on a planet (Melosh, 1985; Melosh`, 1988; Moreno, 1988); (5) simulation experiments revealed that bacterial spores are capable of surviving the ejection and landing forces, which may be associated with interplanetary transfer caused by meteorite impact (Horneck et al., 2001; Burchell et al., 2003; Burchell et al., 2004); (6) the survival of bacterial spores over extended periods in space provided they are shielded against intensive solar UV light by e.g. layers of clay, rocks or meteorite material (Horneck et al., 1994; Horneck et al., 1995; Horneck et al., 2001; Rettberg et al., 2002); (7) increased UV resistance of microorganisms at simulated low temperatures of deep space (Weber and Greenberg, 1985) (8) the likelihood of directed panspermia (exospermia) by man’s space missions to other planets (Mautner, 2004; Tepfer and Leach, 2006; Tepfer, 2008).

3.2. Physical factors that determine survival in space and extraterrestrial environments

The space environment is generally considered as being extremely hostile for all known forms of life, thus limiting the chances of life being propagated throughout the solar system and beyond. It is characterized by different physical factors including a high vacuum, an intense solar electromagnetic radiation and ionizing particle radiation of both solar and galactic origin, extreme temperature fluctuations, and microgravity. The parameters of the environment of interplanetary space and in Low Earth Orbit (LEO) environments are presented in **Table 3**.

Table 3. Major deleterious factors of the interplanetary space and low Earth orbit (LEO) environment (modified from Horneck et al, 2000).

Space parameter	Interplanetary space	Low Earth orbit
Space vacuum		
Pressure (Pa)	10^{-14}	10^{-7}–10^{-4}
Residual gas (part cm^{-3})	1H atom	10^{4}–10^{5} H
		10^{4}–10^{6} He
		10^{3}–10^{6} N
		10^{3}–10^{7} O
Solar electromagnetic radiation		
Irradiance (W m^{-2})	Different values [a]	1360
Spectral range (nm)	Continuum	Continuum
Cosmic ionizing radiation		
Dose (Gy $year^{-1}$)	≤ 0.1 [b]	400–10 000 [c]
Temperature (K)	> 4 [a]	Wide range [a]
Microgravity (g)	< 10^{-6}	10^{-3}–10^{-6}

[a] Depending on orientation and distance from the Sun

[b] Depending on shielding; highest values at mass shielding of 0.15 gcm^{-2}

[c] Depending on altitude and shielding; highest values at high altitudes and shield of 0.15 gcm^{-2}

3.2.1. Deleterious wavelengths of solar electromagnetic radiation

Our Sun is a G2-type star that emits photons over a wide range of wavelengths that span several orders of magnitude, from short-wavelength X-rays (occasionally even shorter wavelengths, γ-rays, which are emitted during solar flares) up to radio frequencies, as seen in **Fig. 1** (Grieder, 2001a; Hasan, 2008). At the mean Earth-Sun distance (1 astronomical unit = 1

AU), the Sun's total radiative output is approximately 1365 Wm^{-2} (± 1.0), which is termed the solar "constant", in spite of smaller variability in energy flux observed during the 11-year cycle of solar activity (Lean, 2008). Out of the total electromagnetic radiation emitted from the Sun, a large fraction is attributed to infrared radiation (IR, λ > 800 nm) and visible radiation (VIS, λ = 400 - 800 nm), which make up about 37% and 43% of the total solar radiant output, respectively (Nicholson et al., 2005). However, potentially deleterious radiation for all known biological systems is that of the short-wavelength part of the solar spectrum, including highly energetic UV radiation, X-rays and γ-rays.

3.2.1.1. Ultraviolet (UV) radiation

Ultraviolet radiation (UV, λ = 100 – 400 nm) constitutes only about 7% of the total solar output (Nicholson et al., 2005; Baglioni et al., 2007). Yet, this part of the spectrum has an important impact on survival in space and extraterrestrial environments. In contrast to the Earth's environments, a full spectrum of solar UV radiation, including highly energetic UV-C and VUV wavelengths can be encountered in interplanetary space. Solar UV radiation has been found to be one of the most deleterious factors in space as tested with dry preparations of viruses, bacterial and fungal spores (Hotchin et al., 1968; Lorenz et al., 1968; Bücker et al., 1974; Spizizen et al., 1975; Horneck et al., 1984a; Horneck et al., 1984b; Horneck, 1993; Horneck et al., 1994; Horneck et al., 1995). Because it is one of the most important factors that limit dispersal of life through space, detailed information about the effects of UV radiation on biological systems, as well as the UV regimes on Earth and other extraterrestrial environments are given in section **3.3.**

3.2.1.2. Ionizing electromagnetic radiation: X-rays and γ-rays

The Sun emits a small portion of highly energetic photons with wavelengths shorter than those of UV radiation. These wavelengths are entirely filtered out by the Earth's atmosphere, but they are present in the space environment. Although the effects of X- and γ-rays may be more lethal than UV photons, their total energy input is generally orders of magnitude lower than that of the UV (Weber and Greenberg, 1985).

The X-ray region of the electromagnetic spectrum extends from the wavelength of 0.01 nm to the short-wavelength side of the UV region. Since X-rays are very energetic, they are usually defined in energy terms ranging from 1 to 100 keV (Smith, 2000). The photons carrying energies of 1-10 keV are usually classified as "soft " X-rays due to their relatively modest penetrating

power, while those with high energies of 10-100 keV are known as “hard” X-rays due to their remarkable penetrating abilities through solid objects. Similarly to UV radiation, the X-ray emission of the Sun varies significantly over the 11-year cycle of solar activity. During periods of higher solar activity, the Sun can emit powerful bursts of X-rays and other high-energy radiation. X-ray bursts accompany essentially every solar flare event, which occurs many times per day during times of great solar activity (Smith, 2000; Hasan, 2008). In addition to a solar source, X-rays can also originate from other sources in the Universe, including quasars and compact objects such as white dwarf stars, neutron stars and black holes. Nevertheless, the contribution of X-ray fluxes that comes from these extrasolar sources is relatively small in comparison to the Sun, which is the brightest source of X-rays in our solar system (Smith, 2000).

The γ-rays are the shortest and the most energetic electromagnetic waves, exceeding an energy of 100 keV (Smith, 2000). Their contribution to the radiation environment of our solar system is extremely small. They are occasionally emitted from the Sun, being generated in the nuclear reactions during solar flares (Hasan, 2008). γ-rays can also be emitted from other highly energetic cosmic sources, including pulsars, supernovas remnants, interstellar clouds etc. (Smith, 2000; Grieder, 2001b).

Both X- and γ-rays are ionizing radiations, since they are energetic enough to detach electrons from any atom or molecule that they strike. Therefore they are potentially hazardous for all biological systems. For X- and γ-rays it is characteristic that they produce ionization homogenously within the matter that they penetrate and the deposit energy declines exponentially with penetration depth (Baumstark-Khan and Facius, 2002; Nelson, 2003). The main biological effect of ionizing radiation is the production of highly reactive free radicals (e.g. $H^{\bullet}$, $^{\bullet}OH$, H_2O^{+}) in irradiated cells that mostly originate from ionized water molecules. Besides indirect damage through interactions with radicals, X- and γ-rays can also induce direct damage to the DNA molecule, causing DNA-strand breaks that may lead to serious chromosome aberrations (Baumstark-Khan and Facius, 2002; Nelson, 2003; Bernhard and Close, 2004). At the cellular level, ionizing electromagnetic radiation induces mutagenesis, malignant alternations and ultimately cellular death (Nelson, 2003; NRC`, 2008).

3.2.2. Ionizing particle radiation: Cosmic radiation

Although X- and γ-rays are present in space, the majority of space ionizing radiation is not in the form of electromagnetic waves, but rather is dominated by the energetic, highly penetrating subatomic particles and ions of galactic and solar origin. The surface of the Earth is largely protected from cosmic radiation thanks to the deflecting effect of the Earth's magnetic field. However, other planetary bodies, which have weak magnetospheres (e.g. Mars) or they lack it (e.g. Moon) are exposed to deleterious cosmic radiation. In interplanetary space, the primary components of the radiation field in our solar system are Galactic Cosmic Rays (GCR) and Solar Cosmic Radiation (SCR) (Horneck and Brack, 1992; Baumstark-Khan and Facius, 2002; Baglioni et al., 2007). In the vicinity of the Earth (e.g. in Low Earth Orbit, LEO), the radiation field comprises the third source of radiation: the Van Allen radiation belts. Two radiation belts, the inner and outer one, result from the interactions of GCR and SCR with the Earth's magnetic field and the atmosphere. These radiation belts consist mainly of trapped protons and electrons, and some low-energy heavy ions (Klecker, 1996; Baglioni et al., 2007; NRC`, 2008). The doses of cosmic radiation in interplanetary space and the LEO are compared in **Table 3**.

GCR originates from outside of our solar system (e.g. supernova explosions and quasars) and their energy range extends from several hundred MeV to tens of GeV (Usoskin et al., 2001; NRC`, 2008). When GCR enter our solar system, they must overcome the outward-flowing solar wind. Since the intensity of the solar wind varies during the 11-year cycle of solar activity, the GCR flux is also modulated according to the solar cycle; it reaches its highest level during minimal solar activity and lowest level during maximal solar activity (Kopp et al., 1999; Baumstark-Khan and Facius, 2002; NRC`, 2008). GCR consist of 98% nuclei and 2% electrons (Baumstark-Khan and Facius, 2002; Baglioni et al., 2007). The former component is composed predominantly of protons (87%), a smaller fraction of α-particles (12%) and a few heavier nuclei (~1%), also called HZE (High charge (Z) and Energy) particles (Horneck and Brack, 1992; Kopp et al., 1999; Baumstark-Khan and Facius, 2002). The HZE particles are defined as cosmic ray primary ions with charges of $Z > 2$ and energies high enough to penetrate at least 1 mm of spacecraft or spacesuit shielding (Horneck and Brack, 1992; Baglioni et al., 2007). Although having only a small contribution to the GCR flux, HZE particles are considered deleterious for living organisms due to the special nature of HZE particle-produced lesions and the inefficiency of shielding (Horneck, 1992; Reitz et al., 1995; Mileikowsky et al., 2000; NRC`, 2008). The very high local concentration of absorbed energy produced by a HZE particle can lead to intense

ionization of matter and it can cause serious biological effects, leading ultimately to cell damage and its death. Compared to ionizing electromagnetic radiation, charged particle radiation interacts with matter in a specific fashion. Charged, accelerated particles penetrate deeply into matter, exhibiting localized tracks. They tend to produce the clusters of ionization and deposit almost all energy at discrete stopping distance, known as the Bragg peak (Baumstark-Khan and Facius, 2002; Nelson, 2003). In addition, penetrating into matter, the charged particles can generate a secondary particle emission (NRC`, 2008). This is of special concern for radioprotection and usage of shielding materials (Mileikowsky et al., 2000; NRC`, 2008).

SCR consists of the low energy solar wind particles (mainly protons) that flow constantly from the Sun and highly energetic particles, known as Solar Particle Events (SPEs) that are emitted sporadically from the Sun as a burst of charged particles during solar flares. SPEs develop rapidly and generally last for no more than a few hours, although some proton events can last over several days (Baumstark-Khan and Facius, 2002; NRC`, 2008). The emitted SPEs can reach very high energies up to several GeV (Baglioni et al., 2007; NRC`, 2008). The SPEs are composed predominantly of protons (90-95%), with a relatively small fraction of α-particles (5-10%), and a minor contribution of heavy ions and electrons (1%) (Horneck, 1992; Baumstark-Khan and Facius, 2002; Baglioni et al., 2007). SPEs are also modulated by the solar cycles. During the solar minimum phase few significant SPE occur, while during each solar maximum phase large events may occur even several times (Baumstark-Khan and Facius, 2002)

3.2.3. Space vacuum

In free interplanetary space, extremely low pressures as low as 10^{-14} Pa can be encountered. Nevertheless, within the vicinity of planetary bodies, the pressure is significantly higher due to the phenomenon of outgassing. Therefore, in the LEO environment, the pressure reaches 10^{-6} to 10^{-4} Pa, and it can further increase in the close vicinity of a spacecraft (Nicholson et al., 2000; Baglioni et al., 2007) (**Table 1**). The major effect of extreme space vacuum is severe desiccation of biological material. Depending on the time of exposure to high vacuum, living cells start first to dehydrate due to the loss of free water. Subsequently the hydrated water, and finally chemically bound water and other volatile molecules may be removed from the cells after prolonged exposure to high vacuum (Horneck and Brack, 1992; Horneck, 1995). Extreme space vacuum is deleterious for many organisms, since it affects the structure and function of many biologically important molecules. It induces the DNA-strand breaks, the formation of DNA-protein complexes, damage to proteins and membranes, changes in carbohydrate structures etc.

(Horneck and Brack, 1992; Cox, 1993; Nicholson et al., 2000; Fekete et al., 2005). However, some of the organisms as we know on Earth are adapted to withstand harsh conditions in the desiccated state. These naturally desiccation-tolerant life forms, such as bacterial and fungal spores, lichens and plant seeds, are capable of surviving exposure to space vacuum (Anikeeva et al., 1990; Alston, 1991; Horneck, 1993; Horneck et al., 1994; Dose et al., 1995; Horneck, 1995; Horneck et al., 1995; Nicholson et al., 2000; Musgrave, 2002; Sancho et al., 2007).

3.2.4. Temperature extremes

The extreme temperatures that are encountered in space and extraterrestrial environments are determined by the extreme frigidity of free space, characterized by a temperature of only 4 K (-269 °C), and on the other hand, by the position of the body towards an energy source (**Table 3**) (Horneck et al., 1984a; Horneck and Brack, 1992). Hence the average surface temperatures of planetary bodies in our solar system decrease with the distance from the Sun and they can range, with the exception of Venus, from +167 ºC on Mercury (~ 0.4 AU) down to -236 ºC on Pluto (~ 39.5 AU) (Faure and Mensing, 2007a). In addition, the temperature of a body in space, which is determined by the absorption and emission of energy, depends also on the size of the body, its mass, surface and albedo (Nicholson et al., 2000). Moreover, the presence of an atmosphere that contains so-called greenhouse gasses (e.g. CO_2, CH_4 and water vapour) also influences the surface temperatures on planetary bodies. That is why Venus (~ 0.7 AU), which has a very dense atmosphere composed mostly of CO_2, exhibits an anomalously high average surface temperature of +464 °C (Faure and Mensing, 2007a). On the other hand, extreme fluctuations of temperatures can be also experienced on bodies that orbit the Sun, since they are periodically shaded from the solar irradiation (Nicholson et al., 2000). The temperatures on the Earth's surface range from -90 ºC up to +58 ºC, while on Mars from -140 ºC up to +20 ºC (Faure and Mensing, 2007a).

The exposure to extreme temperatures can cause many physical and chemical changes in living systems. Freezing leads to cellular destruction due to ice crystals formation, while heating to temperatures close to 100ºC induces denaturation of biomolecules. Although temperature is one of the important limiting parameters for survival, many terrestrial organisms not only tolerate extreme temperatures, but they also grow and develop in extremely hot or cold environments that can be also experienced on an otherwise hospitable Earth. For instance, the most hyperthermophilic terrestrial organism is archaea *Pyrolobus fumarii*, which is capable of growing at the highest temperature of up to +113ºC (Blöchl et al., 1997). On the other hand, many microbes,cell lines and plant seeds can be conserved successfully at temperatures as low as

-196ºC, and many terrestrial microorganisms are known to survive extremely low temperatures in Arctic and Antarctic permafrost (Rothschild and Mancinelli, 2001; Ponder et al., 2004). However, the lowest temperature at which metabolic activity is still recorded in some microbial communities is -18ºC (Rothschild and Mancinelli, 2001; Clarke, 2003). In the resting state, the organisms can survive even more extreme temperatures than in their vegetative forms.

3.2.5. Microgravity

In interplanetary space, a low gravitational force (< 10^{-6} g) is experienced (**Table 3**). At the level of the International Space Station (ISS), which orbits the Earth at an altitude of about 350 km, the gravitational force is reduced to only about 8%, compared to that at the Earth's surface. In order to achieve reduced gravity, the spacecrafts have to accelerate so that the gravitational force and centrifugal force are equal in amount, but with opposite vectors. The resulting microgravity conditions in the spacecrafts are characterized by the acceleration in the range of 10^{-4}-10^{-6} g (Musgrave, 2002; Baglioni et al., 2007). In microgravity, some physical phenomena behave differently than at 1g conditions at the surface of the Earth. For instance, hydrostatic pressure, sedimentation and convection, which are all linearly proportional to gravity, fall to close to zero values in microgravity. Therefore, many biochemical reactions that occur within cells of living organisms will be affected by microgravity (Baglioni et al., 2007). It may also result in altered morphology and physiology of various living systems (Horneck et al., 1996; Ingber, 1999; Musgrave, 2002; Brinckmann, 2007). However, for many terrestrial organisms microgravity is not lethal (Rothschild and Mancinelli, 2001; Musgrave, 2002; Brinckmann, 2007). Microgravity is of even less concern for life forms that have a low water content and that have a significantly reduced metabolic activity, such as dry bacterial spores and plant seeds that experience a temporary state of metabolic quiescence.

3.3. Solar ultraviolet (UV) light as deleterious factor for life

Although only a small portion of electromagnetic radiation emitted from the Sun is assigned to the UV part of the spectrum (~ 7%), compared to the infrared and visible radiation that comprise the majority of the total solar radiant energy (**Fig. 11**), UV radiation has a strong impact on all known biological systems and it is considered as one of the main limitation factor for dispersal of life in space (Horneck, 1995; Horneck et al., 2001; Nicholson et al., 2005).

The UV part of the solar spectrum spans wavelengths from about 100 to 400 nm according to the International Commission on Illumination (CIE) (Braslavsky, 2007; Sliney, 2007). This range is commonly further subdivided into the following four wavebands: UV-A (315-400 nm), UV-B (280-315 nm), UV-C (200-280 nm) and VUV (100-200 nm), as seen in **Fig. 10** (Bolton et al., 1986; Braslavsky, 2007). While in reality a quasi-continuum, these rather arbitrary categories of solar UV radiation have been established on the basis of their biological effects. For instance, UV-A radiation is known to be responsible for changes in human skin that lead to sun tanning, while UV-B radiation can cause skin burning and eventually leads to induction of skin cancer. UV-C radiation is extremely dangerous since it is absorbed by proteins, RNA and DNA and can lead to cell mutations and cell death. UV-C radiation is sometimes called the germicidal UV range since it is effective in inactivating bacteria and viruses. The vacuum UV (VUV) radiation can be absorbed by almost all substances, including water and air, and thus it can be transmitted only in a vacuum (Bolton et al., 1986).

3.3.1. UV radiation on the present-day Earth, on the early Earth and in extraterrestrial environments

Although in interplanetary space the full solar spectrum can be encountered, the UV radiation that reaches the planetary surfaces can vary, both in the terms of absolute flux and spectral quality (Cockell, 2001b). The UV flux at any point on the surfaces of planetary bodies that orbit around the Sun generally depends on a number of factors, including the orbital position of the planet, solar angle, latitude, ground reflection, presence of an atmosphere and possible cloud covers, etc. (Nicholson et al., 2005).

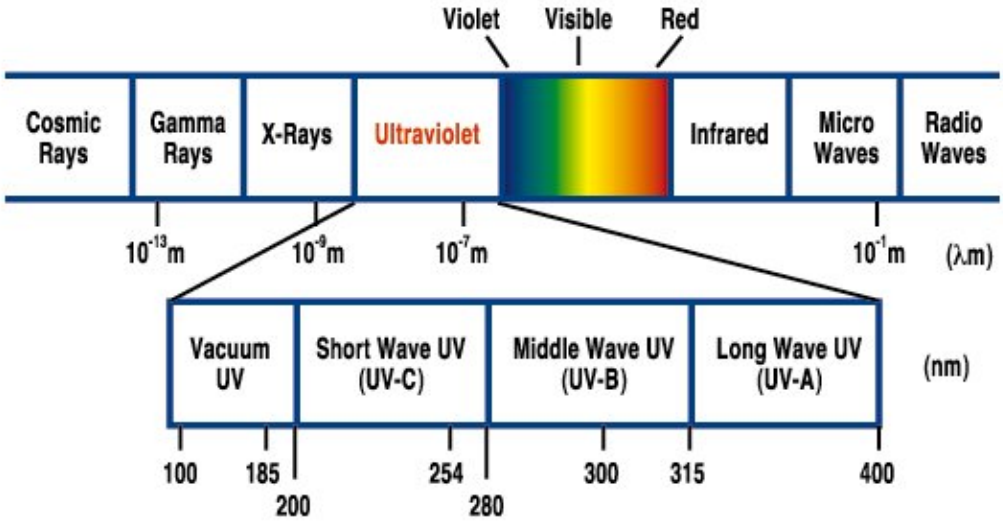

Fig. 10. The spectrum of solar electromagnetic radiation

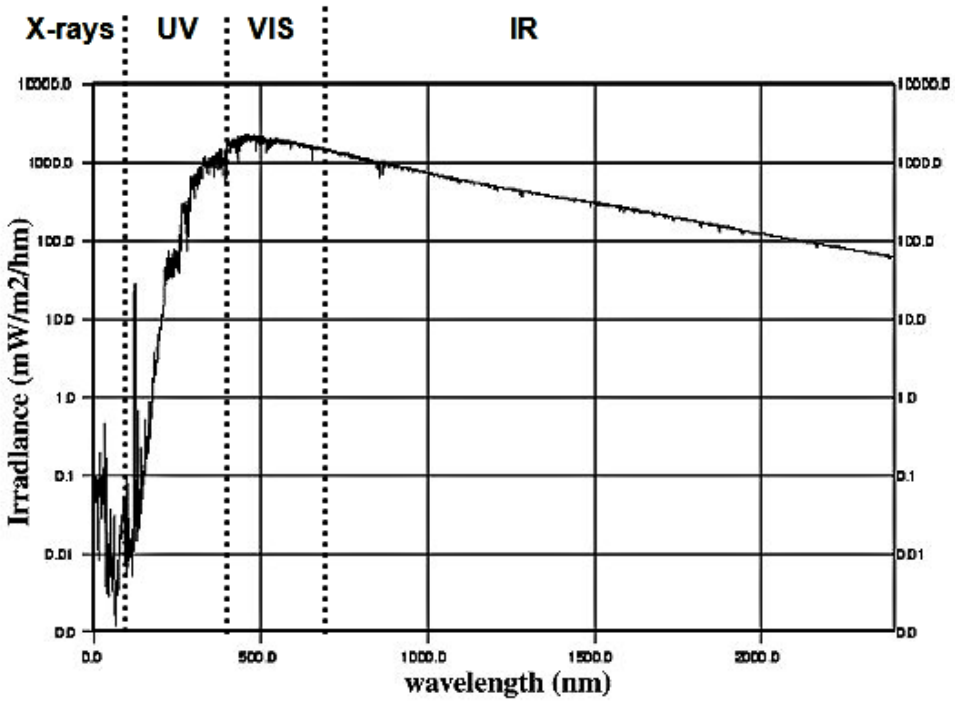

Fig. 11. The extraterrestrial solar irradiance reference spectrum (0.1 nm - 2400 nm). The spectrum is presented in semilogarithmic scale, and it is based on the combined measurements of several instruments during the ATLAS-1 mission. (adapted from Thuillier et al., 2004).
Abbreviations: IR = infrared part of spectrum, VIS = visible part of spectrum, UV = ultraviolet part of spectrum

3.3.1.1. UV radiation on the Earth

Out of the total solar irradiance (see the solar constant above), about one fourth of the energy (~ 341 mW^{-2}) is delivered to the present-day Earth, which in turns reflects about 31% of incoming solar radiation, while the remaining portion is absorbed by the atmosphere or delivered to the Earth's surface (Lean, 2008). The composition of the Earth's atmosphere, which is made up of approximately 78% nitrogen (N_2), 21% oxygen (O_2) and 0.035% carbon dioxide (CO_2), as well as its abundance (the average atmospheric pressure sea level is about 1013 mbar), have an important effect on the attenuation of the solar flux that reaches the Earth's surface, especially in the UV region (Nicholson et al., 2005; Faure and Mensing, 2007b). For instance, UV radiation below 195 nm does not reach the surface of the present-day Earth due to the presence of O_2 and CO_2 (Ogawa, 1971; Cockell, 2001a; Cockell and Raven, 2007). In addition, a portion of the O_2 in the Earth's upper atmosphere interacts with sunlight and is converted into ozone (O_3) (Garcia-Pichel, 1998; Nicholson et al., 2005). The formed stratospheric ozone layer strongly absorbs UV wavelengths shorter than 290 nm (Cockell and Raven, 2007). Therefore, the radiation flux that reaches the surface of the present-day Earth is significantly different from the extraterrestrial spectrum; it is high in the UV-A, decreases sharply in the UV-B region, and it drops to zero in the UV-C and VUV regions, as seen **Fig. 12** (Cockell, 1998).

However, the UV flux regimes during the early history of Earth were likely different from that of the present Earth. Since almost all oxygen in the present-day atmosphere is thought to be produced by photosynthesis (oxygenic photosynthesis), it has been postulated that the atmosphere of the early Earth was poor in oxygen, and consequently lacking the protective ozone shield (Kasting, 1987; Kasting`, 1993). Therefore, the surface of the early Earth was probably exposed to a much higher level of UV radiation than present-Earth, especially in the short-wavelength UV region (Garcia-Pichel, 1998; Cockell and Knowland, 1999; Cockell, 2001a). Four distinct periods of photobiological history of the Earth have been described by Cockell and Knowland (1999).

The first period refers to prebiotic Earth during the Hadean era (>3.9 Ga ago). Although the environment and chemistry on prebiotic Earth are not known with certitude (Leach et al., 2006), it is generally accepted that the Hadean atmosphere was anoxic. High fluxes of relatively unfiltered solar UV radiation that reached the surface of prebiotic Earth, might have been an important driving force for prebiotic chemistry, being involved in molecular complexification,

but it also may have been a limitation factor, having an adverse, destructive photolytic effect (Cockell and Knowland, 1999; Cockell, 2001a).

The second period refers to the Archean era (3.9-2.5 Ga), for which it is believed, according to a diversity of direct geologic and isotopic evidence, that the Earth's atmosphere probably remained essentially anoxic (Kasting, 1987; Kasting`, 1993; Cockell, 2000). However, the early Archean microbial fossil records suggested that life existed on Earth 3.3-3.5 Ga ago (Awramik et al., 1983; Schopf and Packer, 1987; Schopf, 1993; Westall, 2005; Allwood et al., 2006; Westall et al., 2006), and probably even as early as 3.8 Ga (Mojzsis et al., 1996). Many of these microfossils showed strong morphological similarities with present-day cyanobacteria (Schopf, 1994). It suggests that oxygenic photosynthesis may have occurred very early in the Earth's history (for reviews see Awramik et al., 1983; Schopf, 1993; Garcia-Pichel, 1998 and references therein; Des Marais, 2000). However, the reasons for absence of significant levels of O_2 in the Archean atmosphere still remain unclear; either the oxygenic photosynthesis was a later innovation or oxygenic photosynthesis did occur in the Archean, but the possible greater flux of reductants (e.g. hydrogen) mopped up produced O_2, or alternatively, the primary photosynthetic productivity was very low at this time (Cockell, 2001a). Regardless of the possible explanations, the extremely low partial pressure of O_2 in the Archean atmosphere, which was assumed to be at most ~ 1 x 10^{-4} PAL (present atmospheric level, ~210 mb), was likely insufficient to give rise to a significant ozone column that would have protected the early Earth from UV radiation (Cockell, 2001a). In an effort to determine the UV flux that likely reached the surface of the early Earth, Cockell (1998) and Cockell and Raven (2007) used the radiative transfer models, taking into account the luminosity of the early Sun and the composition of the Archean atmosphere (Cockell, 2001a). Although without direct evidences it is difficult to comprehend the early history of Sun's activity, indirect evidences provided by the observation of sun-like early stars, indicated that solar luminosity might have been reduced during the Archean era for approximately 25-30% of present values (Zahnle and Walker, 1982; Cockell, 1998; Cockell, 2001a). However, this would not be sufficient to compensate for the increase in UV radiation at the surface of the Earth caused by the lack of ozone in the Archean atmosphere (Cockell, 1998). In addition, since early stars often emit considerably more UV radiation, it was assumed that during the formation of the Earth and its early history, our Sun was emitting UV radiation of intensity that was considerably greater than today (Canuto et al., 1982; Zahnle and Walker, 1982; Cockell, 2001a). The composition of the Archean atmosphere is not well known, but it was assumed that it contained very little or no O_2, a similar level of N_2 as in the present atmosphere (0.8 bar), and CO_2 at approximately 1 bar, although the pressure of 10 bar as an upper limit, and

values as low as 40 mb have also been suggested (Walker, 1985; Cockell, 2000; Cockell, 2001a). The atmospheric CO_2 would screen the wavelengths below 195 nm (VUV part of spectrum), while nitrogen would probably contribute only to a smaller extent by global scattering of sunlight, without any wavelength-specific filtering of the UV part of spectrum (Cockell and Raven, 2007). According to these assumptions, the theoretical models showed that the surface of Archean Earth was probably exposed to much higher fluxes of UV-B light than the present Earth, in addition to highly deleterious UV-C that is not presently encountered on the Earth's surface (**Fig. 12**) (Cockell, 1998; Cockell`, 2000; Cockell, 2001a). In contrast, the values of the UV-A flux are in orders of magnitude comparable to that of the present Earth (**Fig. 12**), although a continuous increasing tendency of UV-A flux during the Earth history is assumed due to increasing luminosity of the Sun (**Fig. 13**).

The third period in the photobiological history of the Earth refers to the Archean-Proterozoic transition phase. During the early Proterozoic period (~2.5 - 2 Ga ago), the atmospheric O_2 partial pressure began to rise as a result of biological activity (oxygenic photosynthesis) and geologic changes (Cockell, 2001a). As a consequence, a significant level of protective ozone column started to accumulate in the Earth's upper atmosphere (stratosphere). It is assumed that the ozone shield began to form approximately 2 Ga ago (Kasting, 1993; Cockell, 2000). At the level of atmospheric O_2 of about 10^{-3} PAL, the UV-C flux on the Earth's surface probably began to decline, while at about 0.1 PAL (~ 2% O_2), the O_2 levels are thought to be likely sufficient to give rise to an effective ozone shield (Kasting, 1987; Cockell, 2000; Cockell, 2001a). Due to progressive ozone accumulation, the biological effective UV irradiance probably dropped to a level similar to its present-day value, about 1-1.5 Ga ago (**Fig. 13**) (Cockell, 2000).

The fourth period refers to the Proterozoic and Phanerozoic era (2.5 Ga ago to the present), during which flourishing life quickly evolved, protected from deleterious UV radiation thanks to the formed abundant ozone column (Cockell and Knowland, 1999; Cockell, 2000; Cockell, 2001a). The VUV and UV-C wavelengths were entirely filtered out, and the fluxes of UV-B radiation were significantly reduced (**Fig. 13**).

However, throughout this period, alternations in UV-B radiation regimes have occurred as a result of seasonal and long-term changes in ozone abundance, caused by a number of natural events, including volcanism, asteroid and comet impact events, close cosmic events etc. (**Fig. 13**) (Cockell and Knowland, 1999; Cockell, 2000; Cockell, 2001a). Recently, human activity is

found to have a considerable impact on progressive ozone depletion, particularly significant in the Earth's polar regions (Rozema et al., 2002; Sinha and Häder, 2002`, and references therein).

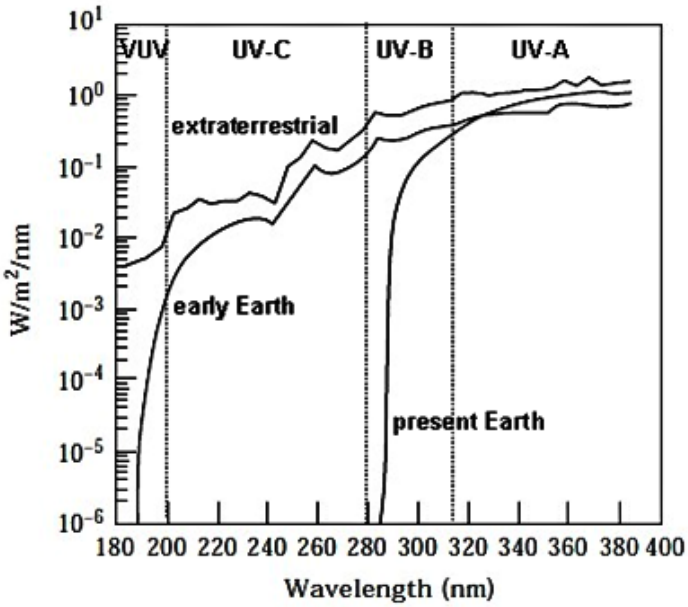

Fig. 12. Solar UV irradiance curves: the extraterrestrial spectrum from Earth orbit (Nicolet, 1989), the theoretical spectrum at the surface of the early Earth ~ 3.8 Ga ago (assuming a worst-case scenario with no other atmospheric attenuation and 40 mbar CO_2 in the atmosphere), and the spectrum at the surface of the present-day Earth, seen at the equator during the summer (adapted from Cockell, 1998).

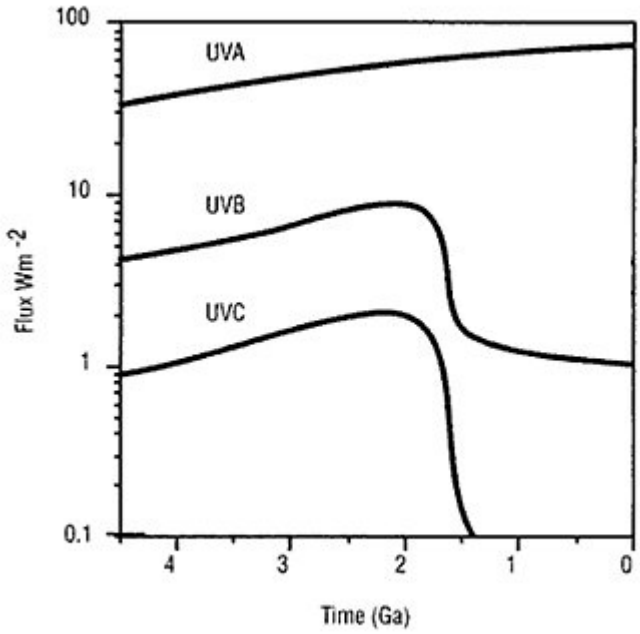

Fig. 13. The photobiological history of Earth showing changes in UV-A, UV-B and UV-C radiation fluxes at the Earth's surface from 4.5 Ga to the present . The UV flux that has been reaching the surface of the Earth was probably influenced by the Sun's luminosity and the composition of the atmosphere, particularly by the presence of ozone (O_3) layer. Besides here presented calculated generalized trend of UV flux, Earth has been also subjected to certain fluctuations in UV regimen throughout its history due to depletion of atmospheric O_3, caused by the natural seasonal and diurnal variations, stochastic "catastrophic" changes (asteroid and comet impacts, volcanic eruptions, close cosmic catastrophes, solar flares etc.), as well as present-day human activity (not presented here) (modified from Cockell, 2001).

3.3.1.2. UV radiation in extraterrestrial environments

The UV radiation fluxes in extraterrestrial environments are substantially different from those encountered on the surface of the Earth (Cockell, 2001c). Depending on the atmospheric composition and their distance from the Sun, extraterrestrial environments encounter different intensities and spectra of solar UV radiation. Here are some examples of extraterrestrial environments that, beside their proximity to the Earth, are also of astrobiological interest.

Despite its greater distance from the Sun, and thus lower solar constant (43% of that of the Earth's), Mars is exposed to a much higher surface flux of UV radiation than the Earth (Nicholson et al., 2005). Mars has an atmosphere one hundredth of the total atmospheric pressure of Earth, and it is mainly composed of CO_2 (~ 95%) (Cockell, 2001b). It has also low levels of N_2 (~2.7%) and extremely low levels of O_2 (~ 0.13%). Neither of these two gasses nor the presence of water vapour (0.03%) contribute significantly to attenuation of UV light at column abundances present in the Martian atmosphere (Cockell, 2001b; 2001c). In contrast to the Earth, Mars does not have a significant ozone column, although some smaller ozone build-up occurs at the poles during the winter and in early spring (Barth et al., 1973; Barth and Dick, 1974; Cockell, 2001b; Cockell, 2001c). Therefore, UV-B and UV-C radiation reaches the surface of Mars relatively unattenuated (**Fig. 14**). The UV-B levels on Mars are about four times greater than on Earth at the subsolar point[1], and there is also substantially greater UV-C flux on Mars (Cockell, 2001b). In contrast, the UV-A radiation fluxes are lower than on Earth (~ 55% of terrestrial levels at comparable latitudes) (Cockell, 2001b; Cockell, 2001c). Due to the presence of high CO_2 concentrations in the Martian atmosphere, the wavelengths below 195 nm are efficiently absorbed, and thus highly damaging VUV radiation does not reach the surface of Mars (Cockell, 2001c; Córdoba-Jabonero et al., 2003). Due to extremely cold surface temperatures on Mars, a significant percentage of atmospheric CO_2 freezes into solid CO_2 at the poles during winter and then resublimates in the spring and summer, resulting in seasonal swings of about 40% in the mean atmospheric pressure (between ~6 and 10 mbar) (Nicolet, 1989; Cockell, 2001c). These CO_2 partial pressure fluctuations also cause slight variations of the UV flux reaching the Martian surface (Nicolet, 1989).

[1] Subsolar point refers here to the latitude where the Sun's rays are perpendicular to the surface of the Earth (or any other planet) at noon. It is a point at which the Sun is exactly overhead (at the zenith) (McIntyre et al., 1991).

The photobiological history of Mars has been suggested to be almost exclusively determined by the increase in solar luminosity and the change in the partial pressure of atmospheric CO_2, which probably gradually declined over time (from initial 0.5-3 bar, over 0.5-1 bar at 3.8 Ga to the present-day surface pressure of 6 mbar). A putative ultraviolet history of Mars is presented in **Fig. 15** (Cockell, 2000; Cockell, 2001b).

In contrast to Earth and Mars, the Moon has no atmosphere and thus the UV flux reaching the lunar surface is very similar to that of the extraterrestrial solar spectrum (**Fig. 14**). The UV-B is about nine times higher on the Moon than on the Earth's surface. Highly deleterious UV-C wavelengths also reach the lunar surface, as well as VUV radiation, since there is no CO_2 or O_2 atmosphere (Cockell, 2001c).

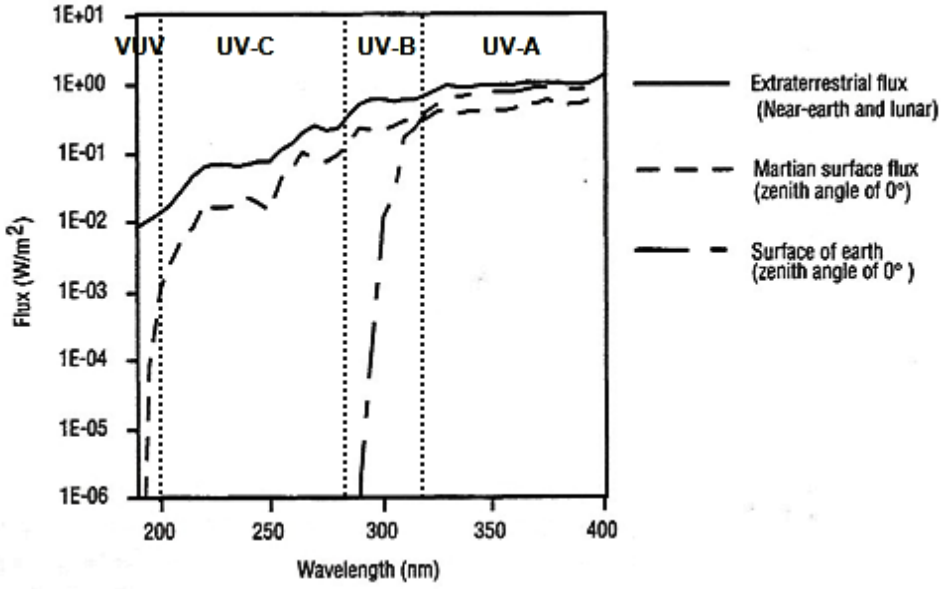

Fig. 14. Solar UV irradiance curves at the surface of present-day Mars and Earth at a zenith angle of 0°. For comparison, the spectrum of full solar extraterrestrial radiation that is encountered at near-Earth orbit and at the surface of Moon (adapted from Cockell, 2001b).

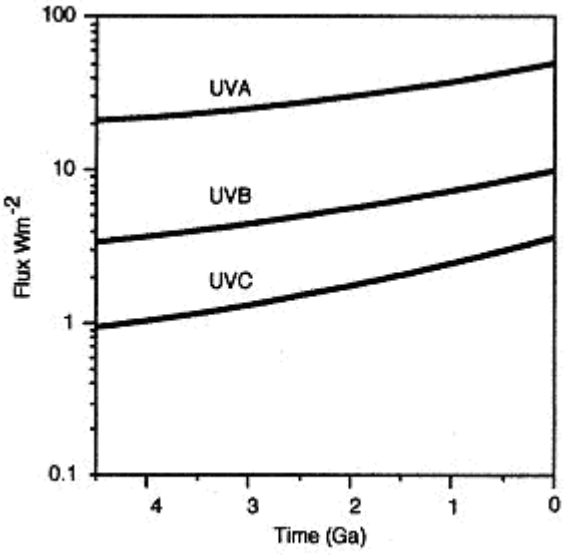

Fig. 15. The ultraviolet history of Mars showing changes in UV-A, UV-B and UV-C radiation fluxes at the Earth's surface from 4.5 Ga to the present. (taken from Cockell, 2001b).

3.3.2. Biological effects of high UV radiation flux

UV radiation has been a deleterious to life since its emergence on Earth. It had a strong influence on ecosystems and organisms that have evolved on Earth (Caldwell et al., 1998; Cockell and Blaustein, 2001). UV radiation is potentially detrimental to all organisms due to its strong mutagenic and cytotoxic effects. It can cause a variety of sublethal effects, and ultimately mortality in many organisms. UV radiation is also known to inhibit photosynthesis and other metabolic processes, and reduce the growth and reproductive capacities of organisms (for reviews see Diffey, 1991; Stapleton, 1992; Caldwell et al., 1998; Castenholz and Garcia-Pichel, 2000; Cockell and Blaustein, 2001). At the cellular level, it causes damage to a wide variety of biologically important macromolecules and cellular complexes, inducing DNA damage, protein destruction, membrane damage, chloroplast damage, hormone inactivation etc. (for reviews seeTevini and Teramura, 1989; Diffey, 1991; Stapleton, 1992; Rozema et al., 1997b; Caldwell et al., 1998). This is due to the fact that UV light is readily absorbed by many macromolecules as diverse as nucleic acids, proteins and lipids (Caldwell et al., 2003). The absorbed energy is than transferred to these molecular targets, causing lesions that can be detrimental to their functions. For molecules such as proteins and lipids, UV-induced damage can be in some cases be compensated by their *de novo* synthesis, which in turn represents a significant energetic cost to the cell (Cockell and Raven, 2007). On the other hand, UV-induced damage to DNA is heritable. Since any structural or chemical change to DNA may interfere with RNA transcription and DNA synthesis (replication), UV-induced damage can ultimately lead, depending on the size and location of the lesion, to mutation or even death (Wynn-Williams and Edwards, 2002; Cockell and Raven, 2007).

Not all UV wavelengths have the same capacity to cause biological damage or stimulate photochemical reactions. The biological effectiveness of UV radiation generally increases with decreasing wavelength (Xenopoulos and Schindler, 2001). In biological systems, the most damaging effects are attributed to the short-wavelength VUV and UV-C radiation. Neither VUV nor UV-C reach the Earth's surface (Fig. 12), and therefore this part of the spectrum is considered as of no ecologically relevance for biota on present-day Earth. Nevertheless, this short-wavelength UV radiation is considered as an important limitation factor for dispersal of life through space and it was likely an obstacle for emergence and expansion of life on the early Earth. Although unfiltered solar emission in the short wavelengths is relatively weak (**Fig. 11** and **Fig. 16A**), the VUV and UV-C part of the spectrum is the most biologically damaging because of the high energies involved and because biological targets often strongly absorb in

these UV regions. For instance, nucleic acids (DNA and RNA) are considered the prime targets for UV damage due to their strong absorption in the UV-C and VUV (**Fig. 16B**) (Zalar et al., 2007c).

Generally, the effect of UV radiation on biological systems can be represented by action spectra. An action spectrum is a plot of a relative biological effect (usually some measure of damage) as a function of the wavelength of radiation (Cockell and Raven, 2007). The most widely accepted reference action spectra are those for erythema in human skin or sunburn (McKinlay and Diffey, 1987), DNA damage (Setlow, 1974; Green and Miller, 1975) and chloroplast photoinhibition (Jones and Kok, 1966). These action spectra span the 280-400 nm region, and most of them are rarely recorded below 280 nm because of the lesser ecological relevance of short-wavelength UV radiation for conditions on present-day Earth. However, by measuring the inactivation of Bacillus subtilis spores and formation of DNA lesions in actual and simulated space conditions, Lindberg and Horneck (1991), Horneck et al. (1995) and Horneck (1993) extended the action spectra down to wavelengths below 280 nm. The action spectrum of the formation of photoproducts can be expected to resemble the absorption spectrum of the molecules responsible for these photoproducts (Jagger, 1985; Diffey, 1991). For instance, the action spectra for DNA damage roughly follow the DNA absorbance profile (**Fig. 16**). The action spectra for whole organisms depend on the combined effects of photoinduced damage, as well as repair and protection mechanisms (Cockell, 1998). Nevertheless, in microorganisms, the action spectrum for decline in viability often follows the absorption spectrum profile of DNA, indicating that DNA is the primary target for UV radiation damage (Jagger, 1985; Diffey, 1991; Horneck, 1993).

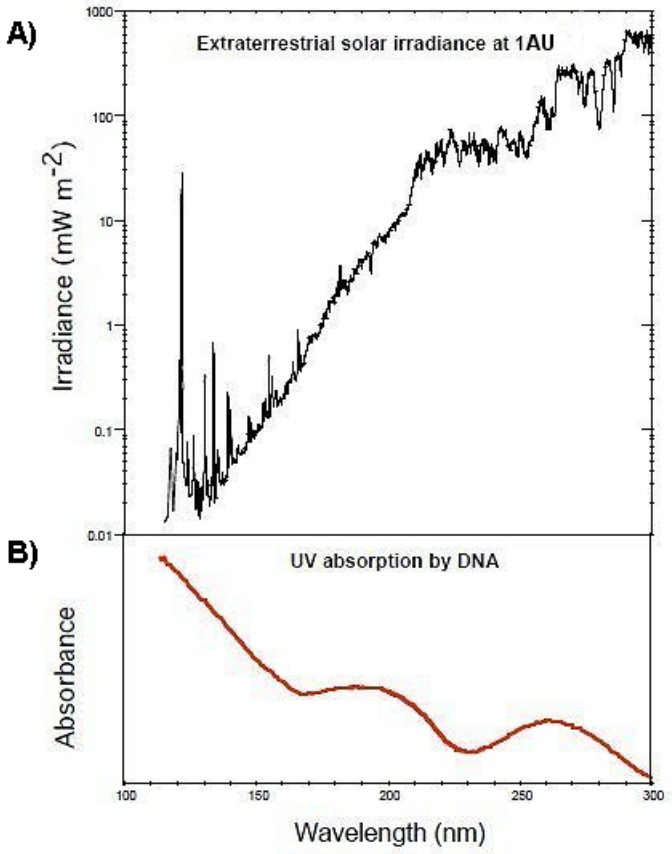

Fig. 16. A) Solar UV emission spectrum recorded at 1 AU. The full reference spectrum of extraterrestrial solar irradiance (0.1 nm - 400 nm) is presented in **Fig. 11** (adapted from Thuillier et al., 2004). B) UV absorption spectrum of DNA (taken from Zalar, 2007a; 2007c).

3.3.3. DNA as a prime target for UV damage

All known life forms depend on DNA to store their genetic information, and despite the relative stability of their genomes, DNA represents a prime target to damage. DNA damage can be caused by different physical factors (UV and ionizing radiation), as well as chemical agents (e.g. nucleic base analogs, intercalating and alkylation agents etc.) (Friedberg et al., 1995; Britt, 1996). Among those, UV radiation is one of the most DNA-damaging environmental factors.

UV radiation can cause both chemical and structural changes to DNA, which may have mutagenic effects (because of base mispairing), as well as cytotoxic effects (because it blocks DNA replication and transcription) (Tuteja et al., 2001; Sinha and Häder, 2002). UV radiation induces different types of DNA damages, including formation of various nucleic base photoproducts, oxidative DNA modification, single- and double-strand DNA breakes, as well as

DNA-protein and DNA-DNA cross-links (Friedberg et al., 1995; Kielbassa et al., 1997; Britt, 1999). Solar radiation can give rise to cellular DNA damage either by direct excitation of DNA or by the indirect mechanisms that involve the excitation of other cellular chromophores (endogenous photosensitizers) (Kielbassa et al., 1997). The most common, and probably the most significant DNA lesions are various types of pyrimidine dimers, such as cyclobutane pyrimidine dimers (CPDs) and pyrimidine (6-4) pyrimidinone dimers ((6-4) photoproducts), which are generated by direct excitation of UV irradiated DNA (Clingen et al., 1995; Friedberg et al., 1995; Britt, 1996; Britt, 1999; Sinha and Häder, 2002). Both types of lesions produce different types of structural distortions within DNA; CPDs induce a slight bending of the DNA helix, while (6-4) photoproducts cause greater bending, as well as unwinding of DNA strains. Therefore, both UV-induced lesions inhibit DNA replication and transcription, and they also promote mutagenesis (Tuteja et al., 2001).

CPDs generally make up the bulk of the total UV-induced damage, and depending on UV wavelength and DNA nucleobase sequence, they may represent approximately 75% of the total DNA damage. The CPDs are formed by the dimerisation of two adjacent pyrimidine bases (TT, TC, CT and CC) on the same strand of DNA (Friedberg et al., 1995; Tuteja et al., 2001; Hollósy, 2002). They arise from a [2+2] cycloaddition of the C5-C6 double bonds of neighbouring pyrimidine bases, as seen in **Fig. 17A** (Ravanat et al., 2001). The CPDs are formed preferentially at TT sites, and to the lesser extent TC sites, whereas CT and CC dimers are poorly photoreactive (Friedberg et al., 1995; Cadet et al., 2005). However, CC photoproducts, although generated in low yields, exhibit a high mutagenic potential (Cadet et al., 2005).

The (6-4) photoproducts are the second most frequent class of UV-induced DNA lesions. These photoproducts are formed by a [2+2] cycloaddition of the C5-C6 double bond of the 5'-end pyrimidine and C4 carbonyl group of the 3'-end thymine, or rarely cytosine, as seen in **Fig. 17B** (Ravanat et al., 2001). Depending upon the UV wavelength and adjacent sequence, (6-4) photoproducts can be formed between adjacent TC and CC, and less frequently TT bases, while CT products were not observed in irradiated DNA (Friedberg et al., 1995; Tuteja et al., 2001). Upon the absorption of UV light, unstable intermediates, oxetane (3'-end base is thymine) or azetedine (3'-end base is cytosine), are first formed. It is by their spontaneous rearrangements that (6-4) photoproducts are finally formed in an irradiated DNA molecule. Absorbing UV-B light at wavelengths longer than 290 nm, (6-4) photoproducts are able to photoisomerize into related Dewar valence isomers, as seen in **Fig. 17B** (Clingen et al., 1995; Friedberg et al., 1995; Tuteja et al., 2001; Sinha and Häder, 2002).

In addition to CPDs and (6-4) photoproducts, other UV-induced lesions have been also observed, but they occur at very low frequency in irradiated DNA. These include photohydration of cytosine, oxidation of guanine into 8-oxo-7,8-dihydroguanine (8-oxoGuo) and the formation of adducts between two adjacent adenine bases or between adenine and thymine bases (Cadet et al., 2005).

Under anhydrous conditions, such as within bacterial spores (e.g. *Bacillus subtilis* spores), a distinct type of UV-induced photoproduct, called spore photoproduct (SP) can occur between two adjacent thymine residues (**Fig. 18**), in addition to CPDs and (6-4) photoproducts, which are present in small quantities. Instead of TT pyrimidine dimers, SPs are the major deleterious DNA lesions found in *Bacillus spores*, as well as in a purified dehydrated DNA (Friedberg et al., 1995; Nicholson et al., 2000; Douki and Cadet, 2003; Douki et al., 2003; Setlow et al., 2006; Moeller et al., 2007a). The formation of this lesion appears to be related to the state of hydration of DNA. In the dry state, DNA is mostly in the A conformation, rather than in the B conformation. It is suggested that irradiated DNA in A-form favours the formation of spore photoproducts, as well as inter-strand photoproducts (Douki and Cadet, 2003; Douki et al., 2003).

Short-wavelength UV radiation has mainly direct deleterious effects, inducing mostly pyrimidine dimmers (CPDs and (6-4) photoproducts), as seen in **Fig. 19**. It was observed that the action spectrum for the induction of pyrimidine dimers in purified DNA follows the absorption spectrum of DNA. Therefore, these lesions are induced most efficiently by UV-C radiation (about 2-10 lesions/ 10^6 bases per Jm^{-2}, Ravanat et al., 2001), particularly at wavelengths close to 260 nm, which is one of the two absorption maxima of DNA, as seen in **Fig. 16B** (Britt, 1996). UV-B radiation also induces large quantities of dimeric pyrimidine photoproducts, although less efficiently than UV-C light (1 lesion/ 10^7 bases per Jm^{-2}, Ravanat et al., 2001). Compared to UV-C radiation, UV-B produces a significantly higher yield of Dewar valence isomers (Clingen et al., 1995). In addition to these direct effects, UV-B radiation can also cause damage to DNA through indirect mechanisms that involve photooxidation reactions, **Fig. 19** (see below). Since DNA has no chromophore for UV-A radiation absorption, indirect mechanisms are thought to be responsible for DNA damage and genotoxic effects observed at these wavelengths, as seen in **Fig. 19** (Kielbassa et al., 1997; Ravanat et al., 2001). It is likely that UV-A light is first absorbed by yet unidentified endogenous photosensitizers, which can damage DNA through the secondary photooxidation reactions (Kielbassa et al., 1997; Ravanat et al., 2001; Sinha and Häder, 2002). There are two types of photooxidation reaction that occur in the cellular systems (**Fig. 19**). In a type I reaction (one-electron oxidation or hydrogen abstraction), an excited endogenous

photosensitizer molecule reacts directly with a DNA molecule without involvement of intermediates. In type II reactions, oxidative DNA modifications are induced via reactive oxygen species (ROS), mostly singlet oxygen ($^1O_2$) and hydroxyl radicals ($^{\bullet}OH$) that are generated upon the absorption of UV light by the endogenous photosensitizers (Kielbassa et al., 1997; Ravanat et al., 2001). Among the four nucleic bases, guanine represents the preferential target for photooxidative damage (both type I and II), giving rise to 8-oxoGua, which is an ubiquitous biochemical marker of oxidative stress (Ravanat et al., 2001).

3.3.4. Strategies for coping with damaging UV light

Prior the build up of atmospheric oxygen, and thus a protective ozone shield, the effective UV irradiance to free DNA would have been approximately three orders of magnitude higher than on present-day Earth, as suggested in the theoretical study by Cockell (1998). Therefore, UV radiation has been a likely limitation factor for emerging life on the surface of the early Earth. Any primary colonizers on the Earth, which were probably some kind of phototrophic organism (e.g. phototrophic bacteria, cyanobacteria-like organisms etc.), would be particularly vulnerable to the effects of an enhanced flux of solar UV radiation because at the same time, for energy requirements they need exposure to a relatively high flux of photosynthetically active radiation (PAR, 400-700 nm). Ever since then, solar radiation is the primary source of energy for life on the Earth. Although the current solar UV flux that reaches the Earth's surface is significantly attenuated by the stratospheric ozone layer, particularly at short wavelengths, UV radiation is still an important stressor for many life forms on Earth. Contemporary photosynthetic organisms, such as photosynthetic bacteria, cyanobacteria, algae and higher plants, are considered to be particularly sensitive to continuous exposure to sunlight. Evolving on Earth, organisms developed different strategies for resisting UV radiation, including avoidance, protection by UV screens and damage repair (Margulis et al., 1976; Cockell and Knowland, 1999; Castenholz and Garcia-Pichel, 2000).

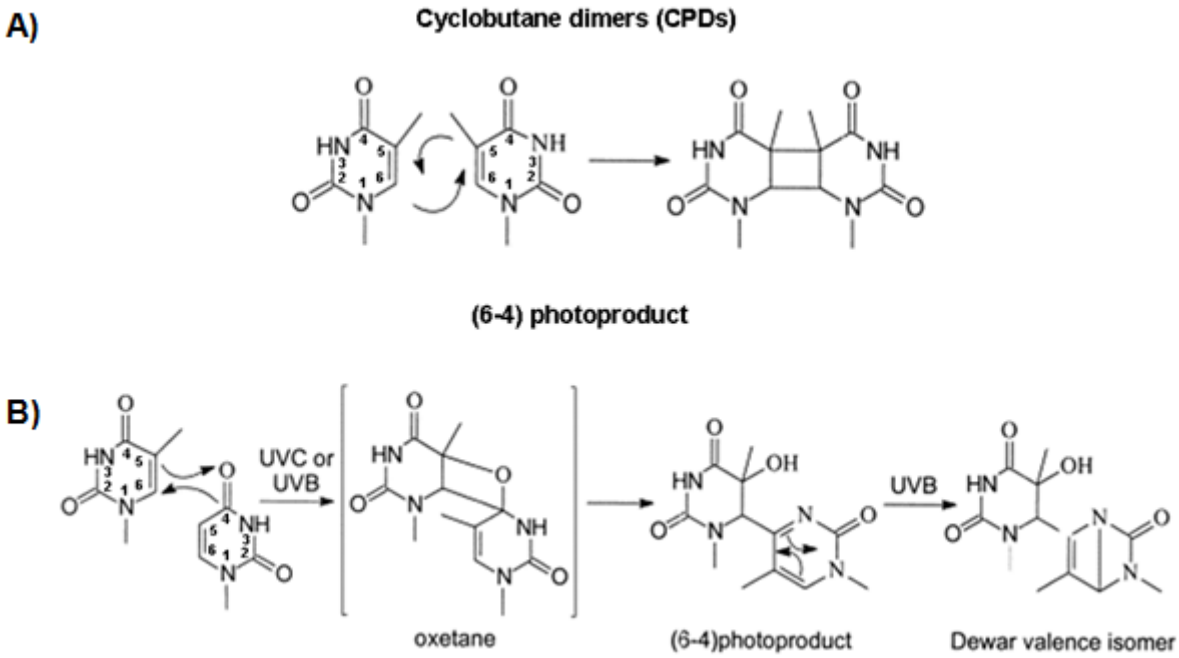

Fig. 17. Formation of two major UV-induced lesions in irradiated DNA. A) Thymine cyclobutane dimer, CPD (TT pyrimidine dimer). B) Pyrimidine (6-4) pyrimidinone dimer ((6-4) photoproduct). Here is presented TT (6-4) photoproduct, which is formed via an unstable intermediary (oxetane). Absorption of UV-B light by the (6-4) photoproduct leads to photoisomeration into a Dewar valence isomer (adapted from Ravanat et al., 2001).

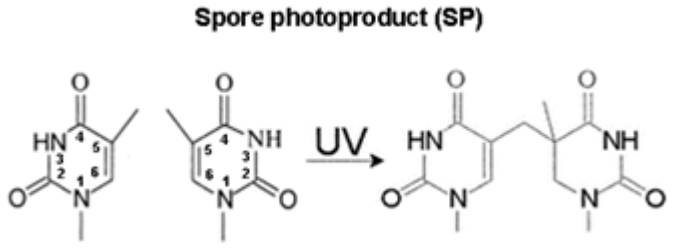

Fig. 18. Principal UV-induced photoproduct in dry *Bacillus subtilis* spores and dehydrated DNA.

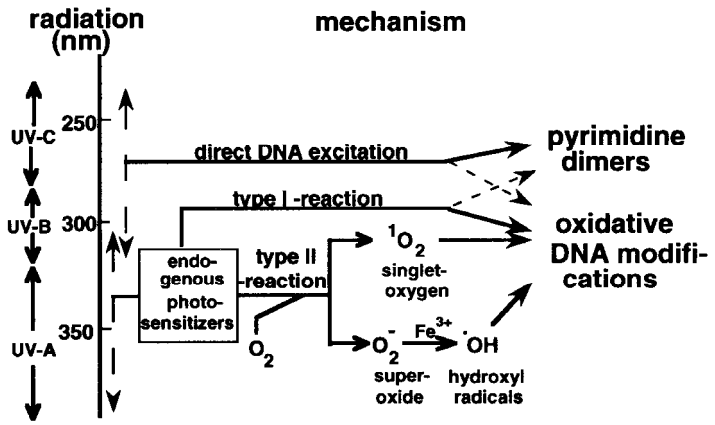

Fig. 19. Direct and indirect mechanisms for the induction of pyrimidine dimers and oxidative DNA modifications by UV radiation (taken from Kielbassa et al., 1997).

3.3.4.1. Avoidance of UV light

Many organisms are able to avoid UV radiation completely, or attenuate UV radiation reaching particular parts of organisms. Some simple single-cell organisms may respond by reversing direction (negative phototaxis) whenever the intensity of solar light increases, thus moving and remaining out of sunlight (NRC`, 1973). Negative phototaxis is observed in many planktonic organisms, as well as in many cyanobacterial mat communities (Margulis et al., 1976; Castenholz and Garcia-Pichel, 2000). The active migration away from the source of UV light may be modulated diurnally (Cockell and Knowland, 1999). Many animals developed specific behavioural responses to increased levels of solar radiation. Few animals remain exposed to full sunlight, unless they possess some means (e.g. hair, feathers, scales or shells) for preventing the entry of light into their skin (NRC`, 1973). Some animals hide by day in rocks, burrows and deep water. These animals exhibit usually increased activity at dusk and become again inactive at dawn. On the other hand, plants, as sedentary organisms, can only partially attenuate UV light by moving their leaves to position of minimal exposure to sunlight. Although avoidance of sunlight may reduce damaging effects of UV light, it is not an entirely satisfactory strategy, especially for sedentary, as well as photosynthetic organisms that require exposure to sunlight for their energy requirements. Therefore, other, more specific mechanisms are necessary for reducing deleterious effect of UV radiation (see below).

3.3.4.2. Protection by UV screens

In spite of the fact that all known terrestrial organisms possess relatively efficient, and sometimes complex systems for repairing UV-induced damage, UV screens represent a first line of defence before damage occurs. UV screens provide passive protection; UV light is absorbed and its energy is dissipated away from sensitive cellular targets (Zalar et al., 2007c). Therefore, UV screening may represent an energetic advantage by reducing the need for constantly active avoidance and biochemical repair processes (Cockell and Knowland, 1999). UV screening protection can be physical or biological (Cockell, 1998; Cockell and Knowland, 1999). A comprehensive review about the role of UV screening compounds in different species and their role throughout the history of life on the Earth is given by Cockell and Knowland (1999). Here is presented only a brief overview of known and putative physical and biological UV screens.

3.3.4.2.1. Physical UV screens

A variety of physical substrates (e.g. atmospheric compounds, water, soil, rocks etc.), can screen sunlight passively by absorption or scattering, thus protecting inhabiting organisms from deleterious UV radiation (Cockell, 1998; Cockell and Knowland, 1999).

Although the early Earth's atmosphere probably lacked a significant ozone column, the presence of other compounds in the early atmosphere might have had an important influence on the UV regime at the Earth's surface (Sagan, 1973; Kasting et al., 1989). For instance, it was suggested that a sulfur haze in the early atmosphere, formed by the photolytic production of sulfur from SO_2 (sulfur dioxide) and H_2S (hydrogen sulfide) volcanic out gassing, might have provided some attenuation of UV radiation reaching the Earth's surface (Sagan, 1973; Kasting et al., 1989; Cockell and Knowland, 1999; Cockell, 2001a). In addition, CH_4 (methane), produced either by methanogenic organisms or abiologically, has been also suggested as one of the possible contaminants in the early Earth atmosphere that might have provided some level of attenuation of UV radiation (Cockell, 2001a). Moreover, an organic haze formed from the molecules that have been delivered from space (e.g. interplanetary dust particles, meteorites etc.) might have also played an important role in the attenuation of UV light reaching the early Earth (Sagan, 1973; Cockell, 2001a). Interplanetary dust particles (micormeteorites) have been suggested as the major carriers of extraterrestrial carbon-rich compounds reaching the Earth. The mass flux of small micrometeorites of sizes about 50-200 μm reaching the present-day Earth is reported as about 2×10^4 tons $year^{-1}$ (Maurette et al., 1995). The delivery of carbon into the terrestrial atmosphere by the small meteorites is estimated in the range $3\text{-}6 \times 10^5$ kg $year^{-1}$ (Chyba and Sagan, 1992; Maurette et al., 1995). Larger size meteorites has considerably smaller mass flux on Earth, reaching about 10^2 tons $year^{-1}$ (Maurette et al., 1995). However, the infall of organics by meteorites and micrometeorites might be even more important during the period of heavy bombardment ~ 4 Ga ago(Chyba and Sagan, 1992; Maurette et al., 1995).

UV screening protection by liquid water as a physical substrate has been also suggested (Sagan, 1973; Margulis et al., 1976). However, because pure water has a low absorption coefficient for UV radiation, several tens of meters of water column would be necessary to act as an efficient shield from UV radiation (Sagan, 1973; Garcia-Pichel, 1998). In addition, a disadvantage of a deep water column is that it attenuates the flux of sunlight unspecifically, meaning that beside UV light, it also reduces the PAR, necessary for photosynthetic organisms. In many waters today, the euphotic zone (the zone at which the rate of photosynthesis equals that

of respiration) is about 3-8 times deeper than the depth at which the flux of UV-B radiation is reduced to 1%. However, the greater incidence of UV-B and UV-C light on the early Earth would cause their greater penetration in the water column. On the other hand, the fainter young Sun probably emitted less PAR, which may have caused the euphotic zone to be closer to the surface, thus causing the rising up of the photosynthetic organisms closer to the zone of UV penetration. Therefore, UV light would be likely a limitation factor for an early photosynthetic organism that inhabited aquatic environments (Cockell, 1998).

However, the presence of inorganic salts, such as nitrogenous and iron-containing salts, which absorb in the UV region, might have assisted in the specific attenuation of short-wavelength UV radiation in the early oceanic water column (Margulis et al., 1976; Olson and Pierson, 1986; Garcia-Pichel, 1998; Cockell, 2001a). In addition, the occurrence of organic impurities in water substrates may have provided additional reduction of UV flux that penetrates through the water column. Many cyclic or conjugated organic compounds absorb efficiently in the UV part of spectrum, and therefore they have been suggested as potentially important UV screening compounds in the early oceans. Although the early oceans have been thought to be relatively poor in dissolved organic carbon due to low or no biological activity, a significant quantity of organics and aromatic compounds (e.g. polycyclic aromatic hydrocarbons, PAHs) may have been however delivered from space by interstellar dust particles, meteorites and comets (Chyba and Sagan, 1992).

The physical substrates in the terrestrial habitats can also provide protection to some organisms by screening the UV light. Different types of rocks provide microenvironments for endolithic microbial communities that are hidden from UV light. Even though the PAR is significantly reduced in these habitats, the light levels are still high enough to support a slow growth of some photosynthetic organisms, such as cyanobacteria and lichens. Sand particles can also screen the UV light, protecting microorganisms in desert habitats. Ferric iron (Fe(III)) impurities can also provide good protection for organisms inhabiting the soil substrates. Olson and Pierson (1986), Pierson et al. (1993) and Gómez et al. (2007) suggested iron as an efficient inorganic UV shield that might have protected life on the early Earth. They found that ferric iron (Fe(III)) strongly absorbs in the wavelength range 220-270 nm, while ferrous iron (Fe(II)), although absorbing in a similar wavelength range, absorbs UV-C radiation less strongly. Both forms of iron were probably present in Precambrian sediments. In addition, iron-containing compounds provide efficient protection that not only screen UV light, but at the same time, they specifically allow transmission of PAR. This was demonstrated by Pierson (1993) who revealed

that a 1 mm layer of 0.1% $FeCl_3$ is sufficient to reduce the incident UV-C (λ = 254 nm) light to 1%, while transmitting most of the visible light.

Some extreme environments on the Earth can be occupied by organisms that, by becoming adapted to such harsh conditions, benefit from the UV protection provided by such physical substrates. For instance, crystalline sodium chloride (NaCl), which is a relatively good UV absorber, can provide protection to halophilic microorganisms that naturally inhabit the evaporite crusts of halite (Rothschild, 1990; Rothschild et al., 1994; Mancinelli et al., 1998; Fendrihan et al., 2009). Thin layers of elemental sulfur that can be generated abiologically or by sulfide-oxidizing organisms, and deposited on top of the microbial mats (e.g. thermophilic microorganisms in hot springs) can provide relatively good protection, since elemental sulfur absorbs well in the UV-C and partially in the UV-B region, although it absorbs weakly in the UV-A part of the spectrum (Cockell, 1998).

3.3.4.2.2. Biological UV screening strategies

Since most of physical UV screens also exhibit nonspecific attenuation of sunlight, particularly in the visible part of the spectrum, evolving life on the Earth had to develop more efficient ways of coping with UV. Among those, the matting habits that are characteristic for some microorganisms have been proposed as one of the strategies for coping with UV on the early Earth (Margulis et al., 1976; Cockell, 1998; Cockell and Knowland, 1999; Castenholz and Garcia-Pichel, 2000). Many current cyanobacteria are found to grow within the mats, where dead or living upper layers protect lower layers from damaging UV radiation (Margulis et al., 1976; Cockell and Knowland, 1999). However, a more efficient and more UV-specific mode of protection involves the active biosynthesis of UV screening compounds, which are found in a wide variety of organisms within distinct phylogenetic groups. The advantage of the organisms that can synthesise their own UV-protecting compounds is that they can occupy a greater diversity of habitats (Cockell and Knowland, 1999).

The UV-screening protection of DNA, as one of the most sensitive cellular targets (see sections **3.3.2** and **3.3.4**), can be achieved at several levels, depending on the structural and chemical complexity of the cell (**Fig. 20**). In the simplest case, DNA is concentrated in the interior of the cell, as far as possible from the incident light, and it is surrounded by UV absorbing molecules that are ubiquitous in all cells (potential UV screens), such as proteins, tyramine and polyamines, which stabilize DNA, forming compact structures that are less prone

to damage (Zalar et al., 2007a`; 2007c). Another level of protection involves synthesis and accumulation of specialized UV screening compounds within the cells that are exposed to UV light (Zalar et al., 2007b`; 2007c). These compounds are small organic molecules that that are efficient and specific UV absorbers. Most of these compounds possess a π-electron system within conjugated bonds of linear chain molecules, as well as aromatic and many cyclic structures. Generally, the size of molecule (number of conjugated bonds) and the number and type of substituents influence the absorption characteristics of a UV screening compound. For instance, molecules that have longer chains with conjugated bonds have absorption maxima at longer wavelengths. A similar bathochromic shift in the maxima of absorption occurs in aromatic molecules with an increasing number of substituents (Cockell and Knowland, 1999). Some specific UV screens accumulate to high concentrations in response to UV radiation. Absorbing UV light, they filter out from the sunlight spectrum those wavelengths that are potentially damaging for cellular constituents, particularly for DNA. A further level of protection can be achieved by peripheral structures formed around the cell, such as capsules and cell walls, which can accumulate large quantities of specialized UV screens. Physical distance between the shield and DNA is advantageous because it reduces the risk that energy absorbed by the screen is transferred to the target (Zalar et al., 2007c).

The following criteria should be fulfilled for identifying a compound as specialized UV screen: (1) a compound must efficiently absorb UV radiation; the screening effect should be maximal at the wavelengths of maximal absorption and negligible where compound does not significantly absorb, (2) screening activity must be demonstrated *in vivo*, (3) biosynthesis of the UV screen should be inducible by UV light, (4) because of the passive nature of the UV screening effect, the correlation between the concentration of compound and resistance to UV should still be present under conditions of physiological inactivity or quiescence, even when other photoprotection and repair mechanisms are not functioning, (5) loss of protection after artificial removal of compound or its blocked synthesis in a biological system (e.g. mutants lacking putative UV screen) (Garcia-Pichel et al., 1993; Cockell and Knowland, 1999).

Here below are some examples of known specialized UV screens found in current, phylogenetically diverse organisms that inhabit aquatic, as well as terrestrial ecosystems. Details about the UV absorption properties of some of these UV-screening substances, as well as their UV protection capacities are discussed elsewhere (see chapter **3** results I, section **10.** and publications attached therein, Zalar et al., 2007a; 2007b; 2007c).

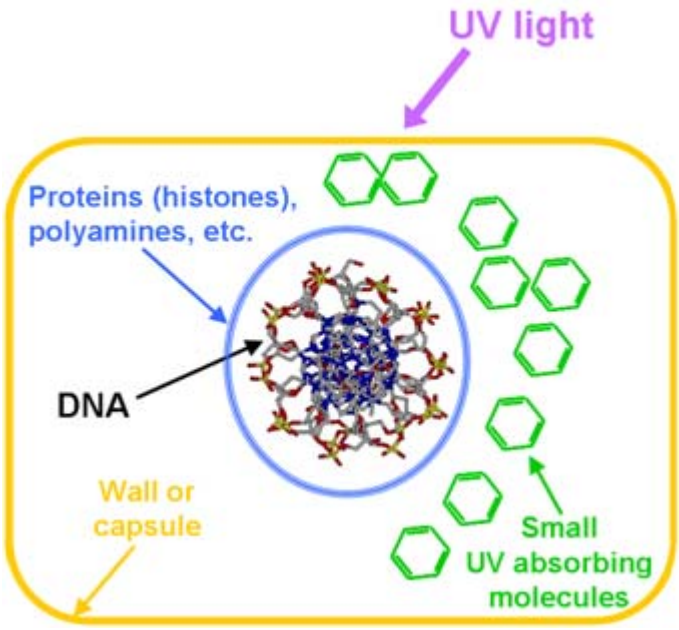

Fig. 20. Schematic representation of UV protection in a hypothetical cell. Ubiquitous molecules with multiple functions, *e.g.* proteins and polyamines, provide constitutive protection. Another level of protection is induced by exposure to UV light, and consists of the accumulation of specialized UV screens, small molecules that are efficient UV absorbers. The cell is further protected by peripheral structures, *e.g.* capsules or cell walls, where these specialized UV screens can accumulate, distancing the screen from the target (Adapted from Zalar et al, 2007c).

Scytonemin is a yellow-brown, lipid-soluble pigment, whose synthesis is induced in cyanobacteria after exposure to UV-A light (Garcia-Pichel et al., 1992). It is a dimeric molecule composed of phenolic and indolic subunits, as described by Proteau et al., 1993 (**Fig. 21A**). Scytonemin accumulates extracelularly in the sheaths of many terrestrial cyanobacteria that forms matting communities, while it is not detected in most planktonic species of cyanobacteria (Cockell and Knowland, 1999; Castenholz and Garcia-Pichel, 2000).

Mycosporine-like amino acids (MAAs) are group of intracellular, water-soluble, colorless compounds that act as UV screen in a wide variety of taxonomically different organisms, including cyanobacteria, marine heterotrophic bacteria, eukaryotic algae, fungi, marine invertebrates, fish and other marine organisms (Cockell and Knowland, 1999; Castenholz and Garcia-Pichel, 2000). MAAs consists of either a cyclohexanone or a cyclohexenimine ring, conjugated to the nitrogen of an amino acid or its imino alcohol (**Fig. 21B**). Depending on their

structure, they exhibit different maxima of absorption. Upon the UV exposure, a complement of several different MAAs can be found accumulated in a single organism, which enables relatively broad-range screening in UV-B and UV-A regions (Cockell and Knowland, 1999; Shick and Dunlap, 2002). In some terrestrial cyanobacteria, MAAs occur together with scytonemin, improving UV screening efficiency (Cockell and Knowland, 1999).

Flavonoids are UV screening pigments in plants (Li et al., 1993; Stapleton and Walbot, 1994; Parr and Bolwell, 2000; Ryan et al., 2002; Treutter, 2006). These polyphenolic compounds are characterized by a flavan ring structure substituted by different functional groups (**Fig. 21C**). Upon UV exposure, they accumulate in plant cells within vacuoles and cell walls. Each plant synthesizes a range of different flavonoid compounds (Le Gall et al., 2005; Routaboul et al., 2006). These pigments exhibit a high level of UV screening capacity, covering UV-C, UV-B and UV-A light (Zalar et al., 2007b`; 2007c). Since flavonoids, as the principle UV protectors in plant seeds, are in the focus of this work, more details about their structure, biosynthesis and functions are given in section **5.2.** The VUV-UV absorption characteristics of flavonoids are presented in chapter **3** results **I**, section **10.2**. (see also the publications attached therein, Zalar et al., 2007b; 2007c).

Melanin pigments are widely distributed in the animal kingdom, and they are also present in fungi, higher plants and some bacteria (Hinojosa-Rebollar et al., 1993). They are highly polymeric compounds, containing indolic subunits (e.g. 5,6-dihydroxyindole (DHI) and 5,6- dihydroxyindole-2-carboxylic acid (DHICA)), as seen in **Fig. 21D** (Pezzella et al., 1997; Wakamatsu and Ito, 2002).The precise structure of natural melanins is not known, because they occur in the large aggregates, usually associated with proteins and lipids (Pezzella et al., 1997; Meredith et al., 2006). They have a strong broad absorption band in the UV and visible regions (Zalar et al., 2007b`; 2007c).

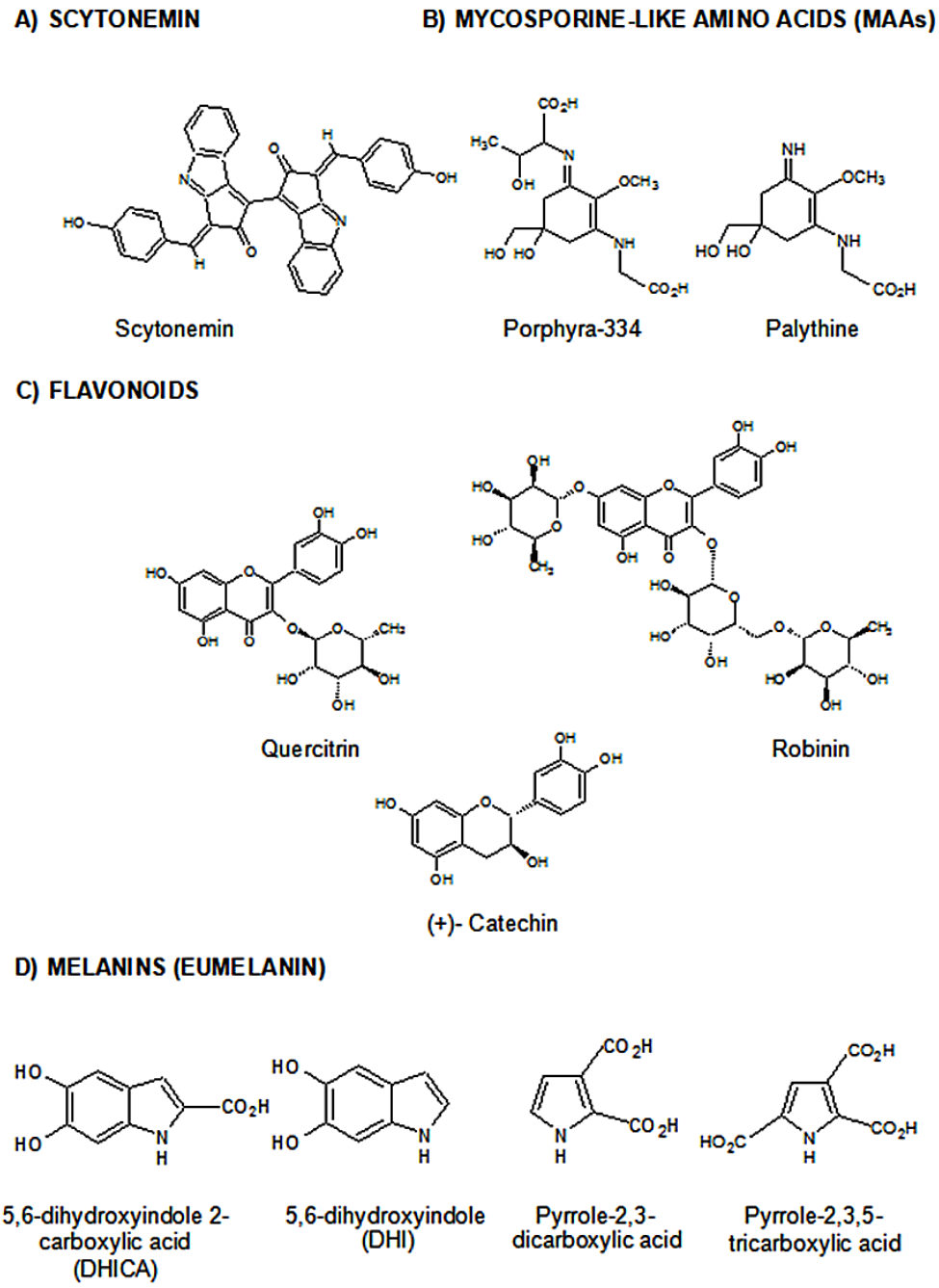

Fig. 21. Chemical structures of some known specialized UV screening compounds: A) scytonemin; B) mycosporine-like amino acids (MAAs); C) flavonoids; D) main building units of melanins (eumelanin) (modified from Zalar et al., 2007b).

3.3.4.3. Repair of UV-induced damage to DNA

For the survival of all organisms, it is crucial that genetic information stored in DNA is transmitted with high accuracy to descendant cells (or organisms). Since avoidance and UV screening are strategies that do not work with absolute efficiency, organisms had to develop DNA repair mechanisms in order to counteract the lethal effects of UV radiation that penetrated into the interior of cell. The principal repair mechanisms of UV-induced DNA lesions include photoreactivation, excision repair, lesion bypass and recombinational repair (Sinha and Häder, 2002).

Photoreactivation (PR) is one of the simplest and probably the oldest DNA repair mechanisms that occurs in a variety of prokaryotic and eukaryotic cells. However, it is not ubiquitous, since many species, including humans, lack this DNA repair system (Tuteja et al., 2001; Sinha and Häder, 2002). PR is a light-dependant repair pathway, which can directly reverse the DNA damage in an error-free manner (Britt, 1996). It is a single-enzyme repair system, which involves DNA photolyases that specifically bind either to CPDs (CPD photolyase) or 6-4 photoproduct (6-4 photolyase). DNA photolyases have two prosthetic chromophors; one of them acts as a light-harvesting antenna, which transfers the absorbed energy to the second chromophore, a two-electron-reduced flavin adenine dinucleotide ($FADH^-$) (Drapkin et al., 1994; Tuteja et al., 2001; Sinha and Häder, 2002). Upon the absorption of a photon of the appropriate wavelength (350-450 nm), the excited $FADH^-$ donates an electron to the pyrimidine dimer, inducing its reversal to monomers (Drapkin et al., 1994; Britt, 1996). PR is very efficient repair system, which generally occurs within a few hours. Once photolyases are bound to DNA lesion, approximately one dimer is split for every photon of UV-A or blue light (Drapkin et al., 1994; Britt, 1996; Walbot et al., 1997).

Excision repair (or “dark” repair) includes the pathways that do not directly reverse damage, but rather involve removal of a DNA lesion, followed by the synthesis of a nucleotide repair patch (Britt, 1996; Walbot et al., 1997; Sinha and Häder, 2002). Compared to photoreactivation, this repair system is more complex and considerably slower (Walbot et al., 1997; Sinha and Häder, 2002). There are two major categories of excision repair pathways: base excision repair (BER) and nucleotide excision repair (NER) (Britt, 1996; Tuteja et al., 2001; Sinha and Häder, 2002). BER mechanism is based on the elimination of a single damaged base residue in DNA. It is catalyzed by a number of different enzymes and involves several steps, including recognition of the DNA lesion, removal of the damaged base, incision of the DNA

strand at 5' or 3' to formed apurinic/ apyrimidinic (AP) site, filling of one-nucleotide gap and finally sealing of repaired DNA strand (Britt, 1996; Tuteja et al., 2001; Sinha and Häder, 2002). The NER pathway acts through a complex of repair enzymes that recognize damaged DNA strand and cut out the damage as a part of an oligonucleotide fragment, usually containing 24-32 nucleotides. The gap in the DNA strand is than filled through DNA synthesis and ligation of the nick (Tuteja et al., 2001). NER is one of the most widespread DNA repair pathways, present in both prokaryotes and eukaryotes (Tuteja et al., 2001). Unlike other DNA repair mechanisms that are lesion-specific, NER is capable of removing a wide range of types of DNA damage, including CPDs, 6-4 photoproducts and spore photoproducts (SPs) (Nicholson et al., 2000; Tuteja et al., 2001; Sinha and Häder, 2002).

Lesion bypass (or mutagenic repair) is a mechanism employed in a case when other DNA repair pathways for some reason do not occur (Sinha and Häder, 2002). As the pyrimidine dimers act as blocks to DNA replication, the only chance of cell to survive is to try to bypass such UV-induced DNA damages, even at the expense of accuracy in the genetic information (Britt, 1996; Tuteja et al., 2001). Some organisms possess modified, low fidelity and usually error-prone DNA polymerases that are capable of bypassing such lesions, and they promote the replication of damaged DNA (Tuteja et al., 2001). These DNA polymerases are involved in the process called the translesion synthesis in which an incorrect nucleotide is inserted opposite the site of the DNA lesion (Britt, 1996; Sinha and Häder, 2002). Since these modified DNA polymerases generally install the adenine residue opposite the lesion, the UV-induced thymidine dimers are usually not mutagenic, but cytosine-containing dimers are (Britt, 1996).

Recombinational repair, in contrast to lesion bypass, fills the daughter strand gap by transferring a preexisting complementary strand from a homologous region of the DNA to the site opposite the damage. However, the lesion is left unrepaired, but the cell manages to get through another round of replication (Britt, 1996). Besides pyrimidine dimers, DNA double-strand breaks and DNA single-strand gaps can be efficiently repaired by cellular mechanisms associated with recombination (Sinha and Häder, 2002).

4. PLANT SEEDS

4.1. Development and structure of plant seeds

Plant seeds are complex structures composed of cells. They undergo a series of cell divisions and differentiation events during the various stages of seed development, being finally organized into the following main seed structures: (1) an embryo, (2) the endosperm, and (3) the seed coat (testa) (Ohto et al., 2007). Seed development comprises three overlapping phases: (1) the embryo development, which is the initial phase characterized by cell division and morphogenesis, (2) seed maturation, a phase which involves the accumulation of storage material, and (3) seed desiccation that is the final phase during which the embryo prepares for desiccation and enters into a state of developmental and metabolic quiescence until germination (West and Harada, 1993; Ohto et al., 2007). Seed development is initiated with fertilization of the ovule, which consists of the embryo sac (female gametophyte) surrounded by the nucellus and one or two enveloping integuments. The point where the integuments meet at the nucellar apex is called the micropyle, which is an opening that serves for entrance of the pollen tube during fertilization. Usually at the opposite (non-micropylar) end, which is called the chalaza, the base of an ovule is attached to the ovary tissue via the structure known as the funiculus (Boesewinkel and Bouman, 1995; Copeland and McDonald, 2001a). In angiosperms, including both monocotyledonous (e.g. maize) and dicotyledonous plants (e.g. *Arabidopsis thaliana*), the process of double fertilization leads to the formation of the main three seed structures, and each of them has a distinct genotype (see **Fig. 22**). The haploid egg cell (n) and the diploid nucleus of the central cell (2n), which is formed prior to fertilization by the fusion of two polar nuclei within the female gametophyte, each fuses with one of the haploid pollen sperm cells (n) to form a zygote and an endosperm nucleus, respectively (Ohto et al., 2007). Therefore, the embryo that develops from a diploid zygote (2n) combines the genotypes of both male and female gametes. On the other hand, a triple nuclear fusion, followed by multiple nuclear divisions and subsequent cellularization, leads to the formation of triploid endosperm tissue (3n), which has two thirds of maternal and one third of paternal origin (Léon-Kloosterziel et al., 1994; Copeland and McDonald, 2001b; Ohto et al., 2007). The seed coat (2n) is entirely of maternal origin, since it is derived from the ovular integuments. (Boesewinkel and Bouman, 1995; Debeaujon et al., 2007).

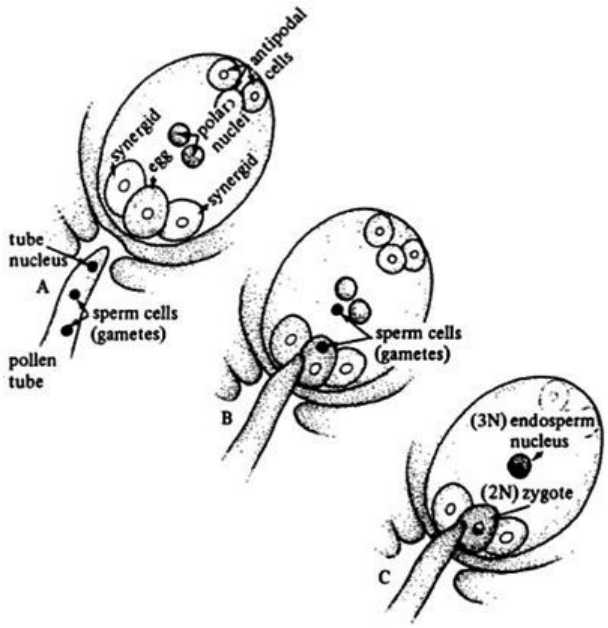

Fig. 22. Schematic representation of double fertilization in angiosperms: (A) Pollen tube with two sperm cells (male gametes) and tube nucleus, passing through the micropyle and approaching the embryo sac (female gametophyte), which contains the egg cell (female gamete) inserted between two synergid cells, two polar nuclei and three antipodal cells. (B) Two sperm cells approach the egg cell and polar nuclei. (C) Double fertilization occurred: the egg cell and the nucleus of the central cell, which is formed by the fusion of two polar nuclei, each fuse with one of the sperm cells to form a diploid (2N) zygote and a triploid (3N) endosperm nucleus, respectively (taken from Copeland and McDonald, 2001).

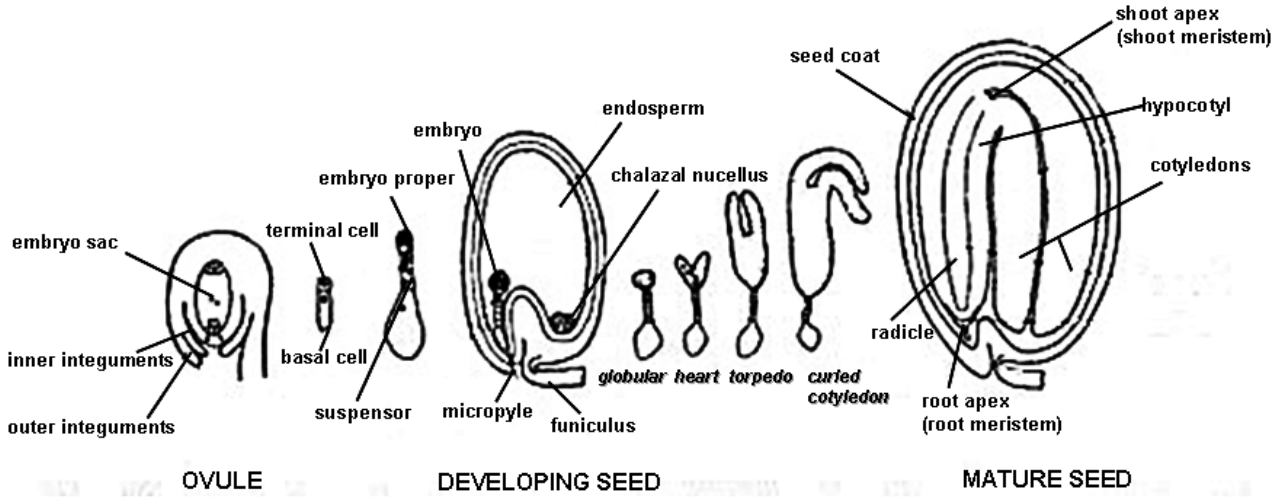

Fig. 23. Overview of embryogenesis and seed development in *Arabidopsis thaliana*. The ovule contains the embryo sac (female gametohyte) surrounded by the nucellus and two integuments. The micropyle is located between the inner integuments. Following double fertilization, the zygote divides into the terminal and basal cells, which give a rise to the embryo proper and the suspensor, respectively. The funiculus attaches the ovule to the central replum of the silique. The suspensor connects the embryo proper to maternal tissue within the ovule. The early embryo in the immature seed is surrounded by the nutritive tissue (endosperm). The growing embryo passes through different developmental stages: the globular, heart, torpedo and curled cotyledon stages. The mature embryo, protected within the seed coat, with established main structures: shoot apex, radicle, hypocotyl and cotyledons (adapted from Castle and Meinke, 1993; Meinke, 1994).

4.1.1. Embryo

Following fertilization, the zygote divides into two separate cells, which have different features and developmental fates; the terminal cell develops into the embryo proper, while the basal cell gives rise to the structure known as the suspensor, which holds the embryo proper fixed to the maternal tissue at the micropylar pole of the ovule (Yeung and Meinke, 1993; Meinke, 1994). Besides this passive role, the suspensor also plays an active role in synthesizing growth factors and transporting nutrients to the early-stage embryo. Nevertheless, the suspensor degenerates in the later stages of embryogenesis and it disappears completely in the mature seeds (Yeung and Meinke, 1993). During embryogenesis, the early embryo undergoes a series of cell divisions and complex morphological and cellular changes that ultimately result in the formation of the mature embryo, which is a new generation plant in miniature. In dicotyledonous plants, the growing embryos have stages of development according to their cell numbers and shapes, and the following stages are commonly distinguished: the octant, globular, heart-shape, torpedo-shape and cotyledonous (West and Harada, 1993; Meinke, 1994). At the latter stage, the basic plan and the polar organisation of the plant body are established; the mature embryo consists of the polar embryonic axis with a distinct shoot apex and radicle (embryonic root) at opposite ends, and the hypocotyl to which the cotyledons (embryonic seeds) are attached (West and Harada, 1993; Bewley and Black, 1994b). Characteristic stages of embryo development within the seed of *Arabidopsis thaliana*, as representative of dicotyledonous plants, are illustrated in **Fig. 22.**

4.1.2. Endosperm

The triploid endosperm tissue is the product of the second fertilization event. The fertilized central cell undergoes a series of free nuclear divisions without cytokinesis to form the endosperm syncytium[2]. Subsequent cellularization leads to the formation of endosperm tissue (Ohto et al., 2007). One of the principal functions of the endosperm is to provide nutritive support for the developing embryo. Depending on the plant species, the endosperm is either a transient or a persistent seed structure. Therefore, seeds can be grouped as endopsermic or nonendospermic in accordance with the presence or absence of the endosperm in the mature seeds (Bewley and Black, 1994b). The endosperm is retained to varying degrees in endopsermic seeds. In many monocotyledonous species (e.g. maize), the endosperm is well-developed and it

[2] Syncytium (pl. syncytia, Gr. *syn* = together + *kytos* = cell) is a cellular structure containing many nuclei in cytoplasm that is not separated into individual cells. Syncytium can be also formed by the cell fusion.

remains abundant throughout embryo development and germination, comprising a major part of the mature seed. In cereal grains and in seeds of some endospermic legumes, the majority of the cells in the well-developed endosperm are non-living due to abundant deposition of the storage material, and only the outermost layer of the endosperm (aleurone layer) consists of the living cells, which do not store many reserves (Bewley and Black, 1994b; Young and Gallie, 2000; Black et al., 2006). In some dicotyledonous plants, the endosperm is either undeveloped or may be consumed by the developing embryo, so that it is completely absent or present only as a very thin layer of tissue in mature seeds. In these cases, other embryonic structures, usually cotyledons, become the primary source of nutrients for embryo growth during germination and emergence (Bewley and Black, 1994b; Boesewinkel and Bouman, 1995).

4.1.3. Seed coat (Testa)

As endosperm and embryo grow, the surrounding maternal tissues form the seed-covering structure, known as the seed coat. The tissue of the seed coat is generally derived from the ovular integuments, but in some species it may be also formed from the chalaza tissue, and sometimes from the layers of nucellus that may be included on the inner side of the seed coat (Boesewinkel and Bouman, 1995). The seed coat is a multifunctional organ that plays an important role in embryo nutrition during seed development (Weber et al., 1996; Debeaujon et al., 2000). It also represents the seed's primary defense against adverse environmental conditions, since the seed coat acts as an efficient physical and chemical barrier between the embryo and external environment. It protects the embryo and the endosperm from various biotic and abiotic stresses, including seed predators, pathogenic microorganisms, UV light, desiccation and mechanical injury etc. (Mohamed-Yasseen et al., 1994; Black et al., 2006). The importance of the seed coat in seed longevity has also been reported, e.g. seeds with hard seed coats are generally long-lived, while seeds with weak seed coats that crack easily are prone to infection by microorganisms that can cause fast seed deterioration (Christiansen et al., 1960; Christiansen and Justus, 1963; Mayne et al., 1969; Bass, 1980; Mohamed-Yasseen et al., 1994). The seed coat has also an important function in regulation of seed germination and dormancy by restricting oxygen and water uptake (see section **4.2.3.3**). In some plant species, the seed coat develops special structures that are used as the means of the seed dispersal (Black et al., 2006). The mechanical resistance of the seed coat is usually provided by the cells that have thickened secondary cell walls with various amounts of deposits of lignin, suberin, cutin or callose substances. Seed coats may contain the mucilage that, upon contact with water (e.g. during imbibition), expands and extrudes from the seed surface, providing a water-retaining barrier around the seeds. The cuticle, often impregnated

with waxes or fats, provides additional protection to the seeds, but it also makes the seed coat impermeable to water, restricting the metabolism and further growth of the embryo (Bewley and Black, 1994b; Boesewinkel and Bouman, 1995; Black et al., 2006). In addition, the coats of numerous seeds contain large amounts of phenolic compounds (Côme, 1982; Corbineau and Côme, 1995), especially flavonoids (e.g. proanthocyanidins, also called condensed tannins). Proanthocyanidins are usually deposited in the tannin vacuoles or in the cell walls in the outer layer of the seeds, but sometimes the tannin cells may also occur in the internal layers of the seed coat (Boesewinkel and Bouman, 1995). These polyphenolic substances improve the mechanical resistance of the seed coat and they make it impermeable to water and oxygen (Côme, 1982; Corbineau and Côme, 1995; Debeaujon et al., 2000; Debeaujon et al., 2007). Due to the toxic properties of many phenolic compounds, seed coats provide additional protection against predators and soil-born pathogenic microorganisms (Mohamed-Yasseen et al., 1994). Many phenolics, including flavonoids, also play important roles in seed physiology (Mohamed-Yasseen et al., 1994; Debeaujon et al., 2000; Debeaujon et al., 2007). More information about the role of testa flavonoids in the regulation of seed dormancy and germination are provided further in this chapter (see section **4.2.3.3**). Since phenolic compounds, notably flavonoids, play an important role in seed protection against various biological and physical stress factors, their chemistry, biosynthesis and physiological functions in plants are described in detail elsewhere (see section **5**).

4.2. Seed physiology: Dormancy and germination

Seeds, as dispersal units of the plants, are structurally and physiologically equipped to sustain the early growth and development of the progeny plants, before they become the self-sufficient, autotrophic organisms (Bewley, 1997). The new plant starts as an embryo within the developing seed. The mature seed separates from the mother plant and the embryo becomes ready to develop further into a young new plant, the seedling, which emerges out from germinating seed. However, many seeds are unable to germinate immediately after reaching maturity, but they rather enter into the quiescent state prior to germination. Quiescent seeds are resting organs generally having low moisture content and drastically reduced, sometimes hardly detectable, metabolic activity. A remarkable property of many seeds is that being in the dry, quiescent state, they can survive extended periods of time, ranging from decades to centuries, and even millennia (Kivilaan and Bandurski, 1981; Steiner and Ruckenbauer, 1995; Shen-Miller et al., 2002; Buitink and Leprince, 2004; Walters et al., 2005; Buitink and Leprince, 2008; Sallon et al., 2008). Soon after the seeds are hydrated and environmental conditions become suitable,

germination may occur, leading to the resumption of normal, high level metabolism and further growth. Nevertheless, some seeds fail to germinate, even if conditions are apparently favourable for germination. Such seeds experience dormancy, a state that can be released by dormancy-breaking factors (Bewley and Black, 1994b) (see section **4.2.3**). In summary, following dissemination from the mother plant, the seeds may enter into one of three states: (1) they are non-dormant and can germinate immediately, (2) they are non-dormant, but in the quiescent state, and (3) they are dormant (Geneve, 1998).

4.2.1. Seed dormancy

The term *dormancy* usually refers to a state of a whole plant or its parts, characterized by a temporal arrest in growth and development. Dormancy was likely acquired during evolution as a strategy for surviving in adverse environmental conditions, such as heat, cold and drought. Seed dormancy results in the absence of germination. However, the absence of germination can have several causes: the seed can be nonviable, the environmental conditions may be insufficient to sustain germination or the seed itself may block germination (Hilhorst, 2007). Seed dormancy has therefore been defined as the incapacity of an intact, viable seed to germinate under conditions that are normally favourable for germination (Bewley, 1997; Finch-Savage and Leubner-Metzger, 2006; Bentsink and Koornneef, 2008). Seed dormancy, as an intrinsic block of germination, is an adaptive trait that allows plants to determine the timing of germination for seeds in a population (e. g. germination at a particular time of the year or preventing pre-harvest germination) (Geneve, 1991; Bewley, 1997; Bentsink and Koornneef, 2008). Seed dormancy is a common condition found in many plant species. It is determined by the genetic factors, but is also influenced by environmental factors, which often act via plant hormones as mediators (Finch-Savage and Leubner-Metzger, 2006).

4.2.1.1. Types of seed dormancy

There are two main categories of seed dormancy based on the timing of the occurrence; these on primary and secondary dormancy (Karssen, 1982). Primary dormancy refers to the innate dormancy possessed by freshly harvested mature seeds. It is acquired prior to seed dispersal as a part of the seed developmental program. On the other hand, secondary dormancy occurs after seed dispersal, when mature imbibed seeds acquire dormancy as a result of the lack of proper conditions for germination. In nature, it is often associated with annual seed dormancy cycles, which can be lost and reintroduced repeatedly as seasons change until favourable

conditions for germination and subsequent plant growth occur (Karssen, 1982; Finch-Savage and Leubner-Metzger, 2006; Hilhorst, 2007). Dormancy is determined both by the physiological and the morphological properties of the seed (Nikolaeva, 2004). Seed dormancy may be related to factors within the embryo (endogenous dormancy) or it may be imposed by the tissues that surround the embryo, e.g. the seed coat (exogenous dormancy) (Hilhorst, 2007). In this respect, Baskin and Baskin (2004) have proposed a classification system for "whole seed" dormancy, which includes five classes: (1) physiological dormancy, (2) morphological dormancy, (3) morphophysiological dormancy, (4) physical dormancy and (5) combinational dormancy.

4.2.2. Germination

The term "germination" generally refers to the process in which the resting forms of life (e.g. seeds, spores and pollen) reinitiate their growth and metabolic activity once they have met the propitious conditions (Nonogaki et al., 2007). Since the term "seed germination" is sometimes used loosely in the scientific literature, it is necessary here to clarify its meaning. Seed quality analysts define seed germination as the process of the emergence and development of the seedling to a stage where the aspect of its essential structures, the root, hypocotyl and cotyledons, indicates whether or not it can develop further into a vigorous plant under favourable conditions (ISTA, 1999). On the other hand, seed physiologists define germination in the strict sense (*sensu stricto*; Perino and Come, 1991) as the process that begins with water uptake by the quiescent dry seed (imbibition) and ends with the elongation of the embryo axis (Bewley and Black, 1994b; Bewley, 1997; Nonogaki et al., 2007). Usually, the visible sign that germination is completed is the penetration of the extended embryo radicle through the covering tissues (e.g. seed coat and endosperm) (Bewley, 1997). Therefore germination *sensu stricto* does not include seedling growth, which begins when germination terminates, as well as the processes that occur in the nascent seedling, such as mobilization of the storage reserves (Bewley and Black, 1994b). Accordingly, the term "seed germination" is used throughout this work only in the strict sense.

In general, germination is constituted of the three processes, seed imbibition, the activation processes and intra-seminal growth that is completed with embryo protrusion (Ranal and de Santana, 2006). It includes numerous events, such as enzyme activation, respiration, subcellular structural changes, repair of DNA and organelles, synthesis of macromolecules (DNA, RNA, proteins etc.), cell elongation etc., as seen in **Fig. 24** (Bewley and Black, 1994b; Bewley, 1997; Nonogaki et al., 2007). However, the crucial step of germination is the imbibition of mature dry seeds in order to resume their metabolic activities. The uptake of water in most seeds is a

triphasic process; it begins with a rapid initial uptake (phase I), followed by the plateau phase of variable duration (phase II) and it ends with resumption of relatively fast water uptake (phase III), which occurs only after germination is completed, as seen in **Fig. 24** (Bewley, 1997; Nonogaki et al., 2007). The initial uptake of water is a physical process driven by the matric potential of the seed and it occurs in both the living and dead cells. It is also thought that the rates of water uptake are controlled initially by the permeability of the seed coat (Nonogaki et al., 2007). During phase I, the influx of water into the cells causes temporary structural perturbations of membranes. Therefore, shortly after the start of water uptake, the leakage of solutes and low molecular weight metabolites can be detected in imbibed seeds (**Fig. 24**). This phenomenon is likely related to a transition process of membrane phospholipids from the gel phase, which is achieved during the seed maturation drying, to the normal, hydrated liquid-crystalline state (Crowe et al., 1984; Crowe et al., 1992; Buitink et al., 2002). However, this process last only until shortly after imbibition, when membranes return to their more stable configuration (Bewley, 1997). Following the initial rapid water uptake, the seed water content is nearly constant during imbibition phase II, where further embryo swelling is prevented either by internal hydraulic pressure (turgor) developed in imbibed embryo, which offsets the osmotic gradient for water uptake, or by the resistance of the tissues that surround the embryo (Nonogaki et al., 2007). In contrast to viable seeds, dead seeds absorb more water during phase II, since they can not develop a turgor due to the loss of membrane integrity in dead cells (Nonogaki et al., 2007). Therefore, dead seeds do not enter into the imbibition phase III. Imbibed dormant seeds also remain in phase II until dormancy is released (Bewley, 1997; Nonogaki et al., 2007).

In viable seeds, metabolism commences as soon as they are hydrated. One of the first changes that occurs after imbibition is the resumption of respiratory activity (**Fig. 24**). Following initial rapid oxygen consumption, the rate declines until the radicle penetrates the enclosing tissues, at which point the respiratory activity increases again steeply (Bewley, 1997).

Proteins are also synthesised in the very early phase of germination. Their synthesis occurs within minutes of imbibition, using preformed mRNAs that remain conserved in dry seeds (Bewley, 1997; Black et al., 2006). In the later germination phases, new mRNAs are transcribed and *de novo* synthesis of proteins occurs (Bewley, 1997). Numerous enzymes are synthesized during germination, including those that are specifically associated with the germination process (Black et al., 2006).

With the resumption of metabolic activity, the repair of existing DNA and organelles occur in germinating seeds, as well as *de novo* synthesis of macromolecules, including DNA. Two discrete phases of DNA synthesis were observed in the radicle cells of germinating seeds. The first occurs soon after imbibition and it is likely preceded by repair of damaged DNA that is caused by maturation drying, rehydration or adverse conditions during seed storage. The second DNA synthesis phase occurs during the late imbibition phase (phase II) and it further continues although the phase III, being associated with postgerminative cell division (Bewley, 1997; Black et al., 2006).

As the emergence of the radicle that protrudes out of the seed coat is considered as the final event of germination, the extension of the radicle is usually associated with cell elongation, which is a turgor-driven process that requires the cell walls of the radicle to yield and expand (Bewley, 1997; Black et al., 2006). Although DNA synthesis may begin in the meristem cells prior to radicle emergence, in most cases cell division does not occur until radicle emergence (Nonogaki et al., 2007). There is also the possibility that in some seeds, for instance in those with coat-imposed dormancy, the structures that surround the radicle tip (micropylar region) start to weaken, allowing the radicle to elongate (Bewley, 1997; Black et al., 2006; Nonogaki et al., 2007). In many endospermic seeds, including those with a single cell endosperm layer (e.g. *Lepidium sativum* and *Arabidopsis thaliana*), germination is a two-step process, where the testa rupture precedes endosperm rupture, as seen in **Fig. 25** (Arcila and Mohapatra, 1983; Müller et al., 2006).

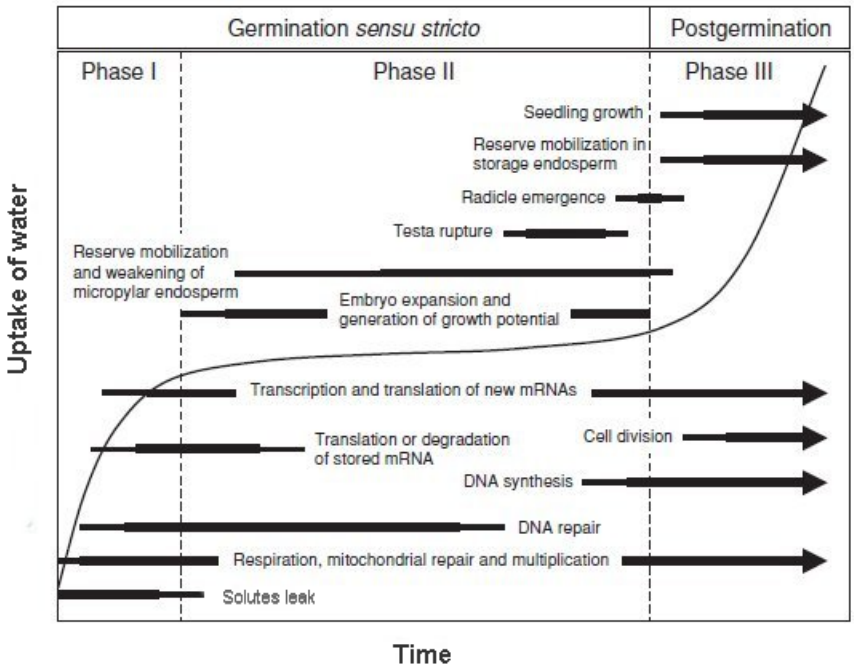

Fig. 24. Time courses of seed imbibition and major events associated with germination and seedling growth as a postgerminative process (adapted from Bewley, 1997 and Nonogaki et al., 2007).

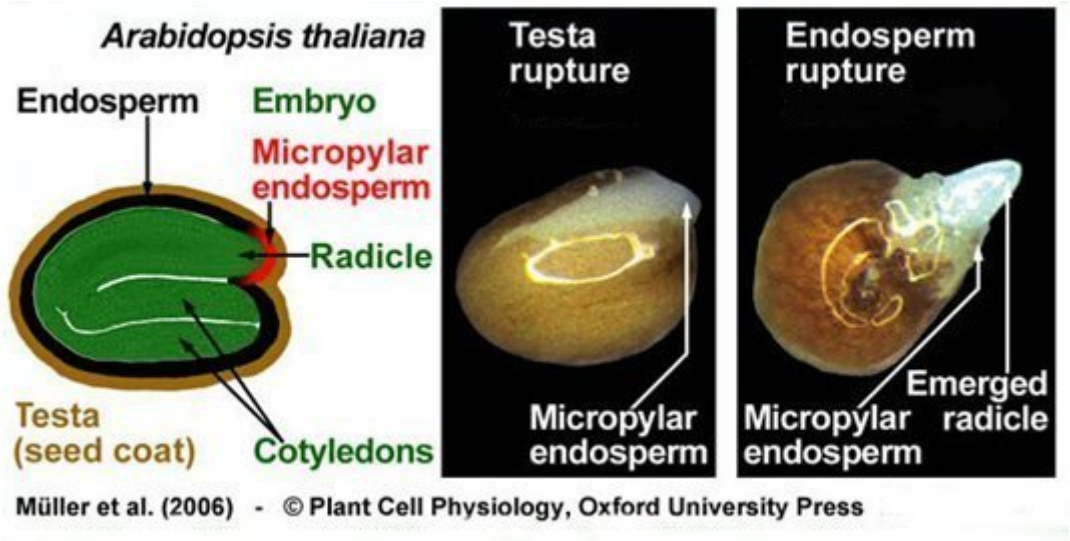

Fig. 25. Germination of *Arabidopsis thaliana* seeds, which is two-step process with distinct testa (seed coat) rupture and endosperm rupture (adapted from Müller et al., 2006)

4.2.2.1. Measurement of germination

Since water uptake and respiration measurements give only a rough indication of the stage of the germination process, and the universal biochemical marker of the germination progress has not yet been found, the only stage that can be relatively precisely determined is the end of the germination process, characterized by visible emergence of the radicle (Bewley and Black, 1994b). The degree to which germination has been completed is usually expressed as a percentage of germinated seeds in the population of sown seeds, observed at time intervals during the germination period (Bewley and Black, 1994b; Ranal and de Santana, 2006).

Generally, germination curves have a similar shape; they are usually sigmoidal and most of them are positively skewed because a greater percentage of seeds germinates in the first half than in the second half of the germination time course (**Fig. 26** and **Fig. 27**) (Bewley and Black, 1994b). However, seed populations may differ in their germination behaviour, having different characteristics that can be measured, including the germination capacity, germination time, germination rate and uniformity. These quantitative germination characteristics vary among species, but also within the same species (e.g. among different cultivars or ecotypes (Black et al., 2006).

Germination capacity refers to the maximal (final) percentage of germinated seeds, which is reached at the end of the germination period (Bewley and Black, 1994b).

The germination time is defined as the period required for the seed population to reach an arbitrary percentage of germinated seeds, usually 50%, or alternatively, to complete the germination process (Bewley and Black, 1994b). Frequently, the mean germination time (MGT) is used to express the average length of time required for maximum germination of a seed population (Ranal and de Santana, 2006). It can be calculated according to the equation of Ellis and Roberts (1981) as follows:

$$MGT = \frac{\sum Dn}{\sum n} \qquad (1)$$

where n is the number of seeds, which were germinated on a particular day/ hour D; D corresponds to number of days/ hours counted from the beginning of germination.

The germination rate (also called the germination speed or germination velocity) can be defined as the reciprocal of the time taken for the germination process to be completed (Bewley and Black, 1994b; Black et al., 2006). It can be determined for individual seeds, but it is more frequently expressed for the whole population, where the mean germination rate (R) is defined as the reciprocal of the MGT. Since in the scientific literature the term "germination rate" has sometimes the other meanings e.g. it may refer to the "cumulative germination percentage" (Black et al., 2006), further in this work we will use only the term "germination speed", in order to avoid any possible confusion.

Germination uniformity represents the degree of synchrony in germination of seeds in the population. A highly uniform seed population is that in which the germination speed of individual seeds is close to the mean germination speed for the population as a whole. The steepness of the germination curve is an indicator of the seed population uniformity, reflecting the fact that the majority of the seeds complete germination over a relatively short time period (Bewley and Black, 1994b).

Some examples of different germination behaviours of seed populations are shown in **Fig. 26** (Bewley and Black, 1994b). The germination curves *a* and *b* represent seed populations with the same germination capacity and highly uniform germination behaviour. Both of them have slightly positive skewed germination as seen from the distribution curves in **Fig. 27** (Bewley and Black, 1994b). However, these two populations differ in germination speed, since the start of the germination is delayed in the population *b*. On the other hand, the germination curve *c* represents a seed population which has the same germination capacity as population *a*, but it lacks uniformity as individual seeds complete their germination in very different periods of

time. The germination curve *d* flattens off when only a low percentage of the seeds has germinated, showing that the population has a low germination capacity, which may be related either to a low viability of seeds, or to a high percentage of dormant seeds, or alternatively, to the environmental conditions that do not favour germination of most of the seeds. Although having a high germination capacity, similar to that of population *a*, the germination curve *e* exhibits poor germination uniformity, where a limited percentage of seeds germinates fairly early, while the remainder germinate only after a delay. It indicates that the population *e* consists of two discrete groups of seeds: the quick and slow germinators (see also a distribution curve *e* in **Fig. 27**).

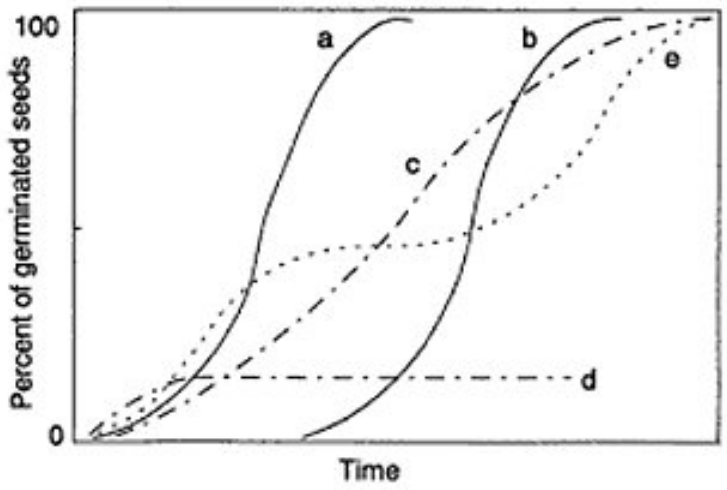

Fig. 26. Some examples of theoretical germination curves for populations of seeds with different germination behaviours (taken from Bewley and Black, 1994b).

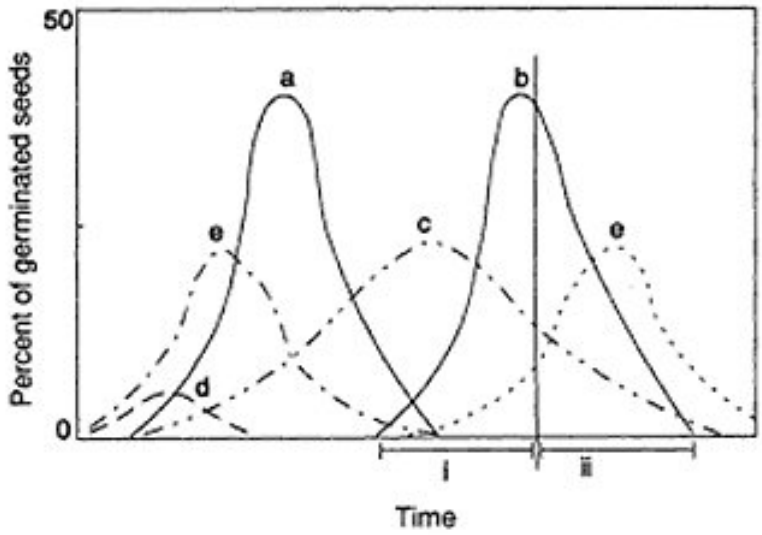

Fig. 27. Distribution of germination with time. The distribution curves are derived from the germination curves presented in **Fig. 5.** The vertical line on the curve b indicates that the germination is positively skewed, where more seeds germinate in the first half (i) than in the second half (ii) of the germination time course (taken from Bewley and Black, 1994b).

4.2.3. Factors affecting seed dormancy and germination

Although the release of dormancy and the subsequent initiation of germination should be considered as two distinct phenomena, sometimes the apparent continuum between these two processes makes it difficult to distinguish the factors that break dormancy from those that induce germination. Usually, one set of environmental factors will release dormancy, while another set of conditions may be required for subsequent germination (Hilhorst, 2007). However, the action of these two sets may overlap. Some of the factors that influence seed dormancy and germination are presented in **Fig. 28**. Certain conditions are essential for germination of all seeds, such as water for rehydration, oxygen for respiration and favourable temperature (Copeland and McDonald, 2001c).

4.2.3.1. After-ripening

After-ripening usually refers to the extended period of dry storage at room temperature of freshly harvested, mature seeds (Finch-Savage and Leubner-Metzger, 2006). It is widely used in seed technology laboratories as a method to release seed dormancy, while in field it occurs in the period between seed shedding and the beginning of germination. Seed after-ripening is influenced by the temperature, seed moisture and oil contents, as well as by the seed-covering structures (Finch-Savage and Leubner-Metzger, 2006). Hydration of seeds often prevents after-ripening and maintains dormancy (Allen et al., 2007). On the other hand, after-ripening is prevented in very dry seeds, in which the threshold value of the moisture content is found to be species-specific (it is lower in oilseeds compared to starchy seeds) (Finch-Savage and Leubner-Metzger, 2006). Although its molecular mechanisms remain still unknown, it is thought that dormancy loss through after-ripening is associated with a breakdown of dormancy imposing factors, e.g. abscisic acid (ABA) (Allen et al., 2007; Hilhorst, 2007).

4.2.3.2. Stratification

In many cases, physiological dormancy may be released in seeds exposed for extended periods to chilling, while in an imbibed state (Copeland and McDonald, 2001c). This stimulatory effect of cool moist conditions has been known for the centuries, and it was in common use for breaking dormancy in many horticultural seeds. Historically, the term stratification originates from the procedure in which the seeds were arranged in layers in moist sand or soil and stored at low temperature prior to planting (Copeland and McDonald, 2001c; Allen et al., 2007).

In nature, seed stratification is an environmental adaptation of many temperate-zone plants, which have seeds that ripen in the fall, remaining over winter in the moist substrate, and germinate in the spring (Geneve, 1998; Allen et al., 2007). Temperature is the most important factor controlling stratification. Temperatures near freezing (1-10°C) are the most effective in so called "cold stratification" (prechilling) (Geneve, 1998). Nevertheless, some seeds require stratification at high temperatures (warm stratification) (Copeland and McDonald, 2001c). The dormancy-breaking effect of stratification is likely achieved through the increased sensitivity of seeds to other environmental factors, such as light and nitrate, and also to gibberellins (GAs), which are the germination stimulating plant hormones (Hilhorst, 2007).

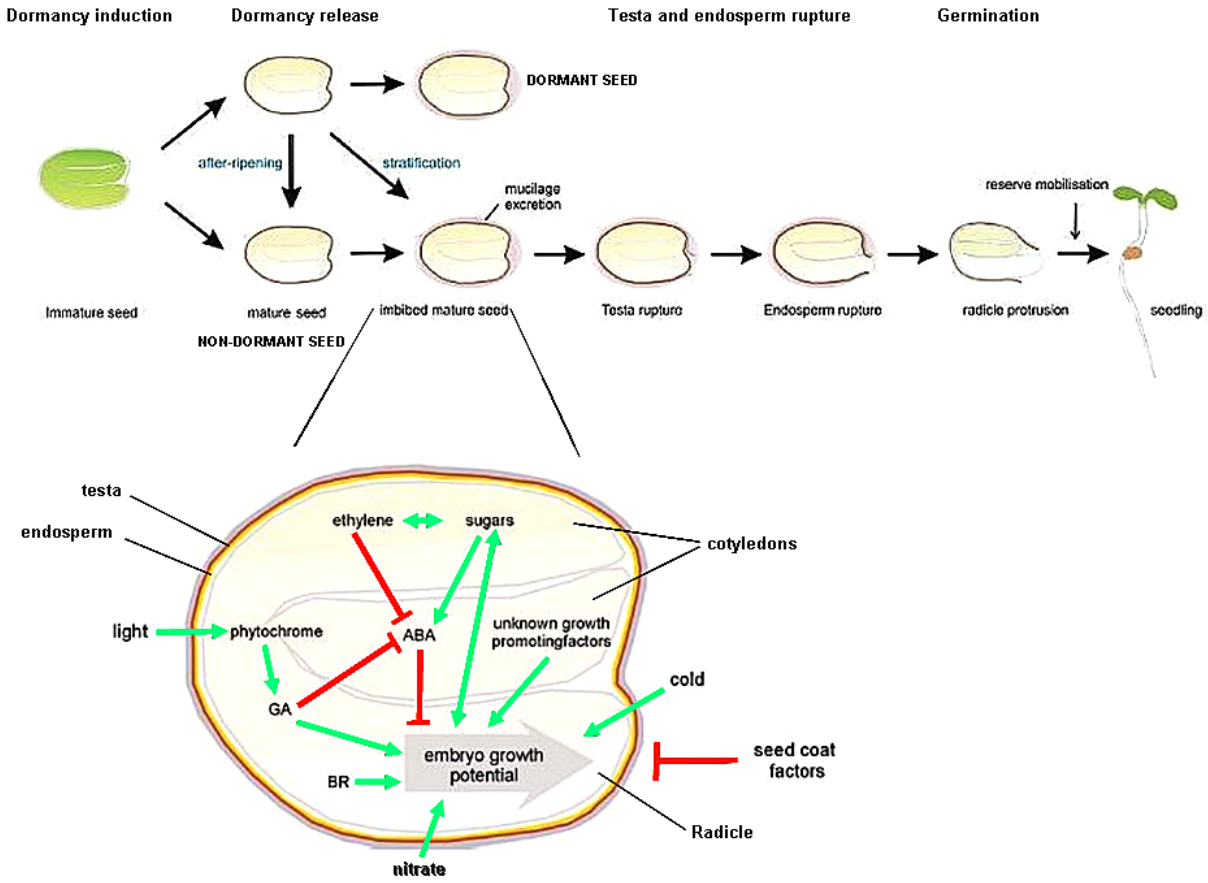

Fig. 28. Schematic presentation of the processes controlling seed dormancy and germination (*Arabidopsis thaliana* seed is here take as an example). The seed can be either in non-dormant or dormant state. Dormant seed will not germinate even when exposed to favourable environmental conditions (e.g. water and light). The seed dormancy can be broken by dry storage (after-ripening) or by cold imbibition (stratification). Germination promoting factors are marked with the green arrows, while germination inhibiting factors are indicated with red arrows (adapted form Bentsink and Koornneef, 2002; 2008).
ABA - abscisic acid, GA - gibberellins, BR – brassinosteroids

4.2.3.3. Coat effects

The tissues surrounding the embryo can influence germination in several ways: (1) by inhibiting water uptake, (2) providing mechanical restraint to embryo expansion and radicle protrusion, (3) limiting gas exchange (particularly oxygen and carbon dioxide), (4) preventing the leakage of germination inhibitors from the embryo, (5) supplying inhibitors to the embryo or (6) filtering out light, which is an environmental factor that affects germination (Geneve, 1998; Debeaujon et al., 2007).

In many seeds the seed coat confers mechanical constraint, which can be overcome either by increased growth potential of the embryo or by testa weakening. Therefore, the germination in many seeds with coat-imposed dormancy may be improved by scarifying or by softening coats, mechanically or chemically. In nature, seed coat weakening may occur by mechanical abrasion, exposure to fire or by alternating freeze - thaw cycles. In addition, seed coats may be softened by the activity of soil-born microorganisms or by the passage of seeds through the digestive tract of animals (Geneve, 1998). Particular arrangements of testa cells and the presence of some chemicals, notably proanthocyanidins (condensed tannins), which are the flavonoid compounds particularly abundant in the seed coats, promote coat-imposed dormancy by increasing the rigidity and mechanical strength of the testa. Being oxidized, proanthocyanidins crosslink with proteins and carbohydrates in the cell wall, resulting in reinforced testa structure (Debeaujon et al., 2007). This also affects the permeability of the seed coat, restricting water entry and gas-exchange (oxygen entry and carbon dioxide escape) (Marbach and Mayer, 1974; Debeaujon et al., 2000; Debeaujon et al., 2007). Phenolic compounds, especially flavonoids, are also efficient antioxidants (Rice-Evans et al., 1997). When present in seed coats, they may fix molecular oxygen through enzymatic and non-enzymatic oxidation, reducing oxygen supply to the embryo (Côme, 1982; Corbineau et al., 1986; Lenoir et al., 1986; Corbineau and Côme, 1995). Therefore, flavonoids and other phenolics (e.g. caffeic, p-coumaric, ferulic, sinapic, vanillic acids and lignans) act as direct or indirect germination inhibitors (Toole et al., 1956; Debeaujon et al., 2007). On the other hand, testa flavonoids play a protective role against solute leakage, imbibition damage and oxidative stress, thus improving seed vigour, germination and longevity (Powell, 1989; Mohamed-Yasseen et al., 1994; Kantar et al., 1996; Debeaujon et al., 2000).

4.2.3.4. Environmental factors

Seedling emergence in the field occurs only when all environmental conditions are within the ranges permissive for seed germination. Some of these conditions are germination-promoting factors, while others are dormancy-release factors (Allen et al., 2007). Nevertheless, some environmental factors are thought to regulate both the dormancy and germination processes or in some cases their roles are difficult to distinguish, due to a continuous transition between the dormancy and nondormancy states (Allen et al., 2007; Hilhorst, 2007). Among different environmental factors, soil water content, temperature, light, gases (air composition) and chemicals (e.g. nitrates), which may act independently or collectively, are thought to have an important role in the control of seed dormancy and germination (Côme and Tissaoui, 1973; Corbineau and Côme, 1995; Allen et al., 2007; Bentsink and Koornneef, 2008).

Water is a basic requirement for germination. Since quiescent seeds have a characteristically low moisture content, water is necessary for the activation of the enzymes related to embryo respiration and growth, as well as the mobilization of reserve storage material during germination (Copeland and McDonald, 2001c). Metabolically activated, imbibed seeds become capable of receiving the external signals that can stimulate germination (e.g. light, temperature variations, chemical signals, etc.) (Bewley, 1997). Therefore, the substrate water potential is one of the most important germination regulatory factors.

Temperature is an important environmental factor that regulates both dormancy and germination (Finch-Savage and Leubner-Metzger, 2006; Hilhorst, 2007). The interactions of temperature with other environmental factors, such as light, moisture of the substrate and gases have been also reported (Côme and Tissaoui, 1973; Cone and Spruit, 1983; Corbineau and Côme, 1995; Bair et al., 2006; Batlla and Benech-Arnold, 2006; Bradford et al., 2007). Great variability in the temperature requirement for germination was found among different species and within species (Toole et al., 1956). The effect of temperature on germination can be generally expressed in terms of the "cardinal temperatures", including the minimum (base), optimum and maximum temperatures at which germination can occur (Toole et al., 1956; Copeland and McDonald, 2001c; Allen et al., 2007). Although the base temperature is sometimes difficult to determine, since the germination may occur, but at a very slow rate, it was found that many seeds can germinate at temperatures close to the freezing point. The optimum temperature for germination of most plant seeds is between 15°C and 30°C, while the maximum temperatures usually range between 30°C and 40°C (Copeland and McDonald, 2001c).

Alternating temperatures is also found to regulate the dormancy status in many seeds. In nature, the changes in seasonal and diurnal temperatures drive dormancy cycling of seeds in soil (Allen et al., 2007; Hilhorst, 2007).

Light can promote, but also inhibit the germination of imbibed seeds (Toole et al., 1956). The majority of seeds need to be exposed to the light, whereas others species require dark conditions to germinate (Toole et al., 1956; Geneve, 1998). While it is widely accepted that light plays a role in the regulation of germination, it still remains unclear whether light can also directly affect seed dormancy (Finch-Savage and Leubner-Metzger, 2006; Hilhorst, 2007). Both light intensity and light quality influence germination. Light is perceived through photoreceptors, the pigments in the phytochrome family. Upon red light irradiation, phytochromes undergo a reversible photoconversion between the red light (R)-absorbing form (Pr) and the far-red light (FR)-absorbing form (Pfr). Phytocromes are synthesized as Pr, a physiologically inactive form, which upon exposure to red light turns into the physiologically active Pfr form that triggers a variety of complex physiological responses, including seed germination. In some seeds, such as *Arabidopsis*, the effects of light on seed germination were found to be interrelated to other factors, such as plant hormones, as seen in **Fig. 28** (Cone and Spruit, 1983; Bentsink and Koornneef, 2008).

Gaseous environment also affects the seed germination and dormancy processes. Most plant species are adapted to an oxygen-rich environment, and require oxygen for seed germination. However, the gaseous composition of the soil may differ from that of the air, since it depends on the structural characteristics of the soil, the diffusion and solubility coefficients of different gases, as well as O_2 uptake and CO_2 and ethylene release by the living soil-born organisms (Corbineau and Côme, 1995). As respiration, an essentially oxidative process, increases sharply during seed germination upon imbibition, most seeds require an adequate supply of O_2 during germination (Copeland and McDonald, 2001c). However, the sensitivity of seed germination to the partial pressure of O_2 depends widely on the plant species, physiological status and the dormancy state of seeds. It is also modulated by other environmental factors, including water potential, light and temperature e.g. the lower the temperature, the less O_2 is required for germination (Corbineau and Côme, 1995; Bradford et al., 2007). Most of seeds in conditions of partial or total deprivation of O_2 have retarded or even inhibited germination. However, some seeds can tolerate hypoxic and anoxic conditions by entering into secondary dormancy (Corbineau and Côme, 1995; Copeland and McDonald, 2001c; Naeem et al., 2009). Other seeds are adapted to germinate at very low O_2 concentrations, e.g. aquatic plants germinate

under water where O_2 is present only in limited concentrations. A few plant species, including rice, are known to germinate under complete anoxia (Corbineau and Côme, 1995, and references therein). Scarification or removal of the seed coat may help germination under hypoxic conditions, where isolated embryos are found to germinate well in an atmosphere containing only 1-3% O_2 (Côme, 1982; Corbineau and Côme, 1995).Carbon dioxide (CO_2) has been shown to stimulate germination, but only at relatively low concentrations (0.5-5%) (reviewed by Corbineau and Côme, 1995). Higher concentrations of CO_2 (above 10%) are found to have inhibitory effects on germination. Nevertheless, in the soil, the concentrations of CO_2 are rarely above 1-2% under natural conditions. Ethylene which is a gaseous phytohormone (see section **4.2.3.5** and **Fig. 28**) also stimulates germination in many plant species. The elevated CO_2 is often associated with enhanced production of ethylene. Both gases possibly stimulate seed germination, acting either in additive or synergistic manner (Corbineau and Côme, 1995).

Nitrate is another factor of the soil environment that can influence germination. Many species are reported to respond positively to low doses of nitrates during laboratory seed quality tests (ISTA, 1999). Although the mechanisms of germination stimulation by nitrate remain still unknown, it is thought that it directly affects the dormancy rather than just promoting seed germination (Finch-Savage and Leubner-Metzger, 2006).

4.2.3.5. Plant hormones

Some phytohormones, such as abscisic acid (ABA), gibberellins (GAs), ethylene and brassinosteroids (BRs) are important regulators of dormancy and germination (**Fig. 28**). ABA and GAs are two types of hormones that act antagonistically; ABA induces dormancy during seed maturation and maintains the dormant state in imbibed seeds, while GAs play a key role in dormancy release and in the promotion of germination (Finch-Savage and Leubner-Metzger, 2006).

In most species, ABA levels increase during the first half of seed development and decline during late maturation, coinciding with the decline in seed water content. In seeds, ABA has been related to different developmental processes, including suppression of precocious germination and induction of desiccation tolerance (Hilhorst, 2007). ABA deficiency during seed development is associated with the absence of primary dormancy, whereas overexpression of ABA biosynthesis genes can increase a seed ABA content and enhance seed dormancy (Finch-Savage and Leubner-Metzger, 2006 and references therein). Upon imbibition of dormant seeds,

the concentrations of endogenous ABA increase (Le Page-Degivry and Garello, 1992; Wilson et al., 1995; Debeaujon and Koornneef, 2000). Therefore, *de novo* biosynthesis of GAs is required during imbibition to overcome this ABA-induced dormant state (Karssen et al., 1989; Nambara et al., 1991).

Two mechanisms have been proposed by which GAs promote germination; the first is the induction of the expression of genes encoding enzymes hydrolyzing the endosperm, which finally leads to endosperm weakening, allowing the radicle to emerge, while the second mechanism consists of a direct stimulating effect on the growth potential of the embryo (Debeaujon and Koornneef, 2000 and references therein). In addition, it was found that a dynamic balance of hormone synthesis and catabolism, which ultimately controls the ABA:GA ratio in seeds, is the major regulator of dormancy/ germination status, rather than the absolute concentrations of these hormones. While dormancy maintenance depends on a high ABA:GA ratio, dormancy release involves a net shift to increased GA biosynthesis and ABA degradation, resulting in low ABA:GA ratios (Finch-Savage and Leubner-Metzger, 2006).

In addition, the effects of some environmental factors, such as light and cold, are mediated by plant hormones. In many seeds, light and GAs can both release dormancy and promote germination (Debeaujon and Koornneef, 2000; Finch-Savage and Leubner-Metzger, 2006; Hilhorst, 2007). In *Arabidopsis* seeds, light-induced phytochrome may induce GA biosynthesis during the early phases of germination, while cold treatment, on the other hand, may increase the sensitivity of the embryo to GAs, finally resulting in the enhanced growth potential of the embryo, as seen in **Fig. 28** (Derkx and Karssen, 1993a; Yamaguchi et al., 1998; Debeaujon and Koornneef, 2000).

4.3. Chemistry of plant seeds

The chemical composition of seeds is basically determined by genetic factors and hence varies widely among species and their varieties. In addition, the environmental conditions that prevail during seed development and maturation may also influence seed chemistry (Bewley and Black, 1994b; Copeland and McDonald, 2001d). Aside from the chemicals that are found in all plant tissues, which play important structural and functional roles, seeds contain large amounts of food reserves that are mobilised during germination, supporting early seedling growth. The seed storage material generally includes carbohydrates, lipids and proteins. Reserves may be stored in different seed parts, including embryonic and extraembryonic tissues. For example, the carbohydrates are mostly located in the endosperm, while the embryos (particularly the cotyledons) may contain large quantities of storage proteins and lipids (Bewley and Black, 1994b). In addition to food reserves, seeds contain smaller amounts of other chemical substances, which have a minor storage role, but a rather important function in the regulation of the growth and metabolism of the developing embryo and early seedling, as well as in seed protection.

4.3.1. Water content

In spite of the fact that plants are composed mainly of water (plant cell protoplasm contains about 85-90% water), the mature seeds are the plant parts that have the least amounts of water (Larcher, 2003). For comparison, the water content in the soft leaves and roots is about 80-90% (fw) and 70-95% (fw), respectively. Freshly cut wood contains about 50% (fw) water. In contrast, most plant seeds have an extremely low water content. It is known that at some point of their development, the seeds of the majority of plant species undergo massive desiccation (Berjak and Pammenter, 2000; Black et al., 2006). Consequently, mature dry seeds contain in average only about 10-15% water (fw), although the water content in some oilseeds may drop down to 5-7% (fw) (Larcher, 2003). In dry state, seeds are capable of surviving for extended periods of time (sometime for decades, or even millennia) (Kivilaan and Bandurski, 1981; Steiner and Ruckenbauer, 1995; Shen-Miller et al., 2002; Walters et al., 2005; Sallon et al., 2008). In most other organisms, the extreme desiccation leads to irreversible injuries to the cellular structures and macromolecules (e.g. membrane disintegration, protein denaturation etc.). Plant seeds developed a particular desiccation tolerance strategy, moreover using it as an ecological advantage for surviving long time periods even under unfavourable environmental conditions. During process of seed drying, cytoplasmic viscosity increases dramatically, and

finally it transforms into so-called glassy state (Buitink and Leprince, 2004). A glass could be defined as an amorphous metastable state that resembles a solid, brittle matter, but retains the disorder and physical properties of the liquid state; it is a highly viscous solid liquid (Buitink et al., 2002; Buitink and Leprince, 2008). The formation of intracellular glasses is indispensable to survive the dry state. Due to a high viscosity, the molecular mobility is extremely limited, thus decreasing the probability of all chemical reactions that depend on molecular diffusion (Buitink and Leprince, 2004; Buitink and Leprince`, 2008). That is why the dry seeds enter in metabolically quiescent state. On the other hand, due to low molecular mobility, generation of ROS and their diffusion is drastically reduced in intracellular glasses, thus leading to decreased oxidative damage and slowing down ageing process in dry seeds (Buitink and Leprince, 2004). Soluble non-reducing sugars (sucrose and oligosaccharides), together with proteins (LEA, HSPs), which are both good glass-formers, play an important role in seed resistance to desiccation (Buitink et al., 2002; Buitink and Leprince, 2004; Boudet et al., 2006) (for details see sections **4.3.2** and **4.3.4**). Nevertheless, not all seeds are tolerant to desiccation. Accordingly, seeds can be generally classified into two groups, the orthodox and the recalcitrant seeds (Basu, 1995). The orthodox seeds are those which can be dried to a low moisture content (≤ 5%, fw), without being damaged, and whose longevity is extended if stored at low moisture content and low temperature (Roberts, 1973; Basu, 1995; Berjak and Pammenter, 2002). The orthodox seeds acquire desiccation-tolerance during their late phase of development, the seed maturation (Leprince et al., 1993). Dry orthodox seeds usually retain their viability for a long time periods, if stored under adequate conditions (Basu, 1995; Doijode, 2001). In contrast, recalcitrant seeds can not be dried and cooled below a certain critical level without being damaged. Therefore, these seeds do not complete maturation drying. They remain desiccation-sensitive both during their development and after harvest, containing a relatively high percentage of water (about 40-80%, fw) (Pammenter et al., 1994; Berjak and Pammenter, 2000). Recalcitrant seeds, which are characteristic of many tropical and subtropical species, can not be stored for long periods, even under favourable conditions (Corbineau and Côme, 1988, , 1989; Basu, 1995; Berjak and Pammenter, 2000; Doijode, 2001; Baskin and Baskin, 2001b).

4.3.2. Carbohydrates

Starch is the most widespread storage carbohydrate that is usually found abundant in seeds, in addition to the soluble sugars and other non-storage carbohydrates, such as cellulose, pectins and mucilages (Bewley and Black, 1994b; Copeland and McDonald, 2001d).

Starch occurs in seeds in two related forms, amylose and amylopectin, which are both polymers of D-glucose; former is a linear-chain molecule, while latter is a branched, high-molecular-weight molecule (**Fig. 29**). Starch is accumulated in small subcellular bodies (2 to 100 μm in diameter), called the starch grains. They are usually composed of about 50-75% amylopectin and 20-25% amylose. Starch grains are found in the endosperm and embryo's cotyledons (Bewley and Black, 1994b; Copeland and McDonald, 2001d).

Free, soluble sugars are rarely the main storage carbohydrates. However, some disaccharides (e.g. sucrose) and some oligosaccharides (e.g. raffinose family oligosaccharides), as seen in **Fig. 30**, are commonly found as minor reserves in embryo and storage tissue of mature seeds (Bewley and Black, 1994b). Nevertheless, soluble carbohydrates, particularly sucrose, are an important source of available carbon and energy, necessary for respiration during germination and early seedling growth. (Hopkins and Hüner, 2004a). They are the principal products of the sugar interconversions that occur in seeds during the mobilization of food reserves in germinating seeds. During the early developmental phase (morphogenesis phase), sucrose is first enzymatically hydrolyzed in seeds, and soluble monosaccharides (glucose and fructose) accumulate in relatively large amounts in the embryo and endosperm. In contrast, during the late phase of seed development (maturation phase), the embryo accumulates predominantly unhydrolyzed sucrose (Weber et al., 1995; Weber et al., 1997; Ohto et al., 2007).

The raffinose family oligosaccharides, RFOs (e.g. raffinose, stachylose, verbascose), occur almost ubiquitously in plant seeds (Peterbauer and Richter, 2001). They are soluble, low-molecular weight chains formed by the $\alpha(1\rightarrow6)$ polymerization of galactose units, attached to the glucose moiety of sucrose (**Fig. 30**). The ROFs accumulate in the late stages of seed maturation and desiccation (Taji et al., 2002). Non-reducing sugars, such as sucrose and RFOs play an important role in seed desiccation-tolerance. Together with late embryogenesis abundant (LEA) proteins (see section **4.3.4**), these non-reducing sugars are involved in the formation of intracellular glassy state, a state that enables seeds to resist almost complete removal of intracellular water and confer an exceptional longevity of seeds in dry state (Buitink and

Leprince, 2004; Buitink and Leprince`, 2008). These non-reducing sugars increase a density of intracellular glasses, thus reducing molecular mobility in the matrix, preventing ultimately from oxidative damage during the long-term storage of seeds. During desiccation process, sucrose and RFOs preserve proteins from unfolding, thus helping in preserving enzyme activity upon re-hydration (Buitink and Leprince, 2004). In addition, these non-reducing sugars act as protectants, being involved in the stabilization of the cell membranes during the dehydration (Crowe et al., 1984; Vertucci and Farrant, 1995; Buitink et al., 2002). A positive relationship between an increase in sucrose and RFO content and the acquisition of seed desiccation-tolerance was demonstrated in various species (Leprince et al., 1990; Bernal-Lugo and Leopold, 1992; Black et al., 1996; Bochicchio et al., 1997; Brenac et al., 1997; Corbineau et al., 2000).

Among non-storage carbohydrates, cellulose, pectins and mucilages can be found in seeds, as well as in other parts of plants. Cellulose and pectins are the two structural carbohydrates that make the matrix of primary cell walls of all land plants. Cellulose is a long, linear polysaccharide chain, constituted of many β(1→4) linked D-glucose units. (Hopkins and Hüner, 2004b). Pectins are complex, heterogeneous mixtures of polysaccharides that are especially rich in galacturonic acid (Bewley and Black, 1994b). Mucilages are chemically complex mixtures, predominantly composed of different polysaccharides (Willats et al., 2001; Copeland and McDonald, 2001d). Their essential components are polyuronides, which are acidic polysaccharides that are mainly composed of D-galacturonic acid, rhamnose, galactose and arabinose, resembling the pectic compounds, (Western et al., 2000; Copeland and McDonald, 2001d; Izydorczyk et al., 2005). Apart from the mucilages, which are sometimes present in rather large amounts in seeds, other non-storage carbohydrates occur in quantities found in other plant organs.

4.3.3. Lipids

The occurrence of large amounts of lipids differentiates the seeds from other plant parts (Bewley and Black, 1994b; Copeland and McDonald, 2001d). The majority of lipids stored in seeds are triacylglicerols, which are esters of glycerol and three molecules of fatty acid (**Fig. 31A**). In addition to these simple lipids, compound and derived types of lipids may also occur in the seeds. The compound lipids are esters of fatty acids, containing additional chemical groups (e.g. phospholipids and glycolipids that constitute the cell membranes), while the derived lipids are hydrolytic products of simple and compound lipids, which include various free fatty acids and some large molecular alcohols, such as sterols (e.g. cholesterol) (Copeland and McDonald, 2001d).

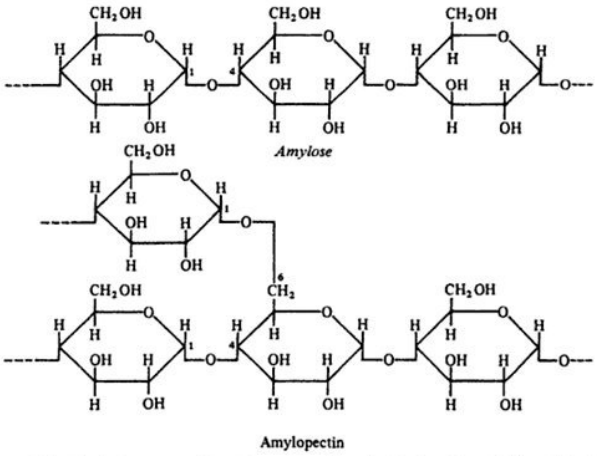

Fig. 29. Chemical structures of amylose and amylopectin, the two components of the starch. Amylose is a long chain of α(1→4)-linked glucose residues. Amylopectin is multibranched polymer of α(1→4)-linked glucose containing α(1→6) branch points (Adapted from Copeland and McDonald, 2001).

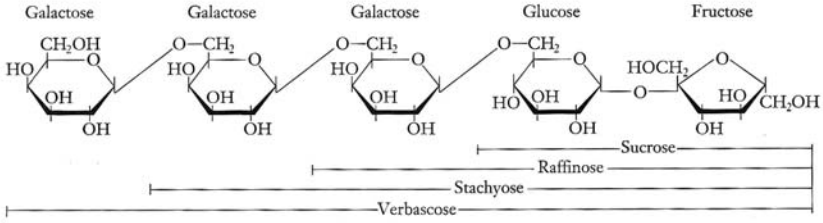

Fig. 30. Chemical structure of soluble sugars ubiquitous in plant seeds: sucrose and raffinose family oligosacharides (raffinose, stachyose and verbascose) that are formed by the α(1→6) polymerization of galactose units, added to the sucrose moiety (Adapted from Hopkins and Hüner, 2004a).

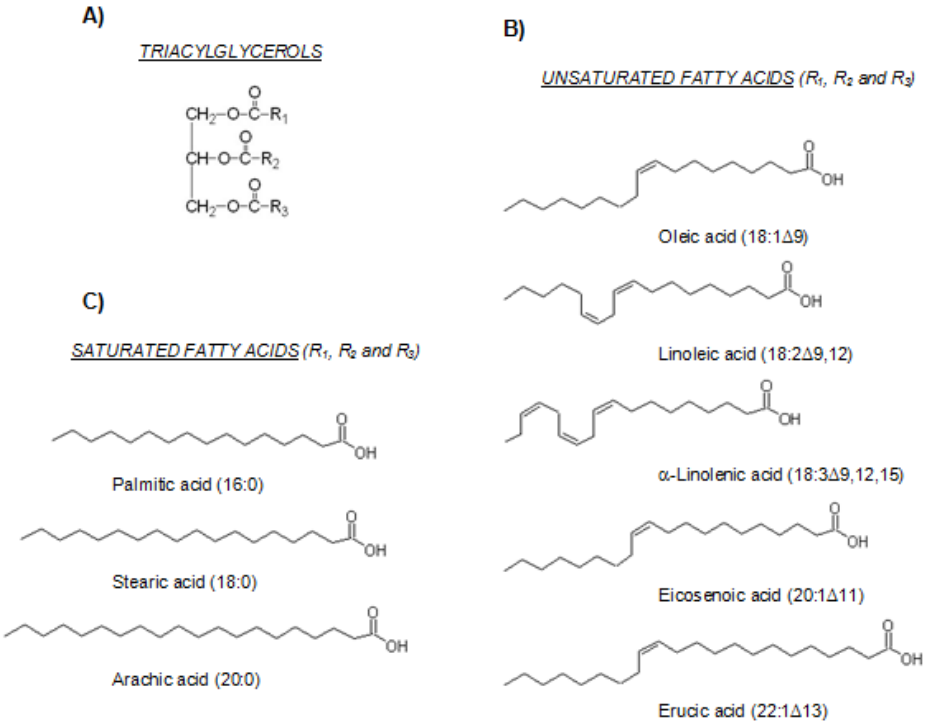

Fig. 31. Chemical structures of triacyglycerols and fatty acids that are commonly found in the storage material of plant seeds. A) Triacylglycerols are composed of glycerol with three attached fatty acids molecules (R_1, R_2 and R_3). Some examples of unsaturated (B) and saturated (C) fatty acids that are frequently found in seeds.

The characteristic of seed storage lipids is their high content of unsaturated and relatively low content of saturated fatty acids. The most common unsaturated fatty acids found in seeds are oleic (18:1Δ9) [3] and linoleic (18:2Δ9,12)[3] acids (**Fig. 31B**). Examples of less common unsaturated fatty acids in seeds are α-linolenic (18:3Δ9,12,15)[3] and erucic (22:1Δ13)[3] acids, as seen in. Among the saturated fatty acids, palmitic acid (16:0)[3] is frequently found in seed storage lipids (**Fig. 31C**) (Bewley and Black, 1994b; Copeland and McDonald, 2001d). In seeds, most of the lipids are stored in the endosperm and the cotyledons, within the small subcellular structures, called oil bodies, which vary in size from 0.2 to 6 μm (Bewley and Black, 1994b). The lipid storage material in many oilseed species is mobilized during the seed germination; the lipids are stepwise hydrolysed by the lipases, and a massive conversion of triacylglycerols to sugars leads to a significant decrease in lipid content and an increase in sucrose content (Copeland and McDonald, 2001d).

4.3.4. Proteins

Proteins comprise an important part of the seed mass, especially in leguminous species, in which they can reach more than 40% of dry seed weigh (Lambert and Yarwood, 1992; Shewry et al., 1995). They provide the embryo with carbon, nitrogen and sulfur resources for subsequent growth and development. The majority of seed proteins are metabolically inactive, serving as nutrient stores, necessary for seed germination and early seedling establishment (Copeland and McDonald, 2001d; Öpik and Rolfe, 2005). Some metabolically inactive proteins play a role in the structural architecture of the seeds. Only a small portion of the total protein content includes proteins that are metabolically active during the phases of seed development and germination. Among these are the enzymes that catalyze all metabolic process related to the respiration, growth and development of the embryo, as well as the storage of food reserves and their mobilization during germination (Copeland and McDonald, 2001d). Dry mature seeds also accumulate particular types of protective proteins, such as late embryogenesis abundant (LEA) proteins and heat shock proteins (HSPs), which are associated with desiccation-tolerance in orthodox seeds (Wehmeyer and Vierling, 2000; Buitink et al., 2002; Buitink and Leprince, 2004; Boudet et al., 2006; Buitink and Leprince, 2008). According to Osborne (1924), seed proteins can be classified on the basis of their solubility into following four groups: albumins (soluble in water), globulins (soluble in saline solutions, but not in water), glutelins (soluble in dilute acid or

[3] Fatty acids (X:YΔn,m,k, …) are identified according to the number of carbon atoms (X), as well as the number of double bonds (Y) and their positions in fatty acid chain (n,m,k,…). Unsaturated fatty acids contain one or more double bonds in their long aliphatic tail, while saturated fatty acids have all carbon-carbon single bonds in their aliphatic chain and therefore are labelled as X:0.

alkali solutions) and prolamins (soluble in aqueous alcohols) (Bewley and Black, 1994b; Shewry et al., 1995; Ogawa and Okita, 2000; Copeland and McDonald, 2001d). Prolamin-type proteins are found only in monocotyledonous seeds (e.g. cereals) (Shewry et al., 1995; Copeland and McDonald, 2001d). Most seed albumins are metabolically active proteins that posses enzymatic activity (Copeland and McDonald, 2001d). Nevertheless, some albumins act as storage proteins (e.g. napins found in *Brassicaceae* family). The globulins are the most widely distributed group of storage proteins in dicotyledonous as well as monocotyledonous seeds (Shewry et al., 1995). Two major classes of seed storage globulins can be identified according to their sedimentation coefficients: 7-8S (the vicilin group) and 11-14S (the legumin group) (Danielsson, 1956; Ogawa and Okita, 2000). Seed storage proteins accumulate primarily in the protein storage vacuoles (PSVs) within the cells of the embryo, as well as in the endosperm, but they can be also deposited within small subcellular structures (1-20 μm in diameter), called the protein bodies (PBs), which contain a mixture of different proteins (Shewry et al., 1995; Herman and Larkins, 1999; Copeland and McDonald, 2001d).

4.3.5. Other chemical substances found in seeds

In addition to structural and storage materials, a variety of other chemical compounds are present in seeds, but they occur in much smaller quantities. Some of these substances are involved in the regulation of embryo growth, germination and subsequent seedling development, while others are involved in seed interactions with the environment, notably in protection against different biotic and abiotic stresses. Many of these substances belong to the class of substance known as plant secondary metabolites, including alkaloids, glycosides, terpenoids and phenolic compounds (Hopkins and Hüner, 2004c). The latter group includes the flavonoids, cinnamic acid and its derivatives (*p*-coumaric, ferulic, caffeic and sinapic acid) (Dixon and Palva, 1995; Hopkins and Hüner, 2004c). Relatively large amount of phenolics, especially flavonoids, are found in plant seeds. Some flavonoids (e.g. condensed tannins) accumulate in large quantities in the seed coats. More information about the role of testa flavonoids in the regulation of seed dormancy and germination are provided in section **4.2.3.3**. Since flavonoids play an important role in seed protection against various biological and physical stresses, including UV radiation, their chemical structures, biosynthesis and physiological roles are discussed in detail elsewhere (see section **5.2**).

4.4. *Arabidopsis thaliana* seeds

4.4.1. Morphology and anatomy of Arabidopsis thaliana seeds

As in other *Brassicaceae*, the seeds of *Arabidopsis thaliana* are produced in fruits, known as siliques. Each silique contains two carpels and a central septum (replum) to which the seeds, arranged into two long rows, are attached by the funiculus that serves as a pipeline for the nutrients coming from the mother plant to developing embryo (Meinke, 1994). Since the life cycle of the *Arabidopsis* plant is relatively short, reproductive development from fertilization to the phase of seed desiccation, as shown in **Fig. 23**, is usually completed in two weeks when plants are grown under optimal conditions (23°C and 16/8-h (light/dark) photoperiod) (Meinke, 1994). The most remarkable feature of *Arabidopsis* seeds is their small size (**Fig. 32**); depending on the seed line, the size of mature dry seed ranges from 300-500 μm and they weight about 20-30 μg (Meinke, 1994; Al-Shehbaz and O'Kane, 2002). Mature wild type *Arabidopsis* seeds have a characteristic brown colour, which originates from flavonoids, particularly proanthocyanidins deposited in the seed coat (**Fig. 32A**). At the surface of mature seeds, some ovular parts can be still recognized: the micropyle region forms a small depression at one of the seed poles, while the hilum, visible as a small white point at the same pole, represents a scar where the funiculus was connected prior to seed detachment (**Fig. 32A** and **Fig. 32B**). Within the seeds, the mature embryo is made of about 15 000 to 20 000 cells that are organised into organs that define the principal pattern of the plant body. These organs, necessary for the subsequent development of young seedlings, are: the shoot apical meristem, the cotyledons, the hypocotyl, the radicle and the root meristem (Jürgens, 1994). In *Arabidopsis* seeds, the radicle tip is situated below the micropyle region (**Fig. 33D**), which facilitates the piercing of the seed coat at germination (Boesewinkel and Bouman, 1995). During early seed development, the establishment of three domains of the endosperm (the micropylar, the peripheral and the chalazal regions) occurs in *Arabidopsis* seeds (Ohto et al., 2007). However, most of the endosperm is absorbed by the growing *Arabidopsis* embryo, so that only little of this tissue remains in the mature seed (**Fig. 33A** and **Fig. 33C**). Therefore, at maturity, the curled embryo occupies most of the volume of the *Arabidopsis* seed (**Fig. 33D**). The embryo is surrounded by a thin hyaline layer and the single-cell layer, known as aleurone layer, which corresponds to reduced peripheral endosperm. The aleurone layer, is tightly associated with the protective seed coat that encapsulates the whole structure (Debeaujon et al., 2000; Debeaujon et al., 2007). In contrast to the seed coat, which contains dead cells, the cells in the aleurone layer remain physiologically active even in the stage of seed maturity (Debeaujon et al., 2000). The *Arabidopsis* seed coat develops from two ovular

integuments and the chalazal tissue (Debeaujon et al., 2007). As seen in **Fig. 33A**, **Fig. 33B** and **Fig. 33C**, the inner integument forms the tegmen that consists of three cell layers, of which the innermost one (ii1), called endothelium, contains the cells specialized in the synthesis of proanthocyanidins (condensed tannins) (Beeckman et al., 2000; Penfield et al., 2001; Debeaujon et al., 2007). These polymeric flavonoid compounds accumulate in the vacuoles of the endotelium cells as colourless compounds at an early stage of seed development (Debeaujon et al., 2007). Yet, during the desiccation stage, they become enzymaticaly oxidized by the polyphenoloxidases into brown pigments that confer the characteristic colour of the mature wild type *Arabidopsis* seeds (Pourcel et al., 2000; Pourcel et al., 2005). The outer integument develops into the two-layered testa (**Fig. 33A**, **Fig. 33B** and **Fig. 33C**). The subepidermal cell layer (outer integument, oi1) undergoes secondary thickening of the inner tangential cell wall and accumulates pale yellow flavonols, a class of flavonoid pigments (Beeckman et al., 2000; Pourcel et al., 2005). The epidermal cells in the outermost layer of the outer integument (oi2) differentiate into mucilage-containing cells, which secrete large quantities of mucilage, deposited in a ring between plasma membrane and primary cell wall. Consequently, the remaining cytoplasm of the epidermal cells is forced into a columnar shape, forming a central elevation called the columella, visible at the surface of *Arabidopsis* seeds (**Fig. 32B**). A thick secondary cell wall is also deposited external to the columella, reinforcing the testa epidermal cells (Beeckman et al., 2000; Western et al., 2000; Penfield et al., 2001; Ohto et al., 2007).

4.4.2. Physiology of Arabidopsis thaliana seeds

Arabidopsis thaliana seeds exhibit physiological non-deep dormancy, meaning that even if the embryos are released from surrounding structures (testa and endosperm tissues), intrinsic factors (e.g. plant hormones, for details see section **4.2.3.5**) keep them in a dormant state (Bentsink and Koornneef, 2008). However, seed dormancy in *Arabidopsis* can be overcome by the common germination promoting factors, including after-ripening (dry storage), moist chilling (stratification) and light (**Fig. 28**). Like in many other seeds, the germination of *Arabidopsis* seeds is under phytochrome mediated photocontrol (**Fig. 28**). Furthermore, applied chemicals, such as KNO_3, NO and treatment with exogenous gibberellins also have germination promoting effects (Derkx and Karssen, 1993a; Derkx and Karssen, 1993b; Bentsink and Koornneef, 2008). The requirement for these exogenous factors depends largely on the genotype. For instance, genetic variations related to the control of germination and dormancy are observed among different natural occurring *Arabidopsis* ecotypes, as well as mutants obtained in the laboratory (Bentsink and Koornneef, 2008).

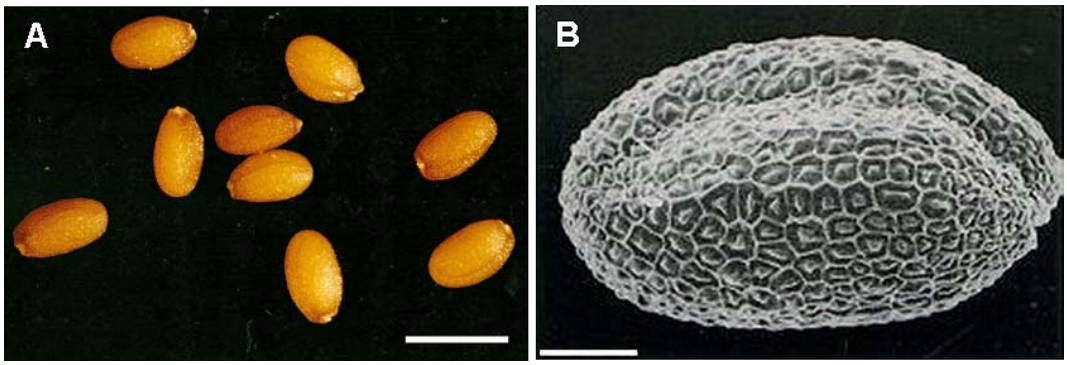

Fig. 32. *Arabidopsis thaliana* wild type seeds. A) Dry mature seeds were photographed at x32 magnification, using Wild Photomakroskp M400. Scale bar: 500 μm (Taken by Andreja Zalar). B) Scanning electron micrograph of a dry seed. Visible are hexagonal epidermal cells that have thickened radial cell walls and central elevations called the columellae. Scale bar: 100 μm (Taken from Western et al., 2000).

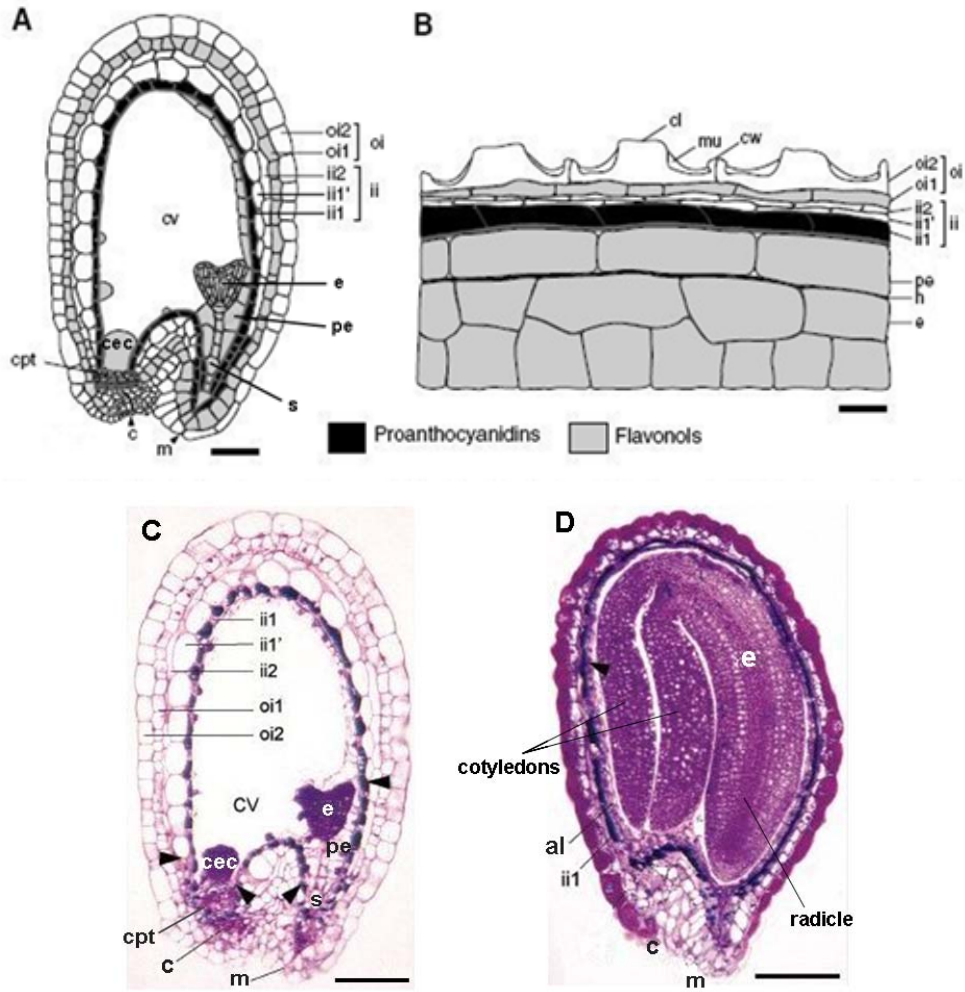

Fig. 33. Anatomy of the *Arabidopsis* seed (Adapted from Debeaujon et al., 2007; Debeaujon et al., 2003). A) Schematic representation of a developing seed at the heart stage embryo (longitudinal section). B) A detail of the mature seed coat (cross section). For A) and B) cells accumulating flavonoid compounds, either proanthocyanidins (condensed tannins) or flavonols are highlighted in black or grey, respectively. C) Micrograph of the longitudinal section of wild-type seed at the heart stage of embryo development (toluidine blue O staining). The innermost inner integument (ii1) (dark coloured), called the endothelium, contains proanthocyanidins. The arrowheads show the limits of the ii1' layer D) Micrograph of the longitudinal section of wild-type seed at the cotyledonary stage of embryo development (toluidine blue O staining). The arrowhead shows the endothelium layer (ii1).
Abbreviations: al - aleurone layer (corresponds to reduced peripheral endosperm); c - chalaza; cec - chalazal endosperm cyst; cl - columella; cpt - chalazal proliferating tissue (remnant of nucellus); cv - central vacuole; cw - cell wall; e - embryo; h - hyaline layer (remnant of central endosperm); ii - inner integument (tegmen); m - micropyle; mu - mucilage; oi = outer integument (testa); pe - peripheral endosperm; s - suspensor
Scale bars: 40 μm in A), 7 μm in B), 65 μm in C) and 80 μm in D).

4.4.3. Chemical composition of Arabidopsis thaliana seeds

The seeds of *Arabidopsis thaliana* are orthodox seeds that withstand a strong desiccation. Harvested, mature seeds have a very low water content, usually around 10% (fw). Yet, *Arabidopsis* seeds withstand drying down to 5-6% (fw) moisture content, which extends the seed longevity during long-term storage (Rivero-Lepinckas et al., 2006). Therefore, more than 90% of the seed mass is made of proteins, lipids and carbohydrates. Since mature dry *Arabidopsis* seeds contain a single-cell layer of vestigial endosperm, surrounded by the thin seed coat, the seed mass is the embryo,where compounds serve as storage materials or they are involved in the structure, development and metabolism of the embryo.

Proteins compose about 47% of the *Arabidopsis* seed mass (e.g. each seed contain about 8 μg of proteins, Focks and Benning, 1998). The bulk of the proteins in mature seeds is represented by different 12S and 2S storage proteins (Focks and Benning, 1998). The 12S α- and 12S β- subunits resemble those of cruciferin, a legumin-type storage globulin, which represent 50-55% of the total proteins in the mature seeds (Koornneef and Karssen, 1994; Gallardo et al., 2002). In contrast to many other seeds, *Arabidopsis* does not contain detectable 7-8S vicilin-type storage proteins in the mature seeds, although a vicilin-like gene is present in its genome (Fujiwara et al., 2002). Instead, the 2S proteins that resemble napin, an albumin-type protein, are the second most abundant group of storage proteins found in mature *Arabidopsis* seeds. The reserve storage proteins are deposited within the protein bodies, which are found both in the hypocotyl and the cotyledons of the mature embryo (Koornneef and Karssen, 1994).

As in most plants of the *Brassicaceae* family, *Arabidopsis* seeds contain large amounts of lipids. The lipid content may reach about 19% (fw) of the total seed weight (3.2 μg of lipids per seed) (Focks and Benning, 1998) . Storage lipids provide the major source of carbon for respiration and growth for developing young *Arabidopsis* seedlings (Eastmond et al., 2000). *Arabidopsis* oilseeds accumulate lipids as triacylglycerols, which represent the major carbon and energy reserves (Koornneef and Karssen, 1994; Focks and Benning, 1998). The triacylglycerols in *Arabidopsis* seeds are mainly constituted from unsaturated fatty acids, predominantly linoleic (18:2Δ9,12), oleic (18:1Δ9) and eicosenoic (20:1Δ11) acid (**Fig. 31B**), which together make about 70% of the total triacylglycerol content (Koornneef and Karssen, 1994; Focks and Benning, 1998). Lower concentrations of unsaturated linolenic (18:3Δ9,12,15) fatty acid and saturated palmitic fatty acids (16:0) are also present, while only small amounts of stearic (18:0), arachic (20:0), behenic (22:0) and erucic (22:1Δ13) acids can be detected in mature *Arabidopsis*

seeds, as seen in **Fig. 31B** and **Fig. 31C** (Focks and Benning, 1998). During development, *Arabidopsis* seeds accumulate lipid storage material in the endosperm, within the oil bodies. Since the endosperm is almost completely resorbed by the developed embryo, in mature seeds, the triacylglycerols are mostly found in the embryonic tissue, notably in the cotyledons, in which oil bodies can occupy about 60% of the cell volume (Patton and Meinke, 1990; Mansfield and Briarty, 1992; Koornneef and Karssen, 1994; Penfield et al., 2004). After germination, the cotyledons in epigeally[4] developed *Arabidopsis* seedlings are progressively transformed into photosynthetic organs (Eastmond et al., 2000).

Mature *Arabidopsis* seeds are relatively poor in storage carbohydrates. Soon after fertilization, developing seeds accumulate starch, but it degrades during the late stages of seed maturation (Caspar et al., 1991; Koornneef and Karssen, 1994). Therefore, mature dry seeds contain only about 1.5% (fw) of starch (0.25 μg per seed, Focks and Benning, 1998), which is stored in the starch grains of embryo cells, but can also be found in the cells of the seed coat (Beeckman et al., 2000). In developing oilseeds, such as *Arabidopsis*, photoassimilates are imported to the embryo in the form of carbohydrates, notably sucrose, but the majority of them are finally converted into the triacylglycerols (Focks and Benning, 1998). Therefore, soluble sugars, including sucrose, glucose and fructose, are present in mature seeds only in small amounts, making together about 3% (fw) of the total seed weight. Sucrose is the main soluble carbohydrate in mature seeds (~ 0.5 μg per seed, Focks and Benning, 1998). Sucrose concentration increases gradually over the course of seed development (Focks and Benning, 1998). In contrast, the concentrations of glucose and fructose are relatively high in the very early stage of seed development, but soon after, their amounts drop steeply to only about 0.06%, which is the final content determined for each monosaccharide in the mature seed (≤ 0.01 μg per seed, Focks and Benning, 1998). In addition to sucrose, as the first major soluble sugar, mature *Arabidopsis* seeds also accumulate the raffinose family oligosaccharides (ROFs), particularly stachyose, and to the lesser extent raffinose, which act as osmoprotectants during *Arabidopsis* seed desiccation (Taji et al., 2002). Interestingly, stachyose does not accumulate in the vegetative parts (e.g. leaves) of *Arabidopsis* plants grown under normal conditions; instead, stachyose is found accumulated only in seeds (Taji et al., 2002; Nishizawa-Yokoi et al., 2008).

[4] Epigeal germination (Gr. *epi* = upon + *gaia* = earth) refers to the emergence of cotyledons above the surface of the soil due to the rapid growth and elongation of the hypocotyl. When above ground, the cotyledons often become photosynthetic as the stored reserves are being depleted. Cotyledons finally dry up and fall off once the seedling becomes an independent plant (Black et al., 2006). (Opposite of hypogeal germination)

In addition to cellulose and lignin, which are the structural elements that reinforce the seed coat, the *Arabidopsis* seed contains considerable amounts of mucilage that is concentrated in the outermost layer of the seed coat (see section **4.4.1** on the Morphology and anatomy of *Arabidopsis thaliana* seeds). The most abundant monomer constituents of *Arabidopsis* seed mucilage are rhamnose and galacturonic acid, indicating that the principal mucilage polysaccharide is rhamnogalacturonan I (RG I) (Goto, 1985; Western et al., 2000). In mature seeds, mucilage is present in a dehydrated form within each epidermal cell. Upon imbibition, mucilage bursts out of the epidermal cells, forming a halo of pectin hydrogel around each seed (Western et al., 2000; Penfield et al., 2001; Ohto et al., 2007).

As in other plant seeds, a broad spectrum of secondary metabolites is also found in *Arabidopsis thaliana* seeds. Most of them have protective functions, but some of them also play important functions in the regulation of dormancy and germination. Among different secondary metabolites, flavonoids are accumulated in relatively large amounts in mature *Arabidopsis* seeds. Depending on *Arabidopsis* ecotype, the total flavonoid content in mature wild type seeds may range between 13 and 15 mg g^{-1} seeds (Lepiniec et al., 2006; Routaboul et al., 2006). Accordingly, flavonoids make about 1.3-1.5% of total weight of dry *Arabidopsis* seed (0.26-0.30 μg per seed, if the weight of one seed is taken as 20 μg). Another important group of secondary metabolites that is found in *Arabidopsis* seeds are the esters of phenolic acids, notably sinapic acid (sinapate esters). According to Ruegger and Chapple (2001), the total concentration of sinapate esters is estimated about 740 pmol mg^{-1} seeds (238 μg g^{-1} seeds). In addition, the glucosinolates, as the third class of important secondary metabolites, can also be found in *Arabidopsis* seeds. Glucosinolates accumulate primarily in the seeds of the *Brassicaceae* family, in which they play a prominent role in plant-herbivore and plant-pathogen interactions. More details about the chemistry and biosynthesis of flavonoids, sinapate esters and glucosinolates that occur in *Arabidopsis* seeds can be found in section **5**.

5. FLAVONOIDS AND OTHER SECONDARY METABOLOTES IN *Arabidopsis thaliana*

Plants are well known producers of a large array of low molecular weight compounds of which most are classified as secondary metabolites. In contrast to primary metabolites, secondary metabolites are compounds that are usually present in specialized cells, and which are not required for the basic functioning of cells, but are rather necessary for plant survival in the environment. The catalogue of known secondary metabolites in higher plants is huge, including at least several hundred thousand compounds. Their structural diversity is usually generated by differential modification of common backbone structures, which enables the production of derivatives with potentially different biological activities (Kliebenstein, 2004). In *Arabidopsis thaliana* plants, as many as 170 secondary metabolites have been identified so far and many more substances are likely to be added to this inventory in the near future (D'Auria and Gershenzon, 2005). *Arabidopsis* seeds contain large amounts of secondary metabolites, of which the great majority are flavonoids, derivatives of hydroxycinnamic acid, and the glucosinolates (**Table 4**).

Phenylpropanoids (including flavonoids and sinapate esters) are the major class of plant secondary metabolites. Due to their high absorption in the UV part of the spectrum, it is generally considered that one of their major roles is UV protection (Kliebenstein, 2004; D'Auria and Gershenzon, 2005). Some phenylpropanoids, such as lignin, are important structural elements of the secondary cell wall, providing mechanical support to land plants (Parr and Bolwell, 2000). Other phenylpropanoids act as pigments, signalling molecules, or protectants against different biotic and abiotic stresses (Weisshaar and Jenkins, 1998). The biosynthesis of phenylpropanoid compounds is activated in specific tissues and cell types, in response to environmental stress, such as UV radiation, wounding, pathogen attack etc. (Dixon and Palva, 1995). Phenylpropanoid synthesis is an ubiquitous pathway in terrestrial plants (Böttcher et al., 2008). All phenylpropanoids are derived from cinnamic acid that is formed from phenylalanine amino acid by the action of phenylalanine ammonia-lyase (PAL), a key enzyme that switches primary metabolism into secondary (phenylpropanoid) metabolism (Dixon and Palva, 1995; Weisshaar and Jenkins, 1998; Parr and Bolwell, 2000). The general phenylpropanoid pathway is schematically presented in **Fig. 34.** Phenylpropanoids are a chemically diverse family of compounds ranging from simple phenolic acids (e.g. *p*-coumaric, caffeic, ferulic and sinapic acids) to very large and complex polymers such as lignin, suberin and tannins (Koes et al., 1994; Parr and Bolwell, 2000). In *Arabidopsis* plants, the principal products of the phenylpropanoid

pathway are: flavonoids, lignin and derivatives of hydroxycinnamic acids, particularly sinapate esters. Structure, biosynthesis and function of flavonoids and sinapate esters will be discussed in detail in sections **5.2** and **5.3.1**, respectively.

Table 4. Major secondary metabolites found in *Arabidopsis thaliana* seeds. The substances were chemically characterized and identified by Böttcher et al., 2008[a] ; Routaboul et al., 2006[b]; Kliebenstein et al., 2001[c].

5.1.1.1.1.1. Metabolite	5.1.1.1.1.2. Compound
5.1.1.1.1.3. 5.1.1.1.1.4. FLAVONOIDS	5.1.1.1.1.5. Quercetin-deoxyhexose[a] (= *Quercetin-*
	5.1.1.1.1.6. Quercitin-rhamnoside dimer 1,2,3,4 [b]
	5.1.1.1.1.7. Quercetin-(deoxyhexose)$_2$ [a] (= *Quercetin-di-*
	5.1.1.1.1.8. Quercetin-deoxyhexose-hexose[a] (= *Quercetin-*
	5.1.1.1.1.9. Quercitin-hexoside-rhamnoside [b]
	5.1.1.1.1.10. Quercetin-hexose[a] (= *Quercetin--3-O-*
	5.1.1.1.1.11. 3'-*O*-methylquercetin-(deoxyhexose)$_2$[a]
	5.1.1.1.1.12. 3'-*O*-methylquercetin -deoxyhexose-
	5.1.1.1.1.13. Kaempferol [b]
	5.1.1.1.1.14. Kaempferol-deoxyhexose[a] (= *Kaempferol--*
	5.1.1.1.1.15. Kaempferol-(deoxyhexose)$_2$[a] (= *Kaempferol--*
	5.1.1.1.1.16. Kaempferol-deoxyhexose-hexose[a] (=
	5.1.1.1.1.17. Kaempferol-3-O-glucoside-7-O-
	5.1.1.1.1.18. Isoramnetin-rhamnoside [b]
	5.1.1.1.1.19. Isoramnetin-di-rhamnoside [b]
	5.1.1.1.1.20. Isoramnetin-hexoside-rhamnoside [b]
	5.1.1.1.1.21. Epicatechin-hexose[a]
	5.1.1.1.1.22. Epicatechin[a]
	5.1.1.1.1.23. Procyanidin oligomers *(n=2-7)* [b]
5.1.1.1.1.24. HYDROXYCINNAMIC ACID ESTERS[a]	*5.1.1.1.1.25. SINAPATE ESTERS* [a] 5.1.1.1.1.26. 1-*O*-Sinapoyl Glucose
	5.1.1.1.1.27. Sinapoyl Choline Isomer 1and 2
	5.1.1.1.1.28. Sinapoyl Choline dehydro dimer Isomer 1
	5.1.1.1.1.30. 4-Hexosyloxycinnamoyl Choline Isomer 1
	5.1.1.1.1.32. 4-Hydroxybenzoyl Choline
	5.1.1.1.1.34. 4-Hexosyloxybenzoyl Choline
	5.1.1.1.1.36. 3-(4-Hexosyloxyphenyl) propanoyl
	5.1.1.1.1.38. Feruloyl Choline
	5.1.1.1.1.40. Unknown Phenolic Choline Ester 1, 2, 3,
	5.1.1.1.1.42. Sinapoyl Choline (4-*O*-β) Guaiacyl
	5.1.1.1.1.44. Syringoyl Choline (4-*O*-β) Guaiacyl
	5.1.1.1.1.46. Feruloyl Choline (4-*O*-β) Guaiacyl
	5.1.1.1.1.48. Feruloyl Choline (5-β) Guaiacyl
5.1.1.1.1.49. **HYDROXYCINNAMIC ACID AMIDES**	5.1.1.1.1.50. Bis(sinapoyl) Spermidine
	5.1.1.1.1.51. Bis(sinapoyl) Spermidine-Hex
5.1.1.1.1.52. 5.1.1.1.1.53. GLUCOSINOLATES[c]	5.1.1.1.1.54. 2-propenyl glucosinolate (allyl)
	5.1.1.1.1.55. 3-butenyl glucosinolate
	5.1.1.1.1.56. 4-pentenyl glucosinolate
	5.1.1.1.1.57. 3-hydroxypropyl glucosinolate
	5.1.1.1.1.58. 3-hydroxybutyl glucosinolate
	5.1.1.1.1.59. 2(*S*)-hydroxy-3-butenyl glucosinolate
	5.1.1.1.1.60. 2(*R*)-hydroxy-3-butenyl glucosinolate
	5.1.1.1.1.61. 3-methylthiopropyl glucosinolate
	5.1.1.1.1.62. 4-methylthiobutyl glucosinolate
	5.1.1.1.1.63. 6-methylthiohexyl glucosinolate
	5.1.1.1.1.64. 7-methylthioheptyl glucosinolate
	5.1.1.1.1.65. 8-methylthiooctyl glucosinolate
	5.1.1.1.1.66. 3-methylsulfinylpropyl glucosinolate
	5.1.1.1.1.67. 4-methylsulfinylbutyl glucosinolate
	5.1.1.1.1.68. 7-methylsulfinylheptyl glucosinolate
	5.1.1.1.1.69. 8-methylsulfinyloctyl glucosinolate
	5.1.1.1.1.70. 3-benzoyloxypropyl glucosinolate
	5.1.1.1.1.71. 4-benzoyloxybutyl glucosinolate
	5.1.1.1.1.72. Indolyl-3-methyl glucosinolate

5.2. Flavonoids: Structure, biosynthesis and biological activity

5.2.1. Chemical structures of flavonoids

Flavonoids are the largest class of polyphenolic secondary metabolites, and they are widespread through the plant kingdom. To date, more than 6000 different flavonoids have been identified in plants, and the list is still growing (Schijlen et al., 2004; Lepiniec et al., 2006). However, they all share the same basic structure, the flavan skeleton (C6-C3-C6), composed of two aromatic rings (ring A and ring B) that are interconnected by a three-carbon bridge, which is cyclized with oxygen, giving rise to the ring C (**Fig. 35**) (Koes et al., 1994; Pourcel et al., 2000; Schijlen et al., 2004). Based on the degree of oxidation of the C ring, flavonoids can be divided into six major subclasses: (1) flavanones (e.g. naringerin), (2) flavonols (e.g. kaempferol, quercetin, myrcetin), (3) flavones, (4) isoflavonoids, (5) anthocyanins and (6) flavanols, which include both flavan-3-ols (e.g. catechin) and flavan-4-ols (precursors of phlobaphenes) (Schijlen et al., 2004; Saraf et al., 2007) (**Fig. 37**). The great diversity in flavonoid structures arises from various modifications of their aromatic cycles, including hydroxylation, methylation, acylation or glycosylation (Koes et al., 1994; Pourcel et al., 2000; Schijlen et al., 2004). In addition, the combination, degree of polymerization and linkages between the basic units allow for the multitude of these compounds characterized in plants (Lepiniec et al., 2006).

5.2.2. Biosynthesis of flavonoids

The first committed step in flavonoid biosynthesis is catalyzed by the enzyme chalcone synthase (CHS), which enables a stepwise condensation of three molecules of malonyl-CoA (derived from carbohydrate metabolism) with one molecule of *p*-coumaroyl-CoA (derived form the general phenylpropanoid pathway, see **Fig. 34**) to form naringenin chalcone (Koes et al., 1994; Parr and Bolwell, 2000; Schijlen et al., 2004). In the majority of plants, chalones are not the end-products, but they are rather converted into a naringenin flavanone by the enzyme chalcone flavanone isomerase (CHI). From these central intermediates, the pathway diverges into several side branches, each resulting in a different class of flavonoids (**Fig. 37**) (Koes et al., 1994).

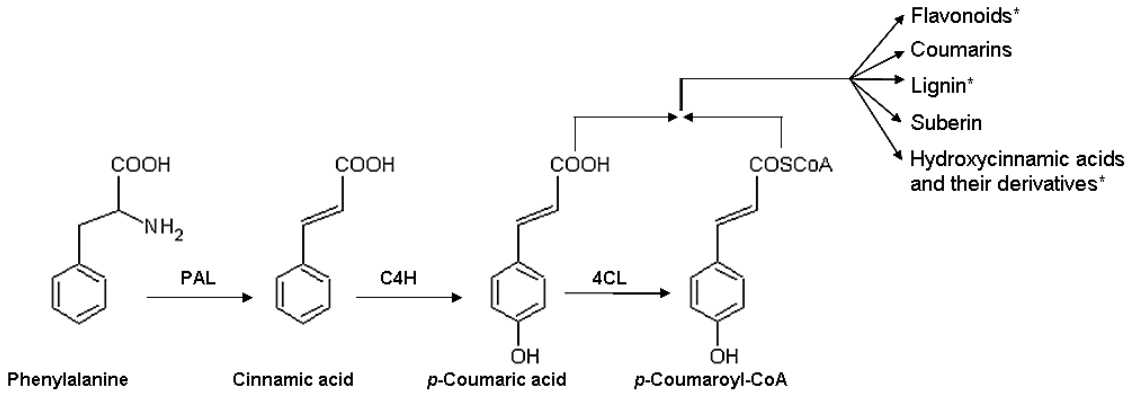

Fig. 34. General phenylpropanoid pathway. The principal phenylpropanoid products in *Arabidopsis* plants are labelled with asterisks. Enzymes involved in the synthesis of phenylpropanoid compounds: phenylalanine ammonia-lyase (PAL),cinnamate-4-hydroxylase (C4H), *p*-Coumaroyl:CoA ligase (4CL).

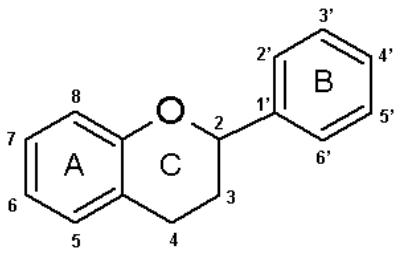

Fig. 35. Basic flavonoid structure (flavan skeleton) and numbering scheme for the flavonoids.

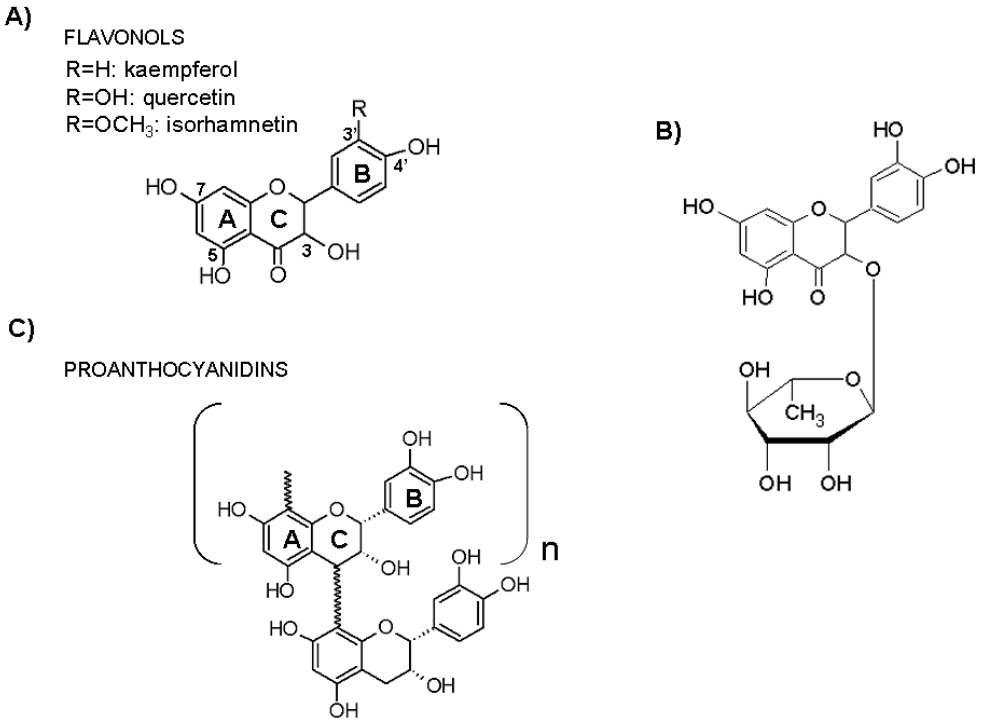

Fig. 36. Chemical structures of flavonoids encountered in *Arabidopsis thaliana* seeds. A) Three principal flavonol aglycones found in *Arabidopsis* seeds: kaempferol, quercetin and isorhamnetin. B) Dominant glycosilated flavonol in *Arabidopsis* seeds, quercetin-3-*O*-rhamnoside (quercitrin). C) Proanthocyanidins (PAs), also known as condensed tannins, which in *Arabidopsis* seeds are composed of polymerized units of epicatechin.

Within the cell, flavonoids usually accumulate in the vacuoles, but some are also found deposited in the cell wall (e.g. in seeds). The type, amount and localization of flavonoids vary according to plant species, developmental stage, as well as plant tissue, and can be modulated by environmental factors (Lepiniec et al., 2006). In plant seeds, large amounts of flavonoids are accumulated in seed coats (see section **4.4.2**). Some flavonoid compounds are ubiquitous, while others are restricted to specific families or species. For instance, aleurones are widespread, but not ubiquitous flavonoids. Some plant species also synthesize specialized forms of flavonoids, such as isoflavonoids, which are colourless compounds found in legumes and in a small number of nonlegume species (Winkel-Shirley, 2001). Phlobaphenes are red coloured flavonoid polymers of flavan-4-ols found in seeds of maize and other monocotyledons (Winkel-Shirley, 2001; Lepiniec et al., 2006). Proanthocyanidins (PAs), also known as condensed tannins, are colourless flavonoid polymers that result from the condensation of flavan-3-ol units (e.g. catechin). PAs specifically accumulate in plant seeds, where being oxidized by the enzymes polyphenol oxidases (PPO), they turn into coloured derivatives that confer a typical brown colour to the mature seeds (Pourcel et al., 2000; Lepiniec et al., 2006; Routaboul et al., 2006). During seed maturation PAs can interact with other phenolics, proteins or cell wall polysaccharides (Lepiniec et al., 2006; Routaboul et al., 2006). Anthocyanins are the major pigments in flowers and fruits, providing them blue, purple or red colouring. They can also contribute to pigmentation of some seeds, where they occurred mainly as copigments with flavonols (Holton and Cornish, 1995; Harborne and Williams, 2000; Winkel-Shirley, 2001; Lepiniec et al., 2006). Flavonols represent one of the most abundant and diverse group of flavonoids that occur abundantly in seeds, as well as in vegetative plant tissues. The most frequent flavonol forms are glycoside derivatives, containing one or more sugar moieties, usually glucose and rhamnose, attached to the positions C-3 and C-7 of the flavan skeleton (Kerhoas et al., 2006; Lepiniec et al., 2006).

Flavonoid biosynthesis in *Arabidopsis thaliana* plants is relatively simple compared with that in many other plants. *Arabidopsis* plants synthesize only three major classes of flavonoids, including flavonols, proanthocyanidins (condensed tannins) and anthocyanins (Owens et al., 2008). However, mature *Arabidopsis* seeds accumulate only two end-products of the flavonoid biosynthesis pathway, flavonols and proanthocyanidins. In *Arabidopsis* seeds, flavonols are present both in the seed coat and the embryo, where they occur in the form of glycoside derivatives of quercetin, kaempferol and isorhamnetin aglycones **(Fig. 36A**) (Kerhoas et al., 2006; Lepiniec et al., 2006; Routaboul et al., 2006). In the wild type, about 85% of the flavonol glycosides from seeds are derived from quercetin, whereas in leaves and flowers the majority of

flavonols are glycosides derivied from kaempferol. Quercetin-3-*O*-rhamnoside, also known as quercitrin is found to be a dominant flavonoid compound in *Arabidopsis* seeds (**Fig. 36B**) (Routaboul et al., 2006). PAs in *Arabidopsis* seeds accumulate exclusively in the seed coat, and unlike many other plants that use catechin, they are composed only of polymerised epicatechin units (**Fig. 36C**) (Lepiniec et al., 2006; Routaboul et al., 2006).

Plant mutants that affect flavonoid synthesis have been widely used to elucidate the flavonoid biosynthetic pathway. They have been isolated in different plant species (e.g. *Arabidopsis*, maize, *Antirhinum*, tobacco and *Petunia*), based on alternations in flower and seed pigmentation (Holton and Cornish, 1995; Winkel-Shirley, 2001; Schijlen et al., 2004). *Arabidopsis thaliana* is a particularly suited genetic model, since all but one enzyme (flavonol synthase, FLS) is encoded by single-copy genes (Winkel-Shirley, 2001; Owens et al., 2008). This lack of redundancy allowed *Arabidopsis* mutants to be identified on the basis of reduced pigmentation in the seed coat. A large collection of *Arabidopsis* mutants with yellow or pale-brown seed colour has been created, and today, it includes 24 members (*tt1-19*, *fls1*, *ban*, *ttg1*, *ttg2* and *aha10*), as seen in **Table 5** (Lepiniec et al., 2006). The mutated *transparent testa* (*tt*) loci were named by Maarten Koornneef (1990), who isolated many of the first mutants, which lack or have a reduced level of pigments in the seed coat (testa). The transparency of the testa reveals the underlying yellow colour of the cotyledons in the mature embryo. The search for new lines producing altered seed pigmentation is still ongoing (Lepiniec et al., 2006). Of special interest in the present study is *Arabidopsis* mutant line *tt4*, which lacks chalcone synthase (CHS) and is thus deficient in all flavonoids, including flavonols, proanthocyanidins (only in seeds) and anthocyanins (only in vegetative parts) (**Fig. 37** and **Table 5**).

Table 5. Loci involved in flavonoid biosynthesis in *Arabidopsis* seeds (adapted from Lepiniec et al., 2006).

Locus	Seed coat color[a]	Gene product	Branch[b]
Structural genes			
tt3	Yellow	Dihydroflavonol reductase (DFR)	P, A
tt4	Yellow	Chalcone synthase (CHS)	P, F, A
tt5	Yellow	Chalcone isomerase (CHI)	P, F, A
tt6	Pale brown spotted	Flavanone-3-hydroxylase (F3H)	P, F, A
tt7	Pale brown spotted	Flavanone-3′-hydroxylase (F3′H)	P, F, A
tt10	Dark yellow/brown C[c]	Polyphenol oxydase (PPO)	P, F
tt12	Pale brown	MATE secondary transporter	P
tt15	Pale brown/brown CM	Glycosyltransferase (GT)	P
tt18/ tds4/ tt11	Yellow	Leucocyanidin dioxygenase (LDOX)[d]	P, A
tt19/tt14	Dark yellow[3]	Glutathione S-transferase (GST)	P, A
ban	Pale gray/gray CM	Anthocyanidin reductase (ANR)	P
aha10	Pale brown	Autoinhibited H^+-ATPase isoform 10	P
Regulatory genes			
tt1	Yellow/brown CM	Transcription factor WIP-type Zn-Finger	P
tt2	Yellow	Transcription factor AtMYB123	P
tt8	Yellow	Transcription factor AtbHLH042	P, A
tt16 /abs	Yellow/brown CM	Transcription factor MADS AtAGL32	P
ttg1	Yellow	Regulatory protein ("WD40" or "WDR")	P, A
ttg2	Yellow	Transcription factor AtWRKY44	P
Other loci			
tt9	Pale gray/dark CM	Unknown	?
tt13	Pale brown	Unknown	?
tt17	Pale brown	Unknown	?
tds1,3, 5, 6	Pale brown	Unknown	P
tds2	Pale brown	Unknown	P, A

[a] Wild-type seed coat colour is brown.
[b] Affected metabolic branch: P, proanthocyanidins (only in seeds); F, flavonols; A, anthocyanins (only in vegetative parts).
[c] Seeds brownish with storage time.
[d] Also called anthocyanidin synthase (ANS).
Abbreviation: C = Chalaze; M= Micropyle.

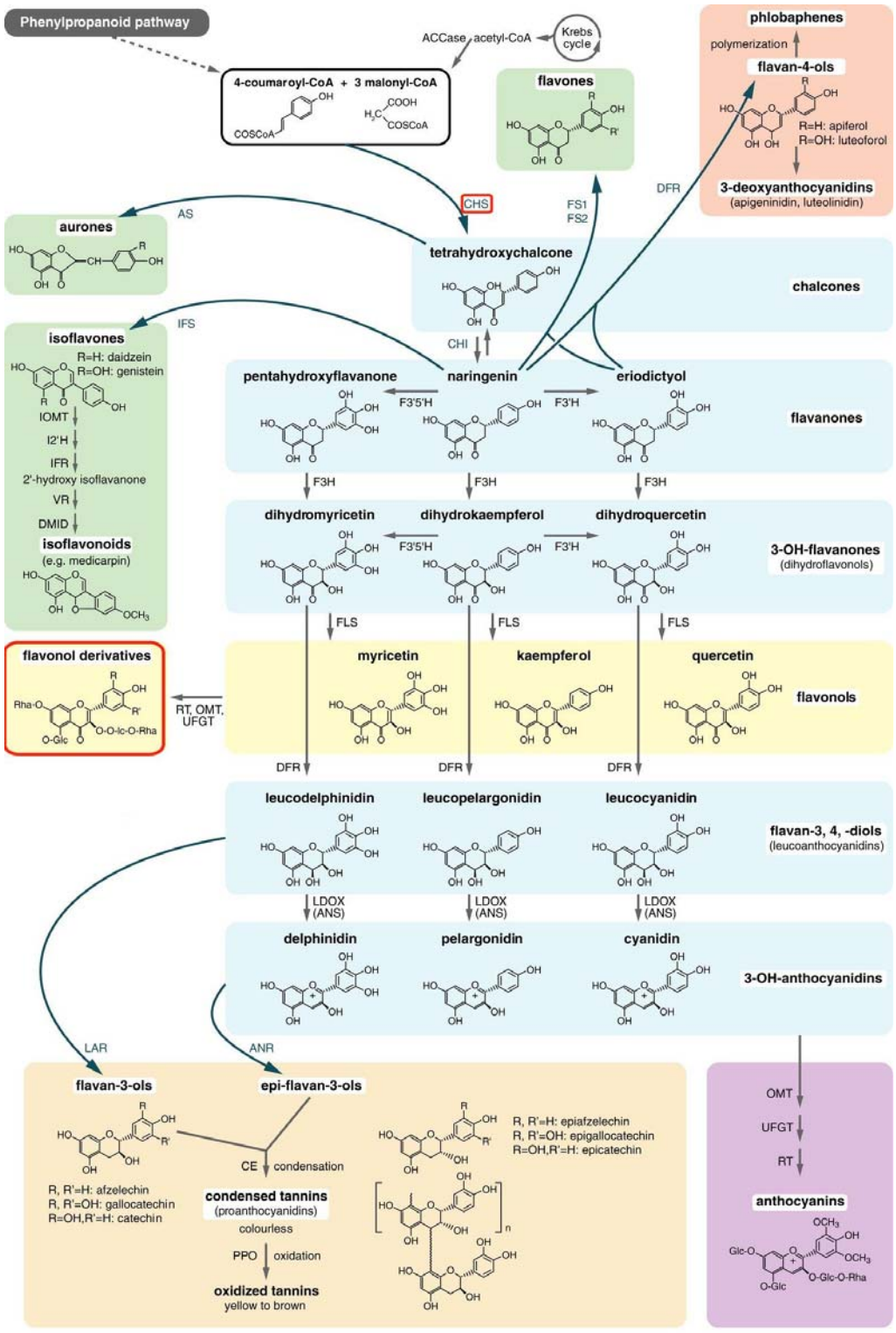

Fig. 37. Flavonoid biosynthetic pathway. The key enzyme, chalcone synthase (CHS), of the first committed step in flavonoid biosynthesis is labelled in red, as well as the glycosilated derivatives of flavonols, which represent the major group of flavonoids in plants. Proanthocyanidins (condensed tannins), together with glycosilated derivatives of flavonols (e.g. qercetin, kaempferol and isorhamnetin) are the only two groups of flavonoids found in *Arabidopsis thaliana* seeds (adapted from Lepiniec et al., 2006).
Enzyme names are abbreviated as follows: acetyl CoA carboxylase (ACCase), anthocyanidin reductase (ANR), anthocyanidin synthase (ANS), aureusidin synthase (AS), condensing enzyme (CE), chalcone synthase (CHS), dihydroflavonol 4-reductase (DFR), 7,2-dihydroxy, 4-methoxyisoflavanol dehydratase (DMID), flavanone 3-hydroxylase (F3H), flavonoid 3'-hydroxylase (F3'H), flavanoid 3'5' hydroxylase (F3'5'H), flavonol synthase (FLS), flavone synthase (FS1/ FS2), isoflavone 2'-hydroxylase (I2'H), isoflavone reductase (IFR), isoflavone synthase (IFS), isoflavone-*O*-methyltransferase (IOMT), leucoanthocyanidin reductase (LAR), leucoanthocyanidin dioxygenase (LDOX), *O*-methyl transferase (OMT), rhamnosyl transferase (RT), UDP flavonoid glucosyl transferase (UFGT), polyphenol oxidase (PPO), vestitone reductase (VR).

5.2.3. Biological activity of flavonoids

In most plant species, flavonoids are found in the leaves, stems, flowers, seeds, fruits and roots. Some flavonoids are found as constitutive compounds, but their synthesis can be induced by various biotic and abiotic stresses, such as UV radiation, a high level of visible light, pathogen attack, low temperature and a low concentration of some nutrients in the soil (Dixon and Palva, 1995). Flavonoids act as important stress protecting agents, feeding deterrents and attractants. To pollinating insects they are also involved in plant-microbe signalling processes, in plant sexual reproduction, as well as in various developmental and physiological functions, including seed physiology.

It is generally considered that photoprotection is a predominant role of flavonoids (Treutter, 2006). Plants expose themselves to sunlight in order to drive their photosynthesis, and since the plants are immobile, they employ some mechanisms that make them resistant to adverse environmental conditions, including UV radiation (Koes et al., 1994; Treutter, 2006). Flavonoids, and in particular the flavones and flavonols, are important UV screens, protecting plants from damage to DNA, proteins and lipids (membranes). This property of flavonoids is attributed to their particular chemical structure, resulting in high absorption of UV light (Parr and Bolwell, 2000). Besides their suitable absorption properties, flavones and flavonols tend to occur in highest levels in plant tissues exposed to strong light (Parr and Bolwell, 2000). Flavonoids accumulate primarily in the epidermal and hypodermal layers of leaves and stems (the most illuminated layers), indicating their function as a protective shield (Koes et al., 1994; Dixon and Palva, 1995). The importance of UV shielding to plant health has been demonstrated by several physiological and genetic studies (Li et al., 1993; Stapleton and Walbot, 1994; Rao et al., 1996; Ryan et al., 2001; Ryan et al., 2002).

Furthermore, the basic chemistry of flavonoids makes them good antioxidants. Catechin- and epicatechin-based flavonoids are particularly efficient antioxidants (Miller, 1996). The interaction of hydroxyl groups of flavonoids with the π-electrons in aromatic rings, gives the flavonoids special properties, notably the ability to generate free radicals where the radical is stabilized by electron delocalisation (Parr and Bolwell, 2000). Therefore, flavonoids may act as efficient scavengers of ROS, which can be produced as result of the indirect reactions of UV light, particularly UV-A wavelengths, with cell components (for details about indirect mechanisms of UV-induced DNA damage see section **3.3.3**).

In addition to their UV protective role, flavonoids have an important function in plant defence against pathogens, such as fungi, viruses, pathogenic bacteria, parasitic plants and insects. Flavonoids can inhibit the growth of pathogenic microbes and they can act as inhibitors of viral replication (Winkel-Shirley, 1998). Condensed tannins have a strong astringent taste and they can precipitate proteins. They accumulate in high concentration in plant seeds, and in leaves of some species, thus acting as efficient herbivore deterrents (Winkel-Shirley, 1998).

However, flavonoids do not act only as repellents. Most flower pigments are flavonoids belonging to the class of red to purple coloured anthocyanins or the yellow coloured aurones and chalcones. Besides, many plant species accumulate flavonols and flavanones in the petals. In most species, flower pigments act as a visual signal to attract pollinating animals (insects and birds) (Koes et al., 1994). Flavonoids are also important compounds in symbiotic plant-microbe interactions. In some leguminous plants, a specific set of different flavonoids is released from plant roots into the soil, which attracts symbiotic bacteria (rhizobia) and contributes in host plant-bacteria recognition (Koes et al., 1994; Treutter, 2006).

Flavonoids have an important function in plant sexual reproduction, since they play an essential role in pollen development and male fertility (Koes et al., 1994). It seems that they are also involved in controlling seed dormancy and germination. In flavonoid-deficient mutants, an increase in germination rate has been found related to a lack of downstream products of flavonoid metabolism (Winkel-Shirley, 1998; Debeaujon et al., 2000).

In man, flavonoids are thought to have health-promoting and disease-preventing properties (Luceri et al., 2008). There is growing evidence that the flavonoids present in some fruits and vegetables posses beneficial antioxidant, antibacterial, antiviral, anti-inflamatory, antiallergic, hepatoportective, antithrombotic and anticarcenogenic activities (Miller, 1996; Saraf et al., 2007`, and references therein)

5.3. Other secondary metabolites found in *Arabidopsis thaliana* plants

5.3.1. Sinapate esters as important derivatives of hydroxycinnamic acids

The second major class of soluble phenylpropanoid compounds found in *Arabidopsis* and other members of *Brassicaceae* are esterified derivatives of hydroxycinnamic acids (*p*-coumaric, caffeic, ferulic and sinapate acids), where sinapic acid represents the major phenolic acid (Kozlowska et al., 1983; Böttcher et al., 2008). The biosynthetic pathway for these monocyclic phenolic acid esters diverges from the general phenylpropanoid pathway prior to the committing step in flavonoid biosynthesis (**Fig. 38**) (Li et al., 1993). The major hydroxycinnamates in *Arabidopsis* plants are the esters of sinapic acid (sinapate esters), which together with flavonoids represent the most abundant secondary metabolites that have an important role in UV protection (Chapple et al., 1992; Landry et al., 1995; Sheahan, 1996). In the angiosperms, sinapic acid is an intermediate in the biosynthesis of so called syringyl lignin. *Arabidopsis* and other members of the *Brassicaceae* accumulate three major sinapate esters: sinapoylglucose, sinapoylmalate and sinapoylcholine. The relative abundance of each of these compounds is tissue-dependant and it varies through the plant developmental cycle. Leaves contain only sinapoylmalate, while seeds accumulate primarily sinapoylcholine (also called sinapine) and smaller amounts of sinapoylglucose, which serves as a common intermediate in the biosynthesis of both sinapoylmalate and sinapoylcholine (Ruegger et al., 1999). Within the cell, the vacuole has been found to be a place of the biosynthesis and deposition of hydroxycinnamic acids and their derivatives, including sinapate esters (Strack and Sharma, 1985). In leaves and seeds, sinapoylmalate and sinapoylcholine are synthesized *de novo* via the phenylpropanoid pathway, while in cotyledons of developing seedlings, sinapoylmalate is derived from seed reserves of sinapoylcholine (Ruegger and Chapple, 2001). Triggered by the imbibition of seeds, a series of interconversion reactions occurs during the germination process. During seed germination and subsequent seedling development, seed sinapoylcholine is first hydrolyzed to sinapic acid, which is than re-esterified by sinapic acid:UCPG sinapoyltransferase (SGT) to form sinapoylglucose. This product has high free energy of hydrolysis, providing the necessary energy for the subsequent transacylation step, in which sinapoylglucose is converted into sinapoylmalate by the enzyme sinapoylglucose:malate sinapoyltransferase (SMT) (Lorenzen et al., 1996; Ruegger et al., 1999) (**Fig. 38**). These interconversions are complete after about 6 days of seedling development, when de *novo synthesis* of sinapoylmalate recommences in developing leaves (Ruegger et al., 1999).

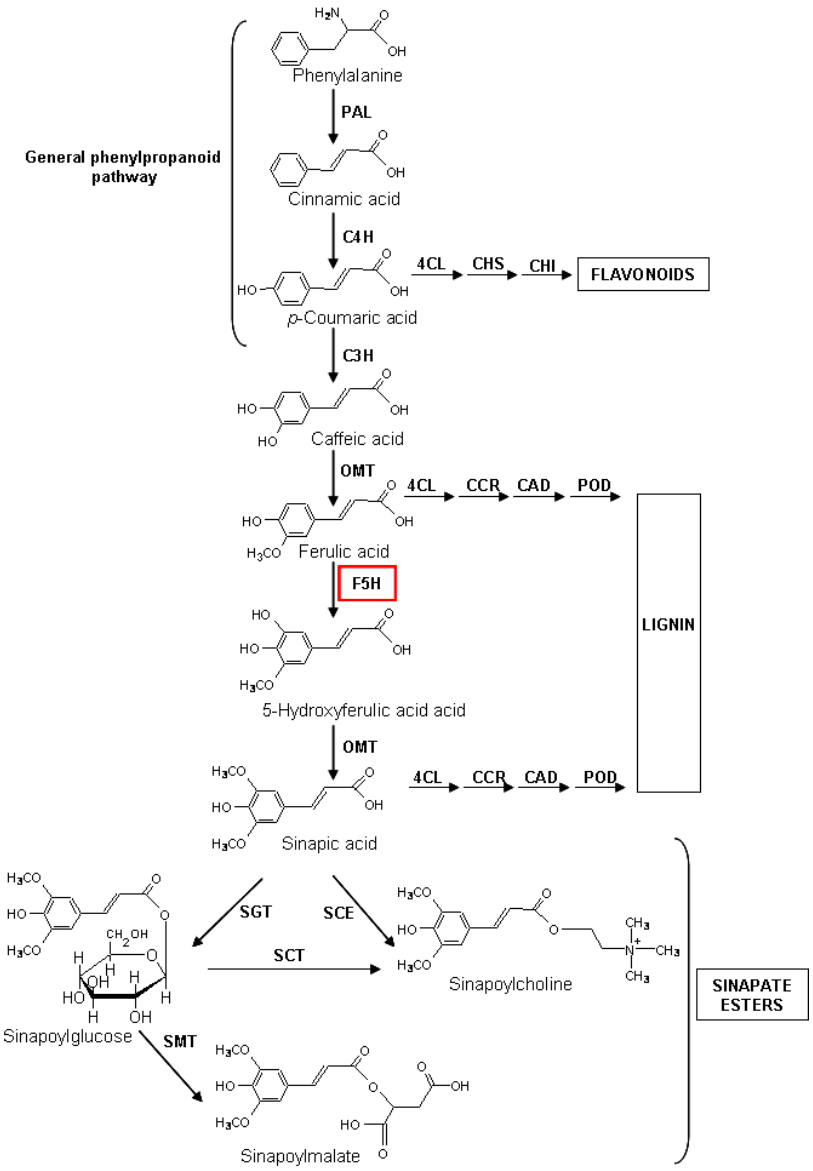

Fig. 38. Biosynthetic pathway of hydroxycinnamic acids and their derivatives in *Arabidopsis thalinana*. A key enzyme for synthesis of sinapate esters, ferulate-5-hydroxylase (F5H) is labelled in red. *Arabidopsis fah1* mutants are blocked in F5H enzyme, thus lack all sinapate esters.
Enzyme names are abbreviated as follows: hydroxycinnamyl alcohol dehydrogenase (CAD), hydroxycinnamyl coenzyme A reductase (CCR), *p*-coumarate-3-hydroxylase (C3H), cinnamate-4-hydroxylase (C4H), *p*-coumarate (hydroxycinnamate) coenzyme A ligase (4CL), chalcone-flavone isomerase (CHI), chalcone synthase (CHS), ferulate-5-hydroxylase (F5H), caffeate/5-hydroxyferulate *O*-methyltransferase (OMT) phenylalanine ammonia-lyase (PAL), peroxidase (POD), sinapoyl glucose:choline sinapoyltransferase (SCT), sinapate:UDP-glucose sinapoyltransferase (SGT), sinapoyl glucose:malate sinapoyltransferase (SMT).

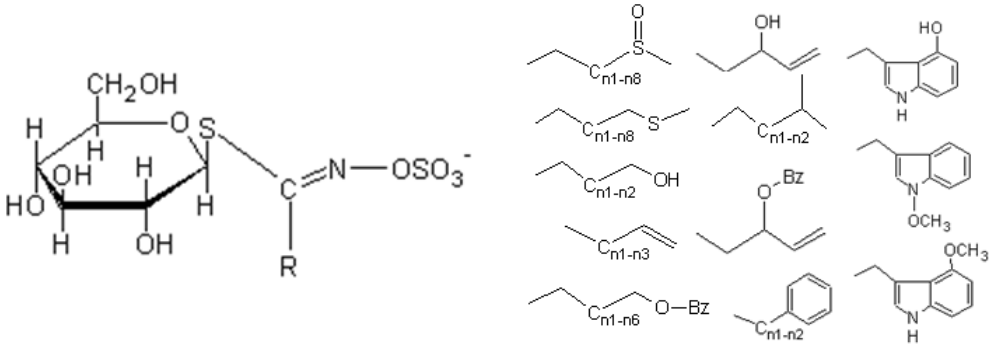

Fig. 39. General structure of glucosinolates and some typical side chains (R) occurring in *Brassicaceae* plants

Although *Arabidopsis* seeds are relatively rich in sinapate esters, the role of these compounds in plants is still unclear. Sinapoylcholine is the major derivative of phenolic acids in *Arabidopsis* seeds, as well as in some other *Brassicaceae* seeds, where it represents more than 80% of all choline esters (Kozlowska et al., 1983; Pokorny and Reblova, 1995; Böttcher et al., 2008). In mature seeds, sinapoylcholine probably serves as a choline reserve, which during germination is used in the biosynthesis of phospholipid membranes in developing seedlings. However, it is still not clear whether this reserve is essential. In addition, sinapate esters have been suggested to play an important role in UV light resistance of plants because they have high absorption in the biologically damaging UV-B part of the spectrum and they are primarily accumulated in the epidermis of plant organs (Chapple et al., 1992; Sheahan, 1996). Similarly to flavonoids, the concentrations of sinapate esters are found to increase in *Arabidopsis* plants as a response to exposure to UV-B light (Li et al., 1993). Mutants defective in sinapate ester synthesis have been also used to study this branch of the phenylpropanoid biosynthetic pathway. Few loci that affect sinapic acid ester biosynthesis have been identified in *Arabidopsis thaliana* (Chapple et al., 1992; Ruegger and Chapple, 2001). Among those, *FAH1* (formerly *SIN1*) locus has been found to encode ferulate-5-hydroxylase (F5H), the enzyme required for synthesis of sinapate esters and sinapic acid-derivied syringyl lignin. Plants homozygous for the *fah1* mutations are blocked at the biosynthetic step catalyzed by F5H, and therefore lack all sinapic acid esters (Chapple et al., 1992). Experiments with *fah1* mutants demonstrated that sinapoylmalate is an important UV-B screen in the vegetative parts of *Arabidopsis* plants (Landry et al., 1995; Sheahan, 1996).

Besides esterified derivatives of phenolic acids, plants contain also small amounts of hydroxycinnamic acid amides, in which phenolic acid is covalently linked to polyamines (e.g. spermine, spermidine and putrescine). Ubiquitous in nature, polyamines are believed to be important growth regulators in both eukaryotic and prokaryotic cells (Tabor and Tabor, 1984; Smith, 1985). Conjugated polyamines are widely distributed in the plant kingdom. The hydroxycinnamoyl substituents of polyamines can be coumaroyl, caffeoyl, feruloyl, hydroxyferuloyl, or sinapoyl acyl groups. Hydroxycinnamic acid amides are closely related to the flowering process and sexual organogenesis, as well as host-pathogen interactions. Conjugation of amines to hydroxycinnamic acids probably has a role in regulation of the level of free polyamines in tissue, which are biological active form of these metabolites (Martin-Tanguy, 1985; Martin-Tanguy`, 2001). In *Arabidopsis* seeds, two derivatives of sinapoyl spermidine have been identified (**Table 5**) (Böttcher et al., 2008; Luo et al., 2009).

5.3.2. Glucosinolates

Glucosinolates are amino acid-derived secondary metabolites that are found almost exclusively in plants of the order *Capparales*, including the family *Brassicaceae* (Chen and Halkier, 2000; Brown et al., 2003). In spite of their large diversity, glucosinolates share the same general structure, containing a thioglucose group linked to a side chain (R-group) through a sulfonated oxime group (**Fig. 39**). Over 100 different side chains, and thus glucosinolates, have been identified (Elfakir et al., 1994). These compounds are classified as aliphatic, aromatic and indole glucosinolates, depending on whether their side chain is derived from methionine, phenylalanine and tyrosine, or tryptophan, respectively (Halkier and Du, 1997). Glucosinolates are present in all parts of the plant, but their types and abundance vary in different tissues and different developmental stages, and are influenced by environmental factors (Chen and Halkier, 2000). Within the cells, glucosinolates are usually localized in vacuoles (Halkier and Du, 1997). *Arabidopsis thaliana*, as a member of *Brassicaceae* family, also possesses glucosinolates. In *Arabidopsis* seeds, 18-19 different glucosinolates have been isolated (**Table 5**) (Kliebenstein et al., 2001; Brown et al., 2003). Compared to the vegetative parts, the glucosinolates of *Arabidopsis* seeds are distinguished by their high concentration, unique aliphatic constituents and the low level of indole-containing compounds. The majority of glucosinolates in *Arabidopsis* seeds belong to the aliphatic class, where 4-methyltiobutyl glucosinolate (4MTB) is the predominant compound, representing about 41% of the total seed glucosinolate content. The aromatic glucosinolates make about 18% of the total seed glucosinolate content, while indolic glucosinolates occur only in a small amounts (~ 2%) in *Arabidopsis* seeds (Brown et al., 2003).

All plant species containing glucosinolates also contain a specific set of enzymes, thioglucosidases, also called myrosinases, which can hydrolyze glucosinolates (Brown et al., 2003). Glucosinolates and myrosinases are spatially separated within the plant, but they can be brought into contact by a tissue damage that yields a variety of toxic hydrolysis products, such as thiocyanates, isothiocyanates and nitriles, which are biologically active substances that act as deterrents to many pathogens and herbivores (Kliebenstein et al., 2001; Lambrix et al., 2001; Brown et al., 2003). Therefore, glucosinolates are believed to have important role in plant defence (Chen and Halkier, 2000; Brown et al., 2003).

Chapter 2

METHODS AND MATERIALS

6. BIOLOGICAL MATERIAL

6.1. Plant material

Arabidopsis thaliana seeds were used as an experimental model for testing resistance of plant seeds to UV light. Seven different genotypes were used in this study, including three wild ecotypes: Wassilevskija (Ws-2), Columbia (Col-0) and Landsberg erecta (Ler-0), as well as three mutant types of seeds: a mutant line dyx (*dyx*), *transparent testa* 4-8 *(tt4-8*), *transparent testa 4-1* (*tt4-1*) and ferulate-5-hydroxilase mutant (*fah1-2*). Wild type seeds Ws-2 and Col-0, together with transgenic mutants *tt4-8* (DFW34) and *dyx* (Bouchez et al., 1993), both prepared in Ws-2 background, were obtained from the Versailles *Arabidopsis thaliana* Resource Centre (INRA, Versailles, France). The Ler-0 wild type seeds (NASC: NW20), as well as nontransgenic mutant seeds *tt4-1* (NACS: N85) in Ler-0 background and *fah1-2* (NASC: N6172) in Col-0 background, were purchased from The Nottingham *Arabidopsis* Stock Centre (NASC, The University of Nottingham, UK).

A T-DNA[5] insertion mutant *tt4-8* is a flavonoid-lacking mutant, due to the absence of chalcone synthase (CHS), one of the key enzymes in the central pathway of flavonoid synthesis. The absence of flavonoids in seed coat results in yellow-coloured appearance of *tt4-8* seeds (**Fig. 40**). A transgenic *dyx* line carries a T-DNA inserted in it its genome, with no known alternations in flavonoid accumulation. The *dyx* seeds appear brown, like the seeds of wild type Ws-2 background (**Fig. 40**); they thus served as T-DNA insertion control for the *tt4-8* seeds. Moreover, a T-DNA of both *tt4-8* and *dyx* mutant, carries a bacterial kanamycin resistance gene (*nptII*) as a selectable marker. A nontransgenic *tt4-1* line was produced by chemical mutagenesis (ethylmethane sulfonate treatment), and it is a flavonoid-deficient mutant with altered flavonoid metabolism(Koornneef et al., 1982; Shirley et al., 1995). The seeds of the *tt4-1* mutant appear yellow, similarly to *tt4-8* seeds (**Fig. 40**). Another nontransgenic *fah1-2* line, previously named *sin1-2* (Chapple et al., 1992), is a sinapate ester-deficient mutant, with altered phenylpropanoid

[5] The T-DNA (transfer DNA) is about 20 kbp long DNA segment of the tumor-inducing (Ti) or root-inducing (Ri) plasmid, carried by the soil bacteria *Agrobacterium tumefaciens* and *Agrobacterium rhizogenes*, respectively (Chilton et al., 1982; Tepfer, 1983, , 1984, , 1995; Hansen and Chilton, 1999). It derives its name from the naturally occurring process, where the bacterium transfers the T- DNA fragment into the nuclear DNA of the host plant. Today, the *Agrobacterium*-mediated T-DNA transfer is widely used in laboratory to introduce a foreign gene of interest, usually together with a selectable marker gene (e.g. *nptII* gene), into the genome of the host organism. Hence this method is widely used as one of the most efficient biotechnological tools for the production of transgenic plants (Tepfer, 1995; Galun and Galun, 2001). The same principle of the T-DNA transfer can be used in so called T-DNA mutagenesis, where the gene of the interest in the host genome is disrupt by the insertion of the T-DNA fragment (Sessions, 2005).

metabolism, probably lacking the conversion of ferulate to 5-hydroxyferulate catalyzed by ferulate-5-hydroxylase (F5H).

Arabidopsis plants were cultivated during the spring and summer, under controlled greenhouse conditions. Three months after planting, the seeds were harvested from dry siliques of mature plants, air-dried at room temperature and stored at 4°C.

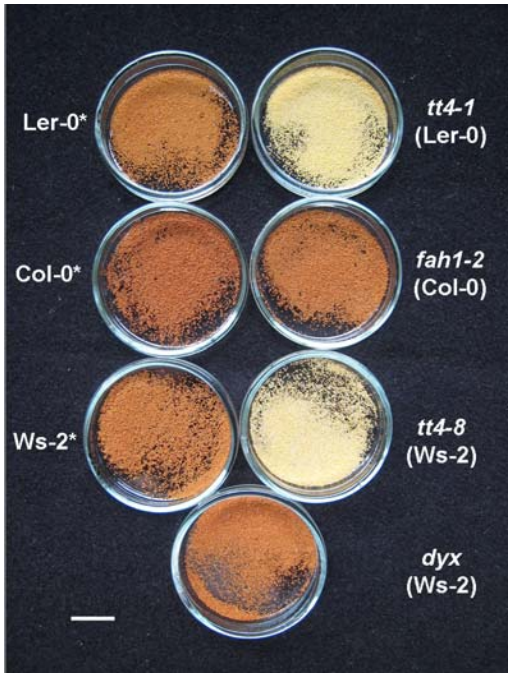

Fig. 40. Different genotypes of *Arabidopsis* seeds used in experiments to test resistance to UV light: Landsberg erecta (Ler-0) ecotype, flavonoid-deficient nontransgenic mutant *transparent testa 4-1* (*tt4-1*), Columbia (Col-0) ecotype, sinapate ester-deficient mutant that lacks ferulate-5-hydroxilase (*fah1-2*), Wassilevskija (Ws-2) ecotype, flavonoid-deficient T-DNA insertion mutant *transparent testa 4-8 (tt4-8*), T-DNA insertion mutant *dyx*. The wild type lines are shown on the left and marked with asterisks. Mutant lines are labelled on the right, and their background ecotypes are noted in parentheses. Scale bar: 1 cm.

6.2. *Bacillus subtilis* spore culture

Dry spores of *Bacillus subtilis* wild type strain WT 168 were kindly provided by the German Aerospace Center (DLR), Institute of Aerospace Medicine, Cologne, Germany. Vegetative *Bacillus* cells were first propagated in 5 ml of Luria-Bertani (LB) medium inoculated with a stock culture of dry *Bacillus* spores. The preculture was grown overnight at 37°C and aerated by shaking at 300 rpm. 3 ml of growing vegetative cells were further inoculated in 300 ml of sporulating medium, consisting of LB medium (tryptone 10g l^{-1}, yeast extract 5g l^{-1} and NaCl 10g l^{-1}), supplemented with salts from Schaeffer'Sporulation Medium (SSM), including KCl (1 g l^{-1}) and $MgSO_4$ x $7H_2O$ (0.25 g l^{-1}), as described in (Schaeffer et al., 1965). After adjusting the pH to 7.0 and autoclaving, filter sterilized solutions of the following SSM salts were added to the medium: $CaCl_2$ (5 x 10^{-4} M), $FeSO_4$ x $7H_2O$ (1 x 10^{-6} M) and $MnCl_2$ x $4H_2O$ (1 x 10^{-5} M). The spore culture was grown for 73 hours at 37°C, with shaking at 225 rpm, and sporulation was confirmed by microscopic examination as described below. Growth of the spore culture was monitored by measuring the optical density (OD) of the culture at 560 nm[6], reaching the stationary state (OD_{560} = 2.0), when spores were harvested (Horsburgh et al., 2001; Kreuzer-Martin et al., 2003; Duport et al., 2004). The spore culture was first incubated on ice and spores were collected by centrifuging at 8,000 rcf for 10 min at 10°C. The pellet was twice resuspended in 1/2 volume (150 ml) of sterile water, followed by centrifugation at 8,000 rcf for 10 min at 10°C. The spore culture was than resuspended in 1/4 volume (75 ml) of sterile water, recentrifuged, and finally resuspended in 1/5 volume (60 ml) of sterile water. The cell lysis step, where spore culture was heat-treated for 10 min at 80°C in the water bath, was performed in order to remove remaining vegetative cells and to facilitate release of endospores from the sporulating cells. Spores were purified by incubation at 37°C and shaking (250-300 rpm) in sterile water for at least one week, centrifuging each day for 20 min at 20,000 rcf and resuspending the resulting pellet (Nicholson and Setlow, 1990). Finally, the spore pellet was resuspended in 1 ml sterile water and stored at 4°C. The purity of the spore culture was determined by microscopic examination (described below), scoring 99.4% free spores, 0.6%

[6] Besides optical density (OD) determined at 600 nm, which is commonly used to measure the density of cells in suspension (turbidity), the OD at 560 nm is also proposed as a reference for measuring the turbidity of *Bacillus* spores in culture (Levinson and Hyatt, 1970; Horsburgh et al., 2001; Kreuzer-Martin et al., 2003; Duport et al., 2004). When light passes through bacterial culture, it will be scattered more or less by the cells depending on the cell density. Bacteria cells scatter the light in the visible wavelengths rather than absorbing it, explaining why bacteria cultures appear turbid. Light scattering of a particle is a function of its size, shape and concentration, as well as the wavelength of the incident light: the smaller wavelength, the more intense scattering and more sensitive the detection. It also depends on chemical composition and colour of the culture medium The short wavelengths above 400 nm are used to measure the turbidity of the cells suspended in buffer or saline (colourless solutions), while the wavelengths at 530-600 nm are preferable for broth cultures since these media contain the materials that absorbs strongly at short wavelengths (Carlberg, 2005).

sporulating cells and 0% vegetative cells. No spore aggregates were observed. The number of spores in prepared culture was determined by plating diluted spore suspensions on LB agar plates. After 12 hours of incubation at 37°C, *Bacillus* spores were quantified as colony forming units (CFU), reaching finally 3.1 x 10^8 spores/ml suspension.

6.2.1. Microscopy

The sporulation process of *Bacillus subtilis* in prepared liquid culture was followed by regularly microscopic inspection of *Bacillus subtilis* dry mounts stained by methylene blue and malachite green/safranin stains (Harisha, 2006). The purity of the spore culture was determined by microscopic examination of dry mounts stained by the Fulton & Schaeffer method (Schaeffer and Fulton, 1933).

6.2.1.1. Methylene blue staining

The heat-fixed smears from the *Bacillus subtilis* spore culture were flooded with 2.5% (w/v) solution of methylene blue (Sigma-Aldrich, France) for 1 min (Aneja, 2003; Harisha, 2006). After rinsing with distilled water, samples were examined using oil-immersion microscopy under bright field at x 2000 magnification. Growing vegetative cells were stained blue, while free spores and endospores found in sporulating cells remained unstained due to impermeable nature of the spore coat to methylene blue solution (Levinson and Sevag, 1953).

6.2.1.2. Schaeffer-Fulton staining

The samples of *Bacillus subtilis* spore culture were prepared as heat-fixed smears on microscopic slides. Small pieces of filter paper were placed above each smear and saturated with a 5% (w/v) solution of malachite green (Sigma-Aldrich, France). The smears were heat treated over a steam bath for 5 min. Stained smears were rinsed thoroughly with distilled water for at least 30 sec in order to decolorize the vegetative cells. The samples were counterstained for 1 min with safranin (ready Gram's safranin solution purchased from Fluka, France) (Harisha, 2006). The smears were rinsed briefly with distilled water, gently blotted dry and examined using oil-immersion microscopy under bright field at x 2000 magnification. Since endospores retained malachite green, they appeared green, and they could be easily differentiated from red/ pink coloured vegetative cells that were counterstained with safranin (Schaeffer and Fulton, 1933).

7. CHEMICAL AND SPECTROSCOPIC ANALYSES OF COMPOUNDS FROM *ARABIDOPSIS THALIANA* SEEDS, INCLUDING UV SCREENS

7.1. Determination of moisture content in *Arabidopsis thaliana* seeds

The seed moisture content is usually expressed as a percentage of the weight loss determined after seeds are dried in accordance with the prescribed rules. The seed moisture content is one of the important parameters, which influence the seed quality and longevity. Although dry seeds have drastically reduced metabolic activity, the ageing process is suspended in seeds with low moisture content (Harrington, 1972; Copeland and McDonald, 2001e; Buitink and Leprince, 2004). Low moisture content in anhydrobionts[7] is closely related to increased desiccation tolerance, as well as heat and freezing-stress resistance (Buitink et al., 2002; Wharton, 2002; Buitink and Leprince, 2004; Buitink and Leprince`, 2008). It may also play a role in seed resistance to UV light and ionizing radiation, since dry seeds are likely more resistant than hydrated seeds (Torres et al., 1991; Qin et al., 2007).

Seed moisture content was determined by the oven drying method prescribed by the International Seed Testing Association (ISTA, 1999). Moisture content is defined as the loss of weight when seeds are dried in accordance with the prescribed rules. It is expressed as a percentage of the fresh weight (fw) of the sample prior to drying. Small glass Petri dishes (∅ 4.5 cm, 1 cm high), fitted with covers, were used as drying containers. Petri dishes were first pre-dried in the oven for 30 min at 130°C and cooled afterwards in desiccators for 30 min. Empty pre-dried dishes were weighed and then filled with 100 mg (fw) of seeds. The total mass of each loaded dish was determined and each open dish with seeds was immediately placed in the oven, on top of its cover, and dried using a low constant temperature method, in which seeds were heat-treated for 18 hours at 103°C. After drying, Petri dishes with seed samples were immediately closed and placed in the desiccator on a top of thick metal plate.

[7] Anhydrobionts (anhydobiosis, from the Greek for "life without water") are the organisms with ability to reversibly lose almost all intracellular water. These organisms are capable to withstand extended periods of dehydration entering in metabolically quiescent state (Hochachka and Guppy, 1987; Crowe et al., 1992).

After cooling for 45 min, Petri dishes with dried seeds were rapidly weighed and seed moisture content was determined according to the following formula (ISTA, 1999):

$$M(\%) = \frac{(M2 - M3)}{(M2 - M1)} x100 \qquad (2)$$

where *M*(%) stands for determined moisture percentage (fw) in seeds, *M1* represents a weight (in grams) of empty container and its cover, *M2* is weight (in grams) of container, cover and its content before drying and *M3* represents the weight (in grams) of container, cover and its content after drying.

All experiments were performed in triplicate (n=3) and moisture content in seed samples was determined as a mean value. Variability around the mean was represented as ± standard deviation.

7.2. Preparation of crude extracts from *Arabidopsis thaliana* seeds

Crude extracts from *Arabidopsis* seeds were prepared from 100 mg (fw) of Ws-2 and *tt4-8* seeds that were frozen in liquid nitrogen and ground to a powder with mortar and pestle. Ground seeds were extracted with 600 µl of 75% (v/v) methanol and the resulting suspension was sonicated for 5 min (Transsonic TP690, Prolabo), followed by centrifugation at 14.1 rpm for 5 min (Eppendorf Mini Speed centrifuge). The supernatant was collected and stored at -20°C until analysis.

7.3. Flavonoid extraction

Flavonoids were isolated from 1.358 g (fw) of Ws-2 *Arabidopsis* seeds. Crude extracts were prepared in 8.148 µl of 75% (v/v) methanol following the procedure described above. After centrifugation, 7.2 ml of supernatant was diluted in 120 ml ultrapure water (Milli-Q® purified, Millipore) and defatted by three successive extractions with 120 ml cyclohexane. The aqueous phase was further purified by Solid-Phase Extraction (SPE) in order to remove coextracted non-flavonoid compounds. SPE was performed using a 200 mg C18 cartridge (Alltech, Templemars, France), which was conditioned by rinsing twice with 100% (v/v) methanol, followed by a washing step where the C18 matrix was rinsed twice with ultrapure water. A flavonoid- extract was than applied to the top of the C18 packing bed and pushed through the column at a flow rate of 1-5 ml min^{-1}. The SPE cartridge was than washed with ultrapure water and flavonoids were

eluted twice with 1 ml of 100% (v/v) methanol. Two flavonoid-containing elutes were pooled together and stored at -20°C until further analyses. Flavonoids were further purified by High Performance Liquid Chromatography (HPLC) as described below.

7.4. Glucosinolate extraction

A crude extract from Ws-2 *Arabidopsis* seeds was prepared in a 75% (v/v) aqueous solution of acetonitrile as described in Kerhoas et al., 2006. Further purification and extraction of glcosinolate compounds was performed by SPE using cation and anion exchange cartridges (see details below). The pH of the aqueous extract was first adjusted to 2.5 using 0.1 N HCl and purified on a strong cation exchanger, 400 mg-cartridge Chromafix® PS-H^+ (Macherey-Nagel, Hoerdt, France), in order to eliminate coextracted cationic compounds. The resulting acidic extract was than neutralized with 0.1 N NaOH and diluted to 500 ml with ultrapure water. The extract was applied to a 1g-cartridge SAX Bond Elut® (Varian, les Ulis, France), used as strong anion exchanger (Kerhoas et al., 2006). Since glucosinolates are negatively charged molecules in neutral medium, carrying a sulphonic acid group, they were retained by the SAX cartridge, while coextracted flavonoids and other neutral compounds were eluted from the anion exchanger. The packing bed of the SAX cartridge was then washed with ultrapure water. Glucosinolate elution was performed by through a stepwise increasing ionic strength gradient (from 0 to 0.5 M NaCl) and a stepwise decreasing pH gradient (0.1M Tris-HCl buffer from pH 8.0 to pH 7.4) in the eluent solution. Glucosinolates were further purified by HPLC as described below.

7.5. High-Performance Liquid Chromatography (HPLC)

7.5.1. Purification and separation of flavonoid-containing fractions

The flavonoids-containing extract, obtained from Ws-2 *Arabidopsis* seeds (see above), was further purified by semipreparative HPLC. Two millilitres of methanolic extract were dried under a stream of nitrogen and the residue was redissolved in a 10% (v/v) methanol solution. HPLC was performed with a Waters 600 multisolvent delivery system, using a reverse phase Kromasil C18 column (250 x 21.2 mm i.d., 10 μm particle size, Alltech, Templemars, France). The mobile phase consisted of acetonitrile and pure water at flow rate of 15 ml min^{-1}. HPLC solvents were filtered through 0.45 μm Millipore filters and degassed by flushing through with helium. The C18 column was first stabilized with 10% (v/v) acetonitrile (initial conditions),

followed by 20 min linear gradient of acetonitrile from 10% to 90% (v/v). The column was than washed with 90% (v/v) acetonitrile for 2 min and equilibrated for 16 min at 10% (v/v) acetonitrile. Data were acquired with a Waters 990 photodiode array detector set at 330 nm for chromatographic data and λ = 190-400 nm for spectroscopic data. The total volume of flavonoid-containing extract was divided in two aliquots that were purified by HPLC separately in two batches. Separated HPLC fractions were manually collected and matching fractions from two batches were pooled together. Eight fractions were evaporated until dryness and the resulting residues were weighed and redissolved in 1 ml of the following methanolic solutions. The residue of fraction F1 (2.33 mg) was dissolved in 33.3 % (v/v) methanol, while fractions F2 (1.6 mg), F3 (0.5 mg), F4 (≤ 0.17 mg) and F5a (1.5 mg) were dissolved in 100 % (v/v) methanol. Fraction F5b (0.25 mg) was redissolved in 50 % (v/v) methanol and fractions F6 (0.5 mg) and F7 (≤ 0.125 mg) were dissolved in 12.5% (v/v) methanol. All prepared fractions were stored at -20°C until further analysis.

7.5.2. Purification and separation of glucosinolate-containing fractions

The extract containg glucosinolates was purified by semipreparative HPLC, using the same instrumental system described above. The mobile phase consisted of a mixture of acetonitrile and pure water at flow rate of 15 ml min^{-1}. However, chromatographic conditions were different from those used for purification and isolation of flavonoids. After stabilization with 5% (v/v) acetonitrile, the C18 column (250 x 21.2 mm i.d., 10 μm particle size, Alltech, Templemars, France) was first eluted with 5% (v/v) acetonitrile for 20 min under isocratic conditions, followed by 30 min linear gradient of acetonitrile from 5 % to 50% (v/v). During the washing step, the column was rinsed with 50% (v/v) for 2 min and finally equilibrated to initial conditions with 5% (v/v) acetonitrile. The data were acquired with UV detector set at 230 nm for chromatographic data and λ = 190-400 nm for spectroscopic data. Seven separated HPLC fractions were collected manually and the dry residues of evaporated fractions were weighed and redissolved in 1 ml of pure water, pure methanol or methanolic solutions. The HPLC fractions G-F1 (83.3 mg), G-F2 (8 mg), G-F3 (10 mg) were redissolved in pure water and fractions G-F4 (6 mg), G-F5 (7.4 mg), G-F6 (5.7 mg) were redissolved in 50% (v/v) methanol, while fraction G-F7 (0.4 mg) was dissolved in 100% methanol. HPLC fractions were immediately stored at -20°C.

7.6. Sinapate ester detection

Sinapate esters display a bright blue fluorescence under long wave UV light (Lorenzen et al., 1996; Sheahan, 1996), allowing easy preliminary detection of these compounds directly in crude extracts of *Arabidopsis* seeds, as well as HPLC purified fractions. Crude extracts of Ws-2, Col-0 and *fah1-2* lines were prepared from 50 mg (fw) of seeds extracted in 75% methanol or 75% acetonitrile, according to the protocol described above. 10 µl of each sample was applied to chromatography paper (Whatman® Chromatography paper 3 MM, Maidstone, UK), used only as a support for the samples, and dried under a stream of cool air. Standard solutions of sinapic acid (0.6 mg/ml), quercitrin (3 mg/ml), kaempferol-3-*O*-rutinoside (2 mg/ml) and epicatechin (3 mg/ml) were prepared in 100% methanol and 10 µl of each standard was applied to chromatography paper, together with the seed extracts. Dried dots of samples were examined for blue fluorescence under UV-A light, using VL-4L lamp (Vilber Lourmat, Marne-la-Vallée, France) as a source of UV (λ = 365 nm) light. Sinapate esters were further detected and identified by mass spectrometry (LC-MS), as described below.

7.7. Liquid Chromatography - Mass Spectrometry (LC-MS)

Mass analysis was conducted on 5 µl aliquots of flavonoid-containing HPLC fractions, as well as glucosinolates-containing HPLC fractions. Each purified fraction of flavonoids was diluted in 250 µl of acetonitrile: water (80:20) solution, containing finally 50-100 µg of analyte. LC-MS was performed according the procedure described in (Routaboul et al., 2006), using an Alliance 2695 (Waters, Milford, USA) reverse phase separation module coupled to Quadro LC instrument (MicroMass Co, Manchester, UK) with an electrospray ionization (ESI) "Z-spray" interface. Data acquisition and analyses were performed by MassLynx software. Separation was carried out on a C18 Uptisphere column (150 x 2 mm i.d., 5µm particle size, Interchrom, Montluçon, France), connected to a Waters 2487 UV detector set at 290 nm for flavonoid detection or 229 nm for glucosinolate detection. The column was eluted at a flow rate of 0.15 ml/min, with a mobile phase comprised of a mixture of solvent A (acetonitrile : water, 95 : 5, v/v, acidified with 0.5% acetic acid) and solvent B (acetonitrile : water, 5 : 95, acidified with 0.5% acetic acid). The gradient profile comprised: initial conditions with 10 : 90, v/v (A : B) for 5 min, a linear gradient up to 70 : 30 v/v (A : B) over 35 min, a washing step 100 : 0, v/v (A : B) for 15 min, followed by the final equilibration of the column with 10 : 90, v/v (A : B) for 20 min. Nitrogen was used as nebulization (100 l/h) and desolvation gas (500 l/h) at 400°C. Argon was used as collision gas at 3.5 x 10^{-3} mbar. Formed ions were detected in positive and/ or negative

modes of operation. Chemical compounds were identified by analysis of data for molecular weight and retention times of formed ions. The data were compared with those of known compounds (standards) and previously reported data (Routaboul et al., 2006). When necessary, the mass fragmentation patterns were subsequently obtained by collision induced dissociation (CID) MS-MS experiments, where collision energy of 2.5 - 40 eV was employed to achieve the fragmentation of molecules.

7.8. Spectroscopy

The UV absorption properties of DNA and its components (mononucleotides and oligonucleotides), ubiquitous putative UV screening compounds (amino acids, proteins, polyamines) and substances associated with UV resistance in phylogenetically distinct groups of organisms (scytonemin, mycosporine-like amino acids, β-carotene, dipicolinic acid, melanin and flavonoids) were determined by two spectroscopic methods: conventional UV absorption spectroscopy in solution and VUV-UV absorption spectroscopy in dry films. Besides spectroscopic analysis of chemically pure standard samples, the UV absorption spectra were also measured in crude extracts from *Arabidopsis* seeds, and their flavonoid-containing, sinapate ester-containing and glucosinolate-containing fractions isolated and purified by HPLC. The VUV-UV spectra were also determined for derivatives of cinnamic acid, which are involved in the phenylpropanoid biosynthetic pathway, and could be considered as molecules that have a potential UV screening role in plants.

7.8.1. Conventional UV-VIS absorption spectroscopy in solution

Prior to the VUV-UV absorption spectroscopy, where samples were prepared in dry films, all samples were first analysed in solution by conventional UV absorption spectroscopy, using a Shimadzu Multipurpose Recording HPS-2000 spectrophotometer. About 5 - 20 μl of each sample were diluted in 1 ml of the appropriate solvent and UV absorption spectra were recorded in the range λ = 200 - 400 nm, using a 1 ml-quartz cuvette with a 1 cm path length.

A DNA sample was prepared by amplifying a 773 bp long sequence, carrying the greater part of kanamycin resistance gene (*nptII*), by Polymerase Chain Reaction (PCR). The *nptII* PCR product was synthesized using Hybaid thermal cycler (Thermo Fisher Scientific, US) according to the following amplification protocol: initial denaturation step at 95°C for 5 min, followed by

35 amplification cycles consisted of 1 min at 95°C (denaturation), 1 min at 55°C (annealing) and 2 min at 72°C (extension), with a final extension step at 72°C for 5 min.

The primers for the *nptII* sequence were 5'-GAACAAGATGGATTGCACGC-3' (forward) and 5'-AGAAGGCGATAGAAGGCGATGC-3' (reverse). The *nptII* PCR product was first analysed by agarose gel electrophoresis and obtained the 773 bp PCR product was purified using QIAquick PCR purification kit (Qiagen, France). The final concentration of DNA (10 ng μl^{-1}) was determined by measuring the OD at 260 nm. 10 µl of the DNA stock solution were diluted to 1 ml and the UV absorption spectrum was recorded using conventional UV absorption spectroscopy.

Two types of proteins, bovine serum albumin (BSA) and histones (unfractioned whole histones from calf thymus, type II-A), both purchased from Sigma-Aldrich, France, were prepared as standard stock solutions (10 mg ml^{-1} in pure water, pH 7.5). 5 µl of BSA and 20 µl of histones were diluted up to 1 ml prior the UV spectroscopic analysis.

Standard solutions of polyamines, spermine (Sigma-Aldrich, France), spermidine (Sigma-Aldrich, France) and putrescine (Fluka, France), were freshly prepared in pure water pH 7.5. 10 µl of a stock solution of spermine (30 mg ml^{-1}), spermidine (30 mg ml^{-1}) and putrescine (50 mg ml^{-1}) were analysed and their UV absorption spectra were recorded. An aromatic amine, tyramine (Sigma-Aldrich, France), was prepared in 100% (v/v) methanol as a stock solution (30 mg ml^{-1}) and 10 µl of a standard solution was analysed by conventional UV absorption spectroscopy.

The flavonoids analysed in this study were: quercitrin (Quercetin-3-*O*-rhamnoside), nicotiflorin (kaempferol-3-*O*-rutinoside), robinin (kaempferol-3-*O*-robinoside-7-*O*-rhamnoside), (+)-catechin (+ 3,3',4',5,7,-pentahydroxyflavan) and condensed tannins (oligomeric proantocyanidins extracted from apples). Standard stock solutions (3 mg ml^{-1}) of quercitrin (Sigma-Aldrich, France), nicotiflorin (Extrasynthese, Genay, France), (+)-catechin (Extrasynthese, Genay, France), condensed tannins (kindly provided by Dr Nour-Eddine Es-Safi) were prepared in 100% methanol (v/v), while a standard stock solution of robinin (2 mg ml^{-1}) was prepared in pure water. Prior the spectroscopic measurements, stock solutions of flavonoids were diluted to the concentration of 0.3 mg ml^{-1} and 10 µl of each diluted standard solution was analysed. Beside the UV absorption data measured in the range of 200 - 400 nm, absorption spectra of the flavonoids were also measured in visible (VIS) region from 400 - 800 nm.

A standard stock solution (1 mg ml^{-1}) of β-carotene (Extrasynthese, Genay, France) was prepared in 100% (v/v) ethylacetate and stored at - 20°C, protected from light. 25 µl of standard solution was diluted up to 100 µl in ethyl acetate and UV absorption was measured using a 100 µl-submicro cell cuvette. The absorption spectrum was recorded in the region 260 - 700 nm, avoiding the interference of ethyl acetate solvent, which had strong absorption in the UV region at 200 - 260 nm.

Melanin (Sigma-Aldrich, France) was purchased as a synthetic melanin, made by the oxidation of tyrosine with hydrogen peroxide. A standard stock solution (1 mg ml^{-1}) of melanin was prepared in 1 N NH_4OH and 10 µl of diluted (0.3 mg ml^{-1}) melanin solution was used for measuring UV absorption properties of melanin. The absorption spectrum was also measured in the 400 - 600 nm VIS region.

Dipicolinic acid (DPA) was purchased from Sigma-Aldrich, France. A standard solution (4 mg ml^{-1}) of DPA was prepared in 100% (v/v) methanol. The calcium chelate of DPA (Ca-DPA) was made by mixing (1:1) equimolar volumes of the DPA standard solution and aqueous solution of $CaCl_2$ ($2.4x10^{-2}$ M). 10 µl of prepared stock solution of Ca-DPA was used for measuring the UV absorption, as well as the absorption in the VIS part of the spectrum (400 - 800 nm).

Scytonemin was extracted from UV-A induced cells of the cyanobacterium *Chroococcidiopsis* (generously provided by Prof. Richard Castenholz), purified by HPLC and analyzed by LC-MS as described elsewhere (Zalar et al., 2007b). A standard solution (0.5 mg ml^{-1}) of scytonemin was prepared in 100% (v/v) ethyl acetate and 100 µl of two times diluted solution was analyzed using a 100 µl-submicro cell cuvette. UV/VIS absorption spectrum was measured in 260 - 700 nm region, avoiding the interference of ethyl acetate solvent, which had strong absorption in 200 - 260 nm UV region.

Two samples of mycosporine-like amino acids (MAA), generously provided by Prof. Donat-Peter Häder, were isolated from the marine red alga *Corallina officinalis*. The MAAs were identified by LC-MS and mass spectra showed that sample MAA-9 contained essentially porphyra-334, while MAA-6 sample contained palythine (Zalar et al., 2007b). MAA samples were prepared in 0.2% (v/v) acetic acid and 10 µl of MAA-9 and 20 µl of MAA-6 were analysed by conventional UV absorption spectroscopy. The absorption properties of MAA samples were also analysed in the VIS part of spectrum (400 - 800 nm).

Crude extracts from Ws-2 and *tt4-8 Arabidopsis* seeds were prepared as stock solutions in 75% (v/v) methanol and 20 µl of each crude extract was used for UV absorption spectroscopy analysis.

Flavonoid-containing HPLC fractions F1, F2, F3, F5a, F5b and F6 were diluted to a concentration of 0.125 mg ml^{-1}, where the F2, F3 and F5a fractions were prepared in 100% (v/v) methanol, while the F1, F5b and F6 fractions were prepared in 33.3% (v/v), 50% (v/v) and 12.5% (v/v) methanolic aqueous solutions, respectively. Fractions F4 (0.17 mg ml^{-1}) and F7 ($\leq$ 0.125 mg ml^{-1}) were used as undiluted solutions prepared in 100 % (v/v) and 12.5% (v/v) methanol, respectively. 10 µl of the F2, F3, F4, F5a, F5b and F7 fractions, as well as 20 µl of F1 and F7 fractions were used to measure UV absorption spectra by conventional UV spectroscopy in solution.

Glucosinolate-containing HPLC fractions G-F2 (8 mg ml^{-1} in water), G-F3 (10 mg ml^{-1} in water), G-F4 (6 mg ml^{-1} in 50% methanol), G-F5 (7.4 mg ml^{-1} in 50% methanol), G-F6 (5.7 mg ml^{-1} in 50% methanol) and G-F7 (0.4 mg ml^{-1} in 100% methanol) were analysed as undiluted stock solutions, while a stock solution of the G-F1 fraction (83.3 mg ml^{-1} in water),was diluted ten times prior the spectroscopic analysis. The UV absorption spectra were recorded using 10 µl of each glucosinolate-containing HPLC fraction.

7.8.2. VUV-UV absorption spectroscopy in dry films

7.8.2.1. Experimental setup and procedures

The VUV-UV absorption spectroscopy measurements were performed at the UV1 beamline at the synchrotron radiation source ASTRID (**Fig. 41**), at the Institute for Storage Ring Facilities (ISA), University of Aarhus, Denmark. Synchrotron radiation was the light source for measuring absorption spectra in the range from 125 nm to 340 nm. The VUV-UV absorption spectra were measured in a vacuum and samples were prepared as thin, solid films in order to avoid background absorption from organic solvents, which absorb strongly below 200 nm. Since all spectroscopic measurements were performed in a high vacuum, all samples were in a dehydrated state. Thin films of samples were prepared by drying substances onto MgF_2 windows. Four MgF_2 discs were than placed in a sample holder (**Fig. 42b**), which was inserted vertically in the vacuum chamber of the UV1 absorption spectroscopy installation (**Fig. 42a**).

In each experiment, one MgF_2 window was kept blank and used as a reference, while three MgF_2 windows carried dried samples. The samples were placed perpendicular the beam, one at a time. Monochromatized light from the beamline passed through the entrance LiF window into the vacuum chamber containing the samples. Transmitted light exited the sample chamber through the exit MgF_2 window and it was detected by a VUV-UV sensitive photomultiplier tube (shown in **Fig. 42a**). For wavelength scans below 200 nm, helium was flushed through the small gap between the photomultiplier tube and the exit window, in order to prevent any UV absorption by air, which could interfere with the VUV-UV spectra measurements.

The resulting spectra were based on transmission measurements and the absorption was calculated from:

$$A = \log\left(\frac{I_0}{I_t}\right) \qquad (3)$$

where A stands for the absorption of sample, I_0 represents the intensity of the light transmitted through the reference (blank window) and I_t is the intensity of the light transmitted through the sample.

Recorded spectra were the result of two phenomena, absorption and scattering, but for the sake of simplicity and due to the small contribution from scattering, all spectra were called absorption spectra. The scattering problems of dry films are discussed elsewhere (Zalar et al., 2007a).

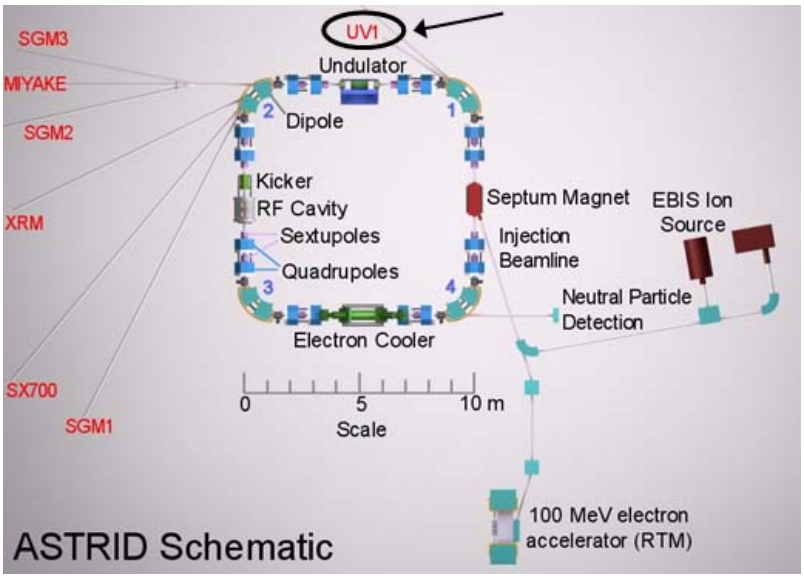

Fig. 41. Schematic representation of the ASTRID storage ring facility at the Institute for Storage Ring Facilities (ISA), University of Aarhus, Denmark. Arrow shows the position of the UV1 beamline. (Layout of ASTRID taken from http://www.isa.au.dk/facilities/astrid/astrid.html).

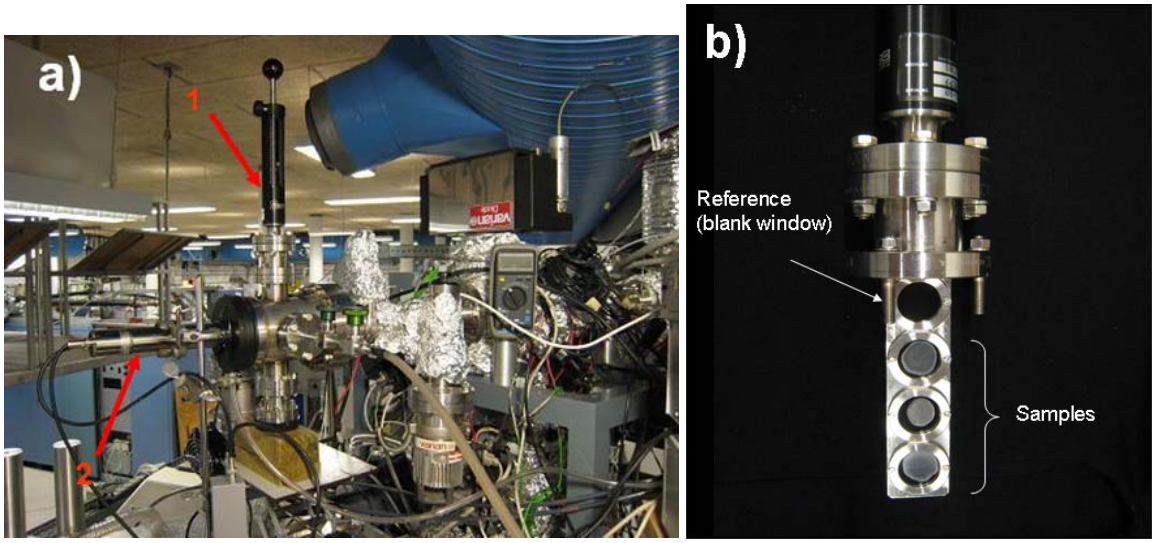

Fig. 42. a) The VUV-UV absorption spectroscopy installation at the UV1 beamline. (1) shows the sample holder, carrying the samples inserted vertically into the vacuum chamber. The UV beam passes horizontally through the sample, and transmitted light is detected by a VUV-UV sensitive photomultiplier tube (2). b) A detail of the sample holder, carrying three samples dried onto MgF_2 discs and one blank MgF_2 window that served as a reference for spectroscopy measurements.

7.8.2.2. Preparation of samples

All samples used in VUV-UV spectroscopy were prepared as thin, sold films, which were air dried onto MgF_2 windows (∅ 23 mm, thickness 1.5 mm). Samples of specialized UV screens and some putative UV screens were prepared from their stock solutions (see section **7.8.1**).

For the VUV-UV absorption spectroscopy, a sample of salmon sperm DNA (Sigma-Aldrich, France) was prepared and purified from proteins as previously described in (Zalar et al., 2007a). DNA was air-dried onto MgF_2 windows. Since VUV-UV absorption measurements were performed in high vacuum, DNA was considered to be in the dehydrated state.

Dry films of mononucleotides (dATP, dGTP, dTTP, dCTP, as well as ATP) and synthesized 20-mer homooligonucleotides (oligoA, oligoG, oligoT and oligoC) were prepared as described in Zalar et al. 2007a. The samples of complementary 20-mer homooligonucleotides (oligoA_{20} + oligoT_{20} and oligoG_{20} + oligoC_{20}) were obtained by mixing (1:1) equimolar volumes of oligoA_{20} with oligoT_{20} and oligoG_{20} with oligoC_{20}. All homooligonucleotides (Genosys-Sigma, France) were prepared as 100 μM solutions in pure water (pH 7.5). Synthetic 60-mer oligonucleotides **(Fig. 43**) with different G+C contents (30%, 50% and 63%), purchased from

Genosys-Sigma, France, were designed to encode the same protein, containing one of each of the 20 amino acids. In order to mimic the contribution of both DNA strands, equimolar (25 µM) mixtures of sense + antisense strands were prepared.

Fig. 43. Synthetic 60-mer oligonucleotides with different G+C content (30%, 50% and 63%), represented by the coding sense (+) strand and the complementary antisense (-) strand. These oligonucleotides have different nucleotide compositions and sequences, but they encode the same peptide, which contains one of each of 20 different amino acids. The amino acid sequence is presented under each oligonucleotide pair. (Zalar et al., 2007c).

Dry films of putative ubiquitous UV screens, such as proteins (histones from calf thymus and bovine serum albumin), amino acids (L-arginine, L-valine, L-aspartic acid and L-tryptophan), polyamines (spermine, spermidine and putrescine) and the aromatic amine, tyramine, were prepared as described in Zalar et al. 2007a.

Thin solid films of known specialized UV screens, including flavonoids (quercitrin, isoquercitrin, robinin and catechin), melanin, β-carotene, scytonemin and two samples of mycosporine-like amino acids (MAA-6 and MAA-9) were prepared as described elsewhere (Zalar et al., 2007b), as is the preparation of dry films of chlorophyll *a* and *b*, as well as Ca-DPA chelate.

Standard solutions, containing 0.5 mg ml^{-1} of t-cinnamic acid and its derivatives (p-coumaric acid, ferulic acid and caffeic acid) were prepared in 50% (v/v) methanol. Dry films were made with 9 x 500 µl of t-cinnamic acid, 4 x 500 µl of p-coumaric acid and 7 x 500 µl of ferulic acid, as well as caffeic acid standard solutions that were dried stepwise on MgF_2 windows. The final mass per MgF_2 window was 2.25 mg of t-cinnamic acid, 1 mg of p-coumaric acid, 1.75 mg of ferulic acid and 1.75 mg of caffeic acid.

Beside chemically pure substances (standards), dry films of seed extracts and their purified HPLC fractions were also prepared. Dry films of crude extracts from *Arabidopsis* seeds were produced by air-drying 500 µl of Ws-2 and *tt4-8* extracts (prepared in 75% (v/v) methanol) on the surface of a MgF_2 window.

Samples of flavonoid-containing HPLC fractions, F1 (2.33 mg ml^{-1}), F2 (1.6 mg ml^{-1}), F3 (0.5 mg ml^{-1}), F4 ($\leq$ 0.17 mg ml^{-1}), F5a (1.5 mg ml^{-1}), F5b (0.25 mg ml^{-1}), F6 (0.5 mg ml^{-1}) and F7 ($\leq$ 0.125 mg ml^{-1}), were prepared by air-drying 500 µl of each stock solution on a MgF_2 window.

Stock solutions of glucosinolate-containing HPLC fractions were diluted in pure water (fractions G-F1, G-F2 and G-F3), 50% (v/v) methanol (fractions G-F4, G-F5 and G-F6) or 100% (v/v) methanol (fraction G-F7) and 500 µl of each solution was air-dried on MgF_2 window. The solid films contained 3.36 mg of G-F1, 2 mg of G-F2, 0.45 mg of G-F3, 3.25 mg of G-F4, 1.85 mg of G-F5, 1.4 mg of G-F5 and 0.2 mg of G-F7 per MgF_2 window.

In order to exclude the background absorption by the remaining traces of solvents in the dry samples, 500 µl of the different solvents used in this study, including water (pH 7.5), 0.2 % (v/v) acetic acid, 1N NH_4OH, 100% (v/v) methanol, methanolic solutions of different concentrations, 100% (v/v) ethyl acetate and a solution of $CaCl_2$ (1.2×10^{-2} M) in 50% (v/v) methanol, were dried onto MgF_2 windows and the VUV-UV absorption was measured. No background absorption was detected for all tested solvents.

8. TESTING UV RESISTANCE OF *ARABIDOPSIS THALIANA* SEEDS AND *BACILLUS SUBTILIS* SPORES

8.1. UV irradiation of *Arabidopsis thaliana* seeds and *Bacillus subtilis* spores

The UV resistance of *Arabidopsis* seeds was tested in experiments that were divided in two parts, depending on the source of UV light: the UV-C exposure experiments, where a UV_{254} lamp was used as a source of quasi-monochromatic UV light, and simulated solar UV exposure experiments, where solar simulators SOL1000 and SOL2000 were used as sources of polychromatic UV light (λ = 200-400 nm). *Bacillus subtilis* spores, known to possess a high level of UV resistance (Horneck et al., 1994; Setlow, 1995; Slieman and Nicholson, 2001; Nicholson et al., 2002; Nicholson and Galeano, 2003), were exposed to UV-C light. These experiments served as a laboratory control for optimization of UV-C exposure conditions. In this work, *Bacillus subtilis* spores were not used in experiments with polychromatic simulated solar UV light, since they were the object of other studies in the context of joint Experiment Verification Tests (EVT). This is of direct interest for collaborators from the Institute of Aerospace medicine, DLR, Cologne, Germany.

8.1.1. Irradiation experiments with quasi-monochromatic UV-C_{254} light

The UV-C irradiation of *Arabidopsis* seeds and *Bacillus subtilis* spores was performed using quasi-monochromatic sources of UV_{254} light, with a sharp peak of emitted light at λ = 254 nm. Besides the predominant (about 90%) UV-C_{254} output, the lamp emitted a smaller portion of UV-B_{312} and UV-A_{365} light, together about 10% of the total UV light. The details about UV_{254} sources, as well as UV exposure conditions, are given here below.

Since the two terms “irradiance” and “fluence” are used throughout this work, and because the physical terms used to describe exposures and dosimetric concepts frequently vary throughout scientific literature, we reasoned first to define these two terms.

The term “irradiance” of UV light is defined here as the total UV radiant power from all upward directions incident upon a small element of flat surface containing the point under consideration divided by the area of the element (IUPAC, 1997; Braslavsky, 2007; Kowalski, 2009). In our experiments, the irradiance of UV light was measured in units of $mWcm^{-2}$.

The term "fluence" of UV light is here used in a sense of the UV dose, and it refers to the amount of UV radiant energy falling on a unit surface area summed over a given exposure time (McDonald, 2003). According to the recommendations of the International Union of Pure and Applied Chemistry (IUPAC, 1997) and the International Ultraviolet Association (IUVA, http://www.iuva.org), and for the reason that the term "dose" is usually used in other contexts to describe the absorbed energy, rather than the incident energy impinging upon an irradiated object, the "fluence" is here preferred as more appropriate term for the photobiological and photochemical context. The UV fluence (H, Jm^{-2}) was here calculated as the product of the UV irradiance (E, Wm^{-2}) and the exposure time (t, seconds) as follows (Linden, 2003):

$$H = E \times t \qquad (4)$$

Samples of *Arabidopsis* seeds and *Bacillus subtils* spores were prepared in monolayers, placed on the flat bottom of the round cavities (∅ 15 mm), in a glass plate, dimensions 11 x 56 cm (VWR International, France), which was used as a sample carrier in all UV-C exposure experiments (**Fig. 44**). The plate was supported on glass ridges that let air flow beneath, preventing the overheating of samples placed under the UV lamp. The samples were covered with three types of different UV cut-off filters: aluminium foil that cut off all emitted light (dark control), a glass filter that cut off UV-C light (samples exposed to UV-B + UV-A light) and a quartz filter that transmitted all the incident UV light (samples exposed to UV-C containing about 10% UV-B + UV-A). The 1 mm-thick glass filters (denoted *Glass*) were prepared by cutting a 2.5 x 2.0-cm piece of microscope slide, made of soda lime glass (Erie Scientific Co., USA). A dark control filter (denoted *Alu*) was made by sticking a thin aluminium foil onto a glass window. A 1 mm-thick quartz window (denoted *Quartz*), dimensions 1.9 x 1.9 cm, was used to transmit UV-C + (UV-B + UV-A) light. The transmittance (T%) of different UV cut-off filters was measured using a Shimadzu Multipurpose Recording HPS-2000 spectrophotometer and T% for UV-C_{254}, UV-B_{312} and UV-A_{365} was determined from obtained transmission spectra (**Fig. 45** and **Table 6**).

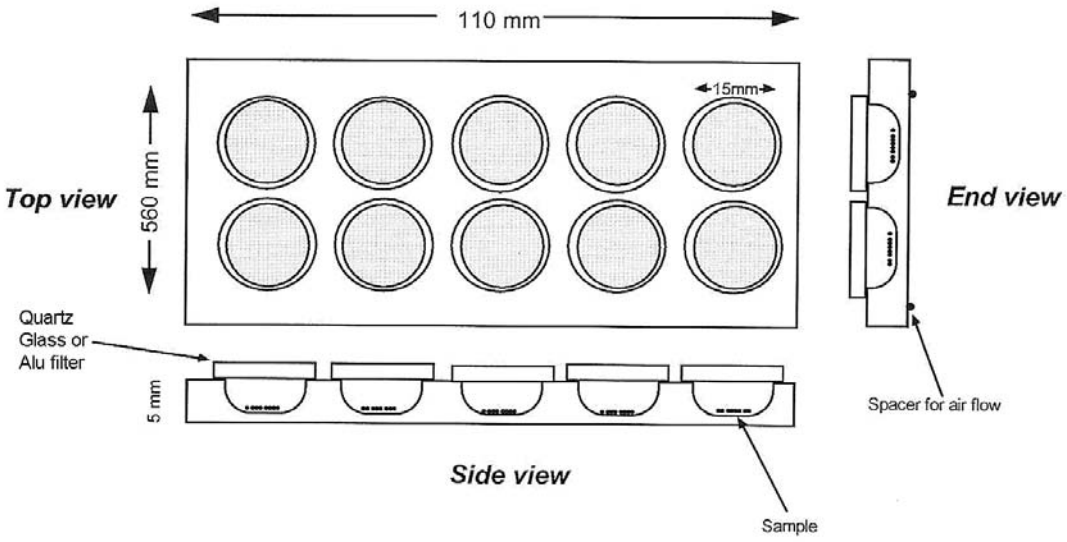

Fig. 44. Sample carrier for UV exposure experiments with *Bacillus subtilis* spores and *Arabidopsis* seeds. Samples were prepared as monolayers on the flat bottom of each cavity and covered with different UV cut-off filters: aluminium foil stuck onto a glass slide (Alu), a microscopy glass slide (Glass) and quartz window (Quartz). The thickness of each filter was about 1 mm, except for the aluminium foil.

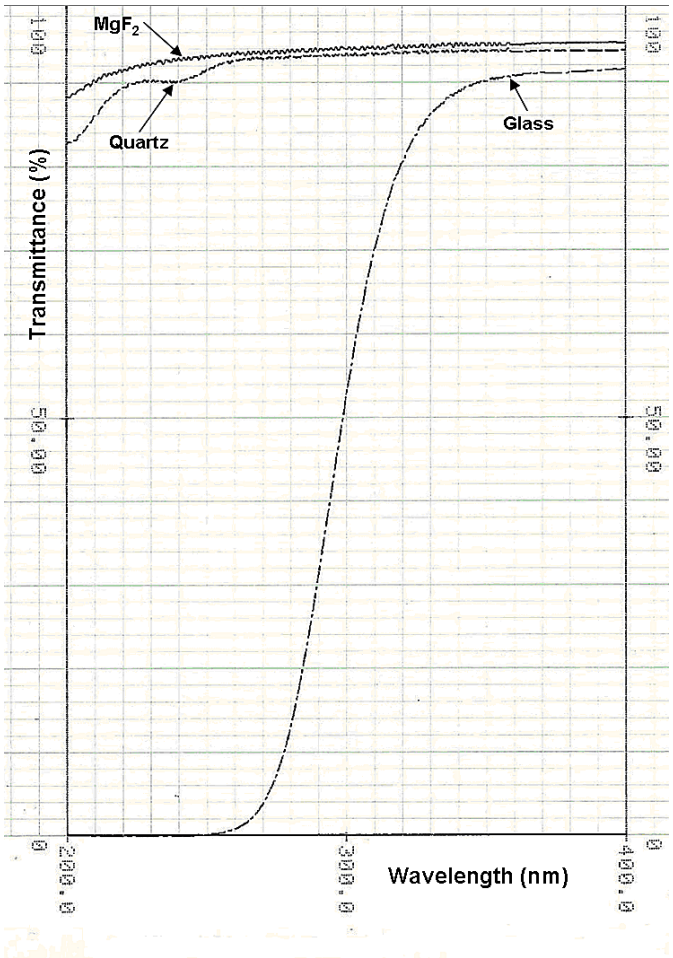

Fig. 45. Transmission spectra for three types of UV cut-off spectra: *Glass* - 1 mm-thick microscopy slide made of soda lime glass, *Quartz* - 1 mm-thick quartz filter, *MgF_2* - 1.5 mm-thick magnesium fluoride window.

Table 6. Transmittance (T%) of UV light at λ = 254 nm, 312 nm and 365 nm for four types of UV cut-off filters used in UV-C experiments: *Alu* - thin aluminium foil stuck onto a glass slide, *Glass* - 1-mm thick microscopy slide made of soda lime glass, *Quartz* - 1-mm thick quartz filter, MgF_2 - 1.5-mm thick magnesium fluoride window. T% values for Glass, Quartz and MgF_2 filters were determined from transmittance spectra (**Fig. 45**)

UV CUT-OFF FILTER	TRANSMITANCE (T%)		
	UV-C_{254}	**UV-B_{312}**	**UV-A_{365}**
Alu	0	0	0
Glass	0	73	91
Quartz	92	94	94
MgF_2	93	94	95

8.1.1.1. UV irradiation of Bacillus subtilis spores

Prior to determining the UV-C resistance of *Arabidopsis* seeds, dry *Bacillus subtilis* spores were exposed to UV_{254} light in order to optimize the conditions of UV exposure experiments and calibrate the UV_{254} lamp.

8.1.1.1.1. Sample preparation of *Bacillus subtilis* spores

For UV irradiation experiments, samples of *Bacillus subtilis* WT 168 spores were prepared as thin dry films. All experiments and procedures were carried out under sterile conditions, including the appropriate use of sterile instruments and tools. A stock suspension of *Bacillus subtilis* purified spores, prepared as described above, was diluted in sterile water to the concentration of 1.5 x 10^6 spores/ml suspension. The aliquots of 80 µl of aqueous spore suspension, containing 1.2 x 10^5 spores/aliquot, were dried onto the flat bottom of the round cavities, in a sterile glass plate that was used as a sample carrier in UV-C exposure experiments (**Fig. 44**). Thin films of *Bacillus* spores were dried overnight under a flow of sterile air at room temperature. The fraction of non-shadowed spores was calculated using the following equation:

$$f_{NS} = \frac{m \times e^{-m}}{1 - e^{-m}} \qquad (5)$$

where f_{NS} stands for the fraction of non-shadowed spores and m is the ratio of the area covered by spores ($\overline{S}$) to the total area of exposure (P) (Lindberg and Horneck, 1991). If the area covered by an individual spore is approximated as 1 μm^2 (Horneck et al., 2001), then we

calculated $\overline{S}$ = 1.2 x 10^5 μm^2 and P = 176.625 x 10^6 μm^2 for dry films prepared in 15 mm ∅ cavities. Using **equation 5**, we calculated f_{NS} = 99.9%, which indicated that almost all spores were non-shadowed by the other spores in prepared dry films. Thus the dry films of *Bacillus* spores were considered to be monolayers.

8.1.1.1.2. UV irradiation conditions

Dry monolayers of *Bacillus* spores were exposed to quasi-monochromatic UV-C emitted from a UV_{254} low-pressure mercury lamp with a sharp peak of emission at λ = 254 nm (VL-4C, Vilber Lourmat, France). The UV lamp was placed in a laminar flow hood, 14.65 cm above the surface of the samples. The energy output of the UV source was monitored by digital radiometers (VLX-254, VLX-312 and VLX-3W, Vilber Lourmat, France), equipped with sensors for 254 nm, 312 nm and 356 nm. The average UV irradiance was UV-C_{254} = 0.207 mWcm^{-2} (± 0.020), UV-B_{312} = 0.016 mWcm^{-2} (± 0.001) and UV-A_{365} = 0.0043 mWcm^{-2} (± 0.0006). The energy output of the UV_{254} source was thus composed of 91% UV-C_{254}, 7% of UV-B_{312} and 2% of UV-A_{365} light. The measurement of the temperature was performed during UV exposure experiments and the average value was 26°C (± 0.7). The area under the lamp exposed to UV was 10 x 5 cm. Each sample carrier with dry films of *Bacillus* spores was placed under the UV lamp, fitting exactly the exposure area. Since small variations in UV irradiance were measured over the UV exposed surface, the sample carrier was rotated at regular time periods in order to expose the samples to a relatively homogeneous fluence of UV light. Dry monolayers of *Bacillus* spores were covered with three types of UV cut-off filters: aluminium foil (*Alu*), glass filter (*Glass*) and quartz filter (*Quartz*). Samples of dry *Bacillus* spores were prepared in triplicate and irradiated with UV light from 16 sec to 300 sec. According to the duration of UV exposure and measured UV irradiance, fluences for UV-C_{254}, UV-B_{312} and UV-A_{365} were calculated using **equation 4** and corrected for the T% values for each UV cut-off filter. Corrected values of UV fluence represented the total amount of UV radiant energy that reached the samples placed under the quartz, glass and aluminium foil filters (**Table 7**).

Table 7. The UV irradiation conditions during UV-C exposure experiments with *Bacillus subtilis* spores. Fluences of UV light calculated according to the duration of UV exposure and measured irradiance of incident light emitted from the quasi-monochromatic UV_{254} source (No filter). The energy output of the UV_{254} source was composed of 91% UV-C_{254}, 7% of UV-B_{312} and 2% of UV-A_{365} light. Fluences of UV-C_{254}, UV-B_{312} and UV-A_{365} were corrected (CORR.) according to T% values (**Table 6**) for each cut-off filter: *Alu* - thin aluminium foil stuck onto glass slide, *Glass* - 1 mm thick microscopy slide made of soda lime glass, *Quartz* - 1 mm thick quartz window.

URATION (sec) OF UV EXPOSURE		FILTER	FLUENCE (Jm^{-2}) UV-C_{254}	UV-B_{312}	UV-A_{365}
16		No filter	34.880	2.560	0.767
	CORR.	*Quartz*	32.090	2.410	0.721
		Glass	0	1.870	0.698
		Alu	0	0	0
50		No filter	109.3	7.500	2.405
	CORR.	*Quartz*	100.6	7.050	2.261
		Glass	0	5.480	2.189
		Alu	0	0	0
100		No filter	197.5	15.700	4.345
	CORR.	*Quartz*	181.7	14.760	4.084
		Glass	0	11.460	3.954
		Alu	0	0	0
150		No filter	343.5	22.500	7.557
	CORR.	*Quartz*	316.0	21.150	7.104
		Glass	0	16.430	6.877
		Alu	0	0	0
300		No filter	571.5	45.000	12.573
	CORR.	*Quartz*	525.8	42.300	11.820
		Glass	0	32.850	11.441
		Alu	0	0	0

8.1.1.2. UV irradiation of Arabidopsis thaliana seeds

About 15 mg of dry *Arabidopsis* seeds were loaded in each round cavity of the glass plate that served as a sample carrier for the UV-C exposure experiments (**Fig. 44** and **Fig. 46A**). Seed samples were prepared in the form of monolayers on the flat bottom of the round cavities. The monolayers were inspected under a dissecting microscope and cleaned from impurities, such as the remains of plant parts, which could interfere by shadowing the incident UV light. The samples were prepared in triplicate and covered by one of three types of UV cut-off filters: aluminium foil (*Alu*), glass filter (*Glass*) and quartz filter (*Quartz*). The sample carriers were placed under a UV_{254} low-pressure mercury lamp (VL-100G, Vilber Lourmat, France) that was used as a source of quasi-monochromatic UV-C light. The UV exposure experiments were performed in a chemical fume hood that drew air across the sample and shielded the exterior with a glass sash (**Fig. 46B**). No UV-C_{254}, UV-B_{312} or UV-A_{365} radiation was detected outside

the protective glass sash. The distance between UV lamp and the surface of samples was 2.3 cm and the UV exposure area was 22 x 7 cm, accommodating two sample carriers at a time. The energy output of the UV_{254} lamp was monitored by digital radiometers (VLX-254, VLX-312 and VLX-3W, Vilber Lourmat, France), equipped with sensors for 254 nm, 312 nm and 356 nm. During the exposure experiments, the irradiance of emitted UV light was regularly measured at three positions on the exposure area (left side, middle and right side). At the end of the long-term UV exposure experiments, the average UV irradiance was calculated for the Ws-2 and *dyx* samples (UV-C_{254} = 12.46 mWcm^{-2} (± 0.57), UV-B_{312} = 1.128 mWcm^{-2} (± 0.113) and UV-A_{365} = 0.249 mWcm^{-2} (± 0.009)), as well as for the Col-0 and *fah1-2* samples (UV-C_{254} = 10.46 mWcm^{-2} (± 1.41), UV-B_{312} = 0.909 mWcm^{-2} (± 0.100) and UV-A_{365} = 0.217 mWcm^{-2} (± 0.016)). In the short-term UV exposure experiments with *tt4-8* seeds, the calculated average UV irradiance was UV-C_{254} = 14.77 mWcm^{-2} (± 1.97), UV-B_{312} = 1.336 mWcm^{-2} (± 0.184) and UV-A_{365} = 0.297 mWcm^{-2} (± 0.040). The measurements of UV irradiance, both in the long term and the short term exposure experiments indicated that the emitted light from the UV_{254} source consisted predominantly of UV-C_{254} light (90%) and a small portion of UV-B_{312} (8%) and UV-A_{365} (2%) light. Since small variations in UV irradiance were measured over the UV exposed surface, sample carriers were regularly rotated and their positions were frequently exchanged in order to obtain relatively homogeneous fluence of incident UV light.

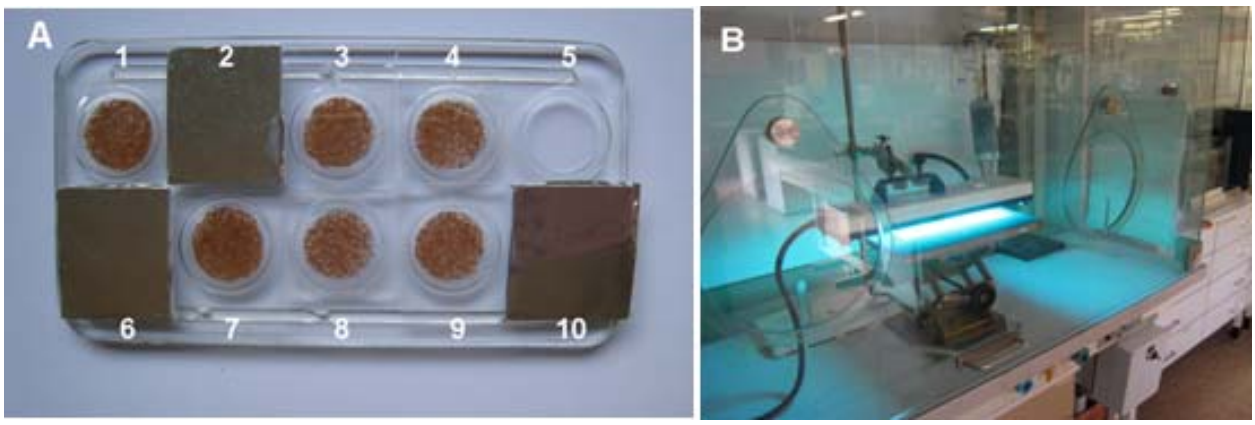

Fig. 46. An experimental setup for UV-C irradiation of *Arabidopsis* seeds.
A) Sample carrier for UV-C experiments, loaded with dry *Arabidopsis* seeds that formed monolayers. Samples were covered with three different types of UV cut-off filters: *Alu*-aluminium foil filter (sample positions N^{o} 2, 6 and 10), *Glass* filter (sample positions N^{o} 3, 7 and 9) and *Quartz* filter (sample positions N^{o} 1, 4 and 8). A sample position N^{o} 5 is shown unloaded.
B) The UV-C exposure setup showing a low-pressure mercury lamp (VL-100G, Vilber Lourmat, France) as a source of quasi-monochromatic UV_{254} light, which was placed above two UV exposure carriers loaded with seed samples.

The temperature and irradiance of UV light were regularly measured during UV exposure experiments. An average temperature of 28°C (±1.1) was measured during long term UV-C exposure experiments with Ws-2 and *dyx* samples, while 24.4°C (±2.1) in the experiments with Col-0 and *fah1-2* seeds. The average temperature under the UV lamp reached 26.3°C (±2.4) in short-term experiments with *tt4-1* seeds. Long-term UV-C exposure experiments were performed in a way that Ws-2 and *dyx* seeds were irradiated with UV for 30 and 60 days, while Col-0 and *fah1-2* seeds were exposed to UV for 40 and 60 days (**Table 8**). Flavonoid-lacking mutant seeds (*tt4-8)* were exposed to UV for shorter time periods, ranging from 0.5 hours to 139 hours (**Table 9**). According to the duration of UV exposure and measured UV irradiance, UV-C_{254}, UV-B_{312} and UV-A_{365} fluences were calculated (**equation 4**), and corrected for the T% values for each UV cut-off filter. Corrected values of UV fluence represented the total amount of UV radiant energy that reached the samples placed under the quartz, glass and aluminium foil filters (**Table 8** and **Table 9**). Samples covered with the *Alu* filter served as a dark control. The seeds covered with the *Glass* filter were exposed to UV-B + UV-A light, while the samples covered with *Quartz* filter were exposed to UV-C + (UV-B + UV-A) light. After the experiment, irradiated samples and their dark controls were immediately stored at 4°C until further analysis.

Table 8. The UV irradiation conditions during long-term UV-C exposure experiments with *Arabidopsis* seeds (Ws-2, *dyx*, Col-0 and *fah1-2* genotypes). Fluences of UV light were calculated according to the duration of UV exposure and the measured irradiance of incident light emitted from quasi-monochromatic UV_{254} source (No filter). The output of the UV_{254} source was composed of 90% UV-C_{254}, 8% UV-B_{312} and 2% UV-A_{365} light. Fluences of UV-C_{254}, UV-B_{312} and UV-A_{365} were corrected (CORR.) according to T% values (**Table 6**) for each cut-off filter: *Alu* - thin aluminium foil stuck to a glass slide, *Glass* - 1 mm thick microscopy slide made of soda lime glass, *Quartz* - 1 mm thick quartz window. Ws-2 and *dyx* seed samples were exposed to UV light for 30 and 60 days, while Col-0 and *fah1-2* seed samples were exposed for 40 and 60 days. The wild type seed lines are marked with asterisks.

DURATION OF UV EXPOSURE		FILTER	FLUENCE (kJm^{-2}) UV-C_{254}	UV-B_{312}	UV-A_{365}	SAMPLE
30 days		**No filter**	3.325×10^5	3.096×10^4	6.650×10^3	**Ws-2*&** ***dyx***
	CORR.	***Quartz***	3.059×10^5	2.910×10^4	6.251×10^3	
	CORR.	***Glass***	0	2.260×10^4	6.052×10^3	
	CORR.	***Alu***	0	0	0	
60 days		**No filter**	6.555×10^5	5.934×10^4	1.311×10^4	
	CORR.	***Quartz***	6.031×10^5	5.578×10^4	1.232×10^4	
	CORR.	***Glass***	0	4.332×10^4	1.193×10^4	
	CORR.	***Alu***	0	0	0	
40 days		**No filter**	3.805×10^5	3.169×10^4	7.610×10^3	**Col-0*&** ***fah1-2***
	CORR.	***Quartz***	3.501×10^5	2.979×10^4	7.153×10^3	
	CORR.	***Glass***	0	2.313×10^4	6.925×10^3	
	CORR.	***Alu***	0	2.313×10^4	6.925×10^3	
60 days		**No filter**	5.208×10^5	4.645×10^4	1.042×10^4	
	CORR.	***Quartz***	4.791×10^5	4.366×10^4	9.795×10^3	
	CORR.	***Glass***	0	3.391×10^4	9.482×10^3	
	CORR.	***Alu***	0	0	0	

Table 9. The UV irradiation conditions during short-term UV-C exposure experiments using *Arabidopsis* seeds (flavonoid lacking mutant *tt4-8*). Fluences of UV light were calculated according to the duration of UV exposure and the measured irradiance of incident light emitted from quasi-monochromatic UV_{254} source (No filter). The output of the UV_{254} source was composed of 90% UV-C_{254}, 8% UV-B_{312} and 2% UV-A_{365} light. Fluences of UV-C_{254}, UV-B_{312} and UV-A_{365} were corrected (CORR.) according to T% values (**Table 6**) for each cut-off filter: *Alu* - thin aluminium foil stuck to a glass slide, *Glass* - 1 mm thick microscopy slide made of soda lime glass, *Quartz* - 1 mm thick quartz window.

DURATION (hours) OF UV EXPOSURE	FILTER		FLUENCE (kJm^{-2})		
			UV-C_{254}	UV-B_{312}	UV-A_{365}
0.5	No filter		3.004×10^2	27.036	6.008
	CORR.	*Quartz*	2.764×10^2	25.414	5.648
		Glass	0	19.736	5.467
		Alu	0	0	0
1	No filter		5.728×10^2	51.552	11.456
	CORR.	*Quartz*	5.270×10^2	48.459	10.769
		Glass	0	37.633	10.425
		Alu	0	0	0
2	No filter		1.169×10^3	1.052×10^2	23.38
	CORR.	*Quartz*	1.076×10^3	98.888	21.977
		Glass	0	76.796	21.276
		Alu	0	0	0
3	No filter		1.797×10^3	1.617×10^2	35.94
	CORR.	*Quartz*	1.653×10^3	1.520×10^2	33.784
		Glass	0	1.180×10^2	32.7054
		Alu	0	0	0
5	No filter		3.069×10^3	2.762×10^2	61.38
	CORR.	*Quartz*	2.824×10^3	2.596×10^2	57.697
		Glass	0	2.016×10^2	55.856
		Alu	0	0	0
10	No filter		4.360×10^3	3.924×10^2	87.20
	CORR.	*Quartz*	4.011×10^3	3.689×10^2	81.97
		Glass	0	2.865×10^2	79.35
		Alu	0	0	0
24	No filter		1.140×10^4	1.026×10^3	2.280×10^2
	CORR.	*Quartz*	1.049×10^4	9.644×10^2	2.143×10^2
		Glass	0	7.490×10^2	2.075×10^2
		Alu	0	0	0
48	No filter		2.252×10^4	2.027×10^3	4.504×10^2
	CORR.	*Quartz*	2.072×10^4	1.905×10^3	4.234×10^2
		Glass	0	1.480×10^3	4.099×10^2
		Alu	0	0	0
139	No filter		6.382×10^4	5.744×10^3	1.276×10^3
	CORR.	*Quartz*	5.871×10^4	5.399×10^3	1.199×10^3
		Glass	0	4.193×10^3	1.161×10^3
		Alu	0	0	0

8.1.2. Simulated solar UV exposure experiments (Experiment Verification Tests - EVT)

The UV exposure experiments with polychromatic simulated solar UV light (λ = 200 - 400 nm) were performed as part of an Experiment Verification Test (EVT) in the preflight programme for the EXPOSE-E space mission. The EVT experiments were carried out at the German Aerospace Center (DLR), Institute of Aerospace Medicine, Cologne, using multi-user simulation facilities, such as solar simulators SOL1000 and SOL2000, and the vacuum facility, PSI 2 (**Fig. 47** and **Fig. 48**). The objective of the EVT was to prepare for the space flight experiments by subjecting different organisms to certain simulated space conditions. Fungi, lichens, cyanobacteria, halophilic archeabacteria, *Bacillus* spores and plant seeds were tested, since they had been selected as candidates for the EXPOSE-E mission. Testing the response of plant seeds to simulated space conditions was the objective of our experiment (SEEDS), which was a part of the multi-user EVT programme. *Bacillus* spores were not an experimental object of SEEDS, since their resistance to simulated space conditions was tested in the context of two other experiments (ADAPT and PROTECT), led by two research teams from DLR, Cologne, Germay. Two Experiment Verification Tests, EVT-E1 and EVT-E2, were performed in the period from September 2006 to January 2007. The EVT experimental setup and conditions are described below.

8.1.2.1. Preparation of seed samples for EVT experiments

Prior the EVT experiments, samples of *Arabidopsis* seeds, including Ws-2 and Ler-0 wild types, as well as *tt4-1*mutant, were prepared in the laboratory at INRA, Versailles, France. According to the biosafety regulations on genetically modified organisms (GMOs) at the Institute of Aerospace Medicine, DLR, Cologne, the EVT with transgenic seeds, including flavonoid-lacking mutant *tt4-8*, were not feasible. Therefore, a *tt4-8* mutant was replaced by a nontransgenic *tt4-1* line*, i.e.* another flavonoid deficient mutant. The background Ler-0 seeds were also included in the EVT. Dry *Arabidopsis* seeds were loaded into small glass Petri dishes (∅ 3.2 cm, height 1 cm), that were used as exposure carriers. Loading a small quantity of *Arabidopsis* seeds (30 -35 mg per dish), resulted in uniform monolayers of seeds over the flat bottom of glass dish. Small dishes that contained seed samples were covered with paper coated glass lids, sealed and properly packed for sending to DLR, Cologne, Germany.

8.1.2.2. EVT experimental conditions

Upon their arrival at DLR, Cologne, seed samples were stored at 4°C until the EVT experiments started. Before exposure to simulated space conditions, sample dishes were unsealed, the protective glass lids were removed and seed monolayers were prepared manually by spreading the seeds over the flat bottom of each sample dish. All samples were exposed to simulated space conditions in the open carriers, since the glass lids were not UV transparent at lower wavelengths. Seeds were exposed simultaneously with the other biological samples to be used in the EXPOSE-E mission. After the exposure, all sample carriers were closed and sealed before sending back to INRA, Versailles, France. The following exposure parameters were tested separately or in the combination:

- polychromatic UV radiation
- simulated space vacuum
- polychromatic UV radiation and simulated space vacuum
- simulated Mars CO_2 atmosphere
- polychromatic UV radiation and simulated Mars CO_2 atmosphere

The EVT experiments also included the laboratory controls that were kept in the dark at room temperature under atmospheric pressure.

8.1.2.2.1. Irradiation with polychromatic UV light

The irradiation experiment with the seed samples exposed to polychromatic simulated solar UV under atmospheric pressure was conducted as a part of EVT-E1 (Rabbow, 2007a). Samples were placed on a cold copper plate inside a non-evacuated vacuum facility PSI 2 (**Fig. 47A**), and illuminated under the solar simulator SOL2000 (**Fig. 47B**). The PSI 2 chamber was closed using a lid with a UV transparent quartz window (**Fig. 47B**). The UV emission spectrum (λ = 200-400 nm) of the SOL2000 source is presented on **Fig. 48B.** The measured integrated UV irradiance for SOL2000 was 479.2 Wm^{-2}. The duration of UV irradiation was 87 hours, corresponding to the UV fluence of 1.5 x 10^5 kJm^{-2}. This fluence for irradiation with polychromatic UV light was selected to simulate the full UV irradiation, in the range of 200 - 400 nm, expected for the EXPOSE-E experiments on the ISS for 1.5 years of mission duration. Since the infrared radiation (IR) of the solar simulator leads to overheating of the

irradiated samples, sample carriers were continuously cooled by the cold plate kept at 10°C. Temperature was continuously monitored by a sensor attached to the sample carriers and measured temperature was below 30°C during the whole experiment.

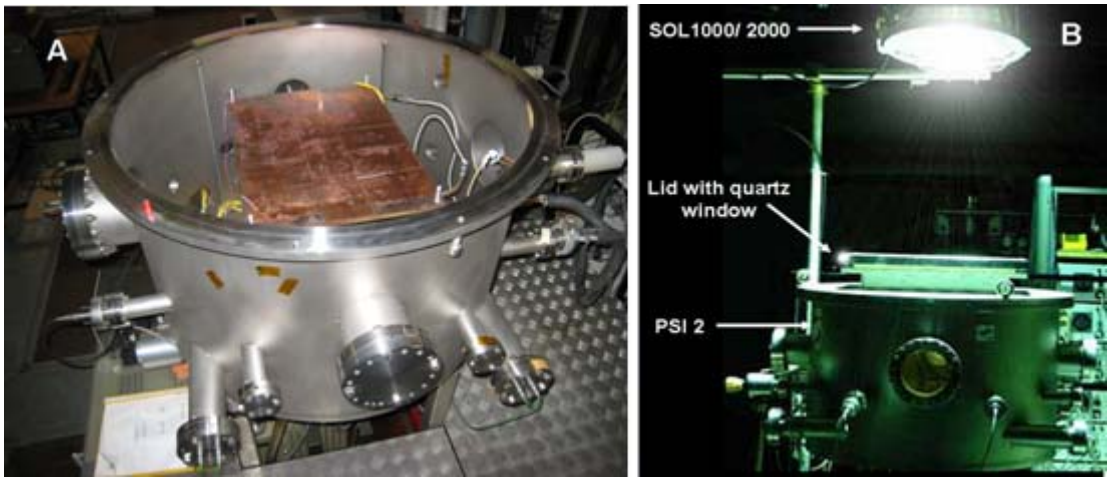

Fig. 47. Experimental setup for EVT experiments at DLR, Cologne, Germany.
A) PSI 2 vacuum simulation facility. The cold copper plate and sensors for measuring temperature and vacuum pressure are placed inside the vacuum chamber of the PSI 2 facility.
B) The samples are accommodated into the PSI 2 facility, which is closed by lid with UV transparent quartz window, and placed below a SOL1000 solar simulator or SOL2000 solar simulator. The solar simulators emitted polychromatic UV light in the range of 200 - 400 nm. Photograph by ©Elke Rabbow /DLR, Cologne, Germany (Rabbow, 2007b).

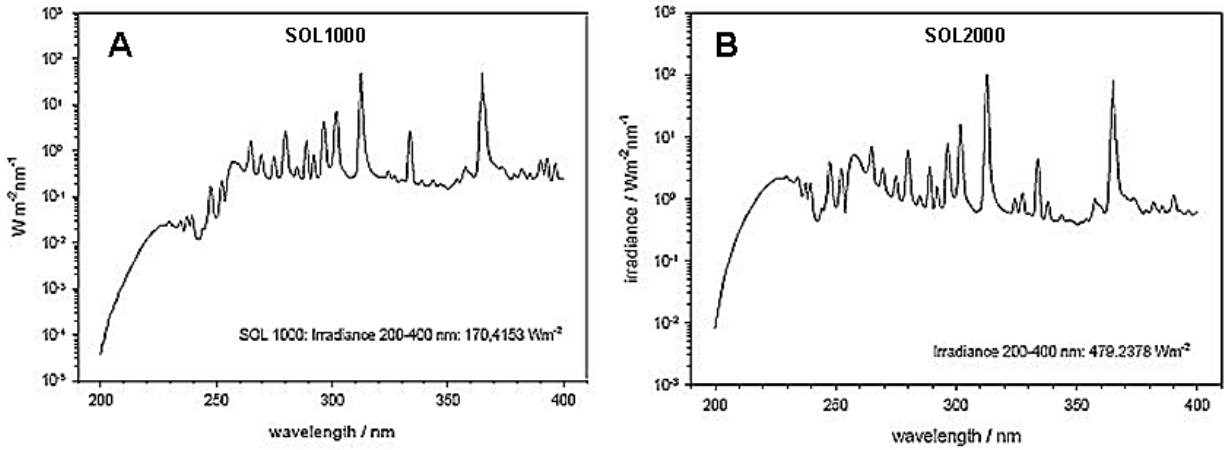

Fig. 48. The UV emission spectra of solar simulators SOL1000 (A) and SOL2000 (B). Both solar simulators were the source of polychromatic UV light (λ = 200 -400 nm), with the energy output of 170.4 Wm^{-2} and 479.2 Wm^{-2} for SOL1000 and SOL2000, respectively. The UV irradiance was integrated over the wavelength range of 200 - 400 nm (Taken from Rabbow, 2007b).

8.1.2.2.2. Exposure to simulated space vacuum

This experiment was performed as dark control for the experiment where seeds were exposed simultaneously to both polychromatic UV light and simulated space vacuum (for details see above). Seed samples exposed only to high vacuum (dark control), were placed in closed, but unsealed, small Petri dishes that were in a vacuum chamber of the PSI 2 facility (**Fig. 47A**), together with UV irradiated samples. The vacuum exposed samples (dark controls) were placed on the second cold plate, beneath the samples exposed to UV placed on the upper cold plate. In this way, control samples were hidden from UV light by the upper cold plate. In both experiments, the UV exposure experiment under the vacuum and dark control experiment under the vacuum, were performed simultaneously in the same simulation facility. The samples were exposed to simulated space vacuum in the dark for 22 days, where final pressure was 10^{-5} Pa.

8.1.2.2.3. Irradiation with polychromatic UV light under simulated space vacuum

This experiment was performed as a part of EVT-E2 experiments (Rabbow, 2007b). The samples were placed in the chamber of vacuum facility PSI 2, on top of a cold copper plate (**Fig. 47A**). The PSI 2 chamber was closed by a lid with quartz window and it was evacuated, reaching a final pressure of 10^{-5} Pa, which was the air pressure expected during the EXPOSE-E mission on the outside of the ISS. The vacuum was monitored by a Pirani cold cathode inserted into the PSI 2 chamber. The samples were irradiated with polychromatic UV light (λ = 200-400 nm), emitted from the solar simulator SOL1000 (**Fig. 47A**). The UV emission spectrum of SOL1000 is shown on **Fig. 48A** and the integrated UV irradiance was 170.4 Wm^{-2}. The temperature was monitored by a sensor attached to the sample carriers, and an increase in temperature at the sample level was detected during UV irradiation. Since the heat cannot be removed from the surface by convection in a vacuum environment, and heat exchange by contact conduction between carrier and cold plate appeared less efficient, this UV irradiation experiment was performed in the cycles that consisted of approximately a 20 min-irradiation period, followed by a 40 min-cooling period. Therefore, the total duration of the experiment was 22 days and an effective duration of UV irradiation was 244.5 hours, corresponding to a final fluence of 1.5 x 10^5 kJm^{-2}. This fluence of polychromatic UV radiation matched the integrated fluence of solar UV irradiation in the range of 200 - 400 nm, expected for the EXPOSE-E experiments on the ISS for 1.5 years of mission duration. Temperature was maintained below 40°C.

8.1.2.2.4. Exposure to a simulated Mars CO_2 atmosphere*

This EVT-E2 experiment was performed as a dark control for the exposure experiment to polychromatic UV carried out under a simulated Mars CO_2 atmosphere*[8] (see section Error! Reference source not found.). The simulated Mars CO_2 atmosphere* was composed of 95.56% (v/v) carbon dioxide, 2.72% (v/v) nitrogen, 1.56% (v/v) argon and 0.16% (v/v) oxygen (gas mixture provided by Linde Gas, Germany). **Table 10** shows the gas composition of simulated CO_2 Mars atmosphere* that was used in our experiment, compared to the composition of present-day Mars and Earth atmospheres. Both experiments, a dark control and a UV exposure experiment, were conducted simultaneously in the same simulation facility. The samples were placed in the PSI 2 camber (**Fig. 47A**) and accommodated onto the second cold plate placed beneath the cold copper plate with UV irradiated samples. The vacuum facility was flooded with a CO_2-containing gas mixture and samples were exposed to the simulated Mars atmosphere* at 1 atm, in the dark for 21 days. Due to technical problems related to the overheating of the irradiated samples (for details see section **8.1.2.2.5**), the EVT-E2 experiments were performed under CO_2-rich atmosphere at 1 atm (101.3 kPa) instead 600 Pa. Therefore, it is important to note that Mars atmosphere was here simulated only in view of its composition, but not the pressure that prevails at the Martian surface.

(Faure and Mensing, 2007b)

Table 10. Principal gaseous constituents of present-day Earth and Mars atmospheres, compared to a gas mixture used as a simulated Mars CO_2 atmosphere* in EVT-E2 experiment.

PRINCIPAL CONSTITUENTS AND PRESSURE	EARTH ATMOSPHERE (AIR) % [a]	MARS ATMOSPHERE % [a]	SIMULATED MARS ATMOSPHERE*[4] %
Nitrogen (N_2)	78.08	2.7	2.72
Oxygen (O_2)	20.94	0.13	0.16
Carbon dioxide (CO_2)	0.035	95.32	95.56
Argon (Ar)	0.93	1.6	1.56
Carbon monoxide (CO)	0.00002	0.07	–
Water vapour	0-4	0.03	–
PRESSURE	101.3 kPa[b] (1 atm)	600 Pa[c]	600 Pa → 1 atm[d]

[a] Adapted from Faure and Mesing (2007b)
[b] The average air pressure at the sea level
[c] The mean surface level pressure
[d] Due to technical problems related to the overheating of the samples, EVT-E2 experiments were performed in 1 atm instead 600 Pa simulated Mars atmosphere

[8] Mars atmosphere was simulated only in view of its composition (95.56% CO_2, 2.72% N_2, 1.56% Ar and 0.16% O_2), but not the pressure, since all experiments were performed at 1 atm (101.3 kPa) instead of 600 Pa.

8.1.2.2.5. Irradiation with polychromatic UV light under simulated Mars CO_2 atmosphere*

As a part of EVT-E2, the seed samples were exposed to polychromatic simulated solar UV radiation in combination with the conditions of a simulated Mars CO_2 atmosphere* (**Table 10**). The open sample carriers were placed into the PSI 2 vacuum facility, directly onto a cold copper plate (**Fig. 47A**). The chamber was closed using a lid with UV transparent quartz window, and it was flooded with a simulated Mars CO_2 atmosphere*, reaching the pressure of 600 Pa. The samples were irradiated with polychromatic light (λ = 200 - 400 nm) emitted from the solar simulator SOL2000 (**Fig. 47B**). Since the removal of heat by convection and contact conduction appeared insufficient at 600 Pa, the vacuum chamber was filled stepwise with the Mars CO_2 atmosphere*, reaching finally the pressure of 1 atm. In addition, the SOL2000 solar simulator was exchanged for a weaker SOL1000 solar simulator (UV emission spectra compared in **Fig. 48**), in order to reduce the IR portion of the spectrum of emitted light. Only under these conditions the temperature at the sample level remained below 40°C. The UV irradiation experiment under simulated Mars CO_2 atmosphere* was performed in the cycles consisting of irradiation and cooling periods, over 21 days. The effective time of $UV_{200-400}$ exposure included 18 min of irradiation with a flux of 479.2 Wm^{-2} using the SOL2000 solar simulator, and 243.7 hours of irradiation with flux of 170.4 Wm^{-2} using the SOL1000 solar simulator. Thus, the final fluence of polychromatic $UV_{200-400}$ was 1.5 x 10^5 kJm^{-2}.

8.2. Analyses of UV irradiated samples of *Arabidopsis thaliana* seeds and *Bacillus subtilis* spores

8.2.1. Analysis of Bacillus subtilis spores exposed to quasi-monochromatic UV-C_{254} light

Immediately after UV-C exposure, dry monolayers of *Bacillus* spores were overlaid with 120 µl of 10% (w/v) aqueous solution of polyvinyl alcohol (PVA) and dried in a laminar flow hood. Dry films of PVA, together with attached *Bacillus* spores, were peeled off with a sterile forceps and placed into a tube with 1 ml of sterile distilled water. This procedure was repeated twice with an additional 120 µl of PVA, in order to increase the efficiency of spore recovery. Dry PVA films with the spores were completely resuspended by vigorous vortexing for at least 5 min. Ten-fold serial dilutions of spores were prepared in sterile water and 100 µl aliquots were inoculated on plates with LB medium. Colonies were scored after 12 hours of incubation at 37°C. The number of CFU per millilitre of suspension was determined on plates inoculated with a spore suspension at 10^{-2} dilution, containing more than 30, but less than 300 colonies, with the exception of samples exposed to high fluences of UV-C, where CFU values were determined at 10^{-1} and 10^{0} dilutions. The efficiency of recovery of spores, using PVA films, was determined by comparing CFU values of spores in dry films (1.2×10^5 spores/dry film) and CFU of spores in 10-fold diluted starting suspension (1.2×10^5 spores/ml). Determined average recovery (± SD) of spores from dry films was 60.8% (±6.9).

8.2.2. Analyses of Arabidopsis thaliana seeds exposed to quasi-monochromatic UV-C_{254} and simulated solar polychromatic UV light

8.2.2.1. Seed germination assays

8.2.2.1.1. Seed germination under optimal conditions

All UV exposed *Arabidopsis* seeds, together with their dark controls, were plated in triplicate on 9-cm ∅ Petri dishes, containing 0.8% (w/v) aqueous agar medium (Bacto-agar, Difco). For UV-C irradiation experiments, 50 seeds were sown per plate, while 40 seeds per

plate were sown for the experiments with simulated solar UV light (EVT experiments). Petri dishes were sealed with strip of plastic wrap and placed in the dark at 4°C. All seed lots were cold treated while imbibing for exactly 72 hours. This stratification procedure was performed in order to break seed dormancy and synchronize seed germination, obtaining consistent and comparable results. Plates with cold stratified seeds were transferred into a culture room at 25°C and exposed to light for 1 hour in order to stimulate germination, followed by an 8 h dark period. Seed germination was further conducted under controlled conditions at an average temperature of 25.7°C ± 1.0 (day temperature) and 24.8°C ± 0.9 (night temperature), with a 16/8-h (light/dark) photoperiod provided by cool-white fluorescent tubes. Germination was observed under a dissecting microscope and germinated seeds were scored periodically over time for 5 days. The results were expressed as the percentage of the total number of seeds sown per plate, where n = 50 for UV-C exposure experiments and n = 40 for EVT exposure experiments. All germination tests were performed in triplicates (Baskin and Baskin, 2001a).

8.2.2.1.2. Seed germination under suboptimal conditions

The germination experiments were performed in 9-cm ∅ Petri dishes, sowing the seeds on a 0.8% (w/v) aqueous agar medium (BactoAgar, Difco). The UV exposed *Arabidopsis* seeds (Ws-2, *dyx*, Col-0 and *fah1-2* seeds exposed to quasi-monochromatic source of UV_{254}), together with their dark controls, were plated in triplicate, with 40 seeds per each plate. The seeds were stratified for 72 hours in the dark at 4°C. Sealed plates were than placed in a growth chamber (Forma Scientific) at a distance of 25 cm under the source of cool-white light (2 fluorescent tubes Sylvania F 15W/133, Germany), with 16/8-h (light/dark) photoperiod. Seed germination was conducted under suboptimal conditions at 10°C day/night-constant temperature. Seed samples were observed for germination daily and germinated seeds were scored over a period of 10 days. The results were expressed as the percentage of total number of seeds sown per plate (n = 40). The germination tests were performed in triplicates (Baskin and Baskin, 2001a).

8.2.2.2. Tetrazolium assay

The tetrazolium (TZ) test is a biochemical method to examine seed viability. This viability test can be used as a supplement to germination tests in order to determine the quality of seeds that have not germinated during the standard germination procedure. The TZ test is based on the principle of metabolic reduction of tetrazolium salts into highly coloured end-products called formazans by NADH-dependent reductases in metabolically active cells.

The viability of *Arabidopsis* seeds that were exposed to quasi-monochromatic UV-C_{254}, as well as polychromatic simulated solar UV, was examined by the TZ test according to the procedure described by Warton (1955). At the end of germination tests, ungerminated seeds were transferred from agar plates into a water-filled well of polystyrene 24-multiwell plate, dimensions 128 x 86 mm (Nunc, Thermo Fisher Scientific, Rochester, US). In addition to UV exposed seed samples, positive control samples (untreated seeds stored in the dark at 4°C), as well as negative control samples (non-viable seeds inactivated by autoclaving for 20 min), were also used in the TZ test. Already imbibed seeds were soaked in sterile water for additional two hours at room temperature. After the removal of water, 500 µl of 1% (w/v) aqueous solution of 2,3,5-triphenyltetrazolium chloride (Sigma-Aldrich, France) was added in each well containing seed samples. Closed multiwell plates were sealed with a parafilm and samples were incubated at 30°C in darkness for 48 hours. Du to the activity of dehydrogenases in the living cells, pale yellow solution of 2,3,5-triphenyltetrazolium chloride was reduced to bright red triphenylformazan. Seed samples were examined under a dissecting microscope, where red-coloured *Arabidopsis* seeds represented viable seeds and unstained seeds were determined as non-viable seeds.

Since the seed coats of flavonoid-containing *Arabidopsis* seeds, including Ws-2, Col-0 and Ler-0 wild types, as well as *fah1-2* mutant, appeared impermeable to tetrazolium solution, the TZ test was performed only on intact seeds of flavonoid-lacking mutant lines *tt4-8* and *tt4-1* (Debeaujon et al., 2000). These mutants had a transparent seed coat that allowed efficient penetration of tetrazolium salt and relatively easy detection of coloured embryo inside the seed coat. Alternative methods for the exposure of tissues prior to staining, such as piercing or removing of the seed coat, seed cutting and excision of the embryo, were not applicable due to very small size of *Arabidopsis* seeds, ranging from 0.3 -0.5 mm (Al-Shehbaz and O'Kane, 2002).

8.2.2.3. Early-seedling stage experiments

After the germination stage, which is known as a principal growth stage 0.0 (Boyes et al., 2001), *Arabidopsis* UV exposed seeds developed into the seedlings that were further cultured *in vitro* under the controlled conditions. The following parameters at early-seedling stage (principal growth stage 1.0 by Boyes et al., 2001) were observed and measured: percentage of ungerminated seeds, percentage of normally and abnormally developed seedlings, and the length

of the primary roots. Abnormally developed seedlings were further inspected for the characteristic seedling damage.

8.2.2.3.1. Quantification and characterization of seedling damage

Following the germination test under optimal conditions, the same UV exposed seed samples were further cultured under controlled conditions in the culture room at 26/24°C (day/night temperature) and under a 16/8-h (light/dark) photoperiod. The seedlings were grown in sealed dishes placed 27 cm under the source of cool-white light (4 fluorescent tubes Philips TL-D 36W/33-640, France). The 14-day-old (17 DAI)[9] Ws-2, *dyx* and *tt4-8* seedlings, as well 19-day-old (22 DAI)[5] Col-0 and *fah1-2* seedlings, all reaching a principal growth stage 1.0 (seedlings with fully opened cotyledons according to Boyes et al., 2001), were observed under a dissecting microscope and examined for seedling damage. The 15-day-old (18 DAI)[5] seedlings developed from seeds used in the EVT experiments (Ws-2, Ler-0 and *tt4-1* seeds exposed to simulated solar UV), were also inspected for the damage observed in essential seedling structures. The images of *Arabidopsis* seedlings were acquired using a digital camera (SONY HYPER HAD color video camera), attached to a dissecting microscope (NIKON SMZ-10A).

According to the recommendations of the International Seed Testing Association (ISTA, 1999), seedlings were quantified and grouped into following three categories: normal seedlings, abnormal seedlings and ungerminated seeds. The abnormal seedlings were examined in detail, and characterized and classified into further subgroups according to the observed defects, occurring separately or in the combination, on essential seedling structures such as the primary root, hypocotyl and cotyledons (ISTA, 1999). All observations were scored and expressed as the percentage of the total number of seeds sown per plate (n = 50 for UV-C exposure experiments and n = 40 for EVT exposure experiments).

8.2.2.3.2. Measurement of primary root length

The UV exposed Arabidopsis seeds, together with their dark controls, were sown in 12 x 12 cm plates, containing 0.8% (w/v) aqueous agar medium (BactoAgar, Difco). The seed samples were prepared in triplicate with 22 seeds per plate, arranged regularly in two rows, with 5 cm spacing between rows and a distance of 1 cm between adjacent seeds. Such seed arrangement enabled regular growth of primary roots, minimizing possible interactions between

[9] DAI = days after imbibition

adjacent seedlings. Immediately after sowing, plates were sealed with strip of plastic wrap and placed at 4°C in the dark and seeds were stratified for 72 hours. The plates were than moved to a culture room, where seeds germinated and seedlings grew at 26/24°C (day/night temperature) and under a 16/8-h (light/dark) photoperiod under cool-white fluorescent tubes. The plates were placed vertically on a rack so that the roots grew downward on the medium surface. The length of primary roots was measured in 10 day-old (13 DAI)[5] seedlings that had reached principal growth stage 1.0, a phase where seedlings developed fully opened cotyledons, according to BBCH scale adapted for Arabidopsis (Boyes et al., 2001; Kjemtrup et al., 2003). The results were scored only for normally developed primary roots with a minimal length of ≥ 3 mm, while smaller roots were considered as damaged roots (retarded roots). In addition, seedlings with developed secondary roots were not taken in account, since they had outgrown stage 1.0, reaching the stage R6 (Boyes et al., 2001). Root growth was observed under a dissecting microscope and tracked by marking the root length on the back surface of each plate. The plates were than photocopied at 150% magnification; root length was measured directly on paper copies and results were scaled down to the real root lengths.

8.2.2.4. Plant development stage and greenhouse experiments

The UV exposed *Arabidopsis* seeds were first sown on Petri dishes containing 0.8% (w/v) aqueous agar medium (BactoAgar, Difco). The stratification step was performed *in vitro*, instead of directly in soil, in order to increase the number of germinated seeds and to synchronize seed germination. Seeds were imbibed and cold-treated at 4°C in the dark for 72 hours. *In vitro* imbibed seeds were than sown in 6 x 6-cm pots containing a peat moss-based soil mixture (Floradur B fine®, Floragard, Germany). Each sample was prepared in triplicate, with n=8 seeds per pot. All seed samples were sown on the same day and all *Arabidopsis* plants were grown in the greenhouse at the same time (from April to May 2008), under approximately the same conditions, at a daily temperature 21-27°C and a night temperature of 17-20°C, under natural day/night cycles, extended to 16 h days using artificial light. Plants were watered every 2-3 days with a nutritive solution using the sub-irrigation method (Scholl et al., 1998; Anderson and Wilson, 2000; Rivero-Lepinckas et al., 2006). Plant growth was observed through different growth stages, including the mature plant stage, defined as principal growth stage 8.0 (plants with the first silique shattered), according to the BBCH scale adapted for *Arabidopsis* (Boyes et al., 2001). After 45 days (48 DAI)[5] of cultivation, a total number of plants at different growth stages, as well as the number of developed mature plants at the stage 8.0, were scored and expressed as a percentage of the total number of seeds sown per pot (n = 8). In addition, the

height of mature plants (principal growth stage 8.0) was also measured. The height of *Arabidopsis* plants was measured by placing the ruler alongside the plants and determining the distance upward from the soil surface at the plant's base to the highest point of the stem.

8.2.3. Statistical analyses

All statistical analyses of the data were performed using GraphPad InStat version 3.06 for Windows, GraphPad Software, San Diego California USA, http://www.graphpad.com.

8.2.3.1. UV exposure experiments with Bacillus subtilis spores

The UV exposure experiments with *Bacillus* spores were performed in triplicate (n = 3). The average CFU value for each UV fluence was determined by four repeated inoculations of spores on LB plates. Data were compared by one-way analysis of variance (ANOVA) to detect significant differences between means. Means differing significantly were compared using the Tukey-Kramer multiple comparison post-hoc test at the level of significance $\alpha = 0.05$. Variability around the mean was represented as ± standard deviation.

8.2.3.2. UV exposure experiments with Arabidopsis thaliana seeds

The *in vitro* experiments, including germination tests and early-seedling stage experiments, were performed in triplicate (n = 3), observing 50 seeds per sample, exposed to quasi-monochromatic UV_{254} or with 40 seeds per sample, exposed to simulated solar UV radiation (EVT experiments) (Baskin and Baskin, 2001a). Mean values were analysed by one-way ANOVA, when the UV exposed samples were compared to their dark controls. Means that were considered statistically different at the level of significance $\alpha = 0.05$ were further compared using the Tukey-Kramer multiple comparisons post-hoc test. An unpaired t-test at the level of significance $\alpha = 0.05$ was used when mean values between two UV exposed samples were compared. The variability around the mean was represented as ± standard deviation. The ANOVA assumes that the standard deviations of the groups are equal and that data follow a Gaussian distribution. Since no Bartlett's test, which examines the assumption of standard deviation equality, no Kolmogorov-Smirnov test, which is test for normality, nor nonparametric tests could be performed due to the requirement of minimal number of repeats $n \geq 5$, the data of germination tests were transformed prior the ANOVA. The data for the germination capacity

tests could be performed due to the requirement of minimal number of repeats $n \geq 5$, the data of germination tests were transformed prior the ANOVA. The data for the germination capacity ($G_{max\%}$) were statistically analyzed using untransformed and $\arcsin\sqrt{\%}$ transformed values, while the data for mean germination time (MGT), $T_{25\text{-}75\%}$ and $T_{50\%}$ were transformed into square-root values.

The data for root length measurements were obtained in triplicate, with n = 22 observed seedlings per sample. The mean values (untransformed data) of three repeats were compared statistically and the data were pooled when no statistical difference was observed. Bartlett's test and the Kolmogorov-Smirnov test were performed prior to the ANOVA and Tukey-Kramer multiple comparison post-hoc test ($\alpha = 0.05$). The mean values of root length were also compared by nonparametric Kruskal-Wallis and Mann-Whithey tests at the $\alpha = 0.05$ level of significance.

The data from greenhouse experiments (stage of plant development) were obtained in triplicate, with n = 8 seeds per sample. The mean values were analyzed by one-way ANOVA and the Tukey-Kramer multiple comparison post-hoc test ($\alpha = 0.05$). Since calculated mean values of total percentage of developed plants and percentage of mature plants were obtained from three independent experiments, Bartlett's test, Kolmogorov-Smirnov test, as well as nonparametric tests, all requiring at least five repeats, could not be performed. Instead, the results obtained by one-way ANOVA were compared to those obtained using $\arcsin\sqrt{x}$ transformed, as well as log (x+1) transformed data. On the other hand, untransformed data for plant height ($n \geq 5$) were analyzed by ANOVA, while testing the equality of standard deviation (Bartelett's test) and normal distribution (Kolmogorov-Smirnov test). In addition, nonparametric Kruskal-Wallis test ($\alpha = 0.05$) was performed to analyze the plant height data.

PART I:

CHEMICAL BASIS FOR UV PROTECTION IMPLIED THROUGH ABSORPTION SPECTROSCOPY

Chapter 3

RESULTS I

9. DNA AS A TARGET FOR UV DAMAGE: THE VUV-UV SPECTROSCOPIC CHARACTERISTICS OF DNA AND ITS COMPONENTS (Article 1 and Article 3)

Life on early Earth or in potentially habitable exoenvironments must cope with the full spectrum of Solar UV light, including the UV-A (315-400 nm), UV-B (280-315 nm), UV-C (200-280 nm) and vacuum UV, VUV (< 200 nm). Although unfiltered solar light in the short wavelength regions (VUV and the UV-C) is relatively weak, this part of the spectrum is particularly damaging. Nucleic acids are prime targets due to their high absorption in the UV-C and VUV part of spectrum. We used synchrotron light to measure VUV-UV absorption spectra (125-340 nm) for thin dry films of DNA and its components (oligonucleotides and mononucleotides). In this work we extended the energy range of previously reported spectra that were generally not known below 200 nm. Therefore, besides its astrobiology context related to the origin and evolution of life, this work represents the first comprehensive study of VUV-UV absorption characteristics of DNA and its components, providing the original spectroscopic data in the VUV part of spectrum.

Dry genomic DNA showed absorption maxima at 264 nm (region I), at 192 nm (region II) and continuously increasing absorption towards the 125 nm (region III) (Zalar et al., 2007a). We also compared the absorption spectra of DNA in dry and hydrated states, where the latter showed a small hypsochromic shift of the peak I at 260 nm.

Polymerized homonucleotides (short tracts of single-stranded DNA), containing 20 identical nucleotides (oligoA_{20}, oligoT_{20}, oligoC_{20} and oligoG_{20}) showed differences in their absorption spectra (Zalar et al., 2007a). Just as for DNA, their absorption peaks could be grouped into three regions. However, these oligonucleotides showed more spectral features than genomic DNA. In addition, a bathochromic shift of the absorption peak in region I for oligoC_{20} and oligoG_{20} was observed, when compared to oligoA_{20} and oligoT_{20}, as well as genomic DNA. This result suggested that DNA sequences rich in G+C nucleotides could have its absorption maximum in the region I shifted towards 280 nm.

We further measured the VUV-UV spectra for equimolar mixtures of two complementary homonucleotides (oligoA+T and oligoC+G), which represented two extremes in G+C content, 0% and 100%, respectively (Zalar et al., 2007c). Significant differences in the absorption were

observed between oligoA+T and oligoC+G spectra. Both spectra differed from that of genomic DNA (41.2% G+C).

In addition, we examined the absorption properties of equimolar mixtures of complementary sense and antisense strands for synthetic 60-mer oligonucleotides with different G+C content (30%, 50% and 63%) (Zalar et al., 2007c). These oligonucleotides had different nucleotide composition and sequence, but they encode the same peptide, which contained one of each of 20 aminoacids. Although no major differences in the overall absorption spectra were observed for these oligonucleotides, a bathochromic shift in the region I was correlated with increasing G+C content.

The results on the VUV-UV spectroscopic characteristics of DNA and its components are presented in the following two publications (see chapter **9**):

Article 1

Zalar A, Tepfer D, Hoffmann SV, Kenney JM, Leach S (2007a) Directed exospermia: I. Biological modes of resistance to UV light are implied through absorption spectroscopy of DNA and potential UV screens. International Journal of Astrobiology **6:** 229-240

Article 3

Zalar A, Tepfer D, Hoffmann SV, Kollmann A, Leach S (2007c) VUV-UV absorption spectroscopy of DNA and UV screens suggests strategies for UV resistance during evolution and space travel. *In* BH Richard, VL Gilbert, YR Alexei, CWD Paul, eds, Instruments, Methods, and Missions for Astrobiology X, Vol 6694. Proceedings of SPIE, pp 66940U (1-15)

10. UV SCREENING COMPOUNDS AND THEIR VUV-UV ABSORPTION PROPERTIES

Due to its absorption properties and biological importance, DNA is a particularly sensitive target to UV damage. Thus evolving life developed different mechanisms for resisting UV radiation. One of the mechanisms is passive protection by UV screens, the substances that absorb the UV light and dissipate the energy away from sensitive targets. Thus, we evaluated the potential UV screening effectiveness for different substances according to the degree of similarity between their VUV-UV absorption spectra and that of DNA. Within the group of biological UV screens (substances that are synthesised by living organisms), we were interested in the VUV-UV absorption properties of molecules that are ubiquitously present in all organisms (potential UV screens), as well as known UV screens that are found in phylogenetically distinct groups of organisms (specialized UV screens). Using synchrotron light, we measured VUV-UV absorption spectra (125-340 nm) for thin dry films of different potential and specialized UV screens. Since little is known about absorption characteristics of these compounds below 200 nm, this work provides valuable spectroscopic data extend into the VUV part of spectrum

10.1. Ubiquitously occurring potential UV screens (Article 1)

Among the substances that are ubiquitous in all organisms, we studied the VUV-UV spectra for thin dry films of mononucleotides, proteins and selected amino acids, as well as polyamines (aliphatic amines) and tyramine (aromatic amine) (Zalar et al., 2007a).

Nucleotides are monomer units of nucleic acids that are abundant in all cells. Besides their use in information storage, they also play important roles in energy transfer and cell signaling processes. The VUV-UV absorption spectra of all four monomer nucleotides (A, T, G, C monophosphates and triphosphates) were similar to those for polymerized oligonucleotides, except in the case of cytidine nucleotide. The accumulation of free nucleotides could contribute to protection of DNA against UV radiation. Among the four nucleotides, ATP had an absorption curve that best matched that of DNA. We suggested that primitive cells might have used ATP as a UV screen, before or at the same time as a “molecular currency” of intracellular energy transfer.

Proteins are macromolecules, composed of amino acids. Although proteins themselves represent a target for UV damage, some of them could provide direct protection (by UV screening or physical compaction of DNA) or indirect protection (enzymatic repair). We measured the VUV-UV absorption spectra for histones (positively charged proteins that interact with DNA), as well as bovine serum proteins, BSA (a small, neutral protein). These proteins could provide efficient UV screening protection to DNA in the VUV part of spectrum, but they would provide poor protection in region I, due to the bathochromic shift in the maximum of absorption at 280 nm.

We further examined the influence of selected amino acids on the UV absorption of proteins by measuring the VUV-UV spectra for valine (neutral and hydrophobic amino acid), arginine (basic amino acid), aspartic acid (acidic amino acid) and tryptophan (neutral, hydrophobic representative of aromatic amino acids). Valine, arginine and aspartic acid showed absorption maxima in the VUV, but they absorbed poorly above 210 nm. In contrast, the UV screening protection to DNA in the region I might be provided by aromatic amino acids, such as tryptophan, which showed a complex broad peak at 287 nm, with a shoulder at 272 nm.

Polyamines are small, cationic molecules that play important roles in the regulation of cell growth in both prokaryotic and eukaryotic cells. Due to their positive charge at physiological pH, they interact closely with negatively charged nucleic acids. Here we examined the VUV-UV spectroscopic properties of ubiquitous polyamines, putrescine, spermidine and spermine. Due to the strong absorbance below 200 nm, and very low absorbance in UV-C, UV-B and UV-A regions, these aliphatic polyamines could act as UV screens only in the VUV part of spectrum. In contrast, the ubiquitously occurring aromatic amine, tyramine, showed a prominent and broad peak at 282 nm in addition to strong absorbance at wavelengths below 220 nm. Thus, tyramine could serve as a UV screen, protecting DNA in all three regions.

The results on the VUV-UV spectroscopic characteristics of ubiquitously occurring potential UV screens are presented in the following publication (see chapter **9**).

Article 1

Zalar A, Tepfer D, Hoffmann SV, Kenney JM, Leach S (2007a) Directed exospermia: I. Biological modes of resistance to UV light are implied through absorption spectroscopy of DNA and potential UV screens. International Journal of Astrobiology **6:** 229-240

10.2. Specialized UV screens from phylogenetically distinct groups of organisms (Article 2 and Article 3)

Besides ubiquitous putative UV screens, we analyzed the VUV-UV absorption properties of known, specialized UV screens found in diverse organisms. The synthesis of these UV screens, which are efficient and specific UV absorbers, is usually induced by UV light. In this study we measured the VUV-UV absorption spectra of thin dry films of specialized UV screens, including scytonemin, mycosporine-like amino acids (MAAs), β-carotene, melanin and flavonoids. On the basis of the similarity with the absorption spectrum of DNA, we evaluated the likely effectiveness of these substances in screening DNA against UV radiation (Zalar et al., 2007b). The photosynthetic system is also considered to be a sensitive target for UV damage, leading to bleaching of photosynthetic pigments. Therefore, we compared VUV-UV absorption spectra of specific UV-screens, found in photosynthetic organisms, with the spectra for pigments, chlorophyll a and b (Zalar et al., 2007c).

Scytonemin is a yellow-brown extracellular pigment that accumulates in sheaths of cyanobacteria after their exposure to UV-A light. Scytonemin absorbs strongly in the UV-A (prominent peak at 386 nm), as well as UV-B and UV-C parts of spectrum. The VUV-UV absorption spectra showed that scytonemin would provide efficient protection to the DNA regions III and II (peak at 195 nm), but region I would be less protected due to weaker absorption and a hypsochromic shift at 253 nm. On the other hand, the scytonemin UV absorption curve matched both the chlorophyll a and b curves, indicating efficient UV screening protection for these photosynthetic pigments.

The MAAs are intracellular, UV inducible compounds, found in taxonomically diverse organisms, notably marine species. We analyzed the VUV-UV spectra of two MAAs, porphyra-334 and palythine, which showed qualitative spectral similarities. The VUV-UV absorption curves indicated that these MAAs would protect DNA in regions II and III, but would not provide sufficient protection in region I (264 nm), since they exhibited minima of absorption in the UV-C part of the spectrum. In addition, the VUV-UV spectra showed that MAAs would protect chlorophyll a and b from VUV, but not from UV-C radiation.

Carotenoids are pigments synthesized by plants, algae and some bacteria. Their absorption maxima occur mainly in the visible part of spectrum, with an extension into the UV-A region. The VUV-UV spectra indicated that β-carotene would provide protection to DNA only in the

VUV (regions II and III), while DNA region I would remain unprotected, since only a small peak at 277 nm was observed. Similarly, β-carotene would protect chlorophyll a and b only in the VUV.

Melanin pigments are found in animals, fungi, higher plants and in some bacteria. Melanins have strong absorption in the UV and visible parts of the spectrum. Our absorption spectra showed uniform absorption in the VUV-UV region, with two poorly resolved peaks. However, an exponential increase of absorbance was observed at wavelengths below 145 nm. This monotonic absorption profile, with poor spectral features, can be explained by the chemical complexity of melanin compounds. Thus, melanins could provide efficient, but not specific UV screening protection.

Flavonoids are known UV screens in plants that accumulate in cell vacuoles and walls. Their synthesis is induced by UV-A and UV-B light. We have examined the VUV-UV absorption characteristics of glycosylated flavonols, including quercitrin, isoqercitrin and robinin. These three flavonoids shared similar spectral features, showing prominent peaks in DNA regions I and II, a steep increase in absorbance towards lower wavelengths at 125 nm (region III), as well as increased absorbance towards higher wavelengths at 340 nm. The broad peak in the UV-A region (~350 nm) was confirmed by conventional spectroscopy in solution. In addition, all these three glycosylated flavonoids exhibited a remarkable similarity to the VUV-UV absorption spectrum of DNA. Thus, we suggested that gycosylated flavonoids would act as ideal UV screens for DNA. Here we also studied the UV absorption properties of catechin, an aglycone flavonoid that is the monomer unit of condensed tannins. Catechin showed a broad peak of absorption in region II (at 204 nm), as well as increased absorbance in region III. However, its absorption minimum at 254 nm (region I) and shifted peak at 280 nm would make catechin a poor UV screen for DNA. Instead it might be better suited for protection of proteins.

In addition to DNA protection, we also considered the role of flavonoids in the UV screening protection of photosynthetic pigments. Comparing VUV-UV spectra, we suggested that glyosylated flavonoids would act as efficient UV screens for chlorophyll a and b in the VUV and UV-C region, but they would provide weaker protection in the UV-B region. On the other hand, catechin would be less suited to protect chlorophyll a and b, except in the VUV part of spectrum.

The results on the VUV-UV absorption characteristics of specialized UV screens and their role in the protection of DNA and photosynthetic pigments are presented in the following two publications (see chapter **9**):

Article 2

Zalar A, Tepfer D, Hoffmann SV, Kenney JM, Leach S (2007b) Directed exospermia: II. VUV-UV spectroscopy of specialized UV screens, including plant flavonoids, suggests using metabolic engineering to improve survival in space. International Journal of Astrobiology **6:** 291-301

Article 3

Zalar A, Tepfer D, Hoffmann SV, Kollmann A, Leach S (2007c) VUV-UV absorption spectroscopy of DNA and UV screens suggests strategies for UV resistance during evolution and space travel. In BH Richard, VL Gilbert, YR Alexei, CWD Paul, eds, Instruments, Methods, and Missions for Astrobiology X, Vol 6694. Proceedings of SPIE, pp 66940U (1-15)

11. CHEMICAL AND SPECTROSCOPIC CHARACTERIZATION OF UV SCREENING COMPOUNDS FROM *Arabidopsis thaliana* SEEDS WITH EMPHASIS ON FLAVONOIDS AND SINAPATE ESTERS

Flavonoids comprise the most common group of polyphenolic plant secondary metabolites and they are abundant constituents of most plant seeds. Over 6000 different falvonoids have been reported, which are divided into different subclasses, including flavonols, flavones, flavanols, flavanones, isoflavonoids and anthocyanins (Schijlen et al., 2004; Saraf et al., 2007). For details about the chemical structure, biosynthesis and biological activity of flavonoids see chapter introduction, section **5.1**. Seeds are rich sources of flavonoid compounds. Due to their strong absorption in the VUV-UV part of the spectrum, flavonoids are considered efficient UV screens (see section **10.2**.). The second major class of phenolic compounds in plants are the hydroxycinnamic acids (for details see chapter introduction, section **5.2.1**). Sinapate esters represent the most abundant hydroxycinnamic acid derivatives in *Arabidopsis* plants, which accumulate three major sinapate ester compounds: sinapoylmalate, sinapoylcholine and sinapoylglucose (Sheahan, 1996; Ruegger et al., 1999). In the literature, sinapate esters are described as good UV screens, providing efficient UV protection to plants (Chapple et al., 1992; Landry et al., 1995; Sheahan, 1996). Besides flavonoids and sinapate esters, glucosinolates also represent important secondary metabolites in *Arabidopsis thaliana* plants (see **Table 4**, chapter **1**, section **5.**). Glucosinolates play an important role in plant defence system, being involved in plant-herbivore and plant-pathogen interactions (Lambrix et al., 2001; Brown et al., 2003; Kliebenstein, 2004). It is still unknown, whether glucosinolated may also play a role in plant UV protection.

In the present work, we used *Arabidopsis thaliana* seeds as a model for studying UV resistance in plant seeds. Due to the observed extreme resistance of *Arabidopsis* seeds to UV radiation (see part II, chapters **5** and **6**), we examined their chemical compounds that might be involved in UV-screening protection. We also analyzed the UV absorption properties of these compounds in order to estimate their UV screening effectiveness.

11.1. Detection and identification of flavonoids and sinapate esters in crude extracts from *Arabidopsis* wild type Ws-2 seeds

11.1.1. HPLC analysis of crude extract from Ws-2 seeds

A crude extract from Ws-2 seeds was analysed and fractionated by HPLC as a preliminary screen for compounds that could serve as UV screens, with focus on flavonoids and sinapate esters. An HPLC chromatogram (λ = 330 nm) of crude Ws-2 seed extract is presented in **Fig. 49**, together with the UV absorption spectra (λ = 190-400 nm) of each separated chromatographic peak. Eight purified fractions (F1, F2, F3, F4, F5a, F5b, F6 and F7) that corresponded to seven prominent HPLC peaks were collected. Among those, peak No 12 (RT[1] = 31.35 min) exhibited a particularly strong signal. Thus, the content of this peak was collected in two separate fractions, F5a and F5b, which corresponded to ascendant and descendant part of the peak. This dominant HPLC peak showed an absorption spectrum that is typical for flavonols (a group of flavonoids), with two absorption maxima at 250-280 nm and at 350-380 nm (Bohm, 1998). Three other less prominent HPLC peaks, No 7 (RT = 19.55 min), No 9 (RT = 22.75 min) and No 10 (RT = 26.05 min), exhibited similar UV absorption features that are characteristic for flavonoids. These three peaks corresponded to collected fractions F2, F3 and F4, respectively. On the other hand, the HPLC peaks No 5 (RT = 16.05 min), No 14 (RT = 37.64 min) and No 17 (RT = 43.39 min), had a UV absorption profiles that did not resemble that of flavonoids, but were more like those of sinapic acid derivatives, which show absorption maxima at ~240 nm and ~320 nm (Lee, 2000). These peaks corresponded to the HPLC-purified fractions F1, F6 and F7, respectively.

In order to determine more precisely their chemical composition and characteristics, all collected fractions were further subjected to comprehensive LC-MS and spectroscopic analyses (see further the results).

[1] RT = retention time

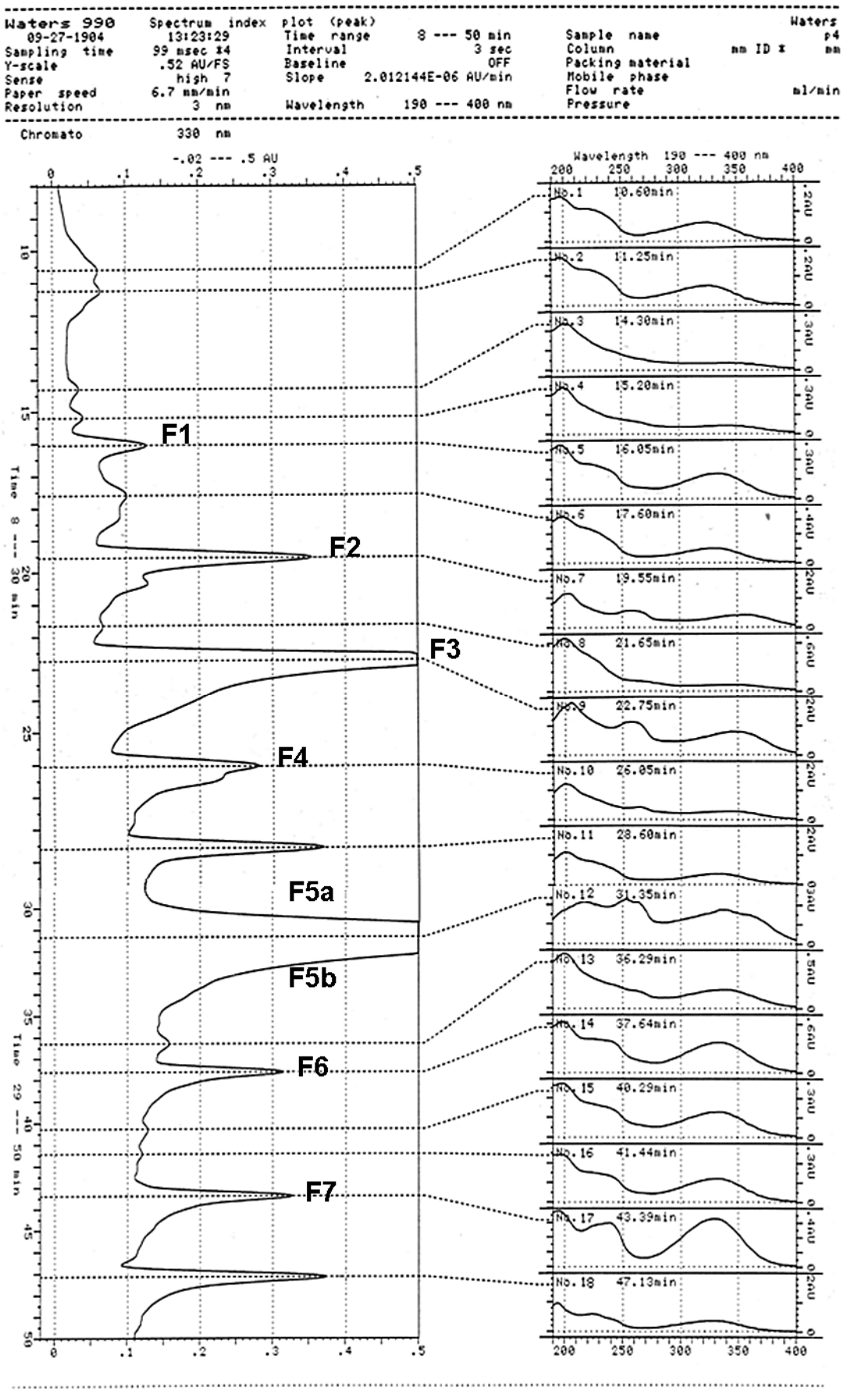

Fig. 49. HPLC chromatogram (λ = 330 nm) of crude extract from whole seeds of *Arabidopsis* Ws-2 wild type line. Eight purified fractions (F1, F2, F3, F4, F5a, F5b, F6 and F7) that correspond to seven prominent HPLC peaks (No 5, 7, 9, 10, 12, 14 and 17) were collected and subjected to further LC-MS and spectroscopic analyses.

11.1.2. Fluorescence detection of flavonoids and derivatives of sinapic acid in HPLC- purified fractions from Ws-2 seed extract

Prior to MS analyses, the HPLC-purified fractions from the Ws-2 seed extract were inspected visually under UV-A light (λ = 365 nm), as shown in **Fig. 50**. For comparison, we also examined standard solutions of flavonoids quercetin-3-*O*-rhamnoside (quercitrin), kaempferol-3-*O*-rutinoside (kaempferol-3-*O*-di-rhamnoside, nicotiflorin) and (-)-3,3',4',5,7-pentahydroxyflavan (epicatechin), as well as standard solution of 3,5-dimethoxy-4-hydroxycinnamic acid (sinapic acid). Quercitrin was chosen as a representative of flavonol-monoglycosides, with quercetin as an aglycone moiety, while nicotiflorin was selected as a representative of flavonol-diglycosides within the group of kaempferol derivatives. In addition, quercitrin is the most abundant flavonoid compound in Ws-2 seeds (see the results below, as well as previously reported data by Routaboul et al., 2006). Epicatechin is a monomer unit of proanthocyanidins (PAs), also known as condensed tannins, which are present in large quantities in the *Arabidopsis* seed coat. *Arabidopsis*, unlike many other plants, uses exclusively epicatechin instead of catechin in synthesis of PAs (Routaboul et al., 2006).

Excited by UV-A_{365} light, the sample of sinapic acid showed a bright blue fluorescence, while flavonol-glycosides quercitrin and nicotiflorin exhibited brown fluorescence (**Fig. 50**), as described in Harborne, 1998. The sample of epicatechin standard showed a weak greyish colour when exposed to UV-A_{365} light.

The HPLC-purified F1 and F6 fractions showed an intensive blue fluorescence under UV-A_{365} light, indicating the presence of sinapic acid (Harborne, 1998) or its derivatives such as sinapate esters (Chapple et al., 1992; Lorenzen et al., 1996; Sheahan, 1996). The F7 fraction also exhibited blue fluorescence, but with low intensity (**Fig. 50**). This result was in agreement with the UV absorption spectra for HPLC peaks F1, F6 and F7 (see HPLC chromatogram in **Fig. 49**) that showed sinapate specific absorption maximum at 320 nm and the shoulder at 240 nm (Lee, 2000). The fraction F2 did not exhibit bright blue fluorescence, but a weak dark blue to gray colour was observed (**Fig. 50**). On the other hand, the fractions F3, F5a and F5b showed intensive brown colour under the UV-A_{365} light, characteristic for the flavonol-glycosides (Harborne, 1998). Interestingly, the colour of F5a fraction matched exactly that of the quercetin-3-*O*-rhamnoside (quercitrin) standard. The fraction F4 exhibited a faint brown to mauve colour under the UV-A_{365} light, which did not correspond to any of the pure substances (standards) examined here.

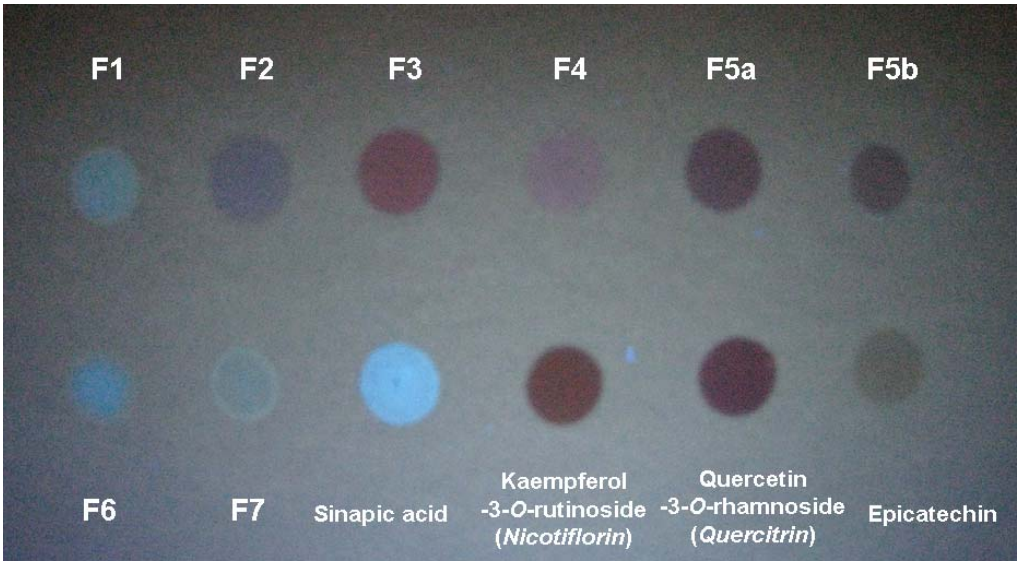

Fig. 50. Fluorescence detection in the HPLC-purified fractions, obtained from a crude extract of *Arabidopsis* Ws-2 wild type seeds. Equal volumes of each sample were dried and visualized under UV-A_{365} light.
The fraction contained following concentrations of analytes: 2.33 mg/ml (F1), 1.6 mg/ml (F2), 0.5 mg/ml (F3), ≤ 0.17 mg/ml (F4), 1.5 mg (F5a), 0.25 mg/ml (F5b), 0.5 mg/ml (F6), ≤ 0.125 mg/ml (F7). The fraction F1 was prepared in 33.3%, the F2, F3, F4, F5a in 100%, the F5b in 50%, while the F6 and F7 in 12.5% methanol solution. The sinapic acid standard (0.3 mg/ml), as well as the flavonoid standards, kaempferol-3-*O*-rutinoside (2 mg/ml), quercetin-3-*O*-rhamnoside (3 mg/ml) and epicatechin (3 mg/ml), were used as the references. All standard solutions were prepared in 100% methanol.

11.1.3. Identification of the main flavonoid and sinapate ester compounds in Ws-2 seed extract using liquid chromatography - mass spectrometry (LC-MS)

Eight HPLC-purified fractions, obtained from *Arabidopsis* Ws-2 seed extract (see above), were further analyzed using LC-MS. The compounds were putatively identified using the mass-to-charge ratio (*m/z*) spectra, obtained in the positive and/ or negative modes, and comparing the mass fragmentation patterns, as well as the retention times to previously reported data (Kerhoas et al., 2006; Routaboul et al., 2006; Böttcher et al., 2008). The MS spectra were recorded from *m/z* 150 up to 850. In the positive mode, the $[M+H]^+$ ions were detected in the MS spectra, together with the cationized adducts $[M+Na]^+$ and the fragment ions, while the $[M-H]^-$ ions were observed in the negative mode. The summarized results of LC-MS analysis of HPLC fractions F1 - F7 are presented in **Table 10**. The results are elaborated in detail here below.

Fraction F1

This fraction contained two compounds with the retention times (RT) at 7.24 and 7.36 min. The first compound was characterized by a strong signal at *m/z* 310 $[M]^+$ in the positive mode, which easily dissociated into the fragment ion at *m/z* 251. The loss of 59 u (mass unit) corresponded to the choline moiety. An additional fragmentation ion was detected at *m/z* 207.

In the positive mode, the second compound exhibited a strong signal at *m/z* 409 characteristic for the $[M+Na]^+$ adduct, which gave rise to fragment ions at *m/z* 225 (loss of glucose moiety) and 207. In addition, the $[M]^+$ ion was detected at *m/z* 386 in the positive mode, while the $[M-H]^-$ ion at *m/z* 385 was observed in the negative mode.

Since both compounds dissociated into the characteristic *m/z* 207 ion, further tandem mass spectrometry (MS-MS) analysis was performed using the collision energies from 5 to 40 eV. The MS-MS spectra in the positive mode indicated further dissociation of the *m/z* 207 ion into the fragment ions at *m/z* 175, 147, 119, 91, 76 and 65. The same MS-MS fragmentation pattern was observed for the sinapic acid standard, which is characterized by the $[M+H]^+$ ion at *m/z* 225 that dissociates into the characteristic fragment ion at *m/z* 207. These results indicated that both compounds in fraction F1 contained a sinapoyl moiety. Thus the first compound (RT = 7.24) is identified as sinapoyl choline (Mw = 310) and the second (RT = 7.36) as sinapoyl glucose (Mw = 386). No other compounds, even at low concentrations, were detected in the F1 fraction.

Fraction F2

The major compound in F2 fraction, with RT = 12.57 min, exhibited a strong $[M+H]^+$signal at *m/z* 611 in the positive mode, with a fragmentation pattern at *m/z* 449 (loss of 162 u corresponds to the elimination of glucose moiety) and *m/z* 303 (loss of 149 u corresponds to the elimination of the rhamnose moiety). The characteristic *m/z* 303 fragment ion was identified as the quercetin $[aglycone + H]^+$ part of the molecule. In addition, the $[M+Na]^+$ adduct at *m/z* 633 was observed in the positive mode, while the $[M-H]^-$ ion at *m/z* 609 was observed in the negative mode. These MS results were in agreement with previously reported data for the flavonoid compound quercetin-glucoside-rhamnoside (Q-Glu-Rha) (Kerhoas et al., 2006; Routaboul et al., 2006).

Besides this dominant component, the F2 fraction contained trace amounts of two compounds. The first one (RT = 6.44 min) was identified as an isomer of sinapoyl choline, according to the same fragmentation pattern as described above (see the fraction F1). The isomer forms of sinapoyl choline were also reported by Böttcher et al., 2008. The second compound (RT = 23.06) was assigned as a glucosinolate with Mw = 477 (for details see section **11.3**).

Fraction F3

This fraction contained three major compounds. The first compound was eluted at RT = 15.28 min, and it was detected by a strong $[M-H]^-$ signal at *m/z* 593 in the negative mode, and signals for the $[M+Na]^+$ adduct at *m/z* 617 and $[M+H]^+$ ion at *m/z* 595 in the positive mode. Two fragment ions were detected at *m/z* 433 and 287, indicating two successive losses of sugar moieties from the $[M+H]^+$ species, corresponding to the initial loss of glucose (162 u) and then of rhamnose (146 u) moieties. The resulting *m/z* 287 fragment ion was characteristic for the kaempferol [aglycone + H]$^+$ part of molecule. Thus, compared to previously reported data this flavonoid compound was identified as kaempferol-3-*O*-glucoside-7-*O*-rhamnoside (K-Glu-Rha) (Kerhoas et al., 2006; Routaboul et al., 2006).

The second major compound was detected at RT = 15.30 min, with a $[M-H]^-$ signal at *m/z* 593 in the negative mode, while in the positive mode this compound showed signals for the $[M+H]^+$ ion at *m/z* 595 and fragment ions at *m/z* 449 and 303. The latter corresponded to quercetine [aglycone + H]$^+$species, which resulted from two successive losses of rhamnose moieties (- 146 u) from the protonated molecule $[M+H]^+$. This fragmentation pattern was in agreement with literature values for the flavonoid compound quercetin-di-rhamnose (Q-Rha-Rha) (Kerhoas et al., 2006; Routaboul et al., 2006).

The third compound found in a large quantity in the F3 fraction was detected at RT = 15.62 min, showing the $[M-H]^-$ ion at *m/z* 623, the $[M+H]^+$ ion at *m/z* 625 and the $[M+Na]^+$ adduct at *m/z* 647. The fragmentation pattern of the protonated molecule gave rise to fragment ions at *m/z* 463 and 317, resulting from the successive elimination of glucose (-162 u) and rhamnose (- 146 u) moieties. The characteristic *m/z* 317 fragment ion corresponded to the isorhamnetin [aglycone + H]$^+$ part of molecule. On the basis of previously reported data this flavonoid compound was identified as isorhamnetin-glucoside-rhamnoside (I-Glu-Rha) (Routaboul et al., 2006).

Beside those three major flavonoid compounds, the fraction F3 contained trace amounts of the Q-Glu-Rha flavonoid, which was identified as described above (see the fraction F2). In addition, a small amounts of the component with RT = 16.26 min, together with a trace amount of the component eluted at RT = 13.53 min, was detected in fraction F3. Both compounds showed a signal only in the negative mode at *m/z* 446 $[M-H]^-$, which putatively derive from the same big anion with z = 2 charge. These two compounds might represent dissociation fragments of the same big molecule with calculated Mw = 894, which is present in the F3 fraction in two isomeric forms. Since the MS spectra were acquired up to *m/z* 850, the intact big molecule was not detected.

Fraction F4

One major compound in the F4 fraction was detected at RT = 17.22 min, which showed a strong signal at *m/z* 577 $[M-H]^-$ in the negative mode and the signals from the $[M+H]^+$ and $[M+Na]^+$ species at *m/z* 579 and 601 in the positive mode, respectively. The protonated molecule dissociated into fragment ions at *m/z* 433 and 287, corresponding to the two successive losses of rhamnoside moieties (-146 u). The resulting *m/z* 287 ion was characteristic for the kaempferol $[aglycone + H]^+$ part of molecule. According to previously published data, this flavonoid compound was identified as kaemperol-3,7-di-*O*-rhamnose (K-Rha-Rha) (Kerhoas et al., 2006; Routaboul et al., 2006).

Besides the dominant K-Rha-Rha compound, the fraction F4 contained small amounts of flavonoids K-Glu-Rha and Q-Rha-Rha, as well as a trace amount of Q-Glu-Rha, which were identified according to the fragmentation patterns described above (see the fraction F3). A flavonoid compound isorhamnetin-di-rhamnoside (I-Rha-Rha) was also detected in fraction F4, but at low concentration. This molecule was identified according to the signals at *m/z* 607 $[M-H]^-$ in the negative mode and *m/z* 609 $[M+H]^+$ in the positive mode, together with fragment ions at *m/z* 463 and 317 (isorhametin aglycone), which resulted from two successive losses of rhamnose moieties (-146 u). This result was in agreement with previously reported data (Routaboul et al., 2006).

In addition, two isomers of the same putative big anion (z = 2), which give rise to the $[M-H]^-$ signal at *m/z* 446, and which was previously observed in the fraction F3 (see for details above), were also detected in the F4 fraction at RT = 15.26 min (small amounts) and RT = 13.53

min (trace amounts), together with the third isomer form detected at RT = 17.17 min (small amounts).

The fraction F4 also contained trace amounts of two components at RT = 4.41 min and RT = 23.06, which likely corresponded to glucosinolate compounds with Mw = 493 and Mw = 477, respectively (for details see section **11.3**).

Fraction F5a

This fraction represented the ascendant part of the dominant peak observed in the HPLC chromatogram. The MS analysis showed that the F5a fraction contained only one compound (RT = 19.32 min), which was present at very high concentration. This compound showed very strong signals at *m/z* 447 $[M-H]^-$ in the negative mode and *m/z* 449 $[M+H]^+$ in the positive mode, together with the weak signal for the $[M+Na]^+$ adduct at *m/z* 471. The protonated molecule $[M+H]^+$ gave rise to the fragment ion at *m/z* 303, characteristic for the quercitin $[aglycone + H]^+$ part of the molecule. The loss of 146 u corresponded to the elimination of the rhamnoside moiety. This result corroborates the previously reported data for the flavonoid compound quercetin-3-*O*-rhamnoside (Q-Rha) (Kerhoas et al., 2006; Routaboul et al., 2006).

Fraction F5b

Together with the fraction F5a, this fraction composed the dominant HPLC peak, taken from the descendant part of the peak. The major compound observed in the high concentration was identified as flavonoid quercetin-3-*O*-rhamnoside (Q-Rha), according to the same MS characteristics and the fragmentation pattern observed in the fraction F5a (for details see above).

Unlike the F5a fraction, the F5b fraction contained the trace amounts of flavonoids Q-Rha-Rha and K-Rha-Rha, identified according to the fragmentation patterns described above (for details see the fractions F3 and F4, respectively). In addition, all three isomers of the same putative big anion (z = 2) with the $[M-H]^-$ signal at *m/z* 446 were detected at RT = 13.53 min, RT = 15.26 min and RT = 17.17 min (for details see above the fractions F3 and F4). However, these compounds were present in the fraction F5b only in the trace amounts.

Fraction F6

Two compounds were detected in fraction F6 and they were present in relatively high concentrations. The first compound was detected at RT = 19.32 and its MS properties in both positive and negative mode, as well as its fragmentation pattern, resembled those of the flavonoid Q-Rha (for details see the fraction F5a).

The second compound (RT = 24.03) showed different MS characteristics, compared to the flavonoid compounds. The MS spectra showed signals at *m/z* 591 $[M-H]^-$ in the negative mode, while the positive mode showed signals for the $[M+Na]^+$ adduct at *m/z* 615 and the $[M]^+$ ion at *m/z* 592. The $[M]^+$ ion dissociated into fragment ions at *m/z* 369 and 207, which resulted from the successive losses of the sinapic acid (-223 u) and glucose (-162 u) moiety, respectively. The tandem MS-MS spectra in the positive mode indicated further dissociation of the *m/z* 207 ion into the same fragment ions observed for sinapoyl choline and sinapoyl glucose, as well as for sinapic acid standard (for details see the fraction F1). Thus, this compound was putatively assigned as di-sinapoyl glucose (Mw = 592).

Fraction F7

This fraction contained only one compound (RT = 26.40), present in relatively high concentration. The MS spectra showed a signal at *m/z* 237 $[M-H]^-$ in the negative mode, while the positive mode showed a signal at *m/z* 239 for the $[M+H]^+$ species, which dissociated into the fragment ion at *m/z* 207, characteristic of the sinapoyl moiety. The fragmentation pattern of the *m/z* 207 ion was the same as observed in the case of sinapoylcholine, sinapoyl glucose and sinapic acid standard (for details see the fraction F1). However, the loss of 32 u (putatively corresponding to the elimination of protonated methoxy group) from the $[M+H]^+$ species remained unexplained. Therefore, the analyzed compound was classified as an unidentified sinapate ester.

The MS results for the eight HPLC-purified fractions were in agreement with previously reported MS data for flavonoids isolated from *Arabidopsis* Ws-2 seeds (Routaboul et al., 2006). Identified flavonoid and sinapate ester compounds from Ws-2 seed extract are listed in the **Table 11**, according to their increasing retention times.

Table 10. Chemical compounds identified by LC-MS and their relative abundance in the HPLC-purified fractions (F1-F7), obtained from the crude extract of *Arabidopsis* Ws-2 wild type seeds. The retention times, RT (min), which were determined by LC-MS, are indicated in parentheses under each compound.
Identified flavonoid compounds: Quercetin-glucoside-rhamnoside (Q-Glu-Rha), Kaempferol-3-*O*-glucoside-7-*O*-rhamnoside (K-Glu-Rha), Quercetin-di-rhamnoside (Q-Rha-Rha), Isorhamnetin-glucoside-rhamnoside (I-Glu-Rha), Kaempferol-3,7-di-*O*-rhamnoside (K-Rha-Rha), Isorhamnetin-di-rhamnoside (I-Rha-Rha), Quercetin-3-*O*-glucoside (Q-Glu), Quercitin-3-*O*-rhamnoside (Q-Rha).

	IDENTIFIED COMPOUNDS		
FRACTION	**MAJOR COMPOUND**	**LOW CONCENTRATION**	**TRACES**
F1	Sinapoylcholine *(RT = 7.24)* Sinapoyl glucose *(RT = 7.36)*		
F2	Q-Glu-Rha *(RT = 12.57)*		Sinapoylcholine *(RT = 6.44)* Glucosinolate Mw = 477 [c] *(RT = 23.06)*
F3	K-Glu-Rha *(RT = 15.28)* Q-Rha-Rha *(RT = 15.30)* I-Glu-Rha *(RT = 15.62)*	Big anion (z=2) [b] *(RT = 16.26)*	Q-Glu-Rha *(RT = 12.57)* Big anion (z=2) [b] *(RT = 13.53)*
F4	K-Rha-Rha *(RT = 17.22)*	K-Glu-Rha *(RT = 15.24)* Q-Rha-Rha *(RT = 15.30)* I-Rha-Rha *(RT = 17.55)* Big anion (z=2) [b] *(RT = 16.26)* Big anion (z=2) [b] *(RT = 17.17)*	Q-Glu-Rha *(RT = 12.57)* Big anion (z=2) [b] *(RT = 13.53)* Glucosinolate Mw = 493 [c] *(RT = 4.41)* Glucosinolate Mw = 477 [c] *(RT = 23.06)*
F5a	**Q-Rha** [a] *(RT = 19.32)*		
F5b	Q-Rha *(RT = 19.32)*		Q-Rha-Rha *(RT = 15.30)* K-Rha-Rha- *(RT = 17.22)* Big anion (z=2) [b] *(RT = 13.53)* Big anion (z=2) [b] *(RT = 16.26)* Big anion (z=2) [b] *(RT = 17.17)*
F6	Q-Rha *(RT = 19.32)* di-Sinapoylglucose *(RT = 24.03)*		
F7	Unidentified sinapate ester *(RT = 26.40)*		

[a] The fraction F5a contained only Q-Rha in high concentration, thus defined as almost pure fraction.
[b] The fragment of the molecule, detected as a big anion with (z=2) charge, which was present in three isomer forms.
[c] Unidentified glucosinolate compounds with determined molecular weight (Mw).

Table 11. Flavonoid and sinapate ester compounds identified by LC-MS, with determined retention times (RT) and molecular weights (Mw).

RT (min)	COMPOUNDS		Mw
	LABEL	NAME	
6.44	Sinapoyl-Ch	Sinapoylcholine	310
7.24	Sinapoyl-Ch	Sinapoylcholine	310
7.36	Sinapoyl-Glu	Sinapoylglucose	386
12.57	Q-Glu-Rha	Quercetin-glucoside-rhamnoside	610
13.53	Big anion (z=2)	?[a]	894?[a]
15.28	K-Glu-Rha	Kaempferol-3-*O*-glucoside-7-*O*-rhamnoside	594
15.30	Q-Rha-Rha	Quercetin-di-rhamnoside	594
15.62	I-Glu-Rha	Isorhamnetin-glucoside-rhamnoside	624
16.26	Big anion (z=2)	?[a]	894?[a]
17.17	Big anion (z=2)	?[a]	894?[a]
17.22	K-Rha-Rha	Kaempferol-3,7-di-*O*-rhamnoside	578
17.29	Q-Glu	Quercetin-3-*O*-glucoside	464
17.55	I-Rha-Rha	Isorhamnetin-di-rhamnoside	608
17.66	Big anion (z=2)	?[a]	894?[a]
19.32	Q-Rha	Quercetin-3-*O*-rhamnoside	448
24.03	di-Sinapoyl-Glu	di-Sinapoylglucose	529
26.40	Sinapoyl-Me	Methyl-containing sinapate ester	238

[a] The structure of the compound was not determined, although the occurrence of a big anion with (z=2) charge was detected in LC-MS negative operating mode. This anion might be a dissociating fragment of the bigger molecule with putative Mw = 894. Comparing the relative retention times determined in this study and in agreement with rescaled values from Routaboul et al, 2006, the unidentified compound with Mw = 894 might represent four isomer forms of quercetin-rhamnoside dimer .

11.2. Detection of sinapate esters in *Arabidopsis* mutant *fah1-2* seeds

11.2.1. Fluorescence detection in fah1-2 seed extracts

The *fah1-2 Arabidopsis* line (previously named *sin1-2*) is a mutant with a defect in the general phenylpropanoid pathway, caused by the mutation in the gene that encodes for ferulate-5-hydoxylase (F5H) enzyme (Chapple et al., 1992; Ruegger et al., 1999). As a consequence, this mutant has blocked biosynthesis of sinapate esters. Aiming to determine the role of sinapate esters, as compared to flavonoids, in the UV protection of *Arabidopsis* seeds (see part II, chapter **5**, section **16**), we examined the accumulation of sinapate esters in seeds of the *fah1-2* mutant (Col-0 accession). Extracts from *fah1-2* mutant seeds and wild type Col-0 seeds were prepared in two different solvents (methanol and acetonitrile) in order to exclude the effect of solvent polarity on extraction efficiency. When excited by long wave UV light, the sinapoyl esters exhibit a bright blue fluorescence (Chapple et al., 1992; Lorenzen et al., 1996; Sheahan, 1996), allowing easy preliminary detection of these compounds. Thus the crude extracts from *fah1-2*, as well as background Col-0 seeds, were visually inspected for the fluorescence under UV-A light (λ = 365 nm).

The Col-0 seed extract, prepared in both solvents, showed intensive blue fluorescence (**Fig. 51**). For comparison, the crude seed extract of another wild type line (Ws-2) was also examined, exhibiting intensive blue fluorescence that indicated the presence of sinapate esters. This result was in agreement with the occurrence of sinapoylcholine and sinapoylglucose in the Ws-2 seed extract, which were detected and identified by MS analyses (see **Table 10** and **Table 11**). Since the blue fluorescence was observed in a methanolic solution of sinapic acid standard, this effect was attributed to the sinapoyl moiety of sinapate ester molecules.

In contrast, no fluorescence was observed in both extracts of *fah1-2* seeds, consistent with the lack of sinapate esters, as well as free sinapic acid (**Fig. 51**). The *fah1-2* seed extracts were further examined in detail by MS (see below).

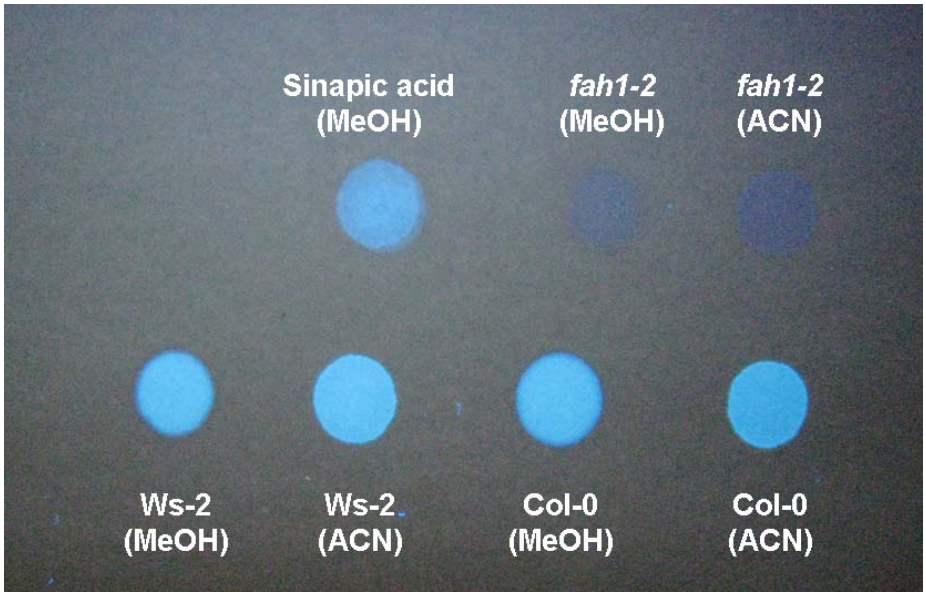

Fig. 51. Preliminary detection of sinapic esters in crude seed extracts from three *Arabidopsis* lines (*fah1-2*, Col-0 and Ws-2). Samples were prepared from 50 mg seeds extracted either with 75% methanol (MeOH) or 75% acetonitrile (ACN) solution. Extracts were visualized under UV-A_{365} light. The sample of sinapic acid standard (0.3 mg/ ml in 100% methanol) was used as a reference.
The plant genotypes were: a sinapate ester mutant (*fah1-2*) in the Col-0 accession, a wild type Columbia (Col-0) and a wild type Wassilewskija (Ws-2).

11.2.2. LC-MS analysis of sinapate esters in fah1-2 seed extracts

Crude extracts from mutant *fah1-2* and wild type Col-0 seeds, prepared in both methanol and acetonitrile, were examined for the presence of sinapate esters using MS. The following substances were screened: sinapoylcholine (Mw = 310), sinapoylglucose (Mw = 386), sinapoylmalate (Mw = 340) and sinapic acid (Mw = 224). In the positive MS operative mode, both Col-0 extracts showed a strong signal at *m/z* 310, characteristic for the $[M]^+$ species of sinapoylcholine. The sinapoylglucose $[M+H]^+$ signal at *m/z* 387 was not detected. Instead, the Col-0 extracts exhibited a weak $[M]^+$ signal at *m/z* 386 and a strong $[M+Na]^+$ signal at *m/z* 409, the characteristic signals for sinapoylglucose that were previously observed in the HPLC-purified fractions from Ws-2 seeds (see section **11.1.3**). No sinapoylmalate was detected in both Col-0 seed extracts, since no signal at *m/z* 341 $[M+H]^+$ nor at *m/z* 340 $[M]^+$ was observed. The Col-0 seed extracts also showed the signal at *m/z* 225, characteristic of the $[M+H]^+$ species of free sinapic acid or sinapoyl moiety, resulting from the fragmentation of the sinapoylglucose $[M+Na]^+$ adduct (for details see the fraction F1 in section **11.1.3**). The MS spectra showed a

signal at *m/z* 239 in the methanolic Col-0 extract, which was also observed in the F7 fraction of the Ws-2 seed extract, putatively representing a [M+H]+ species of an unidentified sinapate ester (see section **11.1.3**).

On the other hand, both *fah1-2* seed extracts showed no MS signals at *m/z* 310, 386/ 409 and 225 that would correspond to the positive mode signals for sinapoylcholine, sinapoylglucose and sinapic acid, respectively, detected in the Col-0 seed extracts. In addition, no signals in the positive MS mode at *m/z* 341 (sinapoylmalate) and 239 (unidentified sinapate ester in methanolic Ws-2 and Col-0 extracts) were detected in extracts from *fah1-2* seeds.

11.3. Detection and characterization of glucosinolates isolated from *Arabidopsis* wild type Ws-2 seeds

Glucosinolates are sulfur-rich plant secondary metabolites whose basic skeleton consists of a β-thioglucose residue, an N-hydroxyiminosulfate moiety and a variable side chain (for chemical structure see **Fig. 39**, chapter **1**, section **5.2.2.**). Plants synthesise a large variety of glucosinolates, and many of them are still unidentified. Although some smaller amounts of glucosinolates were co-extracted from *Arabidopsis* seeds together with flavonoids and sinapate esters (**Table 10**), due to their hydrophilic and anionic nature, and in order to obtain their higher yields, glucosinolates were extracted and analysed separately from flavonoids and sinapate esters, using better suited purification protocols. The extract from whole Ws-2 seeds was first analysed by HPLC, and seven separated fractions (from G-F1 to G-F7), corresponding to seven prominent HPLC peaks were collected and than subjected to LC-MS analysis.

The LC-MS analyses of glucosinolate-containing fractions were performed recording mass spectra from *m/z* 225 up to 575 for parent and daughter ions in both the positive and negative ionization modes. In spite of large number of the *m/z* signals and great diversity of fragmentation patterns, all substances belonging to the glucosinolate class shared common LC-MS features. All glucosinolates had relatively low retention times (RT), appearing close to the peak of injection. This indicated their polar, anionic nature. Glucosinolates generally responded well only in a negative ionization mode, showing a prominent signal of intact parent $[M-H]^-$ ion. Characteristically, this parent ion appeared very stable and its fragmentation was not observed under standard experimental conditions (e.g. at the collision energy of 25 eV). Due to the

presence of at least two sulfur atoms, all glucosinolates showed a specific isotopic pattern[1]. In positive mode, the signal of an intact parent $[M+H]^+$ ion or possible molecular adducts $[M+Na]^+$ or $[M+K]^+$ was difficult to detect, since they readily fragmented into the daughter ions. Depending on the collision energy, the fragmentation of the parent $[M+H]^+$ ion occurs usually in two steps. In the first step, a typical loss of 80 u that corresponded to the loss of SO_3^- group was observed. Formed daughter ion was further fragmented, loosing 162 u, what is characteristic for the elimination of glucose moiety. Detailed fragmentation pattern for glucosinolates contained in each HPLC purified fraction is given her below. The summarized results of LC-MS analysis of glucosinolate-containing HPLC fractions are presented in Table 12.

Fraction G-F1

This fraction contained one dominant component (RT = 2.56 min), which was identified as glucosinolate with Mw = 423, together with traces amounts of other unidentified molecules. In the negative mode, intensive signal of the *m/z* 422 was observed for stable $[M-H]^-$ ion, while in the positive mode, the parent $[M+H]^+$ ion was first fragmented into the *m/z* 344 ion (- 80 u), and subsequently into *m/z* 182 daughter ion (-162 u). According to the determined Mw and the fragmentation pattern, we suggested that this substance might be an aliphatic glucosinolate, 3-methylsulfinylpropyl glucosinolate, 3-MSOP (known as glucoiberin), which was also previously reported to occur in leaves, roots, inflorescences and seeds of *Arabidopsis thaliana*, as well as in other related species of *Brassicaceae* (Kliebenstein et al., 2001; Brown et al., 2003; Bennett et al., 2004; Le Gall et al., 2005).

Fraction G-F2

This fraction appeared as a complex mixture of different molecules. However, two compounds prevailed in G-F2 fraction, one was yet unidentified glucosinolate with Mw = 488 (RT = 2.47 min), and other was assigned a putative glucosinolate with Mw = 369 (RT = 7.08 min). These compounds, together with other substances found in small concentrations or trace

[1] Most elements appear in nature as isotope mixtures. These isotopes are responsible for the peaks in the mass spectrum appearing as isotopic clusters that are characteristic of the elemental composition of particular organic compound. These clusters may contain signals that differ for 1 u, such as M, M+1, M+2, M+3 etc. The intensity of the *m/z* peaks depends on the relative abundance of each isotope in nature. Naturally occurring carbon, for instance, is a mixture of two isotopes ^{12}C and ^{13}C that represent 98.9% and 1.1%, respectively. Some atoms have isotopic compositions that are more obvious, such as chlorine, bromine, selenium and sulfur. In nature, sulfur has four isotopes, ^{32}S, ^{33}S, ^{34}S and ^{35}S, with relative abundances of 95.02%, 0.75%, 4.21% and 0.02%, respectively (de Hoffmann and Stroobant, 2007).

amounts, exhibited the typical glucosinolate signatures (a strong signal in negative mode for $[M-H]^-$ ion and an isotopic pattern). In positive mode, first glucosinolate (Mw = 488) showed a weak signal for the $[M+H]^+$ ion at *m/z* 489 and the fragmentation ion at *m/z* 409 (-80 u). In contrast, the fragmentation of the second putative glucosinolate (Mw = 369) was not observed.

Fraction G-F3

Besides the trace amounts of different unidentified molecules, this fraction contained one major compound, which was identified as a glucosinolate with Mw = 493 (RT = 3.41 min). According to the *m/z* signal of molecular ions detected in negative and positive ionization modes, where stable $[M-H]^-$ ion exhibited a strong signal with the typical isotopic pattern, and $[M+H]^+$ ion dissociated into fragment ions at *m/z* 414 (- 80 u), 252 (-162 u) and 202, we suggested that this substance is likely an aliphatic glucosinolate, 8-methylsulfinyloctyl glucosinolate (8-MSOO), also known as glucohirsutin. This glucosinolate was previously reported to occur in different vegetative organs of *Arabidopsis thaliana*, and particularly in mature seeds (Kliebenstein et al., 2001; Brown et al., 2003; Le Gall et al., 2005).

Fraction G-F4

This fraction contained particularly abundant and almost pure substance, which was identified as glucosinolate compound with Mw = 481 (RT = 8.31 min). In the negative mode, it showed a strong signal of stable $[M-H]^-$ ion, with typical isotopic pattern. In the positive mode, the parent $[M+H]^+$ ion readily dissociated giving rise to the daughter ions at *m/z* 402 (-80 u), 240 (-162 u), 118 and 105. It indicated that this substance is an aromatic glucosinolate, 3-benzoyloxypropyl glucosinolate (3-BzOP), also known as glucomalcomiin. This fragmentation pattern correlated well with that of another analogous aromatic glucosinolate, 4-benzoyloxybutyl glucosinolate (4-BzOP), reported by Graser et al. (2001). The fragmentation pattern and the structure of 3-BzOP was further confirmed by tandem mass spectrometry (MS-MS), using the collision energy from 2.5 to 40 eV to dissociate further the first-order daughter ions (*m/z* 402, 240, 118). The occurrence of 3-BzOP in *Arabidopsis* seeds was also reported by Graser et al., 2001; Kliebenstein et al., 2001; Brown et al., 2003.

Fraction G-F5

The major compound in G-F5 fraction was identified as glucosinolate with Mw = 477 (RT = 21.02 min), since it exhibited a strong and stable $[M-H]^-$ ion at *m/z* 476 in the negative ionization mode, and a weak $[M+H]^+$ ion at *m/z* 478 in the positive ionization mode, which readily dissociated into the daughter ions at *m/z* 398 (-80 u), 236 (-162 u), 186 and 138. According to determined Mw and fragmentation pattern, we suggested that this substance is likely an aliphatic glucosinolate, 8-metylthiooctyl glucosinolate (8-MTO), which is a common glucosinolate found in different organs, including the seeds of *Arabidopsis thaliana* (Kliebenstein et al., 2001; Brown et al., 2003). It is also found in other related *Brassicaceae* species (Bennett et al., 2004).

Fraction G-F6

This fraction represents a mixture of different, yet unidentified molecules, as well as two dominant compounds that were identified as glucosinolates. The first glucosinolate was characterized by Mw = 493 (RT = 4.42 min), and its fragmentation pattern in the positive ionization mode resembled that of 8-methylsulfinyloctyl glucosinolate, the substance found in fraction G-F3 (Table 12). However, these two substances had different retention times, probably indicating that they might be two isomer forms of the same glucosinolate. The second glucosinolate with Mw = 477 had similar fragmentation pattern and retention time (RT = 21.19 min) as glucosinolate identified in G-F5 fraction, thus indicating probably the occurrence of 8-metylthiooctyl glucosinolate in fraction F-G6.

Fraction G-F7

This fraction contained only one substance, which did not exhibit the LC-MS features characteristic for glucosinolates. Instead, it was identified as flavonoid kaempferol-rhamnoside (Mw = 432, RT = 21.45 min). In the positive ionization mode, it exhibited a strong $[M+H]^+$ ion at *m/z* 433 and the fragment ion at *m/z* 287, characteristic for kaempferol aglycone. The loss of 146 u resulted from the elimination of rhamnose moiety. The fragmentation pattern of kaempferol-rhamnoside was also confirmed by the analysis of the *m/z* spectra in the negative ionization mode. This result corroborated with MS data for kaempferol-rhamnoside found in *Arabidopsis* Ws-2 seeds extracts, which was reported by Routaboul et al. (2006).

Table 12. Glucosinolates and other chemical compounds characterized by LC-MS and their relative abundance in the HPLC-purified fractions (from G-F1 to G-F7) obtained from the seed extract of *Arabidopsis* Ws-2 wild type seeds. Molecular weights (Mw) and the retention times (RT, min) were determined by LC-MS. For compounds that prevail in each fraction, the mass-to-charge ratio (*m/z*) was indicated for deprotonated molecular ions, [M-H]-, as well as protonated molecular ions, [M+H]+, observed in the negative and positive ionization modes, respectively. Fragmentation pattern of parent [M+H]+ ions was recorded in the positive ionization mode. The HPLC-purified fraction G-F4 (marked with asterisk) contained almost pure and highly concentrated 3-BzOP.
Identified substances: 3-MSOP = 3-methylsulfinylpropyl glucosinolate (glucoiberin), 8-MSOO = 8-methylsulfinyloctyl glucosinolate (glucohirsutin), 3-BzOP = 3-benzoyloxypropyl glucosinolate (glucomalcomiin), 8-MTO = 8-metylthiooctyl glucosinolate, K-Rha = kaempferol-rhamnoside flavonoid.

FRACTION	MAJOR COMPOUND	Mass spectra (*m/z*)			LOW CONCENTRATION	TRACES
		$[M-H]^-$	$[M+H]^+$	Fragmentation ions (positive mode)		
G-F1	Glucosinolate Mw=423 *(RT=2.56)* **3-MSOP**	422	424	344, 182		Various unidentified molecules
G-F2	Glucosinolate Mw=488 *(RT=2.47)*	487	489	409	Possible Glucosinolate Mw=390 *(RT=2.41)*	Possible Glucosinolate Mw=450, 518, 520, 620
	Possible Glucosinolate Mw=369 *(RT=7.08)*	368			Possible Glucosinolate Mw=470 *(RT=2.59)*	
G-F3	Glucosinolate Mw=493 *(RT=3.41)* **8-MSOO**	492	494	414, 252, 202		Various unidentified molecule
G-F4*	Glucosinolate Mw=481 *(RT=8.31)* **3-BzOP**	480	482	402, 240, 118, 105		
G-F5	Glucosinolate Mw=477 *(RT=21.02)* **8-MTO**	476	478	398, 236, 186, 138	Unidentified molecule Mw=164 *(RT=15.00)*	Glucosinolate Mw=493 *(RT=4.36)*
G-F6	Glucosinolate Mw=493 *(RT=4.42)*	492	494	414, 252, 202	Various unidentified molecules	
	Glucosinolate Mw=477 *(RT=21.19)*	476	478	398, 236, 186		
G-F7	**K-Rha** Mw=432 *(RT=21.45)*	431	433	287		

11.4. Absorption spectroscopy of compounds found in *Arabidopsis thaliana* seed extracts

The UV absorption characteristics of HPLC-purified fractions, obtained from *Arabidopsis* Ws-2 seed extracts, were further studied using conventional UV absorption spectroscopy (λ = 200-400 nm) in solution and VUV-UV absorption spectroscopy (λ = 125-340 nm) in dry, thin films.

11.4.1. Conventional UV absorption spectroscopy of crude extracts and HPLC-purified fractions from Arabidopsis thaliana seeds

Prior to the VUV-UV absorption spectroscopy, crude extracts from *Arabidopsis* seeds, as well as and purified fractions extracted from Ws-2 whole seeds, were examined by conventional UV absorption spectroscopy in solution. The absorption spectra were measured in a wavelength range from 200 to 400 nm.

11.4.1.1. UV absorption spectra of crude extracts from wild type Ws-2 and mutant tt4-8 seeds

The results in the present work revealed extreme UV resistance of Ws-2 wild type seeds, compared to the seeds of flavonoid-lacking *tt4-8* mutant (see part II, chapter **6**, section **18**). Our previous HPLC studies revealed no flavonoid accumulation in the seeds of the *tt4-8* mutant (Zalar, 2004). Using conventional spectroscopy in solution, we first measured the UV absorption spectra (200-400 nm) for two crude extracts that were obtained from Ws-2 and *tt4-8* seeds. Both samples were prepared in parallel, using the same extraction protocol. The Ws-2 and *tt4-8* seed extracts exhibited significant differences in their UV absorption features (**Fig. 52**).

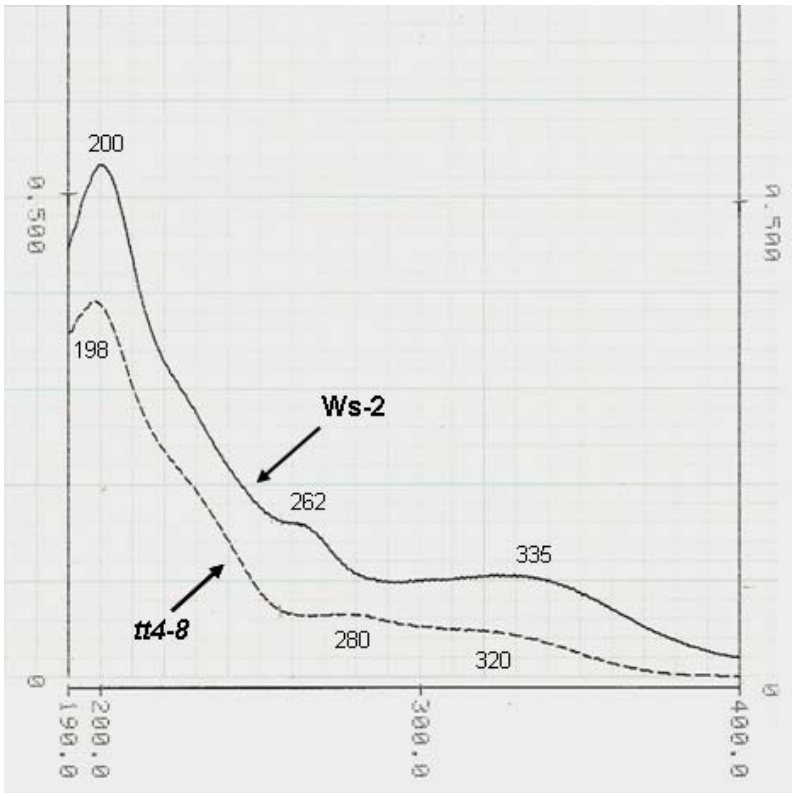

Fig. 52. The UV absorption spectra of crude methanolic extracts obtained from *Arabidopsis* seeds Ws-2 (wild type) and *tt4-8* (flavonoid deficient mutant). Both samples were prepared from 100 mg seeds, using the same extraction protocol. The spectra were recorded in 15% methanol solution, using 20 µl of each seed extracts.

11.4.1.2. UV absorption spectra of flavonoid- and sinapate ester-containing purified fractions from Ws-2 seeds

After determining the content by LC-MS, the UV absorption characteristics of eight HPLC-purified Ws-2 seed fractions (section **11.1**) were first examined by conventional absorption spectroscopy in solution. Absorption spectra for each fraction are presented separately in **Fig. 53D** and **Fig. 54A-D**.

The fraction F1, prepared as a 33.3% methanolic solution, showed one weak maximum of absorption at about 275 nm (**Fig. 53A**). Although LC-MS analysis revealed that this fraction contained sinapate esters, sinapoyl choline and sinapoylglucose, conventional UV absorption spectra did not show a sinapate specific absorption maximum at about 320 nm (Lee, 2000).

The fraction F2, prepared in 100% methanol, showed two absorption maxima, a stronger peak at 262 nm and one weaker peak at 350 nm (**Fig. 53B**). This absorption profile was characteristic for flavonol-containing compounds with *O*-alkyl or *O*-glycosyl moiety (Bohm, 1998). This result was in agreement with LC-MS results (see chapter **3**, section **11.1.3.**).

Flavonoid-containing fraction F3 (in 100% methanol) exhibited two strong absorption maxima at 255 nm and 345 nm (**Fig. 53C**), indicating the presence of flavonols with the *O*-alkyl or *O*-glycosyl moiety *O*-alkyl or *O*-glycosyl moiety (Bohm, 1998). This fraction was composed of the mixture of three flavonoid compounds (see **Table 10,** chapter **3,** section **11.1.3**).

The fraction F4, prepared in 100% methanol, absorbed strongly at 262 nm and 340 nm, indicating the presence of a dominant flavonol compound (**Fig. 53D**).

Both fractions, the F5a (in 100% methanol) and the F5b (50% methanolic solution), which corresponded to the ascendant and descendent parts of the dominant HPLC peak, absorbed strongly in the UV region. These fractions contained flavonoid queretin-3 *O*-rhamnoside (quercitrin) in very high concentration, thus absorbing strongly at 262 nm and in the region around 350 nm (**Fig. 54A** and **B**). The absorption curves of the F5a and F5b fractions were compared to those for queretin-3 *O*-rhamnoside (quercitrin) standard (**Fig. 55A**).

The fractions F6 and F7 (12.5% methanolic solutions) showed an absorption maximum at 320 nm (**Fig. 54C** and **D**). In addition, the F7 fraction exhibited a prominent shoulder at 240 nm, while the F6 fraction had only a weak shoulder at the same wavelength. This UV absorption profile was characteristic for the substances containing a sinapoyl moiety (Lee, 2000).

Fig. 55B illustrates the UV absorption characteristics of a typical flavonoid compound (e.g. quercitrin from the fraction F5a and F5b) and a sinapoyl-containing compound (fraction F7), both isolated from Ws-2 seeds. These absorption curves are compared to the absorption curve of a DNA sample which had a typical absorption maximum at 260 nm. A shoulder observed at about 220 nm in the DNA absorption curve likely originates from the impurities (e.g. chaotropic slats such as quanidine hydrochloride in phosphate buffer) that remained after the purification step of DNA sample (*nptII* PCR product) using the QIAquick® PCR purification kit.

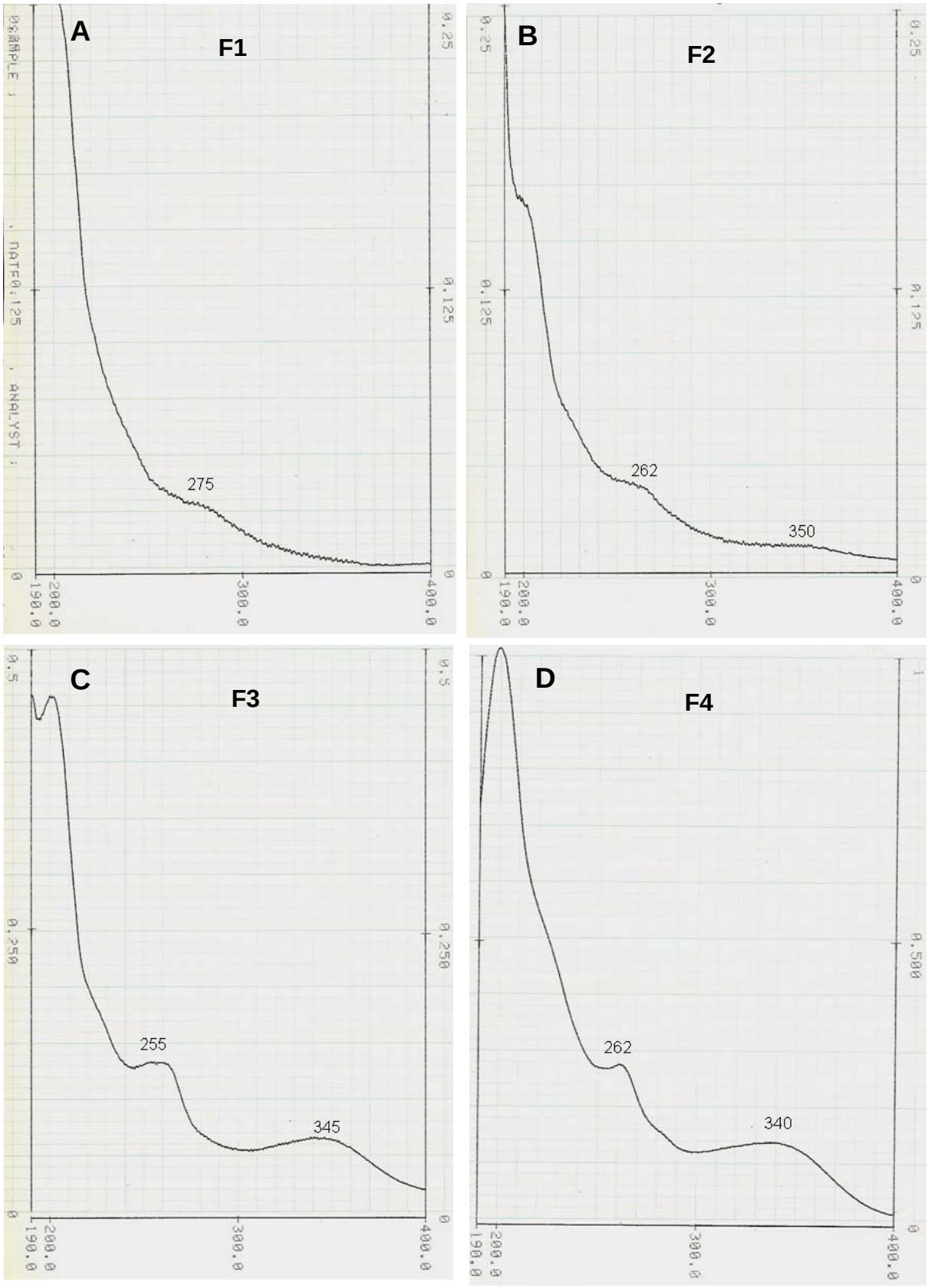

Fig. 53. The absorption spectra of HPLC fractions F1, F2, F3 and F4 purified from the Ws-2 seed extract, measured by conventional UV spectroscopy in solution.
(A) The F1 fraction (0.125 mg/ml in 33.3% methanol, 20µl). (B) The F2 fraction (0.125 mg/ml in 100% methanol, 10µl). (C) The F3 fraction (0.125 mg/ml in 100% methanol, 10µl). (D) The F4 fraction (≤ 0.17 mg/ml in 100% methanol, 10µl).

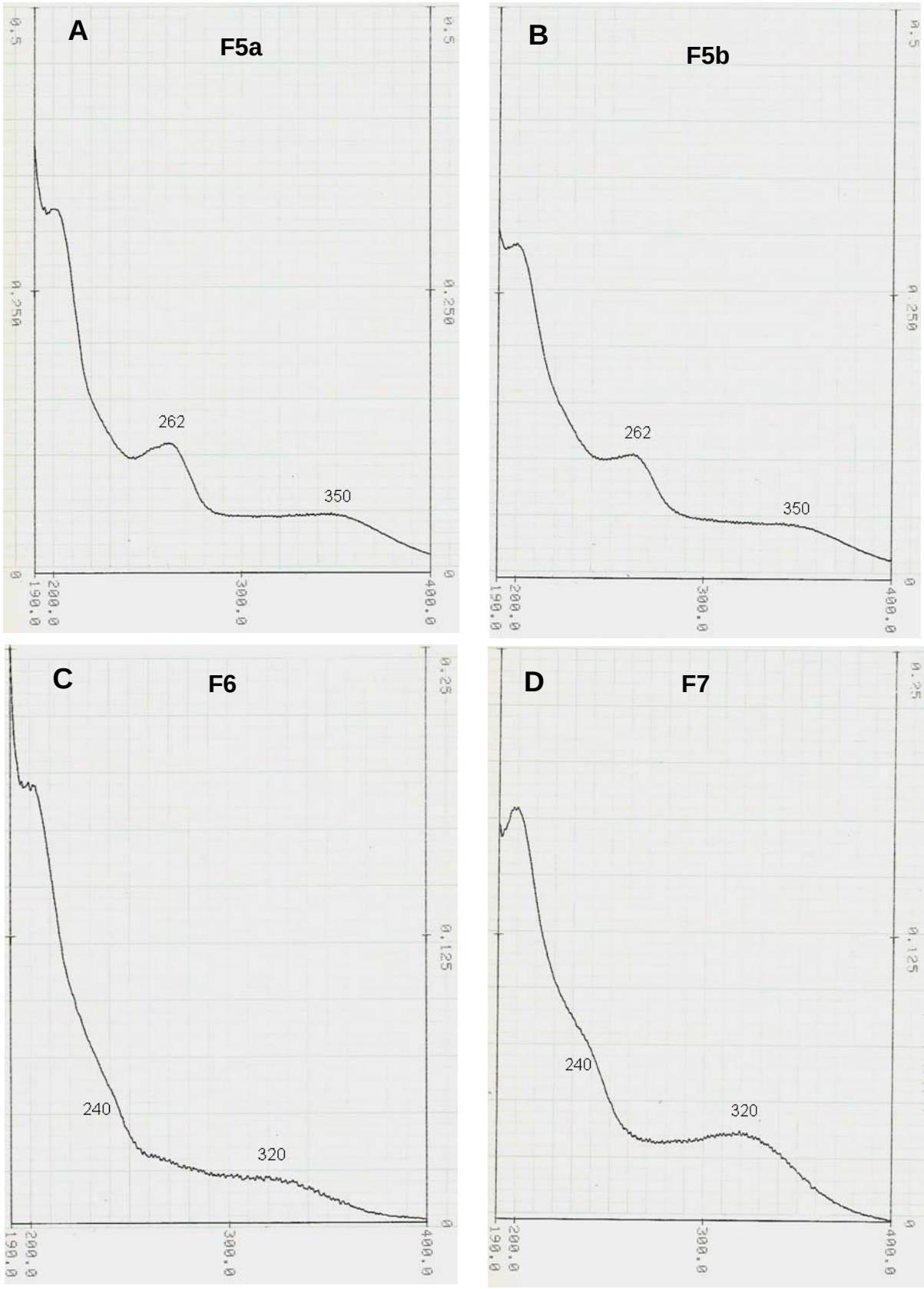

Fig. 54. The absorption spectra of HPLC fractions F5a, F5b, F6 and F7 purified from the Ws-2 seed extract, measured by conventional UV spectroscopy in solution.
(A) The F5a fraction (0.125 mg/ml in 33.3% methanol, 10µl) represents an ascendant part of the dominant HPLC peak. (B) The F5b fraction (0.125 mg/ml in 50% methanol, 10µl) represents a descendant part of the dominant HPLC peak. (C) The F6 fraction (0.125 mg/ml in 12.5% methanol, 20µl). (D) The F7 fraction (≤ 0.125 mg/ml in 12.5% methanol, 10µl).

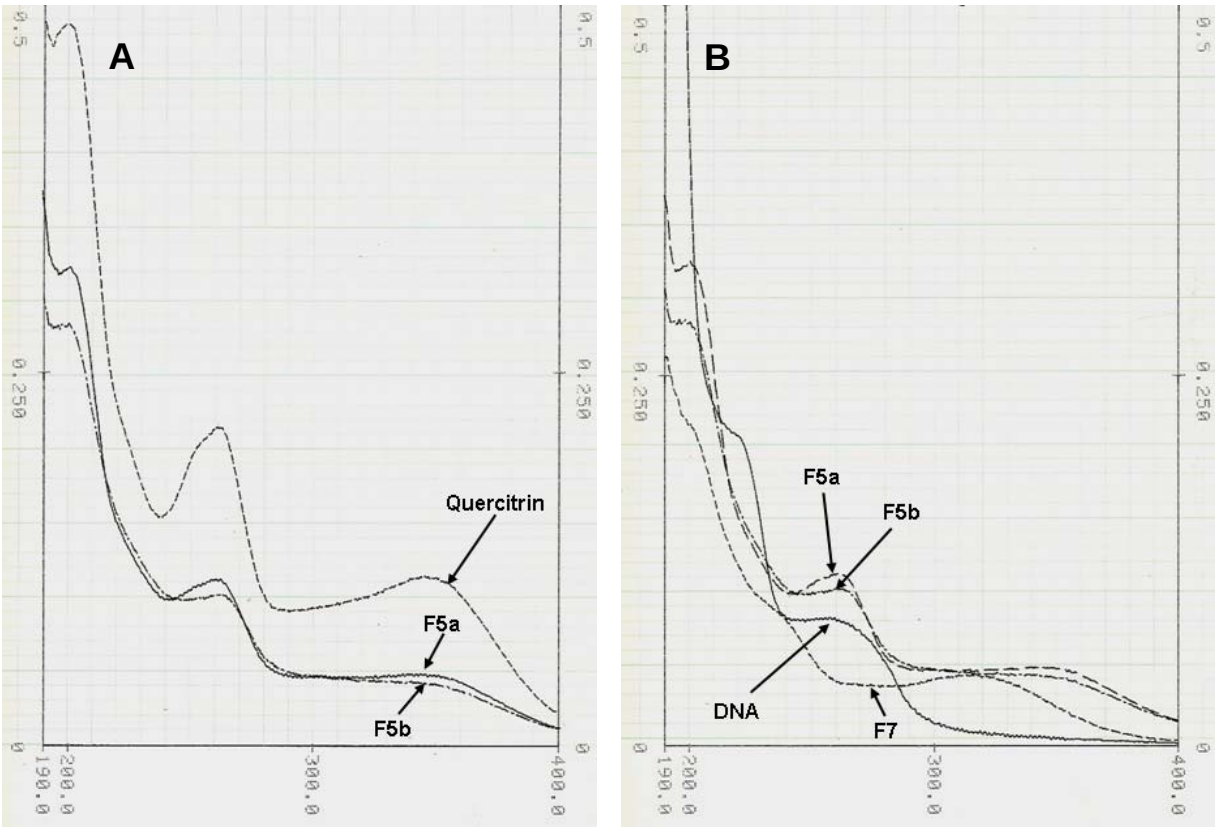

Fig. 55. The absorption spectra of HPLC fractions F5a and F5b purified from the Ws-2 seed extract, and measured by conventional UV spectroscopy in solution.
(A) The absorption curves for the F5a fraction (0.125 mg/ml in 100% methanol, 10µl) and the F5b fraction (0.125 mg/ml in 50% methanol, 10µl) are compared to those for quercetin-3 *O*-rhamnoside (quercitrin) standard, prepared as 0.3 mg/ml solution in 100% methanol (10µl). The F5a and F5b fractions correspond to the ascendant and descendant parts of the dominant HPLC peak, respectively, which contains quercitin in high concentration. (B) The absorption spectra of the flavonoid-containing fractions, the F5a (0.125 mg/ml in 100% methanol, 10µl) and the F5b (0.125 mg/ml in 50% methanol, 10µl), as well as a sinapoyl-containing fraction F7 (≤ 0.125 mg/ml in 12.5% methanol, 10µl), are compared to the absorption curve of a DNA sample (10 ng/µl of purified *nptII* PCR product in water, 10µl).

11.4.1.3. UV absorption spectra of glucosinolate-containing purified fractions from Ws-2 seeds

Following LC-MS analysis, UV absorption spectra of seven HPLC-purified fractions (from G-F1 to G-F7) were first measured in solution, in the 200 - 400 nm wavelength range. Their UV absorption features are presented in Table 13. Generally, these glucosinolate-containing fractions, with exception of fraction G-F7 that contained flavonoid kaempferol-rhamnoside, did not absorb in the UV part of the spectrum above 270 nm. On other hand, the absorption of glucosinolates steeply increased below ~250 nm. Here we single out 3-benzoyloxypropyl glucosinolate (3-BzOP) as the only glucosinolate compound that exhibited a well resolved peak above 270 nm, with λ_{max} = 273 nm and a shoulder at 280 nm. This correlated with the aromatic structure of this glucosinolate.

Table 13. Spectral features of glucosinolate-containing fractions obtained from *Arabidopsis* Ws-2 seed extract. Fractions were separated by HPLC and analysed by conventional UV absorption spectroscopy (λ = 200-400 nm) in aqueous (G-F1, G-F2, G-F3), 50% methanol (G-F4, G-F5, G-F6) or 100% methanol (G-F7) solutions. The dominant compounds in each fraction were determined by LC-MS as follows: 3-MSOP = 3-methylsulfinylpropyl glucosinolate (glucoiberin), 8-MSOO = 8-methylsulfinyloctyl glucosinolate (glucohirsutin), 3-BzOP = 3-benzoyloxypropyl glucosinolate (glucomalcomiin), 8-MTO = 8-metylthiooctyl glucosinolate, K-Rha = kaempferol-rhamnoside flavonoid. Fraction G-F4 contained high concentration of almost pure 3-BzOP (marked with asterisk). Abbreviations: Is = small inflection, M = local minimum of absorption, Ms = small local minimum of absorption, P = absorption peak, Pb = broad absorption peak, Ppr = poorly resolved small peak, SH = shoulder

FRACTION	MAJOR COMPOUND	SPECTRAL FEATURES (nm)
G-F1	3-MSOP	260 → 200 steep increase of absorption
G-F2	Glucosinolate 1 (Mw=488) ? Glucosinolate 2 (Mw=369)	330 (Ppr) 270 → 200 steep increase of absorption 260 (Is) 230 (Is) 210 (Is)
G-F3	8-MSOO	260 → 222 steep increase of absorption 222 (P) 200 (M)
G-F4*	**3-BzOP**	280 (SH) 273 (P) 260 (Ms) 230 (P) 208 (M) 208 →200 steep increase of absorption
G-F5	8-MTO	250 → 223 steep increase of absorption 223 (P) 210 (Ms) 210 → 200 steep increase of absorption
G-F6	Glucosinolate 1 (Mw=493) 8-MTO	250 → 223 steep increase of absorption 224 (P) 212 (Ms) 212 → 200 steep increase of absorption
G-F7	K-Rha	350 (Pb) 320 (M) 263 (P) 245 (M) 245 → 200 steep increase of absorption

11.4.2. VUV-UV absorption spectroscopy of Arabidopsis thaliana seed extracts and HPLC-purified fractions

In order to better examine the UV-B, UV-C, as well as far UV spectroscopic characteristics of compounds found in *Arabidopsis* seeds, thin dry films of crude seed extracts, as well as HPLC-purified seed fractions were analyzed by VUV-UV absorption spectroscopy. Using synchrotron light, the VUV-UV absorption spectra were measured in a wavelength range from 125 to 340 nm. In this way, we extended our previously measured UV absorption spectra (see the section above) into the vacuum UV region (VUV). In addition to conventional solution UV spectroscopy, the VUV-UV spectra revealed more information about the UV absorption characteristics of analyzed substances in dry state, which would resemble the conditions in a dry seeds. Using qualitative similarity with DNA absorption spectra, we evaluated potential UV screening effectiveness of compounds found in *Arabidopsis* seeds.

11.4.2.1. VUV-UV absorption spectra of crude extracts from wild type Ws-2 and mutant tt4-8 seeds

Conventional spectroscopy in solution revealed differences in the UV absorption characteristics of Ws-2 and *tt4-8* seed extracts (see section **11.4.1**). In an attempt to extend the absorption spectra below 200 nm, and to investigate the absorption characteristics of seed compounds in the dry state, we further measured the VUV-UV absorption spectra of Ws-2 and *tt4-8* seed extracts **(Fig. 56**). Both samples were prepared in parallel, using the same extraction protocol, and thin films were prepared by drying the same volume of the Ws-2 and *tt4-8* seed extracts. The Ws-2 crude extract absorbed strongly in the VUV-UV region, showing a broad and prominent peak at 204 nm (region II), a small, poorly resolved peak at about 265 nm (region I), and increased absorbance towards the longer wavelengths at the end of spectrum (340 nm). The *tt4-8* crude extract showed a well resolved peak at 202 nm (region II), which was less intense than the peak at 204 nm in the Ws-2 extract. However, the *tt4-8* sample lacked the week peak that was observed in region I for the Ws-2 sample. Instead, an absorption minimum at 260 nm was observed. Unlike for the Ws-2 sample, the absorption curve for *tt4-8* extract was flat towards 340 nm. Both seed extracts, the Ws-2 and *tt4-8*, exhibited a steep increase in absorbance in the VUV part of spectrum (below 200 nm), which corresponds to the previously described region III.

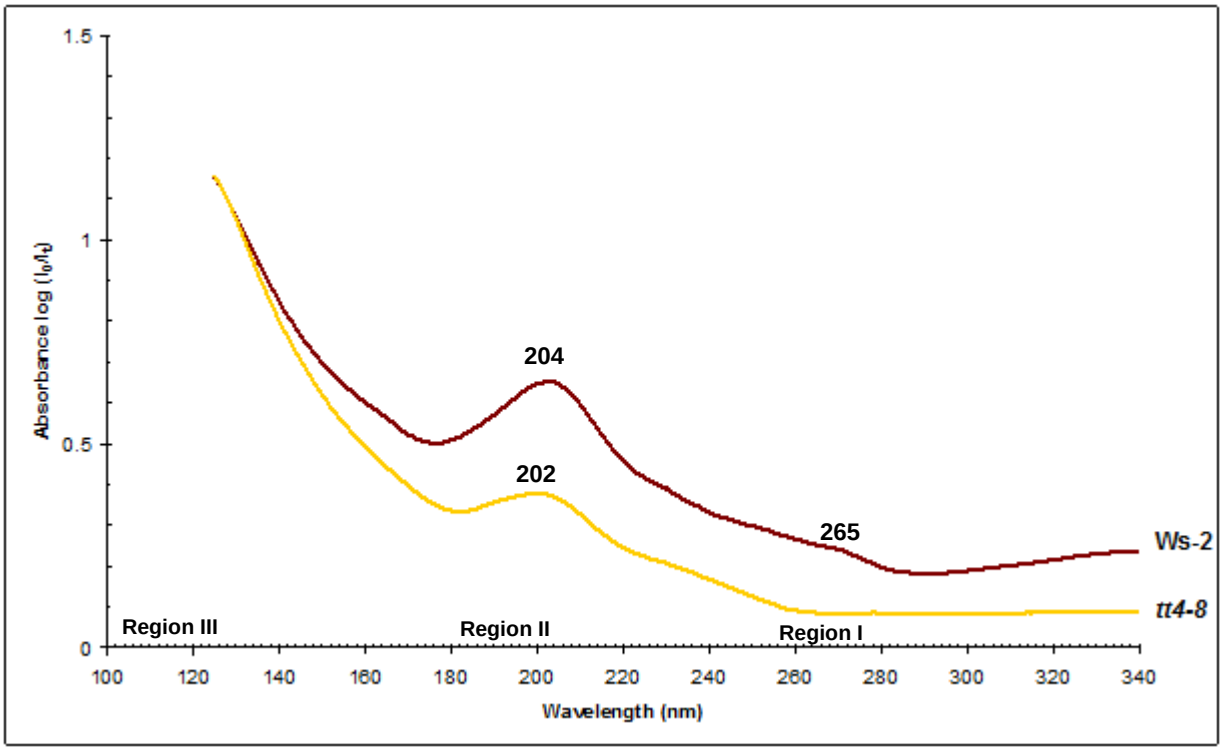

Fig. 56. VUV-UV absorption spectra of methanolic crude extracts obtained from *Arabidopsis* seeds Ws-2 (wild type) and *tt4-8* (flavonoid deficient mutant). The spectra of samples were recorded in thin, dry films. Both samples were prepared from 100 mg seeds, using the same extraction protocol. The thin films were prepared drying the same volume (500 µl) of the Ws-2 and *tt4-8* seed extracts.

11.4.2.2. VUV-UV absorption spectra of HPLC-purified fractions from Ws-2 seeds, containing flavonoids and sinapate esters

The VUV-UV absorption curves of eight purified fractions from Ws-2 seeds, as well as for DNA as the reference, are presented in parallel in **Fig. 43A**.

Fraction F1, which contained sinapoylcholine and sinapoylglucose (sinapate esters), exhibited a weak absorption in the VUV-UV part of the spectrum. The absorption curve revealed two poorly resolved peaks at 164 and 202 nm, as well as a faint shoulder at 245 nm, which was previously detected at 240 nm by conventional spectroscopy in solution (for comparison see above **Fig. 53A**). This fraction also exhibited a local minimum of absorption at 270 nm.

Fraction F2 contained flavonoid Q-Glu-Rha as a dominant compound and trace amounts of sinapoylcholine and glucosinolate compounds. The VUV-UV absorption curve exhibited a prominent and broad peak at 204 nm in region II and a smaller peak at 265 nm in region I. The

latter peak was detected at 260 nm by conventional spectroscopy in solution (for comparison see above **Fig. 53B**), indicating the presence of a flavonoid compound. The absorbance increased slightly towards 340 nm, but it increased considerably in region III, where a local absorption maximum was observed at 157 nm. This VUV-UV absorption curve resembled previously reported curves for glycosylated flavonoids (see section **10.2.,** and Zalar et al. 2007b, Zalar et al., 2007c), although a hypsochromic shift was observed for the peak in region III.

Fraction F3 contained a mixture of various flavonoids, including K-Glu-Rha, Q-Rha-Rha and I-Glu-Rha, which are the three major compounds. Therefore, the VUV-UV absorption curve for the F3 fraction resembled the typical absorption curve for glycosylated flavonoid compounds (see section **10.2.,** and Zalar et al. 2007b, Zalar et al., 2007c). Besides the prominent peak at 202 nm (region II), two smaller, but well resolved peaks were observed, including the peak at 162 nm (region III) and the peak at 260 nm (region I). The former peak corresponded to the maximum of absorption at 255, observed by conventional spectroscopy in solution (for comparison see **Fig. 53C**). In addition, the absorbance of the F3 fraction increased considerably both at the lower end (125 nm) and the upper end (340 nm) of the spectrum.

Flavonoid K-Rha-Rha was the main component of the fraction F4, together with the mixture of other flavonoids which were present in lower concentrations (e.g. K-Glu-Rha, Q-Rha-Rha, I-Rha-Rha, Q-Glu-Rha), and trace amounts of glucosinolates. As expected, the VUV-UV spectra revealed the absorption curve characteristic of flavonoid compounds. Interestingly, the shape of the VUV-UV absorption curve of fraction F4 resembled closely that of F2 fraction, showing the same absorption maxima at 265 nm (region I), 204 nm (region II) and 157 nm (region III). However, these two fractions contained different diglycosylated flavonoids, explaining the different position of absorption maxima in the UV-A part of spectrum, detected by conventional spectroscopy in solution (for comparison see above **Fig. 53B** and **D**).

Fractions F5a and F5b corresponded to the ascendant and descendent parts of the dominant HPLC peak, respectively (see HPLC chromatogram in **Fig. 49**). While F5a fraction contained a considerably higher concentration of almost pure flavonoid Q-Rha (quercitrin), the fraction F5b contained the same substance at high concentration, but with trace amounts of other compounds, notably flavonoids. The absorption curves of the F5a and F5b fractions resembled closely those of other flavonoid containing fractions from Ws-2 seeds (**Fig. 57A**). Both fractions, F5a and F5b, showed similarities in their VUV-UV absorption spectra. However, the absorption curve of the F5a fraction was more similar qualitatively and quantitatively to the curve of the quercitrin

standard (**Fig. 57B**), showing peaks at 163 nm, 204 nm and a very broad peak in the region between 258 and 270 nm. As in the quercitrin standard, the absorbance of the F5a fraction increased markedly from 285 nm to longer wavelengths at the upper end of the spectrum (340 nm). Although qualitatively similar to that of the F5a fraction, the VUV-UV absorption curve of the F5b fraction showed some quantitative differences, notably in the occurrence of a particularly prominent peak at 204 nm, stronger absorption peak at 163 nm and a steep increase in absorbance towards the lower end of the spectrum at 125 nm. On the other hand, fraction F5b showed a smaller and less broad peak in region I, with a maximum of absorption at 270 nm.

Fraction F6 contained a mixture of flavonoid Q-Rha and sinapate ester di-sinapoylglucose, thus the VUV-UV absorption curve exhibited altered absorption characteristics, compared to the flavonoid containing fractions (**Fig. 57A**). In region I, the characteristic flavonoid peak at 260-280 nm almost disappeared, and an additional but poorly resolved peak at 245 nm appeared. The corresponding peak, characteristic for sinapoyl-containing compounds, was observed at 240 nm using conventional spectroscopy in solution (see above **Fig. 54C**). The absorption maximum at 204 nm (region II) was characteristic for the flavonoid compound. Fraction F6 absorbed also strongly in the VUV part of the spectrum, showing a peak at 160 nm and a steep increase in absorbance towards the lower end of the spectrum. An increase in absorbance was also observed toward 340 nm.

Fraction F7 contained only sinapoyl ester in high concentration. The shape of the VUV-UV absorption curve was similar to that of the F6 fraction, including the same position of the absorption maxima at 160 nm and 245 nm, as well as a significant increase in absorbance towards 340 nm (**Fig. 57A**). However, fraction F7 exhibited a small hypsochromic shift of the maximum of absorption in region II, where the peak at 202 nm corresponded to that observed in the sinapoyl containing fraction F1.

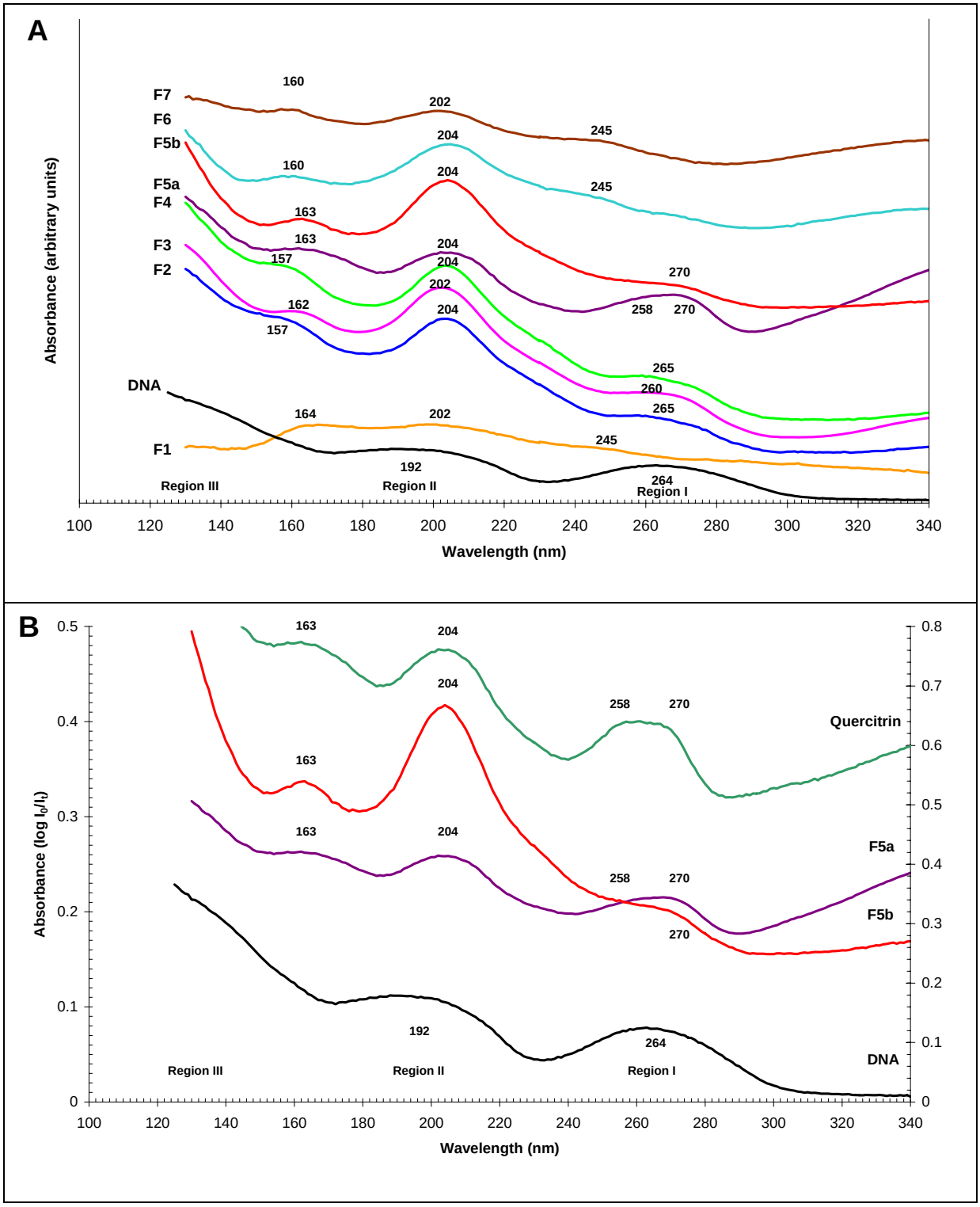

Fig. 57. VUV-UV absorption spectra of the fractions purified by HPLC from a crude extract of *Arabidopsis* Ws-2 wild type seeds. The spectra of samples were recorded in thin, dry films. The spectrum of dry DNA is included as a reference (taken from Zalar et al, 2007a).
(A) Absorption spectra of all eight fractions (F1, F2, F3, F4, F5a, F5b, F6, F7), corresponding to seven prominent HPLC peaks. (B) The absorption spectra of the fractions F5a and F5b, which correspond to ascendant and descendent parts of the dominant HPLC peak, respectively. Their absorption curves are compared to the absorption spectrum of a flavonoid standard, quercitrin (quercetin-3-*O*-rhamnoside = Q-Rha) (0.05 mg per sample). The left side ordinate gives absorbance for F5a, F5b and DNA, while the right side ordinate is for the quercitrin standard.

11.4.2.3. VUV-UV absorption spectra of glucosinolate-containing purified fractions from Ws-2 seeds

In the present work, we also studied the VUV-UV absorption properties of glucosinolates, which besides flavonoids and sinapate esters represent a third group of important secondary metabolites found in *Arabidopsis* seeds. **Fig. 58** shows the VUV-UV absorption spectra of six glucosinolate-rich fractions (from G-F1 to G-F6), purified by HPLC from Ws-2 seeds extract. The fraction G-F7 was not analysed since our MS study showed that it is in fact a flavonoid-containing fraction (see section **11.3.**).

Glucosinolate-rich fractions, with exception of G-F4 fraction, generally showed a weak or no absorption absorption above 260 nm (**Fig. 58A**). Fractions G-F1, G-F2 and G-F6, absorbed poorly throughout the whole VUV-UV spectrum, showing almost featureless absorption curves. Fraction G-F1 contained predominantly 3-methylsulfinylpropyl glucosinolate (3-MSOP), while G-F2 and G-F6 fractions contained the mixtures of two or more glucosinolate compounds (**Table 12**). In contrast to these glucosinolates, fraction G-F3, which contained 8-methylsulfinyloctyl glucosinolate (8-MSOO), showed a steep increase in absorption below 260 nm, exhibiting strong absorption maxima at 225 nm and 156 nm, and a shoulder at 191 nm. Fraction G-F5 contained 8-methylsulfinyloctyl glucosinolate (8-MTO). Its VUV-UV absorption curve showed a strong peak at 227 nm and remarkably steep increase of absorption below 190 nm, towards the lower end of absorption spectrum. In contrast to all here analysed glucosinolate-rich fractions, the G-F4 fraction, which contained almost pure 3-benzoyloxypropyl glucosinolate (3-BzOP) exhibited a particular VUV-UV absorption spectrum. This glucosinolate absorbed strongly below 300 nm and all throughout the VU-C and VUV part of the spectrum, exhibiting at least four fused peaks with high intensity of absorption, characterized by a shoulder at 282 nm and four maxima of absorption at 275 , 233, 196 and 160 nm (**Fig. 58**).

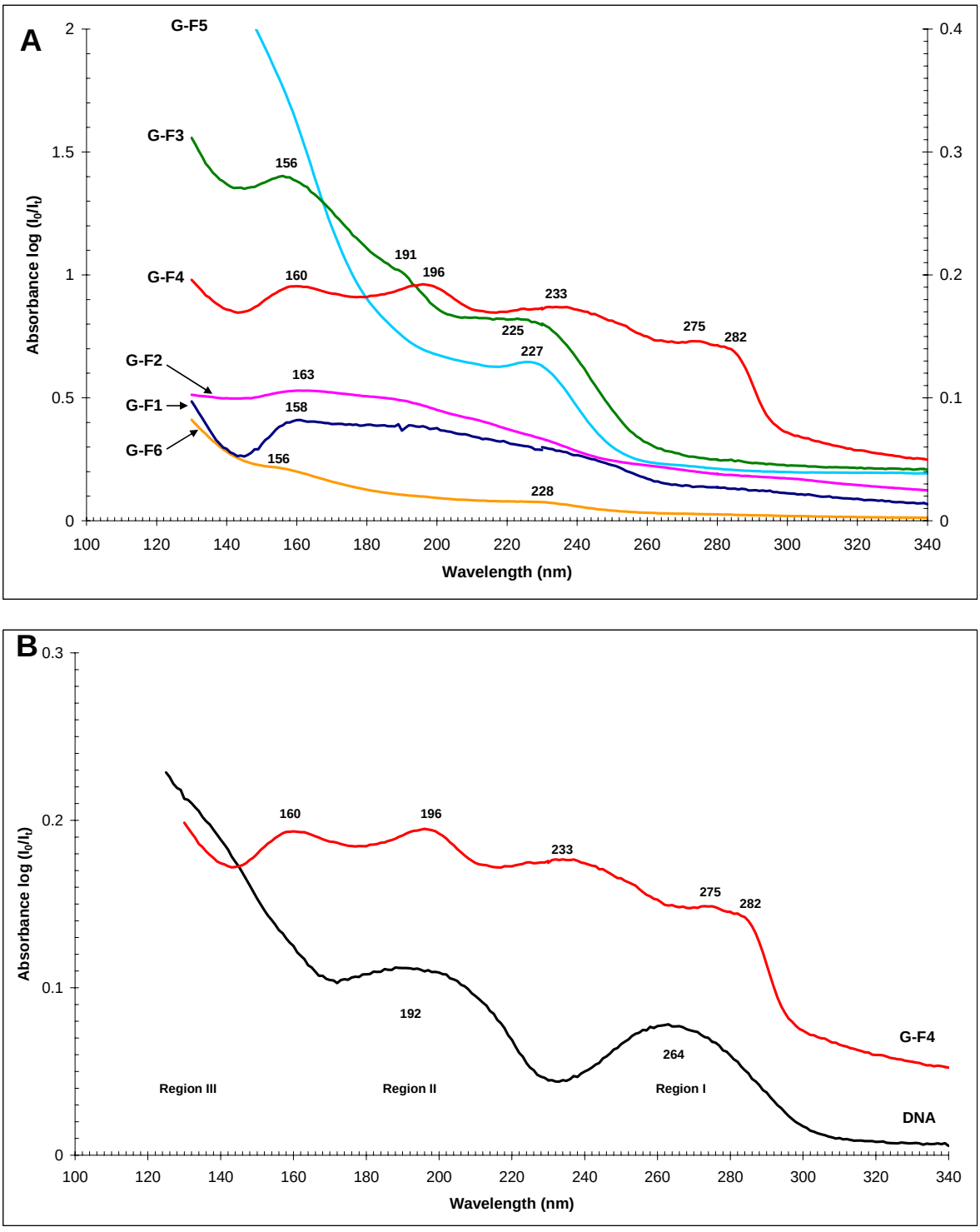

Fig. 58. VUV-UV absorption spectra of glucosinolate-containing fractions separated by HPLC from *Arabidopsis* Ws-2 wild type seeds. The spectra of samples were recorded in thin, dry films. (A) Comparison of absorption spectra of six glucosinolate-containing fractions (from G-F1 to G-F6). Fraction G-F7 was here omitted since it contained almost pure flavonoid kaempferol-rhamnoside. The left side ordinate gives absorbance for G-F2, G-F5 and G-F6 fractions, while the right side ordinate for G-F1, G-F3 and G-F4 fractions. (B) Absorption spectrum of glucosinolate fraction G-F4, containing almost pure 3-benzoyloxypropyl glucosinolate (3-BzOP), also known as glucomalcomiin, compared to absorption spectrum of dry DNA (taken from Zalar et al, 2007).

Chapter 4
DISCUSSION I

The UV radiation is one of the most deleterious factors of the space environment, where the full spectrum of solar UV light is encountered, comprising the UV-A (315 - 400 nm), the UV-B (280 - 315 nm), and highly energetic UV-C (200 - 280 nm) and VUV (< 200 nm). The level of solar UV radiation that reaches the Earth is relatively high in the UV-A and it decreases sharply in the UV-B part of spectrum. Neither VUV nor UV-C reaches the surface of present-day Earth, thanks to filtration by the stratospheric ozone layer. However, the surface of the early Earth was likely exposed to a high flux of short wavelength solar UV until photosynthesis produced enough oxygen for a significant ozone layer to form. Therefore, early organisms probably had to cope with highly damaging UV radiation. Evolving on Earth, organisms developed various mechanisms to resist UV stress. One of these strategies includes the synthesis of small organic compounds that act as UV screens. In an effort to better understand the chemical bases of the resistance to UV light, we first studied the UV absorption characteristics of DNA, which is a key molecule that makes and maintains all life on Earth. Furthermore, we studied the UV absorption spectra of some putative UV screens and those that are known to act as specialized UV screens, in the hope of learning their possible role in the origin and evolution of life and finding possible ways of protecting life during space travel.

Here below are discussed the absorption spectra of DNA and some UV screens. These spectra were measured in the wavelength interval between 125 and 340 nm, and thus included the VUV, the UV-C, the UV-B and a part of the UV-A spectral region. Generally, most of the absorption spectra for different substances, including DNA, are well known above 200 nm, and they are measured using conventional absorption spectroscopy methods. The study of the absorption spectra below 200 nm requires the usage of special techniques and equipment, since air and most solvents, including water, strongly absorb in the VUV region, obscuring the absorption of the sample. Therefore we measured the VUV-UV absorption spectra under vacuum, and all the samples were prepared as dry thin films. Using synchrotron radiation as a light source, we extended the absorption spectra down to 125 nm in the VUV region. For many substances the absorption characteristics in the VUV are less studied or even unknown. Although our spectra are the result of two phenomena, absorption and scattering, for the sake of simplicity and because of the small contribution of scattering, all spectra discussed here are called absorption spectra.

12. DNA AND ITS COMPONENTS

Life as we know it on Earth is based on DNA, which stores essential genetic information about the structure and function of each organism. The DNA polymer is composed of monomer units (nucleotides), which differ in their nucleobases: adenine (A), guanine (G), thymine (T) and cytosine (C). DNA is considered a particularly sensitive target due to its high absorption in the short-wavelength part of the UV spectrum. Being absorbed by DNA, the highly energetic UV photons induce a variety of molecular damage, ranging from the formation of different photoproducts created through the dimerization of two adjacent nucleobases (e.g. cyclobutane pyrimidine dimers and 6-4- photoproduct), induction of cross-links between proteins and DNA, up to severe damage that leads to breaks in DNA backbone (Friedberg et al., 1995; Britt, 1996; Tuteja et al., 2001; Sinha and Häder, 2002). The most frequent UV-induced damage is the formation of photoproducts, particularly thymidine dimers (Clingen et al., 1995; Friedberg et al., 1995; Britt, 1996). The absorption spectrum of DNA roughly correlates with the action spectra for DNA damage and photoproduct formation (Hidea et al., 1986). Therefore, in order to better understand the UV absorption characteristics of DNA and to predict its viability after exposure to UV light, we measured the VUV-UV absorption spectra (125 - 340 nm) of DNA and its components (nucleotides).

In the present study, salmon sperm DNA was used as an example of genomic DNA. Our VUV-UV absorption spectra of dry thin film of DNA revealed two broad bands with the maximum of absorption at 264 nm (region I) and at 192 nm (region II). As expected, VUV-UV absorption spectra showed that DNA does not absorb at wavelengths longer than 310 nm. In addition, we observed that the absorption increased steeply towards the lower end of the spectrum at 125 nm (region III) (see **Fig. 2** in Article **1**, chapter **9**). This result generally agrees with previously published VUV-UV absorption spectra of dry DNA films that exhibit two maxima of absorption, one at about 260 nm and the second in the region covering 190 - 200 nm (Falk, 1964; Inagaki et al., 1974; Sontag and Weigezahn, 1975; Földvári et al., 1982; Ito and Ito, 1986; Gomes et al., 2009). Although published absorption spectra of DNA are all quite similar, they differ however, in relative absorption intensities and they exhibit small differences in the peak wavelengths. This could be due to differences in the source of the DNA (e.g. DNA from salmon sperm, calf thymus, chicken erythrocyte, T7 bacteriophage), as well as the method of sample preparation, the source of UV light and the conditions under which the spectra were recorded. The maxima of absorption of our dry DNA sample agree with those of calf thymus DNA measured by Inagaki et al. (1974). These authors reported three absorption maxima at 4.7

eV (264 nm), 6.5 eV (191 nm) and 13.8 eV (57 nm). The latter was not observed in the present study, since it is out of our measured wavelength range. Nevertheless, the same authors reported a steep rise in absorption above 7.2 eV (172 nm), which correlates with the absorption in region III of the present study. Two absorption peaks that correspond to our region I and region II are attributed to the single-electron excitations of π electrons in the nucleic bases, while increased absorption in region III possibly originates from σ-electron excitations that are mainly associated with the ribose-phosphate chain (Inagaki et al., 1974; Ito and Ito, 1986). The relative absorption intensities of our DNA sample measured at 190, 160 and 150 nm, with respect to the intensity of the 260 nm band, agreed with those for dry calf thymus DNA reported by Sontag and Weigezahn (1975).

Here we also compared the absorption characteristics of DNA in dry and hydrated state (see **Fig. 2** in Article **1**, chapter **9**). In the hydrated sample, the peak at 264 nm was shifted to 260 nm, while the peak at 192 nm was obscured by absorbance of water and only a shoulder at 198 nm could be perceived. A similar hypsochromic shift of the peak at 260 nm was previously reported for both the heat-denatured DNA in heavy-water (D_2O) solution, as well as solid film of DNA at 0% relative humidity, when compared to native DNA in D_2O solution or to highly hydrated films of DNA prepared at 93% relative humidity (Falk, 1964). DNA molecule in solution or in highly hydrated films has a double-helix structure known as the B conformation, while it is in the so-called "disordered" state in solid films at relative humidity below 55%. These structural changes are found to be completely reversible upon rehydration of DNA films. In contrast to denatured DNA in solution, "disordered" DNA in dehydrated solid films maintains a certain rigid structure, where the complementary pairing and the parallel stacking of the DNA bases are largely lost, but the double helical strands remain entwined (Falk, 1964; Inagaki et al., 1974). Since our VUV-UV absorption spectrum of dry DNA film was recorded under vacuum, we assumed that the molecules of DNA were in the "disordered" state. It should be noted that the conditions of DNA as a dry film are different from those of DNA in most of the living cells, which contain generally more than 60% of water (Larcher, 2003; Ling, 2004). However, some life forms occur in nature in highly dehydrated state, such as bacterial spores, plant seeds and pollen grains. They are adapted to resist long time periods under adverse environmental conditions, including UV radiation. Some cyanobacteria are also capable of surviving prolonged periods in extremely desiccated environments (e.g. in hot and cold deserts) (Potts, 1999). Nevertheless, the biophysical properties of macromolecules inside desiccated cells are still poorly understood. Even less is known about the UV sensitivity of DNA molecule within dehydrated cells. Therefore, our VUV-UV absorption spectra of DNA in the dry state could

contribute to a better understanding of the possible effects of UV radiation on DNA in dehydrated cells. However, many anhydrobiotes, including seeds survive extreme desiccation thanks to the cellular transition into the glassy state. Therefore DNA and other biologically important macromolecules in cells of anhydrobiotes are probably embedded into the glassy matrix, made of cell solutes, such as non-reducing sugars and proteins (e.g. LEA) (Buitink and Leprince, 2004`; Buitink and Leprince ; 2008). These glasses probably help in preservation of the structural and functional integrity of macromolecules (Faria et al., 2005; Buitink and Leprince, 2008). Therefore it would be interesting to further investigate whether DNA in the dehydrated cells is in the "disordered" state or more likely in the native state, being protected by intracellular glasses. Since VUV-UV absorption characteristics of DNA may be influenced by its state, it would be interesting to measure the absorption spectra of dry films of DNA embedded into the glassy matrix simulated *in vitro* from the mixtures of proteins (e.g. LEA) and non-reducing sugars (e.g. sucrose and RFOs).

In order to examine the influence of nucleotide composition on overall UV absorption of genomic DNA, we determined the VUV-UV absorption spectra for unpolymerized monomers (nucleotides designated monoA, monoT, monoG and monoC) that make up DNA (see **Fig. 4** in Article **1**, chapter **9**). These spectra were then compared with those of polymerized homonucleotides (short tracts of single-stranded DNA) that consisted of 20 identical nucleotides (oligoA_{20}, oligoT_{20}, oligoG_{20} and oligoC_{20}) (see **Fig. 3** in Article **1**, chapter **9**).

Polymerized homonucleotides (oligohomonucleotides) showed remarkable differences in their VUV-UV absorption spectra. Nevertheless, the absorption peaks in all four oligohomonucleotides could be generally grouped into three regions, corresponding to the absorption peaks observed in genomic DNA: 255-286 nm (region I), 159-220 nm (region II) and below 159 nm (region III). Similarly to the absorption of genomic DNA in region III, all four oligohomonucleotides exhibited continuously increasing absorbance toward the low wavelength end of the spectrum. Therefore, the major differences in VUV-UV absorption spectra were related to region I and II. In addition, we found that the spectra for polymerized A, T and G, with the exception of that for polymerized C, were similar in numbers of bands and peak wavelengths to the VUV-UV absorption spectra of the monomers. This indicated that the interactions among nucleic bases of the same type in homonucleotides oligoA_{20}, oligoT_{20} and oligoG_{20} are relatively small, suggesting that polymerization has little effect on the absorption spectrum in the region we measured, and that the absorption characteristics of oligohomonucleotides in region I and II originate predominantly from nucleic bases. However, monomer nucleotides showed no steep

increase in absorption below 170 nm (corresponding to DNA region III), as was observed in oligohomonucleotides. This result agrees with a previously mentioned hypothesis that absorption in region III is likely associated with σ-electron excitations in the ribose-phosphate backbone (Inagaki et al., 1974; Ito and Ito, 1986).

Furthermore, we found that the VUV-UV absorption spectra of all polymerized homonucleotides differed markedly from that for salmon sperm genomic DNA. The oligohomonucleotides showed more spectral features (peaks and shoulders) than genomic DNA, including differences in the number and positions of the absorption peaks. The oligoT_{20} exhibited three pronounced peaks, while four peaks or shoulders were detected in oligoG_{20} and oligoC_{20}, and five in the oligoA_{20} sample. The purines (A, G) thus showed more features than the pyrimidines (C, T), as expected from their more complex structures. In addition, we observed that purine base oligohomonucleotides (oligoA_{20} and oligoG_{20}) had greater interval between region I peaks and region II peaks, compared to pyrimidine base oligohomonucleotides (oligoT_{20} and oligoC_{20}). We concluded that the broad salmon sperm DNA peaks at 192 and 264 nm can be resolved into oligohomonucleotide spectral families. A particularly interesting difference in UV absorption characteristics was a bathochromic shift in region I for oligoC_{20} (a peak at 278 nm) and for oligoG_{20} (a broad peak with strong shoulder at 286 nm), compared to oligoA_{20} and oligoT_{20}, as well as genomic salmon sperm DNA. These observations suggested that DNA sequences rich in G+C nucleotides might have the absorption maximum in region I shifted toward longer wavelengths. A similar analysis of the absorption properties in region II showed that absorption by DNA sequences rich in A+T nucleotides should occur at shorter wavelengths, compared to G+C rich sequences, but this difference should be less dramatic than for region I. These observations suggested that the overall absorption spectrum of DNA might depend not only on its state of hydration, but also on the relative frequencies of G+C versus A+T base pairs.

Relative G+C content of genomic DNA varies in different organisms, ranging from approximately 25% to 75% (Sueoka, 1962). Salmon sperm DNA belongs to the A+T rich class, having a G+C content of 41.2% (Chargaff et al., 1951). Földvári et al. (1982) observed variations in UV absorption spectra for DNA of different origins. These authors suggested that the variations in absorption might be due to differences in G+C content and in the base sequence for various samples. A similar conclusion was reached by Lewis and Johnson (1974) on the basis of their measurements of vacuum ultraviolet circular dichroism for different DNA samples. Therefore, we examined the possible influence of G+C content on overall VUV-UV absorption properties of DNA. In this respect, we first measured VUV-UV absorption spectra of equimolar

mixtures of two complementary oligohomonucleotides (oligoA+T and oligoG+C) (see **Fig. 6** in Article **3** chapter **9**). These mixtures of single-stranded DNA samples mimicked two complementary strands of homopolymeric double-stranded DNA (dA:dT or dG:dC), representing two extremes in G+C content, 0% and 100%, respectively. The VUV-UV absorption spectra of oligoA+T and oligoG+C differed significantly. Both spectra differed from that of salmon sperm DNA. The oligoG+C showed a complex absorbance in region I, being characterized by one very broad peak (240-315 nm) that was probably formed by the fusion of at least two absorption peaks. In region II, oligoG+C absorbed as a single prominent peak at 185 nm. The pattern of oligoA+T absorbance was reversed, with a complex absorption profile in region II that was likely composed of three fused absorption peaks (155, 177 and 208 nm), and a single, very prominent peak in region I. Here it is important to note that the oligoA+T maximum (263 nm) in region I coincided with peak I in salmon sperm DNA (264 nm), reflecting the A+T rich composition of this genomic DNA. However, compared to oligoA+T, salmon sperm DNA showed less complexity in region II, probably due to the influence of the G and C bases present in genomic DNA. Although extreme nucleotide content of oligoA+T and oligoG+C does not represent in reality the nucleotide content of genomic DNA molecules, since genetic code uses all four nucleotides to encode for 20 essential amino acids, these extreme nucleotide contents , known as homopolymeric DNA tracts, do occur locally in noncoding regions of the genomes of both prokaryotic and eukaryotic organisms (Dechering et al., 1998; Shomer and Yagil, 1999). Long poly(dA:dT) tracts, reaching a size well above 25 base pairs, occur at high frequencies in some eukaryotes, enriching genomes with A and T nucleotides. Other eukaryotic organisms are rather enriched in dG:dC tracts (Dechering et al., 1998). It suggested that local, noncoding segments of genomic DNA might have different UV absorption properties and thus altered wavelength-dependant response to UV radiation, compared to the coding regions of DNA. In prokaryotes, homoplymeric tracts occur, but less frequently since their relatively small genomes contain less noncoding nucleotide sequences (Dechering et al., 1998; Shomer and Yagil, 1999).

Since we concluded that nucleotide content in noncoding DNA regions, can significantly alter the UV absorption of the local segments in genomic DNA, we were further interested to investigate whether the G+C content in the coding DNA regions can influence overall UV absorption properties of genomic DNA. The degeneracy of the genetic code allows significant variations in G+C content. The potential for G use is clear in the genetic code, where in many cases an alternative codon can contribute a supplementary G to the nucleotide sequence, without changing the amino acid sequence in the polypeptide chain. We calculated that a hypothetical gene, encoding a protein that incorporates one of each of the 20 amino acids, can vary in G+C

content by more then twofold (from 30% up to 63% G+C), yet retaining the same amino acid sequence. It seems possible that DNA nucleotide content could evolve as a function of environmental conditions. Three hydrogen bonds in the GC pair, as opposed to two in the AT pair, make the double helix of nucleic acids more stable at high temperatures (Galtier and Lobry, 1997). The formation of different UV-induced lesions depends on wavelength, but also on DNA sequence (Mitchell et al., 1992; Ravanat et al., 2001; Cadet et al., 2005). For instance, nucleotide sequences rich in adjacent thymines are prone to the formation of thymine dimers (TT), the most frequent type of UV damage (Mitchell et al., 1992; Cadet et al., 2005). Other pyrimidine dimers (CT, TC and CC) could be also formed, although at much lower frequencies (Mitchell et al., 1992). According to our observations, the bathochromic shift potentially conferred by a sequence rich in G and C should also confer better UV protection by proteins, particularly those rich in aromatic amino acids, such as tryptophan (see below discussion on ubiquitously occurring potential UV screens). Therefore, in an attempt to understand the relationship between nucleotide frequencies and absorption, we measured VUV-UV absorption spectra for equimolar mixtures of complementary sense and antisense strands for synthetic, protein-encoding DNA that contained 30%, 50% and 63% G+C (see **Fig. 7** in Article **3**, chapter **9**). In spite of their different nucleotide composition and sequences, these 60-mer oligonucleotides encoded the same polypeptide chain. We observed no major qualitative differences in VUV-UV absorption spectra among these synthetic protein-encoding oligonucleotides. However, these spectra revealed a smaller bathochromic shift in region I, which correlated with increasing G+C content of synthetic oligonucleotides. For instance, the maximum of absorption at 262 nm was detected for 30%, at 264 nm for 50% and at 268 nm for 63% of G+C content. At 63% G+C content, peak I was also broader. Nevertheless, these results revealed that differences in the total G+C content in synthetic, protein-encoding DNA had relatively small effect on the UV absorption spectra, while the extreme G+C content of synthetic homopolymeric DNA tracts had an important influence.

Concluding remarks (1)

From the observations discussed above, we concluded that the overall (genomic) G+C content might have a lesser effect on the UV absorption properties of DNA. In contrast, local nucleotide sequence and G+C content might alter UV absorption in noncoding regions of genomic DNA, where sequences are often repeated. In many eukaryotes, a vast majority of the genome is noncoding DNA (e.g. in humans it represents >98% of the genome; Elgar & Vavouri, 2008). Much of this DNA has still unknown biological function and is sometimes referred to as "junk" DNA. Some of noncoding DNA sequences are found to be important in regulation of

transcription and translation processes (Ludwig, 2002). Other noncoding sequences have likely but as-yet undetermined function. It is widely accepted that evolutionary forces drive the architecture of organisms' genomes (Elgar and Vavouri, 2008). The noncoding sequences appeared to be under strong selective pressure (Ludwig, 2002). Therefore we propose that adaptation of DNA sequences to particular UV environments and available UV screens (for details see below) could be one of the functions of this noncoding "junk" DNA in higher organisms.

13. THE VUV-UV ABSORPTION PROPERTIES OF UV SCREENING COMPOUNDS

Highly energetic solar UV radiation was likely an obstacle to the emergence and expansion of life on the early Earth. Organisms evolved different mechanisms for resisting UV radiation, including the synthesis of UV screens, which provide a first line of defence against UV radiation. The protection is passive, since UV screens absorb incident photons and dissipate their energy away from potential cellular targets. Chromosomal DNA is localised in the interior of cells, as far as possible from incident light, and it is surrounded by cellular substances that may protect against UV (see **Fig. 20**, chapter **1**, section **3.3.4.2.2.**). Although extraterrestrial solar emission intensity declines steeply toward short wavelengths, VUV and UV-C radiation represent the most biologically damaging parts of the UV spectrum due to the high energies carried by these photons. DNA strongly absorbs in the VUV and UV-C part of the spectrum (regions I, II and III; for details see above). We assume that an ideal UV screen would absorb UV radiation in a manner similar to DNA. Therefore, according to the degree of VUV-UV spectral similarity between UV screens and the DNA, we evaluated potential UV screening efficiency of different substances.

13.1. Potential, ubiquitously occurring UV screens

Biological molecules of all sorts absorb UV light. They are thus potential UV screens, as well as targets for photodestruction. Here we examined the VUV-UV properties of selected organic compounds that occur in all organisms, including nucleotide monomers, proteins, amino acids and amines (polyamines and tyramine). These compounds have various structural and functional roles in cells, but beside their primary roles, some of them may be involved in the protection of genetic material by screening deleterious UV radiation. In the present study, we call such molecules “potential” UV screens, because they do not fulfil all the criteria that characterize true screens, here termed the “specialized” UV screens (for criteria see chapter **1**, section **3.3.4.2.2.**). Since these compounds are omnipresent in all phylogenetic branches of all three kingdoms (archaea, eubacteria and eukarya), there is a good reason for their presence in the first cells emerging on Earth, when the intensity and spectral quality of UV radiation were likely different from that experienced today. A simple life form could consist of DNA and the molecules it encodes, which would replicate DNA and protect it from UV radiation. The

simplest UV screen for DNA would thus be nucleotide monomers, RNA, free amino acids and proteins.

Nucleotides are the monomer units of nucleic acids (DNA and RNA). They are composed of nucleic base, ribose sugar and phosphate moiety (see **Fig. 1** in Zalar et al., 2007a, part I, chapter **3**, sections **1.** and **2.1.**). They also play important roles in energy metabolism and cell signalling processes. Free nucleotides are therefore abundant in all prokaryotic, as well as eukaryotic cells. Here we suggest that unpolymerized nucleotides can also act as potential, ubiquitously occurring UV screens. We therefore determined VUV-UV absorption spectra for four monomer nucleotides (monoA, monoG, monoT and monoC) and compared them with the absorption spectrum of genomic DNA (see **Fig. 4** in Article **1**, chapter **9**). All four types of nucleoside triphosphates exhibited peaks in the 253-290 nm region and in the 135-232 nm region. We found that VUV-UV absorption spectra of free nucleotides were similar regardless of a degree of phosphorylation (nucleoside 5'-monophosphates and nucleoside 5'-triphosphates) or hydroxilation of ribose moiety (ribonucleoside and 2'-deoxyribonucleoside triphosphates) (our unpublished data). Among the four nucleotides, adenine monunucleotide (ATP) had the absorption curve that best matched that of genomic DNA, showing a peak at about 261 nm (region I) and poorly resolved peaks at 159, 192 and 210 nm (region II). ATP is an essential molecule in all contemporary cells, acting as a primary energy currency in all known living organisms. Therefore, cells contain relatively high amounts of ATP. Adenine nucleic base is one of the most frequently found heterocyclic compounds in the world of modern biochemistry (Maurel et al., 1996). In addition, the importance of adenine nucleic base in possible prebiotic chemistry on primitive Earth has been discussed by many authors (Oró, 1960; Oró`, 1961; Oró and Kimball, 1961; Maurel et al., 1996; Vergne et al., 2000; Orgel, 2004; Lagoja and Herdewijn, 2005; Roy et al., 2007). Adenine derivatives might have played an important role in the emergence of the first genetic system and in the formation of possible prebiotic catalysts (Maurel et al., 1996; Vergne et al., 2000). It seems that adenine can be synthesised in interstellar space, since it was detected, together with other organics of prebiotic importance, in cometary dust (Krueger and Kissel, 1987; Cottin et al., 1999). Adenine was also found in meteorites (Stoks and Schwartz, 1981; Botta and Bada, 2002). Here we suggest that during the early history of life on Earth, when emerging life was possibly exposed to a high flux of energetic UV radiation, primitive cells might have used ATP, in addition to its role in intracellular energy transfer and synthesis of nucleic acids, as an ancient UV screen.

Proteins are macromolecules composed of amino acid monomers. They have catalytic, structural, mechanical and regulatory functions. Although proteins are themselves a sensitive target for UV radiation, some of them assist in coping with UV damage to DNA. For instance, some proteins play an important role as enzymes that efficiently repair DNA damage (Britt, 1996; Tuteja et al., 2001; Sinha and Häder, 2002). Other proteins are capable of interacting with DNA, what leads to large structural changes in the DNA molecule, turning it into more compact structures that are less prone to damaging agents. One group of such proteins are histones, which are small positively charged DNA-binding proteins, abundant in all eukaryotic cells. Analogous proteins with a similar function in bacteria are so-called histone-like proteins (Drlica and Rouviere-Yaniv, 1987). In the present study, we intended to examine whether proteins can protect DNA, acting as efficient ubiquitous UV screens. Comparing the VUV-UV absorption spectra of histones and bovine serum albumin, BSA (a small, neutral non-binding protein) to that of genomic DNA, we found that the UV-screening protection of DNA by proteins would be less obvious than that provided by the other ubiquitously occurring potential UV screens (e.g. free nucleotides, as discusses above). Both proteins had very similar VUV-UV absorption spectra and they showed a characteristic, but weak protein peak at 280 nm (region I), which was visible only in highly concentrated samples (see **Fig. 5** in Article **1**, chapter **9**). Since proteins absorb strongly in region II (peaks at 192 nm and 170 nm) and region III (absorption continuously increases towards the short wavelengths), we suggested that they would provide relatively good screening protection to DNA exposed to highly energetic VUV radiation. In contrast, due to weak absorption in region I and the bathochromic shift of the protein peak (280 nm), compared to the corresponding peak in DNA (264 nm), we concluded that proteins would provide relatively poor UV-C screening protection to DNA, unless the concentration of the screen is so high that the target is protected even at absorption minima. We presume that such a nonspecific opacity to UV radiation would be less efficient than that afforded by a well-matched UV screen.

Free amino acids may also have some role in UV protection. Amino acids might have been involved in the prebiotic chemistry on the early Earth (Miller, 1953; Miller and Urey, 1959; Dyson, 1985; Kobayashi et al., 1998). Some amino acids are found in meteorites, indicating that they can be synthesized in extraterrestrial environments (Cronin and Pizzarello, 1983; Botta and Bada, 2002). Among 20 proteinogenic amino acids, we have studied VUV-UV absorption spectra of four representatives of different amino acid classes: arginine (basic amino acid), aspartic acid (acidic amino acid), valine (hydrophobic amino acid with aliphatic side chain) and tryptophan (hydrophobic amino acid with aromatic side chain) (for chemical structures see **Fig. 1** in Article **1**, chapter **9**). The spectra showed that potential protection of DNA in the VUV part of

spectrum (regions II and III) is the common feature of selected amino acids (see **Fig. 6** in Article **1**, chapter **9**). However, these amino acids, with the exception of the aromatic amino acid, tryptophan, would not provide efficient UV screening protection to DNA in region I. Tryptophan has a prominent, broad peak at 287 nm, with a shoulder at 272 nm, but due to the bathochromic shift relative to DNA peak at 264 nm, we assumed that it would be less suitable UV screen than for instance ATP, unless it occurs in high concentrations. It is interesting to note that among the three proteinogenic aromatic amino acids (tryptophan, tyrosine and phenylalanine), tryptophan is known to have the highest molar extinction coefficient at the maximum of absorption (λ_{max}), and therefore, the absorbance of proteins in the UV-B region is primarily determined by the tryptophan residue and to a lesser extent by the other two aromatic amino acids. Consequently, the absorbance of proteins at 280 nm is approximately proportional to the number of tryptophan residues (Cockell and Airo, 2002). Nevertheless, comparing the percentages of amino acids in the total proteomes of organisms belonging to all three kingdoms (archaea, eubacteria and eukaryotes), aromatic amino acids make up about 8-9%, and of all three aromatic amino acids, tryptophan has the lowest mean abundance (1-1.3%). However, some proteins, such as a light exposed enzyme, photolyase (see chapter **1**, section **3.3.4.3.**) contain higher percentages of tryptophan residues (Cockell and Airo, 2002). Proteins rich in aromatic amino acids are also found in the *Bacillus subtilis* spore coat, where they are thought to play a part in UV resistance (Driks, 1999; Riesenman and Nicholson, 2000). This inspired our idea that protein engineering might be used to improve UV protection *in vivo*. Proteins enriched in tryptophan might provide better protection to DNA, especially those segments rich in G+C base pairs.

Polyamines are another group of potential UV screens that we considered here. They are small, polycationic molecules, present in all prokaryotic and eukaryotic cells. Polyamines play important roles in the regulation of cell growth and differentiation (Tabor and Tabor, 1984; Smith, 1985; Martin-Tanguy, 2001). In cells, they interact with negatively charged molecules, such as nucleic acids, proteins and membrane phospholipids (Martin-Tanguy, 2001). Similarly to histones, polyamines enable folding of DNA and they stabilize condensed DNA conformations (Flink and Pettijohn, 1975; Tabor and Tabor, 1984). Polyamines are found to correlate with increased resistance to radiation and hydrolysis of nucleic acids (Baeza et al., 1992). Since they are relative simple, nitrogen-containing aliphatic molecules, and they are ubiquitously present in all contemporary organisms, we assumed that polyamines or similar molecules might exist in the primitive cells. Baeza et al. (1992) proposed polyamines, such as spermidine, as plausible prebiotic DNA condensing agents, and they considered possible roles of the polyamine-nucleic acid complexes in the evolution of life. Therefore, in the present work, we also investigated

whether polyamines could protect DNA from high fluxes of solar UV radiation, acting as UV screens in primitive cells. Here we examined the VUV-UV absorption properties of three major and ubiquitously occurring polyamines, putrescine, spermidine and spermine (for their chemical structures see **Fig. 1** in Article **1**, chapter **9**). Their VUV-UV absorption spectra revealed high absorption below 180 nm (see **Fig. 7** in Article **1**, chapter **9**). Thus, they would probably protect DNA from VUV radiation. In contrast, polyamines do not absorb in region I, and thus alone they would not provide necessary protection by screening from UV-C and UV-B radiation. However, in plant cells, polyamines often occur as conjugates with hydroxycinnamic acid and its derivatives, which carry an aromatic ring that is a good UV absorber (Martin-Tanguy, 1985; Martin-Tanguy et al., 1991) (for details see chapter **1**, section **5.2.1.** and **Table 1** in section **5.**). We assume that such conjugated forms of polyamines would improve the UV-screening potential, particularly in region I. An interesting finding is that polyamines accumulate in plant cells as a result of different biotic and abiotic stresses, and their synthesis can be induced by UV-B and UV-C radiation (Martin-Tanguy, 2001; An et al., 2004).

In addition to these aliphatic amines, we also examined the VUV-UV properties of tyramine, an aromatic amine that is found to occur in all prokaryotic and eukaryotic organisms (for its chemical structure see **Fig. 1** in Zalar et al., 2007a, part I, chapter results, sections **1.** and **2.1.**). The VUV-UV absorption spectrum of tyramine is presented in **Fig. 7** in Article **1**, chapter **9**. Tyramine absorbs strongly in region III, but it also exhibits a prominent absorption peak at 198 nm and shoulder at 221 nm. In addition, tyramine absorbs strongly at 282 nm, with a shoulder at 267 nm. Therefore we concluded that besides region III, tyramine would provide relatively good protection in both DNA absorption regions I and II, especially for DNA rich in G+C base pairs.

Concluding remarks (2)

Based on degree of similarity of VUV-UV absorption spectra between DNA and different ubiquitously occurring putative UV screens that we examined here, we concluded that free nucleotides, particularly adenosine 5'-triphosphate (ATP) would best protect DNA from incident UV light throughout the DNA absorption spectrum. We suggest that in primitive cells evolving on early Earth, the use of ATP in UV protection might have been as important as the its role in building up the genetic material and its function in energy transfer.

13.2. Known specialized UV screens

It is generally considered that the selective pressure of UV radiation in surface habitats had an important influence on the evolution of the organisms able to synthesize efficient UV-screening and energy-quenching substances to protect their vital molecules such as DNA and proteins (Marcano et al., 2006). Photosynthetic organisms are particularly susceptible to UV-induced damage due to their need for capturing the sunlight as the ultimate source of energy for their survival. In contrast to ubiquitously occurring substances that are constitutively synthesized in all living cells, in which, besides their primary roles, they can putatively act as unspecific UV screens, many surface-inhabiting organisms synthesise specific chemical compounds that are highly efficient in filtration of deleterious UV wavelengths. Most of these specialized UV screens use the UV absorbing properties of π-electron containing chromophores (e.g. conjugated bonds in linear chains and aromatic structures) to screen UV radiation (Cockell and Knowland, 1999). The synthesis and accumulation of these specialized UV screens is usually triggered by the exposure of the organism to UV radiation (Garcia-Pichel et al., 1992; Garcia-Pichel and Castenholz, 1993; Dixon and Palva, 1995; Cockell and Knowland, 1999; Castenholz and Garcia-Pichel, 2000; Treutter, 2006). Since the unspecific, potential UV screens, such as nucleotides, amino acids, proteins and polyamines (see discussion above) are usually dissolved in cytosol or are found in close interaction with chromosomal DNA, one of their main disadvantages is that they possibly carry a risk of transferring the absorbed energy directly to the molecular targets, causing photosensitization rather than protection. Therefore the need to have a spatial distance between the screen and the target DNA has likely contributed to the evolution of cells with specialized UV screens accumulated in extracellular structures, such as cell walls, coats, capsules and sheaths.

Here we discuss the VUV-UV absorption properties of different known specialized UV screens, including mycosporine-like amino acids (MAAs), scytonemin, β-carotene, melanin and flavonoids, which were isolated from phylogenetically distinct groups of organisms. Using similarity with the DNA absorption spectrum, we evaluated the likely effectiveness of these molecules in shielding DNA damaging solar UV radiation. All of these UV screens examined absorbed in the vicinity of DNA absorption regions I, II and III, mostly due to the presence of more or less complex aromatic ring structures (for the chemical structures see **Fig. 21** in chapter **1**, section **3.3.4.2.2.**). Their particularities in VUV-UV absorption characteristics are discussed here below.

The MAAs are a group of structurally diverse, intracellular, colourless compounds, which accumulate in response to UV in certain cyanobacteria and algae, but they are also found in some heteroptrophic bacteria, fungi, lichens and in a variety of marine invertebrates and vertebrates (Castenholz and Garcia-Pichel, 2000; Shick and Dunlap, 2002). For more details about MAAs and their chemical structures, see chapter **1**, section **3.3.4.2.2.** MAAs are reported to have a high molar extinction coefficient in the UV part of the spectrum, exhibiting a single peak with maximum of absorption between 310 and 360 nm (Sinha et al., 1998; Castenholz and Garcia-Pichel, 2000; Shick and Dunlap, 2002). The exact wavelength position of the absorption peak depends on the chemical structure of the particular MAA. In this work, we analysed VUV-UV absorption spectra of two compounds, identified as palythine and porphyra-334 that were isolated from marine red alga *Corallina officinalis*. These two substances are typical MAAs, found in many algae and phytoplanktonic organisms (Sinha et al., 1998). Both MAAs showed qualitative spectral similarities (see **Fig. 2** in Article **2**, chapter **9**). VUV-UV spectra in the thin, solid films revealed a prominent, broad peak at about 335 nm for porphyra-334 and one weak peak at 320-330 nm for palythine. These absorption characteristics correlated with published spectra of porphyra-334 and palythine in solution (Sinha et al., 1998; Xiong et al., 1999). The absorption spectra indicated that porphyra-334 would provide better protection in the UV-B/UV-A region than palythine due to its stronger absorption. In *Corallina officinalis* extracts we identified only these two major MAAs, but other organisms are likely to synthesize several types of MAAs with overlapping maxima of absorption, thus screening more broadly in the UV-A and UV-B wavelength range (Cockell and Knowland, 1999). Furthermore, we were interested to investigate the absorption properties of MAAs below 200 nm, which were before this study practically unknown. Porphyra-334 showed a weak peak at 192 nm and a well resolved peak at 164 nm, while palythine exhibited peaks at 195 nm and 164 nm. Our results indicated that MAAs should screen DNA from VUV radiation (region II and III). However, we concluded that MAAs are not well suited for providing efficient screening in the UV-C part of the spectrum, since they did not absorb the wavelengths between 230 and 300 nm (region I). This would not be relevant for present-day biota, since solar UV-C wavelengths, in contrast to UV-A and UV-B, do not reach the surface of Earth. However, because of their relatively simple chemical structure, and due to their occurrence in a wide range of phylognenetic taxa, which occupy large geographic ranges, one could assume that MAA-like compounds would exist in early evolving organisms. On the other hand, if unfiltered, highly energetic solar UV-C radiation was experienced on Earth during early evolution of life, then it would be difficult to imagine that these organisms used MAA-like screens to protect their genetic material against UV damage,

unless MAAs were complemented with some other type of screening pigment. Indeed, this phenomenon is observed in contemporary cyanobacteria, in which MAAs are often complemented with scytonemin pigment (see discussion below).

Scytonemin is a yellow to brown, extracellular pigment found in many cyanobacteria. The almost exclusive photoautotrophic mode of growth of cyanobacteria requires that they survive in habitats exposed to sunlight, including the visible part of the spectrum, but also UV radiation. Upon exposure to UV-A light, cyanobacteria synthesise large amounts of scytonemin, which acts as a specialized UV screen deposited in cyanobacterial sheaths (Castenholz and Garcia-Pichel, 2000). Due to its relatively complex ring structure (see **Fig. 13**, in chapter **1**, section **3.3.4.2.2**), scytonemin exhibits a specific UV absorption pattern (Proteau et al., 1993). The published absorption spectra measured in solution revealed that scytonemin absorbs most efficiently at the longest wavelengths of the UV spectrum, exhibiting a remarkably prominent and broad peak at 386 nm (UV-A region), in addition to a second prominent peak at 252 nm (UV-C region), and other smaller, fused peaks at 278 nm and 300 nm, as well as at 212 nm (Proteau et al., 1993; Sinha et al., 1998). Our absorption study of scytonemin dry films provided the insight in yet unknown absorption properties of this pigment below 200 nm (see **Fig. 2** in Article **2**, chapter **9**). The VUV-UV absorption spectrum confirmed a reported absorption peak at 253 nm, although it was quite weak. In addition, one prominent peak at 195 nm, and a steep increase in absorption toward 125 nm were also observed. The UV absorption spectra of scytonemin in the dry state may be relevant for desiccation-tolerant cyanobacteria that are capable of surviving in harsh environments, such as hot or cold deserts, used sometimes as analogues for extraterrestrial environments (e.g. Mars) (Liu et al., 2008). Comparing the absorption spectra of scytonemin and DNA, we concluded that scytonemin in the dry state would provide efficient protection to DNA in regions II and III (VUV), but to a lesser extent in region I (UV-C), due to its weaker absorption and the hypsochromic shift of the maximum of absorption of about 10 nm. Thus, the major protection of scytonemin would be provided in the UV-A part of the spectrum, where DNA does not absorb, but other molecules do, leading possibly to the formation of ROS and indirect damage to DNA. In contrast, scytonemin would screen relatively poorly in the UV-B region, and thus providing less protection to the proteins. That is why in many contemporary cyanobacteria, scytonemin occurs together with MAAs, which are good UV-B absorbers (see discussion above). Cyanobacteria belong to an ancient phylogenetic group of phototrophic organisms, and their microfossils possibly date as far as 3.5 Ga ago, when the early Earth's atmosphere was likely poor in ozone that protects present-day Earth from energetic UV

radiation. The occurrence of scytonemin in species belonging to every major taxonomic group of cyanobacteria suggests that scytonemin production might precede the phylogenetic diversification of cyanobacteria, presumably in the Precambrian. Nevertheless, our observations led us to conclude that scytonemin, if it occurred in ancient cyanobacteria, would probably not be alone sufficient to protect cells from unfiltered UV radiation at the early Earth. Similarly to contemporary cyanobacteria, ancient cyanobacteria thus might have used some complementary UV screens in addition to scytonemin. Alternatively, they might have used another kind of efficient, well-suited UV screen, which was lost in present-day cyanobacteria due to the decline in UV selective pressure during the course of evolution. In addition, matting habits, known to be used in present-day cyanobacteria as one of the strategies for coping with UV radiation, might have also been used by the ancient cyanobacteria to attenuate the high fluxes UV radiation probably experienced on Archean Earth.

Beside genetic material and proteins, photosynthetic pigments are also susceptible to UV damage, leading to pigment bleaching (Garcia-Pichel, 1998; Sinha and Häder, 2002). Chlorophyll a is a universal photosynthetic pigment, present in all organisms that carry out oxygenic photosynthesis, including cyanobacteria (Ke, 2001a). Our UV-VIS absorption spectra measured in ethanol solution showed that chlorophyll a absorbs strongly in the visible part of the spectrum at 410 nm and 660 nm (spectra not shown). Extending the absorption spectra into the VUV-UV region, we showed that chlorophyll had absorption maxima at 295 and 193 nm, with an inflection at 250 nm. The absorption of chlorophyll a increased towards the lower, as well as the upper end of measured VUV-UV spectra. Since the scytonemin VUV-UV absorption curve matched that of chlorophyll a (see **Fig. 8** in Article **3**, chapter **9**), we concluded that scytonemin would likely protected chlorophyll a by screening it from the incident UV light. On the other hand, we assumed that due to a strong and broad-band absorption of scytonemin in UV-A (λ_{max} = 386 nm), this cyanobacterial UV screening pigment would probably interfere with the absorption of chlorophyll a at 410 nm. This overlapping in absorption could reduce the effectiveness of chlorophyll a in harvesting sunlight. This might be the reason why contemporary cyanobacteria, in parallel to chlorophyll a, use another chlorophyll-type pigment with a red-shifted absorption spectrum (chlorophyll d), as well as some accessory pigments, such as phycobilins and carotenoids (Ke, 2001a; Larkum and Kühl, 2005). These additional light-harvesting pigments may complement chlorophyll a by absorbing the photons that are not captured, and transferring their energy to chlorophylls. The role of carotenoids as accessory photosyntehtic pigments is discussed below.

Carotenoids are lipid-soluble pigments, synthesized by all photosynthetic organisms and some heterotrophic bacteria and fungi (Armstrong and Hearst, 1996). Carotenoids belong to a group of tetraterpenoids that contain a long polyene chain, terminated by six-member carbon rings. Their chemical structures and the fact that their synthesis is induced by UV radiation, reaching relatively high concentrations in cells, indicated that carotenoids may be involved in UV screening protection (Cockell and Knowland, 1999). Therefore, we analysed the UV absorption properties of β-carotene, a typical representative of carotenoids that is widespread in many photosynthetic organisms, including plants, algae and cyanobacteria.

Our UV-VIS spectrum of β-carotene in solution (ethyl-acetate) coincided with previously published spectra (Miller et al., 1935; Lichtenthaler and Buschmann, 2001), exhibiting a broad and complex absorption band, composed of two strong maxima of absorption at 450 and 478 nm, a shoulder at 430 nm, and one poorly resolved peak at 330 nm (spectra not shown). The spectra revealed that β-carotene, similarly to other carotenoids, absorbs mainly in the visible part of the spectrum (blue light), with an extension into the UV-A (Zscheile et al., 1942; Lichtenthaler and Buschmann, 2001). On the other hand, the UV absorption characteristics of carotenoids below 200 nm are still not well known. Therefore, in the present study we extended the absorption spectrum of β-carotene into the VUV region. According to the literature, the role of carotenoids in UV screening remains still quite controversial (Cockell and Knowland, 1999 and references therein). Therefore, by analyzing the VUV-UV absorption spectrum of β-carotene and comparing it to that of DNA, we aimed to evaluate the putative UV screening effectiveness of carotenoids (see **Fig. 4** in Article **2**, chapter **9**). Dry films of β-carotene exhibited a prominent peak at 195 nm, with steeply increasing absorption towards the lower end of the spectrum (125 nm). In addition to β-carotene, we also measured the absorption spectra of one carotenoid compound that was extracted from UV-A irradiated cells of the cyanobacterium, *Chroococcidiopsis*. This substance was putatively assigned to the carotenoid, lycopene, according to the similarities between our UV-VIS spectra measured in ethyl-acetate solution (λ_{max} = 505, 472 and 450 nm; λ_{min} = 490 and 455 nm) and that reported by Miller et al. (1935). Similarly to β-carotene, the VUV-UV spectra of putative cyanobacterial lycopene showed one prominent peak at 197 nm, and steeply increasing absorption toward the lower end of the measured spectrum (spectra not shown). These observations indicated that carotenoids would provide screening protection to DNA only in the VUV (region I and II), but they would not screen from UV-C and UV-B radiation. We assume that only highly concentrated β-carotene would provide some attenuation of the high-wavelength end of UV-C radiation, but the effective screening protection to DNA would be probably very small, due to weak absorption and a

bathochromic shift of the peak at 277 nm, compared to the DNA peak at 264 nm. β-carotene might provide better protection to proteins rather than the DNA, since the local maximum of absorption for β-carotene (277 nm) matches that for proteins (280 nm), so that we consider that to accomplish adequate UV screening protection to proteins, β-carotene should accumulate in relatively high concentrations. Therefore, our results are consistent with the general opinion that carotenoids play an important role in photoprotection, but acting indirectly as efficient antioxidants and free radical quenchers, rather than passive UV screens (Krinsky, 1979; Cockell and Knowland, 1999). Their role in quenching ROS might have evolved during the early history of life on Earth, when levels of atmospheric oxygen started to increase. The earliest phototrophic organisms might have used carotenoids or similar pigments to cope with toxic by-products of oxygenic photosynthesis (Cockell and Knowland, 1999). Carotenoids are also shown to be important factors in protection of photosynthesis against UV-B damage (Götz et al., 1999). This effect is mostly attributed to their antioxidative ability. Therefore, in the present work, we also examined whether carotenoids might provide UV screening protection to photosynthesis. The photosystem (PS) II reaction centres of plants, algae and cyanobacteria are know to be primary targets of UV damage (Renger et al., 1989; Frisco et al., 1994; Campbell et al., 1998). If present in high concentrations, β-carotene might provide some UV screening protection to protein component of PS II. UV radiation can also induce bleaching of photosynthetic pigments, such as chlorophylls that are part of PS I and II (Garcia-Pichel, 1998; Sinha and Häder, 2002; Wynn-Williams and Edwards, 2002). Comparing the VUV-UV spectra of β-carotene and putative cyanobacterial lycopene with those of chlorophyll a and b (see **Fig. 10** in Article **3**, chapter **9**), we found that carotenoids would provide good UV-screening protection in the VUV, since the absorption spectra of these four pigments are matched perfectly below 200 nm. However, carotenoids would be probably inefficient in the protection of chlorophylls by screening from UV-C, UV-B and UV-A parts of the spectrum. In addition, the absorption characteristics of carotenoids in the visible part of the spectrum revealed that their broad absorption bands overlap partially with the chlorophyll a absorption peak at 410 nm and entirely with the chlorophyll b absorption peak at 450 nm (spectra not presented). This observation can be correlated with the fact that carotenoids do not shade chlorophylls, but rather transfer captured light energy to chlorophylls, contributing to photosynthesis as accessory pigments (Ke, 2001b).

Melanins are known UV screening compounds that are widely distributed in animal kingdom, but they are also found in some eubacteria, fungi and plants (Hinojosa-Rebollar et al., 1993; Césarini, 1996; Riley, 1997). In animals, melanins are accumulated in specialized cells, melanocytes, located in the skin, hair, and in extracutaneous tissues (Césarini, 1996; Cockell and Knowland, 1999). Two classes of melanins, eumelanins (brown-black pigment) and pheomelanins (yellow-reddish) represent highly complex substances, containing indoles and other intermediate products derived from the oxidation of tyrosine (Pezzella et al., 1997; Wakamatsu and Ito, 2002). The chemical structures of main building blocks of melanins are presented in **Fig. 13D**, chapter **1**, section **3.3.4.2.2.** The exact chemical structure of melanins is still unknown, since these highly irregular polymers and usually bound to lipids and proteins, and organized into nanoaggregates (Pezzella et al., 1997; Meredith et al., 2006). In some cells, melanins are synthesized constitutively, but their synthesis can be also induced by UV radiation (e.g. sun tanning of skin).

In this study we also examined the VUV-UV spectra of dry films of eumelanin, which revealed monotonous, almost linear increase in absorption throughout the spectrum from 340 nm to 145 nm, below which the absorption climbed steeply towards the lower end of the measured spectrum see **Fig. 4** in Article **2**, chapter **9**). This almost featureless absorption curve probably results from a highly complex melanin structure in which a diversity of absorbance maxima of the π to π^* electron transitions overlap (Cockell and Knowland, 1999; Meredith et al., 2006). Therefore, we concluded that melanins would provide efficient, but unspecific UV screening protection to biological material (e.g. DNA and proteins), filtering out unselectively all UV wavelengths. However, melanins also attenuate, although to a lesser extent, the visible part of the spectrum, particularly violet and blue light (UV-VIS spectra of melanin in solution are not here presented). Therefore, melanins are less suited UV screens for photosynthetic organisms, which depend on photosynthetic pigments, such as chlorophyll, that capture visible light in the blue and orange-red part of spectrum.

Besides their photoprotective function, melanins also act as efficient antioxidants and free radical scavengers (Césarini, 1996; Riley, 1997). In animals, they play an important role in camouflage and adornment. Very curious is also a property of melanins that can act as intrinsic semiconductors, transforming one kind of energy, for instance light energy, into electrical energy or heat (Césarini, 1996). Therefore, melanins are also important in the thermoregulation of some organisms (Césarini, 1996; Riley, 1997). Nevertheless, the evolutionary importance and possible presence of melanins in the early stages of life on Earth is still unclear. Césarini (1996) suggested that melanins might be present in early life forms, such as archaeobacteria or

thermoresistant eubacteria. In spite of the fact that melanins play multiple roles and that they also occur in prokaryotic organisms, we consider, however, that melanins would be a relatively late evolutionary invention due to their high chemical complexity, requirements for oxygen dependent life (the synthesis of melanins involves oxidative processes), and incompatibility with light-harvesting photosynthetic pigments.

Flavonoids are a large group of phenolic compounds that, together with some other phenolics (e.g. esters of hydroxinamic acid), act as important specialized UV screens in plants (Dixon and Palva, 1995; Parr and Bolwell, 2000; Kliebenstein, 2004). Flavonoids are synthesized from phenylalanine amino acid through the phenylpropanoid pathway (for details about the chemical structure and biosynthesis of flavonoids see introduction chapter, section **5.1.**). Their accumulation in plants is stimulated in response to UV radiation, and mutants plants lacking flavonoids show increased sensitivity to UV light (Li et al., 1993; Fiscus et al., 1999). Besides a direct photoprotective role, flavonoids also play an important role as antioxidants and free radical scavengers (Parr and Bolwell, 2000; Beutner et al., 2001). They constitute an important factor of plant resistance to various biotic and abiotic stresses (see introduction chapter, section **5.1.3.**).

Therefore, we were interested to study VUV-UV absorption properties of different flavonoid compounds and to determine their likely effectiveness in UV screening protection. In the present study, we extended for the first time the absorption spectra of flavonoids below 200 nm. Our VUV-UV spectra revealed the absorption properties of flavonoids in the dry state that is relevant for mimicking the conditions in dry seeds, which generally contain less than 10% water. We measured VUV-UV absorption spectra of four flavonoid chemical standards, including quercitrin, isoquercitrin, robinin and catechin, of which the first three are glycosilated representatives of flavonoids (flavonol class) (for chemical structures see **Fig. 13**, chapter **1**, section **3.3.4.2.2.**). The last one is flavonoid aglycone (flavan-3-ol class), which is a monomer unit of proanthocyanidins (PAs), also called condensed tannins. Among all plant organs, seeds accumulate remarkably large amounts of flavonoids. *Arabidopsis* seeds contain high concentrations of quercitrin (quercetion-3-*O*-rhamnoside) and PAs (Lepiniec et al., 2006; Routaboul et al., 2006). PAs are concentrated exclusively in the seed coat, which protect genetic material carried by embryo (Lepiniec et al., 2006; Routaboul et al., 2006). The concentration of flavonoid UV shields in the seed coat would distance the screen from target DNA carried in the plant embryo, facilitating transfer of the energy absorbed without harm to the target biological molecules.

Our VUV-UV absorption spectra for all three glycosilated flavonoids revealed a remarkable high level of similarity with that of DNA (see **Fig. 5** in Article **2**, chapter **9**). These flavonoids absorb efficiently in the UV-C part of the spectrum, covering with their broad absorption peaks (λ_{max}=269 nm for robinin and λ_{max}=258 nm with shoulder at 270 nm for quercitrin and isoquercitrin) almost perfectly the DNA region I (264 nm). In addition, the absorption spectra also showed prominent and broad peaks in DNA region II (λ_{max}=199 nm for robinin and λ_{max}=204 nm for quercitrin and isoquercitrin), as well as a steep increase in absorption towards the lower end of spectrum (region III). Therefore, we concluded that glycosilated flavonoids would act as ideal UV screens, providing efficient screening protection to DNA from incident UV light throughout the DNA absorption spectrum (VUV and UV-C wavelengths). Although DNA does not absorb in UV-A region, other molecules that are photosensitizers do absorb, causing a potential threat to DNA via indirect oxidative damage. The VUV-UV absorption spectra of glycosilated flavonoids showed a steep increase in absorption towards the upper end of the spectrum (340 nm). This agreed with the spectra measured by conventional UV spectroscopy in solution, as well as in dry films, showing that glycosilated flavonoids are also good absorbers (broad peaks at about 335 nm), thus efficient screening protectors in UV-A part of spectrum.

Catechin showed different VUV-UV absorption profile, compared to glycosilated flavonols (see **Fig. 5** in Article **2**, chapter **9**). However, polymerisation of catechin monomer units into PAs did not alter the VUV-UV absorption properties (spectra not shown). In *Arabidopsis* seeds, PAs are composed of epicatechin, instead of catechin monomer units. Nevertheless, these two stereoisomers did not differ in their VUV-UV absorption profile (spectra not shown). In contrast to glycosilated flavonols, catechin and condensed tannins do not absorb in the UV-A region, and they absorb poorly in the UV-C, showing the local minima at 256 nm. This indicated that catechin would not be a good screening protector for DNA in region I. Since catechin and PAs are strong antioxidants and ROS quenchers, we assume that their role in UV protection would be primarily indirect, preventing oxidative damage to DNA. In addition, we suggest that catechin would provide better UV screening protection to proteins rather than to genetic material, since it exhibits a prominent absorption peak at 280 nm. On the other hand, our results indicated that catechin would provide efficient screening protection in the VUV part of the spectrum, since the absorption curve of catechin matches well the DNA absorption curve in region II (intensive, broad peak at λ_{max}=204 nm with a shoulder at 230 nm), as well as in region III (steep increase in absorption towards 125 nm).

Besides genetic material and proteins, flavonoids accumulated in leaves and other photosynthetic parts of plants can also play an important role in the protection of photosyntetic pigments from UV damage. In addition to ubiquitous chlorophyll a, chlorophyll b represents a plant-specific photosynthetic pigment. Our VUV-UV spectra showed that glycosilated flavonols would be good UV screening protectants for both chlorophyll a and b a (see **Fig. 11** in Article **3**, chapter **9**). Since glycosilated flavonols do not absorb visible light, they should not interfere with photosynthesis. Catechin, and thus PAs, would be less suited to protect chlorophylls from UV radiation, except in the region close to VUV.

Concluding remarks (3)

Based on a qualitative comparison of VUV-UV absorption spectra of DNA and different specialized UV screens that occur in phylogenetically diverse organisms, we came to the conclusion that among all examined screening substances, flavonoids that belong to a group of glycosilated flavonols (e.g. quercitrin) can be considered the ideal UV screens due to the remarkable resemblance of their VUV-UV absorption spectra with that of DNA. In addition, an ideal UV screen should not only provide direct protection of DNA, but also it should protect a variety of substances that absorb at the other wavelengths. Flavonoids also strongly absorb UV-A light, preventing the absorption of these wavelengths by so-called photosensitizers, which can generate ROS, causing an indirect UV-induced damage to DNA. Complemented with catechin containing polymers (PAs), glycosylated flavonols would screen efficiently the VUV, UV-C, UV-B and UV-A parts of the spectrum.

14. VUV-UV ABSORPTION PROPERTIES OF SCREENING COMPOUNDS ISOLATED FROM PLANT SEEDS

According to our VUV-UV spectroscopic studies, we postulated that among all tested chemical compounds, flavonoids (particularly flavonols) can be considered ideal UV screens (see discussion above). However, these VUV-UV absorption spectra were measured using chemically pure flavonoid standards. Plants possess a great capacity to produce a large variety of different secondary metabolites, including flavonoids (Kliebenstein, 2004; D'Auria and Gershenzon, 2005). An individual plant can synthesize a set of chemically different flavonoids, and their composition is usually tissue-specific (Lepiniec et al., 2006). One could expect that these *in situ* mixtures of organic compounds, which might also interact among themselves or with the cellular structures, would exhibit complex UV absorption spectra, with features that are possibly different than that of chemically pure standards. In addition, many of the substances from a vast inventory of plant secondary metabolites are still unidentified. Plant seed are particularly rich sources of flavonoids e.g. in seeds of *Arabidopsis thaliana*, the total amount of flavonoids is about 15 mg g^{-1} seeds (Lepiniec et al., 2006; Routaboul et al., 2006). Seeds are known to resist various harsh conditions, including biotic and abiotic stresses (Rajjou and Debeaujon, 2008). Seeds are also shown to resist exposure to high doses of UV radiation (Zalar, 2004`; see also part II of the present work).

Therefore, we were interested to examine the UV properties of flavonoids that are inherent in seeds. We studied the absorption spectra of crude extracts from *Arabidopsis* seeds using conventional UV spectroscopy in solution (λ = 200-400 nm), but we also extended these spectra into the VUV region by measuring absorption in dry films (λ = 125-340 nm). Most mature seeds contain only a low percentage of water. The water content in our *Arabidopsis* seeds was <7% (see part II, chapter 6, section 18.1.). Seeds survive extreme desiccation thanks to the transition into the state known as the glassy state. The glass formation state occurs in seeds with 10-15% water content, after drying at room temperature (Buitink and Leprince, 2004). The intracellular glass matrix is formed in cytoplasm thanks to the non-reducing sugars and specific proteins (for details see chapter 1, sections 4.3.1., 4.3.2. and 4.3.4.). Nevertheless, most plant secondary metabolites, including flavonoids, sinapate esters and glucosinolates are not accumulated in the cytoplasm, but rather in vacuoles and cell walls, where they probably occur in a near-dry state (Strack and Sharma, 1985; Halkier and Du, 1997; Debeaujon et al., 2007). Therefore, we considered that our VUV-UV spectra of flavonoids and other UV screening compounds,

measured in dry films, should provide a better picture of their absorption characteristics occurring in dry seeds.

In this study, conventional absorption spectroscopy revealed that the crude extract from *Arabidopsis* wild type seeds (Ws-2) absorbs strongly in the UV part of the spectrum, showing a maximum of absorption at 200 nm, one well resolved peak at 262 nm and a broad band in the region 300-360 nm (λ_{max} = 335 nm) (**Fig. 52**, part I, chapter 3, section 11.4.1.1). As already noted in this work, VUV-UV absorption spectra showed a small bathochromic shift (3-5 nm) of absorption peaks, compared to UV absorption spectra measured by conventional spectroscopy in solution. The VUV-UV absorption spectrum of Ws-2 seed extract showed a dominant and broad absorption peak at 204 nm (**Fig. 56**, part I, chapter 3, section 11.4.2.1). It also confirmed the existence of a characteristic peak in the UV-C part of the spectrum, although in the VUV-UV spectrum, this peak (λ_{max} = 265 nm) appeared small and poorly resolved. The absorbance increased towards the upper end of the spectrum (340 nm), but a steep increase in absorbance was more obvious in the VUV part of the spectrum down to 125 nm. These UV absorption features resembled those for flavonoids. In the literature, flavonoids are known to exhibit characteristic absorption spectra, which are used for their identification and quantification (Bohm, 1998; Stefova et al., 2004). Flavonols that are substituted at position C3 (*O*-alkyl or *O*-glycosyl) are reported to have two characteristic maxima of absorption, one in the range 330-360 nm (band I) and the other in the range 250-280 nm (band II) (Bohm, 1998). Sinapate esters, as another major group of secondary metabolites in *Arabidopsis*, are usually characterized by the absorption peak at about 320 nm and shoulder at about 240 nm (Lee, 2000). Our results indicated that, in spite of the fact that crude seed extracts represent a complex mixture of compounds that have probably different chemical and spectroscopic properties, their overall UV absorption spectra are mainly determined by flavonoids, particularly flavonol-glycosilated compounds. This observation was in agreement with previously published data, reporting quercitrin (quercetin-3-*O*-rhamnoside) as a dominant flavonoid in *Arabidopsis* seeds, where it accumulates in high concentrations (Routaboul et al., 2006). Quercitrin is flavonol with an attached rhamnose sugar at position C3 in the ring C of the flavan skeleton (for details about the flavan skeleton and precise chemical structure of quercitrin see **Fig. 35** and **Fig. 36**, respectively, in chapter 1, section 5.1.2.). In addition, the occurrence of quercitrin was also confirmed in our HPLC and LC-MS analyses (**Fig. 49**, **Table 10** and **Table 11** in chapter 3, section 11.1). To corroborate our assumption that flavonoids predominate the overall UV absorption spectrum of seed extract, we compared the absorption characteristics of crude extracts obtained from wild type (Ws-2) and flavonoid-lacking mutant (*tt4-8*) *Arabidopsis* seeds (**Fig. 52**, chapter 3, section 11.4.1.1). We

observed significant differences in UV absorption spectra between these two seed extracts. The absorption of the *tt4-8* seed extract was lower in intensity than that of the Ws-2 extract all through the spectral range, indicating that *tt4-8* seeds contain less UV absorbing compounds, and thus probably less substances that act as UV screens. The most obvious difference, however, was the absence of an absorption peak at 262 nm (the UV-C part of the spectrum that corresponds to DNA peak I). The *tt4-8* seed extract also lacked other spectral features that are characteristic of flavonoids, such as a broad peak around 335 nm, which almost disappeared in the *tt4-8* seed extract. In contrast, some spectral features of *tt4-8* seed extract resembled those of sinapate esters (e.g. peak at 320 nm and a weak shoulder at ~235 nm). VUV-UV absorption spectra recorded in dry films showed similar differences in absorption characteristics of the Ws-2 and *tt4-8* seed extracts (**Fig. 56**, chapter 3, section 11.4.2.1), as was observed by conventional UV absorption spectroscopy. In addition, the *tt4-8* seed extract, although exhibiting a relatively prominent and broad peak at 202 nm, absorbed to much lesser extent than the Ws-2 seed extract in the same region (λ_{max} = 204 nm). This effect is likely related to the lack of flavonoids in the *tt4-8* seed extract. These spectroscopy results corroborate the results of our previous HPLC studies, showing no flavonoid accumulation in the *tt4-8* mutant seeds (Zalar, 2004). The absence of flavonoid compounds in *tt4-8* seeds was also reported by Routaboul et al. (2006) and Luceri et al. (2008).

Comparing VUV-UV absorption curves of *Arabidopsis* seed extracts and DNA, we concluded that compounds in Ws-2 seeds strongly absorb and thus potentially protect DNA by screening in all three regions, I, II and III (for details about the three absorption characteristic regions of DNA and protection by UV screens see the discussion in chapter 4, section 12). In addition, we suggested that compounds found in Ws-2 seeds would also provide efficient UV screening protection in the UV-A part of the spectrum. In spite of the fact that DNA and proteins do not absorb in this part of the spectrum, screening form UV-A radiation would likely minimize the production of ROS and ultimately oxidative damage to biologically important molecules. In contrast, *tt4-8* seeds lack the substances that would efficiently screen UV-A light. The compounds in *tt4-8* seeds would poorly protect DNA in region I (UV-C), since they exhibit a local absorption minimum in the same wavelength range that corresponds to the absorption maximum of DNA. However, DNA in *tt4-8* seeds might be protected from UV damage in regions II and III, although not as efficiently as in Ws-2 seeds.

Further in this study, we aimed to identify and isolate the substances from *Arabidopsis* seed extract that are dominant, not only quantitatively, but also by their particular UV absorption features that would hopefully explain the phenomenon of high UV resistance observed in *Arabidopsis* seeds (for details see part II, chapter 6). Plant crude extracts are usually complex mixtures of chemically different compounds. Our HPLC and LC-MS analyses showed that the *Arabidopsis* crude seed extract is composed of many different substances, including flavonoids, sinapate esters and glucosinolates (**Fig. 49**, **Table 10**, **Table 11** and **Table 12**, chapter 3, section 11.). This observation was in agreement with previous studies on metabolic profiling of *Arabidopsis* secondary metabolites (von Roepenack-Lahaye et al., 2004; Le Gall et al., 2005). However, a great majority of compounds detected in our seed extract belong to the flavonoid class. Out of eight isolated fractions (F1, F2, F3, F4, F5a, F5b and F7), we found that six of them contained flavonoids (**Table 10**, chapter 3, section 11.1.3). All of them were identified as glycosilated derivatives of flavonols, quercetin, kaempherol and isorhamnetin (for chemical structures see **Fig. 36**, chapter 1, section 5.1.1.). In our experiments, the chromatographic and structural features (MS fragmentation pattern) of these compounds were in accordance with those reported by Routaboul et al. (2006) and Kerhoas et al. (2006). Our HPLC and LC-MS analyses revealed that qercetin-3-*O*-rhamnoside (also called quercitrin), which was contained in fractions F5a and F5b (**Fig. 49**, chapter 3, section 11.1.1), is a dominant and remarkably abundant flavonoid in Ws-2 seed extract. This was in agreement with previously published data on the relative abundance of flavonoids in wild type *Arabidopsis* seeds (Kerhoas et al., 2006; Routaboul et al., 2006). Routaboul et al. reported concentrations of qercetin-3-*O*-rhamnoside as high as 3.6 mg per gram of *Arabidopsis* seeds (Routaboul et al., 2006). According to the same authors, more than 90% of the total quercetin-3-*O*-rhamnoside is accumulated in the seed coat. In contrast most di-glycosilated flavonols are concentrated in the embryo. Among these, quercetin-di-rhamnoside, which was contained in our fraction F3 (**Fig. 49** and **Table 10**, chapter 3, section 11.1), is the second most abundant flavonoid in *Arabidopsis* seeds, reaching a concentration up to approximately 1.4 mg g^{-1} seeds (Routaboul et al., 2006). This compound is the main flavonoid in the *Arabidopsis* embryo, in contrast to quercetin-3-*O*-rhamnoside, which is the dominant flavonoid in the seed coat, together with proanthocyanidins (condensed tannins). However, proanthocyanidins were not detected in our experiment since these highly polymerised substances are usually insoluble and difficult to extract from seeds (Routaboul et al., 2006).

In crude seed extract, we also detected smaller amounts of compounds that were identified as sinapate esters (**Fig. 49**, chapter 3, section 11.1.1). They were contained in fraction F1 and F7, while in fraction F6 they were present in the mixture with flavonoid quercetin-3-*O*-rhamnoside.

Fraction F2 contained only trace amounts of sinapate esters. The majority of sinapate esters in *Arabidopsis* seed extract were identified as sinapoyl choline and sinapoyl glucose, while fraction F7 contained yet an unidentified methyl-containing sinapate ester. Sinapoylmalate was not detected in our seed extract, which is in accordance with previously published data (Chapple et al., 1992). In *Arabidopsis* and other members of *Brassicaceae*, sinapoylmalate represents a leaf-specific ester of sinapic acid, while sinapoylcholine, also called sinapine, is a major seed-specific sinapate ester, together with the smaller amounts of its biosynthetic precursor, sinapoylglucose (Chapple et al., 1992; Lorenzen et al., 1996; Ruegger et al., 1999; Ruegger and Chapple, 2001). In addition, we detected an unusual sinapate ester compound in fraction F6, a product that was identified as di-sinapoylglucose. Sinapate ester known as 1,2-di-*O*-sinapoyl-β-glucose, was previously reported to accumulate only in dark-grown seedlings of *Raphanus sativus* and in *Arabidopsis* seedlings with altered sinapate ester biosynthesis, but not in the wild type (Strack et al., 1984; Fraser et al., 2007). Sinapate esters are reported to act as efficient UV-B protectant in plants, and they have been considered even better UV screens than flavonoids (Chapple et al., 1992; Sheahan, 1996; Booij-James et al., 2000).

Besides flavonoids and sinapate esters, glucosinolates make the third group of important secondary metabolites (see **Table 4**, chapter 1, section 5.). These nitrogen and sulfur-containing substances are found almost exclusively in plants of the *Brassicaceae* family and other related families of the order *Capparales* (Kliebenstein et al., 2001; Brown et al., 2003). A large variety of glucosinolates has been found in *Arabidopsis* plants, where they accumulate in leaves, stems, roots, inflorescences, as well as in seeds. The great structural variability of this class of secondary metabolites results from their variable side-chains. Depending on their side-chains, this group of secondary metabolites can be generally classified as aliphatic, aromatic or indole glucosinolates (Brown et al., 2003). The concentration and accumulation of glucosinolates differ among plant organs and depend on the ecotype and developmental stage of the plant (Chen and Halkier, 2000; Brown et al., 2003). Seeds accumulate glucosinolates at concentrations higher than any other plant organ. The great majority of glucosinolates in *Arabidopsis* seeds has been reported to belong to the aliphatic class (Brown et al., 2003). In our experiments, we detected at least six chemically different glucosinolates that were relatively abundant in *Arabidopsis* wild type Ws-2 seeds (**Table 13**, chapter 3, section 11.3). Four of them were identified by LC-MS. These included 3-methylsulfinylpropyl glucosinolate (3-MSOP), also known as glucoiberin, 8-methylsulfinyloctyl glucosinolate (8-MSOO), known as glucohirsutin, 3-benzoyloxypropyl glucosinolate (3-BzOP), also called glucomalcomiin, and 8-metylthiooctyl glucosinolate (8-MTO). Although being reported as a predominant glucosinolate in *Arabidopsis* seeds, 4-

methyltiobutyl glucosinolate (4MTB) was not detected in this work (Brown et al., 2003). Similarly, no indole-containing glucosinolates were detected in our seed extract, which was in agreement with reported low concentration (about 2% of the total glucosinolate content) in mature seeds (Brown et al., 2003). Apart from the majority of aliphatic glucosinolates, we detected only one glucosinolate, 3-BzOP, which posses an aromatic ring structure. Glucosinolates are important secondary metabolites known to be involved in plant defence system, particularly against biotic stress caused by pathogen and herbivore attacks. Reifenrath and Müller (2007) reported that the concentrations of glucosinolates in leaves of two studied *Brassicaceae* species may change in response to the exposure to UV radiation. It is still unclear whether glucosinolates might be also involved in UV protection (Gonzales-Castañeda and Gonzales, 2008). For this reason, it was interesting to investigate whether glucosinolates contribute in the UV protection of *Arabidopsis* seeds.

Further in this part of work, we examined the UV absorption characteristics of the major secondary metabolites that were isolated from *Arabidopsis* seeds, including flavonoids, sinapate esters and glucosinolates. Comparing their absorption spectra with that of DNA, we estimated their potential in providing efficient UV screening protection to seeds.

Conventional spectroscopy (λ = 200-400 nm) in solution revealed that all flavonoid-containing fractions (F2, F3, F4, F5a and F5b), with the exception of fraction F6, exhibit absorption curves typical for flavonoids, having two absorption maxima, one in the range 255-260 nm, and a second in the range 340-350 nm (**Fig. 53** and **Fig. 54**, chapter 3, section 11.4.1.2). Fractions F5a and F5b, which contained a dominant and highly abundant flavonoid, identified as quercetin-3-*O*-rhamnoside (quercitrin), exhibited very similar absorption curves to that of the quercitrin pure chemical standard (**Fig. 55**A). This was also confirmed by VUV-UV spectroscopy (**Fig. 57**B, chapter 3, section 11.3.2.2.). However, the shape of absorption curve for the F5a fraction was more similar qualitatively and quantitatively to the standard curve than the F5b fraction. This could be expected since the fraction F5a contained high concentration of almost pure quercitrin, while fraction F5b contained some smaller amounts of other flavonoids and other substances, in addition to dominant quercitrin.

Fraction F7 was the only fraction that contained relatively pure sinapate ester compound at concentration high enough to exhibit the absorption spectrum characteristic for sinapate esters, with a shoulder at 240 nm and a prominent peak at 320 nm. Other sinapate ester-containing fractions showed either weak absorption features (fraction F1), or they contained sinapate esters in a mixture with other substances (fractions F2 and F6). It remains still unclear why fraction F1,

which contained only sinapoylglucose and sinapoylcholine, did not exhibit absorption characteristics expected for sinapate esters. Since fraction F7 contained almost pure and abundant sinapate ester, we used this fraction as a representative for the sinapate esters group. When the absorption spectra of sinapate ester (fraction F7) and flavonoid-containing fractions, particularly those containing large amounts of quercitrin (fractions F5a and F5b), were compared to the absorption curve of DNA, we observed that the absorption maximum of quercitrin (262 nm) matched almost perfectly to the maximum of absorption of DNA (260 nm) (**Fig. 55B**). In contrast, sinapate ester exhibited a local minimum of absorption at 260 nm. This indicated that sinapate esters, in contrast to flavonoids, would not provide sufficient protection to DNA in the UV-C part of the spectrum (region I), unless they are present in cells in high concentrations. Nevertheless, sinapate esters would be better UV screens against UV-B radiation, due to its characteristic broad absorption peak at 320 nm. Since both flavonoids and sinapate esters had strong absorption in the UV-A region, exhibiting broad peaks with adjacent absorption maxima at 350 and 330 nm, respectively, we concluded that combined together, these two substances would complement well each other in the UV-A part of the spectrum. By absorbing a broader range of UV-A wavelengths, flavonoids and sinapate esters together would efficiently attenuate UV-A radiation, and therefore protect the cells from oxidative damage. Apart from a direct UV screening protection function, flavonoids and sinapate esters are probably also involved in indirect protection from UV-induced oxidative damage, acting as efficient free radical and ROS quenchers.

Similar conclusions about UV screening efficiency of flavonoids and sinapate esters were drawn from VUV-UV absorption spectra (λ = 125-340 nm) that were measured in dry films. All flavonoid-containing fractions (F2, F3, F4, F5a and F5b), except fraction F6, had qualitatively similar absorption curves that are typical for flavonoids, showing one broad peak at 260-270 nm (corresponds to DNA peak I), a prominent peak at 202-204 nm (corresponds to DNA peak II), a small absorption peak in the VUV region at 157-160 nm, and a steep increase in absorption towards the lower end of the measured spectrum (region III). Fraction F6 had a different absorption curve. Since it represents the mixture of quercitrin and di-sinapoylglucose, it combined spectral features of both flavonoids and sinapate esters. Sinapate esters-containing fractions showed relatively weak VUV-UV spectral features, showing a small peak in the 160-164 nm region, one prominent peak at 202-204 nm and a weak shoulder at 245 nm. Compared to the VUV-UV spectrum of DNA, we concluded that sinapate esters would provide relatively poor protection to DNA in region I (UV-C). Depending on their concentration, sinapate esters might better protect DNA in region II (VUV). Flavonoids, particularly quercitrin from fraction F5a that

represents the most abundant flavonoid in our seed extract, showed absorption characteristics that would confer a good protection of DNA in regions I, II, III.

Besides flavonoids and sinapate esters, glucosinolates are the third group of secondary metabolites that was investigated in this study. Conventional UV spectroscopy (λ = 200-400 nm) in solution revealed that majority of glucosinolates isolated from *Arabidopsis* Ws-2 seeds (fractions G-F1, G-F2, G-F3, G-F5 and G-F6) are poor UV absorbers in the region above 250 nm (**Table 13**, chapter 3, section 11.4.1.3). This might be expected from the chemistry of majority of seed glucosinolates, including here detected 3-methylsulfinylpropyl (3-MSOP), 8-methylsulfinyloctyl (8-MSOO) and 8-metylthiooctyl (8-MTO) glucosinolates, which belong to the aliphatic class. Aliphatic functional groups in most glucosinolates contain many saturated covalent bonds, which are generally weak UV chromophores. However, these substances exhibited steeply increased UV absorption towards 200 nm, indicating that they contain heteroatoms, such as sulfur and oxygen that permit $n \rightarrow \sigma^*$ electron transitions. Similar observation was also found by measuring VUV-UV absorption spectra of dry films of glucosinolate-containing fractions from Ws-2 seeds **Fig. 58**, chapter **3**, section **11.4.2.3**). These spectra clearly showed that all glucosinolate fractions, but one, absorbed poorly in the 250-340 nm part of the spectrum. These results clearly indicated that aliphatic glucosinolates, which represent the majority of *Arabidopsis* seed glucosinolates, would provide no specific protection to DNA, proteins or any other cellular target in the UV-A, UV-B or UV-C part of the spectrum. Extending the absorption spectra into the VUV region, we also observed that fractions G-F1, G-F2, and particularly G-F6 were weak absorbers even in the VUV part of the spectrum. In contrast, aliphatic glucosinolate fractions G-F3 (8-methylsulfinyloctyl, 8-MSOO) and G-F5 (8-metylthiooctyl, 8-MTO) were excellent absorbers in the VUV region. However, their maxima of absorption did not match well the DNA peak in the region II. Therefore, they would provide relatively weak specific UV screening protection to DNA.

Here we single out the glucosinolate fraction G-F4, which contained the only aromatic glucosinolate (3-benzoyloxypropyl glucosinolate, 3-BzOP) detected in our seed extract. Thanks to the delocalized π-electron system in the aromatic ring, among all analysed glucosinolates, this compound was relatively good UV absorber. However, conventional UV absorption spectra, as well as VUV-UV absorption spectra in dry state revealed that this compound would not protect from UV-A, nor UV-B induced damage. According to VUV-UV absorption spectra, this substance in dry state exhibit high absorption all through 280 - 140 nm region (UV-C/ VUV part

of spectrum). This substance might have a good potential as UV screen protecting DNA and proteins, but only in UV-C and VUV regions.

Concluding remarks (4)

Here we summarize our observations on VUV-UV absorption properties of UV screening compounds found in *Arabidopsis* seeds. In this work we were particularly interested in absorption properties of UV screens in the UV-C and VUV part of the spectrum, since these wavelengths are highly damaging to DNA and other biologically important molecules. On the other hand, these highly energetic UV wavelengths were probably encountered on early Earth, and they are at the present encountered in the extraterrestrial environments, being limitation factor for life dispersal.

All our absorption spectroscopy results lead us to conclude that flavonoids can be considered as an ideal UV screens. Flavonoids inherent in *Arabidopsis* seeds, such as quercitrin, which is a representative of glycosilated flavonols, are the best suited UV screens, providing efficient direct protection to DNA both in the UV-C, as well as in the VUV region. Due to the high absorption in the UV-A part of the spectrum, flavonoids may also act as efficient protectants against indirect, oxidative damage to DNA and proteins. In addition, flavonoids occur in high concentration in seeds, particularly in the outer protective tissue, the seed coat, filtering out deleterious UV wavelengths prior they reaches the embryo in the interior of seed.

Furthermore, we found that glucosinolates, which accumulate in relatively high concentrations in seeds, would not act as efficient UV screens, except in the case of aromatic glucosinolates, such as glucomalcomiin, 3-benzoyloxypropyl glucosinolate (3-BzOP). However, their abundance in *Arabidopsis* seeds, in contrast to aliphatic glucosinolates, is relatively low (they make about 18% of the total glucosinolate content). Therefore, we assumed that they would have only small contribution in the total UV screening capacity provided by the secondary metabolites contained in *Arabidopsis* seeds.

Here we also conclude that sinapate esters that occur in *Arabidopsis* seeds would be less efficient than flavonoids in providing a direct UV screening protection to DNA particularly in the UV-C part of the spectrum, since they exhibited a local absorption minimum at the wavelengths at which DNA exhibits the maximum of absorption. These observations presumably

disagree with some earlier findings from *in vivo* studies, which indicated that sinapate esters are more effective and predominant UV protectors than flavonoids. However, these studies have not considered primarily the effects of UV-C radiation, but rather UV-B radiation, which is an important environmental factor on present-day Earth. Our absorption spectra showed that indeed, sinapate esters are much better absorbers in the UV-B than in the UV-C part of the spectrum (Chapple et al., 1992; Landry et al., 1995; Sheahan, 1996). However, based on the comparison of UV spectra of sinapate esters with those of flavonoids, it would be hard to conclude that sinapate esters would provide better UV-B screening protection than flavonoids. Nevertheless, they might have another indirect role in the UV protection, being ultimately more efficient protectants *in vivo* than flavonoids. Here we suggested that in plants, sinapate esters act complementarily with flavonoids, providing efficient protection in wider UV-B wavelength range. In addition, previous studies were performed on vegetative parts of plants (seedlings and leaves), rather than on seeds. Different plant tissues accumulate different types and concentrations of secondary metabolites, including flavonoids and sinapate esters. This may also reflect the differences in the level of resistance of seeds and vegetative tissues. Therefore, our UV absorption spectroscopy studies provide only preliminary estimation of UV screening efficiency for different compounds found in seeds. Their role in UV protection is necessary to be further demonstrated in systems *in vivo*. For this reason, in the second part of this thesis (chapters 5 and 6, part II), we tested the UV resistance of *Arabidopsis* seeds that contained normal level of flavonoids (wild type seeds), those that were deficient in flavonoids (*tt4* mutant), as well as those that lack sinapate esters (*fah1-2* mutant).

PART II:

TESTING UV RESISTANCE OF *Arabidopsis* SEEDS AND COMPARISON TO UV RESISTANCE OF *Bacillus subtilis* SPORES

Chapter 5
RESULTS II

15. RESISTANCE OF *Bacillus subtilis* SPORES TO QUASI-MONOCHROMATIC UV-C_{254} LIGHT

Samples of *Bacillus subtilis* spores were irradiated with quasi-monochromatic UV_{254} light for 16, 50, 100, 150 and 300 sec. The measured energy output of the UV lamp consisted predominantly of UV-C_{254} light (91%), and smaller portion of UV-B_{312} (7%) and UV-A_{365} light (2%). Samples of *Bacillus* spores were prepared in dry monolayers, where the calculated fraction of non-shadowed spores was 99.9% (**Equation 5**, chapter **2,** section **8.1.1.1.1.**), indicating that all spores in dry film were UV irradiated. Dry monolayers of *Bacillus* spores were covered with three types of UV cut-off filters: an aluminium foil that totally blocked light (dark control), a glass filter that cut off UV-C light and transmitted only UV-B and UV-A light (UV-B+UV-A), and a quartz filter that entirely transmitted the emitted UV light (UV-C + (UV-B + UV-A)).The minimal fluence[12] of UV-C_{254} light was 32.09 Jm^{-2} and the maximal fluence was 525.8 Jm^{-2}, corresponding to 16 sec and 300 sec of UV exposure under the quartz filter, respectively. Besides UV-C light, *Bacillus* spores covered with a quartz filter received a small amount of combined UV-B + UV-A light, ranging from 2.41 Jm^{-2} to 42.3 Jm^{-2} for UV-B_{312} light and from 0.721 Jm^{-2} to 11.82 Jm^{-2} for UV-A_{365} light. Spore samples covered with the glass filter were exposed only to the UV-B + UV-A portion of the light emitted from the UV source, with fluence ranging from 1.87 Jm^{-2} to 32.85 Jm^{-2} for UV-B_{312} light and from 0.698 Jm^{-2} to 11.441 Jm^{-2} for UV-A_{365} light. The UV resistance of *Bacillus* spores was determined by scoring the total number of colonies (CFU = colony forming unit), developed from exposed spores. Calculated CFU values per dry layer of spores represent a measure for determining the total number of spore survivors in the monolayer. **Fig. 59** shows the results of UV exposure experiments, where CFU units were compared for spore samples covered with aluminium foil (dark control samples), a glass filter (UV-B +UV-A exposed samples) and a quartz filter (UV-C + (UV-B + UV-A) exposed samples).

[12] The term "fluence" here stands for the total radiant energy of UV light falling on a unit surface area summed over a given period of irradiation (for details see chapter **2**, section **8.1.1.**). In photobiology, the term "UV fluence" is recommended instead of the term "UV dose" (IUPAC, 1997; IUVA http://www.iuva.org; Linden, 2003). Fluence (Jm^{-2}) is calculated as a product of irradiance (Wm^{-2}) and exposure time (sec) (see **Equation 4**, chapter **2**, section **8.1.1.**).

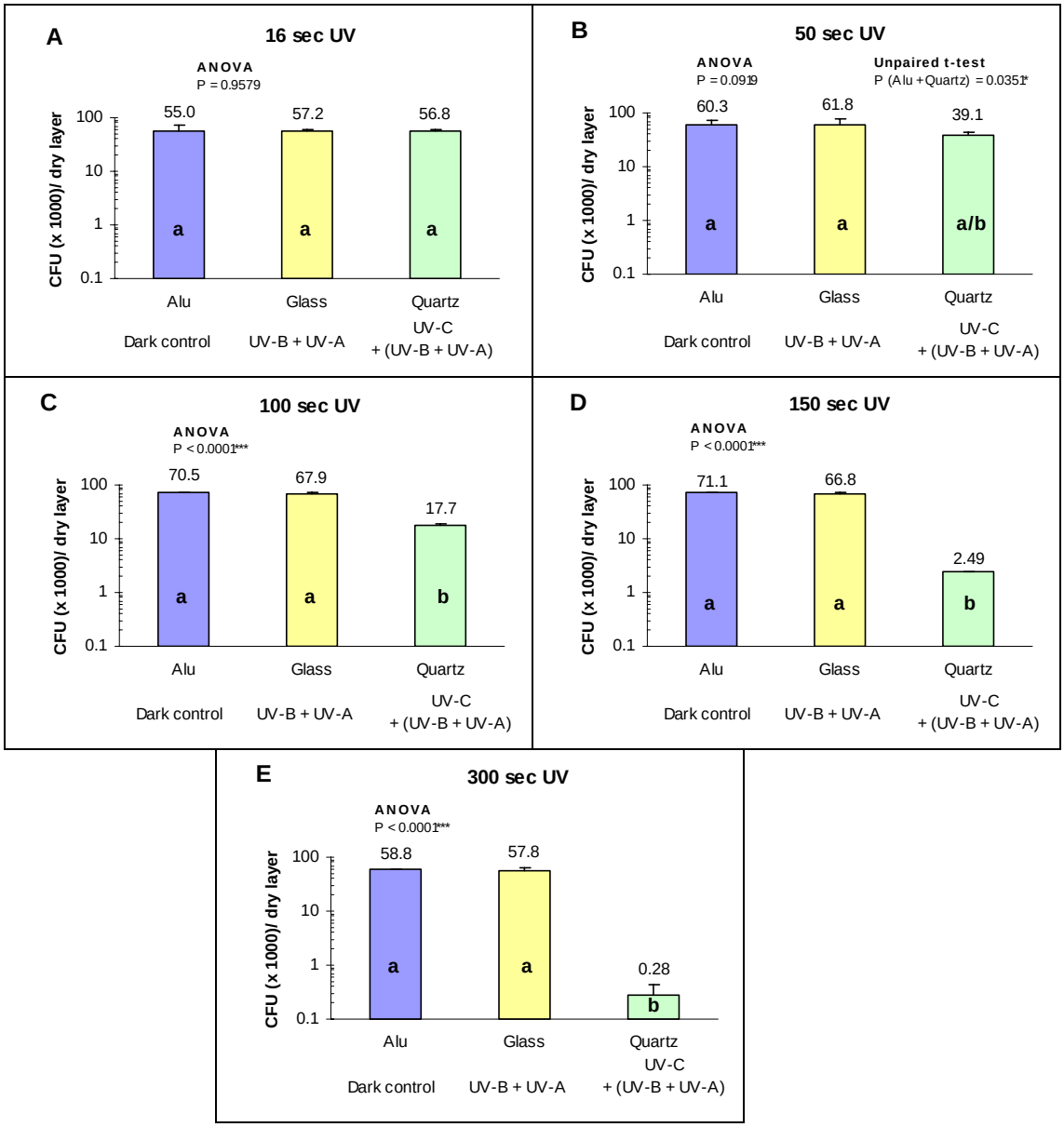

Fig. 59. The effects of entirely transmitted UV-C + (UV-B + UV-A) light and its UV-B +UV-A portion on colony forming ability (CFU = colony forming units) for dry spores of *Bacillus subtilis* WT 168 that were exposed to UV light for 16 (A), 50 (B), 100 (C), 150 (D) and 300 (E) sec. The samples were covered with different UV cut-off filters: aluminium foil (Alu), glass slide (Glass) and quartz window (Quartz).The samples covered with aluminium foil were used as a dark control, while samples covered with glass filter served as UV-B +UV-A control. The samples covered with quartz filters were exposed predominantly to UV-C (~91% of the total energy output) and to a smaller portion of UV-B + UV-A light emitted from the UV-C_{254} source. All values are the mean ± standard deviation of three independent experiments. Bars with different letters denote significant difference at $P < 0.05$ according to ANOVA and an unpaired t-test. The ANOVA p values are indicated above the bars: * = significant difference ($p < 0.05$), ** = very significant difference ($p < 0.01$), *** = extremely significant difference ($p < 0.001$). The UV-C stands for the light at λ = 254 nm, UV-B at λ = 312 nm and UV-A at λ = 365 nm.

At significance level of α = 0.05, the ANOVA results showed no significant difference in CFU values among dark control and samples exposed for 16 sec to UV-B + UV-A and UV-C + (UV-B + UV-A) (**Fig. 59A**), as well as in the case of samples exposed for 50 sec (**Fig. 59B**). However, an unpaired t-test showed a significant difference ($p = 0.0351$) in CFU values between dark control and samples irradiated with UV-C + (UV-B + UV-A) for 50 sec (**Fig. 59B**). Samples covered with quartz filter and exposed for 100, 150 and 300 sec to UV-C + (UV-B + UV-A) light, showed extremely significant differences ($p < 0.0001$) in CFU units when compared to their dark controls (samples covered with aluminium filter) and their UV-B + UV-A controls (samples covered with glass filter) (**Fig. 59C, D** and **E**).

No significant difference ($p = 0.1879$) was observed in CFU values among dark controls used in all UV exposure experiments (data not shown). Therefore, the CFU values for all dark controls were averaged and the mean value was compared to the values obtained for the samples irradiated with increasing fluences of entirely transmitted UV-C + (UV-B + UV-A) light and increasing fluences of the UV-B +UV-A portion of the light (**Fig. 60**).

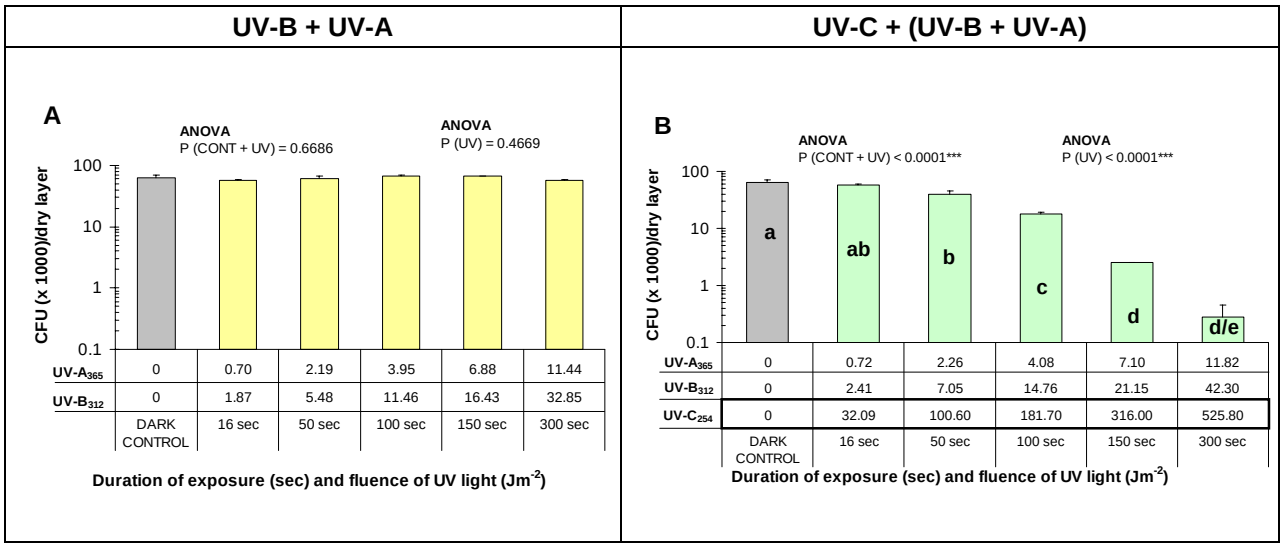

Fig. 60. The effects of UV-B +UV-A and UV-C + (UV-B + UV-A) light on colony forming ability (CFU = colony forming units) for dry spores of *Bacillus subtilis* WT 168 exposed to UV light. The UV-C + (UV-B + UV-A) denotes an entirely transmitted incident light (quartz filter), in contrast to its UV-B +UV-A portion (glass filter), emitted from the UV-C_{254} source. The duration of UV exposure (from 16 sec to 300 sec) and UV fluence (Jm^{-2}) are indicated under each bar. Values are the mean ± standard deviation of three independent experiments. Bars with different letters denote a significant difference at $\alpha < 0.05$ according to ANOVA and unpaired t-tests (UV exposed samples). Precise values from ANOVA are indicated above the bars, where * means a significant level ($P < 0.05$), ** very significant ($P < 0.01$) and *** extremely significant ($P < 0.001$) level of difference.

The CFU values of all samples that were covered with a glass filter and exposed only to UV-B + UV-A light, ranging from 1.87 Jm^{-2} to 32.85 Jm^{-2} for UV-B_{312} and from 0.698 Jm^{-2} to 11.441 Jm^{-2} for UV-A_{365} light, did not differ statistically (p = 0.6686), compared to the dark control. In addition, no significant difference (p = 0.4669) in CFU values was observed within the group of UV-B + UV-A irradiated samples, covered with glass filter (**Fig. 60A**).

On the other hand, UV-C + (UV-B + UV-A) light had extremely significant impact (p < 0.0001) on colony forming ability of irradiated *Bacillus* samples. The total number of *Bacillus* colonies decreased with increasing fluences of UV-C + (UV-B + UV-A) radiation (**Fig. 60B**). Since UV-B + UV-A radiation had no effect on the total number of colony formers, all observed effects of UV-C + (UV-B + UV-A) were attributed to the dominant UV-C component of the emitted light. The Tukey-Kramer post-hoc test (α = 0.05) showed no significant difference between the averaged dark control and the sample covered with quartz filter and exposed to UV-C light for 16 sec. However, statistically very significant decrease (p < 0.001) in CFU value was observed after only 50 sec of UV-C irradiation of *Bacillus* spores (UV-C_{254} fluence = 100.6 Jm^{-2}). The CFU values further decreased with increasing fluence of UV-C light, reaching a minimum CFU = 0.28 at the maximal fluence of UV-C = 525.8 Jm^{-2} after 300 sec of irradiation. Although the Tukey-Kramer post-hoc test showed no statistical difference between CFU values of samples exposed to UV-C light for 150 and 300 sec, a separately performed unpaired t-test inside these two groups clearly indicated statistical difference at the level of p < 0.0001.

Since UV-C light had a strong effect on the total number of *Bacillus* colonies developed from UV exposed spores, the UV_{254} dose response curve of *Bacillus* dry spores was established, where the logarithm of the surviving fraction of spores was plotted against the UV-C_{254} fluence (

Fig. 61). The surviving fraction S(UV) after UV irradiation is given by following equation (Horneck, 1993):

$$S(UV) = N/N_0 \times 100(\%) \qquad (5)$$

where

N = number of colony formers after UV irradiation with a certain fluence (samples covered with quartz filter)

N_0 = number of colony formers at zero fluence (dark control - samples covered with aluminium foil filter)

From the dose response curve, we determined the 10% survival rate (F_{10}) that is the equivalent of the value LD_{90} (lethal dose that inactivates 90% of spores). We found that dry spores of *Bacillus subtilis* WT 168 exposed to UV-C_{254} light had F_{10} (LD_{90}) = 0.245 kJm^{-2} (**Fig. 61**). Similarly, from the dose response curve we also determined the lethal dose that inactivates 50% of spores, LD_{50} = 0.123 kJm^{-2}.

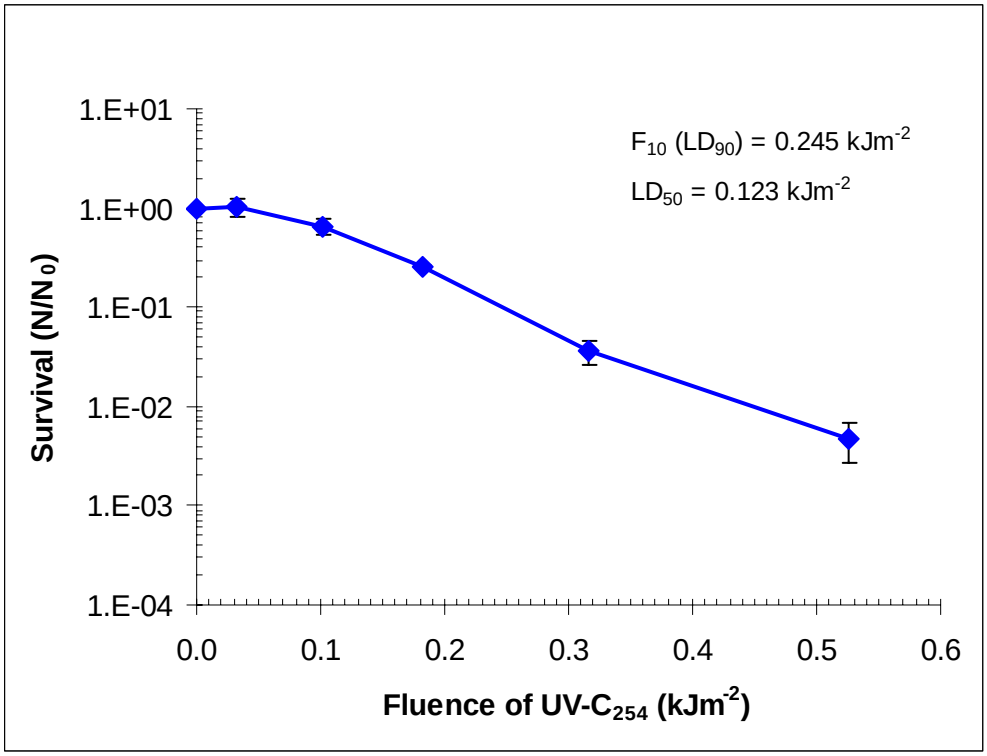

Fig. 61. Dose response curve for dry spores of *Bacillus subtilis* WT 168 exposed to increasing fluences of UV-C light (λ = 254 nm). The survival of spores is determined as N/N_0 where N means the number of colony formers after UV_{254} irradiation and N_0 stands for number of colony formers at zero fluence (dark control). The 10% survival rate F_{10} = 0.245 kJm^{-2} (the equivalent for LD_{90}, lethal dose that kills 90% of spores), as well as LD_{50} = 0.123 kJm^{-2} (lethal dose that kills 50% of spores) were determined from the graph. All values are the means ± standard deviation of three independent experiments.

16. RESISTANCE OF *Arabidopsis thaliana* SEEDS TO QUASI-MONOCHROMATIC UV-C_{254} LIGHT

16.1. General summary of results on the resistance of *Arabidopsis thaliana* seeds to quasi-monochromatic UV-C_{254} light

Dry *Arabidopsis* seeds were exposed to a quasi-monochromatic source of UV_{254} light that consisted predominantly of UV-C_{254} light (90%) and a smaller portion of UV-B_{312} (8%) and UV-A_{365} (2%) light. Monolayers of seeds were placed under the UV lamp, and they were covered with one of three types of UV cut-off filters, an aluminium foil (*Alu*) that blocked all light and therefore used as a dark control, a glass filter (*Glass*) that transmitted only UV-B + UV-A part of light and a quartz filter (*Quartz*) that transmitted almost entirely the incident UV-C + (UV-B + UV-A) light. The UV resistance was tested in five genotypes of *Arabidopsis* seeds, including two different wild ecotypes (Ws-2 and Col-0), genetically modified seeds of the *dyx* line and a flavonoid-lacking *tt4-8* mutant, both carrying a T-DNA with the *nptII* gene inserted in the Ws-2 genome, and nontransgenic *fah1-2* line, which is a sinapate ester-deficient mutant prepared in the Col-0 background. Since the *tt4-8* mutant was prepared by T-DNA mutagenesis, which in some cases may lead to the occurrence of pleiotropic effects, a transgenic *dyx* line was used as a T-DNA insertion control for *tt4-8* seeds.

The resistance of flavonoid-containing Ws-2, Col-0, *dyx* and *fah1-2* seeds was tested after a long-term UV irradiation up to 60 days, while the effects of UV light on flavonoid-lacking *tt4-8* seeds were observed after the short-term irradiation up to 139 hours. After 60 days of UV exposure, the Ws-2 and *dyx* seeds covered with the *Quartz* filter were exposed to maximal fluence[1] of UV-C = 6.0×10^5 kJm^{-2}, and to lesser fluences of UV-B = 5.6×10^4 kJm^{-2} and UV-A = 1.2×10^4 kJm^{-2}. The Col-0 and *fah1-2* seeds that were irradiated for 60 days under the *Quartz* filter, they were exposed to maximal fluence of UV-C = 4.8×10^5 kJm^{-2} and lesser fluences of UV-B = 4.4×10^4 kJm^{-2} and UV-A = 9.8×10^3 kJm^{-2}. The samples that were covered with the *Glass* filter were exposed only to UV-B + UV-A light, and after 60 days of irradiation the maximal fluence received by Ws-2 and *dyx* seeds were UV-B = 4.3×10^4 kJm^{-2} and UV-A = 1.2×10^4 kJm^{-2}, while those that were received by Col-0 and *fah1-2* seeds were UV-B = 3.4×10^4 kJm^{-2} and UV-A = 9.5×10^3 kJm^{-2}.

Table 14. General summary of the effects of UV-B + UV-A and UV-C + (UV-B + UV-A) radiation on different parameters at three developmental stages of *Arabidopsis* plants grown from irradiated seeds. The UV-C + (UV-B + UV-A) denotes an entirely transmitted incident light (quartz filter), in contrast to its minor UV-B +UV-A portion (glass filter), emitted from the UV-C_{254} source.The flavonoid-containing Ws-2, Col-0, *dyx* and *fah1-2* seeds were exposed up to 60 days (long-term UV exposure experiments), while flavonoid-lacking *tt4-8* seeds were irradiated up to 139 hours (short-term UV exposure experiments). The maximal fluences of UV-B + UV-A[13] and UV-C + (UV-B + UV-A)[14] light are indicated in the footnotes, where fluences were measured at λ = 254 nm (UV-C), λ = 312 nm (UV-B) and λ = 365 nm (UV-A).
The plant genotypes were: Wassilewskija (Ws-2), Columbia (Col-0), a control mutant with T-DNA insertion carrying the *nptII* gene (*dyx*), a flavonoid-deficient mutant with a T-DNA insertion carrying the *nptII* gene*(tt4-8*), a sinapate ester-deficient mutant (*fah1-2*). Wild ecotypes are marked with asterisks and background ecotypes are noted under each mutant line.

PLANT DEVELOPMENTAL STAGES	MEASURED PARAMETERS	UV-B + UV-A					UV-C + (UV-B + UV-A)				
		Ws-2*	Col-0*	*dyx* (Ws-2)	*tt4-8* (Ws-2)	*fah1-2* (Col-0)	Ws-2*	Col-0*	*dyx* (Ws-2)	*tt4-8* (Ws-2)	*fah1-2* (Col-0)
Germination	Loss of germination capacity ($G_{max\%}$)	-	-	-	-[a]	-	-	-	-	++++[b]	-
	Increase in mean germination time (MGT)	-	-/+[c]	-/+[c]	+++	++	+	+	++	++++[b]	+++
Early-seedling development	Increase in % of abnormal seedlings	-	-/+	-	-[a]	++	++	+	++	++++[b]	++
	Severity of seedling damage	-	-/+	-	-[a]	+	++	+	++	++++[b]	++
	Reduction in root length	-	-	+	-[a]	-	++	-	++	++++[b]	+
Plant development	Decrease in % of survived plants	-	-	//	+++	-	++	+	//	++++[b]	++
	Decrease in % of fertile plants	-	-	//	+++	-	++	+	//	++++[b]	++
	Reduction in plant height	-	-	//	+++	-	++	+	//	++++[b]	+

[a] No effects observed after 139 hours of exposure to UV-B + UV-A light (short-term UV exposure experiments)[2]. Effects of higher UV fluences after 60 days of irradiation were not determined (long-term UV exposure experiments).
[b] Extreme effects of UV-C + (UV-B + UV-A) radiation observed already at lower UV fluences up to 139 hours of exposure (short-term UV exposure experiments)[3].
[c] Effects of increased MGT values observed only when seeds were germinated under suboptimal conditions

// = effect not determined, - no effect, -/+ possible effect, + small effect, ++ strong effect, +++ very strong effect, ++++ extreme effect

[13] Maximal fluence of UV-B + UV-A light:
- long-term exposure of Ws-2 and *dyx* seeds: UV-B = 4.3 x 10^4 kJm^{-2}, UV-A = 1.2 x 10^4 kJm^{-2}
- long-term exposure of Col-0 and *fah1-2* seeds: UV-B = 3.4 x 10^4 kJm^{-2}, UV-A = 9.5 x 10^3 kJm^{-2}
- short-term exposure of *tt4-8* seeds: UV-B = 4.2 x 10^3 kJm^{-2}, UV-A = 1.2 x 10^3 kJm^{-2}

[14] Maximal fluence of UV-C + (UV-B + UV-A) light:
- long-term exposure of Ws-2 and *dyx* seeds: UV-C = 6.0 x 10^5 kJm^{-2}, UV-B = 5.6 x 10^4 kJm^{-2}, UV-A = 1.2 x 10^4 kJm^{-2}
- long-term exposure of Col-0 and *fah1-2* seeds: UV-C = 4.8 x 10^5 kJm^{-2}, UV-B = 4.4 x 10^4 kJm^{-2}, UV-A = 9.8 x 10^3 kJm^{-2}
- short-term exposure of *tt4-8* seeds: UV-C = 5.9 x 10^4 kJm^{-2}, UV-B = 5.4 x 10^3 kJm^{-2}, UV-A = 1.2 x 10^3 kJm^{-2}

During the short-term UV exposure experiments, the *tt4-8* seeds were irradiated in different time periods from the minimal 0.5 hour (UV-C = 2.8 x 10^2 kJm^{-2}, UV-B = 25.4 kJm^{-2} and UV-A = 5.6 kJm^{-2}) to the maximal 139 hours of exposure (UV-C = 5.9 x 10^4 kJm^{-2}, UV-B = 5.4 x 10^3 kJm^{-2} and UV-A = 1.2 x 10^3 kJm^{-2}). The *tt4-8* samples covered with the *Glass* filter were exposed to UV-B + UV-A light with fluences[1] from UV-B = 19.7 kJm^{-2} and UV-A = 5.5 kJm^{-2} (0.5 hour of irradiation) up to fluences of UV-B = 4.2 x 10^3 kJm^{-2} and UV-A = 1.2 x 10^3 kJm^{-2} (169 hours of irradiation).

The UV resistance of *Arabidopsis* seeds was determined by observing and measuring physiological parameters throughout three different growth stages: the seed germination (principal growth stage 0.5), the early-seedling stage (principal growth stage 1.0) and the stage of plant development (principal growth stage 8.0), described in Boyes et al. 2001 and Kjemtrup et al. 2003.

Summarized results on the effects of UV-C + (UV-B + UV-A) light and UV-B + UV-A part of emitted light on *Arabidopsis* seeds, observed through three developmental stages, are presented in **Table 14**. The results for each separately studied parameter are elaborated in detail further in this work.

16.2. Seed germination stage - effects of quasi-monochromatic UV-C_{254} light

After the UV irradiation of dry *Arabidopsis* seeds, the effects of entirely transmitted incident UV-C + (UV-B + UV-A) radiation, as well as the UV-B + UV-A portion of light emitted from UV-C_{254} source, were first studied on the level of seed germination, which is the first growth stage in plant development. Here we considered the germination *sensu stricto* (Perino and Côme, 1991), which starts at the end of the phase of water uptake by the quiescent dry seeds and terminates by the elongation of the embryonic axis through the surrounding tissue (Bewley, 1997; Nonogaki et al., 2007). Since no universally useful biochemical marker of the progress of germination has been found, the only stage of germination that we can determine quite precisely is its termination (Bewley and Black, 1994b). The visible sign that germination completed is a protrusion of radicle from the seed coat, defined as the principal growth stage 0.5, according to the BBCH growth stage scale adapted for *Arabidopsis* model (Boyes et al., 2001; Kjemtrup et al., 2003).

Different parameters of germination process were studied here: germination capacity, speed of germination and uniformity of germination. Germination capacity of UV irradiated seeds was expressed through the maximal germination percentage ($G_{max\%}$), while germination speed was studied by measuring the mean germination time (MGT). Additional parameters of germination dynamics were also analyzed, such as $T_{50\%}$ and $T_{25\text{-}75\%}$ values, as well as skewness of germination curves (see below).

The resistance of flavonoid-containing seeds (Ws-2, Col-0, *dyx* and *fah1-2* lines) was tested in the long-term UV exposure experiments that lasted up to 60 days. The effects of UV radiation on germination were then studied under optimal and suboptimal temperature conditions. The resistance of flavonoid-lacking *tt4-8* seeds was tested in so-called short-term UV exposure experiments that lasted up to 139 hours, after which the germination was studied only under optimal temperature conditions.

16.2.1. Long-term UV exposure of flavonoid-containing Arabidopsis seeds

16.2.1.1. Germination of UV irradiated flavonoid-containing Arabidopsis seeds under optimal conditions

The germination process of irradiated flavonoid-containing seeds was studied by scoring the percentage of germinated seeds over the time periods and plotting the germination curves (**Fig. 62**). Irradiated seeds were imbibed for exactly 72 hours in the dark at 4°C and germinated under optimal conditions (25-26 °C, 16/8 hours light/dark cycle). The germination time was measured in hours after imbibition (HAI). The germination curves of long-term UV exposed seed samples (**Fig. 62E-H)** and the unexposed control samples (**Fig. 62A-D**) are compared for the Ws-2 and *dyx* samples that were exposed for 30 and 60 days, as well as for the Col-0 and *fah1-2* samples that were exposed for 40 and 60 days. The curves have the typical sigmoidal shape, showing that a minority of the seeds in the population germinated early, then the germination percentage increased more rapidly, and finally just a few late germinators emerged at the end of the germination process.

All samples, including unexposed controls, as well as those exposed to UV-C + (UV-B + UV-A) and UV-B + UV-A light, germinated up to almost 100%, even after 60 days of treatment. In order to investigate possible instability in seed vigour[15] related to the seed aging problem during long-lasting experiments, the germination curves of all dark control samples (seeds exposed to the experimental conditions, but protected from UV light by the *Alu* filter) were compared to the germination curves of laboratory controls (seeds stored in the dark at 4°C), as shown in **Fig. 62A-D**. The germination curves of the dark and laboratory controls were similar in the *fah1-2* mutant line and the background Col-0 line, exposed for 40 and 60 days, as well as in the *dyx* mutant line, exposed to the experimental conditions for 30 and 60 days (**Fig. 62B**, **C** and **D**). These results indicated satisfying stability of seeds during the long-term experiment, as well as adequate consistency of germination results. However, small changes in germination dynamics, but not in germination capacity ($G_{max\%}$) were detected for both Ws-2 dark control samples that were exposed for 30 and 60 days, when compared to the Ws-2 laboratory control (**Fig. 62A**). Nevertheless, this effect was not observed in germination test under stressed

[15] In this work the term *seed vigour* is defined as the sum of the properties, which determine the potential for rapid and uniform seed germination under wide range of experimental conditions (modified from AOSA, 1983). For instance, the high-vigour seeds germinate uniformly and rapidly and grow more resistant seedlings than the low-vigour seeds. The level of seed vigour is determined by three major factors: genetic constitution, environmental factors and storage conditions (Sun et al., 2007). Seeds undergoing natural ageing during storage are likely to lose vigour at a faster rate than they lose viability (Schmidt, 2000).

conditions at suboptimal temperature (for details see section **16.2.1.2**). Since there were no observed major changes in germination behaviour between the two dark controls exposed for 40 and 60 days in the case of Col-0 and *fah1-2* seeds, and 30 and 60 days in the case of Ws-2 and *dyx* seeds, data points were averaged for the two dark controls of the same genotype. The average germination curves for dark controls were plotted and compared to the UV exposed samples for Ws-2, Col-0, *dyx* and *fah1-2* lines (**Fig. 62E-H**).

The Ws-2, *dyx* and Col-0 seeds that were exposed to UV-B + UV-A portion of emitted light (seeds covered with the *Glass* filter) showed no major changes in germination behaviour even after 60 days of UV exposure (**Fig. 62E, F** and **G**), where Ws-2 and *dyx* samples were exposed to fluences of UV-B = 4.3 x 10^4 kJm^{-2} and UV-A = 1.2 x 10^4 kJm^{-2}, while the Col-0 sample was exposed to fluences of UV-B = 3.4 x 10^4 kJm^{-2} and UV-A = 9.5 x 10^3 kJm^{-2}. However, smaller changes in germination behaviour of *fah1-2* seeds was observed after 60 days of exposure to UV-B + UV-A light (UV-B = 3.4 x 10^4 kJm^{-2} and UV-A = 9.5 x 10^3 kJm^{-2}), where the germination dynamics, but not the germination capacity, was affected (**Fig. 62H**).

The UV-C + (UV-B + UV-A) radiation had more pronounced effects on germination dynamics of seed samples (seeds covered with the *Quartz* filter), although the germination capacity ($G_{max\%}$) in all samples was not affected (**Fig. 62E-H**). For instance, the germination behaviour of the Ws-2 seeds was not altered after 30 days, but it was slowed after 60 days of exposure to UV-C + (UV-B + UV-A) radiation (**Fig. 62E**). The germination of the *dyx* seeds was slowed by exposure for 30 days and this effect was even more pronounced after 60 days of exposure to UV-C + (UV-B + UV-A) light, as shown in **Fig. 62F**. The germination of the Col-0 wild type seeds was slightly slower after 40 days of exposure, but it remained unchanged after 60 days of exposure to UV-C + (UV-B + UV-A) light (**Fig. 62G**). The germination dynamics of the sinapate ester-mutant *fah1-2* changed significantly already after 40 days of exposure to UV-C + (UV-B + UV-A) light, although the germination capacity remained unchanged (**Fig. 62H**).

In an effort to better describe the germination process illustrated by the germination curves, and to quantify differences in germination behaviour among samples exposed to UV-C + (UV-B + UV-A) light, as well as UV-B + UV-A portion of light, different germination parameters, including germination capacity and germination speed, were studied separately and the results were analyzed statistically as described below.

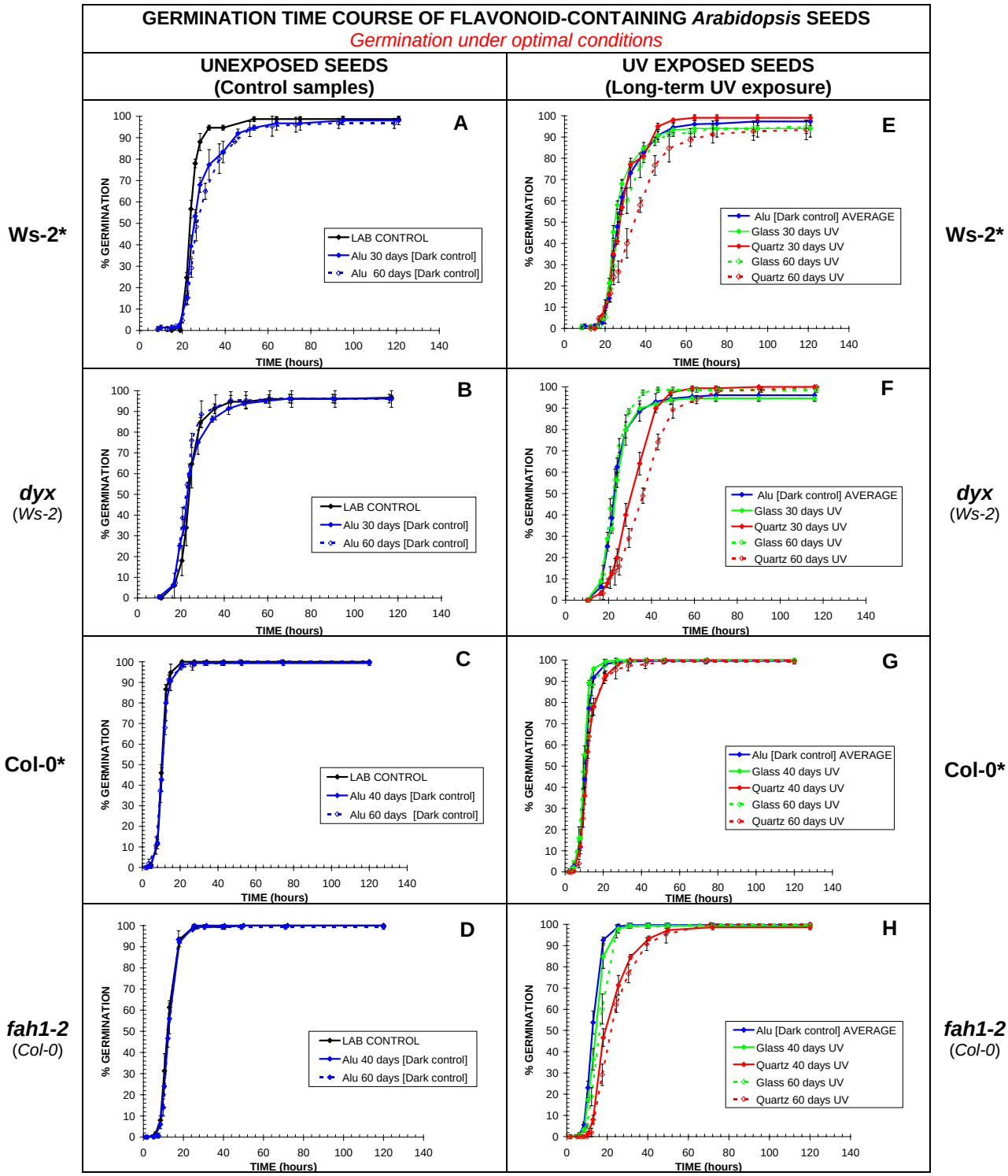

Fig. 62. Effects of UV radiation on germination behaviour of flavonoid-containing *Arabidopsis* seeds germinated under the optimal conditions. The germination curves of seeds that germinated after long-term exposure to UV light (panels E, F, G and H) are compared to the germination curves of unexposed control samples (panels A, B, C and D). Germination time is expressed in hours after imbibition (HAI). Imbibition was performed in the dark at 4°C for 72 hours. Seeds covered with an aluminium foil (*Alu* filter) were protected from the UV light, and they served as dark controls (blue lines), while laboratory controls were untreated seeds, stored in the dark at 4°C over the whole period of the experiment (black lines). Seeds covered with a *Glass* filter were exposed only to the minor UV-B + UV-A portion of emitted light (green lines), while those covered with a *Quartz* filter were exposed to entirely transmitted UV-C + (UV-B + UV-A) light, emitted from the UV-C_{254} source (red lines). The duration of exposure was 30 and 60 days in the case of the Ws-2 and *dyx* seeds, and 40 and 60 days in the case of the Col-0 and *fah1-2* seeds. Data points represent the mean values ± standard deviation of three parallel experiments (n = 50).
The plant genotypes were: Wassilewskija (Ws-2), A and E; a control mutant with a T-DNA insertion, carrying the *nptII* gene (*dyx*), B and F; Columbia (Col-0), C and G; a sinapate ester-deficient mutant (*fah1-2*), D and H. Wild ecotypes are marked with asterisks and background ecotypes are noted in the parentheses under each mutant line.

16.2.1.1.1. Germination capacity ($G_{max\%}$) of seeds exposed to quasi-monochromatic UV-C_{254} light

The germination capacity was expressed through the maximal germination percentage ($G_{max\%}$) achieved at the end of the germination process. The germination capacities of Ws-2, *dyx*, Col-0 and *fah1-2 Arabidopsis* seeds exposed to UV-C + (UV-B + UV-A) and UV-B + UV-A light, were compared as illustrated in **Fig. 63**. The mean values of $G_{max\%}$ obtained from three parallel experiments, observing n = 50 seeds, were analyzed using ANOVA and the unpaired t-test ($\alpha = 0.05$). In the literature, the germination percentage data are usually transformed in $\arcsin\sqrt{\%}$ values prior the analysis of variance (Baskin and Baskin, 2001a). Since we obtained very similar statistical results for transformed and untransformed $G_{max\%}$ data, here are presented only the results obtained directly from untransformed percentage data.

No statistically significant differences ($p > 0.05$) in $G_{max\%}$ values were observed among the control samples, comparing a laboratory control and two dark controls after 30 and 60 days of treatment in the Ws-2 and *dyx* lines or 40 and 60 days in the Col-0 and *fah1-2* lines (results not shown). Since these results indicated good stability of germination capacity in all dark controls even after 60 days of treatment under experimental conditions, the $G_{max\%}$ values for dark controls were averaged in each seed line and these values were further compared to $G_{max\%}$ for UV exposed samples (**Fig. 63**).

The exposure of seeds to UV-B + UV-A light did not affect the germination capacity, even after 60 days of irradiation. It is important to note that all dark controls as well as the samples exposed to UV-B + UV-A light reached the final germination percentage of about 100% (**Fig. 63A-D**). ANOVA ($\alpha = 0.05$) showed no significant difference in $G_{max\%}$ among dark controls and samples exposed to UV-B + UV-A for Ws-2 and Col-0 wild type lines, as well as the transgenic *dyx* line and the sinapate ester mutant, *fah1-2*. In addition, the unpaired t-tests ($\alpha = 0.05$) showed no statistically significant differences in $G_{max\%}$ within the group of UV-B + UV-A exposed samples in the Ws-2, Col-0 and *fah1-2* lines (**Fig. 63A, C** and **D**). Although the unpaired t-test showed a small increase in $G_{max\%}$ ($p = 0.0134$) after 60 days of exposure of *dyx* seeds to UV-B + UV-A light, ANOVA clearly showed no statistical difference ($p = 0.1406$), indicating that UV-B + UV-A had no effect on germination capacity of *dyx* seeds (**Fig. 63B**).

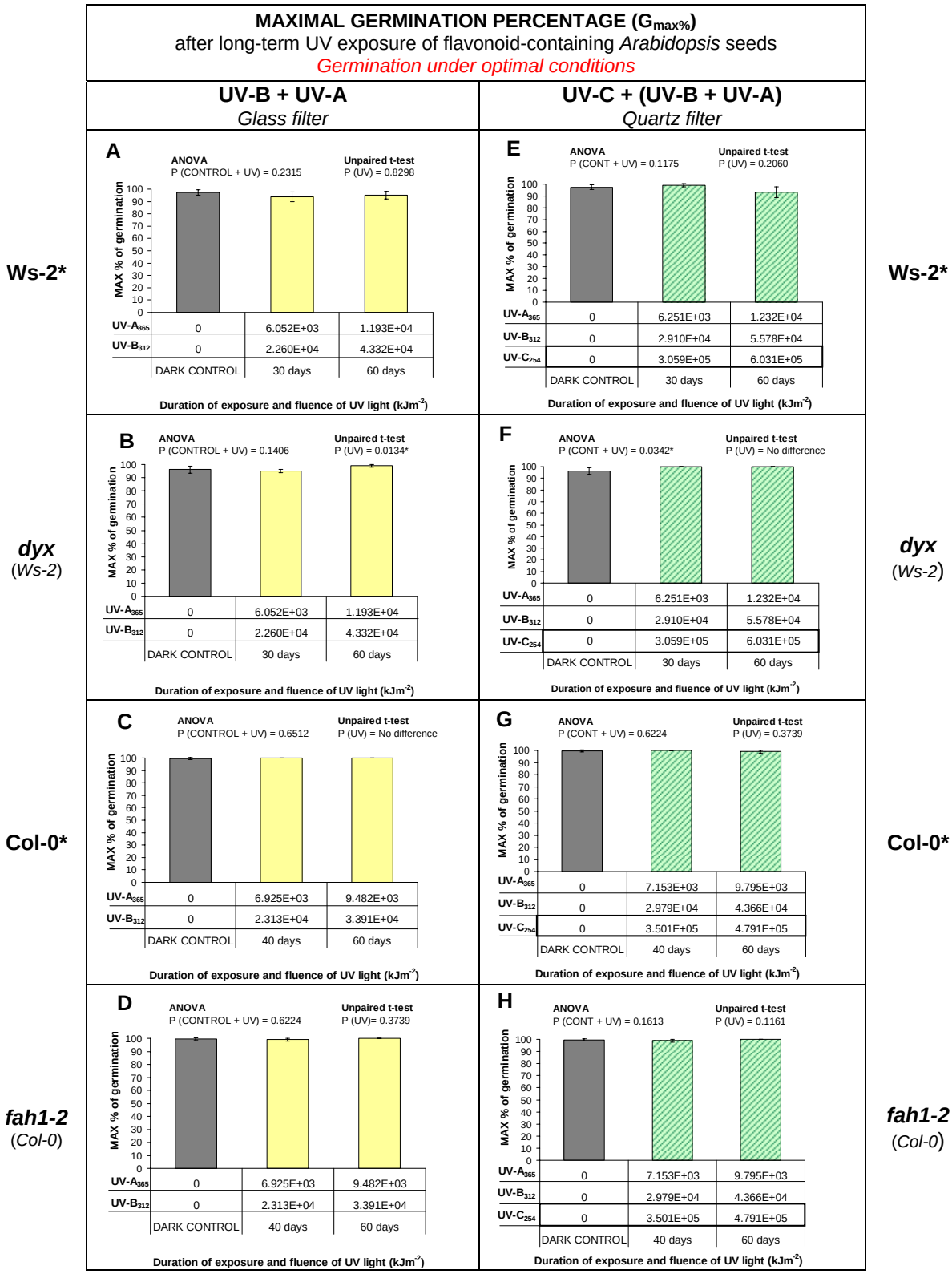

Fig. 63. Maximal germination percentage ($G_{max\%}$) of flavonoid-containing *Arabidopsis* seeds germinated under the optimal conditions after exposure to entirely transmitted UV-C + (UV-B + UV-A) light or only to its minor UV-B + UV-A portion, emitted from the UV-C_{254} source. The $G_{max\%}$ values of UV irradiated seed samples are here compared with those of the unexposed control samples (dark controls). The duration of UV exposure (30 and 60 days for Ws-2 and *dyx* seeds, and 40 and 60 days for Col-0 and *fah1-2* seeds) and UV fluences (kJm^{-2}) are indicated under each bar. After UV exposure, seeds were imbibed in the dark at 4°C for 72 hours. Values are the mean ± standard deviation of three parallel experiments (n = 50). The precise values from ANOVA and the unpaired t-tests are indicated above the bars, where * means a significant level ($P < 0.05$), ** very significant ($P < 0.01$) and *** extremely significant ($P < 0.001$) level of difference.
The plant genotypes were: Wassilewskija (Ws-2), A and E; a control mutant with a T-DNA insertion carrying the *nptII* gene (*dyx*), B and F, Columbia (Col-0), C and G; a sinapate ester-deficient mutant (*fah1-2*), D and H. Wild ecotypes are marked with asterisks and background ecotypes are noted in the parentheses under each mutant line.

The exposure of seeds to UV-C + (UV-B + UV-A) light had no effect on the germination capacity of the Ws-2, *dyx*, Col-0 and *fah1-2*seeds (**Fig. 63E-H**). ANOVA showed no differences in the germination capacity among both UV-C + (UV-B + UV-A) irradiated samples and the dark controls for the Ws-2, Col-0 and *fah1-2* lines, and the unpaired t-tests detected no statistical difference in $G_{max\%}$ values within the group of UV-C + (UV-B + UV-A) exposed samples in these three genotypes (**Fig. 63E**, **G** and **H**). In the case of the *dyx* seeds irradiated for 30 and 60 days, ANOVA indicated a significant increase in $G_{max\%}$ values (p = 0.0342) for both UV-C + (UV-B + UV-A) exposed samples, compared to the dark control (**Fig. 63F**). Since both UV exposed *dyx* samples reached maximal germination percentage at 100 ± 0%, the statistical difference was not taken into account, due to the limitations of ANOVA in the case of to high disparity in the variance among tested groups.

16.2.1.1.2. Mean germination time (MGT) of seeds exposed to quasi-monochromatic UV-C_{254} light

Besides the final percentage of germinated seeds, we also studied the dynamics of the germination process over the whole time period of germination. Mean germination time can be used as a parameter of germination dynamics, as an inverse expression of overall germination speed for the whole seed population, and it corresponds to the reciprocal value of the mean germination rate (Larsen and Bibby, 2004; Ranal and de Santana, 2006). It represents the average length of time required for maximum germination of a seed population (Ranal and de Santana, 2006). Mean germination time (MGT) was calculated according to the equation of Ellis and Roberts (1981) (see **Equation 1**, chapter **1**, section **4.2.2.1**).

The impact of UV-C + (UV-B + UV-A) light, as well as its UV-B + UV-A component on the mean germination time (MGT) of Ws-2, *dyx*, Col-0 and *fah1-2 Arabidopsis* seeds is illustrated in **Fig. 64**. Mean values, obtained from three parallel experiments, observing n = 50 seeds, were calculated and compared for each seed genotype. ANOVA and the unpaired t-test, both at the level of significance α = 0.05, were used for the statistical analysis of the results. Since seeds in the germination process frequently show some deviation from normality, causing a positively skewed germination time course (Bewley and Black, 1994b; Ranal and de Santana, 2006), as detected for *Arabidopsis* seeds (**Table 15**), and in an effort to obtain homogeneous variance in ANOVA, the MGT data were transformed into square-root values, prior the statistical analysis (Larsen and Bibby, 2004).

The stability in vigour of dark control Ws-2, *dyx*, Col-0 and *fah1-2* seeds, treated up to 60 days under the experimental conditions, was examined by comparing their MGT values to that of laboratory control (results not shown). According to ANOVA performed on square-root transformed data, no significant differences ($p > 0.05$) in MGT were observed among the control samples, including the laboratory and two dark controls for the Col-0, *dyx* and *fah1-2* seed lines. However, ANOVA showed an extremely significant difference ($p = 0.0008$) in MGT values for both Ws-2 dark controls (exposed for 30 and 60 days), when compared to the Ws-2 laboratory control. In spite of this, the unpaired t-test showed no significant difference ($p = 0.3514$) between these two Ws-2 dark controls. Thus, the MGT values of the two dark controls were averaged for the Ws-2 line, as well as for the *dyx*, Col-0 and *fah1-2* seed lines. The MGT values of samples exposed to UV-C + (UV-B + UV-A) and UV-B + UV-A light were statistically weighted against averaged MGT values of the dark controls (**Fig. 64**).

Statistical analyses showed that UV-B + UV-A component of light emitted from quasi-monochromatic UV_{254} source had no effect on the mean germination time of the Ws-2, *dyx* and Col-0 seeds (**Fig. 64A-C**), while it had a significant impact on the MGT of the sinapate ester mutant *fah1-2* (**Fig. 64D**). The unpaired t-test showed no significant difference in MGT between two Ws-2 samples exposed to UV-B + UV-A light for 30 and 60 days (**Fig. 64A**). Although the results of unpaired t-test indicated a significant difference within the group of UV-B + UV-A exposed samples in *dyx* ($p = 0.00328$) and Col-0 ($p = 0.0137$) line, ANOVA clearly showed that there is no statistical difference ($p > 0.05$) in MGT values among the seed samples in all three genotypes, Ws-2, *dyx* and Col-0 (**Fig. 64A-C**).

On the other hand, the sinapate ester mutant *fah1-2* showed very different germination behaviour after the exposure of the seeds to lower fluences of UV-B + UV-A light (**Fig. 64D**). Compared to the dark control, ANOVA showed an extremely significant difference ($p < 0.0001$) in MGT values for both UV-B + UV-A exposed *fah1-2* samples irradiated for 40 and 60 days. The Tukey-Kramer post-hoc test showed a very significant ($p < 0.01$) increase in MGT already after 40 days of the exposure of *fah1-2* seeds to UV-B + UV-A light (UV-B = 2.3×10^4 kJm^{-2} and UV-A = 6.9×10^3 kJm^{-2}), and an extremely significant increase ($p < 0.001$) in MGT after 60 days of the exposure (UV-B = 3.4×10^4 kJm^{-2} and UV-A = 9.5×10^3 kJm^{-2}). In addition, the unpaired t-test showed very significant difference ($p = 0.0069$) within the group of UV-B + UV-A exposed *fah1-2* samples. This result indicated increased sensitivity of the sinapate ester-lacking *fah1-2* mutant to UV-B + UV-A radiation, as seen in the slower germination of irradiated seeds.

The UV-C + (UV-B + UV-A) light had a significant impact on the mean germination time in all four tested flavonoid-containing seed lines (**Fig. 64E-H**). ANOVA showed statistically important differences in MGT among dark controls and the samples exposed to UV-C + (UV-B + UV-A) light in all four genotypes, resulting in a very significant difference in the Ws-2 sample ($p = 0.0084$), as shown in **Fig. 64E**, and extremely significant differences in *dyx* ($p < 0.0001$), Col-0 ($p = 0.0005$) and *fah1-2* ($p < 0.0001$) samples (**Fig. 64F, G** and **H**, respectively). This effect of increased MGT was attributed mainly to the dominant UV-C component (it makes about 91% of incident light), since UV-B + UV-A alone did not have an effect on MGT of Ws-2, *dyx* and Col-0 seeds (**Fig. 64A-C**). On the other hand, the observed extremely significant increase in the MGT of the *fah1-2* seeds exposed to UV-C + (UV-B + UV-A) light can be attributed to combined effects of both components of the incident light (dominant UV-C and background UV-B + UV-A), as seen in **Fig. 64D** and **Fig. 64H**.

The Tukey-Kramer post-hoc test ($\alpha = 0.05$) showed no difference in MGT between Ws-2 sample exposed to UV-C + (UV-B + UV-A) light for 30 days (UV-C = 3.1 x 10^5 kJm^{-2}) and the dark control, but increased fluences of UV light (UV-C = 6.0 x 10^5 kJm^{-2}), reached after 60 days, induced a very significant increase ($p < 0.01$) in the MGT of Ws-2 seeds (**Fig. 64E**). The MGT values for both UV-C + (UV-B + UV-A) exposed Ws-2 samples did not differ significantly, according to the unpaired t-test.

The T-DNA insertion mutant *dyx* appeared more sensitive to UV-C + (UV-B + UV-A) light than its Ws-2 background, since the Tukey-Kramer post-hoc test showed an extremely significant increase ($p < 0.001$) in MGT value already after 30 days of exposure (UV-C = 3.1 x 10^5 kJm^{-2}). Increased fluences of UV light (UV-C = 6.0 x 10^5 kJm^{-2}), reached after 60 days, induced a further extremely significant increase ($p < 0.001$) in MGT in this line (**Fig. 64F**). The MGT values for both UV-C + (UV-B + UV-A) exposed *dyx* samples differed very significantly, according to the unpaired t-test.

Compared to the dark control, the Tukey-Kramer post-hoc test showed a very significant increase ($p < 0.01$) in MGT for Col-0 wild type seeds exposed to UV-C + (UV-B + UV-A) for 40 days (UV-C = 3.5 x 10^5 kJm^{-2}), and an extremely significant increase ($p < 0.001$) in MGT for seeds exposed for 60 days (UV-C = 4.8 x 10^5 kJm^{-2}), as seen in **Fig. 64G**. No statistically significant difference was detected in MGT values within the group of UV-C + (UV-B + UV-A) exposed Col-0 samples, using the unpaired t-test.

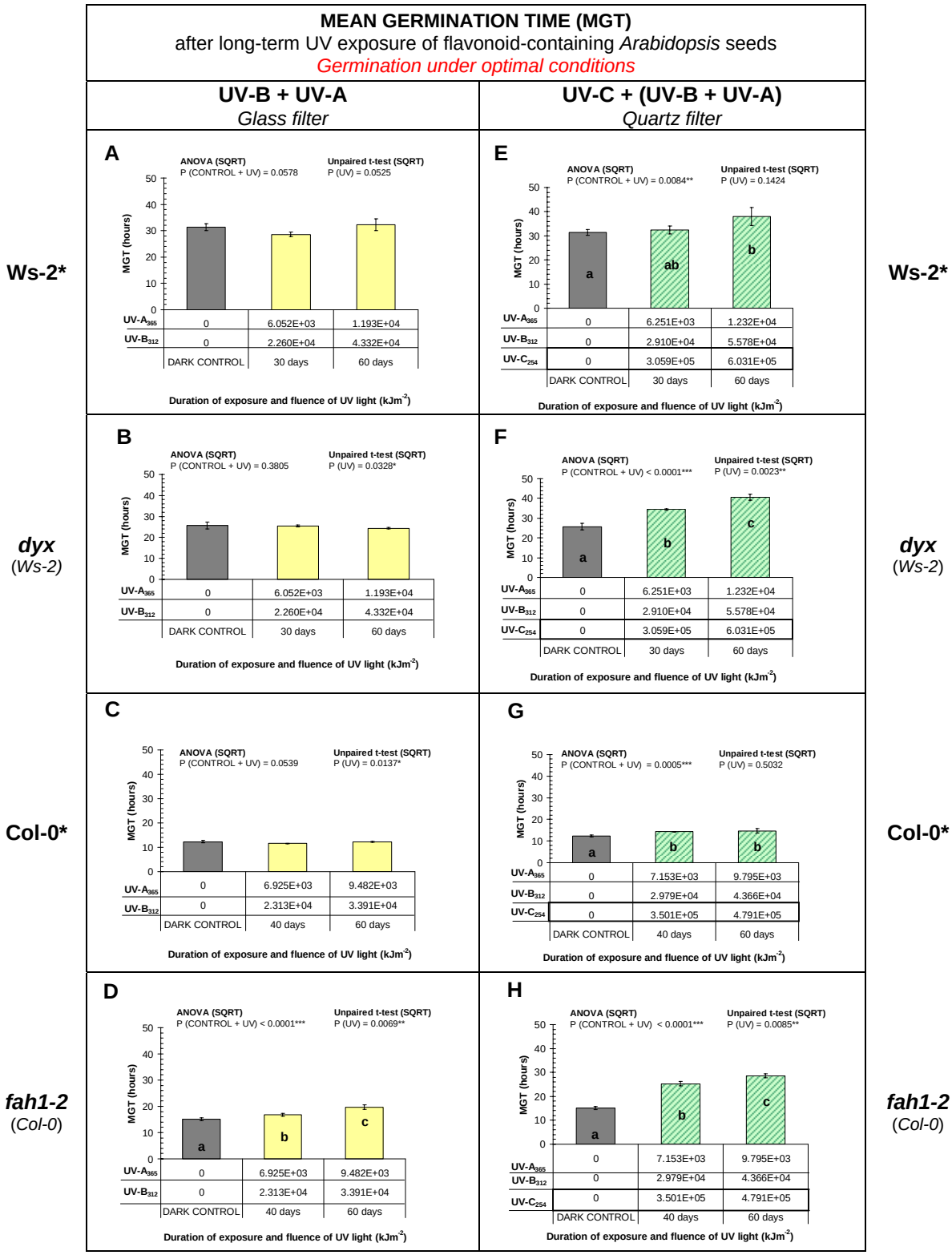

Fig. 64. The mean germination time (MGT) of flavonoid-containing *Arabidopsis* seeds germinated under the optimal conditions after exposure to entirely transmitted UV-C + (UV-B + UV-A) light or only to its minor UV-B + UV-A portion, emitted from the UV-C_{254} source. The MGT values of UV irradiated seed samples are here compared with those of the unexposed control samples (dark controls). The duration of UV exposure (30 and 60 days for Ws-2 and *dyx* seeds, and 40 and 60 days for Col-0 and *fah1-2* seeds) and UV fluences (kJm^{-2}) are indicated under each bar. The seeds were imbibed in the dark at 4°C for 72 hours. Values are the mean ± standard deviation of three parallel experiments (n = 50). Bars with different letters denote significant differences at $\alpha < 0.05$, according to ANOVA and the unpaired t-tests (UV exposed samples), calculated for square-root transformed data. The precise values of statistical tests are indicated above the bars, where * means a significant ($P < 0.05$), ** very significant ($P < 0.01$) and *** extremely significant ($P < 0.001$) level of difference.

The plant genotypes were: Wassilewskija (Ws-2), A and E; a control mutant with a T-DNA insertion carrying the *nptII* gene (*dyx*), B and F; Columbia (Col-0), C and G; a sinapate ester-deficient mutant (*fah1-2*), D and H. Wild ecotypes are marked with asterisks and background ecotypes are noted in the parentheses under each mutant type.

In the case of the sinapate ester mutant *fah1-2* exposed to UV-C + (UV-B + UV-A) light, the Tukey-Kramer post-hoc test showed an extremely significant increase ($p < 0.001$) in MGT value for the sample exposed for 40 days, when compared to the dark control sample (**Fig. 64H**). The MGT value further increased ($p < 0.001$) in the *fah1-2* sample irradiated for 60 days. In addition, both UV-C + (UV-B + UV-A) exposed *fah1-2* samples differed very significantly in MGT values according to the results obtained from the unpaired t-test ($p = 0.0085$).

16.2.1.1.3. Other parameters of germination dynamics in seeds exposed to quasi-monochromatic UV-C_{254} light

Besides the mean germination time, as a reciprocal expression of germination speed, additional parameters of germination dynamics were also considered, such as $T_{50\%}$ and $T_{25\text{-}75\%}$ values, as well as the skewness of the germination curves. A $T_{50\%}$ value represents the time necessary to reach 50% of maximum germination. Together with MGT, it represents the central tendency of germination process (Ranal and de Santana, 2006). A $T_{25\text{-}75\%}$ value is an expression of the spread of germination times between 25% and 75% of maximum germination, and it represents the measure for germination uniformity. A $T_{25\text{-}75\%}$ value is related to the steepness of the germination curve around the median. Thus, a steep germination curve of seeds, with uniform behaviour, indicates that the majority of the seeds complete the germination over a relatively short time period (Bewley and Black, 1994b). Skewness is a measure for asymmetry of the germination curve, and it is calculated from the ratio $T_{50\%}$ / MGT. The calculated value usually lies between 0 and 1. A value 1 means that the curve is symmetric and a value <1 indicates that the curve is asymmetric, meaning that the greater percentage of seeds germinates in the first half of the germination period than the second half.

Precise values and the results of ANOVA ($\alpha = 0.05$) followed by the Tukey-Kramer post-hoc test for different parameters of germination dynamics, including MGT, $T_{50\%}$, $T_{25\text{-}75\%}$ and skewness for Ws-2, Col-0, *dyx* and *fah1-2* seeds irradiated with UV-C + (UV-B + UV-A) and UV-B + UV-A light, are presented in **Table 15**.

Table 15. Effects of long-term exposure to UV-C + (UV-B + UV-A) and UV-B + UV-A radiation on *Arabidopsis* seed germination dynamics, including $T_{25\text{-}75\%}$, $T_{50\%}$, mean germination time (MGT) and skewness of germination curves. The UV-C + (UV-B + UV-A) denotes an entirely transmitted incident light (quartz filter), in contrast to its minor UV-B +UV-A portion (glass filter), emitted from the UV-C_{254} source. Seeds were UV exposed for 30 and 60 days (Ws-2 and *dyx* seed lines) or 40 and 60 days (Col-0 and *fah1-2* seed lines), and subsequently germinated under optimal conditions after imbibition in the dark at 4°C for 72 hours. Values of UV exposed samples are compared to the value of the averaged dark control (unexposed seed sample protected from UV by an aluminium foil filter). Values are the mean ± standard deviation of three independent experiments (n = 50). Different letters denote a significant difference at $\alpha < 0.05$ according to ANOVA and the Tukey-Kramer post-hoc tests performed on square-root transformed data for $T_{25\text{-}75\%}$, $T_{50\%}$, and MGT parameters, and untransformed data for skewness parameter.
The plant genotypes were: Wassilewskija (Ws-2), a control mutant with a T-DNA insertion carrying the *nptII* gene (*dyx*), Columbia (Col-0) and a sinapate ester-deficient mutant (*fah1-2*). Wild ecotypes are marked with asterisks and background ecotypes are noted in parentheses under each mutant type.

GENOTYPE	DURATION OF UV IRRAD.	UV RADIATION	PARAMETERS OF GERMINATION DYNAMICS			
			$T_{25\text{-}75\%}$ (hours)	$T_{50\%}$ (hours)	MGT (hours)	SKEWNESS $T_{50\%}$ / MGT
Ws-2*		Dark control (averaged)	9.5 ***a***	26.0 ***a***	31.4 ***a***	0.8321 ***a***
	30 days	UV-B+UV-A	7.4 ***a***	24.8 ***a***	28.6 ***a***	0.8477 ***a***
		UV-C+ (UV-B+UV-A)	8.8 ***a***	27.3 ***a***	32.4 ***ab***	0.8404 ***a***
	60 days	UV-B+UV-A	11.7 ***ab***	25.9 ***a***	32.3 ***a***	0.8029 ***a***
		UV-C+ (UV-B+UV-A)	16.7 ***b***	33.6 ***b***	38.0 ***b***	0.8581 ***a***
dyx (Ws-2)		Dark control (averaged)	6.7 ***a***	22.0 ***a***	25.7 ***a***	0.8759 ***a***
	30 days	UV-B+UV-A	7.8 ***a***	23.0 ***a***	25.5 ***a***	0.9020 ***a***
		UV-C+ (UV-B+UV-A)	12.5 ***b***	30.8 ***b***	34.4 ***b***	0.8942 ***a***
	60 days	UV-B+UV-A	6.7 ***a***	21.8 ***a***	24.4 ***a***	0.8907 ***a***
		UV-C+ (UV-B+UV-A)	15.0 ***b***	36.2 ***c***	40.7 ***c***	0.8920 ***a***
Col-0*		Dark control (averaged)	3.6 ***a***	11.0 ***a***	12.3 ***a***	0.8565 ***a***
	40 days	UV-B+UV-A	3.1 ***a***	9.9 ***a***	11.6 ***a***	0.8560 ***a***
		UV-C+ (UV-B+UV-A)	5.2 ***b***	11.5 ***b***	14.3 ***b***	0.8014 ***a***
	60 days	UV-B+UV-A	5.0 ***b***	9.9 ***a***	12.3 ***a***	0.8116 ***a***
		UV-C+ (UV-B+UV-A)	5.1 ***b***	11.5 ***b***	14.7 ***b***	0.7867 ***a***
fah1-2 (Col-0)		Dark control (averaged)	4.6 ***a***	13.0 ***a***	15.1 ***a***	0.83302 ***a***
	40 days	UV-B+UV-A	5.5 ***ab***	14.4 ***b***	16.8 ***b***	0.8555 ***a***
		UV-C+ (UV-B+UV-A)	11.2 ***c***	19.1 ***d***	25.3 ***d***	0.7479 ***b***
	60 days	UV-B+UV-A	7.3 ***b***	16.2 ***c***	19.7 ***c***	0.8260 ***ac***
		UV-C+ (UV-B+UV-A)	13.1 ***c***	21.9 ***e***	28.6 ***e***	0.7666 ***bc***

In all four tested genotypes, the Tukey-Kramer test showed a similar distribution of statistical differences in the $T_{50\%}$ values among the dark controls and the UV exposed samples, as it was observed for the MGT values (**Table 15**). The differences in the MGT of irradiated and control seed samples are illustrated in **Fig. 64** and are discussed in details elsewhere (see section **16.2.1.1.2**). Here below are elaborated the results of statistical analyses for the $T_{50\%}$, skewness and $T_{25\text{-}75\%}$ parameters of germination dynamics.

In the case of the Ws-2 and *dyx* lines, ANOVA showed extremely significant differences ($p < 0.0001$) in $T_{50\%}$ values among the dark controls and samples exposed to UV-C + (UV-B + UV-A) light. The *dyx* line appeared more sensitive than the Ws-2 line, since $T_{50\%}$ increased already after 30 days of irradiation. In contrast, UV-B + UV-A light did not affect the $T_{50\%}$ parameter in Ws-2 and *dyx* lines. Extremely significant differences ($p < 0.0001$) in $T_{50\%}$ values were also detected for Col-0 and *fah1-2* samples irradiated for 40 and 60 days. In addition, **Table 15** shows the precise values for $T_{50\%}$, which are lower than MGT values in all cases. Thus, all calculated values for the skewness were below the value 1, indicating slightly asymmetric nature of germination curves in *Arabidopsis* seeds.

ANOVA showed no significant difference ($p > 0.05$) in positively skewed germination behaviour among samples exposed to UV-C (UV-B + UV-A) and UV-B + UV-A light and the dark controls, in the case of the Ws-2, Col-0 and *dyx* seed lines. In contrast, a very significant change ($p = 0.0021$) in germination skewness of *fah1-2* seeds was detected after the exposure to UV-C + (UV-B + UV-A) light for 40 and 60 days. The positive shift in skewness of the germination curve in *fah1-2* samples exposed to UV-C + (UV-B + UV-A) light indicates that the first half of the germination period was much longer than in dark control *fah1-2* seeds. Since this effect was not observed after the exposure of *fah1-2* seeds to UV-B + UV-A light, the change in skewness of germination of *fah1-2* seeds was attributed to the dominant UV-C part of the emitted UV light.

Unlike the MGT and $T_{50\%}$ parameters, the uniformity parameter $T_{25\text{-}75\%}$ had a different distribution of statistically significant variations among the UV exposed samples and the dark controls in all four tested genotypes. ANOVA showed a very significant difference ($p = 0.0026$) in $T_{25\text{-}75\%}$ values among the samples in Ws-2 line, where a decrease in uniformity of germination was detected after 60 days of exposure to UV-C + (UV-B + UV-A) radiation. Lower fluences of UV-C + (UV-B + UV-A) radiation, as well as UV-B + UV-A light, did not affect the uniformity of Ws-2 seed germination. As with the Ws-2 background, UV-B + UV-A light did not change

the germination uniformity of the *dyx* seeds. In contrast, UV-C + (UV-B + UV-A) light had a strong impact on the $T_{25\text{-}75\%}$ parameter in the *dyx* sample exposed for 30 and 60 days, since an extremely significant difference ($p < 0.0001$) in $T_{25\text{-}75\%}$ values was observed among the UV exposed samples and the dark control.

The Col-0 wild type seeds irradiated with UV-C + (UV-B + UV-A) and UV-B + UV-A light showed different behaviour in germination uniformity, compared to the Ws-2 wild type. An extremely significant difference ($p < 0.0001$) in $T_{25\text{-}75\%}$ values among the UV exposed samples and the dark control was observed in Col-0 wild type line. Compared to the Ws-2 line, the Col-0 seeds showed an increased sensitivity to both UV-C + (UV-B + UV-A) and UV-B + UV-A light. The uniformity of germination in the sinapate ester mutant *fah1-2* was extremely affected ($p < 0.0001$) by both UV-B + UV-A and UV-C + (UV-B + UV-A) radiation. The *fah1-2* seeds that were exposed to UV-B + UV-A light for 60 days had a significantly decreased $T_{25\text{-}75\%}$ value, compared to the dark control. The exposure to UV-C + (UV-B + UV-A) light affected the uniformity of *fah1-2* germination already after 40 days of UV exposure.

16.2.1.2. Germination of UV-C_{254} irradiated flavonoid-containing Arabidopsis seeds under suboptimal conditions

The germination tests under suboptimal conditions at low temperature (10°C) were performed in order to further examine the quality of *Arabidopsis* seeds Ws-2, Col-0, *dyx* and *fah1-2*, irradiated with high fluences of UV-C + (UV-B + UV-A) and UV-B + UV-A light. Standard germination tests, which are carried out under optimal conditions, may show relatively high germination performance of low-vigour seeds, while the tests conducted under stressed conditions may show comparatively poor germination (ISTA, 1995). The vigour of seeds, in effect, is a measure of the extent of damage that has accumulated in individual seeds, and one of the obvious signs of this damage is the increased time taken for seeds to germinate, as was observed for UV exposed Ws-2, Col-0, *dyx* and *fah1-2* seeds germinated under optimal conditions (see section **16.2.1.1.2**). Under stressed conditions, such as low temperature, the germination process is slower, making it possible to observe small differences in the vigour of UV irradiated and control seeds. Since the optimal temperature range for *Arabidopsis* germination and growth is 23-25°C (Rivero-Lepinckas et al., 2006), and the estimated base temperature (minimum temperature permitting radicle emergence) for *Arabidopsis* germination is close to 0°C (Gummerson, 1986; Salaita et al., 2005), a low constant temperature of 10°C was used to test the germination capacity and vigour of *Arabidopsis* seeds.

The germination time courses for *Arabidopsis* Ws-2, *dyx*, Col-0 and *fah1-2* seeds that were germinated under suboptimal conditions at 10°C, after they had been exposed to UV light for long time periods, are presented in **Fig. 65**. The panels **A, B, C** and **D** in **Fig. 65** illustrate the germination behaviour of the unexposed control samples that were not exposed to UV light. The panels **E, F, G** and **H** in **Fig. 65** show the germination curves of seeds exposed to UV-C + (UV-B + UV-A) light (samples covered with the *Quartz* filter), as well as the germination curves of seeds exposed only to UV-B + UV-A portion of the emitted light (samples covered with the *Glass* filter).

The results of germination under suboptimal conditions clearly show that the germination capacity of the Ws-2, *dyx*, Col-0 and *fah1-2* seeds was not affected by UV-B + UV-A light, nor by UV-C + (UV-B + UV-A) light. All tested seed samples, including control samples and all UV exposed seeds, reached final germination percentage of about 100%, even if germinated under stressed conditions at 10°C.

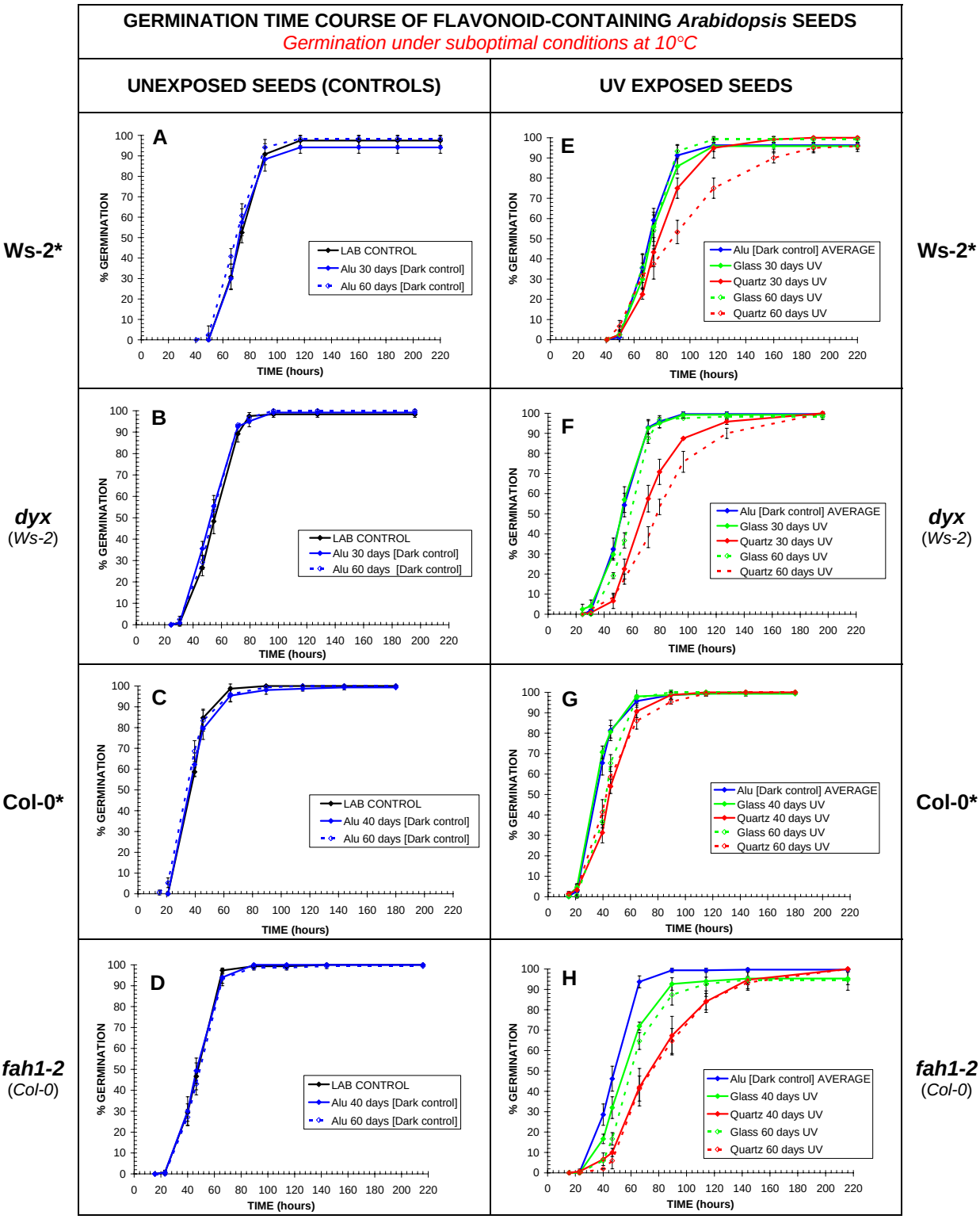

Fig. 65. Effects of UV radiation on germination behaviour of flavonoid-containing *Arabidopsis* seeds germinated under suboptimal conditions at 10°C. The germination time courses of UV irradiated seeds (panels E, F, G and H) are compared to the germination time courses of the control samples that were not exposed to UV light (panels A, B, C and D). Germination time is expressed in hours after imbibition (HAI). Imbibition was performed in the dark at 4°C for 72 hours. Seeds covered with an aluminium foil (*Alu* filter) were protected from the UV light, and they served as dark controls (blue lines), while laboratory controls were untreated seeds, stored in the dark at 4°C over the whole period of the experiment (black lines). Seeds covered with a *Glass* filter were exposed only to the UV-B + UV-A portion of emitted light (green lines), while those covered with a *Quartz* filter were exposed to entirely transmitted UV-C + (UV-B + UV-A) light, emitted from the UV-C_{254} source (red lines). The duration of exposure was for 30 and 60 days in the Ws-2 and *dyx* lines, and 40 and 60 days in the Col-0 and *fah1-2* lines.
The plant genotypes were: Wassilewskija (Ws-2), A and E; a control mutant with a T-DNA insertion carrying the *nptII* gene (*dyx*), B and F; Columbia (Col-0), C and G; a sinapate ester-deficient mutant (*fah1-2*), D and H. Wild ecotypes are marked with asterisks and background ecotypes are noted in the parentheses under each mutant type.

The germination curves of all dark controls for the Ws-2, *dyx*, Col-0 and *fah1-2* lines (seeds protected from UV light by the aluminium foil, *Alu*, filter and exposed to the experimental conditions up to 60 days) fitted perfectly to the germination curves of their laboratory controls (**Fig. 65A-D**), showing the consistency of the germination results. In addition, these results clearly showed good stability of the seeds kept under experimental conditions for up to 60 days, even in the case of Ws-2 dark control seeds (**Fig. 65A**), which showed a small change in germination speed in the germination test perforemd under optimal conditions (see **Fig. 62A**, section **16.2.1.1**). Thus, the average germination curves for Ws-2, *dyx*, Col-0 and *fah1-2*dark controls were plotted and further compared to the germination curves of UV irradiated samples (**Fig. 65E-H**).

As in the experiments under optimal conditions (**Fig. 62**, section **16.2.1.1**), the results of germination tests under suboptimal conditions indicated that UV-C + (UV-B + UV-A) light, as well as its UV-B + UV-A portion of emitted light, did not affect the germinability of Ws-2, *dyx*, Col-0 and *fah1-2* seeds, but rather the seed vigour. Compared to the tests performed under optimal conditions, the observed differences in germination speed were more pronounced if germination was carried out under suboptimal conditions. This was especially significant in the case of the samples exposed to UV-C + (UV-B + UV-A) light, where the differences in germination speed were detected already after 30 days of irradiation of Ws-2 and *dyx* seeds, as well as after 40 days of irradiation of Col-0 and *fah1-2* seeds.

Hovewer, the most pronounced differences in germination speed were observed in the sinapate ester-lacking mutant *fah1-2*, which was more sensitive to UV-C + (UV-B + UV-A) light, as well as UV-B + UV-A portion of emittied light, compared to its background Col-0 ecotype, and the Ws-2 and *dyx* genotypes.

The observed differences in the germination behaviour were further quantified, where the germination capacity, as well as the mean germination time were measured and statistically analysed among UV irradiated samples and the dark controls (see below).

16.2.1.2.1. Germination capacity ($G_{max\%}$) of UV-C_{254} irradiated seeds germinated under suboptimal conditions

As illustrated in **Fig. 65**, the maximal germination percentage ($G_{max\%}$) of Ws-2, *dyx*, Col-0 and *fah1-2* seeds reached about 100% in all the UV exposed and dark control samples. Neither UV-B + UV-A radiation, nor UV-C + (UV-B + UV-A) light affected the germination capacity of all tested samples. The mean values of $G_{max\%}$ obtained from three independent experiments, observing n = 40 seeds, were analyzed using ANOVA and the unpaired t-test, both at the level of significance $\alpha = 0.05$ (results not shown).

Using untransformed $G_{max\%}$ values, ANOVA showed no statistical difference ($p > 0.05$) among the dark and laboratory controls in Ws-2, *dyx*, Col-0 and *fah1-2* seed lines. Since these results indicated seed stability under the experimental conditions, but protected from UV light, the $G_{max\%}$ values for two dark controls were averaged in each seed line and these values were further compared to those of samples exposed to UV light.

No statistical differences ($p > 0.05$) were observed in germination capacity among the averaged dark controls and the Ws-2, *dyx*, Col-0 and *fah1-2* samples exposed to UV-B + UV-A light. Similarly, ANOVA showed no statistical differences ($p > 0.05$) among the Ws-2, *dyx*, Col-0 and *fah1-2* samples exposed to UV-C + (UV-B + UV-A) light, weighted against their averaged dark controls. Similar results for germination capacity of seeds exposed to UV-C + (UV-B + UV-A) and UV-B + UV-A light were obtained when $\arcsin\sqrt{\%}$ transformed data were used in statistical analyses (results not presented).

16.2.1.2.2. Mean germination time (MGT) of UV-C_{254} irradiated seeds germinated under suboptimal conditions

Long-term exposure of Ws-2, *dyx*, Col-0 and *fah1-2* seeds to UV-C + (UV-B + UV-A) and UV-B + UV-A light had a significant effect on germination speed, as determined at suboptimal temperature (**Fig. 66**). The mean germination time (MGT), as an inverse expression of germination speed, was calculated for each sample and the mean values of MGT, obtained from three independent experiments (n = 40), were compared for UV exposed and dark control samples. ANOVA and the unpaired t-tests, both at he level of significance $\alpha = 0.05$, were performed on square-root transformed MGT values due to observed slightly positively skewed germination time course of *Arabidopsis* seeds (for details see section **16.2.1.1.3**).

Germination tests under suboptimal conditions confirmed the stability in seed vigour of all dark controls up to 60 days of treatment under experimental conditions, where no statistical difference ($p > 0.05$) was observed in MGT values among the laboratory controls (seeds that were stored in the dark at 4°C) and the dark controls (seeds exposed to the experimental conditions, but protected from UV light) in all four tested seed lines (results not shown). Thus, further statistical analyses of MGT for both UV-B + UV-A and UV-C + (UV-B + UV-A) exposed samples, were statistically weighted against the averaged MGT values for dark controls, as shown in **Fig. 66**.

Unlike the germination under optimal conditions, the results of germination under stressed conditions at 10°C showed that the UV-B + UV-A component of emitted light had an effect on the mean germination time of the *dyx* ($p = 0.0039$) and Col-0 ($p = 0.0061$) seeds, but only after 60 days of UV exposure (**Fig. 66B** and **C,** respectively). Lower fluences of UV-B + UV-A light, reached after 30 or 40 days of exposure, did not affect ($p > 0.05$) the MGT in irradiated *dyx* and Col-0 seeds. In contrast, the wild type Ws-2 seeds appeared more resistant to UV-B + UV-A light, since no statistically significant difference was observed in MGT among the dark control and exposed samples (**Fig. 66A**). On the other hand, the sinapate ester mutant *fah1-2* was more sensitive than other seed lines to UV-B + UV-A light, since an extremely significant increase ($p < 0.0001$) in MGT was observed in *fah1-2* line already after 40 days of UV irradiation (**Fig. 66D**). The MGT of *fah1-2* seeds further increased after 60 days of UV-B + UV-A exposure. The same effect was also observed in the germination experiments under optimal conditions, but it was less pronounced compared to the suboptimal conditions (see **Fig. 64**, section **16.2.1.1.2**).

The germination experiments under suboptimal temperature conditions revealed a strong impact of UV-C + (UV-B +UV-A) light on the mean germination time, since extremely significant differences ($p \leq 0.0001$) were detected among the dark controls and the samples exposed to UV-C + (UV-B +UV-A) in all tested genotypes (**Fig. 66E-H**). The MGT values for the Ws-2 wild type and *dyx* mutant seeds was very significantly increased ($p < 0.001$) already after 30 days exposure, and the MGT further increased with increased UV fluences (**Fig. 66E** and **F**, respectively). UV-C + (UV-B +UV-A) light induced an extremely significant increase ($p < 0.0001$) in MGT for the Col-0 wild type seeds and the sinapate ester *fah1-2* mutant already after 40 days of irradiation, but the MGT did not further increase with increased fluences of UV-C + (UV-B +UV-A) light (**Fig. 66G** and **H**).

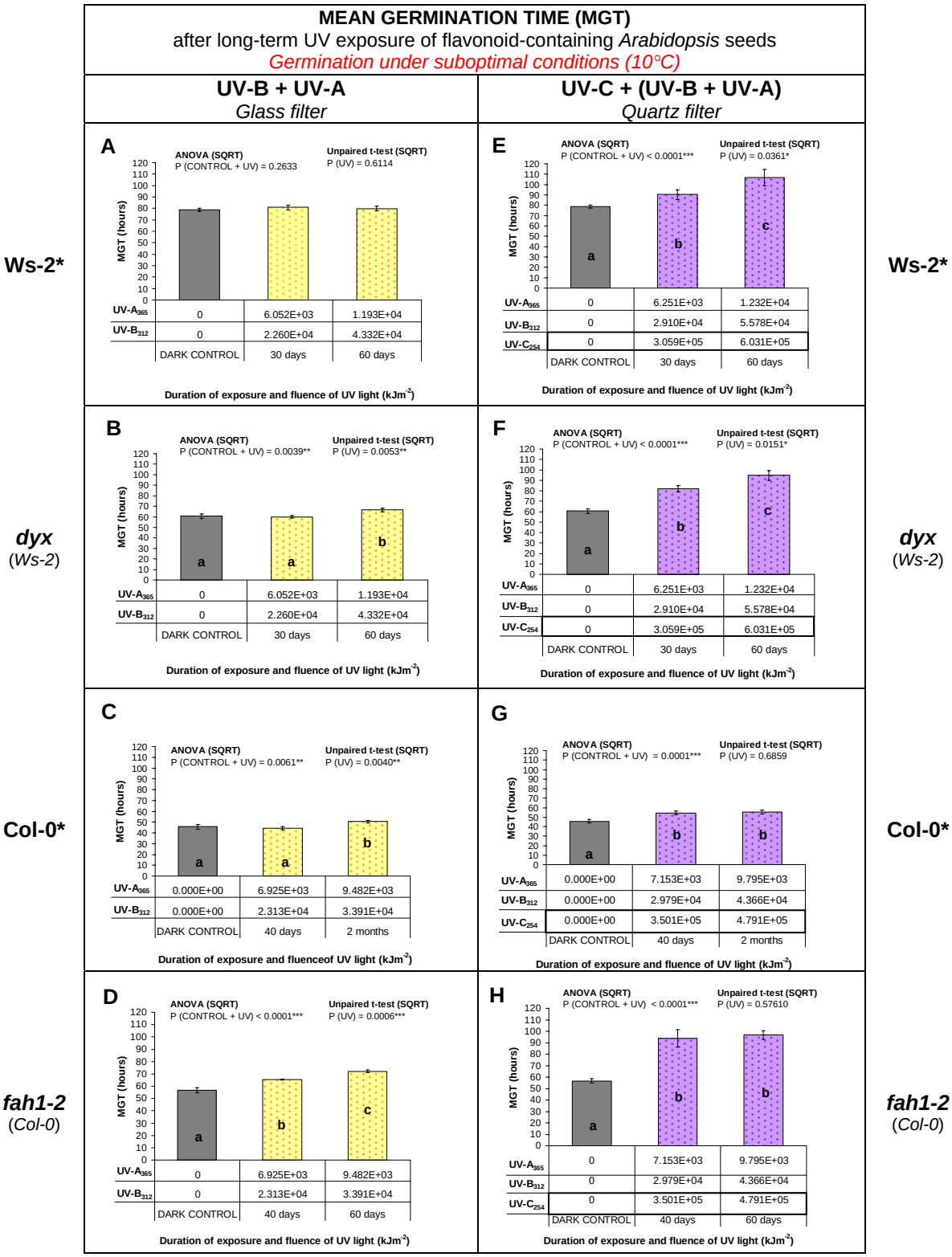

Fig. 66. The mean germination time (MGT) of flavonoid-containing *Arabidopsis* seeds germinated under suboptimal conditions at 10°C after exposure to entirely transmitted UV-C + (UV-B + UV-A) light or only to its minor UV-B + UV-A portion, emitted from the UV-C_{254} source. The MGT values of UV irradiated seed samples are here compared with those of the unexposed control samples (dark controls). The duration of UV exposure (30 and 60 days for Ws-2 and *dyx* seeds, and 40 and 60 days for Col-0 and *fah1-2* seeds) and UV fluences (kJm^{-2}) are indicated under each bar. Prior the germination, seeds were imbibed in the dark at 4°C for 72 hours. Values are the mean ± standard deviation of three parallel experiments (n = 40). Bars with different letters denote a significant difference at $\alpha < 0.05$ according to ANOVA and the unpaired t-tests (UV exposed samples), calculated for square root transformed data. The precise values of statistical tests are indicated above the bars, where * means a significant level ($P < 0.05$), ** very significant ($P < 0.01$) and *** extremely significant ($P < 0.001$) level of difference.
The plant genotypes were: Wassilewskija (Ws-2), A and E; a control mutant with a T-DNA insertion carrying the *nptII* gene (*dyx*), B and F; Columbia (Col-0), C and G, a sinapate ester-deficient mutant (*fah1-2*), D and H. Wild ecotypes are marked with asterisks and background ecotypes are noted n the parentheses under each mutant type.

16.2.2. Short-term UV-C_{254} exposure of flavonoid-lacking tt4-8 Arabidopsis seeds

The resistance of flavonoid-lacking *tt4-8* seeds (Ws-2 accession) to UV-C + (UV-B + UV-A) radiation, as well as the UV-B + UV-A portion of emitted light, was studied by analyzing germination behaviour and seed viability. Compared to the experiments with flavonoid-containing seed lines (see section **16.2.1**), the *tt4-8* seeds were exposed to UV radiation for relatively short time periods, ranging from 0.5 up to 139 hours. The germination tests were performed only under optimal conditions, since pronounced differences in germinability and germination speed were observed already after a short time period of UV exposure (see below). A tetrazolium test, which is used for determination of seed viability, was performed using intact *tt4-8* seeds that remained ungerminated at the end of germination test (for details see further below).

16.2.2.1. Germination of tt4-8 seeds exposed to quasi-monochromatic UV-C_{254} light

The germination curves of *tt4-8* samples exposed to UV radiation for 0.5, 1, 2, 3, 5, 10, 24, 48 and 139 hours, as well as unexposed samples (dark controls), are presented in **Fig. 67**.

UV-B + UV-A radiation did not have an effect on the germination capacity ($G_{max\%}$) of *tt4-8* seeds (samples covered with the *Glass* filter) over the whole range of UV exposure from 0.5 up to 139 hours (the maximal fluences of UV-B = 4.2 x 10^3 kJm^{-2} and UV-A = 1.2 x 10^3 kJm^{-2}) (**Fig. 67A-I)**. In addition, we found that UV-B + UV-A light did not affect the germination speed up to 5 hours of irradiation (**Fig. 67A-E**). However, *tt4-8* seeds exposed for 10 hours to UV-B + UV-A light (UV-B = 2.9 x 10^2 kJm^{-2} and UV-A = 79.4 kJm^{-2}) germinated slower than the dark control, and this effect was more pronounced with increased duration of exposure to UV-B + UV-A light (**Fig. 67F-I**).

UV-C + (UV-B + UV-A) light had an extreme effect on germination behaviour of *tt4-8* seeds (samples covered with the *Quarz* filter), lowering the overall speed of germination and reducing dramatically the final percentage of germinated seeds ($G_{max\%}$) (**Fig. 67A-I)**. Although, the germination capacity ($G_{max\%}$) of *tt4-8* seeds remained unchanged reaching about 100% after 0.5 and 1 hour of UV exposure (**Fig. 67A** and **B**), it decreased rapidly with increased duration of exposure, dropping finally to 13% after 139 hours of irradiation (the maximal fluences of UV-C = 5.9 x 10^4 kJm^{-2}, UV-B = 5.4 x 10^3 kJm^{-2} and UV-A = 1.2 x 10^3 kJm^{-2}) (**Fig. 67C-I**).

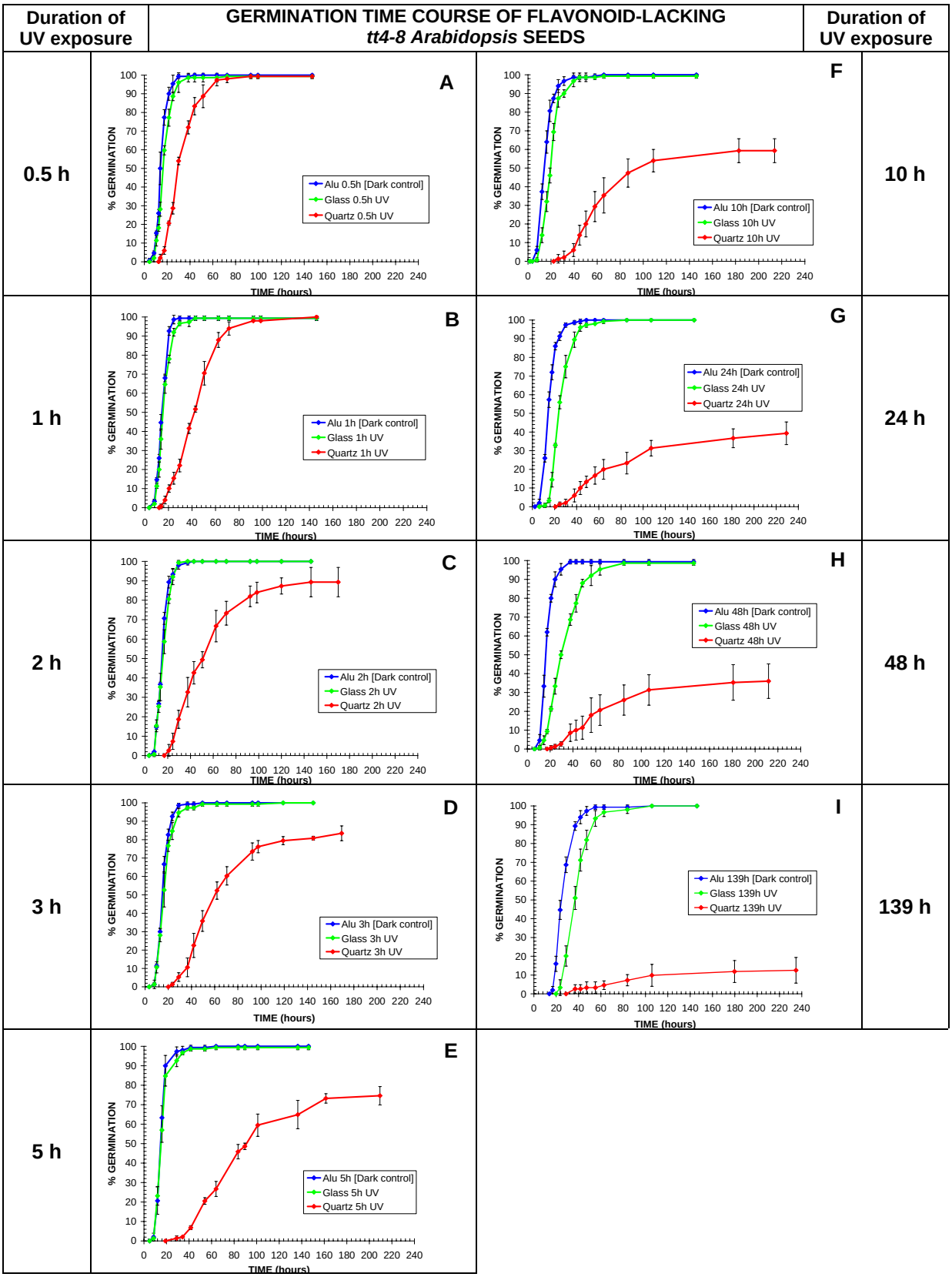

Fig. 67. Time course of germination of flavonoid-lacking *tt4-8 Arabidopsis* seeds after short-term exposure to UV light. The mutant *tt4-8* seeds (Ws-2 accession), were germinated under optimal conditions after they were irradiated for 0.5 (A), 1 (B), 2 (C), 3 (D), 5 (E), 10 (F), 24 (G), 48 (H) and 139 (I) hours. The seeds covered with an aluminium foil (*Alu* filter) were protected from the UV light, and they served as dark controls (blue lines). Seeds covered with a *Glass* filter were exposed only to the minor UV-B + UV-A portion of emitted light (green lines), while those covered with a *Quartz* filter were exposed to entirely transmitted UV-C + (UV-B + UV-A) light, emitted from the UV-C_{254} source (red lines). Data points represent the mean values ± standard deviation of three parallel experiments (n = 50). The time scales represent germination time expressed in hours after imbibition (HAI). After the exposure the imbibition was performed in the dark at 4°C for 72 hours.

On the other hand, the germination speed started to decrease already after only 0.5 hour of exposure of *tt4-8* seeds to UV-C + (UV-B + UV-A) light (UV-C = 2.8 x 10^2 kJm^{-2}, UV-B = 25.4 kJm^{-2} and UV-A = 5.6 kJm^{-2}) (**Fig. 67A**). This effect was even more pronounced with longer time of exposure (**Fig. 67B-I**).

In **Fig. 68** there are presented the germination curves that are compared all together for the dark controls, and the samples exposed to UV-B + UV-A or UV-C + (UV-B + UV-A) light, obtained from nine parallel UV irradiation experiments, ranging from 0.5 hour to 139 hours of exposure.

The germination curves of UV unexposed *tt4-8* seed samples, including a laboratory control and all dark controls from nine parallel UV exposure experiments, are compared all together in **Fig. 68A**. The laboratory control consisted of untreated seeds that were stored in the dark at 4°C during the experiments, while the dark controls were seeds protected from UV light by an aluminium foil (*Alu*) filter and placed under the UV lamp in parallel with UV exposed samples. The germination curves of all dark controls treated up to 48 hours were similar to the germination curve of the laboratory control, indicating the consistency of results and satisfying stability of *tt4-8* seeds under experimental conditions up to 48 hours. Surprisingly, a significant shift in position of the germination curve was observed in *tt4-8* dark control treated for 139 hours. This sample exhibited a delayed start of germination and an increase in the total time necessary to complete germination. This effect of instability in vigour of *tt4-8* seeds, possibly related to the seeds aging problem, should be also taken into account when analysed the irradiated samples that were exposed to the high UV fluences reached after 139 hours. Seed instability in the dark controls was not encountered in flavonoid-containing seeds, even after 60 days of treatment under experimental conditions, when protected from UV light (see section **16.2.1**). Due to the observed instability in the vigour of *tt4-8* seeds, averaged germination curves for the dark controls were not plotted.

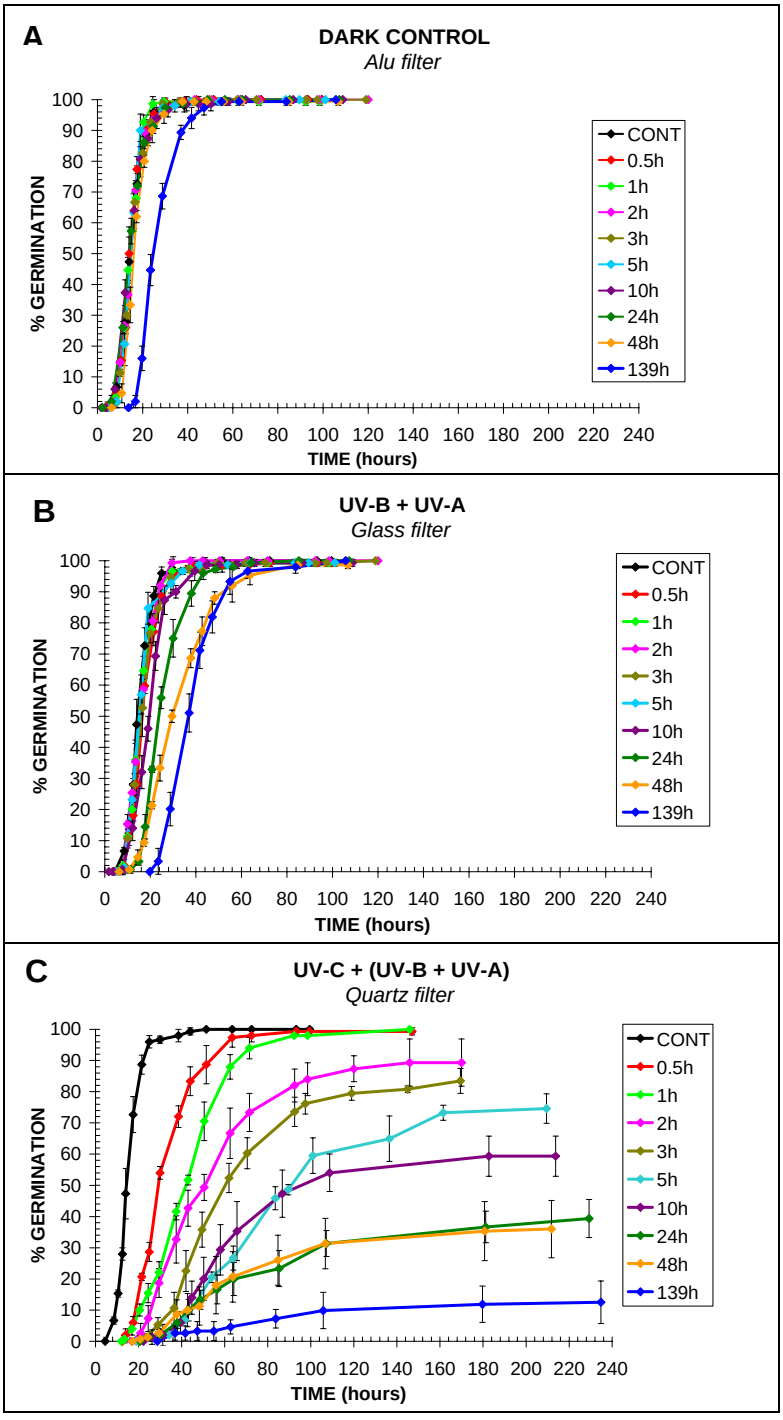

Fig. 68. Time course of germination of flavonoid-lacking *tt4-8 Arabidopsis* seeds after short-term exposure to UV light. The mutant *tt4-8* seeds (Ws-2 background), were germinated under optimal conditions after exposure to UV radiation for 0.5h, 1h, 2h, 3h, 5h, 10h, 24h, 48h and 139h. The time scales represent the germination time expressed in hours after imbibition (HAI), which was performed in the dark at 4°C for 72 hours. Seeds covered with an aluminium foil (*Alu* filter) were protected from the UV light and they served as dark controls (A), while seeds covered with a *Glass* filter were exposed only to the UV-B + UV-A portion of emitted light (B), and those covered with a *Quartz* filter were exposed to entirely transmitted UV-C + (UV-B + UV-A) light, emitted from the UV-C_{254} source (C). The germination curves of UV exposed seeds and dark control seeds were compared to the germination curve of the laboratory control (CONT), which represents untreated seeds that were stored in the dark at 4°C over a period of UV experiment (black lines).

The germination curves of all *tt4-8* samples exposed to UV-B + UV-A light, obtained from nine parallel exposure experiments, were compared to the germination curve for the laboratory control (**Fig. 68B**). All samples that were exposed to UV-B + UV-A light, as well as the control sample, reached maximal percentage of germination about 100%. However, a small shift in the position of the germination curve was observed in the sample exposed for 10 hours. A subsequent decrease in germination speed and delay in germination start was detected with increased UV-B + UV-A fluence.

The germination curves of all nine *tt4-8* samples exposed to UV-C + (UV-B + UV-A) light were compared in parallel and weighed against the laboratory control (**Fig. 68C**). A strong effect of UV-C + (UV-B + UV-A) light on the germination behaviour of *tt4-8* seeds was observed. The UV exposure for 0.5 and 1 hour resulted in changed dynamics of germination, including decreased germination speed and delayed start of germination, while the germination capacity remained unchanged, reaching about 100%. Doses received after 2 hours of UV exposure caused both, change in germination dynamics and in germination capacity of *tt4-8* seeds. Increasing doses of UV-C + (UV-B + UV-A) light caused subsequent decrease in the germination speed and an important decrease in the germination capacity. It is interesting, however, to observe the similarity in the shapes of the germination curves for the samples exposed to UV-C + (UV-B + UV-A) light for 24 and 48 hours, reaching approximately the same final percentage of germinated seeds.

As in the case of long-term UV exposure experiments with flavonoid-containnig Ws-2, Col-0, *dyx* and *fah1-2* seeds (see section **16.2.1**), different germination parameters, such as the germination capacity and the mean germination time, were studied separately in order to better describe the germination process and to quantify the differences in germination behaviour of the samples exposed to entirely transmitted UV-C + (UV-B + UV-A) and the UV-B + UV-A portion of light emitted from the UV-C_{254} source.

16.2.2.1.1. Germination capacity ($G_{max\%}$) of *tt4-8* mutant seeds exposed to quasi-monochromatic UV-C_{254} light

Maximal germination percentage ($G_{max\%}$), as a parameter of germination capacity, was measured in the *Arabidopsis* flavonoid-lacking *tt4-8* mutant seeds, which were exposed for 0.5 up to 139 hours to incident UV-C + (UV-B + UV-A) light, as well as the UV-B + UV-A portion of emitted light (**Fig. 69**). The mean values for $G_{max\%}$ were calculated from three parallel experiments, observing n = 50 seeds. Untransformed $G_{max\%}$ values were analyzed statistically using ANOVA folowed by the Tukey-Kramer post-hoc test ($\alpha = 0.05$).

The stability in germination capacity of *tt4-8* seeds was determined by comparing the $G_{max\%}$ values for the laboratory control and all nine dark controls, exposed from 0.5 up to 139 hours to the experimental conditions in the dark (**Fig. 69A**). No statistically significant differences ($p > 0.05$) in $G_{max\%}$ values were observed among all UV unexposed samples, including the laboratory control and all nine dark controls, as well as within the group of the dark controls. This result showed stability in the germination capacity of the *tt4-8* dark controls up to 139 hours of treatment.

The UV-B + UV-A component of incident light did not have any influence on the germination capacity of *tt4-8* seeds up to 139 hours of exposure (**Fig. 69B**). No statistically significant difference ($p > 0.05$) in $G_{max\%}$ was observed among the averaged *tt4-8* dark control and all nine samples irradiated with UV-B + UV-A light.

In contrast, UV-C + (UV-B + UV-A) light had an extremely significant effect ($p < 0.0001$) on the germination capacity of *tt4-8* seeds (**Fig. 69C**). Since the UV-B + UV-A part of light did not affect the germination capacity of *tt4-8* seeds, a decline in $G_{max\%}$ was attributed to the UV-C component, which made up 90% of the light emitted from the UV_{254} source. The Tukey-Kramer post-hoc test showed no statistical differences in $G_{max\%}$ among the averaged dark control and the samples exposed for 0.5, 1 and 2 hours. The fluence of UV-C light reached after 2 hours of irradiation was 1.1×10^3 kJm^{-2}. Above this value, the germination capacity of *tt4-8* seeds dropped significantly with increasing UV-C fluences. The exposure to UV-C = 1.0×10^4 kJm^{-2} (24 hours of irradiation) caused an important decrease in $G_{max\%}$ down to 39%. Surprisingly, a further increase in UV-C fluence up to $2.1\ 10^4$ kJm^{-2} (48 hours of exposure) did not cause a statistically significant decrease in $G_{max\%}$ value. Nevertheless, after 139 hours of irradiation (UV-C = 5.9×10^4 kJm^{-2}), only 13% of *tt4-8* seeds finaly germinated.

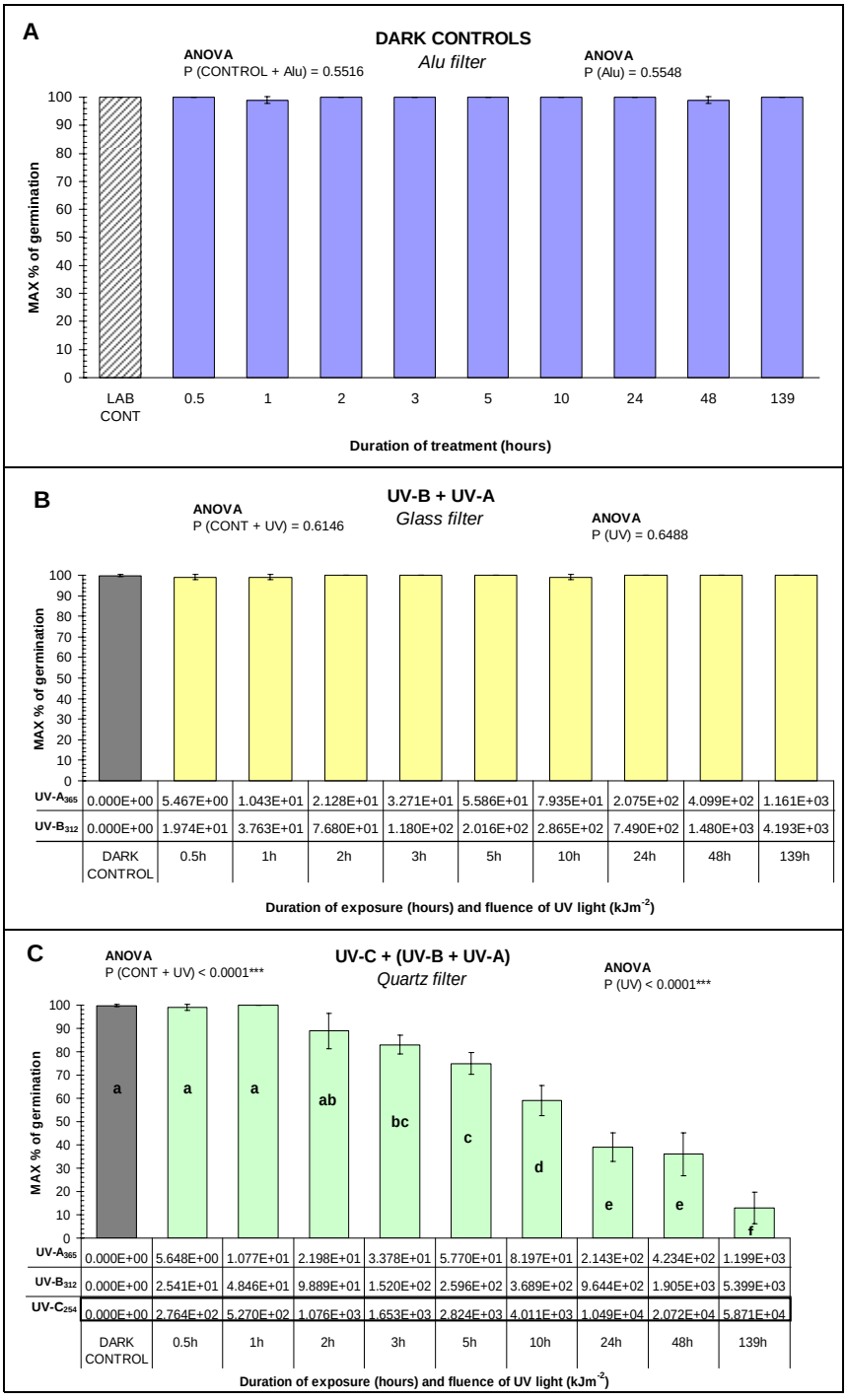

Fig. 69. Maximal germination percentage ($G_{max\%}$) of flavonoid-lacking *tt4-8 Arabidopsis* seeds (Ws-2 accession) after short-term exposure to UV light. The seeds covered with an aluminium foil (*Alu* filter) were protected from the UV light, and they served as dark controls (A). The $G_{max\%}$ for the dark controls are compared to the $G_{max\%}$ of the laboratory control (LAB CONT), which represents untreated seeds that were stored in the dark at 4°C during the experiment. The seeds covered with a *Glass* filter were exposed to only to the minor UV-B + UV-A portion of emitted light (B) and those covered with a *Quartz* filter were exposed to entirely transmitted UV-C + (UV-B + UV-A) light, emitted from the UV-C_{254} source (C). The $G_{max\%}$ values of irradiated samples are compared to the $G_{max\%}$ of an averaged dark control. The duration of UV exposure (hours) and UV fluences (kJm^{-2}) are indicated under each bar. Values are the mean ± standard deviation of three parallel experiments (n = 50). Bars with different letters denote a significant difference at $\alpha < 0.05$, according to ANOVA and the Tukey-Kramer post-hoc test. The precise values of statistical tests are indicated above the bars, where * means a significant level ($P < 0.05$), ** very significant ($P < 0.01$) and *** extremely significant ($P < 0.001$) level of difference.

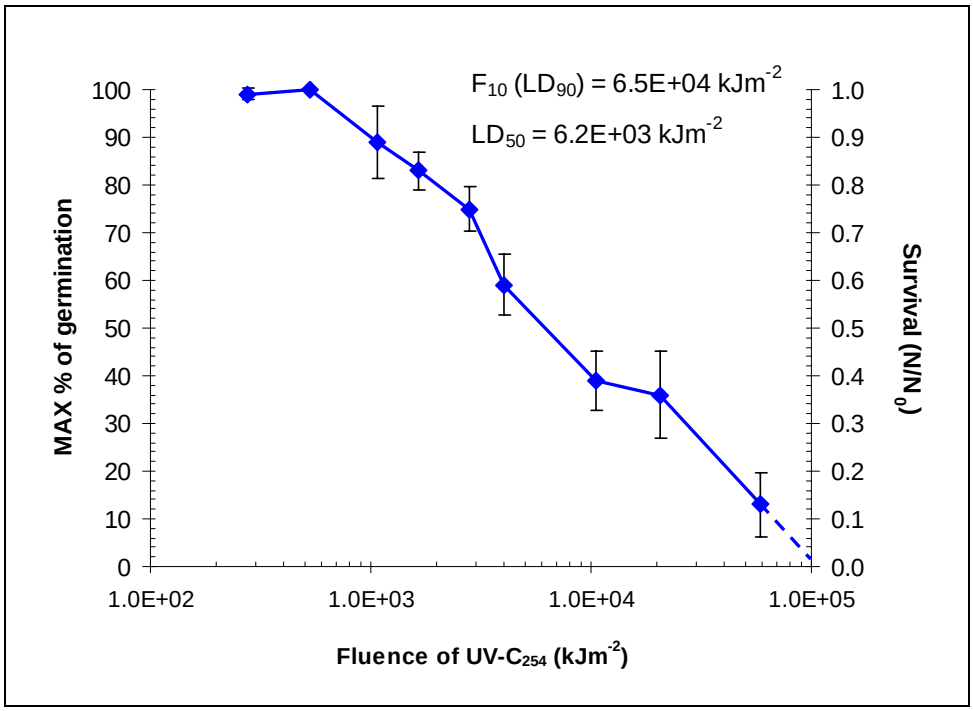

Fig. 70. Dose response curve for the flavonoid-lacking *tt4-8 Arabidopsis* seeds (Ws-2 accession) exposed to increasing fluences of UV-C light (λ = 254 nm). The survival rate of *tt4-8* seeds (scale on the right side) is closely related to the maximal percentage of germination (scale on the left side). Survival was determined from the ratio N/N_0 where N means the number of germinated seeds after UV_{254} irradiation and N_0 stands for the number of germinated seeds at zero fluence (dark control). The lethal UV-C_{254} dose of that kills 50% of seeds was determined from dose response curve, LD_{50} = 6.2 x 10^3 kJm^{-2}. The 10% survival rate F_{10} = 6.5 x 10^4 kJm^{-2}, which is the equivalent for the lethal dose LD_{90}, was determined graphically from the extrapolated part of dose response curve (dashed line). All values are the means ± standard deviation of three parallel experiments (n = 50).

In view of the fact that UV-C (λ = 254 nm) had a very strong impact on the germinability of the *tt4-8* seeds, the UV_{254} dose response curve for *Arabidopsis* flavonoid-lacking *tt4-8* mutant seeds was established, where the values for maximal percentage of germination ($G_{max\%}$) were plotted against the logarithm of UV-C_{254} fluence, ranging from 2.8 x 10^2 kJm^{-2} up to 5.9 x 10^4 kJm^{-2} (**Fig. 70**). The survival rate of *tt4-8* seeds was closely related to the $G_{max\%}$ value at a particular UV_{254} fluence. With anology to the survival rate determined for UV exposed *Bacillus subtilis* spores (see **Equation 5** and **Fig. 61** in section **15**), the survival of *tt4-8* seeds was determined from the ratio N/N_0 where N means the number of germinated seeds after UV_{254} irradiation (samples covered with the *Quartz* filter) and N_0 stands for the number of germinated seeds at zero fluence (dark control samples covered with an aluminium foil filter).

From the dose response curve, we determined the lethal dose of UV-C_{254} radiation that kills 50% of *Arabidopsis* flavonoid-lacking *tt4-8* dry seeds, $LD_{50\%}$ = 6.2 10^3 kJm^{-2} (**Fig. 70**). Furthermore, by extrapolating the dose response curve, we estimated the 10% survival rate (F_{10}) that is equivalent of the value LD_{90} (lethal dose that inactivate 90% of seeds), F_{10} (LD_{90}) = 6.5 x 10^4 kJm^{-2}.

16.2.2.1.2. Mean germination time (MGT) of *tt4-8* mutant seeds exposed to quasi-monochromatic UV-C_{254} light

Mean germination time (MGT), as a parameter of germination dynamics and reciprocal value of germination speed (rate), was determined for *Arabidopsis tt4-8* seeds exposed to incident UV-C + (UV-B + UV-A) light, as well as the UV-B + UV-A portion of emitted light (**Fig. 71**). The mean germination time of *tt4-8* seeds was calculated according to the equation of Ellis and Roberts (1981) (see **Equation 1**, chapter **1**, section **4.2.2.1.**). Mean values of MGT data were calculated from three parallel experiments, observing n = 50 seeds. Square-transformed MGT values were analyzed statistically using ANOVA and the Tukey-Kramer post-hoc test, both at the level of significance $\alpha = 0.05$.

The *tt4-8* dark controls showed extremely significant ($p < 0.0001$) change in the mean germination time (**Fig. 71A**). According to the Tukey-Kramer post-hoc test, the MGT values for *tt4-8* dark control samples were unaffected up to 24 hours of treatment, but the MGT started to increase after 48 hours of treatment. An extremely significant increase ($p < 0.0001$) in MGT was detected after 139 hours of exposure under the experimental conditions in the dark. Thus, the MGT values for all dark controls could not be averaged and further compared to the MGT values for the UV exposed samples. Instead, the MGT of the laboratory control was taken as a reference value.

UV-B + UV-A radiation did not affect the MGT for *tt4-8* seeds exposed up to 5 hours (UV-B = 2.0 x 10^2 kJm^{-2} and UV-A = 56 kJm^{-2}), as shown in **Fig. 71B**. Higher fluences of UV-B + UV-A radiation, starting from 10 hours (UV-B = 2.9 x 10^2 kJm^{-2} and UV-A = 79 kJm^{-2}) up to 139 hours of exposure (UV-B = 4.2 x 10^3 kJm^{-2} and UV-A = 1.2 x 10^3 kJm^{-2}), caused a progressive increase in the MGT values in irradiated *tt4-8* samples. However, this increase in the MGT at higher fluences has to be interpreted with causion, since it might reflect not only the effect of UV-B + UV-A radiation, but also the intrinsic instability of *tt4-8* seeds under experimental conditions (for details see above the results on MGT of the *tt4-8* dark controls).

The impact of UV-C + (UV-B + UV-A) light on the MGT of *tt4-8* seeds is illustrated in **Fig. 71C**. ANOVA results indicated extremely significant differences ($p < 0.0001$) in the MGT among *tt4-8* seed samples exposed to UV-C + (UV-B + UV-A) light. Increased MGT value was detected already after 0.5 hour of exposure and progressive increase in the MGT was observed with increasing fluences up to 5 hours of exposure. Curiously, further increase in UV-C + (UV-B

+ UV-A) fluences, starting with 10 hours of exposure, did not result in a linear increase in MGT, but rather non-linear behaviour of dose response. While the effect of UV-C + (UV-B + UV-A) light on the MGT of *tt4-8* seeds for lower fluences up to 5 hours of exposure could be attributed entirely to the dominant UV-C part of the incident light, the impact of higher fluences on the MGT is a complex problem, which includes combined effects of the dominant UV-C light and the UV-B + UV-A component of light, as well as the effects of seed instability observed in the dark controls.

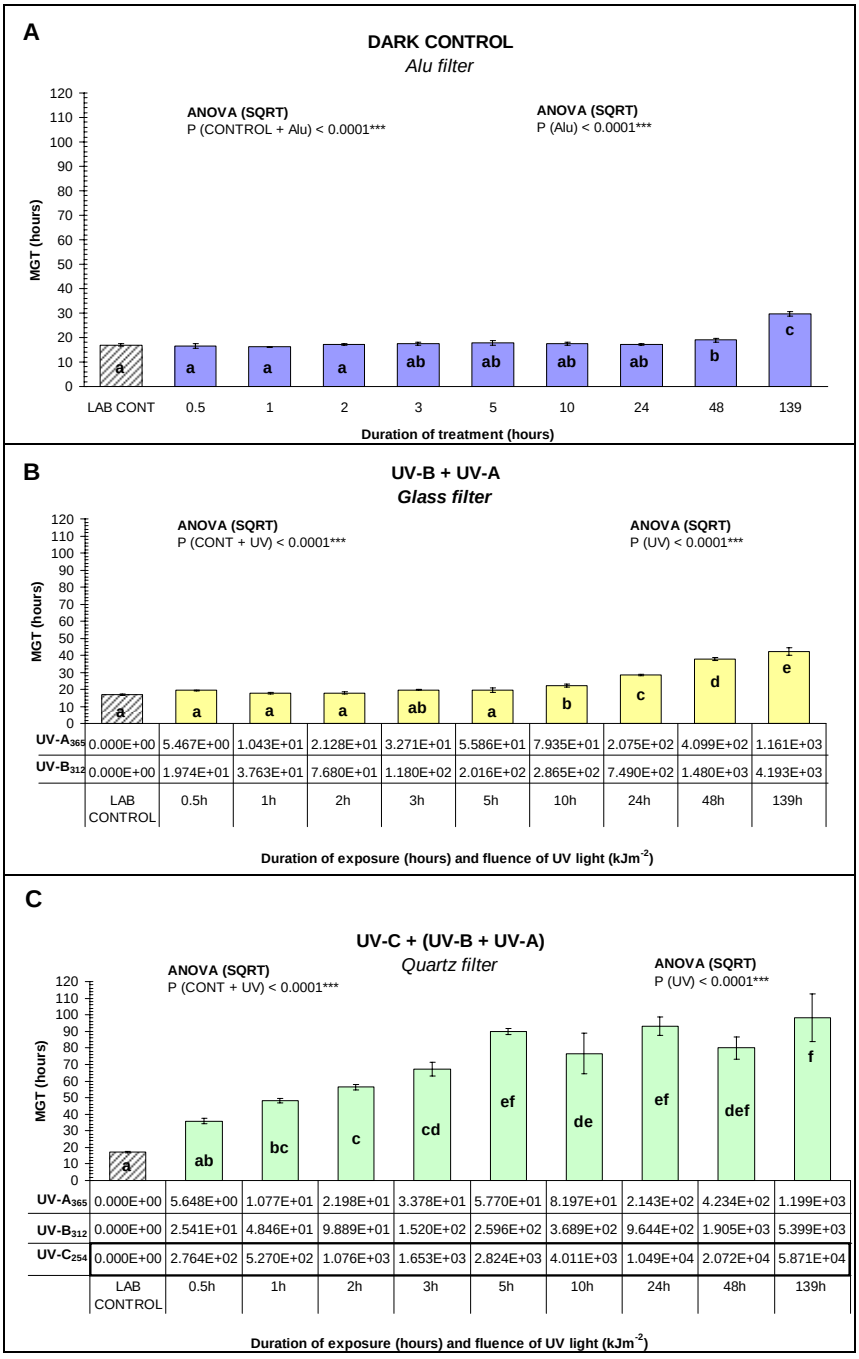

Fig. 71. The mean germination time (MGT) of *flavonoid-lacking tt4-8 Arabidopsis* seeds (Ws-2 accession) after short-term exposure to UV light. Seeds covered with an aluminium foil (*Alu* filter) were protected from the UV light, and they served as dark controls (A). The MGT values for the dark controls were compared to the MGT of the laboratory control (LAB CONT), which represents untreated seeds that were stored in the dark at 4°C during the whole experiment. The seeds covered with a *Glass* filter were exposed only to the UV-B + UV-A portion of emitted light (B), and those covered with a *Quartz* filter were exposed to entirely transmitted UV-C + (UV-B + UV-A) light, emitted from the UV-C_{254} source (C). The duration of UV exposure (hours) and UV fluences (kJm^{-2}) are indicated under each bar. Values are the mean ± standard deviation of three parallel experiments (n = 50). Bars with different letters denote a significant difference at $\alpha < 0.05$, according to ANOVA and the Tukey-Kramer post-hoc test, calculated for square root transformed data. The precise values of statistical tests are indicated above the bars, where * means a significant level ($P < 0.05$), ** very significant ($P < 0.01$) and *** extremely significant ($P < 0.001$) level of difference

16.2.2.1.3. Other parameters of germination dynamics in *tt4-8* mutant seeds exposed to quasi-monochromatic UV-C_{254} light

The parameters of germination dynamics, including $T_{25-75\%}$, $T_{50\%}$, MGT and the skewness of the germination curves were determined for the *tt4-8* seeds exposed to incident UV-C + (UV-B + UV-A) light and to its UV-B + UV-A portion (**Table 16**). The $T_{25-75\%}$, $T_{50\%}$, MGT and skewness values were calculated as means from three parallel experiments, with n = 50 sample size. The results were analyzed using statistical tests, including ANOVA and the Tukey-Kramer post-hoc test at the level of significance $\alpha = 0.05$. Because of a small deviation from the normal distribution and slightly positively skewed germination time course for *tt4-8* seeds, as it was also detected for the Ws-2 background (see section **16.2.1.1.3**), ANOVA and the Tukey-Kramer post-hoc test were performed on square-root transformed data for $T_{25-75\%}$, $T_{50\%}$ and MGT. Skewness parameter was analyzed statistically using untransformed data. Since the *tt4-8* dark controls showed an increase in MGT at longer duration of treatment (**Fig. 71A**), all values for $T_{25-75\%}$, $T_{50\%}$, MGT and skewness parameters, presented in **Table 16**, were weighted against the value of the laboratory control, rather than the averaged dark control.

The results for the mean germination time (MGT), presented in **Table 16A,** indicated that UV-B + UV-A radiation did not affect the MGT of *tt4-8* seeds exposed up to 5 hours, and further increasing fluences of UV-B +UV-A caused a subsequent increase in MGT. It is important to note that statistical tests showed the same tendency in distribution of differences for $T_{50\%}$ (median of germination process), as seen for the MGT parameter. On the other hand, the $T_{25-75\%}$ parameter, which represents the germination uiformity, showed a slightly different statistical distribution. Fluences of UV-B + UV-A radiation corresponding to irradiation up to10 hours did not have an effect on germination uniformity of *tt4-8* seeds. After 24 and 48 hours of exposure, the $T_{25-75\%}$ values increased with increasing UV-B + UV-A fluences, indicating that exposed *tt4-8* seeds germinated less uniformly. Surprisingly, the $T_{25-75\%}$ value decreased in the sample exposed for 139 hours, compared to the sample exposed to UV-B + UV-A light for 48 hours. This effect of slightly improved uniformity of germination in the sample exposed for 139 hours might be related to the effect of delayed start of germination, compared to the sample exposed for 48 hours (**Fig. 68B**). Calculated $T_{50\%}$ /MGT ratio showed the values < 1, indicating a slightly positive skewed germination time course in all samples irradiated with UV-B + UV-A, as well as in the laboratory control. Nevertheless, statistical tests showed no differences in the skewness in germination curves for the samples exposed to UV-B + UV-A light, compared to the laboratory control.

Table 16. A) Effects of the UV-B + UV-A portion of emitted light (samples covered with a *Glass* filter) and B) entirely transmitted incident UV-C + (UV-B + UV-A) light (samples covered with a *Quartz* filter) on different parameters of germination dynamics for flavonoid-lacking *tt4-8 Arabidopsis* seeds (Ws-2 accession). The values for $T_{25\text{-}75\%}$, $T_{50\%}$, mean germination time (MGT) and skewness of germination curves of UV exposed samples are compared to the laboratory control (unexposed seed sample stored at 4°C in the dark). Mean values ± standard deviation were calculated for three parallel experiments (n = 50). Different letters denote a significant difference at $\alpha < 0.05$, according to ANOVA and the Tukey-Kramer post-hoc test performed on the square-root transformed data for $T_{25\text{-}75\%}$, $T_{50\%}$, and MGT, and untransformed data for the skewness.

A)

UV-B + UV-A *Glass filter*				
DURATION OF UV IRRADIATION	**PARAMETERS OF GERMINATION DYNAMICS**			
	$T_{75\text{-}25\%}$ (hours)	**$T_{50\%}$ (hours)**	**MGT (hours)**	**SKEWNESS $T_{50\%}$ / MGT**
Laboratory control	6.7 ***a***	14.4 ***a***	17.0 ***a***	0.8611 ***a***
0.5 h	7.8 ***a***	16.4 ***a***	19.4 ***a***	0.8456 ***a***
1 h	7.0 ***a***	15.2 ***a***	17.9 ***a***	0.8496 ***a***
2 h	7.7 ***a***	15.7 ***a***	17.9 ***a***	0.8801 ***a***
3 h	7.3 ***a***	16.1 ***a***	19.7 ***a***	0.8172 ***a***
5 h	8.3 ***ab***	17.4 ***a***	19.7 ***a***	0.8085 ***a***
10 h	8.7 ***ab***	19.6 ***b***	22.1 ***b***	0.8806 ***a***
24 h	11.3 ***bd***	23.8 ***c***	28.5 ***c***	0.8360 ***a***
48 h	19.4 ***c***	29.5 ***d***	37.7 ***d***	0.7823 ***a***
139 h	13.8 ***d***	36.7 ***e***	42.1 ***e***	0.8717 ***a***

B)

UV-C + (UV-B + UV-A) *Quartz filter*				
DURATION OF UV IRRADIATION	**PARAMETERS OF GERMINATION DYNAMICS**			
	$T_{75\text{-}25\%}$ (hours)	**$T_{50\%}$ (hours)**	**MGT (hours)**	**SKEWNESS $T_{50\%}$ / MGT**
Laboratory control	6.7 ***a***	14.4 ***a***	17.0 ***a***	0.8612 ***a***
0.5 h	16.7 ***ab***	29.3 ***ab***	35.9 ***ab***	0.8537 ***a***
1 h	21.4 ***abc***	42.2 ***bc***	48.2 ***bc***	0.8763 ***a***
2 h	31.4 ***bcd***	45.1 ***bcd***	56.4 ***c***	0.7980 ***ab***
3 h	32.8 ***bcd***	53.9 ***cd***	67.1 ***cd***	0.8037 ***ab***
5 h	45.0 ***de***	74.8 ***ef***	89.9 ***ef***	0.7093 ***b***
10 h	35.4 ***cde***	60.6 ***def***	76.6 ***de***	0.7949 ***ab***
24 h	63.0 ***f***	65.8 ***ef***	93.1 ***ef***	0.7057 ***b***
48 h	44.5 ***de***	59.0 ***cef***	80.0 ***def***	0.7344 ***ab***
139 h	50.5 ***ef***	73.6 ***f***	98.1 ***f***	0.7545 ***ab***

The effects of UV-C + (UV-B + UV-A) light on the other parameters of germination dynamics of *tt4-8* seeds are shown in **Table 16B**. Compared to the MGT parameter, a similar behaviour of $T_{50\%}$ parameter was observed for *tt4-8* seeds irradiated with incident UV-C + (UV-B + UV-A) light, although with the minor differences in statistical distribution of variations. The $T_{50\%}$ /MGT ratio for all samples exposed to UV-C + (UV-B + UV-A) light, as well as the control sample, showed values < 1, indicating a slightly positive skewed germination time course. It is interesting to observe that among all tested samples, two samples that were exposed to UV-C + (UV-B + UV-A) light for 5 and 24 hours, showed a very significant ($p = 0.0018$) positive shift in the skewness, indicating a certain delay in the first half of germination process. The uniformity parameter, $T_{25\text{-}75\%}$, showed different statistical distribution of variations, compared to differences in the MGT and $T_{50\%}$. The $T_{25\text{-}75\%}$ values appeared unchanged after 0.5 and 1 hour of exposure to UV-C + (UV-B + UV-A) light. Similarly to MGT and $T_{50\%}$ parameters, the increasing fluences of UV-C + (UV-B + UV-A) light caused first an increase in $T_{25\text{-}75\%}$ values, indicating a decline in the germination uniformity for the samples irradiated up to 5 hours.This trend was than followed by a non-linear dose response behaviour of $T_{25\text{-}75\%}$ parameter at higher UV fluences.

16.2.2.2. The viability of tt4-8 mutant seeds exposed to quasi-monochromatic UV-C_{254} light (Tetrazolium test)

The tetrazolium (TZ) test was used as a supplement to the germination test in order to examine the viability of ungerminated *tt4-8* seeds that were exposed to incident UV-C + (UV-B + UV-A) radiation, as well as the UV-B + UV-A portion of the light emitted from the UV-C_{254} source. The TZ test is frequently used to determine the viability of individual seeds at the end of a germination test, especially when seed dormancy is suspected. In addition, this test can be used to detect damaged seeds or seeds in an advanced stage of deterioration, with consequence of reduced seed vigour. Thus, even when the germinability of seeds is markedly reduced or lost due to dormancy, ageing or serious seed damage, the results of the TZ test can reveal whether the ungerminated seeds are still viable or not. Upon the entry of the tetrazolium salts into the seeds, the formation of red formazan is an indication of dehydrogenase activity in metabolically active cells, which is in turn an indication of seed viability. Thus, red-stained *tt4-8* seeds were considered as viable, while uncoloured, pale yellow *tt4-8* seeds were classified as dead seeds.

At the end of the germination test, the UV irradiated *tt4-8* seeds that remained ungerminated were further tested for viability using the TZ test. All seeds in three replicas of the positive control (untreated viable seeds) and the negative control (seeds inactivated by autoclaving), which were used in the TZ test in parallel with the UV exposed *tt4-8* samples, stained brightly red or remained unstained, respectively. **Table 17** shows the results of the germination test and TZ test that were presented in parallel, where the final percentage of ungerminated *tt4-8* seeds was compared to the percentage of tetrazolium unstained seeds (negative TZ test result). Dark control samples represented unexposed seeds covered with an aluminium foil (*Alu*) filter, while seed samples covered with a *Glass* filter and a *Quartz* filter were exposed to the UV-B + UV-A portion and entirely transmitted UV-C + (UV-B + UV-A) incident light, respectively.

The results clearly showed that a few dark control seeds, which remained ungerminated after 1 hour and 48 hours of treatment, turned out to be viable. Thus, all *tt4-8* seeds used as a dark control in UV exposure experiments, showed 100% viability even after 139 hours of treatment under the experimental conditions.

In contrast, ungerminated *tt4-8* seeds after 0.5 hour and 10 hours of UV-B + UV-A irradiation remained unstained, but these few detected dead seeds (0.7 % ± 1.2) were considered statistically irrelevant ($p > 0.05$). Thus, the TZ test showed that UV-B + UV-A radiation did not affect the viability of the *tt4-8* seeds.

In addition, the results of the TZ test also indicated that UV-C + (UV-B + UV-A) light did not affect the viability of *tt4-8* seeds after 0.5 and 1 hour of irradiation, but higher fluences of UV-C + (UV-B + UV-A) light, reached from 2 hours (UV-C = 1.1 x 10^3 kJm^{-2}) up to 139 hours of irradiation (UV-C = 5.9 x 10^4 kJm^{-2}), seriously decreased the viability of the *tt4-8* seeds. It is important to note that the results of the germination test did not much differ from those of the TZ test, with the exception of a few viable seeds detected among ungerminated seeds that were irradiated with UV-C + (UV-B + UV-A) light for 3, 48 and 139 hours. Thus, almost all irradiated *tt4-8* seeds that remained ungerminated in the germination test did not stain in the TZ test, and therefore they were classified as dead seeds.

Table 17. The effects of short-term exposure to the UV-B + UV-A and UV-C + (UV-B + UV-A) radiation on the germinability and viability of *Arabidopsis* flavonoid-lacking *tt4-8* seeds (Ws-2 background). Ungerminated seeds at the end of the germination test were used in a tetrazolium (TZ) test in order to determine their viability. The seeds covered with an aluminium foil (*Alu*) filter were protected from UV light (dark control), while seed samples covered with a *Glass* filter were exposed only to the UV-B + UV-A portion of emitted light, with maximal fluences up to UV-B_{312} = 4.2 x 10^3 kJm^{-2} and UV-A_{365} = 1.2 x 10^3 kJm^{-2}. Seeds covered with a *Quartz* filter were exposed to entirely transmitted UV-C + (UV-B + UV-A) light, emitted fro the UV-C_{254} source, with maximal fluences up to UV-C_{254} = 5.9 x 10^4 kJm^{-2}, UV-B_{312} = 5.4 x 10^3 kJm^{-2} and UV-A_{365} = 1.2 x 10^3 kJm^{-2}. Values are the mean ± standard deviation of three parallel experiments.

DURATION OF UV EXPOSURE	GERMINATION TEST Ungerminated seeds (%)			TZ TEST Unstained seeds (%)		
	DARK CONTROL *Alu*	UV-B + UV-A *Glass*	UV-C + (UV-B + UV-A) *Quartz*	DARK CONTROL *Alu*	UV-B + UV-A *Glass*	UV-C + (UV-B + UV-A) *Quartz*
0.5 h	0	0.7 (± 1.2)	0.7 (± 1.2)	–[a]	0.7 (± 1.2)	0
1 h	0.7 (± 1.2)	0.7 (± 1.2)	0	0	0	–[a]
2 h	0	0	10.7 (± 7.6)	–[a]	–[a]	10.7 (± 7.6)
3 h	0	0	15.8 (± 5.4)	–[a]	–[a]	15.1 (± 2.7)
5 h	0	0	25.4 (± 4.7)	–[a]	–[a]	25.4 (± 4.7)
10 h	0	0.7 (± 1.2)	40.7 (± 6.4)	–[a]	0.7 (± 1.2)	40.7 (± 6.4)
24 h	0	0	60.7 (± 6.1)	–[a]	–[a]	60.7 (± 6.1)
48h	0.7 (± 1.2)	0	64.0 (± 9.2)	0	–[a]	62.7 (± 9.5)
139h	0	0	87.4 (± 6.8)	–[a]	–[a]	86.8 (± 7.9)

[a] Tetrazolium (TZ) test was not performed since 100% of germinability was reached and no ungerminated seeds were detected.

16.3. Early-seedling stage - effects of quasi-monochromatic UV-C_{254} light

Following the germination as the first growth stage in plant development (see section **16.2**), *Arabidopsis* seedlings that were developed from irradiated seeds were further grown in controlled *in vitro* conditions. Seedling development was observed during so-called the early-seedling stage that corresponded to the principal growth stage 1.0, which according to the BBCH scale modified for the *Arabidopsis* model, is defined as a stage when seedlings have fully opened cotyledons (Boyes et al., 2001; Kjemtrup et al., 2003).

Germination tests do not provide sufficient information whether or not a germinant is able to develop into normal seedling and further into functional plant. Development and the aspect of essential seedling structures, such as root system (e.g. primary root), shoot axis (e.g. hypocotyl) and cotyledons, determine further the plant growth and development. Accordingly, ISTA suggests organizing the results of germination and early-seedling stage tests into the following three groups: normal seedlings, abnormal seedlings and ungerminated seeds. Normal seedlings are considered to show potential for continued development into satisfactory plants when grown under favourable conditions, while abnormal seedlings include damaged, deformed or unbalanced seedlings, which would unlikely develop into normal plants. Abnormal seedlings are further characterized by the appearance of any of the seedling damages, including weakly developed, physiologically disturbed, deformed, out of proportion, severely damaged, decayed, or even missing essential seedling structures (ISTA, 1999). Therefore, in this section we considered following parameters of early-seedling growth: percentage of normal seedlings, abnormal seedlings and ungerminated seeds (section **16.3.1**), characterization and quantification of types of damage in abnormally developed seedlings (section **16.3.2**), and the length of normally developed primary roots (section **16.3.3**).

16.3.1. Normal seedlings, abnormal seedlings and ungerminated seeds after exposure to quasi-monochromatic UV-C_{254} light

Observing the development of early-stage seedlings (17 DAI-old Ws-2, *dyx*, *tt4-8* seedlings and 22 DAI-old Col-0, *fah1-2* seedlings) that were germinated from seeds exposed to incident UV-C + (UV-B + UV-A) and the UV-B + UV-A portion of light emitted from the UV-C_{254} source, the percentages of normally and abnormally developed seedlings, as well as the percentage of ungerminated seeds were determined in all five *Arabidopsis* lines that were object of study in the long-term (section **16.3.1.1**), as well as the short-term UV-C_{254} exposure experiments (section **16.3.1.2**). Here we point up that the total percentage of sown seeds (100%) equals the sum of the three portions, the percentage of normal seedlings, the percentage of abnormal seedlings and the percentage of ungerminated seeds. Statistical analyses were performed using ANOVA and the Tukey-Kramer post-hoc test, both at the level of significance $\alpha = 0.05$.

Prior to the analysis of the UV exposed samples, the proportion of normally and abnormally developed seedlings, as well as ungerminated seeds, were compared for each genotype among the dark control samples (seeds exposed to experimental conditions but protected from UV by an aluminium foil) and the laboratory control samples (seeds stored at 4°C in the dark during a UV exposure experiment). The percentage of normally developed seedlings in all control samples was above 95% and no statistical difference ($p > 0.05$) was observed among the laboratory control and the dark controls for the Ws-2, Col-0, *dyx*, *fah1-2* and *tt4-8* lines (data not presented).

16.3.1.1. Seedling development after long-term UV-C_{254} exposure of flavonoid-containing Arabidopsis seeds

After long-term UV exposure of the Ws-2 and *dyx* seeds to the UV-B + UV-A component of incident light, where seeds were irradiated for 30 and 60 days, no significant differences in the percentages of developed normal and abnormal seedlings were observed in these lines (**Fig. 72A** and **B**). In contrast, the UV-B + UV-A portion of emitted light induced a small, but statistically significant decrease ($p = 0.0010$) in the percentage of normally developed Col-0 seedlings and a reciprocal small increase ($p < 0.0001$) in the percentage of abnormal (3%) Col-0 seedlings, compared to the dark control (**Fig. 72C**). However, this effect was detected only after 60 days of irradiation (UV-B = 3.4×10^4 kJm^{-2} and UV-A = 9.5×10^3 kJm^{-2}), while lower fluences of UV-B

+ UV-A radiation did not affect seedling development in Col-0 line. A similar effect of higher fluences of UV-B + UV-A radiation, was also observed for the sinapate ester mutant *fah1-2*, with an extremely significant ($p < 0.0001$) change in the percentage of normal (89%) and abnormal (11%) seedlings (**Fig. 72D**). This change was more pronounced than that observed in Col-0 wild type background.

The effects of entirely transmitted UV-C + (UV-B + UV-A) incident light on seedling development in the Ws-2, *dyx*, Col-0 and *fah1-2* lines are presented in **Fig. 72E-H**. Along with the results for $G_{max\%}$ obtained from the germination tests (see section **16.2.1.1.1**), the percentage of ungerminated seeds remained unaltered and at low level in all UV exposed and control samples. On the other hand, UV-C + (UV-B + UV-A) light had an extremely significant ($p < 0.0001$) effect on the development of normal seedlings, and reciprocally on abnormally developed seedlings in all genotypes.

The level of normal seedlings dropped to 48% in the Ws-2 line and 47% in the *dyx* line after 30 days of exposure, reaching 36% in both lines after 60 days of irradiation (**Fig. 72E** and **F**). The percentage of abnormal Ws-2 and *dyx* seedlings increased with increasing fluences of UV-C + (UV-B + UV-A) radiation, reaching 51% and 53% after 30 days, and 57% and 64% after 60 days of exposure, respectively. Since no effect of the UV-B + UV-A portion of light was observed on Ws-2 and *dyx* seedling development, the extreme effect of UV-C + (UV-B + UV-A) light was attributed to its dominant UV-C component, which made about 90% of incident light.

In contrast to the Ws-2 wild type line, normal development of Col-0 wild type seedlings was less affected by incident UV-C + (UV-B + UV-A) light, reaching 93% of normal seedlings after 40 days and 83% after 60 days of irradiation (**Fig. 72G**). Only 7% of seedlings with abnormalities were observed after 40 days of exposure, and the percentage of abnormal seedlings increased to 15% after 60 days of exposure to UV-C + (UV-B + UV-A) light.

Compared to the Col-0 background, UV-C + (UV-B + UV-A) radiation had a more pronounced effect on the sinapate ester *fah1-2* mutant, dropping the level of normal seedlings to 69% after 40 days and to 40% after 60 days of irradiation (**Fig. 72H**). The percentage of abnormal *fah1-2* seedlings increased proportionally with the increase in UV-C + (UV-B + UV-A) fluence, reaching 29% after 40 days and 60% after 60 days of irradiation. Although the *fah1-2* line appeared to be more sensitive than the Col-0 background, regarding the seedling development, it reached almost the same level of abnormal seedlings as the Ws-2 wild type and *dyx* line at the highest fluences of UV-C + (UV-B + UV-A) radiation.

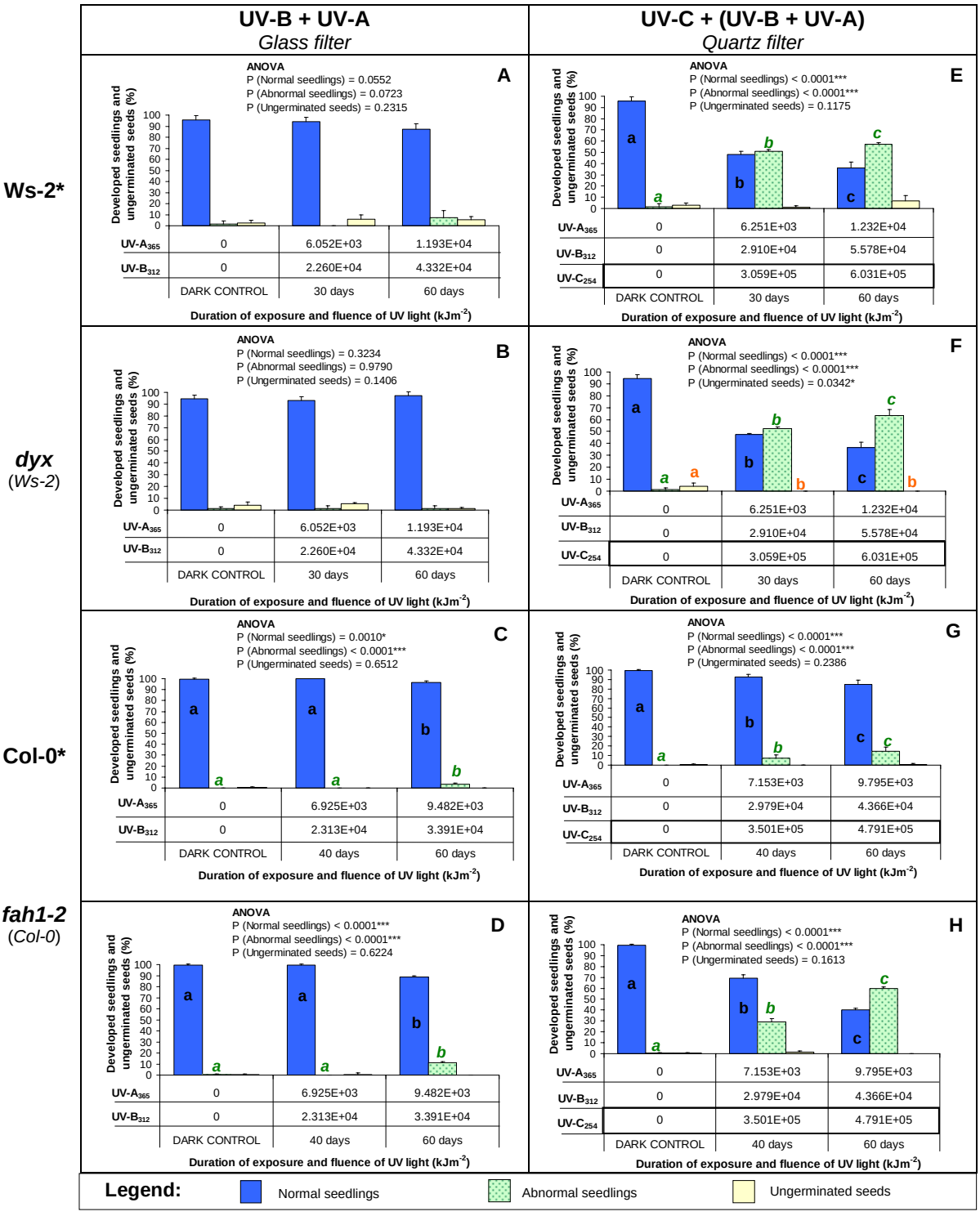

Fig. 72. Impact of UV-B + UV-A and UV-C + (UV-B + UV-A) radiation on germination and development of seedlings after long-term exposure of flavonoid-containing *Arabidopsis* seeds. Seed samples were covered with a *Glass* filter were exposed only to the UV-B + UV-A portion of emitted light, while those covered with a *Quarz* filter were exposed to entirely transmitted UV-C + (UV-B + UV-A) incident light, emitted from the UV-C_{254} source. The duration of UV exposure (30 and 60 days for Ws-2 and *dyx* seeds and 40 and 60 days for Col-0 and *fah1-2* seeds) and fluences of UV light (kJm^{-2}) are indicated under each bar. The percentages of ungerminated seeds, as well as normal and abnormal seedlings developed from UV irradiated seeds are compared to unexposed control samples (dark control). Values are the mean ± standard deviation of three parallel experiments (n = 50 sown seeds). Bars with different letters within the same group denote a significant difference at $\alpha < 0.05$, according to ANOVA and the Tukey-Kramer post-hoc test. The precise values of statistical tests are indicated above the bars, where * means a significant level ($P < 0.05$), ** very significant ($P < 0.01$) and *** extremely significant ($P < 0.001$) level of difference.

The plant genotypes were: Wassilewskija (Ws-2), A and E; a control mutant with a T-DNA insertion carrying the *nptII* gene (*dyx*), B and F; Columbia (Col-0), C and G; a sinapate ester-deficient mutant (*fah1-2*), D and H. Wild ecotypes are marked with asterisks and background ecotypes are noted in the parentheses under each mutant type.

16.3.1.2. Development of flavonoid-lacking tt4-8 Arabidopsis seedlings after short-term UV-C_{254} exposure

Short term exposure of *tt4-8* seeds to the UV-B + UV-A portion of emitted light up to 139 hours did not affect the development of *tt4-8* seedlings **(Fig. 73A)**, where nearly 100% of seedlings developed normally in all exposed samples. Thus, ANOVA showed no statistical differences ($p < 0.05$) in the percentages of normal and abnormal seedlings, as well as ungerminated seeds in all *tt4-8* samples exposed to UV-B + UV-A light, compared to the dark controls.

Regarding the development of the *tt4-8* seedlings from seeds exposed to incident UV-C + (UV-B + UV-A) light (**Fig. 73B**), the flavonoid-lacking mutant exhibited extreme sensitivity ($p < 0.0001$) already at relatively low doses of entirely transmitted incident light. Increasing fluences of UV-C + (UV-B + UV-A) light had the effect of almost linear increase in percentage of ungerminated *tt4-8* seeds, starting from 11% of ungerminated seeds after only 2 hours of irradiation. The exposure to incident UV-C + (UV-B + UV-A) light for 24 and 48 hours had statistically the same effect ($p > 0.05$) on the level of ungerminated *tt4-8* seeds, reaching 61% and 64%, respectively. The UV-C + (UV-B + UV-A) irradiation for 139 hours inhibited the germination of 88% of *tt4-8* seeds.

The percentage of normal *tt4-8* seedlings was inversely related to increasing fluences of UV-C + (UV-B + UV-A) light. A decrease to 74% of normally developed seedlings was detected after only 0.5 hour of exposure. Exposure for 3 and 5 hours had statistically the same effect ($p > 0.05$) on the percentage of normal seedlings, dropping to 39% and 35%, respectively. After 10 hours of UV-C + (UV-B + UV-A) exposure, 10% of *tt4-8* seedlings developed normally. Only 3% of normal seedlings were observed after 24 hours of UV exposure, and no normally developed seedlings were detected after 48 and 139 hours of irradiation.

Surprisingly, the percentage of abnormally developed seedlings had non-linear relationship with increasing fluences of UV-C + (UV-B + UV-A) radiation. At the lowest UV fluence reached after 0.5 hour of irradiation, 25% of seedlings developed abnormal morphology. At the maximal UV fluence reached after 139 hours of exposure, 12% of abnormal seedlings were detected, in addition to 88% ungerminated seeds. Since no effect from the UV-B + UV-A part of the incident light was observed on *tt4-8* seedling development up to 139 hours of irradiation, the extreme impact of UV-C + (UV-B + UV-A) light was attributed to the dominant UV-C part of the incident light, which made about 90% of emitted light from the UV-C_{254} source.

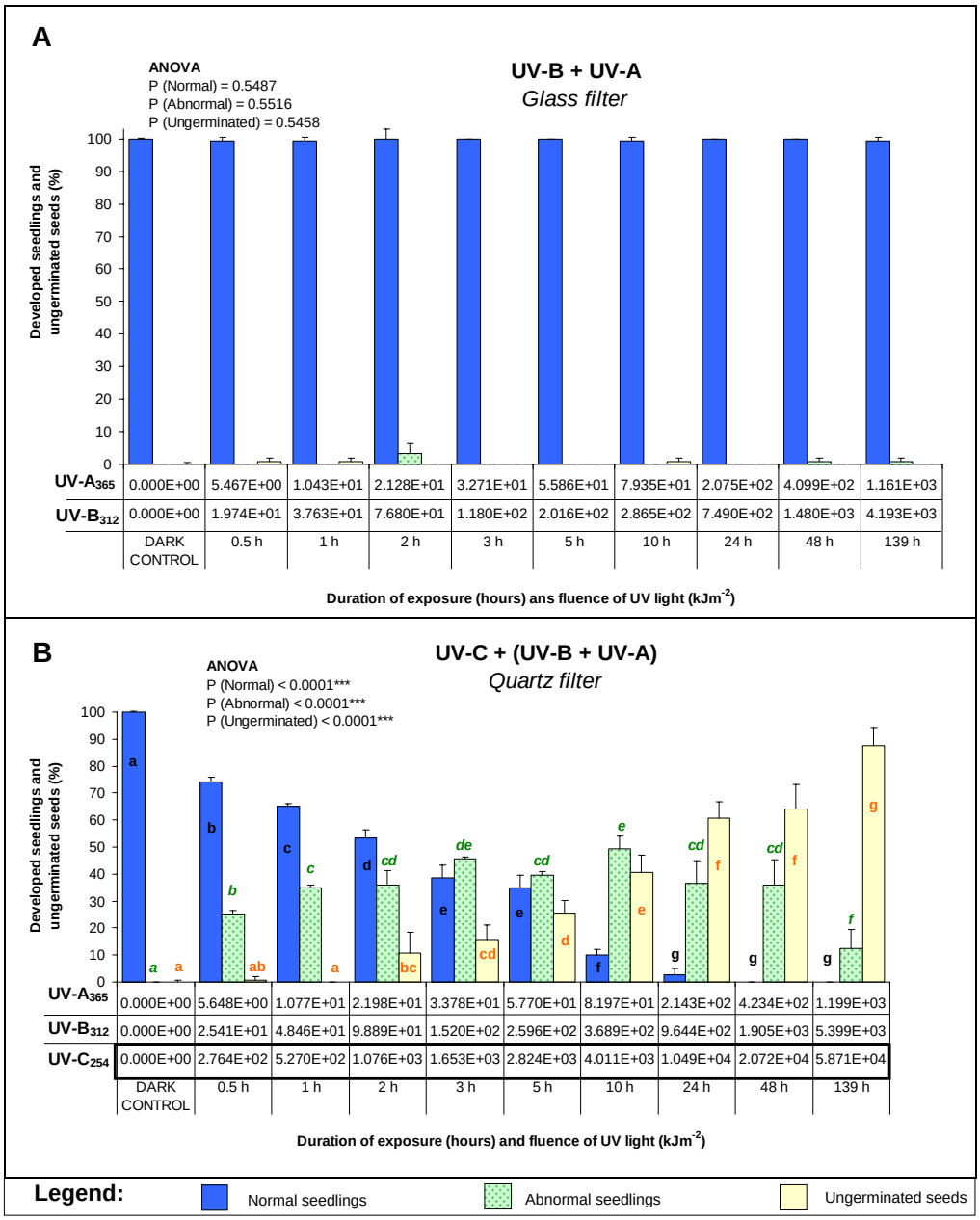

Fig. 73. Impact of short-term UV-B + UV-A and UV-C + (UV-B + UV-A) radiation on germination and development of seedlings after the irradiation of *Arabidopsis* flavonoid-lacking *tt4-8* seeds (Ws-2 accession). The seeds covered with *Glass* filter were exposed only to UV-B + UV-A portion of emitted light (A) and those covered with *Quartz* filter were exposed to entirely transmitted UV-C + (UV-B + UV-A) light emitted from the UV-C_{254} source (B). The duration of UV exposure (hours) and UV fluences (kJm^{-2}) are indicated under each bar. Values are the mean ± standard deviation of three parallel experiments (n = 50 sown seeds). Bars with different letters within the same group, denote a significant difference at $\alpha < 0.05$, according to ANOVA. The precise values of statistical tests are indicated above the bars, where * means a significant level ($P < 0.05$), ** very significant ($P < 0.01$) and *** extremely significant ($P < 0.001$) level of difference.

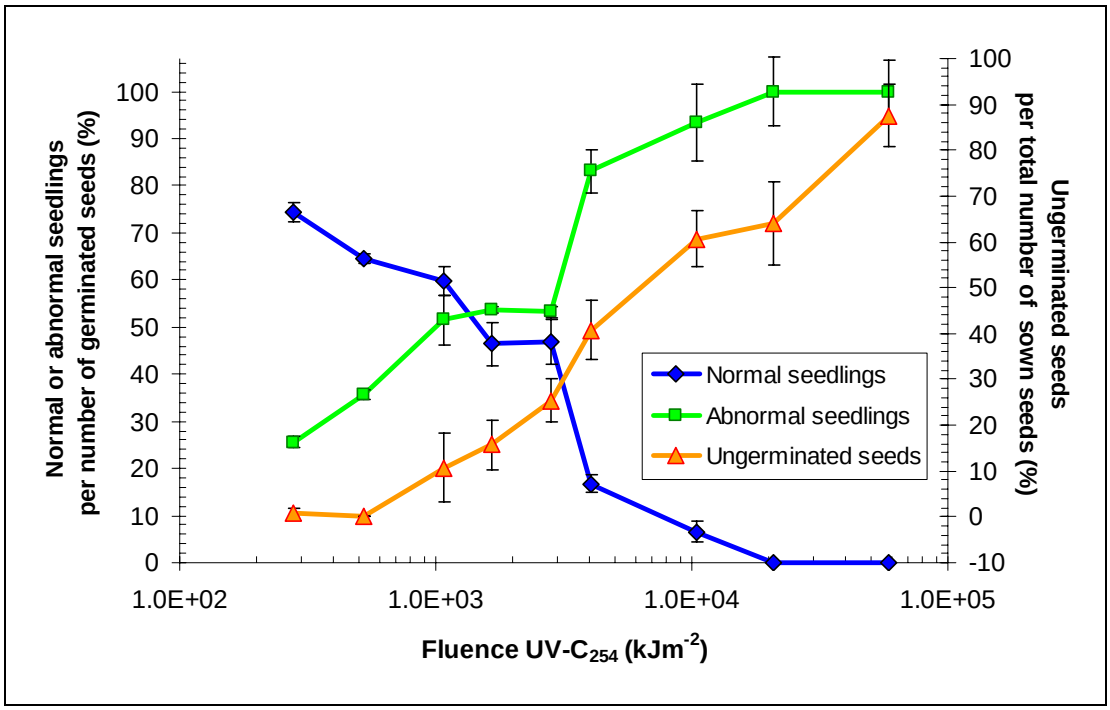

Fig. 74. Effect of UV-C (λ = 254 nm) light on germination and development of seedlings after the irradiation of *Arabidopsis* flavonoid-lacking *tt4-8* seeds (Ws-2 accession). The UV-C_{254} dose response curve for *tt4-8* ungerminated seeds (scale on the right side) is compared to dose response curves for developed normal and abnormal seedlings germinated from UV exposed seeds (scale on the left side). All values are the means ± standard deviation of three parallel experiments (n = 50 sown seeds).

The UV-C (λ = 254) dose response curves for the percentage of ungerminated *tt4-8* seeds, as well as the frequencies of normally and abnormally developed *tt4-8* seedlings from irradiated seeds were therefore plotted against increasing UV fluence (**Fig. 74**). Besides almost linearly increased percentage of ungerminated seeds, we observed an interesting non-linear behaviour of the UV-C dose response curve for the percentage of normal and abnormal seedlings germinated from irradiated *tt4-8* seeds. The percentage of normally developed seedlings decreased progressively up to UV-C fluence of 1.7 x 10^3 kJm^{-2}, remaining at about the same level up to 2.8 x 10^3 kJm^{-2}. A sudden drop to only 17% of normal seedlings occurred at the UV-C fluence of 4.0 x 10^3 kJm^{-2} (corresponds to 10 hours of irradiation). Higher fluences caused further decline in the percentage of normally developed seedlings. Finally, no normal seedlings were detected at UV-C ≥ 2.1 x 10^4 kJm^{-2}.

On the other hand, the percentage of abnormally developed seedlings followed a reciprocal trend, exhibiting a progressive increase up to UV-C = 1.1 x 10^3 kJm^{-2}. Surprisingly, a further increase in UV-C fluence up to 2.8 x 10^3 kJm^{-2} did not significantly alter the percentage of abnormal seedlings. A sudden rise in the percentage of abnormal seedlings occurred at UV-C = 4.0 x 10^3 kJm^{-2} (corresponds to 10 hours of irradiation). Further increase in UV-C fluence caused progressive increase in the percentage of abnormal seedlings. At the fluence of UV-C ≥ 2.1 x 10^4 kJm^{-2}, all germinated seeds developed into abnormal seedlings.

16.3.2. Characterisation and quantification of seedling damage after exposure to quasi-monochromatic UV-C_{254} light

Since abnormal morphology was detected in *Arabidopsis* seedlings developed from UV-C_{254} irradiated seeds (see sections **16.3.1.1** and **16.3.1.2**), we aimed further to characterize and quantify types of damage to essential seedling structures, including the hypocotyl, the primary root and the cotyledons. Seedling defects that occurred single or in the combination were characterized according to ISTA (1999). **Fig. 75** illustrates the types of damage observed in early stage *Arabidopsis* seedlings (17 DAI-old Ws-2, *dyx* and *tt4-8* seedlings, as well as 22 DAI-old Col-0 and *fah1-2* seedlings) developed from seeds exposed to incident UV-C + (UV-B + UV-A) light and its minor UV-B + UV-A component. The primary root was the most sensitive organ, where a slight root shortening in otherwise normally developed seedlings was first detected (**Fig. 75B**). Development of shoot axis was also frequently affected, with a short or twisted hypocotyl (**Fig. 75C**). More severe damage included the combination of abnormal morphology of both the shoot axis and the root system, resulting in the development of abnormal seedlings with a short or twisted hypocotyl, together with a short (**Fig. 75D**), retarded (**Fig. 75E**) or even missing (**Fig. 75F**) primary root. The most severe damage was observed in seedling forms with no developed hypocotyl, and an undeveloped root system, exhibiting the cotyledons that were not fully developed (**Fig. 75G**).

Therefore, we determined the type and severity of seedling damage as a function of UV wavelength and fluence. The percentage of abnormal seedlings within each class of seedling damage is presented together with the total percentage of ungerminated seeds for the Ws-2, *dyx*, Col-0 and *fah1-2* lines (**Fig. 76**, section **16.3.2.1**), as well as for *tt4-8* line (**Fig. 77**, section **16.3.2.2**).

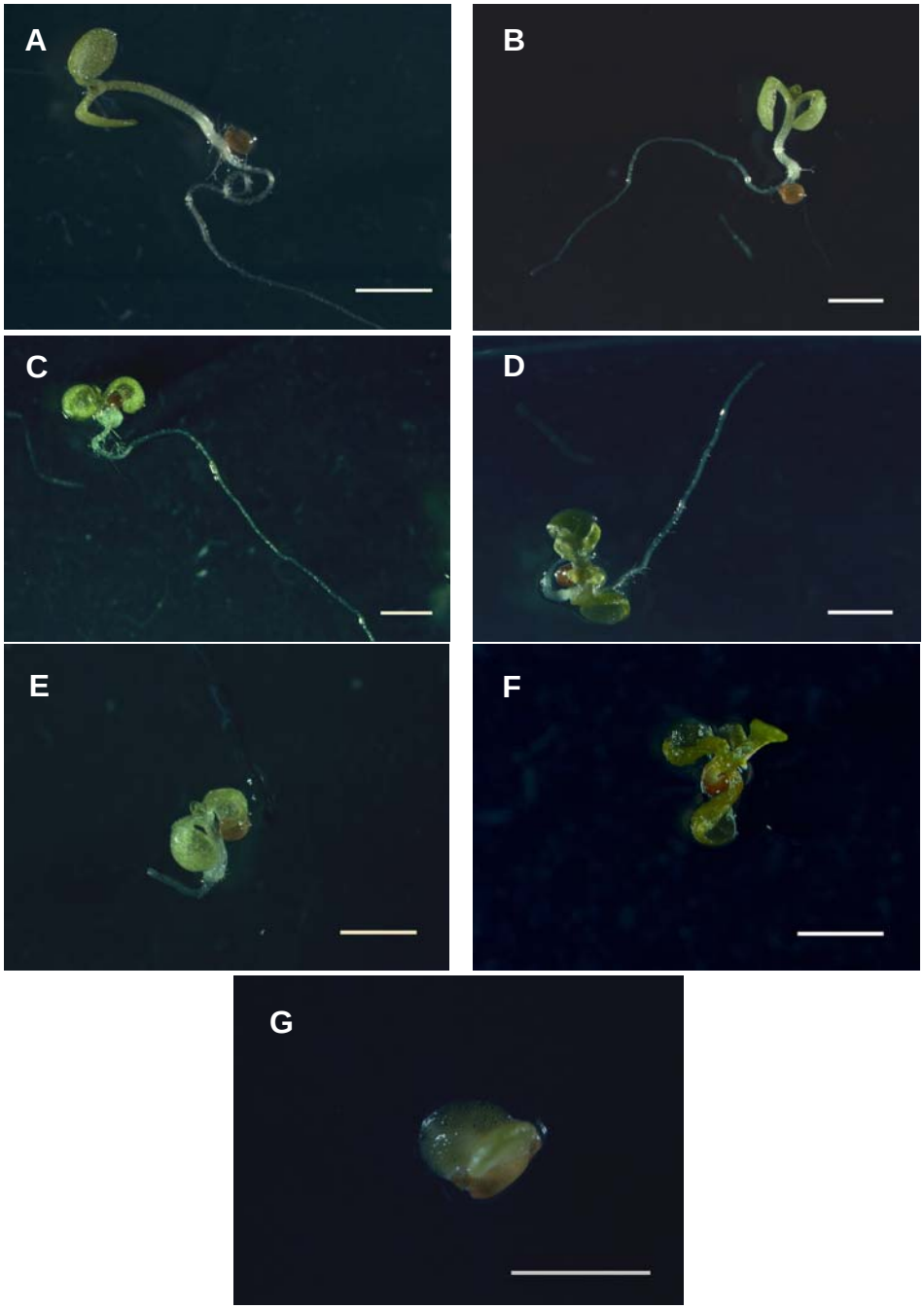

Fig. 75. Types of damage to essential structures of early-stage *Arabidopsis* seedlings, developed from seeds exposed to entirely transmitted UV-C (UV-B + UV-A) light or only to its UV-B + UV-A component, emitted from the UV-C_{254} source.
Type of damage observed on 17 DAI-old (Ws-2, *dyx*, *tt4-8* lines) and 22 DAI-old (Col-0 and *fah1-2* lines) seedlings: (A) normally developed seedling, (B) normal seedling with shorter primary root, (C) damaged seedling with hypocotyl short or twisted, but normally developed primary root, (D) damaged seedling with hypocotyl short or twisted and short primary root, (E) damaged seedling with hypocotyl short and retarded primary root, (F) damaged seedling with short hypocotyl and missing primary root, (G) damaged seedling with missing hypocotyl, missing primary root and cotyledons that are not fully developed. The full length of normally developed primary roots is not presented on pictures in panel A and C. Bars represent 1 mm, DAI = days after imbibitition.

16.3.2.1. Types of seedling damage after long-term UV-C_{254} exposure of flavonoid-containing Arabidopsis seeds

The UV-B + UV-A part of light emitted from the UV_{254} source did not alter seedling development in the Ws-2 wild type and the *dyx* mutant line (**Fig. 76A** and **B**). Only a few seeds remained ungerminated or developed abnormal seedlings, but with no statistical relevance ($p > 0.05$), compared to the dark controls.

In contrast, 60 days of exposure of the Col-0 wild type seeds to UV-B + UV-A light resulted in a small (3%), but statistically important increase ($p = 0.0012$) in percentage of damaged seedlings. In addition, the only type of abnormal morphology observed was seedlings with short or twisted hypocotyls, while cotyledons and roots developed normally. No damage occurred to Col-0 seedlings after the exposure of seeds to lower doses (40 days of irradiation) of the UV-B + UV-A portion of emitted light (**Fig. 76C**).

Similarly, no abnormal seedlings were observed in the *fah1-2* mutant after exposure of seeds to the UV-B + UV-A portion of emitted light for 40 days (**Fig. 76D**). On the other hand, the *fah1-2* seeds that were irradiated for 60 days, receiving higher doses of UV-B + UV-A radiation, exhibited higher level of sensitivity to UV-B + UV-A radiation, compared to the Col-0 background. Abnormal morphology was detected in 11% of developed *fah1-2* seedlings, and two types of seedling damage were observed. An extremely significant increase ($p < 0.0001$) in the percentage of seedlings with short or twisted hypocotyls, as well as a very significant increase ($p = 0.020$) in the percentage of seedlings with short or twisted hypocotyls that developed also short primary roots, was detected in irradiated *fah1-2* samples.

UV-C + (UV-B + UV-A) light had a strong effect on the morphology of seedlings developed from irradiated Ws-2, *dyx*, Col-0 and *fah1-2* seeds, and this effect was observed already at lower fluences of UV-C + (UV-B + UV-A) radiation (**Fig. 76E-H**). Cumulative percentage graphs showed that 30 days of UV-C + (UV-B + UV-A) exposure resulted in 52% abnormally developed seedlings in the case of the Ws-2 wild-type line (**Fig. 76E**) and 53% in the case of the *dyx* T-DNA insertion mutant (Ws-2 accession) (**Fig. 76F**), where three types of seedling damage were observed. The most frequent abnormal morphology was short or twisted hypocotyl, but with normally developed root and cotyledons, which was detected in 32% of the Ws-2 and 35% of the *dyx* seedlings. More severe damage included seedlings with abnormally developed both shoot and root axes, where 14% of the Ws-2 and *dyx* seedlings exhibited short or twisted hypocotyls together with short primary roots, while about 3% of the seedlings developed

short or twisted hypocotyls and retarded primary roots. Less than 2% of the Ws-2 and *dyx* seedlings developed into a seriously damaged seedling form with a short hypocotyl and missing primary root. Sixty days of exposure of the Ws-2 and *dyx* seeds to UV-C + (UV-B + UV-A) radiation resulted in an important increase in the cumulative percentage of seedling damage and ungerminated seeds, reaching the level of 64% for both the Ws-2 and the *dyx* lines (**Fig. 76E** and **F**, respectively). Four types of seedling damage were observed in both the Ws-2 and *dyx* samples, including the most frequent seedling form with a short or twisted hypocotyl in an otherwise normally developed seedling (27% in the Ws-2 line and 28% in the *dyx* line), followed by three abnormal seedling forms exhibiting a short or twisted hypocotyl together with a short, retarded or missing primary root. Comparing the samples irradiated with UV-C + (UV-B + UV-A) for 30 and 60 days, we observed that the percentage of seedlings with a short or twisted hypocotyl, in otherwise normally developed seedlings, decreased in favour of increased percentages of other more severe damage.

On the other hand, seedling development in the Col-0 wild-type line was less affected by UV-C + (UV-B + UV-A) radiation than the Ws-2 wild-type, reaching the cumulative percentage of seedling damage of 7% and 15% for the Col-0 samples irradiated for 40 and 60 days, respectively (**Fig. 76G**). A statistically important increase ($p = 0.0002$) in the percentage of only one type of seedling damage was observed in Col-0 samples. The percentage of seedlings with a short or twisted hypocotyl, but normally developed root and cotyledons reached 5% and 9% in the samples irradiated for 40 and 60 days, respectively. Other types of more severe damage to Col-0 seedlings occurred at low frequency (<1%), having no statistical relevance ($p > 0.05$) compared to the dark control.

The sinapate ester mutant *fah1-2* was more affected by UV-C + (UV-B + UV-A) light, compared to the Col-0 background, but less affected than the Ws-2 and *dyx* lines. The cumulative percentage of damaged *fah1-2* seedlings and ungerminated seeds reached the level of 31% and 60% for samples irradiated for 40 and 60 days, respectively (**Fig. 76H**). A statistically significant increase ($p < 0.0001$) in two types of seedling damage was observed in *fah1-2* line. Seedlings with the short or twisted hypocotyls, but normally developed roots and cotyledons reached the levels of 25% and 42% after 40 and 60 days of irradiation, respectively. In addition, the seedlings with short or twisted hypocotyls in combination with short primary roots reached 4% and 13%, respectively. Other seedling damage observed in the *fah1-2* sample irradiated for 60 days did not differ significantly ($p > 0.05$), compared to the dark control.

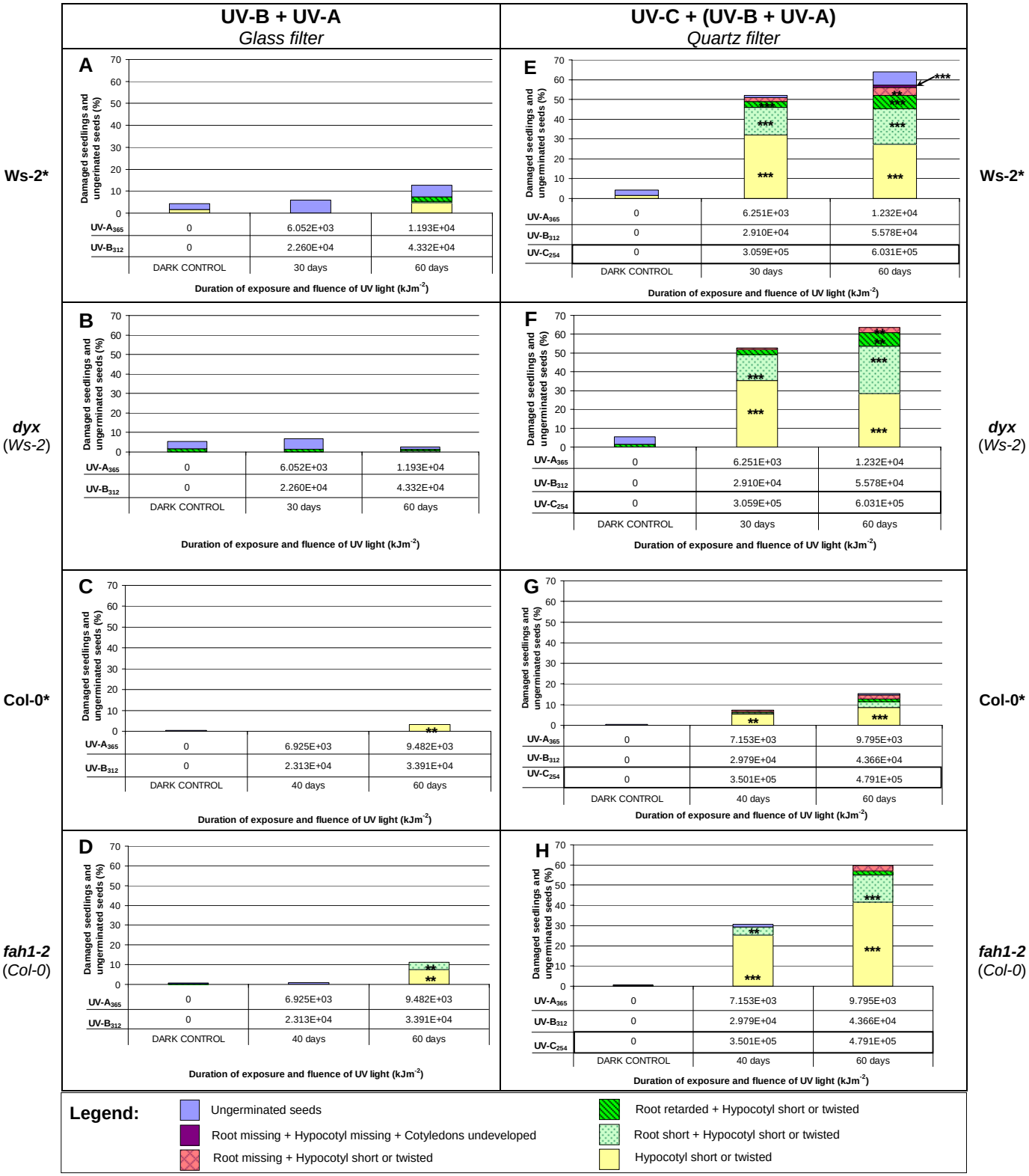

Fig. 76. Damaged early-stage *Arabidopsis* seedlings germinated from seeds exposed to the UV-B + UV-A portion and incident UV-C + (UV-B + UV-A) light emitted from the UV-C_{254} source. Seed samples were covered with the *Glass* or the *Quartz* filter. The duration of UV exposure (30 and 60 days for the Ws-2 and *dyx* seeds and 40 and 60 days for the Col-0 and *fah1-2* seeds) and UV fluences (kJm^{-2}) are indicated under each bar. Percentages of ungerminated seeds and different types of damaged seedlings developed from UV irradiated seeds are compared to unexposed control samples (dark control). Mean values were obtained from three parallel experiments (n = 50 sown seeds) and analyzed by ANOVA ($\alpha = 0.05$), where * means a significant level ($P < 0.05$), ** very significant ($P < 0.01$) and *** extremely significant ($P < 0.001$) level of difference.
The plant genotypes were: Wassilewskija (Ws-2), A and E; a control mutant with a T-DNA insertion carrying the *nptII* gene (*dyx*), B and F; Columbia (Col-0), C and G; a sinapate ester-deficient mutant (*fah1-2*), D and H. Wild ecotypes are marked with asterisks and background ecotypes are noted in the parentheses under each mutant line.

16.3.2.2. Types of damage in flavonoid-lacking tt4-8 Arabidopsis seedlings after short-term UV-C_{254} exposure

Short-term exposure of flavonoid-lacking *tt4-8* seeds to the minor UV-B + UV-A portion of emitted light up to fluences of UV-B = 4.2 x 10^3 kJm^{-2} and UV-A = 1.2 x 10^3 kJm^{-2} (corresponds to 139 hours of irradiation) did not affect development of *tt4-8* seedlings, and no abnormal seedling structures were observed (data not presented).

In contrast, short-term exposure of *tt4-8* seeds to incident UV-C + (UV-B + UV-A) had a dramatic effect on seedling development (**Fig. 77**). Already 0.5 hour of UV-C + (UV-B + UV-A) irradiation of *tt4-8* seeds resulted in an increased percentage of two types of seedling damage: the seedlings with a short or twisted hypocotyls, but normally developed root system and cotyledons (22%), and the seedlings with short or twisted hypocotyls in combination with short primary roots (3%). Flavonoid-lacking *tt4-8* seeds that were exposed to UV-C + (UV-B + UV-A) light for 24 hours, developed all five types of seedling damage: (1) the seedlings with short or twisted hypocotyls, but normally developed root system and cotyledons, the seedlings with short or twisted hypocotyls in combination with short (2), retarded (3) or missing primary roots (4), and seedling forms with undeveloped hypocotyls in combination with a missing primary roots and undeveloped cotyledons (5). Since the UV-B + UV-A component of the incident light did not influence *tt4-8* seedling development, the effect of UV-C + (UV-B + UV-A) light was due to the UV-C dominant component.

In addition, **Fig. 77** illustrates the dynamics in frequencies of *tt4-8* seedling damage, where the peaks in the occurrence of dominant type of seedling damage could be determined in relation to the fluences of UV-C + (UV-B + UV-A) light. Reaching a peak of occurence, the percentage of seedlings with a particular damage started to decrease in favour of increasing percentages of other types of seedling damage. The peak in frequency for seedlings with short or twisted hypocotyls, but normally developed roots and cotyledons, was determined at a dose received after 3 hours of irradiation (UV-C = 1.7 x 10^3 kJm^{-2}). The peaks in frequency for seedlings with short or twisted hypocotyls in combination with short, retarded or missing primary root, was determined at fluences reached after 10 hours (UV-C = 4.0 x 10^3 kJm^{-2}), 24 hours (UV-C = 1.0 x 10^4 kJm^{-2}) and 48 hours (UV-C = 2.1 x 10^4 kJm^{-2}) of irradiation, respectively. The maximal percentage of the most severe seedling damage, an undeveloped hypocotyl in combination with a missing primary root and undeveloped cotyledons, occurred after 139 hours of irradiation (UV-C = 5.9 x 10^4 kJm^{-2}).

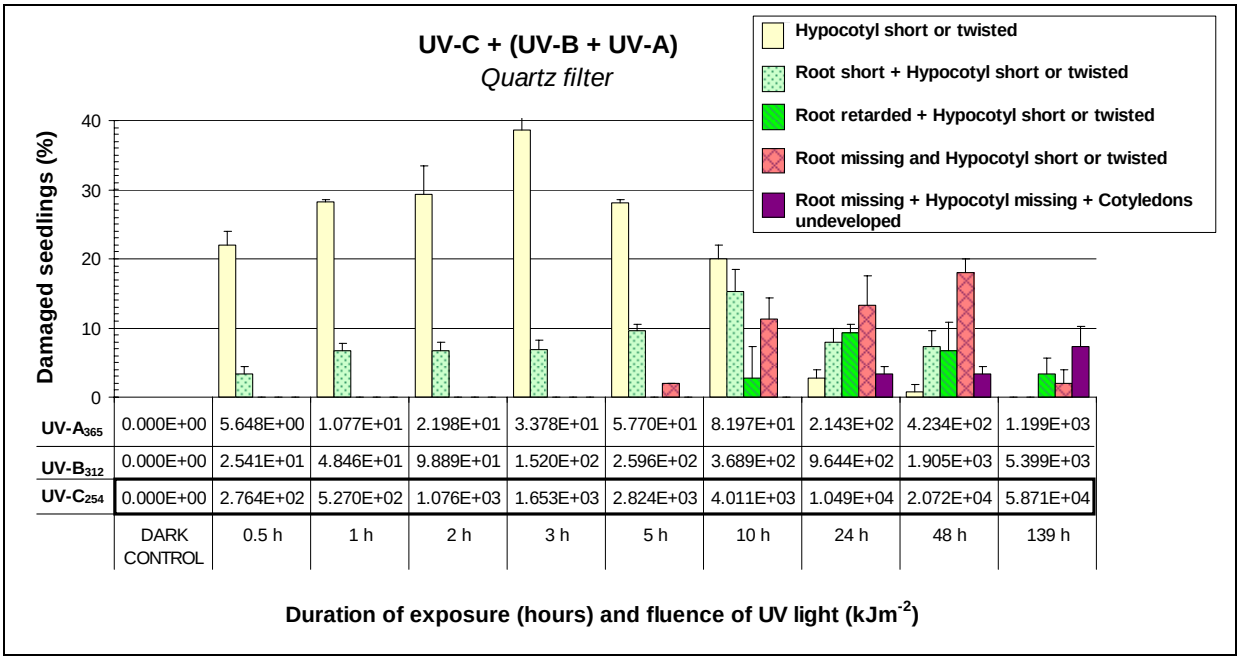

Fig. 77. Dynamics in frequencies of *Arabidopsis tt4-8* seedling damage after the exposure of seeds to entirely transmitted UV-C + (UV-B + UV-A) light emitted from the UV-C_{254} source. Seed samples covered with the *Quarz* filter were irradiated from 0.5 hour to 139 hours with UV fluences (kJm^{-2}) that are indicated under each bar. Percentages of different types of damaged seedlings from UV irradiated seeds are compared to the control sample (dark control), which developed all normal seedlings. Values are the mean ± standard deviation of three parallel experiments (n = 50 sown seeds).

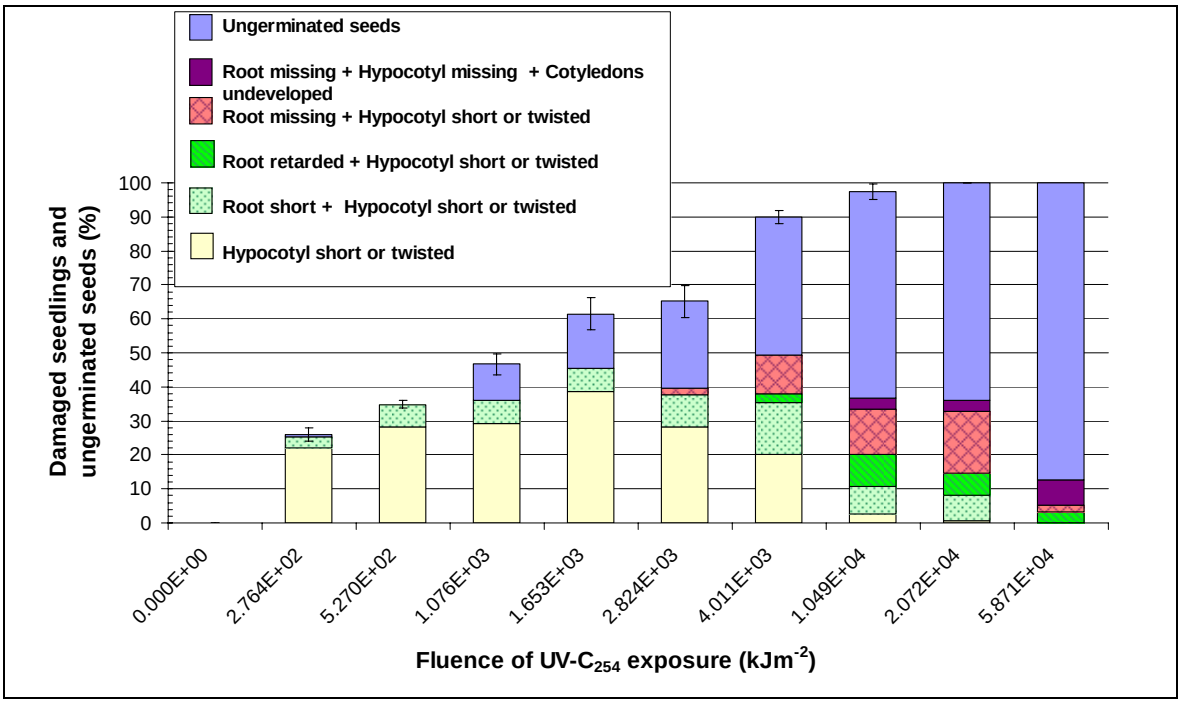

Fig. 78. Effect of UV-C (λ = 254 nm) light on germination and development of *Arabidopsis* flavonoid-lacking *tt4-8* seedlings after the exposure of seeds to UV light. All values are the means obtained from three parallel experiments (n = 50 sown seeds). The error bars represent ± standard deviations in cumulative percentage of damaged seedlings and ungerminated seeds.

The graph in **Fig. 77** does not include the percentage of ungerminated *tt4-8* seeds. Thus, a cumulative percentage graph, presented in **Fig. 78** shows the contribution of each type of seedling damage, as well as the percentage of ungerminated seeds as a function of increasing UV-C (λ = 254) fluence. Increasing UV-C fluence resulted in an increased cumulative percentage of seedling damage and ungerminated *tt4-8* seeds. However, UV-C fluences of 1.6 x 10^3 kJm^{-2} and 2.8 x 10^3 kJm^{-2} caused similar cumulative effects, but the contribution of each type of damage was different. Similarly, the highest UV-C fluences of 2.1 x 10^4 kJm^{-2} and 5.9 x 10^4 kJm^{-2} resulted in the same cumulative percentage of damaged seedlings and ungerminated seeds reaching 100%, although the contribution of each type of damage in the total percentage was different. In addition, **Fig. 78** shows that only 10% of the seedlings developed normally after the exposure of *tt4-8* seeds to UV-C fluence of 4.0 x 10^3 kJm^{-2}, while no normally developed seedlings were observed at UV-C $\geq$ 2.1 x 10^4 kJm^{-2}.

16.3.3. Length of primary roots in seedlings developed form seeds exposed to quasi-monochromatic UV-C_{254} light

Arabidopsis seeds that were exposed to UV light emitted from UV_{254} source frequently produced the seedlings with damaged essential structures. The root axis was a particularly sensitive seedling structure, since the UV exposed seeds frequently germinated into seedlings with short, retarded or even missing primary roots (see above section **16.3.2**). A normal root system is essential for development of functional and vigorous plants. Thus, we considered the root length as one of the important parameters in the early-seedling stage development. The length of normally developed primary roots (≥ 3 mm) was measured in 10 day-old (13 DAI) Ws-2, *dyx*, Col-0 and *fah1-2* seedlings (**Fig. 79**, section **16.3.3**) and *tt4-8* seedlings (**Fig. 80**, section **16.3.3.2**) that germinated from seeds exposed to UV-C + (UV-B + UV-A) light, as well the UV-B + UV-A component of incident light. The germinants that developed into seedlings with retarded or missing roots, as well as ungerminated seeds were not here considered.

16.3.3.1. Effect of long-term UV-C_{254} exposure on primary root length in flavonoid-containing Arabidopsis seedlings

Prior to the analysis of irradiated samples and in order to determine the consistency of the results, measured root lengths were compared among the dark controls (seedlings developed from seeds that were exposed to the experimental conditions, but protected from UV by an aluminium foil filter) and their laboratory control samples (seedlings developed from seeds that were stored at 4°C in the dark during the UV exposure experiment). Parametric tests, such as one-way ANOVA and the unpaired t-test showed no statistical differences ($p > 0.05$) in root length among the dark controls and the laboratory controls, as well as within the group of dark controls for the Ws-2, *dyx*, Col-0 and *fah1-2* lines (results not presented). The same result was obtained using the Kruskal-Wallis and the Mann-Whithey nonparametric statistical tests, showing no statistical differences ($p > 0.05$) among the dark controls and the related laboratory controls, as well as within the group of dark control samples for each tested genotype (results not presented). Thus, the root lengths for two dark control samples were averaged for the Ws-2, *dyx*, Col-0 and *fah1-2* lines. These values were further compared to those of irradiated samples.

The effect of the UV-B + UV-A portion of emitted light on the average length of primary roots in the Ws-2, *dyx*, Col-0 and *fah1-2* seedlings is presented in **Fig. 79A-D**. Compared to the

dark controls, ANOVA showed no statistical differences ($p > 0.05$) in the average root length of Ws-2, Col-0 and *fah1-2* seedlings developed from seeds irradiated up to 60 days (**Fig. 79A, C** and **D**). A similar result was obtained when root length data were analyzed using the nonparametric Kruskal-Wallis statistical test. Surprisingly, an extremely significant difference ($p < 0.0001$), using both ANOVA and the Kruskal-Wallis test, was detected in the average root length of the *dyx* seedlings developed from UV-B + UV-A exposed seeds (**Fig. 79B**). However, this effect was observed only at the highest fluence reached after 60 days of irradiation (UV-B = 4.3 x 10^4 kJm^{-2} and UV-A = 1.2 x 10^4 kJm^{-2}), while no statistical difference ($p > 0.05$) in root length was observed at lower fluence after 30 days of exposure.

The exposure of seeds to entirely transmitted UV-C + (UV-B + UV-A) light had an extremely significant effect ($p < 0.0001$) on the length of primary roots in the Ws-2 and *dyx* seedlings (**Fig. 79E** and **F**), where significant shortening of primary roots occurred in the samples irradiated for 30 days, and the root length decreased further with increased UV-C + (UV-B + UV-A) fluence. Since no effect of the UV-B + UV-A portion of incident light on root length was observed in the Ws-2 wild type samples, this phenomenon of root shortening was attributed to the UV-C dominant component of the emitted light. However, the combined effects of the UV-C part and the UV-B + UV-A component of emitted light should be taken into account for the *dyx* samples, but only at the highest fluences reached after 60 days of irradiation.

Unlike the Ws-2 wild type, the Col-0 wild type appeared more robust in this analysis, since no effect of incident UV-C + (UV-B + UV-A) light on primary root length was observed (**Fig. 79G**). ANOVA, as well as the nonparametric Kruskal-Wallis test, showed no statistical difference ($p > 0.05$) in the average length of roots among the Col-0 samples exposed to UV-C + (UV-B + UV-A) light and the dark control.

On the other hand, the *fah1-2* mutant appeared extremely sensitive to UV-C + (UV-B + UV-A) light, compared the Col-0 background. An extremely significant decrease ($p < 0.0001$) in the average length of the *fah1-2* seedling roots was observed already after 40 days of exposure (UV-C =3.5 x 10^5 kJm^{-2}) (**Fig. 79H**). Higher fluences (UV-C = 4.8 x 10^5 kJm^{-2}) did not cause further decrease in the length of the seedling roots. Since the UV-B + UV-A component of the emitted light did not affect the length of roots in *fah1-2* seedlings, the observed shortening of primary roots in UV-C + (UV-B + UV-A) exposed *fah1-2* samples was related to the effects of the dominant UV-C component of emitted light.

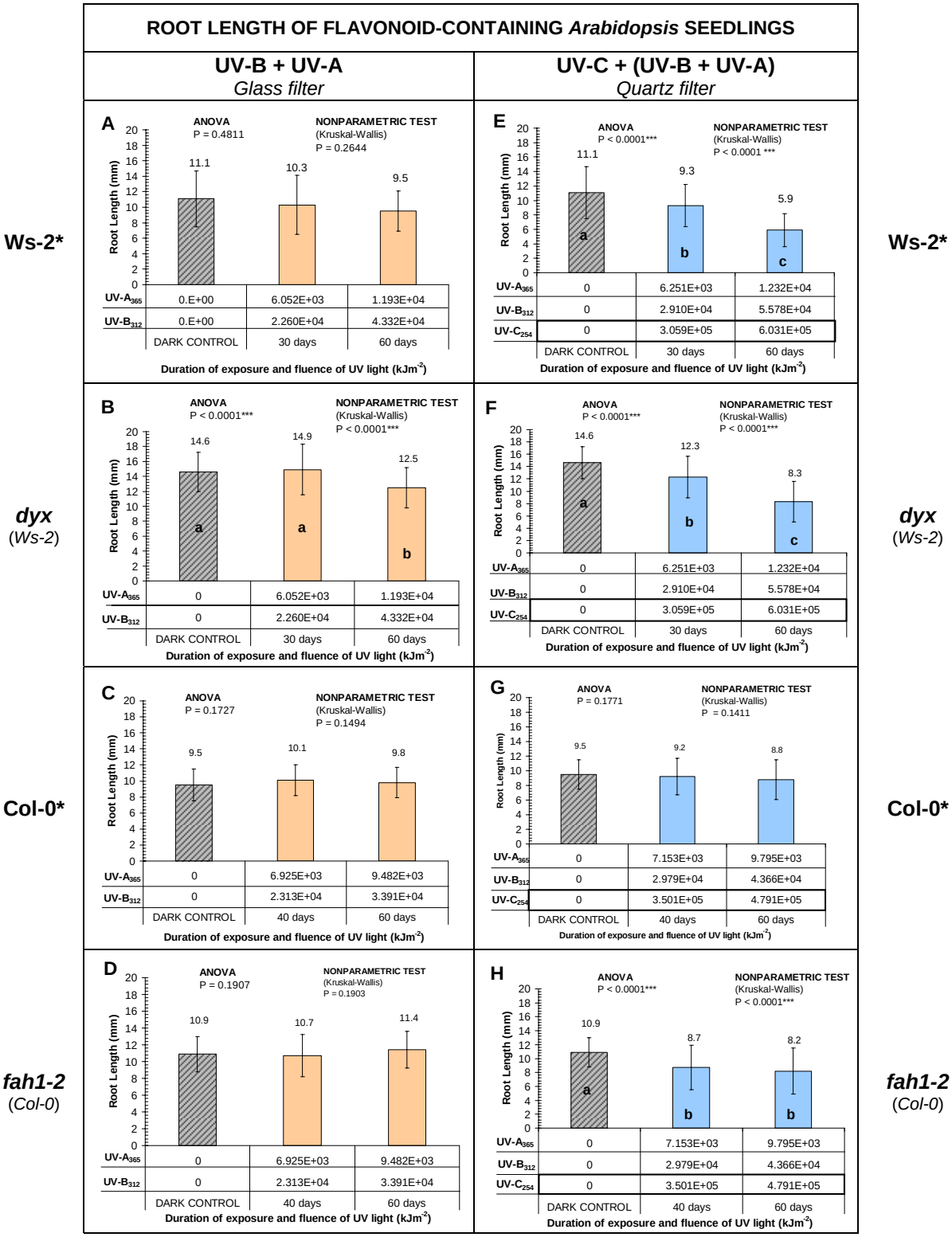

Fig. 79. Root length of 10 day-old *Arabidopsis* seedlings (13 DAI) germinated from the flavonoid-containing seeds exposed to entirely transmitted UV-C + (UV-B + UV-A) light or only to its UV-B + UV-A portion emitted from the UV-C_{254} source. The root length was measured only in germinants that developed normal root ≥ 3 mm. The duration of UV exposure (30 and 60 days for the Ws-2 and *dyx* seeds, and 40 and 60 days for the Col-0 and *fah1-2* seeds) and UV fluences (kJm^{-2}) are indicated under each bar. Values are the mean ± standard deviation of three parallel experiments (n = 22). Bars with different letters denote a significant difference at $\alpha < 0.05$, according to ANOVA (parametric test) and the Kruskal-Wallis test (nonparametric test). The precise values of statistical tests are indicated above the bars, where * means a significant level ($P < 0.05$), ** very significant ($P < 0.01$) and *** extremely significant ($P < 0.001$) level of difference. DAI = days after imbibition.

The plant genotypes were: Wassilewskija (Ws-2), A and E; a control mutant with a T-DNA insertion carrying the *nptII* gene (*dyx*), B and F; Columbia (Col-0), C and G; a sinapate ester-deficient mutant (*fah1-2*), D and H. Wild ecotypes are marked with asterisks and background ecotypes are noted in the parentheses under each mutant line.

16.3.3.2. Primary root length in tt4-8 Arabidopsis seedlings after short-term UV-C_{254} exposure

The consistency of results for seedling root length of *tt4-8* dark control samples was determined by comparing the root length values for all nine dark controls, ranging from 0.5 up to 139 hours of treatment, against the laboratory control (results not presented). ANOVA showed satisfying consistency of the result, since there was no detected significant difference ($p > 0.05$) in root lengths among all tested control samples. Similar result was obtained using the Kruskal-Wallis nonparametric statistical test. Therefore, the root length values for all nine *tt4-8* dark controls were pooled together and the calculated mean value was further compared to the UV exposed samples.

Short-term exposure of the flavonoid-lacking *tt4-8* seeds to the UV-B + UV-A portion of emitted light did not affect the growth of primary roots in the early-stage seedlings (**Fig. 80A**). The root length in all nine UV-B + UV-A exposed samples, irradiated from 0.5 up to 139 hours (maximal fluence up to UV-B = 4.2 x 10^3 kJm^{-2} and UV-A = 1.2 x 10^3 kJm^{-2}), did not differ from that of the averaged dark control. Both one-way ANOVA (parametric test) and the Kruskal-Wallis (nonparametric test) showed no statistical differences ($p > 0.05$). Similarly, no statistically significant difference was detected within the group of all nine UV-B + UV-A exposed samples.

In contrast, short-term exposure of the *tt4-8* seeds to entirely transmitted UV-C + (UV-B + UV-A) light had an extremely significant ($p < 0.0001$) effect, according to both one-way ANOVA and the Kruskal-Wallis test, on growth of primary roots in the *tt4-8* seedlings, where increased fluences of UV-C + (UV-B + UV-A) light caused a decrease in root length (**Fig. 80B**). Since short-term exposure to UV-B + UV-A light alone did not affect the root growth (see above), the observed root shortening was related to the effects of the dominant UV-C component of emitted light. The Tukey-Kramer post-hoc test and the Dunn's multiple comparisons test, showed that as little as 1 hour of irradiation (UV-C =5.3 x 10^2 kJm^{-2}) of *tt4-8* seeds resulted in an extremely significant ($p < 0.0001$) shortening of the primary roots, but UV-C fluence reached after 2 hours of exposure did not cause further decrease in the root length. However, 3 hours of UV exposure (UV-C =1.7 x 10^3 kJm^{-2}) resulted in further shortening of the primary roots. The average root length in *tt4-8* seedlings remained statistically unchanged in samples exposed for 5 and 10 hours. The *tt4-8* seeds that were exposed for 24, 48 and 139 hours (maximal fluence up to UV-C =5.9 x 10^4 kJm^{-2}) did not develop seedlings with measurable primary roots (root length < 3 mm), although the germination capacity reached 39%, 36% and 13%, respectively.

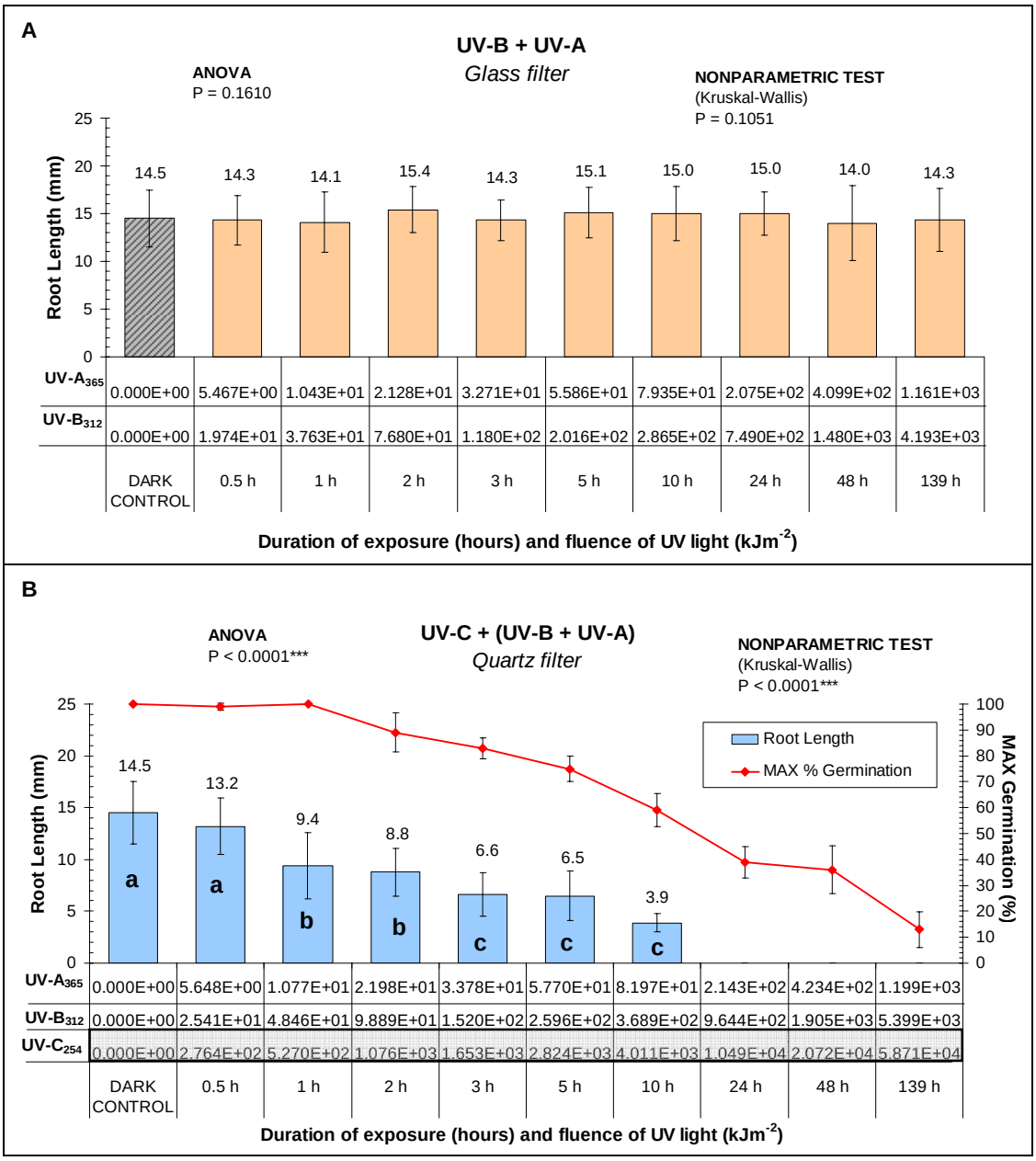

Fig. 80. Root length of 10 day-old (13 DAI) *Arabidopsis tt4-8* seedlings developed from seeds after short-term UV-B + UV-A and UV-C + (UV-B + UV-A) irradiation. A) Seedlings developed from seeds that were covered with a *Glass* filter and exposed to the UV-B + UV-A portion of emitted light. B) Seedlings developed from seeds that were covered with a *Quartz* filter and exposed to entirely transmitted UV-C + (UV-B + UV-A) light, emitted from the UV-C_{254} source. The root length of UV-C + (UV-B + UV-A) exposed samples is compared to the maximal germination percentage ($G_{max\%}$). Samples exposed to UV-C + (UV-B + UV-A) light for 24, 48 and 139 hours did not develop primary roots that could be measured (root length < 3 mm). The duration of UV exposure (hours) and UV fluences (kJm^{-2}) are indicated under each bar. Values are the mean ± standard deviation of three parallel experiments (n = 22). Bars with different letters denote significant differences at $\alpha < 0.05$, according to one-way ANOVA (parametric test) and the Kruskal-Wallis test (nonparametric test). The precise values of statistical tests are indicated above the bars, where * means a significant level ($P < 0.05$), ** very significant ($P < 0.01$) and *** extremely significant ($P < 0.001$) level of difference. DAI = days after imbibition

16.4. Plant development stage - effects of quasi-monochromatic UV-C_{254} light

Following the seed germination (principal growth stage 0.5; see section **16.2**) and the early-seedling stage (principal growth stage 1.0; see section **16.3**), where physiological parameters were observed in cultures *in vitro*, the resistance of *Arabidopsis* seeds to incident UV-C + (UV-B + UV-A) light and its UV-B + UV-A portion was further determined through the plant development stage. After 3-days imbibition *in vitro*, irradiated seeds were germinated in soil and plants were cultivated for 45 days (48 DAI) under greenhouse conditions, reaching different growth stages. The total percentage of grown plants (survivors) from UV irradiated seeds, as well as the percentage of fertile plants that reached the principal growth stage 8.0 (seed producers) was determined for the flavonoid-containing Ws-2, Col-0, *fah1-2* lines (**Fig. 81**, section **16.4.1**) and the flavonoid-lacking *tt4-8* line (**Fig. 82,** section **16.4.2**). The principal growth stage 8.0 is defined as a developmental stage of mature *Arabidopsis* plants with the first siliques shattered (Boyes et al., 2001; Kjemtrup et al., 2003). In addition, the height of the plants grown from irradiated seeds that reached the principal growth stage 8.0 was measured and compared to that of the control plants (**Fig. 81G-I** and **Fig. 82C** and **F**). The plant height is here defined as the perpendicular distance from the soil surface at the plant base to the highest point of the stem in mature plants (Heady, 1957).

16.4.1. Effects of long-term UV-C_{254} exposure on development of plants grown from irradiated flavonoid-containing seeds

The **Fig. 81** shows the effects of UV-C + (UV-B + UV-A) light emitted from the UV-C_{254} source and its UV-B + UV-A portion on the growth of *Arabidopsis* Ws-2, Col-0 and *fah1-2* plants developed from irradiated seeds. The soil-based experiments were omitted for the *dyx* mutant line (a T-DNA insertion control) due to the difficulties related to the handling of a large number of plant samples in a limited greenhouse space. For the same reasons, the Ws-2, Col-0 and *fah1-2* plants were grown in soil only from seeds irradiated with the maximal UV fluences reached after 60 days of exposure.

Out of the total number of nonirradiated Ws-2, Col-0 and *fah1-2* seeds (dark controls) that were sown in soil, 63%, 75% and 83%, respectively, germinated and subsequently developed into the plants (**Fig. 81A-C**). Compared to the percentage of seeds germinated under *in vitro* conditions, where the Ws-2, Col-0 and *fah1-2* dark controls reached $G_{max\%}$ close to 100% (see section **16.2.1.1.1**), we observed lower germinability of the same dark controls when cultivated

in soil under greenhouse conditions. Higher percentage of remaining ungerminated, but putatively viable dark control seeds may be related to the more restrictive greenhouse conditions (e.g. lower air humidity, lower soil water potential, greater variations in temperature, exposure to the microorganisms and insects etc.), compared to the optimal *in vitro* conditions. However, all grown dark control plants in the Ws-2 and Col-0 wild type lines reached the principal growth stage 8.0, capable of producing seeds (fertile plants) (**Fig. 81D** and **E**). Out of the total number of sown *fah1-2* dark control seeds, 75% produced the fertile plants (**Fig. 81F**).

The exposure of seeds to the UV-B + UV-A component of the emitted light did not have an effect on development and growth of the Ws-2, Col-0 and *fah1-2* plants, even after 60 days of exposure. Compared to the dark control samples, ANOVA followed by the Tukey-Kramer multiple comparisons post-hoc test ($\alpha = 0.05$) showed no statistically significant difference ($p > 0.05$) in studied parameters, such as the percentage of survived plants (**Fig. 81A-C**), the percentage of fertile plants (**Fig. 81D-F**) and the plant height (**Fig. 81G-I**). The same result was obtained using ANOVA with $\arcsin\sqrt{\%}$ transformed and log (x+1) transformed data in the case of the percentage of survived plants and the percentage of fertile plants, as well as using the nonparametric Kruskal-Wallis test in the case of plant height parameter.

In contrast, the exposure of seeds to high fluences of entirely transmitted UV-C + (UV-B + UV-A) light, reached after 60 days of exposure, had a strong effect on subsequent development of the Ws-2, Col-0 and *fah1-2* soil-grown plants, resulting in a lower percentage of survived plants (**Fig. 81A-C**), a lower percentage of fertile plants (**Fig. 81D-F**) and a decreased plant height (**Fig. 81G-I**). These effects were related to the dominant UV-C component of emitted light, since its UV-B + UV-A portion had no effect on the growth of the Ws-2, Col-0 and *fah1-2* plants (see above).

Statistical analyses using ANOVA and the Tukey-Kramer post-hoc test ($\alpha = 0.05$) showed a significant differences ($p < 0.05$) in the percentage of survived (**Fig. 81A**) and fertile Ws-2 plants (**Fig. 81D**) that grew from UV-C + (UV-B + UV-A) irradiated seeds. Although a multiple comparison statistical test showed no significant difference ($p > 0.05$) in the percentage of survived Col-0 plants (**Fig. 81B**), the average percentage of fertile Col-0 plants developed from UV-C + (UV-B + UV-A) irradiated seeds differed significantly ($p < 0.05$) from that of the dark control (**Fig. 81E**). The sinapate ester mutant *fah1-2* showed a very significant differences ($p < 0.01$) in the percentage of survived plants (**Fig. 81C**) and in the percentage of fertile plants (**Fig. 81F**) that were grown from UV-C + (UV-B + UV-A) irradiated seeds.

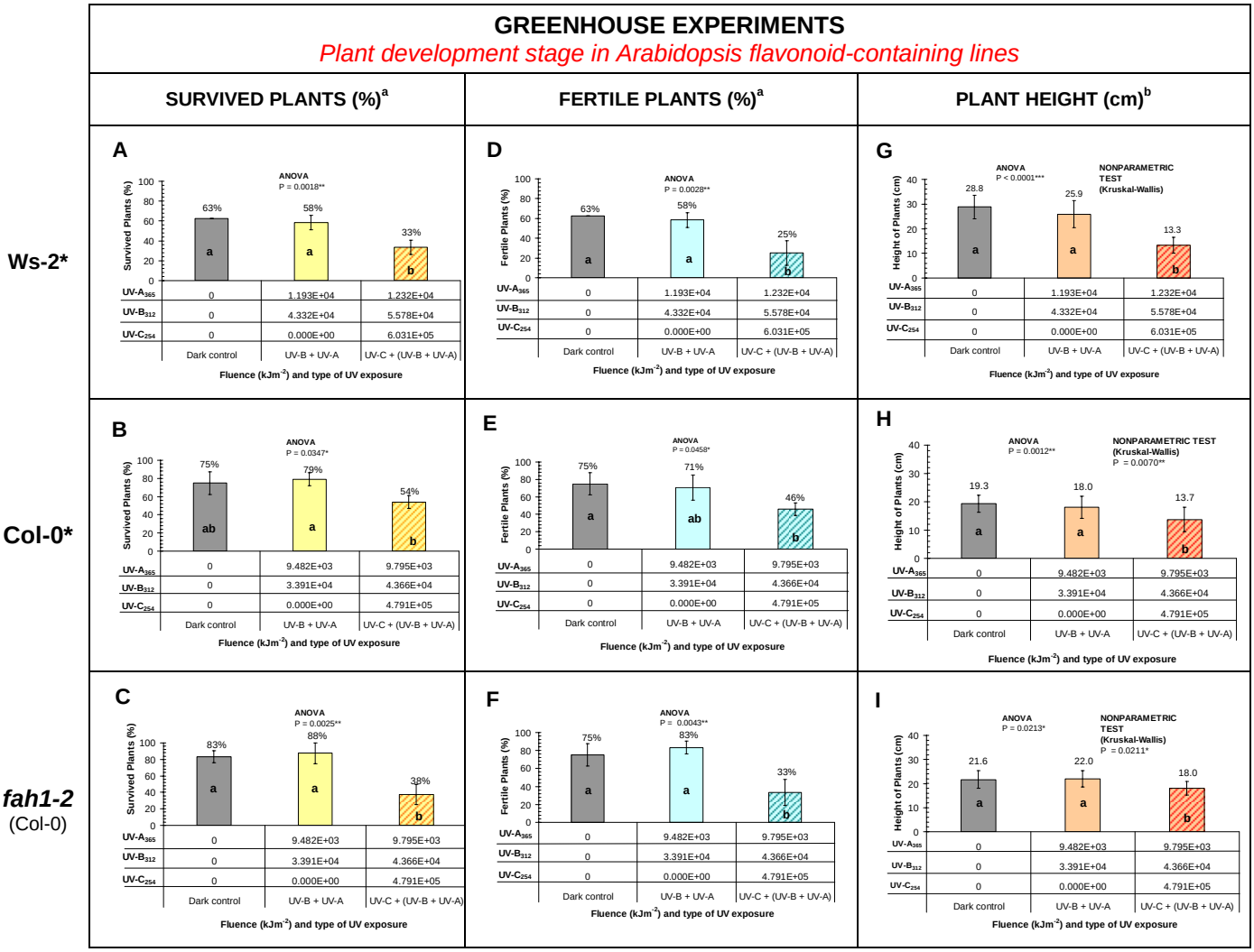

Fig. 81. The effect of incident UV-C + (UV-B + UV-A) light emitted from the UV-C_{254} source or its minor UV-B + UV-A portion on the growth of flavonoid-containing *Arabidopsis* plants developed from seeds irradiated for 60 days. Seeds were germinated in soil and plants were grown in the greenhouse for 45 days (48 DAI), when the percentage of survived plants and the percentage of fertile plants were scored, together with the height of plants that reached the principal growth stage 8.0. The UV fluences (kJm^{-2}) and type of UV exposure are indicated under each bar. Values are the mean ± standard deviation of three parallel experiments, where n = 8 for the percentages of survived and fertile plants. Bars with different letters denote a significant difference at $\alpha < 0.05$, according to ANOVA and the Tukey-Kramer multiple comparisons post-hoc test, as well as the nonparametric Kruskal-Wallis test. The precise values of statistical tests are indicated above the bars, where * means a significant level ($P < 0.05$), ** very significant ($P < 0.01$) and *** extremely significant ($P < 0.001$) level of difference. DAI = days after imbibition.

The plant genotypes were: Wassilewskija (Ws-2), A, D, G; Columbia (Col-0), B, E, H; a sinapate ester-deficient mutant (*fah1-2*), C, F, I. Wild ecotypes are marked with asterisks and background ecotypes are noted in the parentheses under the mutant line.

[a] The percentages of survived and fertile plants were scored out of the total number seeds sown in soil.

[b] The height was measured in mature *Arabidopsis* plants that reached the principal growth stage 8.0. The height of a plant is here defined as the perpendicular distance from the soil surface at the plant base to the highest point of the stem, measured in its natural position (Heady, 1957).

Sixty days of exposure of flavonoid-containing Ws-2, Col-0 and *fah1-2* seeds to UV-C + (UV-B + UV-A) radiation had also a strong impact on height of the plants that reached the principal growth stage 8.0. Compared to the dark controls, ANOVA and the Tukey-Kramer post-hoc test indicated an extremely significant ($p < 0.001$), a very significant ($p < 0.01$) and a significant ($p < 0.05$) differences in the plant height for Ws-2, Col-0 and *fah1-2* irradiated samples, respectively (**Fig. 81G**, **H** and **I**). Although the plant height data passed the Bartlett's test (test for standard deviation equality) and the Kolmogorov-Smirnov test (normality test), justifying the use of the parametric tests, the nonparametric Kruskal-Wallis test was also performed, giving similar result for statistical differences in plant height between irradiated and dark control samples.

16.4.2. Development of tt4-8 Arabidopsis plants after short-term UV-C_{254} exposure of flavonoid-lacking seeds

Short-term UV-B + UV-A and UV-C + (UV-B + UV-A) exposure of flavonoid-lacking mutant *tt4-8* seeds had a strong effect on subsequent growth and development of plants (**Fig. 82**). Due to a large sample size, the study of the plant growth for some *tt4-8* samples was omitted in soil-based experiments, including the samples exposed to UV-B + UV-A radiation from 0.5 up to 5 hours, which showed no difference in germination and early-seedling development, compared to the dark control (see sections **16.2.2.1** and **16.3.1.2**). In addition, *tt4-8* samples that were exposed to UV-C + (UV-B + UV-A) radiation for 0.5 hour and 2 hours were not analyzed in soil-based experiments.

Dark control *tt4-8* seeds that were sown and germinated in the soil developed a total of 78% plants (survived plants) (**Fig. 82A** and **D**). Out of the total number of sown *tt4-8* dark control seeds, 73% plants finally reached the principal growth stage 8.0 (fertile plants) (**Fig. 82B** and **E**).

Unlike flavonoid-containing *Arabidopsis* samples, *tt4-8* mutant seeds exhibited higher sensitivity to the UV-B + UV-A portion of emitted light. A decrease in the percentage of survived plants, the percentage of fertile plants (seed producers) and height of plants that reached the 8.0 growth stage, was detected in UV-B + UV-A irradiated *tt4-8* samples (**Fig. 82A, B** and **C**).

Using untransformed data, ANOVA indicated a significant difference in the percentage of survived plants ($p = 0.0117$) (**Fig. 82A**), as well as in the percentage of fertile plants ($p = 0.0391$) (**Fig. 82B**), when UV-B + UV-A exposed samples were compared to the dark control. A statistically significant decrease in both measured parameters was observed only after 139 hours of irradiation (UV-B = 4.2×10^3 kJm^{-2} and UV-A = 1.2×10^3 kJm^{-2}). These parameters remained unchanged in the samples irradiated up to 48 hours. Similar statistical results for the percentages of survived and fertile plants were obtained using ANOVA with $\arcsin\sqrt{\%}$ transformed and log (x+1) transformed data.

In addition, UV-B + UV-A light had an extremely significant effect ($p < 0.0001$) on the height of survived *tt4-8* plants, where exposure of seeds for 48 hours (UV-B = 1.5×10^3 kJm^{-2} and UV-A = 4.1×10^2 kJm^{-2}) resulted in a statistically significant decrease in the height of plants developed from irradiated seeds (**Fig. 82C**). The height of plants that were developed from *tt4-8* seeds exposed for 139 hours, differed extremely ($p < 0.0001$), compared to dark control plants, but remained statistically unchanged ($p > 0.05$), compared to the sample irradiated for 48 hours.

The exposure of *tt4-8* seeds to entirely transmitted UV-C + (UV-B + UV-A) light had a dramatic effect on subsequent plant development and growth (**Fig. 82D, E** and **F**). Seeds that were exposed to UV-C + (UV-B + UV-A) light from 5 up to 139 hours, produced no plants under greenhouse conditions (**Fig. 82D**). Both statistical tests, ANOVA and the nonparametric Kruskal-Wallis test, showed that lower fluences of UV-C + (UV-B + UV-A) radiation (up to 3 hours of exposure), caused an extremely significant ($p < 0.0001$) decrease in the percentage of survived plants (**Fig. 82D**), the percentage of fertile plants (seed producers) (**Fig. 82E**) and the height of mature plants (**Fig. 82F**). Since low fluences of the UV-B + UV-A portion of emitted light did not have an effect on the growth of *tt4-8* plants developed from irradiated seeds, the effect of low fluences of UV-C + (UV-B + UV-A) light was attributed to the dominant UV-C component of the incident light. Already 1 hour of UV exposure (UV-C = 5.3×10^2 kJm^{-2}) of *tt4-8* seeds induced an extremely significant ($p < 0.0001$) decrease in values of all three studied parameters of plant growth. After 3 hours of exposure (UV-C = 1.7×10^3 kJm^{-2}), 33% of soil-germinated *tt4-8* seeds grew into the plants that reached different developmental stages (survived plants) (**Fig. 82D**), and only 17% of seeds produced the plants that reached the principal growth stage 8.0 (fertile plants) (**Fig. 82E**).

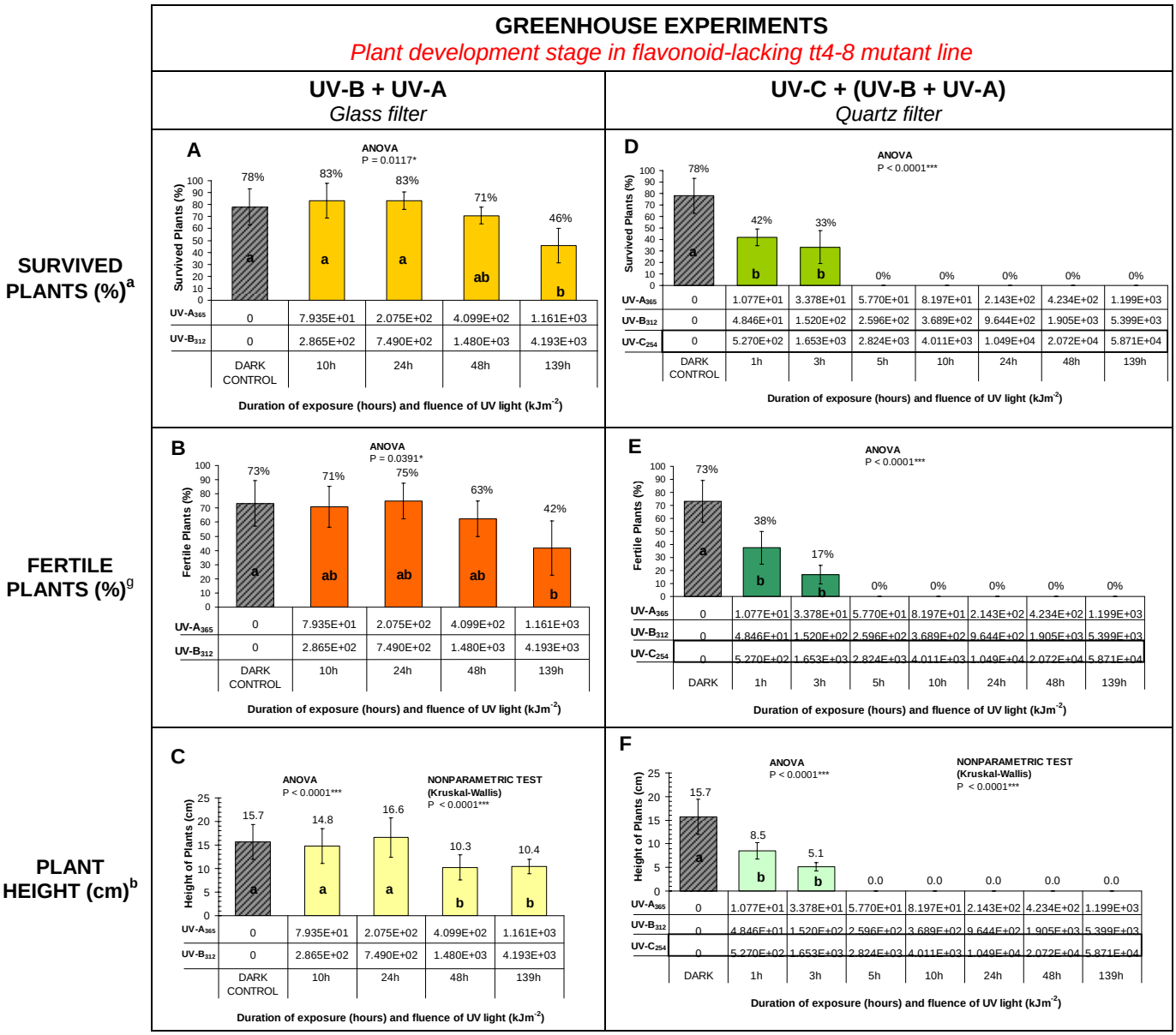

Fig. 82. The effect of short-term exposure to incident UV-C + (UV-B + UV-A) light emitted from the UV-C_{254} source or its minor UV-B + UV-A portion on growth of *Arabidopsis* flavonoid-lacking *tt4-8* plants developed from irradiated seeds. Seeds were germinated in the soil and plants were grown in the greenhouse for 45 days (48 DAI), when the percentage of survived plants and the percentage of fertile plants were scored, together with the height of plants that reached the principal growth stage 8.0. The duration of UV exposure (hours) and UV fluences (kJm^{-2}) are indicated under each bar. Values are the mean ± standard deviation of three parallel experiments (n = 8). Bars with different letters denote a significant difference at $\alpha < 0.05$, according to ANOVA and the Tukey-Kramer multiple comparisons post-hoc test, as well as the nonparametric Kruskal-Wallis test. The precise values of statistical tests are indicated above the bars, where * means a significant level ($P < 0.05$), ** very significant ($P < 0.01$) and *** extremely significant ($P < 0.001$) level of difference. DAI = days after imbibition.

[a] The percentages of survived and fertile plants were scored out of the total number seeds sown in soil.
[b] The height was measured in mature plants that reached the principal growth stage 8.0.

16.5. Survival rates of *Arabidopsis* plants developed from seeds exposed to quasi-monochromatic UV-C_{254} light

Observing two plant developmental stages, the seed germination stage (principal growth stage 0.5; see section **16.2**) and the plant development stage (principal growth stage 8.0; see section **16.4**), survival rates for *Arabidopsis* plants that were grown from seeds exposed to quasi-monochromatic UV-C_{254} source of light, were determined using the same equation as for the surviving fraction S(UV) of *Bacillus* spores exposed to UV radiation (Horneck, 1993). The **Equation 5** (see section **15**) was adapted for the plant survival parameter, where N stands for the maximal percentage of germinated seeds (seed germination stage) or the percentage of survived plants (plant development stage) that developed from irradiated *Arabidopsis* seeds, and N_0 stands for the maximal percentage of germinated seeds (seed germination stage) or the percentage of survived plants (plant development stage), grown from UV unexposed seeds (dark control samples). The average survival rates were obtained from three parallel experiments, where the maximal percentage of germinated seeds was determined from n = 50 sample size, and the percentage of survived plants from n = 8 sample size.

Table 18 shows the survival rates of *Arabidopsis* plants grown from UV irradiated seeds, where surviving fractions were determined at the stage of seed germination (*in vitro* experiments) and at the stage of developed mature plants (soil-based experiments in the greenhouse). Since the quasi-monochromatic UV_{254} source also emitted a small portion of UV-B + UV-A light, the survival rates of samples that were covered with the *Quartz* filter, and thus exposed to entirely transmitted UV-C + (UV-B + UV-A) light, were determined in parallel with the survival rates of samples that were exposed only to a background UV-B + UV-A part of light (samples covered with *Glass* filter). Survival fractions were calculated for Ws-2, *dyx*, Col-0 and *fah1-2* samples, which were exposed to the maximal UV fluences after 60 days of irradiation, as well as for *tt4-8* line that was exposed to short-term UV radiation up to 139 hours. In order to compare the survival rates of *Arabidopsis* plants to that calculated for *Bacillus subtilis* spores, which were irradiated with 5 to 6 orders of magnitude lower UV doses than *Arabidopsis* seeds, all values for UV fluence are here expressed in units of Jm^{-2}.

The results from germination tests (*in vitro* experiments) indicated that the survival rates of seeds exposed to the UV-B + UV-A portion of emitted light reached about 100% in all tested *Arabidopsis* lines. Soil-based experiments in greenhouse showed that the UV-B + UV-A portion did not affect the survival of Col-0 and *fah1-2* plants, but slightly higher UV fluences resulted in slightly decreased the survival rate of Ws-2 plants to 92%. Ten times lower fluences of UV-B +

UV-A radiation (UV-B = 4.2 x 10^6 Jm^{-2} and UV-A = 1.2 x 10^6 Jm^{-2}) had a strong effect on development of *tt4-8* plants under greenhouse conditions, lowering the survival rate to 65%.

The entirely transmitted UV-C + (UV-B + UV-A) light, with the fluence of UV-C from 4.8 x 10^8 Jm^{-2} to 6.0 x 10^8 Jm^{-2}, did not affect the survival of the flavonoid-containing Ws-2, *dyx*, Col-0 and *fah1-2 Arabidopsis* seeds at the germination stage(*in vitro* experiments), where the maximal percentages of survival reached about 100%. However, germination tests showed a strong impact of UV-C + (UV-B + UV-A) light on the survival rate of flavonoid-lacking *tt4-8* seeds (13%), although they were irradiated with ten times lower UV doses (UV-C = 5.9 x 10^7 Jm^{-2}). In addition, soil-based experiments showed a strong effect of UV-C + (UV-B + UV-A) radiation on the survival rate of mature plants developed from irradiated seeds, where a decrease in survival percentage was observed in Col-0 (72%), Ws-2 (53%) and *fah1-2* (45%) lines. The UV-C + (UV-B + UV-A) radiation had a dramatic effect on the survival of *tt4-8* plants, where no plant survivors (0%) were observed in soil-based experiments.

Table 18. The effect of incident UV-C + (UV-B + UV-A) light emitted from the UV-C_{254} source and its UV-B + UV-A portion on survival of *Arabidopsis* plants developed from irradiated seeds. The survival rate is measured at two plant developmental stages: the seed germination stage ($G_{max\%}$) and the plant growth stage (survived plants %). The Ws-2, *dyx*, Col-0 and *fah1-2* seed lines were irradiated up to 60 days, while *tt4-8* seeds up to 139 hours. The maximal UV fluences (Jm^{-2}) are indicated in the table. The survival rate of *Bacillus subtilis* dry spores exposed for up 300 sec to UV-B + UV-A and UV-C + (UV-B + UV-A) is presented for comparison.
The plant genotypes were: Wassilewskija (Ws-2), a control mutant with a T-DNA insertion carrying the *nptII* gene (*dyx*), Columbia (Col-0), a flavonoid-deficient mutant *(tt4-8*) with a T-DNA insertion carrying the *nptII* gene, a sinapate ester-deficient mutant (*fah1-2*). Wild ecotypes are marked with asterisks and background ecotypes are noted in the parenthesis under each mutant line.

	UV-B + UV-A *Glass filter*				**UV-C + (UV-B + UV-A)** *Quartz filter*		
SAMPLES	**FLUENCE (Jm^{-2})**		**SURVIVAL RATE (%)[a] Seed germination stage**	**SURVIVAL RATE (%)[b] Plant development stage**	**FLUENCE (Jm^{-2})**	**SURVIVAL RATE (%)[a] Seed germination stage**	**SURVIVAL RATE (%)[b] Plant development stage**
	$UV\text{-}B_{312}$	**$UV\text{-}A_{356}$**			**$UV\text{-}C_{254}$**		
Ws-2*	4.3 x 10^7	1.2 x 10^7	98	92	6.0 x 10^8	97	53
dyx (Ws-2)	4.3 x 10^7	1.2 x 10^7	100	nd	6.0 x 10^8	100	nd
Col-0*	3.4 x 10^7	9.5 x 10^6	100	100	4.8 x 10^8	99	72
fah1-2 (Col-0)	3.4 x 10^7	9.5 x 10^6	100	100	4.8 x 10^8	100	45
tt4-8 (Ws-2)	4.2 x 10^6	1.2 x 10^6	100	65	5.9 x 10^7	13	0
Bacillus subtilis	32.9	11.4	98		5.3 x 10^2	0.5	

[a] Survival rate ($S = N/N_0$) determined in the germination tests (*in vitro* experiments) from the maximal percentage of germinated seeds. N stands for the percentage of germinated seeds in irradiated sample, while N_0 stands for the percentage of germinated seeds in the dark control

[b] Survival rate of plants determined from $S = N/N_0$, where N represents the percentage of survived plants in UV exposed samples, while N_0 represents the percentage of survived plants in the dark control. The percentages of survived plants were scored out of the total number of seeds sown in soil (greenhouse experiments).
nd = not determined

17. RESISTANCE OF *Arabidopsis thaliana* SEEDS TO POLYCHROMATIC UV RADIATION UNDER SIMULATED SPACE VACUUM AND SIMULATED MARS CO_2 ATMOSPHERE*

17.1. General summary of results on the resistance of *Arabidopsis* seeds to polychromatic UV radiation under simulated space vacuum and simulated Mars CO_2 atmosphere*

The resistance of *Arabidopsis* seeds to simulated space conditions expected at the level of the ISS, which orbits at the low Earth orbit (LEO) altitudes, approximately 400 km above Earth's surface, was tested using space simulation facilities at the German Aerospace Center (DLR), Cologne. In addition, the resistance of *Arabidopsis* seeds to simulated Mars CO_2 atmosphere* was also tested using the same simulation facilities. The exposure experiments were performed as a part of the pre-flight EXPOSE-EVT (Experiment Verification Tests) in order to optimize analytical methods and evaluation before the launch. Due to biosafety regulations at DLR, transgenic *tt4-8* seeds had to be replaced with the nontransgenic flavonoid-lacking *tt4-1*mutant, which has been prepared in the Ler-0 background. Thus, Ws-2 and Ler-0 wild ecotypes, as well as *tt4-1* mutant were used in EVT experiments, where seed samples were exposed to single or combined simulated space conditions or simulated Mars conditions, including polychromatic simulated solar UV radiation (λ = 200 - 400 nm, fluence 1.5 x 10^5 kJm^{-2}), simulated space vacuum[a](10^{-5} Pa) and simulated Mars CO_2 atmosphere* (95.6% CO_2).

Two sets of multiuser EVT experiments were performed: in the EVT-E1, the samples were exposed to polychromatic $UV_{200-400}$ light under atmospheric pressure, while in the EVT-E2, the samples were exposed to simulated space vacuum or simulated Mars CO_2 atmosphere* separately, or in the combination with polychromatic $UV_{200-400}$ light. Unfortunately, due to mishandling during shipping of the exposed seed samples from DLR, some sample carriers arrived heavily damaged, resulting in loss of the EVT-1 samples for the Ws-2 and Ler-0 lines.

* Mars atmosphere was simulated only in view of its composition (95.56% CO_2, 2.72% N_2, 1.56% Ar and 0.16% O_2), but not the pressure, since due to the overheating of the samples, all EVT-E2 experiments were performed at 1 atm (101.3 kPa) instead of 600 Pa (for details see chapter **2**, section **8.1.2.2.5**)

[a] In interplanetary space, the extremely low pressures down to 10^{-14} Pa prevail. However, within the vicinity of a planetary body, the pressure increases due to the outgassing. For instance, at the low Earth orbit (LEO) altitudes (between 200 and 600 km above Earth's surface), the pressure reaches 10^{-7} to 10^{-4} Pa. In the vicinity of a spacecraft, the pressure is further increased e. g. at the level of the ISS it reaches about 10^{-5} Pa (Horneck and Brack, 1992; Horneck et al., 2000; Baglioni et al., 2007).

Only the *tt4-1* sample from the EVT-1 experiments and all the EVT-2 samples were recovered and analyzed.

The resistance of *Arabidopsis* seeds to polychromatic simulated solar UV radiation under simulated space vacuum or simulated Mars CO_2 atmosphere* was determined by studying the germination and subsequent plant development, observing three important developmental stages: the seed germination (principal growth stage 0.5), the early-seedling stage (principal growth stage 1.0) and the mature plant development (principal growth stage 8.0), described in Boyes et al. 2001 and Kjemtrup et al. 2003. Summarized results of these studies are presented in **Table 19**. Detailed results are given in the sections below.

Table 19. General summary of the effects of simulated space and Mars conditions on different parameters at the three developmental stages of *Arabidopsis* plants grown from exposed seeds. The conditions applied separately or in the combination during the Experiment Verification Tests (EVT): simulated polychromatic solar UV radiation (λ = 200 - 400 nm) with a fluence of 1.5 x 10^5 kJm^{-2}, simulated space vacuum at 10^{-5} Pa and simulated Mars CO_2 atmosphere* at 1atm, containing 95.6% CO_2.
The plant genotypes were: Wassilewskija (Ws-2), Landberg erecta (Ler-0) and a flavonoid-deficient mutant (*tt4-1*) in Ler-0 accession. Wild ecotypes are marked with asterisks.

PLANT DEVELOPMENTAL STAGES	MEASURED PARAMETERS	Vacuum			UV + Vacuum			CO_2 Mars			UV + CO_2 Mars		
		Ws*	Ler*	*tt4-1* (*Ler*)	Ws*	Ler*	*tt4-1* (*Ler*)	Ws*	Ler*	*tt4-1* (*Ler*)	Ws*	Ler*	*tt4-1* (*Ler*)
Germination	Loss of germination capacity ($G_{max\%}$)	-	-	-	-	-	++++[a]	-	-	+++	-	++	++++[a]
	Mean germination time (MGT)	-/+[b]	+[b]	-	++	+++	n/a	-	+++	+++	++	++++	n/a
Early-seedling development	% Abnormal seedlings	-	-	-	+	++	n/a	-	-	+	++	++	n/a
	Severity of seedling damage	-	-	-	+	++	n/a	-	-	++	++	+++	n/a
	Reduction in root length	-	-	-	++	+++	n/a	-	+	+	++	+++	n/a
Plant development	Decrease in % of survived plants	-	-	-	+++	++	n/a	//	//	//	//	//	//
	Decrease in % of fertile plants	-	-	-	+++	++	n/a	//	//	//	//	//	//
	Reduction in plant height	-	-	-	-	-	n/a	//	//	//	//	//	//

[a] Extremely negative effect of the exposure to (UV + Vacuum) and (UV + CO_2 Mars) conditions that killed all tested seeds ($G_{max\%}$ = 0%).
[b] Simulated space vacuum had small, but positive effect on seed germination, increasing the speed of germination (MGT decreased).

n/a = not applicable parameter (0 % germinated seeds), // = effect not determined, - no effect, -/+ possible effect, + small effect, ++ strong effect, +++ very strong effect, ++++ extreme effect

17.2. Seed germination stage - effects of polychromatic UV radiation under simulated space vacuum and simulated Mars CO_2 atmosphere*

The resistance of *Arabidopsis* seeds to polychromatic UV radiation under simulated space vacuum and Mars CO_2 atmosphere* was first determined at the level of seed germination, which is the earliest stage in plant development. The germination was scored at the point of its termination when the radicle protruded from the seed coat (the principal growth stage 0.5, according to Boyes et al., 2001 and Kjemtrup et al., 2003), which is the only time point of germination that can be relatively precisely determined. Similar to the experiments with quasi-monochromatic UV-C_{254} light (see above section **16.2**), the following parameters of seed germination were here considered: germination capacity (section **17.2.1**) and germination dynamics, including the mean germination time (section **17.2.2**) and other parameters of germination dynamics, notably $T_{50\%}$, $T_{25\text{-}75\%}$ and the skewness of germination curve (section **17.2.3**). In addition, we also determined the viability of exposed flavonoid-lacking *tt4-1 Arabidopsis* seeds (section **17.2.4**).

After the exposure to simulated space and Mars conditions, including polychromatic $UV_{200\text{-}400}$, high vacuum and simulated Mars CO_2 atmosphere*, imbibed *Arabidopsis* Ws-2, Ler-0 and *tt4-1* seeds were germinated under optimal conditions. The percentage of germinated seeds was plotted against the time required for germination, expressed in hours after imbibition (HAI). **Fig. 83** illustrates the germination curves of the Ws-2, Ler-0 and *tt4-1* seeds after the exposure to simulated space and Mars conditions applied during the EVT-E2 experiments. The samples were irradiated with polychromatic $UV_{200\text{-}400}$ light at the total fluence of 1.5 x 10^{-5} kJm^{-2} under simulated space vacuum at 10^{-5} Pa (UV + Vacuum) or under a simulated Mars CO_2 atmosphere* at 1 atm (UV + CO_2 Mars). In order to distinguish the influence of polychromatic $UV_{200\text{-}400}$ light from the effects of simulated space vacuum and simulated Mars CO_2 atmosphere*, dark control samples were also analysed. They included the seeds that were exposed only to simulated space vacuum (Dark + Vacuum) and the seeds that were exposed only to simulated Mars CO_2 atmosphere* (Dark + CO_2 Mars). The germination curves of exposed Ws-2, Ler-0 and *tt4-1* seeds were compared to the germination curves of the laboratory controls that represent the unexposed seeds stored in the dark at 4°C during the EVT experiments.

All Ws-2 exposed seed samples, including (Dark + Vacuum), (Dark + CO_2 Mars), (UV + Vacuum) and (UV + CO_2 Mars), reached germination maximum of about 100%, similar to the Ws-2 laboratory control (**Fig. 83A**). The exposure of the Ws-2 seeds only to simulated space

vacuum or simulated Mars CO_2 atmosphere* had a small effect on germination speed, but surprisingly, these seeds germinated slightly faster than the unexposed laboratory control seeds. In contrast, the exposure of the Ws-2 seeds to polychromatic $UV_{200-400}$ light in combination with either simulated space vacuum or simulated Mars CO_2 atmosphere* had a strong effect on the germination, causing a delay in germination start and an important decrease in germination speed.

Similarly to Ws-2 line, the Ler-0 wild type seeds that were exposed to simulated space vacuum germinated faster than the laboratory control seeds, and they reached a maximal germination percentage of 100% (**Fig. 83B**). On the other hand, the Ler-0 wild type seeds appeared to be more sensitive to simulated Mars CO_2 atmosphere* than the Ws-2 ecotype, since the exposed seeds germinated much slower than the Ler-0 laboratory control. However, the Ler-0 seeds that were exposed to the simulated Mars CO_2 atmosphere* reached maximal germination percentage of about 100%. The exposure of the Ler-0 seeds to polychromatic $UV_{200-400}$ light under simulated space vacuum conditions caused a remarkable delay (for about 27 hours) in germination, although about 100% of the Ler-0 seeds germinated by the end of the experiment. Polychromatic $UV_{200-400}$ light in combination with simulated Mars CO_2 atmosphere* had a strong impact on the germination behaviour of the Ler-0 seeds, for which decrease in the maximal germination percentage, delayed start of germination and decreased germination speed were detected.

The germination behaviour of the flavonoid-lacking *tt4-1* mutant was unchanged after the exposure of seeds to simulated space vacuum. No differences in maximal germination percentage and germination speed were observed, compared to the laboratory control (**Fig. 83C**). On the other hand, exposure to simulated Mars CO_2 atmosphere* had a strong effect on the germination of *tt4-1* seeds, resulting in decreased maximal germination percentage (60% ± 8), as well as in delayed and slower germination course, compared to the unexposed laboratory control. Polychromatic $UV_{200-400}$ light had a drastic impact on *tt4-1* seeds, both under simulated space conditions and under simulated Mars CO_2 atmosphere*, causing complete inhibition of germination.

The results of the EVT-1 experiment, where *tt4-1* seeds were exposed to simulated polychromatic solar $UV_{200-400}$ radiation (1.5×10^5 kJm^{-2}) in air under atmospheric pressure, are presented in **Fig. 84**. The flavonoid-lacking *tt4-1* seeds appeared extremely sensitive to polychromatic $UV_{200-400}$ light, since no seeds germinated.

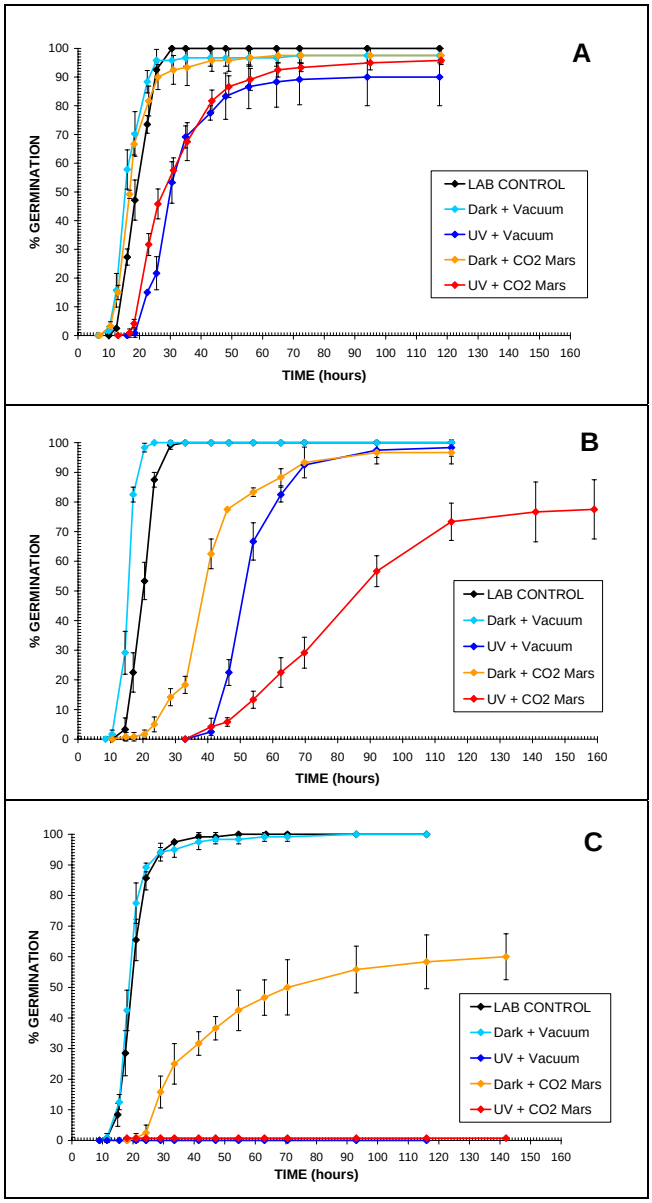

Fig. 83. Time course for *Arabidopsis* seed germination after the exposure of seeds to simulated space and Mars conditions: simulated polychromatic solar UV light (λ = 200-400 nm, fluence 1.5 x 10^5 kJm^{-2}), simulated space vacuum (10^{-5} Pa) and simulated Mars CO_2 atmosphere* at 1 atm (95.6 % CO_2).
The exposure experiments were performed as a part of the EVT-E2 (Experimental Verification Test) programme, where seed samples were exposed to simulated space vacuum in the dark (Dark + Vacuum, a light blue line), polychromatic UV radiation under simulated space vacuum (UV + Vacuum, a dark blue line), simulated Mars CO_2 atmosphere* in the dark (Dark + CO_2 Mars, an orange line), and polychromatic UV radiation under simulated Mars CO_2 atmosphere* (UV + Mars CO_2, a red line). The laboratory controls (black lines) represent the unexposed seeds stored in the dark at 4°C during the EVT experiments.
Germination time is expressed in hours after imbibition (HAI), performed in the dark at 4°C for 72 hours.
The plant genotypes: (A) Wassilewskija (Ws-2), (B) Landsberg erecta (Ler-0) and (C) a flavonoid-lacking mutant in Ler-0 accession (*tt4-1*). Wild ecotypes are marked with asterisks.

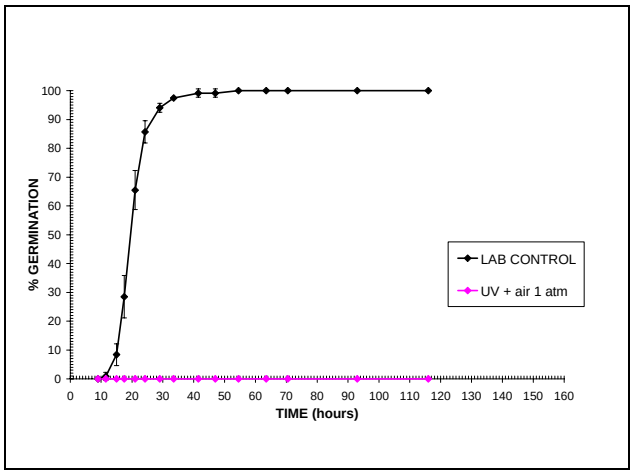

Fig. 84. Time course of seed germination for the *Arabidopsis* flavonoid-lacking, *tt4-1*, mutant after the exposure of seeds to polychromatic simulated solar UV light (λ = 200-400 nm, fluence 1.5 x 10^5 kJm^{-2}). The UV exposure experiment was performed as a part of the EVT-E1 (Experimental Verification Test) programme, where seeds were exposed to UV radiation in air under atmospheric pressure (UV + air 1 atm, a magenta line). The laboratory control (black line) represents the unexposed seeds stored in the dark at 4°C during the EVT experiments. Germination time is expressed in hours after imbibition (HAI), performed in the dark at 4°C for 72 hours.

*17.2.1. Germination capacity ($G_{max\%}$) of seeds exposed to polychromatic UV light under simulated space vacuum and simulated Mars CO_2 atmosphere**

The germination capacity of the Ws-2, Ler-0 and *tt4-1* seeds was expressed as the maximal germination percentage ($G_{max\%}$), reached at the end of the germination process. The mean values of $G_{max\%}$ were obtained from three parallel experiments, observing n = 40 seeds. The $G_{max\%}$ values for the Ws-2, Ler-0 and *tt4-1* samples, which were exposed to polychromatic $UV_{200-400}$ light, simulated space vacuum and simulated Mars CO_2 atmosphere*, were compared to $G_{max\%}$ values for unexposed laboratory control samples that reached 100% in all three tested genotypes (**Fig. 85**). The $G_{max\%}$ data were analyzed statistically using one-way ANOVA and the Tukey-Kramer multiple comparisons test at $\alpha = 0.05$. Since similar statistical results were obtained using untransformed and $\arcsin\sqrt{\%}$ transformed $G_{max\%}$ data, only the results from untransformed percentage data are presented here.

Seeds exposed only to simulated space vacuum (Dark +Vacuum) reached a maximal germination percentage of 98% in the Ws-2 line and 100% in the Ler-0 wild type line, as well as the *tt4-1* mutant line (**Fig. 85A, B** and **C**). Combined exposure to polychromatic $UV_{200-400}$ light and simulated space vacuum (UV + Vacuum) resulted in $G_{max\%}$ values of 92% and 98% in the Ws-2 and Ler-0 samples, respectively (**Fig. 85A** and **B**). ANOVA showed no statistical differences in germination capacity among (Dark + Vacuum), (UV + Vacuum) and unexposed laboratory control for the Ws-2 and Ler-0 wild type lines. Additional t-test showed no statistical differences between (Dark + Vacuum) and (UV + Vacuum) exposed samples in both the Ler-0 ($p = 0.3739$) and Ws-2 ($p = 0.3305$) wild type line. Furthermore, no statistical difference was observed between the *tt4-1* sample exposed to (Dark + Vacuum) and the laboratory control, since both samples reached $G_{max\%}$ of 100% (**Fig. 85C**). In contrast, polychromatic $UV_{200-400}$ light in combination with simulated space vacuum had a drastic effect on the flavonoid-lacking *tt4-1* line, since no germinated seeds ($G_{max\%} = 0\%$) were observed in the samples exposed to (UV + Vacuum).

After exposure to simulated Mars CO_2 atmosphere* (Dark + CO_2 Mars atm), the Ws-2, Ler-0 and *tt4-1* seeds germinated with $G_{max\%}$ values of 98%, 97% and 60%, respectively (**Fig. 85D, E** and **F**). Seeds that were exposed to the combined effects of polychromatic $UV_{200-400}$ light and simulated Mars CO_2 atmosphere* (UV + CO_2 Mars atm) reached $G_{max\%}$ values of 97% in the case of the Ws-2 line and 80% in the case of the Ler-0 line (**Fig. 85D** and **E**). Statistical tests

showed no significant difference in germination capacity within the group of (Dark + CO_2 Mars atm), (UV + CO_2 Mars atm) and laboratory control for the Ws-2 line.

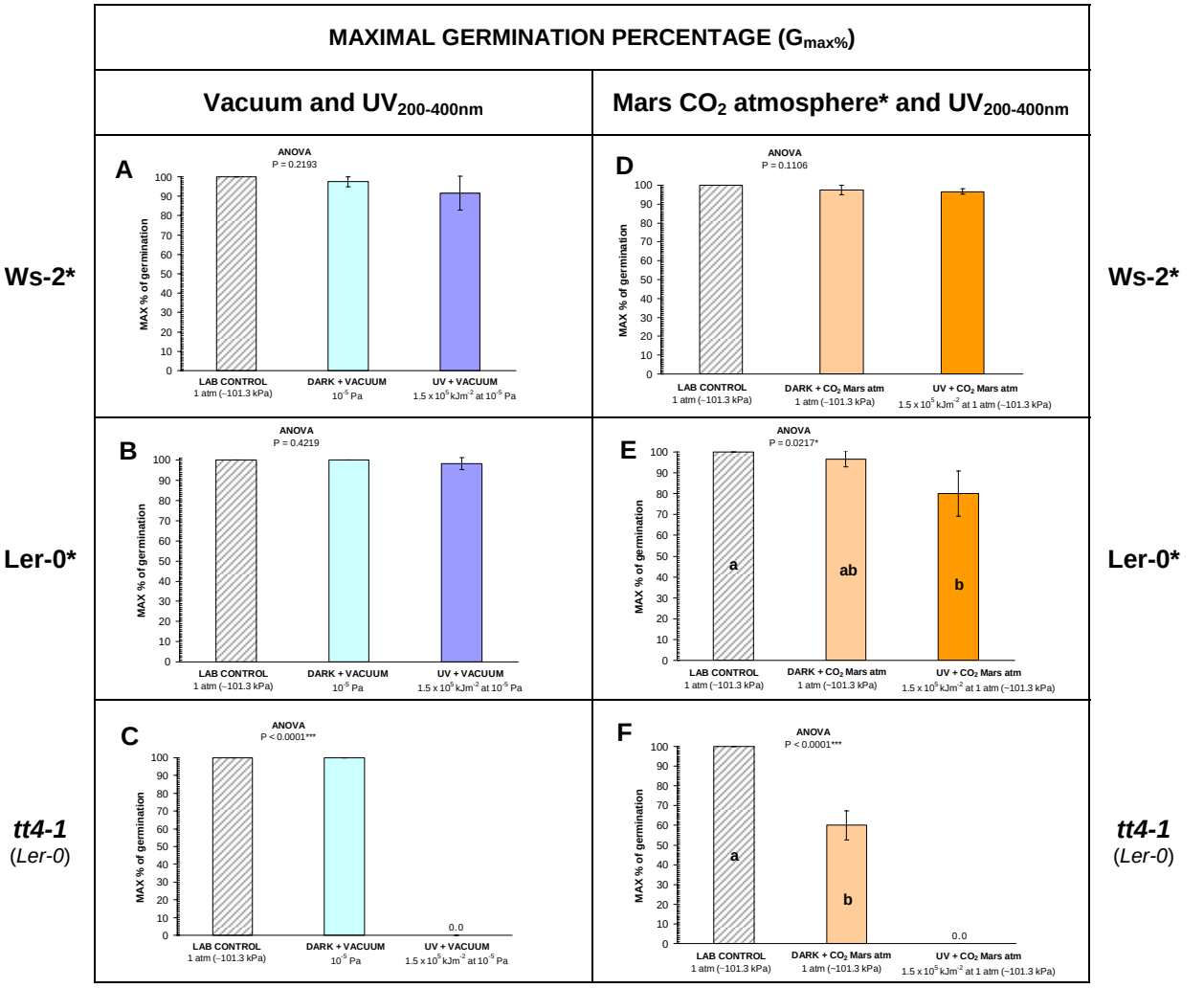

Fig. 85. Maximal germination percentage ($G_{max\%}$) of *Arabidopsis* seeds exposed to simulated space and Mars conditions, including polychromatic solar UV light (λ = 200-400 nm, fluence 1.5 x 10^5 kJm^{-2}), simulated space vacuum (10^{-5} Pa) and simulated Mars CO_2 atmosphere* at 1 atm (95.6 % CO_2). The $G_{max\%}$ values of samples exposed to simulated space conditions were compared to those obtained for the laboratory controls (unexposed seeds that were stored in the dark at 4°C during the EVT experiments). Values are the mean ± standard deviation from three parallel experiments (n = 40). Bars with different letters denote a significant difference at $\alpha < 0.05$, according to ANOVA and the Tukey-Kramer test. The precise values from ANOVA are indicated above the bars, where * means a significant level ($P < 0.05$), ** very significant ($P < 0.01$) and *** extremely significant ($P < 0.001$) level of difference.
The plant genotypes were: Wassilewskija (Ws-2), A and D; Landsberg erecta (Ler-0), B and E; a flavonoid-lacking mutant in Ler-0 accession (*tt4-1*), C and F. Wild ecotypes are marked with asterisks.

In contrast, a significant difference ($p = 0.0217$) was detected for the Ler-0 line, due to decreased $G_{max\%}$ value in sample exposed to (UV + CO_2 Mars atm), while (Dark + CO_2 Mars atm) sample showed statistically unaltered germination capacity. On the other hand, an extremely significant decrease ($p < 0.001$) in germination capacity was observed for flavonoid-lacking *tt4-1* seeds that were exposed to (Dark + CO_2 Mars atm) and no germinated seeds ($G_{max\%} = 0\%$) were observed after the exposure of *tt4-1* samples to (UV + CO_2 Mars atm) (**Fig. 85F**).

The cross-comparison of the effects of simulated space vacuum (Dark + Vacuum) and simulated Mars CO_2 atmosphere* (Dark + CO_2 Mars atm) revealed no statistical difference in $G_{max\%}$ for both Ws-2 (**Fig. 85A** and **D**) and Ler-0 (**Fig. 85B** and **E**) wild type lines. In contrast, an extremely significant decrease ($p < 0.001$) in $G_{max\%}$ was observed for *tt4-1* seeds exposed to (Dark + CO_2 Mars atm), when compared to that exposed to (Dark + Vacuum) (**Fig. 85C** and **F**).

When the combined effects of (UV + Vacuum) were cross-compared to the combined effects of (UV + CO_2 Mars atm), no statistical difference in $G_{max\%}$ was observed for Ws-2 wild type line (**Fig. 85A** and **D**), but significant decrease ($p < 0.05$) in $G_{max\%}$ was detected in Ler-0 sample exposed to (UV + CO_2 Mars atm) (**Fig. 85B** and **E**).

*17.2.2. Mean germination time (MGT) of seeds exposed to polychromatic UV light and simulated space vacuum and simulated Mars CO_2 atmosphere**

In addition to germination capacity (section **17.2.1**), we also studied the dynamics of germination in *Arabidopsis* seeds that were exposed to simulated space and Mars conditions. Mean germination time (MGT), as one of the parameters of germination dynamics, represents an inverse expression of overall germination speed, and thus it indicates seed vigour.

The effects of polychromatic $UV_{200-400}$ light, simulated space vacuum and simulated Mars CO_2 atmosphere* on the MGT of exposed Ws-2, Ler-0 and *tt4-1* seeds are presented in **Fig. 86**. The MGT values of exposed samples are compared to the MGT values of unexposed laboratory control samples. Mean germination time (MGT) was calculated according to **Equation 1** (see chapter **1**, section **4.2.2.1**). Mean values for MGT were obtained from three parallel experiments, observing n = 40 seeds. One-way ANOVA and the Tukey-Kramer post-hoc test ($\alpha = 0.05$) were performed on square-root transformed MGT values due to a slightly positively skewed germination time course (see **Table 20** in section **17.2.3**).

The exposure of seeds to simulated space vacuum (Dark + Vacuum) resulted in faster seed germination in Ws-2 and Ler-0 wild type lines, compared to the laboratory control samples (**Fig. 86A** and **B**). One-way ANOVA and the Tukey-Kramer post-hoc test showed an extremely significant decrease ($p < 0.0001$) in the MGT value for the Ler-0 sample exposed to (Dark + Vacuum). The same result was obtained using an unpaired t-test. In the case of the Ws-2 line, the Tukey-Kramer post-hoc test appeared to be less sensitive to the differences between the sample exposed to (Dark + Vacuum) and the laboratory control, but the unpaired t-test, as well as alternative Student-Newman-Keuls post-hoc test, clearly showed significant decrease ($p < 0.05$) in MGT value for Ws-2 sample exposed to (Dark + Vacuum). Unlike in the Ws-2 and Ler-0 lines, the MGT of *tt4-1* seeds did not change after the exposure of seeds to simulated space vacuum (**Fig. 86C**). The unpaired t-test showed no significant difference in the MGT values between *tt4-1* (Dark + Vacuum) sample and the laboratory control.

Exposure to polychromatic $UV_{200-400}$ light in the combination with simulated space vacuum (UV + Vacuum) had a strong impact on the MGT of exposed seeds, resulting in an extremely significant increase ($p < 0.0001$) in MGT values for Ws-2 and Ler-0 wild type seeds (**Fig. 86A** and **B**) and inhibition of germination in the case of flavonoid-lacking *tt4-1* mutant (**Fig. 86C**).

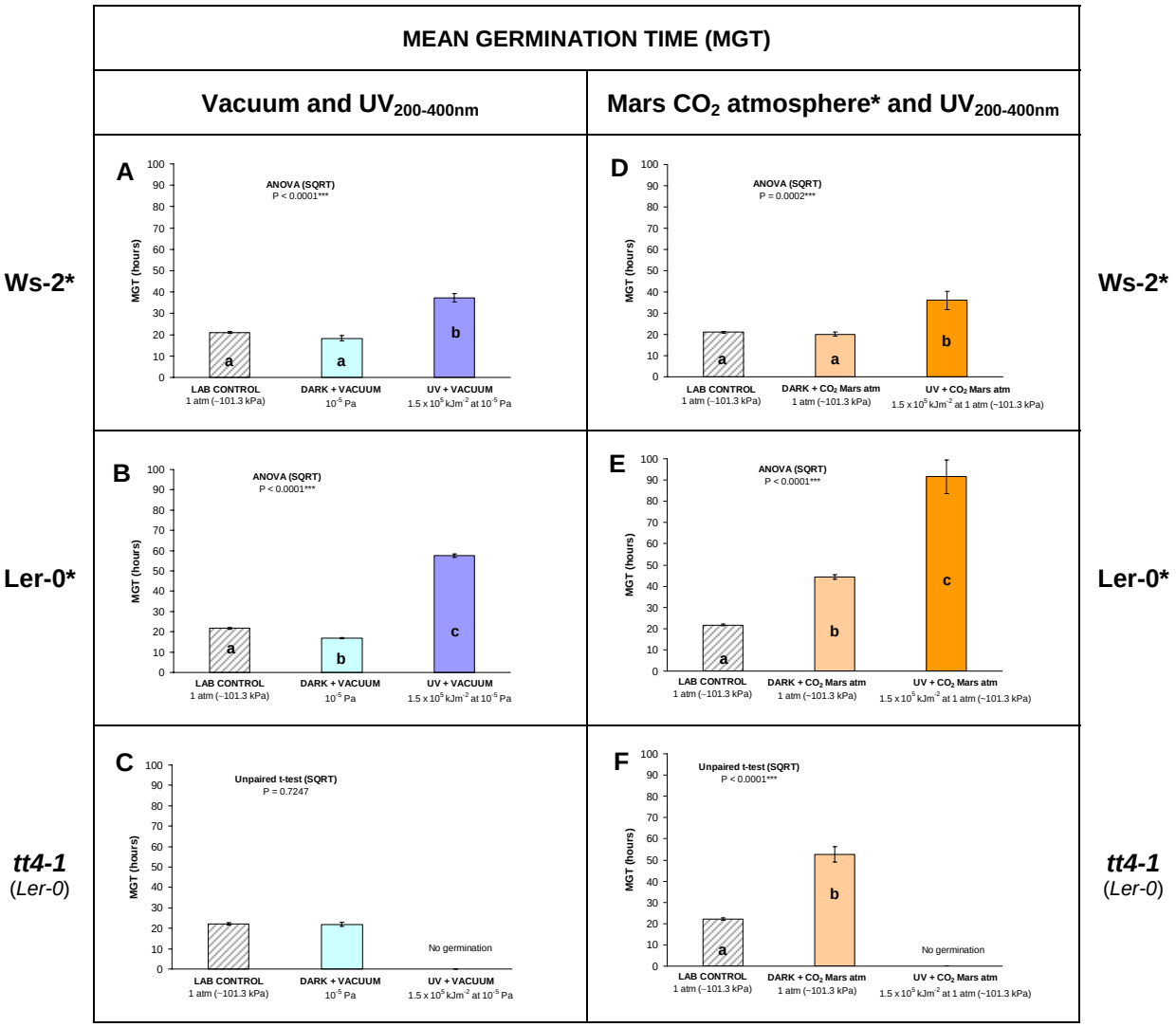

Fig. 86. Mean germination time (MGT) of *Arabidopsis* seeds exposed to simulated space and simulated Mars conditions, including simulated polychromatic solar UV light (λ = 200-400 nm, fluence 1.5 x 10^5 kJm^{-2}), simulated space vacuum (10^{-5} Pa) and simulated Mars CO_2 atmosphere* at 1 atm (95.6 % CO_2). The MGT values of samples exposed to simulated space conditions are compared to those obtained for laboratory controls (unexposed seeds that were stored in the dark at 4°C during the EVT experiments). Values are the mean ± standard deviation of three parallel experiments (n = 40). Bars with different letters denote a significant difference at $\alpha < 0.05$, according to ANOVA and the Tukey-Kramer test, as well as the unpaired t-test in the case of *the tt4-1* samples, calculated for square-root transformed data. The precise values from ANOVA and the unpaired t-test are indicated above the bars, where * means a significant level ($P < 0.05$), ** very significant ($P < 0.01$) and *** extremely significant ($P < 0.001$) level of difference.
The plant genotypes were: Wassilewskija (Ws-2), A and D, Landsberg erecta (Ler-0), B and E; a flavonoid-lacking mutant in Ler-0 accession (*tt4-1*), C and F. Wild ecotypes are marked with asterisks.

The exposure of seeds to simulated Mars CO_2 atmosphere* (Dark + CO_2 Mars atm) had no effect on the MGT of the Ws-2 seeds **(Fig. 86D**), but it had a strong effect on the germination behaviour of Ler-0 and *tt4-1* seeds (**Fig. 86E** and **F**). Compared to the MGT values of laboratory controls, ANOVA and the Tukey-Kramer test showed an extremely significant increase ($p < 0.0001$) in MGT values for both the Ler-0 wild type line and the flavonoid-lacking *tt4-1* mutant.

The mean germination time of seeds that were exposed to polychromatic $UV_{200-400}$ light in combination with simulated Mars CO_2 atmosphere* (UV + CO_2 Mars atm) increased even more than in the case of seeds exposed only to simulated Mars CO_2 atmosphere*. Due to the combined effects of $UV_{200-400}$ radiation and increased level of CO_2, Tukey-Kramer post-hoc test indicated an extremely significant increase ($p < 0.0001$) in MGT values for both Ws-2 and Ler-0 wild type lines, compared to the samples exposed to (Dark + CO_2 Mars atm) and unexposed laboratory controls (**Fig. 86D** and **E**). The exposure of flavonoid-lacking *tt4-1* seeds to polychromatic $UV_{200-400}$ light under simulated Mars CO_2 atmosphere* had a dramatic effect on germination, since no germinated *tt4-1* seeds were observed after the exposure to (UV + CO_2 Mars atm) (**Fig. 86F**).

Cross-compared the effects of simulated space vacuum (Dark + Vacuum) and simulated Mars CO_2 atmosphere* (Dark + CO_2 Mars atm) on MGT, revealed no statistical difference in the Ws-2 wild type line (**Fig. 86A** and **D**), while an extremely significant difference ($p < 0.001$) was observed in the case of the Ler-0 wild type line (**Fig. 86B** and **E**) and the *tt4-1* mutant line (**Fig. 86C** and **F**).

Similarly, when the combined effects of (UV + Vacuum) were cross-compared to the combined effects of (UV + CO_2 Mars atm), no statistical difference was observed in MGT for the Ws-2 wild type line (**Fig. 86A** and **D**), while an extremely significant difference ($p < 0.001$) was observed in the case of the Ler-0 wild type line (**Fig. 86B** and **E**).

*17.2.3. Other parameters of germination dynamics in seeds exposed to polychromatic UV under simulated space vacuum and simulated Mars CO_2 atmosphere**

In addition to the mean germination time (section **17.2.2**), other parameters of germination dynamics, such as $T_{50\%}$, $T_{25\text{-}75\%}$ and the skewness of the germination curves, were determined for *Arabidopsis* seeds exposed to simulated space and simulated Mars conditions. The precise values for these parameters, as well as the statistical distribution of significant differences ($\alpha = 0.05$) according to one-way ANOVA and the Tukey-Kramer post-hoc tests for the Ws-2, Ler-0 and *tt4-1* seed samples, exposed to polychromatic $UV_{200\text{-}400}$, simulated space vacuum and simulated Mars CO_2 atmosphere*, are presented in **Table 20**.

The value $T_{50\%}$ represents a central tendency of the germination process and it corresponds to the time necessary to reach 50% of the germination maximum. Compared to $T_{50\%}$ values of unexposed samples (laboratory controls), ANOVA showed an extremely significant ($p < 0.0001$) decrease in $T_{50\%}$ values for Ws-2 and Ler-0 seed samples that were exposed to simulated space vacuum (Dark + Vacuum), as well as for the Ws-2 seeds exposed to simulated Mars CO_2 atmosphere* (Dark + CO_2 Mars atm). On the other hand, extremely significant ($p < 0.0001$) increase in $T_{50\%}$ values was observed in the Ler-0 and *tt4-1* samples exposed to simulated Mars CO_2 atmosphere* (Dark + CO_2 Mars atm), as well as in all samples exposed to polychromatic $UV_{200\text{-}400}$ light in the combination with simulated space vacuum (UV + Vacuum) or simulated Mars CO_2 atmosphere* (UV + CO_2 Mars atm). Unlike the Ler-0 wild type line and the *tt4-1* mutant line, which showed the same statistical distribution of differences in variance for MGT and $T_{50\%}$, an altered distribution of differences in variance for these two parameters was observed in the Ws-2 line.

Skewness of the germination curves was calculated from the ratio $T_{50\%}$ / MGT. Since the observed $T_{50\%}$ values for the Ws-2, Ler-0 and *tt4-1* lines appeared lower than MGT values in all cases, the calculated values for skewness <1 indicated a slightly asymmetric nature of *Arabidopsis* germination curves, as it was previously observed in experiments with quasi-monochromatic UV-C_{254} light (**Table 15** in section **16.2.1.1.3** and **Table 16** in section **16.2.2.1.5**). Compared to the laboratory control, ANOVA showed no statistically significant difference in positively skewed germination behaviour for all Ler-0 samples exposed to simulated space and simulated Mars CO_2 conditions.

Table 20. The effects of simulated space and simulated Mars conditions on parameters of germination dynamics of *Arabidopsis* seeds, including $T_{25\text{-}75\%}$, $T_{50\%}$, mean germination time (MGT) and skewness of germination curves. Seeds were exposed to simulated space vacuum (10^{-5} Pa) or simulated Mars CO_2 atmosphere* at 1 atm (95.6 % CO_2) in the dark or in combination with simulated polychromatic solar UV light (λ = 200-400 nm, fluence 1.5 x 10^5 kJm^{-2}). The values for $T_{25\text{-}75\%}$, $T_{50\%}$, MGT and germination curve skewness of samples exposed to simulated space and simulated Mars conditions are compared to those obtained for the laboratory controls (unexposed seeds that were stored in the dark at 4°C during the EVT experiments). Values are the mean ± standard deviation of three parallel experiments (n = 40). Different letters denote a significant difference at $\alpha < 0.05$, according to ANOVA and the Tukey-Kramer post-hoc test performed on square-root transformed data for $T_{25\text{-}75\%}$, $T_{50\%}$, and MGT parameters, and untransformed data for the skewness parameter.
The plant genotypes were: Wassilewskija (Ws-2), Landsberg erecta (Ler-0) and the flavonoid-lacking mutant (*tt4-1*) in the Ler-0 accession. Wild ecotypes are marked with asterisks.

GENOTYPE	EXPERIMENTAL CONDITIONS	PARAMETERS OF GERMINATION DYNAMICS			
		$T_{25\text{-}75\%}$ (hours)	**$T_{50\%}$ (hours)**	**MGT (hours)**	**SKEWNESS $T_{50\%}$ / MGT**
Ws-2*	LAB CONTROL	6.8 ***ab***	18.9 ***a***	21.0 ***a***	0.8983 ***a***
	Dark + Vacuum	5.7 ***a***	15.3 ***b***	18.3 ***a***	0.8372 ***ab***
	$UV_{200\text{-}400}$ + Vacuum	9.7 ***b***	29.4 ***c***	37.3 ***b***	0.7897 ***b***
	Dark + CO_2 Mars atm	6.3 ***ab***	16.7 ***b***	20.1 ***a***	0.8306 ***ab***
	$UV_{200\text{-}400}$ + CO_2 Mars atm	16.3 ***c***	27.3 ***c***	36.1 ***b***	0.7596 ***b***
Ler-0*	LAB CONTROL	5.1 ***ab***	20.2 ***a***	21.7 ***a***	0.9310 ***a***
	Dark + Vacuum	2.7 ***a***	15.6 ***b***	16.9 ***b***	0.9230 ***a***
	$UV_{200\text{-}400}$ + Vacuum	11.1 ***c***	51.4 ***c***	57.5 ***c***	0.8937 ***a***
	Dark + CO_2 Mars atm	9.8 ***bc***	38.5 ***d***	44.3 ***d***	0.8692 ***a***
	$UV_{200\text{-}400}$ + CO_2 Mars atm	36.2 ***d***	78.3 ***e***	91.6 ***e***	0.8589 ***a***
tt4-1 (Ler-0)	LAB CONTROL	5.2 ***a***	19.7 ***a***	22.2 ***a***	0.8872 ***a***
	Dark + Vacuum	4.2 ***a***	18.7 ***a***	21.9 ***a***	0.8529 ***a***
	$UV_{200\text{-}400}$ + Vacuum	n/a	n/a	n/a	n/a
	Dark + CO_2 Mars atm	31.1 ***b***	***b***	52.7 ***b***	0.7724 ***b***
	$UV_{200\text{-}400}$ + CO_2 Mars atm	n/a	n/a	n/a	n/a

n/a = not applicable parameter (0% germinated seeds)

In contrast, a statistically significant ($p < 0.05$) positive shift in skewness of the germination curve was detected in the Ws-2 seeds exposed to (UV + Vacuum) and (UV + CO_2 Mars atm). Thus the first half of the germination time course in the Ws-2 samples exposed to $UV_{200-400}$ light was longer than in the control sample. Unlike the Ler-0 background genotype, the flavonoid-lacking *tt4-1* mutant showed a statistically significant ($p < 0.05$) positive shift in germination skewness for the sample that was exposed to (Dark + CO_2 Mars atm). This effect was not observed in the *tt4-1* samples exposed to (Dark + Vacuum).

The $T_{25-75\%}$ parameter is the measure of germination uniformity. It corresponds to a time period between 25% and 75% of maximum germination, and thus it is related to the steepness of germination curve around the median. The statistical distribution of differences in variance for $T_{25-75\%}$ parameter in the *tt4-1* line is equal to those for MGT and $T_{50\%}$ parameters, while an altered statistical distribution of differences in variance for $T_{25-75\%}$ parameter was detected in the Ws-2 and Ler-0 wild type lines. The Tukey-Kramer post-hoc test indicated that simulated space vacuum (Dark + Vacuum) or simulated Mars CO_2 atmosphere* (Dark + CO_2 Mars atm) did not affect germination uniformity of the Ws-2 and Ler-0 seeds. In contrast, the exposure of *tt4-1* seeds to (Dark + CO_2 Mars atm) resulted in an extremely significant ($p < 0.001$) increase in $T_{25-75\%}$ value, while simulated space vacuum (Dark + Vacuum) had no effect on germination uniformity of the *tt4-1* seeds. The germination uniformity of the Ws-2 samples exposed to (UV + Vacuum) was not different from that of the laboratory control, but it differed significantly ($p < 0.05$), when compared to the Ws-2 sample exposed to (Dark + Vacuum). The exposure of the Ws-2 seeds to (UV + CO_2 Mars atm) resulted in an extremely significant ($p < 0.001$) increase in the $T_{25-75\%}$ value. In the case of the Ler-0 wild type line, both (UV + Vacuum) and (UV + CO_2 Mars atm) affected the germination uniformity, resulting in a significant ($p < 0.05$) and extremely significant ($p < 0.001$) increases in $T_{25-75\%}$, respectively.

17.2.4. The viability of flavonoid-lacking tt4-1 Arabidopsis seeds exposed to polychromatic UV under simulated space vacuum and simulated Mars CO_2 atmosphere (Tetrazolium test)*

After the germination test, the viability of ungerminated *Arabidopsis tt4-1* seeds was determined by the tetrazolum (TZ) test. Since dormant, deteriorated or seriously damaged seeds demonstrate drastically reduced or even lost germination capacity, the TZ test can be used as a method for detection of potentially viable seeds among ungerminated seeds. The conversion of tetrazolium salts into bright red formazan end-product indicates the metabolic activity of viable cells. Due to the impermeability of the seed coat observed in flavonoid-containing Ws-2 and Ler-0 *Arabidopsis* seeds, the evaluation of seed viability by the TZ test was feasible only for flavonoid-lacking *tt4-1*mutant, which has a transparent seed coat that allows efficient penetration of the tetrazolium salt solution. Thus, red-stained *tt4-1* seeds were considered viable, while uncoloured *tt4-1* seeds were determined as dead seeds.

Since the exposure to polychromatic simulated solar $UV_{200-400}$ radiation, applied alone or in combination with simulated space vacuum and simulated Mars CO_2 atmosphere*, had dramatic effects on the germination capacity of exposed *tt4-1* seeds ($G_{max\%}$ = 0%), as seen in **Fig. 85**, the viability of ungerminated *tt4-1* seeds was further determined by the TZ test (**Fig. 87**). All three replicas of seed samples in positive TZ (+) control (untreated viable seeds) and negative TZ (-) control (seeds inactivated by autoclaving) stained brightly red or remained unstained, respectively. Dark control seeds, which were not exposed to UV radiation and were kept in the air at a pressure of 1 atmosphere, stained red at the level of 100% in all three replicas. In contrast, all *tt4-1* seeds that remained ungerminated after the exposure to polychromatic $UV_{200-400}$ radiation alone (UV + air) or in combination with simulated space vacuum (UV + Vacuum) and simulated Mars CO_2 atmosphere* (UV + CO_2 Mars atm), remained unstained in all parallel replicas. This result clearly showed that viability of the *tt4-1* seeds was entirely lost after the exposure to polychromatic simulated solar $UV_{200-400}$ radiation at fluence of 1.5×10^5 kJm^{-2}.

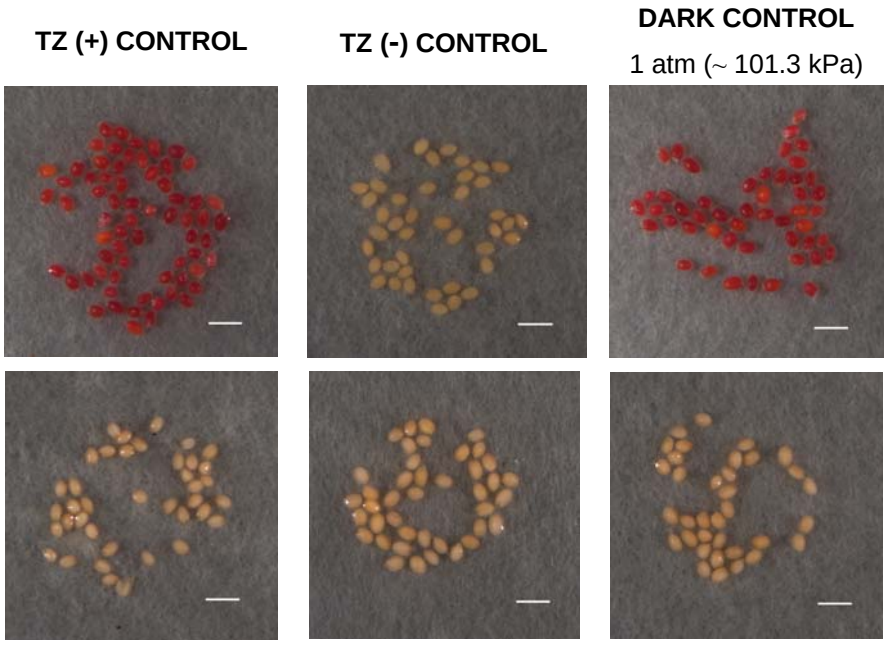

Fig. 87. The effect of polychromatic UV radiation under simulated space vacuum and simulated Mars CO_2 atmosphere* on the viability of *Arabidopsis* flavonoid-lacking *tt4-1* seeds exposed to simulated polychromatic solar UV light (λ = 200-400 nm, fluence 1.5 x 10^5 kJm^{-2}) alone or in the combination with simulated space vacuum (10^{-5} Pa) and simulated Mars CO_2 atmosphere* at 1 atm (95.6 % CO_2). The inviability of the *tt4-1* seeds (Ler-0 accession) that remained ungerminated at the end of germination assay was confirmed by the tetrazolium (TZ) test. Bars represent 2 mm.

17.3. Early-seedling stage: effects of polychromatic UV under simulated space vacuum and simulated Mars CO_2 atmosphere*

Following the germination stage (principal growth stage 0.5; see section **17.2**) of *Arabidopsis* seeds that were exposed to polychromatic UV light under simulated space vacuum and simulated Mars CO_2 atmosphere*, the germinants were further grown under *in vitro* conditions and development of early-stage seedlings was observed at the principal growth stage 1.0 (Boyes et al., 2001; Kjemtrup et al., 2003). In order to predict whether germinants, which have been developed from the Ws-2, Ler-0 and *tt4-1* seeds exposed to polychromatic $UV_{200-400}$ radiation, simulated space vacuum and simulated Mars CO_2 atmosphere*, had the capacity to develop into functional and healthy plants, the development and morphology of essential seedling structures, such as root system (e.g. primary root), shoot axis (e.g. hypocotyl) and cotyledons, were further studied. Similarly to the experiments with quasi-monochromatic UV-C_{254} light (see section **16.3**), here we studied the following parameters of early-seedling growth: percentage of normal seedlings, abnormal seedlings and ungerminated seeds (section **17.3.1**), characterization and quantification of types of damage in abnormally developed seedlings (section **17.3.2**), and the length of normally developed primary roots (section **17.3.3**).

*17.3.1. Normal seedlings, abnormal seedlings and ungerminated seed occurrence after exposure of seeds to polychromatic UV light under simulated space vacuum and simulated Mars CO_2 atmosphere**

According to the rules for seed testing (ISTA, 1999), the results of early-seedling stage experiments were grouped into the following three categories: normal seedlings, abnormal seedlings and ungerminated seeds. The total percentage of sown seeds (100%) was thus equal to the sum of the percentages for these three groups. Normal seedlings are defined as those that show potential for continued development into satisfactory plants, when grown under favourable conditions, while abnormal seedlings include damaged, deformed or unbalanced seedlings, which would unlikely develop into normal plants (ISTA, 1999). Observing the development of 15-day-old *Arabidopsis* seedlings that were grown from seeds exposed to simulated space and simulated Mars conditions, the percentage of normal and abnormal seedlings, as well as ungerminated seeds was determined for the Ws-2, Ler-0 and *tt4-1* lines (**Fig. 88**). One-way

ANOVA and the Tukey-Kramer post-hoc test were performed, both at the level of significance $\alpha = 0.05$, where calculated mean values were obtained from three parallel experiments with n = 40 sample size.

Laboratory controls (unexposed seeds) in the Ws-2, Ler-0 and *tt4-1* lines developed 100% normal seedlings, where neither abnormally developed seedlings nor ungerminated seeds were observed (**Fig. 88A-F**).

The exposure of seeds only to simulated space vacuum (Dark + Vacuum) had no effect on subsequent development of early-stage seedlings in the Ws-2 and Ler-0 lines, as well as the *tt4-1* mutant, since almost all seeds germinated into normal seedlings (**Fig. 88A-C**).

In contrast, the exposure of seeds to polychromatic $UV_{200-400}$ light in combination with simulated space vacuum (UV + Vacuum) had a strong effect on Ws-2 and Ler-0 seedling development (**Fig. 88A** and **B**), resulting in a very significant decrease ($p = 0.0054$) in the percentage of the Ws-2 normal seedlings (72%), and extremely significant decrease ($p < 0.0001$) in percentage of normal Ler-0 seedlings (59%). The percentage of abnormal seedlings in (UV + Vacuum) samples increased, reaching 20% and 39% for the Ws-2 and Ler-0 line, respectively. No statistically significant increase in the percentage of ungerminated seeds was observed in the Ws-2 and Ler-0 wild type seeds exposed to (UV + Vacuum). Polychromatic $UV_{200-400}$ light in combination with simulated space vacuum inhibited the germination of *tt4-1* seeds, since all exposed seeds remained ungerminated (**Fig. 88C**).

Statistical tests showed that the exposure of wild type seeds to simulated Mars CO_2 atmosphere* (Dark + CO_2 Mars atm) had no effect on seedling development, where the percentage of normal seedlings reached the level of 94% and 89% in the Ws-2 and Ler-0 line, respectively **(Fig. 88D** and **E**). The low percentage of abnormal seedlings and ungerminated seeds in the case of the Ws-2 and Ler-0 samples exposed to the (Dark + CO_2 Mars atm) had no statistical significance, compared to the laboratory controls. In contrast, the exposure of flavonoid-lacking *tt4-1* seeds to (Dark + CO_2 Mars atm) had a marked effect on early-stage seedling development (**Fig. 88F**). An extremely significant decrease ($p < 0.0001$) in the percentage of normal seedlings (55%) was observed, and the percentage of abnormal seedlings (5%) and ungerminated seeds (40%) increased after the exposure of the *tt4-1* seeds to (Dark + CO_2 Mars atm).

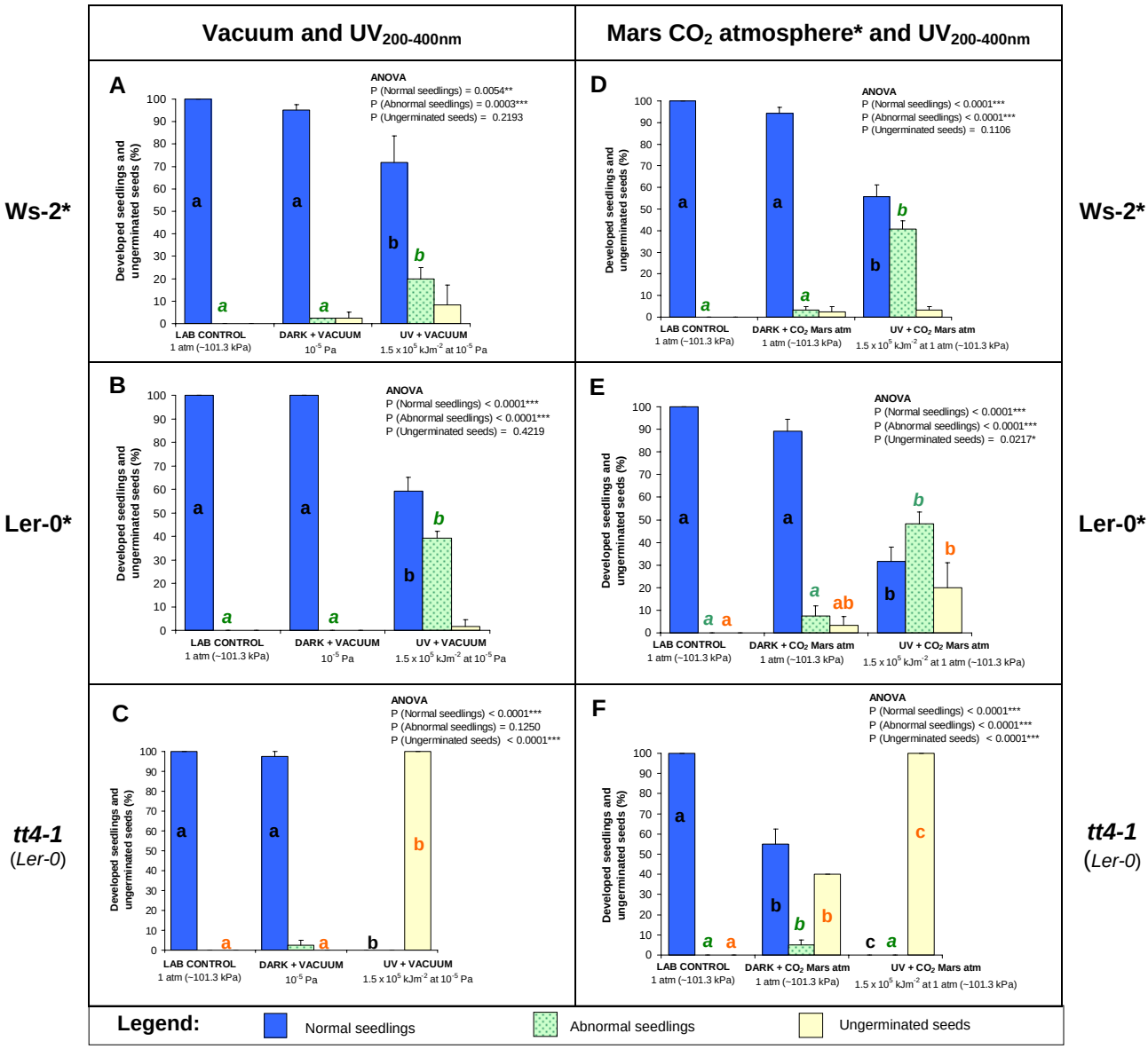

Fig. 88. The effect of simulated space and simulated Mars conditions on the germination and development of *Arabidopsis* seedlings after exposure of seeds to polychromatic simulated solar UV light (λ = 200-400 nm, fluence 1.5 x 10^5 kJm^{-2}), simulated space vacuum (10^{-5} Pa) and simulated Mars CO_2 atmosphere* at 1 atm (95.6 % CO_2). Percentages of ungerminated seeds, as well as normal and abnormal seedlings developed from seeds exposed to simulated space and Mars CO_2 conditions were compared to the laboratory control samples (seeds that were stored in the dark at 4°C during the EVT experiments). Values are the mean ± standard deviation of three parallel experiments (n = 40). Bars with different letters within the same group, denote a significant difference at $\alpha < 0.05$, according to ANOVA and the Tukey-Kramer post-hoc test. The precise values of ANOVA are indicated above the bars, where * means a significant level ($P < 0.05$), ** very significant ($P < 0.01$) and *** extremely significant ($P < 0.001$) level of difference.
The plant genotypes were: Wassilewskija (Ws-2) in A and D; Landsberg erecta (Ler-0) in B and E; a flavonoid-lacking mutant in Ler-0 accession (*tt4-1*) in C and F. Wild ecotypes are marked with asterisks.

The exposure of seeds to polychromatic $UV_{200-400}$ light in combination with simulated Mars CO_2 atmosphere* (UV + CO_2 Mars atm) had a strong effect on development of normal seedlings in all three *Arabidopsis* lines. An extremely significant decrease ($p < 0.0001$) in the percentage of normal Ws-2 and Ler-0 seedlings was observed, dropping to 56% and 32%, respectively (**Fig. 88D** and **E**). The percentage of abnormal Ws-2 and Ler-0 seedlings, which were grown from seeds exposed to (UV + CO_2 Mars atm), increased significantly ($p < 0.0001$), reaching 41% and 48%, respectively (**Fig. 88D** and **E**). Only a few Ws-2 seeds (3%) remained ungerminated after exposure to (UV + CO_2 Mars atm), having no statistical significance, compared to the laboratory control. In contrast, a statistically significant increase ($p < 0.05$) in the percentage of ungerminated seeds was observed in the Ler-0 sample exposed to (UV + CO_2 Mars atm), reaching 20% (**Fig. 88E**). Polychromatic $UV_{200-400}$ light in combination with simulated Mars CO_2 atmosphere* completely inhibited the germination of the flavonoid-lacking *tt4-1* seeds (**Fig. 88F**).

*17.3.2. Characterisation and quantification of seedling damage after exposure of seeds to polychromatic UV light, simulated space vacuum and simulated Mars CO_2 atmosphere**

Early-stage *Arabidopsis* seedlings that were grown from seeds exposed to simulated space and simulated Mars CO_2 conditions frequently developed an abnormal morphology of essential seedling structures, such as the primary root, hypocotyl and cotyledons. **Fig. 89** shows different types of damage observed in 15-day-old seedlings, developed from exposed Ws-2 and Ler-0 wild type seeds. As in the case of seeds exposed to quasi-monochromatic UV-C_{254} light (see section **16.3**), the root appeared to be the most sensitive organ in seedlings developed from seeds exposed to simulated solar polychromatic $UV_{200-400}$ light. The shortening of primary roots in otherwise normally developed seedlings was first observed (**Fig. 89B**). An altered morphology of the shoot axis was also frequently found, where seedlings developed an abnormally short or twisted hypocotyl (**Fig. 89C**). Seriously damaged seedlings showed morphological abnormalities in both the shoot axis and the root system. For instance, abnormal Ws-2 and Ler-0 seedlings that developed a short or twisted hypocotyl, showed at the same time a short (**Fig. 89D**), retarded (**Fig. 89E**) or even missing (**Fig. 89F**) primary root. Heavily damaged seedlings with missing hypocotyl and root system in combination with undeveloped cotyledons, which were observed after exposure to quasi-monochromatic UV-C_{254} light (see **Fig. 75G** in section **16.3.2**), were not here detected.

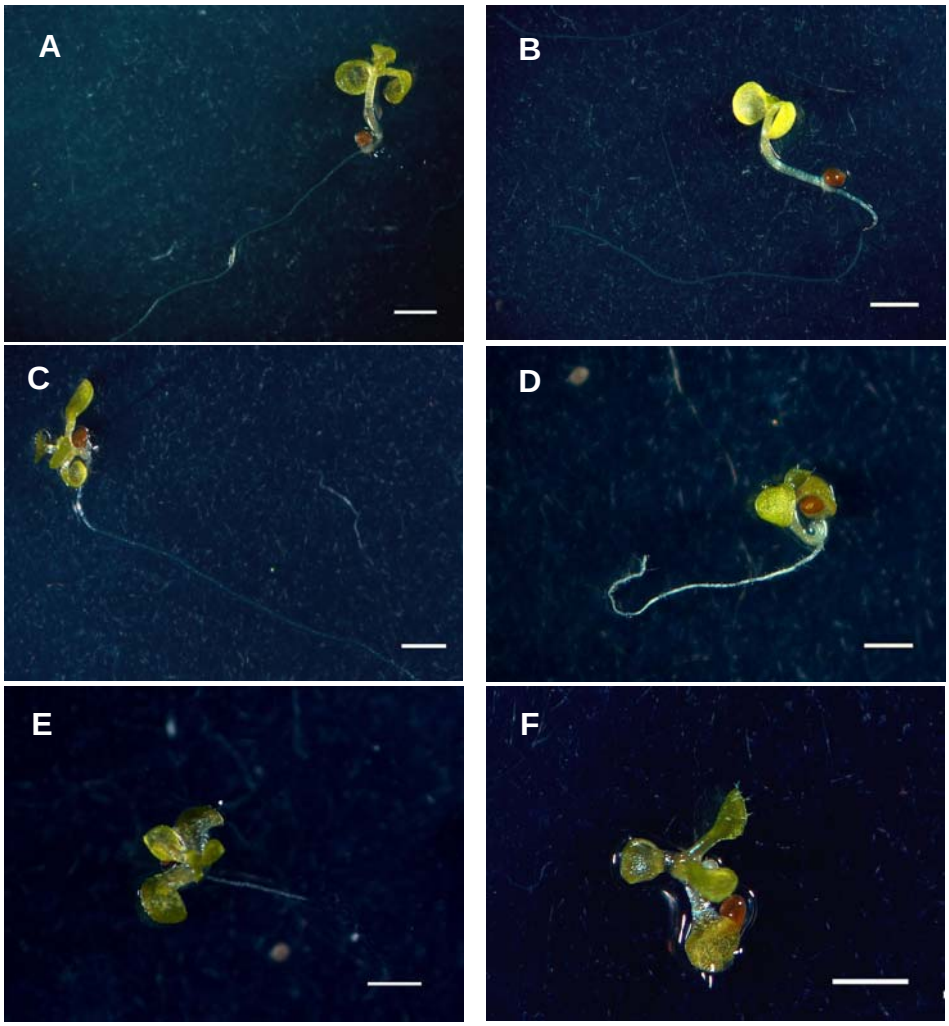

Fig. 89. Types of damage to essential structures of early-stage *Arabidopsis* seedlings, developed from seeds exposed to simulated space and Mars conditions, including polychromatic simulated solar UV light (λ = 200-400 nm, fluence 1.5 x 10^5 kJm^{-2}), simulated space vacuum (10^{-5} Pa) and simulated Mars CO_2 atmosphere* at 1 atm (95.6 % CO_2). Morphological changes in 15-day-old seedlings: normally developed seedling (A), normal seedling with shorter primary root (B), damaged seedling with hypocotyl short or twisted, but normally developed primary root (C), damaged seedling with hypocotyl short or twisted and short primary root (D), damaged seedling with hypocotyl short and retarded primary root (E), damaged seedling with short hypocotyl and missing primary root (F). The full length of normally developed primary roots is not presented on pictures in panel A and C. Bars represent 1 mm. (Here presented photographs show Ws-2 *Arabidopsis* seedlings).

In order to determine the relative contribution of each type of seedling damage in relation to the EVT exposure conditions, aberrant seedling forms were quantified and statistically analyzed using ANOVA and the Tukey-Kramer post-hoc test ($\alpha = 0.05$). The percentages of seedlings with different types of damage were graphed in stacked bars, together with the percentage of ungerminated seeds for the Ws-2, Ler-0 and *tt4-1* lines (**Fig. 90**). Thus, the cumulative percentage of damaged seeds represented the sum of individual percentages for each category of seedling damage and the percentage of ungerminated seeds. In all three analyzed genotypes, neither damaged seedlings, nor ungerminated seeds were observed in unexposed samples (laboratory controls).

The exposure of seeds to simulated space vacuum (Dark + Vacuum) had no effect on subsequent development of early-stage seedlings, since neither seedlings with aberrant morphology nor ungerminated seeds were detected in the Ler-0 samples (**Fig. 90B**), and only a few damaged seedlings or ungerminated seeds that were observed in the Ws-2 and *tt4-1* samples had no statistical relevance, compared to the laboratory controls (**Fig. 90A** and **C**).

The irradiation of seeds with polychromatic $UV_{200-400}$ light under simulated space vacuum (UV + Vacuum) affected subsequent seedling development, where 28% of the Ws-2 and 42% of the Ler-0 seeds developed either into the seedlings with aberrant morphology or they remained ungerminated (**Fig. 90A** and **B**). The most frequent type of damage was in the form of seedlings with a short or twisted hypocotyl, but with a normally developed primary root and cotyledons, observed in 14% of the Ws-2 and 30% of the Ler-0 seedlings developed from exposed seeds. More severe damage included seedlings with abnormally developed both shoot and root axes, where 4% of the Ws-2 and 5% of the Ler-0 seedlings had a short or twisted hypocotyl, together with a short primary root. The low percentage of the Ws-2 and Ler-0 seedlings that developed a short or twisted hypocotyl together with retarded primary root, as well as Ler-0 seedling with a short hypocotyl and missing primary root, showed no statistical difference, compared to laboratory controls. As demonstrated before (see section **17.3.1**), the percentages of ungerminated Ws-2 and Ler-0 seeds had no statistical relevance, compared to laboratory controls. In contrast, the *tt4-1* seeds exposed to (UV + Vacuum) were seriously damaged to the point that all seeds remained ungerminated (**Fig. 90C**).

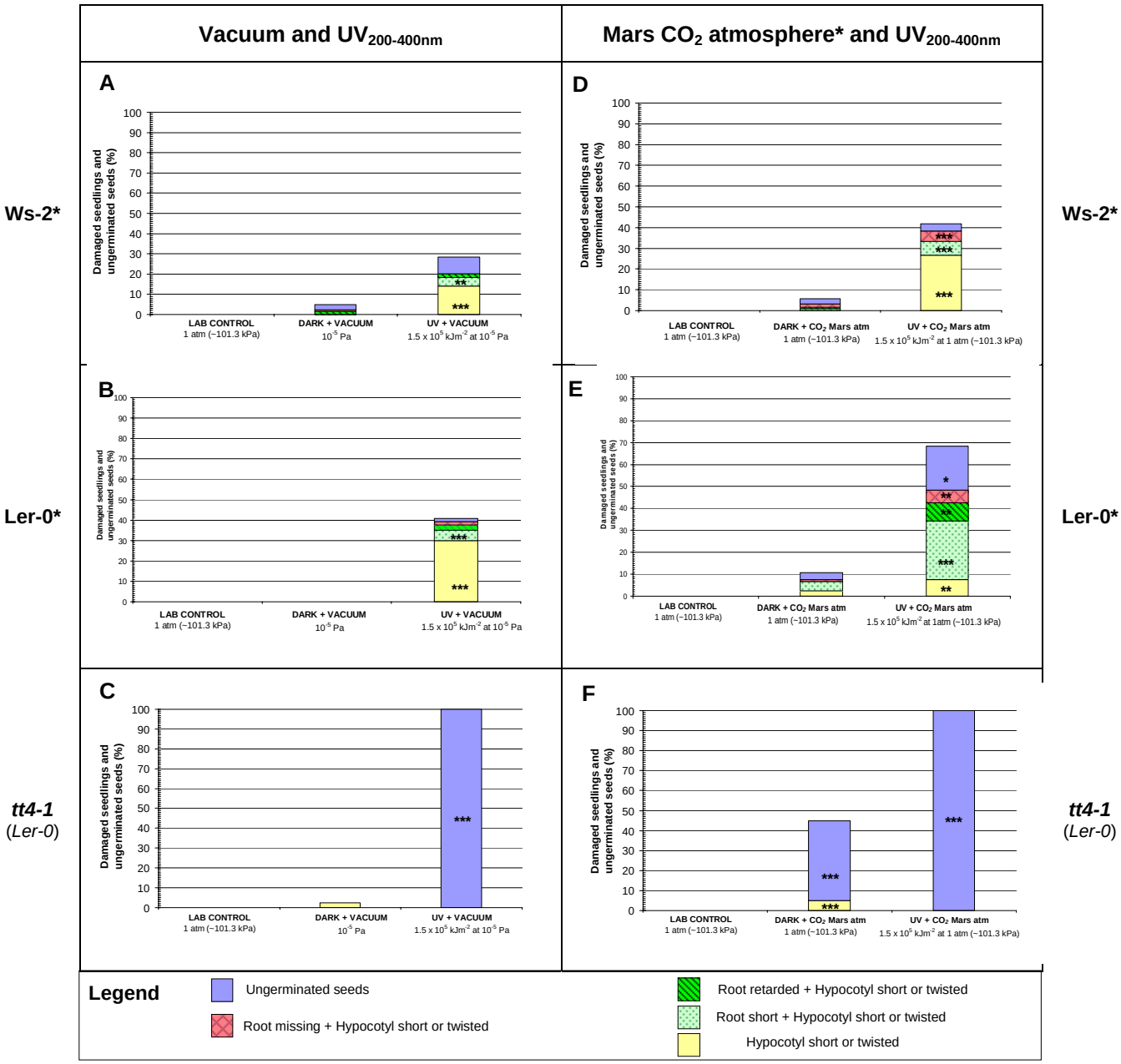

Fig. 90. Damaged *Arabidopsis* early-stage seedlings germinated from seeds exposed to simulated space and simulated Mars conditions: simulated polychromatic solar UV light (λ = 200-400 nm, fluence 1.5 x 10^5 kJm^{-2}), simulated space vacuum (10^{-5} Pa) and simulated Mars CO_2 atmosphere* at 1 atm (95.6 % CO_2). Percentages of ungerminated seeds and different types of damaged seedlings developed from seeds exposed to simulated space conditions are compared to the laboratory control samples (unexposed seeds that were stored in the dark at 4°C). Mean values were obtained from three parallel experiments (n = 40) and analysed by ANOVA and the Tukey-Kramer post-hoc test (α = 0.05), where * means a significant level ($P < 0.05$), ** very significant ($P < 0.01$) and *** extremely significant ($P < 0.001$) level of difference.
The plant genotypes were: Wassilewskija (Ws-2), A and D; Landsberg erecta (Ler-0), B and E; a flavonoid-lacking mutant in Ler-0 accession (*tt4-1*), C and F. Wild ecotypes are marked with asterisks.

Although cumulative percentages of damaged seeds reached 7% in the Ws-2 and 11% in the Ler-0 samples exposed to simulated Mars CO_2 atmosphere* (Dark + CO_2 Mars atm), individual percentages for each type of seedling damage and the percentage of ungerminated seeds remained low, showing no statistical difference, compared to the laboratory controls (**Fig. 90D** and **E**). After exposure of the *tt4-1* seeds to Dark + CO_2 Mars atm, a total of 45% of the seeds were damaged (**Fig. 90F**), resulting in an extremely significant increase ($p < 0.0001$) in the percentage of seedlings with a short or twisted hypocotyl (5%), as well as in the percentage of ungerminated seeds (40%).

The exposure of seeds to polychromatic $UV_{200-400}$ light in combination with simulated Mars CO_2 atmosphere* (UV + CO_2 Mars atm) had a strong impact on early-stage seedling development. The Ws-2 wild type line appeared more resistant to (UV + CO_2 Mars atm) than the Ler-0 wild type line, since the cumulative percentages of damaged seedlings and ungerminated seeds reached 42% and 69%, respectively (**Fig. 90D** and **E**). The most frequent abnormality in exposed Ws-2 samples (27%) were seedlings with a short or twisted hypocotyls and normally developed primary roots, as well as cotyledons. The same type of damage reached only 8% in exposed Ler-0 samples. However, more severe seedling damage that occurred in the form of seedlings with a short or twisted hypocotyl and short primary roots appeared to be the most frequent damage in exposed Ler-0 samples (28%). In addition, 8% of Ler-0 seedlings exhibited short or twisted hypocotyl and retarded primary roots. This type of seedling damage was not observed in the exposed Ws-2 samples. In both Ws-2 and Ler-0 samples that were exposed to (UV + CO_2 Mars atm), a statistically important increase in the percentage of seriously damaged seedlings with short or twisted hypocotyl and missing root system was observed, reaching 5% in the Ws-2 and 6% in the Ler-0 line. As demonstrated previously (see section **17.3.1**), the percentages of ungerminated Ws-2 seeds had no statistical relevance, compared to the laboratory controls, while a statistically significant increase in the percentage of ungerminated seeds (20%) was observed in the Ler-0 line. All *tt4-1* seeds exposed to (UV + CO_2 Mars atm) were heavily damaged, so that all remained ungerminated (**Fig. 90F**).

17.3.3. Effects of exposure to polychromatic UV light under simulated space vacuum and simulated Mars CO_2 atmosphere on primary root length*

One of the first morphological changes in the early-stage *Arabidopsis* seedlings t grown from the exposed seeds was observed on the root axis. Since damaged seedlings frequently exhibited shorter, retarded or even missing primary roots (**Fig. 89**), the root system was considered as one of the most critical points in plant development. Therefore, we measured the length of normally developed primary roots in 10-day-old Ws-2, Ler-0 and *tt4-1* seedlings that were grown from seeds exposed to simulated space vacuum or simulated Mars CO_2 atmosphere* alone, or in combination with polychromatic simulated solar $UV_{200-400}$ light (**Fig. 91**). The mean values for root length were obtained from three parallel experiments observing n = 22 seedlings per sample. Using parametric tests (ANOVA and unpaired t-test) and nonparametric tests (Kruskal-Wallis and Mann-Whitney tests), both at the level of significance $\alpha = 0.005$, the mean values for the root length of exposed samples were statistically compared to those obtained for unexposed samples (laboratory controls).

As shown in **Fig. 91A-C**, the exposure of seeds to simulated space vacuum (Dark + Vacuum) had no effect on the growth of the primary roots in the Ws-2, Ler-0 and *tt4-1* seedlings. Parametric tests, as well as nonparametric tests, showed no statistical differences in the root length between exposed samples and the laboratory controls in all three genotypes.

The exposure of the seeds to polychromatic $UV_{200-400}$ light in combination with simulated space vacuum (UV + Vacuum) was associated with reduction in root length in the Ws-2, as well as in the Ler-0 seedlings **(Fig. 91A** and **B**). ANOVA, as well as the Kruskal-Wallis test, indicated an extremely significant differences ($p < 0.0001$) in root length among samples exposed to (UV + Vacuum), (Dark + Vacuum) and the laboratory controls in both wild type lines.

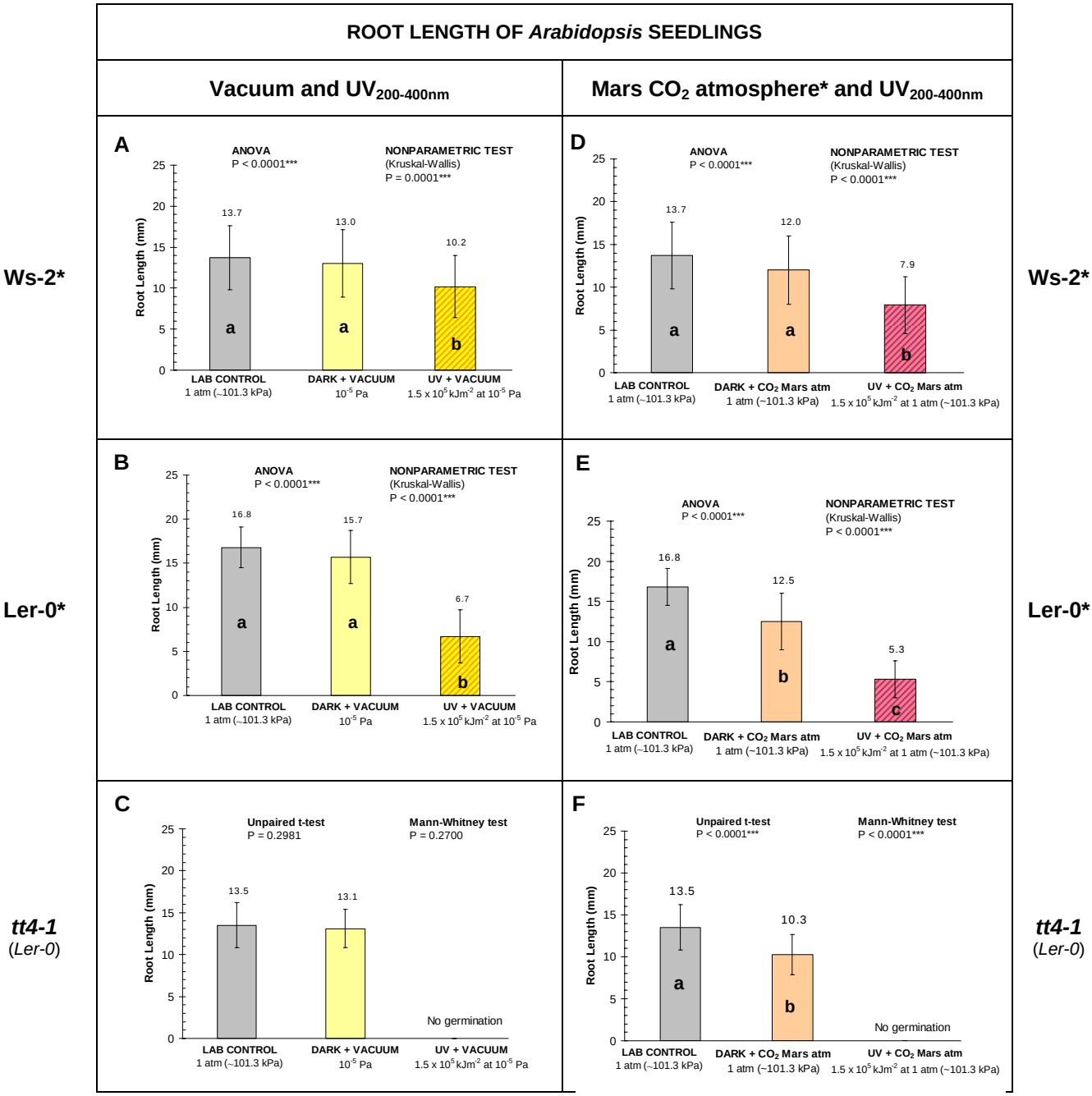

Fig. 91. The length of primary roots in 10-day-old *Arabidopsis* seedlings germinated from the seeds that were exposed to simulated solar UV light (λ = 200-400 nm, fluence 1.5 x 10^5 kJm^{-2}), simulated space vacuum (10^{-5} Pa) and simulated Mars CO_2 atmosphere* at 1 atm (95.6 % CO_2). The root length of samples exposed to simulated space and simulated Mars conditions are compared to the laboratory controls (unexposed seeds that were stored in the dark at 4°C) Values are the mean ± standard deviation of three parallel experiments (n = 22). Bars with different letters denote a significant difference at $\alpha < 0.05$ according to ANOVA (parametric test) and the Kruskal-Wallis test (nonparametric test), as well as the unpaired t-test (parametric test) and the Mann-Whitney test (nonparametric test) in the case of *tt4*-1 samples. The precise values of statistical tests are indicated above the bars, where * means a significant level ($P < 0.05$), ** very significant ($P < 0.01$) and *** extremely significant ($P < 0.001$) level of difference.
The plant genotypes were: Wassilewskija (Ws-2) in A and D, Landsberg erecta (Ler-0) in B and E, and a flavonoid-lacking mutant in Ler-0 accession (*tt4-1*) in C and F. Wild ecotypes are marked with asterisks.

Simulated Mars CO_2 atmosphere* had no effect on the growth of primary roots in the Ws-2 seedlings, since no statistical difference in root length was observed between (Dark + CO_2 Mars atm) sample and the laboratory control (**Fig. 91D**). In contrast, the Ler-0 wild type line, as well as the *tt4-1* mutant line, appeared to be more sensitive to simulated Mars CO_2 atmosphere*, since both genotypes developed shorter primary roots (**Fig. 91E** and **F**). ANOVA followed by the Tukey-Kramer post-hoc test (parametric statistical tests) showed an extremely significant difference ($p < 0.001$) in root length between the Ler-0 sample exposed to (Dark + CO_2 Mars atm) and the laboratory control. A similar result was obtained using the Kruskal-Wallis test followed by the Dunn post-hoc test (nonparametric statistic tests), but at the very significant level of difference ($p < 0.01$). In the case of the *tt4-1* line, both the parametric test (unpaired t-test) and the nonparametric test (Mann-Whitney test) indicated an extremely significant difference ($p < 0.0001$) in root length between the sample exposed to (Dark + CO_2 Mars atm) and the laboratory control.

The Ws-2 and Ler-0 seeds that were irradiated with polychromatic $UV_{200-400}$ light under simulated Mars CO_2 atmosphere* (UV + CO_2 Mars atm) developed seedlings with significantly shorter primary roots (**Fig. 91D** and **E**). Both ANOVA (parametric statistical test) and the Kruskal-Wallis test (nonparametric statistical test), showed an extremely significant differences ($p < 0.0001$) in the root length among samples exposed to (UV + CO_2 Mars atm), (Dark + CO_2 Mars atm) and the laboratory controls in the both wild type lines.

17.4. Plant development stage: effects of simulated space conditions, including polychromatic UV light and simulated space vacuum

We recall that according to the BBCH scale, the plant development is conventionally divided into number of principal growth stages, each coded with the number from 0-9 (Boyes et al., 2001; Kjemtrup et al., 2003). In the present work, we were interested in putative changes in development of *Arabidopsis* plants that were grown from exposed seeds, and we measured different physiological parameters throughout three principal growth stages: the seed germination (principal growth stage 0.5), the early-seedling stage (principal growth stage 1.0) and the mature plant development (principal growth stage 8.0). The results related to the resistance of *Arabidopsis* seeds to the effects of simulated space and simulated Mars conditions, observed at the level of the seed germination and the early-seedling stage are presented above (see sections **17.2** and **17.3**, respectively). In this section we are focused at the level of the development of mature *Arabidopsis* plants grown from exposed seeds.

Our aim was to determine whether the germinants grown from exposed *Arabidopsis* seeds were able to develop into functional and healthy plants. This was tested during the soil-based experiments performed under greenhouse conditions. The seeds were first imbibed *in vitro* and than transferred to the soil where they were let to germinate. The plant growth and development was further studied in *Arabidopsis* plants, reaching the principal growth stage 8.0, which is defined as a developmental stage of mature *Arabidopsis* plants with the first siliques shattered (Boyes et al., 2001; Kjemtrup et al., 2003). After 45 days of plant cultivation, the percentage of survived plants, the percentage of fertile plants, as well as the average height of mature plants was determined for the Ws-2, Ler-0 and *tt4-1* samples exposed to simulated space conditions (**Fig. 92**). The percentage of survivors comprised all the germinants that at least reached the principal growth stage 3.0, characterized by the growth of rosette leaves (Boyes et al., 2001; Kjemtrup et al., 2003), and it included the plants that passed through subsequent stages, up to the principal growth stage 8.0. The percentage of fertile plants (seed producers) included only the mature plants with developed siliques that reached the principal growth stage 8.0. Due to a large number of samples, the plant growth and development was studied only in the samples exposed to simulated space conditions, including simulated space vacuum and polychromatic solar $UV_{200-400}$ light, while the samples that were exposed to simulated Mars conditions were not analysed in these soil-based experiments.

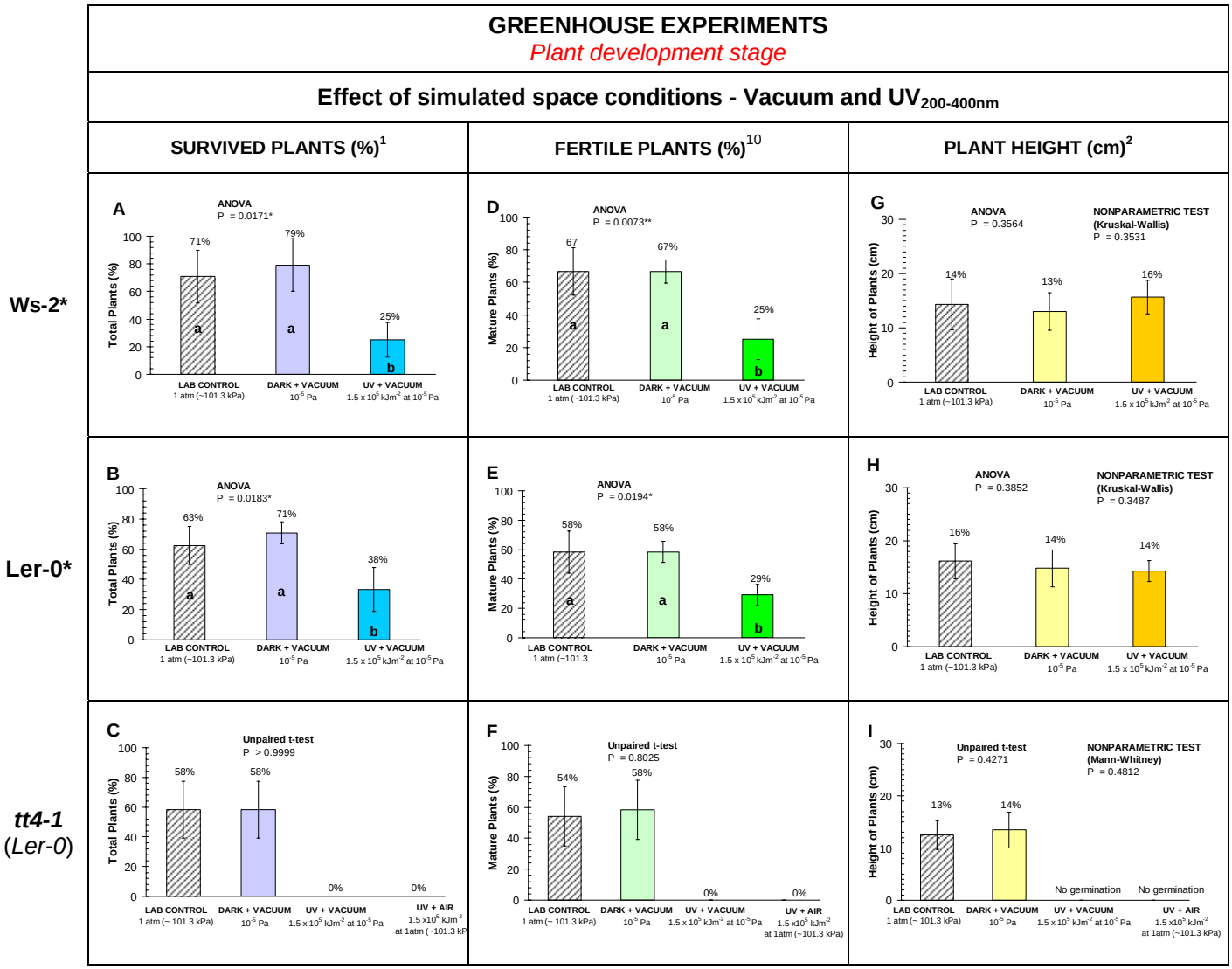

Fig. 92. The effects of simulated space conditions on the growth of *Arabidopsis* plants developed from seeds exposed to simulated polychromatic solar UV light (λ = 200-400 nm, fluence 1.5 x 10^5 kJm^{-2}) and simulated space vacuum (10^{-5} Pa). Seeds were germinated in the soil and plants were grown in the greenhouse for 45 days (48 DAI) when the percentage of survived plants, percentage of fertile plants and plant height of fertile plants were determined. Values are the mean ± standard deviation of three parallel experiments, with n = 8 sample size. Bars with different letters denote a significant difference at $\alpha < 0.05$, according to ANOVA (parametric test) and the Kruskal-Wallis test (nonparametric test), as well as unpaired t-test (parametric test) and the Mann-Whitney test (nonparametric test) in the case of *tt4*-1 samples. The precise values of statistical tests are indicated above the bars, where * means a significant level ($P < 0.05$), ** very significant ($P < 0.01$) and *** extremely significant ($P < 0.001$) level of difference. DAI = days after imbibitition.
The plant genotypes were: Wassilewskija (Ws-2), A, D and G; Landsberg erecta (Ler-0), B, E and H; and a flavonoid-lacking mutant in Ler-0 accession (*tt4-1*), G, H and I. Wild ecotypes are marked with asterisks.

[1]The percentages of survived and fertile plants were scored out of the total number seeds sown in soil.
[2]The height was measured in mature plants that reached the principal growth stage 8.0.

Out of the total number of sown seeds, 71% of Ws-2, 58% of Ler-0 and 63% of *tt4-1* unexposed seeds (laboratory control) germinated and finally developed into plants (**Fig. 92A-C**). As it has been already observed in this work (see section **16.4**), the germinability of unexposed *Arabidopsis* seeds was markedly lower in soil-based experiments, compared to the *in vitro* germination assay. This phenomenon is probably related to more restrictive greenhouse conditions, including lower humidity and substrate water potential, greater temperature variations and growth in non-axenic environment. However, all developed plants in the Ler-0 laboratory control reached the growth stage 8.0 (seed producers), while 67% of Ws-2 and 54% of *tt4-1* unexposed seeds finally developed into fertile plants (**Fig. 92D-F**).

The exposure of seeds to simulated space vacuum (Dark + Vacuum) alone had no effect on subsequent plant development and growth in the Ws-2, Ler-0 and *tt4-1* lines. ANOVA ($\alpha = 0.05$) showed no statistical differences in the percentage of survived plants (**Fig. 92A-C**), the percentage of fertile plants (**Fig. 92D-F**) and the average height of fertile plants (**Fig. 92G-I**) between the samples exposed to (Dark + Vacuum) and the laboratory controls. The same result was obtained using an unpaired t-test with $\arcsin\sqrt{\%}$ transformed or log (x+1) transformed data for percentages of survived and fertile plants, as well as nonparametric tests (Kruskal-Wallis and Mann-Whithey tests), in the case of the plant height parameter.

In contrast, the exposure of seeds to polychromatic simulated solar $UV_{200-400}$ light under simulated space vacuum (UV + Vacuum) had a strong effect on plant development in all three genotypes. The percentage of survived Ws-2 and Ler-0 plants after the exposure to (UV + Vacuum) dropped to the level of 25% and 38%, respectively (**Fig. 92A** and **B**). This was confirmed by ANOVA, which showed a statistically significant decrease in the percentage of survived plants in exposed samples for both the Ws-2 ($p = 0.0171$) and Ler-0 ($p = 0.0183$) lines. The development of fertile plants (seed producers) was also strongly affected by exposure to (UV + Vacuum), where 25% of the Ws-2 and 29% of the Ler-0 plants reached finally the growth stage 8.0 (**Fig. 92D** and **E**). Comparing the laboratory controls, statistical tests indicated a significant reduction in the percentage of fertile plants in the samples exposed to (UV + Vacuum). Statistical difference was detected at a significant level ($p = 0.0194$) in the Ler-0 line and at very significant level ($p = 0.0073$) in the Ws-2 line. Since the exposure of *Arabidopsis* seeds only to simulated space vacuum (Dark + Vacuum) had no impact on subsequent plant growth and development (see above), the phenomenon of reduced percentage of survived, as well as fertile plants in samples exposed to (UV + Vacuum) was attributed to the effects of polychromatic $UV_{200-400}$ radiation.

No survivors, and thus no fertile mature plants, were observed in the *tt4-1* sample exposed to (UV + Vacuum) (**Fig. 92C** and **F**). The exposure of the *tt4-1* seeds only to polychromatic simulated solar $UV_{200-400}$ light under atmospheric pressure (UV + Air), resulted also in complete inhibition of germination of the *tt4-1* seeds (**Fig. 92C, F** and **I**).

The height of mature plants in the Ws-2 and Ler-0 lines was not affected by the exposure to (UV + Vacuum) (**Fig. 92G** and **H**). This was confirmed by ANOVA (parametric statistical test), as well as the Kruskal-Wallis test (nonparametric statistical test), which revealed no statistically significant difference in the plant height between (UV + Vacuum) exposed and laboratory control samples for both Ws-2 and Ler-0 wild type lines.

17.5. Survival rates of *Arabidopsis* plants developed from seeds exposed to polychromatic UV light under simulated space vacuum and simulated Mars CO_2 atmosphere*

After the exposure of *Arabidopsis* seeds to simulated space conditions and simulated Mars conditions, which included exposure to simulated space vacuum (10^{-5} Pa) or simulated Mars CO_2 atmosphere* at 1 atm (95.6 % CO_2) applied alone or in combination with polychromatic simulated solar UV light (λ = 200-400 nm, fluence 1.5 x 10^5 kJm^{-2}), the survival rates for the Ws-2, Ler-0 and *tt4-1* lines were determined at two developmental stages, the seed germination stage (germination experiments *in vitro*) and the plant development stage (soil-based experiments in greenhouse), as shown in **Table 21**. The survival rates of *Arabidopsis* plants developed from exposed seeds were calculated using the formula for surviving fraction S(UV) of *Bacillus* spores exposed to UV radiation (Horneck, 1993), which was modified for the plant model (see **Equation 5** in section **15** and the details about its modification in section **16.5**). The average survival rates were calculated from three parallel experiments, where the maximal percentage of germinated seeds (germination experiments *in vitro*) was determined from n = 40 sample size, while the percentage of survived plants (soil-based experiments in greenhouse) from n = 8 sample size.

Germination tests *in vitro* indicated that seeds that were exposed to simulated space vacuum survived at very high level, reaching 98% in the Ws-2 wild type line, and 100% in both the Ler-0 wild type line and the flavonoid-lacking *tt4-1* mutant line. After the exposure to polychromatic $UV_{200-400}$ light in combination with simulated space vacuum, the survival rate of the Ws-2 seeds slightly decreased to 92%, while reaching a high level (98%) in the Ler-0 line. In contrast, no survived germinants (0%) were detected in the *tt4-1* samples that were exposed to polychromatic $UV_{200-400}$ light in combination with simulated space vacuum. The Ws-2 and Ler-0 wild type seeds survived the exposure to simulated Mars CO_2 atmosphere*, reaching 98% and 97%, respectively. The flavonoid-lacking *tt4-1* seeds were more sensitive to the exposure to simulated Mars CO_2 atmosphere*, since the survival rate dropped to the level of 60%. The exposure to polychromatic $UV_{200-400}$ light under simulated Mars CO_2 atmosphere* had no effect on the survival rate (100%) of Ws-2 seeds germinated *in vitro*, while a decreased survival rate (80%) was detected in the Ler-0 line. No germinants (0%) were detected in the *tt4-1* sample that was exposed to polychromatic $UV_{200-400}$ light under simulated Mars CO_2 atmosphere*.

The survival rates at the plant development stage were determined only for the samples exposed to simulated space conditions, including simulated space vacuum applied alone or in combination with polychromatic $UV_{200-400}$ light, while the survival rates of samples exposed to simulated Mars conditions were not determined. The soil-based experiments indicated that the exposure of seeds to simulated space vacuum had no effect on the survival of *Arabidopsis* plants, where 100% survival was detected in all three tested genotypes. In contrast, the exposure of seeds to polychromatic $UV_{200-400}$ light in combination with simulated space vacuum had a strong effect on the survival of plants grown in the soil, where the survival rates dropped to 36% in the Ws-2 line and 53% in the Ler-0 line. No survived plants (0%) were detected in the *tt4-1* sample exposed to polychromatic $UV_{200-400}$ light under simulated space vacuum. Since the exposure to simulated space vacuum did not affect the survival of soil-grown plants, the effect of decreased survival rate after the exposure to combined conditions of polychromatic $UV_{200-400}$ light and simulated space vacuum was attributed to the effects of UV radiation.

Table 21. The effects of simulated space and Mars conditions on the survival of *Arabidopsis* plants developed from seeds exposed to simulated polychromatic solar UV light (λ = 200-400 nm, fluence 1.5 x 10^5 kJm^{-2}), simulated space vacuum (10^{-5} Pa) and simulated Mars CO_2 atmosphere at 1 atm (95.6 % CO_2). The survival rates were measured at two plant developmental stages: the seed germination stage ($G_{max\%}$) and the plant growth stage (% survived plants).
The plant genotypes were: Wassilewskija (Ws-2), Landsberg erecta (Ler-0) and a flavonoid-lacking mutant (*tt4-1*) in Ler-0 accession. Wild ecotypes are marked with asterisks.

	SURVIVAL (%)[a] Seed germination stage				SURVIVAL (%)[b] Plant growth stage			
SAMPLES	Vacuum	UV + Vacuum	CO_2 Mars	UV + CO_2Mars	Vacuum	UV + Vacuum	CO_2 Mars	UV + CO_2Mars
Ws-2*	98	92	98	100	100	36	nd	nd
Ler-0*	100	98	97	80	100	53	nd	nd
tt4-1 (Ler-0)	100	0	60	0	100	0	nd	nd

[a] Survival determined in the germination tests (*in vitro* experiments) from the maximal percentage of germinated seeds.
[b] The percentage of survived plants scored out of the total number of seeds sown in soil (greenhouse experiments).
nd = not determined

Chapter 6
DISCUSSION II

According to our UV spectroscopy results, elaborated in part **I**, chapters **3** and **4**, we postulated that among different potential and known UV screening compounds, flavonoids were particularly suited to protect DNA from deleterious direct effects of UV (including VUV) radiation. However, using the similarity with DNA absorption spectra as a primary criterion, the spectroscopy results provided just a preliminary evaluation of the potential effectiveness of these screens. Therefore, it was further necessary to demonstrate the UV-protection capacity of flavonoids in experiments *in vivo*.

There is good evidence that flavonoids protect plants from the effects of UV-B radiation by acting as sunscreens (Teramura, 1983; Cen and Bornman, 1993; Jordan, 1996; Reuber et al., 1996; Bornman et al., 1997; Greenberg et al., 1997). Previously reported results demonstrated that flavonoid-deficient *Arabidopsis* plants, as well as mutants with a reduced level of flavonoids, had higher sensitivity to the deleterious effects of UV-B radiation (Li et al., 1993; Lois and Buchanan, 1994; Landry et al., 1995; Rao et al., 1996). Stapelton and Walbot (1994) reported that DNA in flavonoid-containing *Zea mays* plants was better protected from UV-B and UV-C induced damage than that in flavonoid-deficient plants. In addition, Koostra (1994) directly demonstrated the UV screening capacity of some flavonoids that were capable of preventing the UV-B-induced damage to DNA. Flavonoids also have an important role as antioxidants and free radical scavengers (Miller, 1996; Parr and Bolwell, 2000), protecting DNA and other macromolecules in plant cells from oxidative damage, resulting from the indirect effects of UV radiation (Landry et al., 1995; Rao et al., 1996; Saraf et al., 2007). Upon UV exposure, flavonoids are found to accumulate in plants in relatively high amounts (Vierstra et al., 1982).

Plant seeds contain high concentrations of flavonoids e.g. *Arabidopsis* seeds contain about 15 mg g^{-1} seed of total flavonoids, including flavonols and proanthocyanidins, each representing approximately a half of the flavonoid content (Lepiniec et al., 2006; Routaboul et al., 2006). Yet, little is known about the resistance of plant seeds to UV radiation. Most previous studies were focused on the effects of UV radiation on the vegetative rather than the reproductive parts of plants. Few studies concerned the effects of UV radiation, especially in the UV-B part of the spectrum, on seed germination and early seedling development (Musil, 1994; Tosserams et al., 1997; Musil et al., 1998; Dai and Upadhyaya, 2002; Farokh et al., 2010). Even less is known about the effects of UV-C radiation on plant seeds, since this part of the solar spectrum does not reach the surface of the present-day Earth, and thus it is of less ecological concern. Many seeds

tolerate harsh environmental conditions, provided they are in a dry state. The lifespan of seeds can be remarkably long, ranging from decades to centuries, and even millennia (Buitink and Leprince, 2004, and references therein). During seed drying, the cellular viscosity increases dramatically, and reaching the dry state, the cytoplasm transforms into so-called glassy state (Buitink et al., 2002; Buitink and Leprince, 2004; Buitink and Leprince, 2008). For more information about seed water content and formation of glassy state in dry seeds see chapter **1**, section **4.3.1**. Due to its high viscosity, intracellular glasses have been shown to slow down severely molecular diffusion and to decrease the probability of chemical reactions (Buitink and Leprince, 2008). It explains why seeds in dry state have drastically reduced metabolic activity, however, they retaining their ability to germinate (Rajjou and Debeaujon, 2008). Due to the low moisture content in seeds, free radicals and reactive oxygen species (ROS) that are involved in UV-induced oxidative stress might have lower mobility and therefore limited access to the target molecules, such as DNA, proteins and lipids. In addition, molecules of water in hydrated tissues can act as a direct source of free radicals (e.g. highly reactive hydroxyl radical), which are readily generated through the photohydrolytic reactions. Thus, lower moisture content might be related to a lower level of macromolecular damage and higher resistance in dry seeds. On the other hand, being in a metabolically quiescent state, dry seeds accumulate damage all through the period of exposure to stress conditions, and due to lower molecular mobility their ability to detoxify ROS and to repair DNA damage enzymatically might be seriously reduced (Bailly, 2004). Thus, accumulation of non-enzymatic antioxidant components and UV screening molecules play an important role in the longevity and the high resistance of dry seeds (Buitink et al., 2002; Bailly, 2004; Rajjou and Debeaujon, 2008).

In this work we have chosen *Arabidopsis* seeds as a terrestrial model for testing resistance to the harsh conditions found in space, particularly to highly energetic UV radiation. Due to their small size (0.3-0.5 mm, Al-Shehbaz and O'Kane, 2002), *Arabidopsis* seeds were particularly suitable for our space experiments (EXPOSE-EuTEF and EXPOSE-R, see chapter **1**, section **2**), where the limited available space in sample holders was of great concern. Therefore, our primary aim was to determine the resistance of *Arabidopsis* seeds to UV radiation and other simulated space conditions. *Arabidopsis thaliana* seemed an appropriate model plant because of its small, sequenced genome, rapid life cycle, and because of availability of extensive information concerning the genetics, biosynthesis and chemistry of diverse secondary metabolites. These advantages have enabled the creation of a large collection of *Arabidopsis* mutants that are defective in synthesis of specific chemical compounds. In order to examine the role of certain secondary metabolites in the UV resistance of seeds, we used *Arabidopsis* mutants with altered

phenylpropanoid biosynthetic pathways, which were defective in the ability to synthesise specific UV absorbing compounds, such as flavonoids and sinapate esters that represent two major classes of UV screens in plants. We studied the resistance of *Arabidopsis* seeds through three plant developmental stages: the germination stage, the stage of early-seedling development and the stage of mature plant development. In this work, we discuss the biological endpoints of survival observed during one generation cycle (M_1) of *Arabidopsis* from exposed seed up to the stage of mature plant, capable of producing the next-generation seeds. Up to now, little attention has been paid to seed germination and early-seedling growth processes as a response to UV radiation, particularly the UV-C part of the spectrum.

The germination stage in seeds exposed to stress e.g. UV radiation, is a critical step in plant development, since the direct damage to DNA, as well as oxidative damage on macromolecules that have been progressively accumulated in quiescent seeds, will be expressed all at once at the moment of seed imbibition and subsequent phase of germination. This may ultimately lead to reduced vigour[4], low germinability or even seed death. The plant seed contains an embryo with a preformed radicle, hypocotyl and cotyledons, encapsulated all together in the protective seed coat. During germination, the growth of the embryo will proceed from two meristems, one in the root and one in the shoot apex. These meristems, consisting of few initial cells, are sensitive targets for radiation-induced damage. The enzymatic repair of accumulated DNA lesions, as well as enzymatic detoxification of accumulated ROS and free radicals, largely depend on the successful reactivation of metabolic processes following seed imbibition (Bailly, 2004; Rajjou and Debeaujon, 2008). The detoxification and DNA repair potential of exposed seeds can be strongly reduced if these enzymes, as well as other proteins are targets on their own to directly or indirectly induced UV damage. In addition, seed germination is a potentially harmful process *per se* due to increased respiratory activity and a greater influx of oxygen into the imbibed seeds, which leads to the oxidative damage through the formation of ROS in germinating seeds (Bailly, 2004). The increased mobility of molecules in rehydrated seeds leads to improved accessibility of enzymes to their substrates, but it also leads to increased activity of ROS and free radicals which have better access to the target molecules. As a result, reduced or even lost germinability of seeds exposed to UV occurs as a result of an imbalance between the accumulated damage and the efficiency of the repair and detoxification systems, activated in imbibed seeds. In order to determine the effect of UV radiation and other simulated space conditions on the germination of *Arabidopsis* seeds, we measured following endpoints: the germination capacity ($G_{max\%}$) and parameters of germination dynamics, including the mean

germination time (MGT), the median of germination ($T_{50\%}$), the germination uniformity ($T_{25\text{-}75\%}$) and the skewness of the germination curve ($T_{50\%}$/ MGT).

The early-seedling stage is the second critical step in plant development, since it reveals whether or not the germinants are able to grow into normal seedlings with fully developed essential seedling structures, such as root system, hypocotyl (shoot axis) and cotyledons (first seedling leaves) (ISTA, 1999). Within the plant life cycle, the seedling stage is one of the most vulnerable stages, usually showing the highest mortality rates (Fenner, 1987). Thus, we also aimed to determine the effects of UV exposure of *Arabidopsis* seeds on subsequent seedling development. To this purpose, we measured the percentage of normally developed seedlings, as well as the percentage of abnormal seedlings and the percentage of remaining ungerminated seeds. We also characterized and quantified the types of damage to essential seedling structures. In addition, we measured the length of the primary roots in seedlings germinated from exposed seeds, since root growth and development are sensitive to many environmental stresses and growth factors (Gregory, 2006; Qi et al., 2007).

We were also interested in the stage of mature plants, in order to determine whether or not *Arabidopsis* seedlings that were grown from UV exposed seeds, further developed into functional and healthy plants, capable of producing progeny. Plants were grown in soil, under greenhouse conditions. We determined the percentage of surviving plants, as well as the percentage of fertile plants (seed producers), which developed from exposed seeds. It was reported that increased levels of solar UV radiation inhibited growth and reduced total biomass in a variety of plant species (reviewed in Teramura, 1983; Greenberg et al., 1997; Murphy, 1997; Day, 2001). Thus, we also measured the height of the mature plants that were grown from seeds exposed to UV light.

18. RESISTANCE OF *Arabidopsis* SEEDS TO QUASI-MONOCHROMATIC UV-C_{254} LIGHT

In the present work, we first determined the effects of UV-C radiation on the resistance of *Arabidopsis* seeds. The source of quasi-monochromatic UV-C light emitted predominantly at λ = 254 nm, the wavelength of particular interest due to its proximity to the maximum of absorption of DNA in region I (λ ≈260 nm) (see chapter **3**, section **9** and chapter **4,** section **12**). Since the action spectrum for the induction of DNA pyrimidine dimers roughly follows the absorption spectrum of DNA (Britt, 1996), we assumed that above 200 nm, the maximal biological damage would be caused by UV-C radiation at wavelengths close to 260 nm. Although the UV-C part of the solar spectrum does not reach the surface of present-day Earth because of atmospheric absorption, a high flux of unattenuated UV-C radiation was probably present on the early Earth, prior the build-up of the ozone layer (Cockell, 1998; Cockell, 2001a). Highly energetic UV-C radiation is present in space, as well as in extraterrestrial environments e.g. on the Moon and on Mars (Cockell, 2001c), where it represents one of the most important obstacles to the emergence of life and its propagation.

In our experiments, the source of UV-C_{254} light was not strictly monochromatic due to a small contribution of UV-B_{312} (8%) and UV-A_{365} (2%) light, in addition to the predominant UV-C_{254} (90%) part of the emitted light. The effects and type of damage are wavelength dependent, due to differences in the energy carried by the UV photons, absorption spectra of key biological molecules and various photophysical and photochemical mechanisms involved in damage induction and repair. For instance, short-wave UV-C radiation causes a direct damage to DNA, generating predominantly cyclobutane pyrimidine dimers (CPDs) and (6-4) photoproducts as a result of direct excitation of DNA (Kielbassa et al., 1997). Similarly, UV-B radiation induces the formation of dimeric pyrimidine photoproducts (Kielbassa et al., 1997; Cadet et al., 2005), but besides this direct damage, it also induces an indirect damage to DNA through the production of ROS that are generated in photooxidation reactions. Due to a strong absorption at 280 nm, UV-B/UV-C radiation is also potentially very damaging to proteins. Because DNA is a weak chromophore for UV-A radiation, the photons in this range are absorbed in the cells by other biologically important molecules, which can act as endogenous photosensitizers, causing the indirect damage to DNA by ROS and free radicals (Ravanat et al., 2001).

Therefore we found it necessary to examine and distinguish the effects of the dominant UV-C_{254} light on *Arabidopsis* seeds from that caused by the relatively minor UV-B_{312} and UV-

A_{365} component of the emitted light. We thus employed three types of cut-off filters: a quartz filter that transmitted essentially all of the UV light emitted by the source, here marked as the UV-C + (UV-B + UV-A) light, a glass filter that filtered out the dominant UV-C light, thus transmitting only background UV-B + UV-A part of light, and an aluminium foil filter that blocked all emitted light. Since we did not use the Mylar UV-B cut-off filter, we could not distinguish between the effects of UV-B and UV-A components of emitted background radiation. Nevertheless, here is important to note that the UV-A component had only a minor contribution (2%) to the emitted light.

In this work, we studied the effects of quasi-monochromatic UV-C_{254} light on seeds in two *Arabidopsis* wild type lines, Ws-2 and Col-0, and we compared the resistance of these seeds to that of two mutant lines that were defective in the biosynthesis of UV-screening compounds, flavonoids in the *tt4-8* line (Ws-2 accession) and sinapate esters in the *fah1-2* mutant (Col-0 accession).

The transgenic *tt4-8* mutant carries a T-DNA insertion, resulting in the disruption of the gene for chalcone synthase (CHS), a key enzyme for flavonoid synthesis. This mutant does not accumulate flavonoids, explaining the yellow colour of the *tt4-8* seeds (Debeaujon et al., 2003; Pourcel et al., 2005). Our previous HPLC analysis revealed the absence of flavonoids in *tt4-8* seeds (Zalar, 2004). Recent LC-MS studies confirmed that *tt4-8* seeds were deprived of flavonols, proanthocyanidins (characteristic for the seed coat) and anthocyanins (characteristic for the vegetative parts), the three classes of flavonoid compounds that normally accumulate in *Arabidopsis* wild type lines (Routaboul et al., 2006; Luceri et al., 2008). In addition, Luceri et al. (2008) reported that other phenolics are not obviously affected in the *tt4-8* mutant.

In order to examine possible pleiotropic effects that sometimes accompany T-DNA mutagenesis (Bentsink and Koornneef, 2008), which ultimately might interfere with the effects of UV radiation on *tt4-8* seeds, we also examined a transgenic control mutant, a *dyx* line. This mutant carries the same T-DNA fragment inserted in the genome of the Ws-2 background, but without disruption of gene for CHS.

The second mutant line was a sinapate ester-deficient mutant, *fah1-2* (Col-0 accession), previously called *sin1-2* (Chapple et al., 1992), which has a dysfunctional ferulate-5-hydroxylase (F5H), an enzyme important in the synthesis of sinapate esters (Ruegger et al., 1999). Sinapate esters are derivatives of hydroxycinnamic acids, and they strongly absorb in the UV-B part of the

spectrum, and thus together with flavonoids, are considered as major UV-B protectants in *Arabidopsis* plants (Chapple et al., 1992; Li et al., 1993; Landry et al., 1995; Sheahan, 1996). For detailed discussion about UV absorption properties of flavonoids and sinapate esters see chapter **4**, section **14**. Excited under long-wave UV-A light, sinapic acid and sinapate esters exhibit a bright blue fluorescence (Chapple et al., 1992; Lorenzen et al., 1996; Sheahan, 1996). Our results clearly showed that the sinapate ester mutant was totally deprived of sinapate esters, since no blue fluorescence was detected in *fah1-2* seed extracts (**Fig. 51,** chapter **3,** section **11.2.1**). This result was further confirmed by LC-MS analysis, since no sinapoyl choline, sinapoyl glucose, sinapoyl malate or free sinapic acid were detected in *fah1-2* seed extracts (see chapter **3**, section **11.2.2**) In addition, LC-MS showed that *fah1-2* seeds contained normal levels of flavonoid compounds, comparable to those found in the Col-0 wild type (results not presented).

In our UV-C_{254} exposure studies, the flavonoid-containing seeds were irradiated for long time periods, to achieve exposures to extremely high fluences of UV light. The UV-C fluences were 3-6 orders of magnitude higher than those in previous studies on the effects of UV-C radiation on vegetative parts of plants, seeds and fruits (Jenkins et al., 1995; Danon and Gallois, 1998; Brown et al., 2001; Narayanasamy, 2006; Iriti et al., 2007; Kunz et al., 2008; Bashandy et al., 2009). In addition, the doses of UV-C_{254} light that we previously used to test the extreme resistance of *Bacillus subtilis* spores were 6 orders of magnitude lower than those used in our experiments with *Arabidopsis* seeds (Horneck et al., 1984a; Horneck et al., 1984b; Weber and Greenberg, 1985; Riesenman and Nicholson, 2000; Slieman and Nicholson, 2001; Moeller et al., 2005; Moeller et al., 2007b). The Ws-2 and *dyx* seeds were irradiated for 30 and 60 days, reaching the maximal fluence of UV-C = 6.0×10^5 kJm^{-2}. Due to the observed decrease in UV lamp output with such long periods of continuous operation, the irradiation of the second set of samples, the Col-0 and *fah1-2* seeds, was extended up to 40 days for the lower range of fluence, while the maximal fluence achieved after 60 days of exposure was UV-C = 4.8×10^5 kJm^{-2}, reaching unfortunately the end of the lamp's lifetime. Since previous studies indicated that flavonoid-lacking mutant lines are more sensitive to UV light, the *tt4-8* seeds were irradiated for shorter time periods, from 0.5 to 139 hours (UV-C = 2.8×10^2 - 5.9×10^4 kJm^{-2}). This means that the *tt4-8* seeds were exposed to 1-3 orders of magnitude lower fluences of UV light compared to the flavonoid-containing seeds.

In the present study, we determined the germination capacity and the seed vigour of UV irradiated seeds, performing the germination tests both under optimal and suboptimal (10ºC) temperature conditions. Standard germination tests, usually performed under optimal conditions,

sometimes show a relatively high germination performance of the seeds with affected vigour. Under suboptimal conditions, the germination process is slower, enabling the detection of relatively small differences in seed quality (ISTA, 1995). Although ISTA (1999) recommends using paper or sand substrates in standardized germination tests for various plant species, in this work we used 0.8% agar medium (agar-solidified ultrapure water) as a substrate for *Arabidopsis* seed germination. Depending on their concentration, gelling agents might affect *in vitro* performance, e.g. higher concentrations of gelling agent lead to lower water potential (ψ_w), thus reducing water availability (Smith and Spomer, 1995). It was reported that a small reduction in ψ_w (down to -0.6 MPa) may cause a slight delay in the initiation of germination, but without reduction in the maximal germination percentage (Bradford, 1990; Chon et al., 2004). Reported ψ_w for 0.8% agar medium is about -0.45 MPa (Beruto et al., 1999), while the matric potential is found to contribute only 1-2% to the total water potential of agar medium (Beruto et al., 1995).

Although the usage of a water-saturated paper substrate is well recommended due to its ψ_w close to 0 (ψ_w = 0 for pure distilled water), our preliminary germination tests on special germination filter paper (Filtres Durieux®) showed a lower consistency of germination results than on 0.8% agar support (results not presented). This observation might be related to the several problems experienced during germination of very small-sized *Arabidopsis* seeds on water-saturated filter paper, including the problem of easy displacement of small seeds over the surface of the moistened filter paper, seed clumping, and higher sensitivity of small seeds to the local differences in water availability, caused by the differences in the fine structure of the filter paper surface. All of these problems were largely overcome by using the agar-solidified substrate. In addition, using the agar-solidified medium it allowed us, besides the germination tests, to proceed directly with further *in vitro* studies, observing the stage of seedling development. The usage of agar-solidified medium enabled also *in situ* measurements of seedling roots. By positioning vertically the culture plates with germinated seeds, it enabled the seedling roots to grow straight down over the surface of solid medium, making easier the measurement of the length of rather thin *Arabidopsis* seedling roots. For all of these reasons, we considered the usage of agar-solidified substrate is better suited than moisten germination filter paper for studying the germination and development of *Arabidopsis* seedlings. We assumed that the possible slight delay in the start of germination would be of less concern in our studies, since all seed samples were analyzed in the same manner, and thus here we interested only in the relative differences between the control and UV exposed samples, rather than in absolute values of germination parameters.

18.1. Testing the stability of *Arabidopsis* dark control seed samples

The quasi-monochromatic UV-C_{254} exposure experiments were performed over long time periods, and besides the damaging effects of UV radiation, prolonged exposure to potentially unfavourable conditions might lead to accelerated seed ageing. Deterioration of seeds is manifested through progressive loss of seed quality with time (Coolbear, 1995). When seeds deteriorate, they lose vigour, become more sensitive to stress conditions and ultimately become unable to germinate (Rajjou and Debeaujon, 2008). Many factors contribute to seed deterioration, including storage conditions, where relative humidity and temperature represent two most important factors (Buitink and Leprince, 2004; Buitink and Leprince, 2008). Storage stability of seeds is closely related to the molecular mobility and packing density of the intracellular matrix (Buitink et al., 2002; Buitink and Leprince, 2004). Therefore, the formation of intracellular glasses is necessary for providing the stability for long-term survival of seeds (Buitink and Leprince, 2004). The water content at which the cytoplasm transforms into a glassy state during drying depends on the temperature; the lower the temperature of drying, the higher the cellular water content at which the cytoplasm becomes glassy (Buitink and Leprince, 2008). According to generalized rules proposed by Harrington (1972), seed life is halved by each 1% increase in seed moisture content, as well as by each 5ºC increase in temperature. The optimal storage conditions for *Arabidopsis* seeds are at room temperature or at 4ºC for the short- to medium-term storage, as well as at -20ºC for long-term storage, and 5-6% (fw) seed moisture content (Anderson and Wilson, 2000). Prior the UV exposure experiments, we determined the moisture content of *Arabidopsis* seeds that we used in the present study. We found that the moisture content of all seeds was close to the suggested optimal range: Ws-2 (5.7%), *dyx* (4.7%), Col-0 (5.3%), *fah1-2* (5.2%), *tt4-8* (6.6%) (results not presented).

Before studying the effects of UV radiation on seed resistance, it was first necessary to determine the quality and performance of dark control seed samples. The dark controls referred to the seeds that were exposed to the experimental conditions, but protected from UV light by the thin aluminium foil filter. Placed under the UV lamp, which also emitted some infrared light, the seeds were exposed to higher average temperatures (up to 28°C) than that suggested as the optimal storage temperature range. Therefore, it was necessary to test whether these non-storage conditions might affect the germination performance of *Arabidopsis* dark control seeds. This was particularly important for the long-term UV exposure experiments in order to exclude possible interference of the effects of accelerated seed ageing after prolonged exposure to unfavourable non-storage conditions and that caused by UV radiation.

Our results indicated that all flavonoid-containing dark control seeds, including the Ws-2 and Col-0 wild type lines, as well as the *dyx* and *fah1-2* mutant lines, showed high performance and good stability in seed quality, even after 60 days of treatment (**Fig. 62A-D**). High germination capacity ($G_{max\%}$ = 96-100%), and high vigour of the Ws-2, Col-0, *dyx* and *fah1-2* dark control seeds, which was measured through different parameters of germination dynamics, including MGT, $T_{75-25\%}$, $T_{50\%}$ and the germination skewness, did not differ from those for the laboratory controls (seeds stored in the dark at 4°C), with the exception of slightly slower germination observed in the Ws-2 dark control samples (**Fig. 62A**). Germinating under suboptimal conditions at 10ºC, all flavonoid-containing dark control *Arabidopsis* seeds exhibited an excellent performance and unaltered germination behaviour, even in the case of the Ws-2 dark control (**Fig. 65A-D**). These results confirmed the high stability of *Arabidopsis* seeds after relatively long time periods of exposure to experimental conditions. We concluded that, besides UV radiation as a parameter of our direct interest, the other parameters of the experimental conditions in the present study did not influence the germinability and the vigour of all flavonoid-containing *Arabidopsis* seeds.

On the other hand, dark control samples of the flavonoid-deficient *tt4-8* mutant, showed some differences in germination behaviour after relatively short-term treatment of seeds under control experimental conditions (**Fig. 68A**). Although the germination capacity ($G_{max\%}$) did not alter with time, remaining at about 100% all through the period of experiment duration (**Fig. 69A**), the germination dynamics of the *tt4-8* dark control seeds was altered after 48 and 139 hours of treatment (**Fig. 71A**). Compared to the laboratory control samples (seeds stored at 4°C), the *tt4-8* dark control showed only a small increase in MGT after 48 hours of treatment. However, after 139 hours of treatment, a significant decrease in the seed vigour was detected in the *tt4-8* dark control seeds. A 13-hour-increase in MGT resulted from both a delayed start of germination and decreased uniformity of germination in seeds treated for 139 hours. These results indicated a possible seed ageing problem and the beginning of seed deterioration process in the *tt4-8* dark controls after prolonged exposure to experimental, non-storage conditions. A similar result was also reported in our previous work, where we observed an altered germination dynamics for the *tt4-8* seeds that were used as a negative control (unexposed seeds) in the UV-C_{254} exposure experiments (Zalar, 2004). We reported therein a decline in germination speed for the *tt4-8* control seeds after prolonged exposure to the experimental conditions (seeds protected from UV-C light and kept at 25-30°C), starting from 45 hours up to the maximal 115 hours of treatment.

Oxidative stress is probably one of the important processes involved in seed ageing (Bailly, 2004; Rajjou and Debeaujon, 2008). The supply of oxygen to the embryo largely depends on the structure, the thickness and the biochemical properties of the seed coat (Corbineau and Côme, 1995). Pigments that are accumulated in large amounts in seed coats are mainly flavonoid compounds, and particularly proanthocyanidins (condensed tannins). These phenolic compounds fix molecular oxygen through reactions catalyzed by polyphenoloxidases and some other, non-enzymatic processes (Côme, 1982; Corbineau and Côme, 1995; Debeaujon et al., 2007). In this way, oxidized flavonoid polymers limit the oxygen supply to the embryo during the storage, thus preventing ROS formation and oxidative damage (Corbineau and Côme, 1993). Therefore, as efficient antioxidants and free radical scavengers, flavonoids have beneficial effects on seed longevity (Rice-Evans et al., 1997; Debeaujon et al., 2007; Rajjou and Debeaujon, 2008). In addition, oxidized flavonoids make seed coats impermeable to water, thus acting as germination inhibitors, but also as protectors against imbibition damage (Debeaujon et al., 2000; Debeaujon et al., 2007). It was reported that *Arabidopsis* pigmentation mutants (e. g. *transparent testa* mutants), which are defective in the testa flavonoids, exhibit more seed deterioration than their wild type lines (Debeaujon et al., 2000). Generally these mutants show a reduced germination capacity and a higher rate of seedling abnormalities after the long-term ambient storage or controlled deterioration tests (Debeaujon et al., 2000; Clerkx et al., 2004). In addition, the pigmentation mutants exhibit a reduced dormancy, compared to wild type seeds (Debeaujon et al., 2000; Debeaujon et al., 2007). This phenomenon was also observed in our experiments, since the *tt4-8* laboratory control seeds started to germinate 12.5 hours earlier than that in the Ws-2 wild type line. This was also reported in our previous work, where we observed a faster germination in the *tt4-8* mutant seeds, compared to the wild type seeds (Zalar, 2004). In addition, the storage stability of *Arabidopsis* seeds was also found to correlate with density of the cytoplasmic molecular matrix (Buitink et al., 2002; Buitink and Leprince, 2004). The fast-dried embryos exhibit a less tight hydrogen-bonding network, which is likely associated with more loosely packed glassy structure (Buitink and Leprince, 2004). The differences in stability under experimental control conditions between flavonoid-lacking *tt4-8* and wild type Ws-2 seeds might reflect an altered seed composition (e.g. changes in accumulation of LEA proteins) or might be caused by possibly faster drying of *tt4-8* embryos due to more permeable flavonoid-lacking seed coat, which allows faster water loss and easier gas exchange. This may be also correlated with observed lower resistance of *tt4-8* seeds on dry-heating at high temperatures, compared to the Ws-2 wild type (see **Annex C**).

In spite of observed change in vigour of the *tt4-8* dark control seeds exposed to the experimental conditions up to 139 hours, further seedling development was not affected in all *tt4-8* dark control samples, as well as in the flavonoid-containing dark controls (Ws-2, Col-0, *dyx* and *fah1-2*). More than 95% of seeds in all dark control samples germinated into normal seedlings, showing no difference in percentage of normal seedlings (chapter **5**, section **16.3.1**), as well as primary root growth (chapter **5**, section **16.3.3**).

Concluding remarks (5)

Dry *Arabidopsis* seeds that served as dark controls in the UV exposure experiments exhibited a good stability in seed quality after prolonged exposure, up to 60 days, to the experimental, non-storage conditions. Their stability in quality was characterized by the high germination capacity and high seed vigour, measured through different parameters of germination dynamics, including the mean germination time (MGT), the germination uniformity ($T_{75-25\%}$) and the skewness of germination curve.

In contrast, seeds that lack flavonoids (*tt4-8* mutant seeds) showed lower stability than the wild type seeds. Although the *tt4-8* dark control seeds retained a high germination capacity all through the experiment, their vigour started to decline already after 48 hours of exposure to the experimental, non-storage conditions. These results indicated possible beginning of seed deterioration process in the *tt4-8* dark control seeds and their higher susceptibility to seed ageing, compared to flavonoid-containing seeds. Further experiments, however, would be necessary to determine the level of possible oxidative stress related to the accelerated seed ageing in *tt4-8* mutant e.g. by direct measuring the production of different types of ROS species using selective fluorescent ROS probes (APF, HPF, DCFH-DA etc.) or by measuring the activity of antioxidant enzimes (CAT, POD, SOD etc.). In plants, flavonoids are known as good antioxidants. Here we suggest that flavonoids play an important role in protection of seeds against oxidative stress, thus preventing accelerated seed ageing.

18.2. Influence of the UV-B + UV-A portion of emitted light on germination performance, and development of early-stage seedlings and mature plants

Although the UV-C_{254} source emitted only about 10% of UV-B + UV-A light, it was first necessary to determine the possible effects of this part of emitted light on the germination of *Arabidopsis* seeds, as well as on seedling development, and subsequent development of mature plants. The UV-B doses used in this study were, nevertheless, 2-3 orders of magnitude higher than those used in previously published work on the effects of UV-B radiation on the vegetative parts of plants (Mirecki and Teramura, 1984; Murali et al., 1988; Barnes et al., 1990; Rao and Gill, 1993; Landry et al., 1995), and about 1-2 orders of magnitude higher than UV-B doses used in previous studies on seed resistance (Musil, 1994; Musil et al., 1998; Dai and Upadhyaya, 2002). Therefore our study provided new data about responses of *Arabidopsis* seeds to high doses of UV-B + UV-A radiation. Using *Arabidopsis* seeds as a plant model, these experiments may have ecological and agronomical implications, given the reduction of the stratospheric ozone layer and subsequent effects of increased solar UV-B flux on terrestrial biota.

The germination stage

Our results revealed a high resistance of *Arabidopsis* seeds to the UV-B + UV-A portion of emitted light, since the germination capacity ($G_{max\%}$) was found unaltered in all flavonoid-containing seeds, including Ws-2, *dyx*, Col-0 and *fah1-2* seed lines (**Fig. 62E-H** and **Fig. 63A-D**). All flavonoid-containing seeds exhibited high germinability ($G_{max\%}$ = 95-100%), even after 60 days of UV exposure (**Fig. 63A-D**). These results were also confirmed by the germination tests performed under suboptimal temperature conditions (**Fig. 65E-H**). In addition, we also found that the seed vigour, which was expressed through the mean germination time (MGT), was not affected by UV-B + UV-A light in the Ws-2, *dyx* and Col-0 seeds germinated under optimal conditions (**Fig. 64A-C**). Besides MGT, other parameters of germination dynamics, such as $T_{50\%}$, $T_{25\text{-}75\%}$ and germination skewness, remained unchanged after exposure of the Ws-2, *dyx* and Col-0 seeds to UV-B + UV-A radiation. The only exception was increased $T_{25\text{-}75\%}$ value in the Col-0 seeds irradiated with the maximal UV fluence (**Table 15**). This indicated that after 60 days of UV exposure, the Col-0 seeds had lower germination uniformity than the control seeds. When irradiated seeds were germinated under suboptimal conditions, the Ws-2 line showed no differences in MGT, even after 60 days of exposure (**Fig. 66A**). However, the *dyx* and Col-0 seeds that were exposed to the maximal UV fluences showed a small increase in MGT, when germinated under suboptimal temperature conditions (**Fig. 66B** and **C**). These small differences

in the germination dynamics, observed mostly under suboptimal germination conditions, revealed a slightly higher resistance in the Ws-2 wild type seeds, compared to the *dyx* mutant (Ws-2 accession) and the Col-0 wild type line. Although all three seed lines are supposed to contain normal levels of flavonoids and sinapate-ester compounds, the observed slight changes in UV resistance indicated possible differences in the chemical and biochemical composition of seeds, the efficiency in ROS and free radical detoxification or differences in the activity of their repair mechanisms. Previously it was found that the naturally occurring genetic variation in various plant species, including *Arabidopsis*, may cause not only differences in their morphological and physiological traits, but also variations in the tolerance to diverse biotic and abiotic stress factors, such as pathogens, freezing temperatures, drought, UV radiation, high/low CO_2 concentrations, oxidative factors and high concentrations of salt and metals (Koornneef et al., 2004). Slight differences in the response to UV-B + UV-A radiation between the two different *Arabidopsis* ecotypes, Ws-2 and Col-0, detected at the level of germination speed, are likely related to the genetic variations that occur among different ecotypes. Torabinejad and Caldwell (2000) reported the occurrence of variations in morphological responses to enhanced UV-B radiation among seven different *Arabidopsis* ecotypes. Ecotypic variations in plant growth as response to enhanced polychromatic UV-A and UV-B + UV-A were also observed among *Arabidopsis* Ws, Col and Ler wild types (Cooley et al., 2001). Various levels of UV-absorbing compounds in different ecotypes are among the factors that may contribute to the observed variations in UV tolerance (Torabinejad and Caldwell, 2000). Previous studies reported naturally occurring variations in flavonoid content in the seeds of Ws-2, Col-0 and Ler-0 *Arabidopsis* ecotypes (Lepiniec et al., 2006; Routaboul et al., 2006). Our results from UV-B + UV-A exposure experiments also showed small differences in seed vigour between a T-DNA insertion control mutant, *dyx*, and the Ws-2 background. This observation might be in relation to possible pleiotropic effects, caused by T-DNA insertion, which perhaps resulted in unexpected, small alternations in the level of UV protective compounds and/or repair and detoxification mechanisms.

Regardless of the small effects on the seed vigour, our results demonstrated a high resistance of *Arabidopsis* seeds to UV-B + UV -A radiation up to doses of UV-B = 4.3 $x10^4$ kJm^{-2} and UV-A = 1.2 x 10^4 kJm^{-2}. Relatively little information is available in the literature on the seed germination response to enchanted levels of UV-B radiation, despite its agronomic and ecological relevance. Previous studies revealed different, and sometimes opposed responses of seeds to UV-B radiation, depending on plant species, and the intensity and the quality of UV-B light. For instance, Dai and Upadhyaya (2002) reported that UV-B doses of 1.1 x 10^2 kJm^{-2} (10

days of irradiation, 8 hours day^{-1}) do not inhibit seed germination in various weedy species. The study of Tosserams et al. (1997) revealed no adverse effects of enhanced polychromatic UV-B radiation (9.18 $kJm^{-2}day^{-1}$) on seeds in several plant species from dune grasslands. On the other hand, enhanced polychromatic UV-B radiation (7.1 $kJm^{-2}day^{-1}$) was found to reduce germination in radish and cucumber seeds (Tevini et al., 1983). Surprisingly, enhanced ambient UV-B radiation (280-320 nm) at a maximal fluence of 1.5 x 10^3 kJm^{-2} is found to improve germination in seed morphs of *Dimorphotheca pluvialis* (Musil, 1994). A faster germination in UV-B irradiated safflower seeds was also reported by Farokh et al. (2010). A non-linear UV-B+UV-A dose response was observed in dry seeds of *Leucadendron laureolum* (Musil et al., 1998).

Although our experiments revealed a high level of UV-B + UV-A tolerance in wild type *Arabidopsis* seeds, the mutant seeds that were deficient in major UV-absorbing compounds (flavonoids and sinapate esters) showed increased sensitivity to UV-B + UV-A radiation.

The sinapate ester mutant, *fah1-2*, showed a high germination capacity (nearly 100%) that was unaltered even after 60 days of irradiation (**Fig. 63D**). It remained at a high level even when seeds were germinated under suboptimal conditions (**Fig. 65H**). However, the vigour of the *fah1-2* seeds was altered after exposure to UV-B + UV-A light. Compared to the dark control sample, a small, but statistically significant decrease in germination speed for 1.7 hours (11.3% increase in MGT) was detected already after 40 days of irradiation (UV-B = 2.3 x10^4 kJm^{-2} and UV-A = 6.9 x 10^3 kJm^{-2}), as shown in **Fig. 64D**. The germination was further slowed for 4.6 hours (30.5% increase in MGT) in *fah1-2* samples exposed for 60 hours (UV-B = 3.4 x10^4 kJm^{-2} and UV-A = 9.5 x 10^3 kJm^{-2}). This effect was even more pronounced when irradiated *fah1-2* seeds germinated under suboptimal temperature conditions, since MGT increased for 8.6 and 15.6 hours after 40 and 60 hours of UV exposure, respectively (**Fig. 66D**). As *fah1-2* seeds lacked sinapate esters, but contained normal levels of flavonoids (see discussion above and chapter **3**, section **11.2**), the difference in seed vigour between *fah1-2* seeds and the Col-0 background indicated the importance of sinapate-esters in the UV-B + UV-A protection. Due to their high absorbance in the UV-A and UV-B part of the spectrum, sinapate esters are considered efficient UV protectors. The broad absorption peak at 320 nm (**Fig. 55B,** chapter **3**, section **11.4.1.2**) indicated that sinapate esters would provide major protection against UV-B light (Sheahan, 1996). Since they absorb to a lesser extent around 260 nm, sinapate esters would provide more screening protection to proteins than to DNA, and they could protect other molecules that absorb in the UV-B and UV-A regions (see discussion in chapter 4). In addition, they probably play a role in indirect protection, acting as efficient antioxidants (Landry et al.,

1995). Several authors reported the importance of sinapate esters in the UV-B protection of *Arabidopsis* seedlings (Chapple et al., 1992; Li et al., 1993; Landry et al., 1995; Sheahan, 1996). However, UV-B doses used in these studies were about two orders of magnitude lower than those used in our experiments on *Arabidopsis* seeds.

We also examined the UV-B + UV-A tolerance of the flavonoid-lacking *tt4-8* mutant seeds. We found that UV exposure up to 139 hours (UV-B = 4.2 $x10^3$ kJm^{-2} and UV-A = 1.2 x 10^3 kJm^{-2}) did not affect the germination capacity ($G_{max\%}$) of the *tt4-8* seeds, which reached about 100% in all examined samples (**Fig. 69B**). However, seed vigour was altered in the irradiated *tt4-8* seeds, but only at the higher UV-B + UV-A fluences (**Fig. 71B**). After 10 hours of irradiation (UV-B = 2.9 $x10^2$ kJm^{-2} and UV-A = 79 kJm^{-2}), MGT started to increase significantly and germination was slower for 5.1 hours. Germination further slowed in seeds irradiated with increasing fluences of UV-B + UV-A radiation. After 139 hours of UV exposure, germination slowed down for 25.1 hours (148% increase in MGT). Since flavonoid-lacking *tt4-8* dark control seeds exhibited reduced seed vigour after 48 and 139 hours of exposure to experimental conditions (see above), we assumed that the lower germination speed of the *tt4-8* seeds irradiated with high UV fluences is likely the result of combined effects of UV-B + UV-A radiation and possible oxidative damage involved in seed ageing, which is may be enhanced in flavonoid-lacking seeds (Debeaujon et al., 2000).

Taking into account the differences in germination speed, our results clearly indicated that flavonoid-lacking *tt4-8* seeds were two orders of magnitude more sensitive to UV-B + UV-A light than the sinapate ester mutant *fah1-2* line, while germination capacity remained unaffected in both mutants. This result implied that the flavonoids in *Arabidopsis* seeds provided greater UV-B + UV-A protection than sinapate esters. To our knowledge, this is the first comparative study on the effects of UV-B + UV-A radiation on *Arabidopsis* seeds of different genotypes, including the mutants deficient in major UV-protective compounds. Here we report for the first time *in vivo* evaluation of the effectiveness of flavonoids and sinapate esters in the protection of dry *Arabidopsis* seeds from UV-B + UV-A light. Previous studies were not focused on the UV resistance in seeds, but rather on the vegetative parts or tissues in *Arabidopsis* plants and seedlings, and they came to disparate conclusions about the UV-B protection efficiency of flavonoids and sinapate esters. Landry et al. (1995) reported that hydroxycinnimate esters (sinapate esters) are more efficient UV-B protectants than flavonoids, due to the increased sensitivity of *Arabidopsis fah1* seedlings to UV-B radiation in comparison to the *tt4* mutant. Sheahan (1996) communicated that sinapate esters provide better UV-B attenuation in leaves of

Arabidopsis seedlings than flavonoids, since sinapate-deficient mutants suffered from greater epidermal penetration of UV-B light than the flavonoid-deficient mutant, causing enhanced chlorophyll excitation. On the other hand, Li et al. (1993) demonstrated *in vivo* the significance of both flavonoids and sinapate esters in the UV-B protection of *Arabidopsis* seedlings. According to Rao et al. (1996), UV induced flavonols are predominant UV-B protectants in *Arabidopsis* seedlings. Possible variations in the UV response and protection mechanisms in different developmental stages (seeds, seedlings and plants) are likely related to temporal and spatial differences in the types and concentrations of accumulated UV protective compounds, notably flavonoids and sinapate esters. For instance, significantly higher amounts of sinapate esters are detected in *Arabidopsis* seedlings (1000 pmol seedling^{-1}) than in dry seeds (300 pmol seed^{-1}), as reported by Lorenzen et al. (1996). Sinapoyl choline is a major sinapate ester accumulated in *Arabidopsis* seeds, together with smaller amounts of sinapoyl glucose, while sinapoyl malate is found exclusively in leaf tissues (Chapple et al., 1992; Ruegger et al., 1999). In mature *Arabidopsis* seeds, quercetin-3-*O*-rhamnoside (quercitrin) is the major flavonol compound, which accumulates in seed coats in particularly high concentrations (Kerhoas et al., 2006; Lepiniec et al., 2006; Routaboul et al., 2006). In contrast to seeds, which accumulate predominantly glycosylated derivatives of quercetin, *Arabidopsis* leaves, stems, flowers and seedlings mainly accumulate glycosylated derivatives of kaempferol (Veit and Pauli, 1999; Lepiniec et al., 2006). Quercetin derivatives have a higher antioxidant potential, and are therefore considered more effective UV-protectors than other flavonols (Montesinos et al., 1995; Ryan et al., 2001; Ryan et al., 2002; Owens et al., 2008). Moreover, proanthocyanidins (also known as condensed tannins), which occur exclusively in seeds, accumulate in high concentrations in seeds coats. These flavonoid polymers exhibit high antioxidant capacity, and are considered efficient free radical scavenging agents (Miller, 1996; Bors and Michel, 1999; Lepiniec et al., 2006; Routaboul et al., 2006).

The early-seedling stage

Reduced plant growth, visible through stunting, reduced root weight, reduced leaf area etc. is known to occur as a response of seedlings and mature plants to elevated UV-B or UV-B + UV-A radiation (Teramura, 1983; Cooley et al., 2001; Day, 2001). However, in our study we did not expose directly the seedlings and plants to UV radiation, but rather we were interested in subsequent development of seedlings that were grown from UV-B + UV-A irradiated seeds.

We found that the UV-B +UV-A component of emitted light did not influence subsequent seedling growth and development in the Ws-2 and *dyx* (Ws-2 accession) lines, since almost all irradiated seeds germinated into normal seedlings (**Fig. 72A** and **B**). In addition, all Ws-2 seedlings developed normal primary roots and their average length did not differ from that of the dark control sample (**Fig. 79A**). Surprisingly, a small reduction in root length (about 14%) was observed in *dyx* seedlings that were grown from irradiated seeds, but only at the highest UV-B + UV-A fluences (60 days of irradiation) (**Fig. 79B**). The higher sensibility of root development in *dyx* samples, compared to the Ws-2 wild type, might be due to genotypic differences related to a T-DNA insertion and possible, as-yet uncharacterized pleiotropic effects in this mutant line. Genotype effects related to differences in UV-B + UV-A response were also observed in the Col-0 wild type line, where a small, but statistically significant increase in the percentage of abnormal seedlings (3%) was detected in the samples that were irradiated for 60 days (**Fig. 72C**). Morphological changes in the Col-0 seedlings were manifested through a short or twisted hypocotyl, while other seedling structures appeared unaffected (**Fig. 75C** and **Fig. 76C**). For instance, seed exposure to UV-B + UV-A light did not affect the primary root growth in the Col-0 early-stage seedlings (**Fig. 79C**). The effect of inhibited hypocotyl elongation in seedlings exposed to UV-B light was also reported in other plant species, including cress, tomato and cucumber (Steinmetz and Wellmann, 1986; Lercari et al., 1990; Ballaré et al., 1991). As already observed in our germination tests, this result indicated a slightly higher sensitivity of the Col-0 wild type seeds to UV-B + UV-A radiation, compared to the Ws-2 wild type. This might be explained by the possible differences in seed biochemistry of these two *Arabidopsis* lines, as discussed above.

In contrast, the sinapate ester mutant, *fah1-2*, appeared more sensitive than the background Col-0 wild type line, since UV-B + UV-A radiation significantly affected *fah1-2* seedling development. This result again demonstrated the importance of sinapate esters in the protection of seeds from UV-B + UV-A radiation. The occurrence of abnormal seedlings increased by 11%, but only at higher doses received after 60 days of irradiation (**Fig. 72D**). Two types of damaged seedlings were observed: (1) seedlings with short or twisted hypocotyls, but with normally developed other structures (**Fig. 75C** and **Fig. 76D**) and (2) seedlings with short or twisted hypocotyls and short primary roots (**Fig. 75D** and **Fig. 76D**). However, the average root length in the population of *fah1-2* seedlings grown from irradiated seeds did not differ from that of the dark control sample (**Fig. 79D**).

On the other hand, the development of flavonoid-lacking *tt4-8* seedlings appeared unaffected by the exposure of seeds to UV-B + UV-A light up to 139 hours. Almost all irradiated *tt4-8* seeds developed into normal seedlings (**Fig. 73A**), and their primary roots grew normally, without reduction in average root length (**Fig. 80A**). Although we found no changes in *tt4-8* seedling development, it is however important to note that the maximal UV-B + UV-A fluence in this case was 12.4 times lower than the maximal fluence to which the sinapate ester mutant (*fah1-2*) was exposed. Since the response of *tt4-8* samples to the higher fluences of UV-B + UV-A light (equivalent to that used with *fah1-2* samples) remain unknown, it is difficult to compare more precisely the UV-B + UV-A protection capacities of flavonoids and sinapate esters at the level of early-seedling development.

The plant development stage

Enhanced solar UV-B radiation has been shown to affect anatomical and morphological traits in plants (e. g. plant architecture, biomass allocation, leaf structure), as well as plant phenology (e.g. emergence, flowering, reproduction and senescence)(Rozema, 2000). However, our results showed a high resistance of *Arabidopsis* to UV-B + UV-A radiation, even at the stage of mature plant development. Here is important to note that in our experiments, the vegetative parts of plants were not directly exposed to UV light, but rather the seeds, which subsequently grew into plants.

When UV-B + UV-A irradiated *Arabidopsis* seeds were germinated in the soil and than allowed to grow into mature plants under greenhouse conditions, we observed no effects on subsequent plant development in all examined flavonoid-containing *Arabidopsis* lines, including the Ws-2, Col-0 and *fah1-2* lines. In all of these lines, the measured parameters of plant growth and development, such as the percentages of survived plants, the percentages of fertile plants (plants capable of producing next-generation seeds) and the height of mature plants did not differ between UV exposed and dark control samples (**Fig. 81A-I)**.

In contrast, the exposure of flavonoid-lacking *tt4-8* seeds to the maximal doses of UV-B + UV-A light had an effect on subsequent plant development (**Fig. 82A-C**). The exposure of seeds for 139 hours resulted in a reduction in plant survival and fertility (**Fig. 82A** and **B**). Plant growth was also inhibited in samples irradiated for 48 and 139 hours, where plant height was reduced by 58% in both cases (**Fig. 82C**). This result indicated that at the level of the plant development stage, the flavonoid lacking *tt4-8* mutant was at least 29 times more sensitive than

the wild type Ws-2 line, as well as the sinapate ester mutant, *fah1-2*. For comparison, the germination difference between Ws-2 wild type and *tt4-8* mutant ranged over about two orders of magnitude at the germination stage.

Concluding remarks (6)

Arabidopsis seeds showed high resistance to UV-B + UV-A portion (10%) of light emitted from the quasi-monochromatic UV-C_{254} source. This was confirmed at the three different developmental stages: the seed germination, the early-seedling stage and the mature plant development stage.

At the germination stage, all examined seed lines, including flavonoid-containing Ws-2, *dyx*, Col-0, as well as the sinapate ester mutant, *fah1-2* and the flavonoid-lacking mutant, *tt4-8*, retained a high germination capacity after the exposure to UV-B + UV-A light. However, the differences in the response to UV-B + UV-A light among different seed lines were observed through the smaller changes ingermination dynamics. Compared to the Ws-2 wild type line, small changes in germination speed in the Col-0 wild type line and the control T-DNA insertion mutant, *dyx*, were only obvious when seeds were germinated under stress conditions (suboptimal temperature).

The effects of UV-B + UV-A light were more pronounced in the *fah1-2* line, which exhibited lower seed vigour and higher percentage of abnormally developed seedlings. This indicated the importance of sinapate esters in the UV protection.

The seed vigour in flavonoid-lacking *tt4-8* line was more seriously affected by UV-B + UV-A radiation, showing about 100 times higher sensitivity, compared to *fah1-2* seeds. We concluded that in *Arabidopsis* seeds, flavonoids provide greater protection than sinapate esters against UV-B + UV-A radiation.

Furthermore, our results showed that the germination and the early-seedling stages are the two critical and very sensitive phases in plant development. They reveal whether or not plants can cope with damage accumulated in the quiescent seeds. Depending on the degree and type of damage, on the one hand, and the efficiency in protection and damage repair, on the other hand, these early developmental phases are decisive for further plant development. All putative molecular and cellular damages that accumulated in dry seeds during UV-B + UV-A irradiation were either reversed or successfully repaired in all flavonoid-containing *Arabidopsis* lines, since plants continued with their normal development, reaching maturity. This was not the case in the flavonoid-lacking *tt4-8* mutant, in which UV-B + UV-A radiation affected the plant survival, vegetative growth and reproductive capacity.

18.3. Effects of UV-C radiation on *Arabidopsis* seeds, determined at three plant developmental stages

The aim of our experiments was to determine the response of *Arabidopsis* seeds to highly energetic UV-C (λ = 254 nm) radiation, observing three different stages of plant development: the germination stage, the early-seedling stage and the stage of plant development. Little is known about the response of plant seeds to UV-C light, which does not endanger present-day terrestrial biota. However, the effects of highly energetic UV-C light are of great photobiological and astrobiological concern (see chapter **1**, section **3.3**). We were especially interested in this part of spectrum in the context of the preparation for the EXPOSE-EuTEF and EXPOSE-R space experiments (for details see chapter **1**, section **2**), in which our seed samples were exposed to the full solar UV emission spectrum at λ>110 nm, including the highly energetic UV-C wavelengths. The expected UV fluence in the EXPOSE experiments was about 1.5 x 10^5 kJm^{-2}, which was calculated for 377.4 solar constant hours (1.5 years of a mission duration), and integrated for the UV range 200-400 nm (Rabbow, 2007a). We reasoned that UV-C (λ = 254 nm) light is among the wavelengths that causes the most damaging effects due to the high absorbance of DNA in the region around 260 nm, which leads to a direct excitation of DNA and induction of severely damaging lesions. Therefore, in our laboratory experiments we attempted to simulate a worst-case scenario by exposing *Arabidopsis* seeds to monochromatic UV-C_{254} light with exceptionally high fluences in the range of 10^5 kJm^{-2}, which corresponded to the integrated fluence of polychromatic solar UV light (λ = 200-400 nm), expected in the EXPOSE experiments. The Ws-2 and *dyx* seeds were irradiated for 30 days (UV-C = 3.1 x 10^5 kJm^{-2}) and 60 days (UV-C = 6.0 x 10^5 kJm^{-2}), while the Col-0 and *fah1-2* seeds were exposed for 40 days (UV-C = 3.5 x 10^5 kJm^{-2}) and 60 days (UV-C = 4.8 x 10^5 kJm^{-2}). UV-C light represented 90% of the incident light in our experiments, and since we were unable to filter out the remaining concurrent part of UV-B + UV-A light, we actually measured the combined effects of UV-C + (UV-B + UV-A) light. UV-B + UV-A light represented only a minor part of incident light. Nevertheless, comparing the results from the UV-B + UV-A exposure experiments and that obtained from the UV-C + (UV-B + UV-A) experiments, we concluded about the effects of the dominant UV-C part of the emitted light.

The germination stage

Our results clearly demonstrated the extreme resistance of dry *Arabidopsis* seeds to quasi-monochromatic UV-C_{254} light, since neither UV-C + (UV-B + UV-A) nor the UV-B + UV-A part of the emitted light affected the germination capacity ($G_{max\%}$) in all examined flavonoid-containing seed lines (Ws-2, *dyx*, Col-0 and *fah1-2*), as seen in **Fig. 62E-H**. On exposure to extremely high fluences of UV-C light, up to 6.0 x 10^5 kJm^{-2} (Ws-2 and *dyx* lines) or 4.8 x 10^5 kJm^{-2} (Col-0 and *fah1-2* lines), all these seed samples exhibited high values of $G_{max\%}$ (93-100%), which did not differ from those of the respective dark control samples (**Fig. 63E-H**). This result was further confirmed in germination tests performed under suboptimal temperature conditions (**Fig. 65E-H**). A high UV-C resistance of dry *Arabidopsis* wild type seeds was also described by A. B. Britt (personal communication), where no inhibition of germination is observed in seeds irradiated for 96 hours at the UV-C fluence of 8.986 x 10^3 kJm^{-2}. Although it is considered a particularly high fluence, in comparison to those used previously in the UV-C exposure studies on seedlings and plants (Jenkins et al., 1995; Murphy, 1997; Tiunaitienė et al., 2002; Preuss and Britt, 2003; Iriti et al., 2007), the fluences used in our study are about two orders of magnitude higher than that used by A. B. Britt. It is important to note that even these extreme fluences of UV-C light did not have an inhibitory effect on the germination of *Arabidopsis* seeds.

Although the germination capacity was not affected, our results showed that UV-C + (UV-B + UV-A) radiation had, however, an effect on the vigour of the Ws-2, *dyx*, Col-0 and *fah1-2* seeds (**Fig. 62E-H**). The germination process in irradiated seeds was slowed down, as measured by the increase in the mean germination time (MGT) (**Fig. 64E-H**). Since the UV-B + UV-A part of the incident light had no effect on the MGT in the Ws-2 line, and only slight effects in the *dyx* and Col-0 lines (see discussion above in section **18.2**), changes in MGT after irradiation of seeds with entirely transmitted UV-C + (UV-B + UV-A) light was essentially attributed to the dominant UV-C component.

The wild type Ws-2 and Col-0 seeds appeared the most resistant. The Ws-2 seeds showed no change in germination speed was observed after 30 days of UV-C exposure (**Fig. 64E**). However, at the highest fluence of UV-C light (6.0 x 10^5 kJm^{-2}) the germination of Ws-2 seeds slowed down for 6.6 hours (20.5% increase in MGT). In the Col-0 irradiated seeds, the MGT increased for 16.3% already after 40 days of UV-C exposure (3.5 x 10^5 kJm^{-2}). At the maximal UV-C fluence, reached after 60 days of irradiation, the MGT increased for 19.5% (**Fig. 64G**). The differences in the germination speed became more pronounced in seeds that were

germinated under temperature suboptimal conditions (**Fig. 65E** and **G**, as well as **Fig. 66E** and **G**). Comparing the UV-C response of two wild type Ws-2 and Col-0 seeds that were germinated at suboptimal temperature (10°C), we found that the latter appeared more resistant, since at the maximal UV-C fluence achieved after 60 days of irradiation, the MGT increased for 34.5% and 20.3%, respectively. Slight differences in seed vigour between these two ecotypes were also observed in the UV-B + UV-A exposure experiments, although they were detected only under suboptimal conditions (see discussion above, section **18.2**). These differences in UV response were likely due to naturally occurring genetic variations, observed in many plant species, including different *Arabidopsis* ecotypes (Torabinejad and Caldwell, 2000; Cooley et al., 2001; Koornneef et al., 2004). These differences could be due to small variations in the chemical composition of the seeds and/or the efficiency of detoxification and repair systems. The water content might be one of the important factors in determining the level of resistance in seeds (see discussion above). The Ws-2 and Col-0 seeds that were used in our UV exposure experiments had a similar water content, 5.7% and 5.3%, respectively, thus we concluded that it was not the cause of the observed variations in UV-C sensitivity. Variations in the types and amounts of UV absorbing compounds might play an important role in the level of UV protection in different plant ecotypes. For instance, Lepiniec et al. (2006) reported differences in the total flavonoid content in *Arabidopsis* seeds of the Ws-2 (~ 15 mg g^{-1} seed) and Col-0 (~ 13.2 mg g^{-1} seed) ecotypes.

A T-DNA control mutant, *dyx*, appeared more sensitive to UV-C light than the Ws-2 background (**Fig. 64F**), since germination was slowed down already after 30 days of exposure (33.9% increase in MGT). Comparing the germination speed as the measure for the seed vigour, we found that the *dyx* seeds were 2.85 times more sensitive to UV-C_{254} light than the Ws-2 background. This unexpected difference in the vigour of the Ws-2 and *dyx* seeds could be related to pleiotropic effects caused by the random insertion of a T-DNA into the Ws-2 genome. This in turn might affect the chemical and biochemical composition of the seeds and/or the activity of the systems involved in coping with UV-induced damage. Further genetic, metabolic and chemical studies are necessary to determine the effects of T-DNA insertion on the gene expression, chemical content and physiology of *dyx* seeds.

In addition to observed extreme resistance of *Arabidopsis* dry seeds to UV-C radiation, in this work we also determined *in vivo* the contribution of UV-absorbing compounds, including flavonoids and sinapate esters, in such a high level of UV-C tolerance. Many studies in the literature describe the UV-B protective capacities for these two groups of UV-screening

compounds (Chapple et al., 1992; Li et al., 1993; Landry et al., 1995; Rao et al., 1996; Sheahan, 1996). In addition, these studies focused on the UV protection efficiency of flavonoids and sinapate esters in the vegetative and aerial parts of plants, rather than in seeds. In our work, this is extended in the UV-C part of spectrum by testing the UV resistance of two *Arabidopsis* mutant seeds, *fah1-2* and *tt4-8*, former deficient in sinapate esters and latter in flavonoids.

Our results showed high UV-C resistance in sinapate ester-lacking seeds, *fah1-2*, since the germination capacity ($G_{max\%}$) remained at the maximal level (about 100%), even after 60 days of irradiation (UV-C = 4.8 x 10^5 kJm^{-2}), as seen in **Fig. 63H**. However, the exposure of *fah1-2* seeds to UV-C + (UV-B + UV-A) light affected markedly germination dynamics in this mutant line (**Fig. 62H**). The *fah1-2* seeds exhibited an increase in MGT of 67.5% (10.2 hours of delay in germination) after 40 days of irradiation (**Fig. 64H**). These sinapate ester-lacking seeds showed 4.78 times higher sensitivity to UV-C + (UV-B + UV-A) radiation than the Col-0 background. Germination under suboptimal conditions revealed even more pronounced differences in vigour between the irradiated and the dark control *fah1-2* seeds (**Fig. 66H**). Since the UV-B + UV-A component of the incident light was found to have an effect, although to a lesser extent, on the germination speed of *fah1-2* seeds, the results of the UV-C + (UV-B + UV-A) exposure experiments should be interpreted with caution, taking into account possible combined effects of dominant UV-C light and the background UV-B + UV-A light on seed vigour. Other parameters of germination dynamics were similar to the MGT parameter (**Table 15**). An interesting effect of UV-C + (UV-B + UV-A) light was observed on the skewness of the *fah1-2* germination curve. In contrast to the Col-0, Ws-2 and *dyx* seeds, a positive shift in germination skewness was observed in the irradiated *fah1-2* samples, indicating that the germination process in these seeds was seriously delayed, mostly in the first half of the germination period. This phenomenon was not detected after the exposure to only UV-B + UV-A portion of incident light. It suggested that after UV-C exposure, the *fah1-2* seeds suffered from a larger amount of accumulated damage to DNA and other essential macromolecules (RNAs, proteins and lipids), so that the time required to detoxify, repair or to *de novo* synthesise damaged molecules in the beginning of the germination period (see chapter **1**, section **4.2.2**) probably slowed down seriously the germination process.

Our study on *fah1-2* seeds clearly demonstrated the role of sinapate esters in the UV protection. The differences in seed vigour of irradiated *fah1-2* and Col-0 seeds suggested that sinapate esters provide important protection against extremely high fluences of UV-C light. Sinapate esters are described in the literature to provide efficient direct UV-B screening

protection in *Arabidopsis*, as well as indirect protection, acting as antioxidant agents and free radical scavengers (Landry et al., 1995; Sheahan, 1996). Here we evaluated for the first time the efficiency of sinapate esters in the UV-C protection of dry *Arabidopsis* seeds. However, since germination of sinapate ester-deficient seeds was not inhibited by the high fluences of UV-C radiation or by the UV-B + UV-A component of emitted light, we suggest that other protective compounds in *fah1-2* seeds, such as flavonoids, could provide an additional level of UV protection.

In contrast to the *fah1-2* seeds, we demonstrated that the flavonoid-lacking *tt4-8* seeds were extremely sensitive to UV-C + (UV-B + UV-A) light. It affected not only the germination speed, as seen in other flavonoid-containing seeds, but it also had a strong adverse effect on germination capacity ($G_{max\%}$), as seen in **Fig. 68C** and **Fig. 69C**. A statistically significant decrease in $G_{max\%}$ (83%) was observed already after 3 hours of exposure (UV-C = 1.7 x 10^3 kJm^{-2}), as seen in **Fig. 69C**. At the maximal UV-C fluence of UV-C = 5.9 x 10^4 kJm^{-2}, which corresponded to 139 hours of irradiation, the $G_{max\%}$ dropped to only 13%. Almost all *tt4-8* seeds that remained ungerminated after exposure to UV-C light were dead, since no metabolic activity was detected by the tetrazolium viability test (**Table 17**). As the UV-B +UV-A part of the light did not affect germination capacity (**Fig. 69B**), the inhibitory effect on seed germination was attributed to the highly energetic UV-C part of emitted light. These results showed that the flavonoid-lacking *tt4-8* seeds were at least two orders of magnitude more sensitive to UV-C radiation than the flavonoid-containing seeds, including the Ws-2 (background line), the *dyx* (T-DNA insertion control mutant) and the Col-0 wild type, as well as the sinapate ester mutant, *fah1-2*. It is important to note that in contrast to the *tt4-8* mutant, all of flavonoid-containing seeds did not exhibit reduced germination capacity even at the highest fluences reached after 60 days (1 440 hours) of exposure to UV-C radiation. In addition to $G_{max\%}$, the exposure to UV-C + (UV-B + UV-A) light slowed the germination speed of the *tt4-8* seeds (**Fig. 71C**). The low fluences of UV-B + UV-A light did not affect the germination dynamics of the *tt4-8* seeds (**Fig. 71B** and **Table 16**). Therefore, the effects observed up to 5 hours of irradiation, were due to the dominant UV-C part of the incident light. The exposure to very low UV fluences, reached after only 0.5 hours of irradiation, resulted in a significant delay in germination for 18.9 hours (111% increase in MGT), as seen in **Fig. 71C**. The germination of irradiated *tt4-8* seeds further slowed, as the duration of UV exposure increased up to 5 hours (UV-C = 2.8 x 10^3 kJm^{-2}). Surprisingly, at the higher fluences of UV-C + (UV-B + UV-A) radiation, after more than 5 hours of exposure, the MGT followed a nonlinear dose-response trend. This phenomenon might be explained by the complex interaction of several factors acting concurrently at the higher UV fluences. One of the

possible reasons might be the partial overlap of two UV response phenomena, the slowing down of germination and the decrease in the maximal percentage of germinated seeds. The nonlinear dose-response behaviour of the MGT parameter at higher UV fluences might also result from possible combined effects, which are not necessarily additive, of the dominant UV-C part of light (**Fig. 71C**), the UV-B + UV-A component of light (**Fig. 71B**) and the problem of accelerated ageing of the *tt4-8* seeds, observed after 48 and 139 hours of treatment (**Fig. 71A**). Other parameters of germination dynamics, such as $T_{50\%}$ and $T_{75\text{-}25\%}$, also showed nonlinear response in the *tt4-8* seeds exposed to the higher UV doses (**Table 16**). A nonlinear UV dose-response behaviour is often observed in complex biological systems, in contrast to the linear dose-response known for many photochemical reactions studied *in vitro* systems (Setlow, 1974; Sutherland, 2002). In biological systems, the UV dose response represents the sum of different photochemical and photobiological processes; it includes no only the processes of damage induction to different types of molecules, but it also involves various detoxification mechanisms, as well as repair systems.

The results from our study clearly demonstrate the importance of flavonoids in UV protection, especially in the highly energetic UV-C part of the spectrum. Observing the germination stage, we found that flavonoids provided at least two orders of magnitude higher UV-C protection to *Arabidopsis* seeds than sinapate esters. Flavonoids also exhibited a greater effectiveness, by 2 orders of magnitude, than sinapate esters in protection of *Arabidopsis* seeds from UV-B + UV-A radiation (for details see discussion above, section **18.2**). These findings corroborated our results from UV absorption spectroscopy studies, performed both in solution and in dry films (**Fig. 55B** and **Fig. 57A,** chapter **3,** for details see discussion **I**, chapter **4**, section **14**). It supported our hypothesis that flavonoids could be considered as ideal UV screens (Zalar et al., 2007b; Zalar et al., 2007c). A flavonol, quercetin-3-*O*-rhamnoside (quercitrin), and the proanthocyanidins (condensed tannins) are the major flavonoid constituents of *Arabidopsis* seeds. They are predominantly concentrated in the seed coat, protecting the embryo and its genomic DNA from damage (Lepiniec et al., 2006; Routaboul et al., 2006). Our UV absorption studies indicated that glycosylated flavonoids, such as quercitrin, due to high absorption in the UV-C part of the spectrum and an absorption maximum close to that of DNA in region I, would provide efficient direct screening protection (**Fig. 55A** and **Fig. 57**, chapter **3**, sections **11.4.1.2** and **11.4.2.2**, respectively). Furthermore, our spectroscopy studies implied that glycosylated flavonoids would also screen efficiently in the UV-B and UV-A regions due a of broad absorption peak in the 300-400 nm region, with the local maximum at about 350 nm. Additional evidence for the importance of seed coat and flavonoids in direct UV screening protection is

reported in our previous work (Zalar, 2004). For instance, the exposure of the flavonoid-deficient *tt4-8* seeds to UV-C_{254} light that was filtered through dry layers of different flavonoids, placed above the seeds, showed that these compounds can improve the UV resistance of the *tt4-8* seeds. Furthermore, in the same work it was demonstrated that the removal of the seed coat from both the *tt4-8* mutant and the Ws-2 wild type embryos increases their sensitivity to UV-C_{254} light. Besides screening protection, both groups of flavonoids, glycosylated flavonoids and condensed tannins, are known to act as strong antioxidant agents and free radical scavengers, also providing efficient indirect protection to DNA and other biologically important molecules (Landry et al., 1995; Montesinos et al., 1995; Ryan et al., 2001; Lepiniec et al., 2006).

The early-seedling stage

The analysis of the early-seedling stage was undertaken to determine whether the exposure of seeds to UV-C + (UV-B + UV-A) light affected subsequent growth and development of *Arabidopsis* seedlings. Although we found that UV-B + UV-A light had no effect (Ws-2 and *dyx*) or just a small effect (Col-0) on subsequent seedling development, the exposure of *Arabidopsis* seeds to UV-C + (UV-B + UV-A) light affected significantly seedling development in the Ws-2 and *dyx* lines, and surprisingly, to a much lesser extent the development of seedlings in the Col-0 line (**Fig. 72E-G**). We concluded that the observed abnormal development was caused mostly by UV-C light. After 30 days of irradiation (UV-C = 3.1 x 10^5 kJm^{-2}), more than 50% of the exposed Ws-2 and *dyx* seeds developed abnormal seedlings. This was even more pronounced at the maximal UV-C fluence reached after 60 days of irradiation (6.0 x 10^5 kJm^{-2}), where irradiated seeds developed 57% (Ws-2) and 64% (*dyx*) of abnormal seedlings, respectively (**Fig. 72E** and **F**).Different types of seedling damage were observed in the UV-C exposed samples, mostly concerning hypocotyl and root growth (**Fig. 75** and **Fig. 76E-G**). The majority of abnormal Ws-2 and *dyx* seedlings exhibited short or twisted hypocotyls, but normally developed roots (**Fig. 75C**). Some of seedlings, besides having damaged hypocotyls, they developed short roots (**Fig. 75D** and **Fig. 76E-F**), or even seriously retarded roots (**Fig. 75E** and **Fig. 76E-F**). These findings are in accordance with several previous studies on the effects of UV-C light on seedling growth and development. Like the effects of UV-B exposure, UV-C radiation induced an inhibition of hypocotyl elongation in the irradiated seedlings of several plant species, including lettuce, tobacco, radish and cucumber (Lapointe et al., 1996; Kobzar et al., 1998; Hirokazu et al., 1999; Shinkle et al., 2005). There is also evidence that UV-C radiation affects root growth in *Arabidopsis* seedlings (Al Khateeb and Schroeder, 2009). However, in all of these studies, seedlings were directly exposed to UV-C radiation, as opposed to seedlings

grown from irradiated seeds (the present report). Among the most serious damage in the Ws-2 and *dyx* lines, we observed seedlings with short hypocotyls and missing roots (**Fig. 75F** and **Fig. 76E**). In addition, a small, but statistically significant percentage of the Ws-2 seeds that were exposed to the maximal UV-C fluence developed into heavily damaged seedling forms with no hypocotyl, no roots and undeveloped cotyledons (**Fig. 75G** and **Fig. 76E**). Besides the increased number of seedlings with morphological abnormalities, our results demonstrated that UV-C light has an inhibitory effect on the growth of primary roots in normal Ws-2 and *dyx* seedlings, developed from irradiated seeds (**Fig. 79E** and **F**). After exposure to a lower UV-C dose, the Ws-2 and *dyx* samples developed 16% shorter primary roots, while more than a 43% reduction in the length of the seedling roots was observed in samples that were irradiated for 60 days. Similar inhibitory effects of UV-C radiation on root growth was described in *Arabidopsis* wild type seedlings that were directly irradiated with UV-C light at fluences as low as 0.5-1.5 kJm^{-2} (Al Khateeb and Schroeder, 2009). Our results indicate that the seeds of the Ws-2 wild type and the T-DNA insertion control (*dyx*) had, in spite of the genetic difference, similar growth responses to UV-C radiation.

Surprisingly, the Col-0 wild type appeared more robust than the Ws-2 line to the effects of UV-C light on early-seedling development, since only 15% of the irradiated Col-0 seeds developed abnormal seedlings after 60 days of exposure (**Fig. 72G**), and UV-C radiation induced less severe seedling damages than in the Ws-2 line. The major type of UV-C induced seedling damage in the Col-0 line concerned the development of the hypocotyl (short or twisted hypocotyl), while other seedling structures remained mostly unaffected (**Fig. 75C** and **Fig. 76G**). In addition, the exposure of the Col-0 seeds to UV-C radiation did not affect the growth of primary roots in developed early-stage seedlings (**Fig. 79G**). Thus, although the Col-0 and Ws-2 wild type seeds exhibited asimmilar level of UV resistance at the germination stage (see discussion above), the Col-0 line appears to be more resistant to the effects of UV-C at the early-seedling stage. This indicates that Col-0 seeds, although containing to some extent less (~12%) flavonoids (Lepiniec et al., 2006; Routaboul et al., 2006), this wild type line might have more efficient detoxification and/or damage repair systems than the Ws-2 line. The repair of DNA and organelles, as well as *de novo* synthesis of macromolecules, occurs in the early phases of germination process prior the radicle protrusion (see **Fig. 24**, chapter **1**, section **4.2.2.**). It could explain why irradiated seeds required a longer time to germinate in order to repair more efficiently all accumulated damage and to replace damaged molecules by the newly-synthesised molecules, prior the radicle emergence and further development of seedlings. However, further comparative studies at molecular level would be necessary in order to determine the origin of

ecotypic differences between the Ws-2 and the Col-0 line, including the quantification and determination of the types of DNA lesions, as well as studying the expression and activity of antioxidant enzymes POD, CAT and SOD in irradiated dry seeds and developed seedlings.

Unlike the Col-0 background, the sinapate ester mutant, *fah1-2*, appeared less resistant to UV-C + (UV-B + UV-A) radiation, not only at the level of germination, but also at the level of subsequent early-seedling development. After 60 days of UV exposure, 60% of the irradiated *fah1-2* seeds developed into abnormal seedlings (**Fig. 72H**). Most of the damaged seedlings exhibited an altered hypocotyl morphology (short or twisted hypocotyl), which occurred alone or in combination with short primary roots (**Fig. 75C-D** and **Fig. 76H**). Although more sensitive than the Col-0 background, irradiated *fah1-2* seeds did not develop seedlings with the heavily damaged essential structures, observed in the Ws-2 wild type (**Fig. 76E-H**). Even though we found that the UV-B + UV-A component of the incident light had some effects on seedling development after 60 days of irradiation of the *fah1-2* seeds (**Fig. 72D**, for details see discussion above, section **18.2**), its contribution was relatively small in comparison to the effects of UV-C + (UV-B + UV-A) light (**Fig. 72H**). Therefore, we suggested that these effects might be mainly due to the dominant UV-C light, but the possibility to the combined effects of UV-C and UV-B + UV-A radiation, which might not be simply additive, has also to be taken into consideration. In contrast to the Col-0 line, UV-C radiation has an inhibitory effect on the root growth of normal *fah1-2* seedlings developed from irradiated seeds (**Fig. 79H**). The UV-B + UV-A part of the light did not contribute to this effect (**Fig. 79D**). The average root length in the population of *fah1-2* seedlings decreased after 40 days of irradiation, and exposure to the maximal fluence of UV-C radiation (60 days of exposure) resulted in a 25% reduction of root length. In spite of differences in the UV-C response at the stage of the early-seedling development, between the Col-0 and *fah1-2* lines, this sinapate ester-deficient mutant exhibits a relatively high resistance to UV-C radiation, in comparison to the flavonoid-deficient mutant (see below). We suggested that the flavonoids, as the major UV-screening and detoxification compounds, largely contributed to this phenomenon.

Similarly to the germination stage, the flavonoid-lacking mutant, *tt4-8,* exhibited a high level of UV-C sensitivity with respect to subsequent seedling development and primary root growth. The root growth in seedlings that developed from irradiated *tt4-8* seeds was seriously inhibited by UV-C radiation (**Fig. 80B**). We found that the UV-B + UV-A part of the incident light, after 139 hours of exposure, did not affect the development of essential seedling structures nor the growth of primary roots in exposed *tt4-8* samples (**Fig. 73A** and **Fig. 80A**). Increasing

UV-C fluences from 2.8 x 10^2 kJm^{-2} (0.5 hours of exposure) up to 5.9 x 10^4 kJm^{-2} (139 hours of exposure) caused a decrease in the percentage of normal seedlings and, as expected, a progressive increase in the percentage of ungerminated seeds (**Fig. 74**). The percentage of abnormal *tt4-8* seedlings increased linearly up to 2 hours of UV-C exposure. Surprisingly, at the higher doses the percentage of abnormally developed seedlings did not follow the linear trend in the UV-C dose-response (**Fig. 74**). A non-linear behaviour was also observed at the germination stage, measuring the parameters of germination dynamics, MGT, $T_{75\text{-}25\%}$ and germination skewness (**Fig. 71C** and **Table 16B**). From the dose-response curve presented in **Fig. 74**, it can be observed that the percentage of abnormal seedlings remained constant in the UV-C fluence range between 1.7 x 10^3 kJm^{-2}and 2.8 x 10^3 kJm^{-2}, corresponding to irradiation from 3 to 5 hours. The same fluence range is paralleled by the prominent increase in MGT and $T_{75\text{-}25\%}$ values, and significant decrease in germination skewness (**Fig. 71C** and **Table 16B**). This might indicate that the slowing down of germination occurred, especially in the first half of the germination period, possibly due to the activation of detoxification/repair systems, which enabled keeping relatively constant the number of abnormal seedlings. Above the threshold UV-C fluence, reached after 10 hours of exposure (4.0 x 10^3 kJm^{-2}), the efficiency in damage repair might have declined in germinating *tt4-8* seeds, since sudden increase in percentage of abnormal seedlings up to 83% was paralleled with sudden faster germination speed (decrease in MGT and $T_{75\text{-}25\%}$ and increase in skewness) (**Fig. 71C** and **Fig. 74**). The non-linearity phenomenon of UV dose-response functions for biological endpoints was also discussed by Setlow (1974) and Sutherland (2002). These authors pointed out that although many photochemical reactions are linear within the biologically relevant range of UV doses, many biological responses exhibit a more complex, non-linear dose-response due to the combined effects of direct DNA damage, repair and multiple interactions of photochemical reactions, such as photoreactivation and the induction of indirect DNA damage.

In our study, we found that the exposure of the *tt4-8* seeds to increasing fluences of UV-C light induced a variety of different types of seedling damage, ranging from the less severe at the lowest UV-C dose, such as altered hypocotyl morphology (hypocotyl short or twisted), up to seriously damaged seedlings with missing hypocotyls, missing roots and undeveloped cotyledons, observed at the higher fluences (**Fig. 75** and **Fig. 78**). After 10 hours of UV-C exposure (4.0 x 10^3 kJm^{-2}), the *tt4-8* seeds were seriously damaged, so that the percentage of heavily damaged seedlings and ungerminated seeds increased markedly. No normal *tt4-8* seedlings developed from the seeds irradiated with UV-C fluences greater than 2.1 x 10^4 kJm^{-2}.

This means that further development of mature plants is hardly to be expected in the *tt4-8* samples exposed to high doses of UV-C radiation.

Compared to the effects of seed irradiation on the subsequent development of the Ws-2 and *fah1-2* seedlings, these results confirm the importance of flavonoids in UV-C protection. They appear to be more efficient UV-C protectors in *Arabidopsis* seeds than sinapate esters.

The plant development stage

We also examined whether or not irradiated seeds are capable of developing into healthy, mature plants. The chances of plant survival largely depend on the degree and the type of damage, as well as on the efficiency in protection and damage repair during the early-seedling stage. Therefore, irradiated seeds were germinated in the soil and the growing seedlings were allowed to develop under greenhouse conditions up to the stage of mature plants.

We found that in contrast to the UV-B + UV-A component of the incident light, the exposure of seeds to UV-C + (UV-B + UV-A) radiation had a strong inhibitory effect on subsequent plant growth and development in all examined *Arabidopsis* lines. Therefore, the dominant UV-C part of the incident light is responsible for the significant decrease in the percentage of survived Ws-2, Col-0 and *fah1-2* plants grown from 60-day irradiated seeds (**Fig. 81A-C**). The plant survival rates indicate that the Col-0 line (72% survival) is more resistant to UV-C radiation than the Ws-2 line (53% survival), but that both wild type lines are more resistant than the sinapate ester mutant, *fah1-2* (45% survival), as seen in **Table 18**. These results showed that sinapate esters are important UV-C protective compounds in *Arabidopsis* seeds, capable of improving the survival rates of plants grown from irradiated seeds.

Like at the stage of early-seedling development, the plant development stage showed that the Col-0 line better tolerates exposure to UV-C radiation. Compared to the Ws-2 line, the higher plant survival rate in the Col-0 line suggested that this wild type line might have a more efficient repair system, in spite of a putatively lower UV screening capacity related to the lower concentration of flavonoids in the Col-0 seeds (Lepiniec et al., 2006; Routaboul et al., 2006). Besides the plant survival rate, the exposure of seeds to UV-C radiation also affected the vegetative growth and reproductive output of *Arabidopsis* plants (**Fig. 81**). Exposure of *Arabidopsis* seeds to high fluences of UV-C (up to 60 days of exposure) inhibited the growth of developing plants. Significantly reduced height of mature plants was detected in all studied

genotypes (**Fig. 81G-I**). In addition, the exposure of seeds to UV-C led to a reduction in the percentage of fertile plants (**Fig. 81D-F)**. Similar effects on plant growth and reproductive output were previously reported in numerous studies concerning plant responses to an enhanced level of UV radiation (reviewed by Day, 2001). The reduced plant growth under enhanced UV radiation is likely related to the costs involved in the production of secondary metabolites, the repair of DNA or membrane damage and the scavenging of free radicals (Rozema et al., 1997b; Treutter, 2006).

The exposure of the *tt4-8* seeds to UV-C light had an extreme inhibitory effect on subsequent plant growth and development in this flavonoid-lacking mutant (**Fig. 82D-F**). The plant survival rate in the *tt4-8* line was seriously reduced (54% survival) after only 1 hour of irradiation (5.3 x 10^2 kJm^{-2}), and fluences above 2.8 x 10^3 kJm^{-2} resulted in 0% plant survivors (**Fig. 82D**).These results indicate that the flavonoid-deficient mutant is about 1000 times more sensitive than the Ws-2 background, and about 300 times more sensitive than the sinapate ester mutant.

Concluding remarks (7)

Our results revealed the extreme resistance of dry *Arabidopsis* seeds to quasi-monochromatic light emitted from the UV-C_{254} source. We found that even after 60 days of irradiation (UV-C fluences up to 6 x 10^5 kJm^{-2}), *Arabidopsis* seeds retained a high and unaltered germination capacity. To our knowledge, this is the first report of such a high UV-C resistance encountered among all known terrestrial life forms. Nevertheless, in spite of their high germinability, irradiated seeds started to show a decline in the seed vigour, which was manifested through a slightly slower germination process and a lower germination uniformity. Small differences in vigour of UV-C irradiated seeds, observed between two wild type lines, Ws-2 and Col-0, were likely due to naturally occurring genetic variations that are common among different *Arabidopsis* ecotypes e.g. occurrence of differences in seed physiology, their chemical composition and efficiency in repair and detoxification systems. Further comparative chemical analyses of seed content, particularly of the major UV screening compounds in seeds (flavonoids and sinapate esters), would be necessary to elucidate small differences in the UV response of the Ws-2, Col-0 and *dyx* seeds. Greater differences in seed vigour, observed between the sinapate ester mutant, *fah1-2*, and the wild type line, indicated the importance of sinapate esters in protection of seeds against UV-C radiation.

Unlike all tested flavonoid-containing seeds, the flavonoid-lacking mutant, *tt4-8*, exhibited a remarkably higher sensitivity to UV-C radiation. The UV-C fluences as low as 1.7×10^3 kJm^{-2} affected significantly the germination capacity of the *tt4-8* seeds, and only 13% of seeds germinated after exposure to UV-C = 5.9×10^4 kJm^{-2}. The present study clearly demonstrates the importance of flavonoids in the UV-C protection. Observing the germination stage, we found that flavonoids provide at least 2 orders of magnitude higher UV-C protection in *Arabidopsis* seeds, compared to sinapate esters. These *in vivo* results are in good agreement with our UV spectroscopy results (see discussion **I**, chapter **4**, section **14**).

At the germination stage, we determined the scale of UV-C tolerance for different seed lines as follows: Col-0 ≥ Ws-2 > *dyx* > *fah1-2* >> >*tt4-8*.

Our study also demonstrated that the exposure of *Arabidopsis* seeds to the high UV-C fluences had an important impact on subsequent seedling development, increasing the number of abnormal seedlings. Damaged seedlings exhibited mostly changes in hypocotyl and root growth. At the early-seedling stage, the Col-0 wild type appeared more resistant than the Ws-2 line. We suggested that in spite of lower seed flavonoid content, the Col-0 line might have more efficient detoxification and/or repair mechanisms. However, further studies at molecular level would be necessary to determine the differences in the number and types of UV-induced damage among different genotypes. The molecular damage should be measured before imbibition (in dry irradiated seeds) and after the germination (in early-stage seedlings). The efficiency of detoxification mechanisms could be further determined by mesuring the ROS production (e.g. by using ROS specific probes), as well as by measuring the activity of detoxification enzymes (POD, CAT, SOD etc.) in both the irradiated dry seeds and early-stage seedlings.

At the stage of early-seedling development, the flavonoid-lacking *tt4-8* mutant exhibited, as expected, a high sensitivity to UV-C radiation, developing a high percentage of seriously damaged seedlings. No normal seedlings developed from *tt4-8* seeds that were exposed to UV-C at fluences above 2.1×10^4 kJm^{-2}.

At the stage of early-seedling development, we determined the following scale of UV-C resistance for different *Arabidopsis* genotypes: Col-0 > Ws-2 = *dyx* ≥ *fah1-2* >> > *tt4-8*.

Our in-soil experiments demonstrated that UV-C light had a strong inhibitory effect on vegetative growth and reproductive output in *Arabidopsis* plants developed from irradiated

seeds. We determined a higher plant survival rate in the Col-0 (72%) than in the Ws-2 (53%) line, suggesting that the former wild type line exhibited a higher level of the UV-C resistance, possibly due to more efficient detoxification and/or repair systems (see above). Comparing the UV-C resistance at the stage of plant development for the sinapate ester-lacking mutant, *fah1-2*, and the flavonoid-lacking mutant, *tt4-8*, we confirmed that flavonoids, as the major UV screens in *Arabidopsis* seeds, provide more efficient UV-C protection than sinapate esters.

At the stage of plant development, we determined the scale of UV-C resistance for different *Arabidopsis* genotypes as follows: Col-0 > Ws-2 > *fah1-2* >> >*tt4-8*.

18.4. UV-C resistance of *Arabidopsis* seeds compared to other highly resistant life forms, including *Bacillus subtilis* spores

According to present study, dry seeds can be considered as extremely resistant terrestrial life forms, which can survive exposure to particularly high fluences of damaging UV-C light. Plant vegetative forms, such as seedlings and mature plants that are directly subjected to UV-C radiation show severe damage even at much lower UV doses that those used in our seed exposure experiments. For instance, the exposure of *Arabidopsis* seedlings to UV-C fluences of 10-50 kJm^{-2} is found to induce apoptotic-like changes and DNA fragmentation. Jenkins (1995) reported that exposure of *Arabidopsis* seedlings to UV-C fluence as low as 3.2 kJm^{-2} has a lethal effect on 50% of wild type seedlings (LD_{50}). Compared to this, our results showed that wild type *Arabidopsis* seeds have at least 2 x 10^5 times higher UV-C resistance than seedlings, since no lethal effect was detected in irradiated seeds at fluences as high as UV-C = 6.0 x 10^5 kJm^{-2}. In contrast, flavonoid-lacking mutant seeds appeared much more sensitive to UV-C radiation (see chapter **5**, section **16.2.2**). Nevertheless, determining the LD_{50} from the UV-C dose response curve for *Arabidopsis tt4-8* seeds (LD_{50} = 6.2 x 10^3 kJm^{-2}) (**Fig. 70**), we found that even UV sensitive flavonoid-deficient seeds were about 2 x 10^3 times more resistant than irradiated flavonoid-containing vegetative forms (wild type seedlings).

Arabidopsis dry seeds were also found to be extremely UV resistant in comparison to other organisms and life forms, in particular those which are used in astrobiological studies as terrestrial models known to withstand extreme conditions. For instance, we found that wild type

Arabidopsis seeds were at least 10^6 times more resistant than dry spores of *Bacillus subtilis*. Our experiments showed that a UV-C fluence as low as 0.5 kJm^{-2} killed 99.6% of *Bacillus subtilis* WT 168 spores (**Fig. 60B**). From the UV-C dose response, we also determined a lethal dose that inactivated 50% (LD_{50} = 0.123 kJm^{-2}), as well as 90% (LD_{90} = 0.245 kJm^{-2}) of *Bacillus subtilis* WT 168 spores (**Fig. 61**). The latter value is equivalent to the parameter F_{10} (10% survival rate), which is sometimes used in literature to express the sensitivity of organisms to absorbed doses of radiation. Our LD_{90} (F_{10}) value for *Bacillus subtilis* WT 168 spores was in close agreement with previously reported values for the same strain, obtained for the spores exposed to UV-C_{254} light either in a dry state or in suspension (Horneck et al., 1984a; Weber and Greenberg, 1985; Nicholson et al., 2000; Moeller et al., 2007a; Moeller et al., 2007b). Other *Bacillus subtilis* wild type strains that were used in photobiological and astrobiological studies exhibit similar or slightly lower LD_{90} values for UV-C irradiated spores (Horneck et al., 1984b; Horneck et al., 1995; Riesenman and Nicholson, 2000; Bernardini et al., 2003; Link et al., 2004). For comparison, 6 orders of magnitude higher UV-C doses had no effect on the germinability of *Arabidopsis* seeds. Comparing the UV-C dose response curves and LD_{90} values for *Bacillus subtilis* spores and *tt4-8* seeds (**Fig. 61** and **Fig. 70**), we found that even flavonoid-lacking seeds were 2.7 x 10^5 times more resistant to deleterious effects of UV-C radiation. *Arabidopsis* seeds are thus shown to be far more resistant even than spores of *Bacillus pumilus* SAFR-032, an isolate obtained from an ultraclean spacecraft assembly facility, for which was reported the highest degree of spore UV-C_{254} resistance observed by any *Bacillus* spp. encountered to date (LD_{90} = 1.7 kJm^{-2}) (Link et al., 2004). Another example of high resistance is known in bacterium *Deinococcus radiodurans*, which exhibits an extraordinary ability to tolerate the lethal effects of a variety of DNA-damaging agents, including UV radiation. This organism survives UV-C_{254} doses up to 1 kJm^{-2} (Battista et al., 2000; Chen et al., 2000), which makes this extremophile at least 10^5 times more sensitive to UV radiation than *Arabidopsis* seeds. We found that even the flavonoid-lacking *tt4-8* seeds were highly UV-C_{254} resistant, compared to these stress-tolerant organisms. We suggest that several factors contribute to such extreme resistance of plant seeds, including the fact that they are multicellular life forms, they contain particularly low water content, the protective role of the seed coat, the shielding effect of the multicellular endosperm rich in proteins that may absorb UV light, the occurrence of redundancy in genetic information that is common in plant genomes, and high efficiency of detoxification and repair systems. In this work we demonstrated that UV screening compounds, which accumulate in high concentrations in plant seeds, provide an additional level of UV resistance and that flavonoids, as the major UV protective compounds in plant seeds, increase the level of UV-C resistance of seeds by at least 2 orders of magnitude.

19. RESISTANCE OF *Arabidopsis* SEEDS TO SIMULATED POLYCHROMATIC SOLAR $UV_{200-400}$ RADIATION

Due to its high energy and efficient absorption by many biologically important macromolecules, solar UV is considered one of the most deleterious components of solar radiation (Nicholson et al., 2005). The UV portion of the extraterrestrial solar spectrum spans the wavelength range from about 100 to 400 nm. The highly energetic wavelengths below 290 nm currently do not reach the Earth, thanks to the absorption by the protective ozone shield in the upper atmosphere. Space experiments have shown that solar UV radiation is the main cause of inactivation of microorganisms, such as viruses, bacterial spores and fungal spores, where the UV spectral range between 200 and 300 nm was found to have the highest biological effectiveness (Lorenz et al., 1969; Horneck et al., 1984a). DNA is considered a prime target for UV damage, since the action spectra for decline in viability of microorganisms roughly follow the absorption curve of DNA (Horneck, 1993; Horneck et al., 1995; Nicholson et al., 2000). Although previous studies on *Bacillus* spores have shown that UV-C radiation, especially at λ = 254 nm, is more effective than UV-B and UV-A light (Riesenman and Nicholson, 2000; Slieman and Nicholson, 2000; Slieman and Nicholson, 2001; Moeller et al., 2005), we were interested, however, to also examine possible combined effects of the range of wavelengths (λ = 200-400 nm) occurring in polychromatic extraterrestrial sunlight. This we considered an important issue, especially in view of the simultaneous accumulation of different types of molecular damage, including direct and indirect mechanisms of damage to DNA and other essential molecules, as well as induction of oxidative damage, for which the wavelength dependence was previously demonstrated by Kielbassa et al. (1997) and Ravanat et al. (2001) (for details see chapter **1**, section **3.3.3** and **Fig. 19**). In addition, some UV wavelengths play an important role in the light-dependant repair processes, which can reverse the DNA damage caused by the highly energetic UV radiation (e. g. UV-A light activates the photolyase enzyme, involved in the photoreactivation repair) (Britt, 1996; Tuteja et al., 2001; Sinha and Häder, 2002).

In extraterrestrial environments, deleterious UV radiation is encountered together with other harsh conditions. In space, extremely high vacuum can be encountered, which can cause a complete desiccation of cells and ultimately death. Acting in combination, polychromatic solar UV radiation and high vacuum were found to have a synergistic effect in inactivation of different types of microorganisms (Bücker et al., 1974; Horneck et al., 1984b; Weber and Greenberg,

1985; Horneck, 1993; Dose et al., 1996; Fekete et al., 2005). On Mars, which has an atmosphere rich in CO_2 (~95%), but poor in oxygen and lacking efficient gaseous UV absorbers (e.g. ozone shield), high fluxes of deleterious solar UV radiation (λ ~ 200-400 nm) reach the surface of the planet. Up to date, little is known about the combined effects of polychromatic solar UV radiation and high concentrations of CO_2.

Therefore, in the present study, we further examined the resistance of dry *Arabidopsis* seeds to simulated polychromatic solar $UV_{200-400}$ light, at fluence as high as 1.5 x 10^5 kJm^{-2}, which corresponded to the expected total fluence of extraterrestrial solar $UV_{200-400}$ light in the EXPOSE experiments after 1.5 years of space mission outside the International Space Station (ISS) (for details see chapter **1**, section **2**). In addition, the integrated fluence of polychromatic $UV_{200-400}$ light was in the range close to that used in our laboratory experiments with quasi-monochromatic UV-C_{254} radiation (see discussion above, section **18**). However, it is important to mention that the partial fluence at λ = 254 nm in simulated polychromatic solar $UV_{200-400}$ light was about 1400 times lower than that for the same wavelength emitted from our monochromatic UV-C_{254} source. Furthermore, we examined the effects of simulated space vacuum and simulated CO_2 rich Mars atmosphere on dry *Arabidopsis* seeds, separately, as well as in combination with simulated polychromatic solar $UV_{200-400}$ light. The exposure experiments were performed as part of the pre-flight EXPOSE-EVT (Experiment Verification Tests), where two flavonoid-containing *Arabidopsis* wild type lines, Ws-2 and Ler-0 were used, together with the flavonoid-deficient *tt4-1* mutant line (Ler-0 accession). The impact of polychromatic $UV_{200-400}$ light and high vacuum or simulated CO_2 rich Mars atmosphere was determined at the three plant developmental stages: the seed germination, the early-seedling stage and the mature plant development.

19.1. Effects of simulated polychromatic solar $UV_{200-400}$ radiation and simulated space vacuum on seed resistance

Since an extreme space vacuum *per se* represents one of the limiting factors for transfer of life through space, prior to studying the combined effects of simulated polychromatic solar $UV_{200-400}$ and simulated space vacuum (10^{-5} Pa), we first examined separately the effects of high vacuum on dry *Arabidopsis* seeds.

19.1.1. Effects of high vacuum

Exposure to space vacuum causes extreme desiccation, leading to a high rate of mutations and ultimately to cell death. The mechanisms of DNA damage due to the exposure to vacuum are mostly based on desiccation damage, where the removal of water induces changes in the structure of DNA, leading to single-strand (ss) and double-strand (ds) breaks. Extreme desiccation also affects the integrity of proteins and it may lead to the formation of DNA-protein complexes (Nicholson et al., 2000; Tuteja et al., 2001; Fekete et al., 2005). Previous studies on the effects of simulated space conditions revealed that extreme desiccation at 10^{-6} Pa for 24 hours results in complete killing of *Escherichia coli* and *Halobacterium halobium* cells, while 55% of *Clostridium mangenoti* spores and 75% of *Bacillus subtilis* spores survived the exposure to a high vacuum (Koike et al., 1992; Nicholson et al., 2000). Space experiments during the EURECA mission showed that up to 25% of *Bacillus subtilis* spores survived after 327 days of exposure to high space vacuum (~ 10^{-5} Pa) (Horneck et al., 1995). However, only 1-2% of non-protected *Bacillus* spores resisted after 6 years of exposure to space vacuum during the long duration exposure LDEF mission, while embedding of the spores in glucose and salt crystals significantly improved their survival (Horneck et al., 1994; Horneck et al., 1995; Horneck, 1999). Data from several space experiments suggested that there is a slow, but progressive loss in the survival of spores as a function of the duration of exposure to high vacuum (Horneck et al., 1984b; Horneck et al., 1994; Horneck et al., 1995). On the other hand, it is known that many plant seeds are desiccation-tolerant life forms, which have developed efficient mechanisms to withstand the loss of the major portion of their water content and are able to survive in the dry state for prolonged periods thanks to the formation of intracellular glasses (Tuteja et al., 2001; Buitink and Leprince, 2004; Buitink and Leprince 2008; Rajjou and Debeaujon, 2008; and references herein). Furthermore, the longevity of many orthodox seeds is improved by desiccation and storage under low vacuum and/or cold, permitting long-term seed preservation

(Tauer, 1979; Yeh et al., 2005; Sastry et al., 2007). However, little is known about the effects of high vacuum on the viability and germination performance of plant seeds.

Our results clearly showed that exposure to a simulated space vacuum (10^{-5} Pa) for 22 days had no adverse effects on *Arabidopsis* seed germination (**Fig. 83A-C**), as well as on the subsequent development of early-stage seedling (**Fig. 88A-C, Fig. 90A-C** and **Fig. 91A-C**) and the growth of the mature plants (**Fig. 92A-I**). The germination tests revealed that seeds exposed to vacuum retained their high germination capacity ($G_{max\%}$) at about 100% in all three examined *Arabidopsis* lines, including wild type lines Ws-2 and Ler-0, as well as flavonoid-lacking mutant, *tt4-1* (**Fig. 83A-C** and **Fig. 85A-C**). These results are in accordance with previously reported data, which indicated that a high vacuum environment at 10^{-7} Torr (1.33×10^{-5} Pa) has no effect on seed germinability in five Japanese crop species (Hashimoto, 2001).

In addition, our results also revealed that high vacuum had a small, but surprisingly positive effect on germination speed in *Arabidopsis* wild type lines, resulting in a slightly faster germination of the Ws-2 seeds, while the vacuum treated Ler-0 seeds germinated significantly faster (22% decrease in MGT) than the control samples (**Fig. 83A-B**, **Fig. 86A-B** and **Table 20**). The inducing effect of high vacuum on germination may be explained by possible mechanical weakening (cracking) of the seed coat in treated seeds. It is well known that the scarification or removal of the seed coat can promote germination in many plant seeds (Toole et al., 1956; Corbineau and Côme, 1995; Geneve, 1998). Depending on their structure and chemical composition, seed coats represent the germination constraints mostly by being impermeable to water and gases (notably oxygen), or by their mechanical resistance to radicle protrusion (Corbineau and Côme, 1995; Debeaujon et al., 2000). For details about seed coat effects on seed germination see chapter **1**, section **4.2.3.3**. Besides a direct physical effect on seed germination, other effects of exposure to vacuum, related to oxygen deprivation and extreme desiccation should be also considered. The response of seeds to anoxia is generally species-dependent, e.g. some nondormant seeds lose their ability to germinate because they enter into secondary dormancy, while some dormant seeds in other species become able to germinate when subjected to anoxic conditions (Côme, 1982; Côme et al., 1991; Corbineau and Côme, 1995). Oxygen deprivation may result in the production of ethanol by fermentation. Ethanol accumulation in anoxic conditions might break dormancy and stimulate germination in various seeds. (Corbineau et al., 1991; Corbineau and Côme, 1995). In addition, oxygen deprivation likely promotes the production of ethylene, once the seeds have been removed from anoxic conditions and exposed to the air (Lieberman, 1979; Corbineau and Côme, 1995). The increased production of ethylene,

which is an important phytohormone, may facilitate the germination in many plant seeds (Corbineau and Côme, 1995). On the other hand, the exposure of seeds to high vacuum may lead to a massive water loss, as reported by Hashimoto (2001), who observed an important weight reduction in seeds that were kept under high vacuum. Since the water potential gradient between the seed and its surrounding is a driving force for the water uptake, which is necessary for promoting germination, drier seeds that were exposed to vacuum may exhibit faster germination due to a greater water potential gradient (Bewley and Black, 1994a). In contrast, drying of seeds beyond the critical water content may result in a higher level of desiccation damage, particularly by inducing irreversible peroxidative damage to membrane lipids, DNA damage and alternations in protein structures (Tuteja et al., 2001; Walters et al., 2002). Nevertheless, most plant seeds possess a high desiccation tolerance (Tuteja et al., 2001; Buitink et al., 2002; Walters et al., 2002; Buitink and Leprince, 2004). Seeds are rich in soluble carbohydrates, such as sucrose and raffinose family oligosaccharides (RFOs), which together with a specific group of proteins (e.g. LEA proteins), form an intracellular glassy matrix, which improves the stability of macromolecules and their complexes within desiccated cells (Bewley and Black, 1994a; Buitink et al., 2002; Buitink and Leprince, 2004; Buitink and Leprince, 2008). Thus, mature dry seeds are adapted to tolerate a low water content that occurs under normal physiological conditions, e. g. *Arabidopsis* seeds in our experiment contained only 6-7% water prior to the vacuum treatment.

Our results further indicated that even the flavonoid-lacking *tt4-1* seeds exhibit a high level of resistance to simulated space vacuum, since both the germination capacity and the seed vigour remained unaltered after the treatment. Unlike in the wild-type Ws-2 and Ler-0 seeds, the vacuum treatment of the *tt4-1* seeds did not result in faster germination speed (**Fig. 83C** and **Fig. 86C**). This could be explained by initially greater permeability of the flavonoid-lacking seed coats to water and oxygen in untreated *tt4-1* seeds, in contrast to the impermeable seed coats of the wild type seeds.

Since we expected that during the EXPOSE space missions outside the ISS, our seed samples would be exposed to a pressure of about 10^{-5} Pa, we concluded that space vacuum alone would probably not be detrimental factor for the survival of *Arabidopsis* seeds. This estimation is consistent with results obtained from previous space experiments, which showed that various plant seeds survived exposure to space vacuum for the almost 6 years of the LDEF mission (Alston, 1991; Musgrave, 2002). In addition, Anikeeva et al. (1990) reported that vacuum and

low temperatures alone were not among those space environment factors that had the adverse effects on *Arabidopsis* seeds flown for 13 days aboard the biosatellite Kosmos 1887.

19.1.2. Combined effects of polychromatic $UV_{200-400}$ light and high vacuum

The space experiments, as well as simulation experiments, revealed that the inactivating effect of polychromatic solar UV radiation was increased by simultaneous exposure to space vacuum (Horneck et al., 1984b; Weber and Greenberg, 1985). For instance, there was reported a tenfold increase in the UV-sensitivity of *Bacillus subtilis* spores when they were simultaneously exposed to space vacuum and solar UV radiation, compared to the samples that were exposed solely to solar UV light (Bücker et al., 1974; Horneck et al., 1995; Horneck, 1999). It was previously suggested that the formation of "vacuum-specific" photoproducts in DNA, as well as DNA protein cross-linking and DNA strand breaks are among the most severe injuries that are less amenable to cellular repair processes (Lindberg and Horneck, 1991; Horneck, 1993; Horneck et al., 1995). The same effect of increased photosensitivity due to desiccation damage caused by simultaneous exposure to vacuum was also described for bacterial cells of highly resistant *Deinococcus radiodurans*, conidia of fungus *Aspergillus ochraceus*, viral particles of bacteriophage T7 and dry films of DNA (Dose et al., 1995; Dose et al., 1996; Fekete et al., 2005). We therefore examined the combined effects of simulated polychromatic solar $UV_{200-400}$ (1.5×10^5 kJm^{-2}) and simulated space vacuum (10^{-5} Pa) on dry *Arabidopsis* Ws-2, Ler-0 and *tt4-1* seeds (Ler-0 accession).

The germination stage

Simultaneous exposure to polychromatic $UV_{200-400}$ light (1.5×10^5 kJm^{-2}) and high vacuum had no effects on germination capacity of the flavonoid-containing Ws-2 and Ler-0 wild type seeds, which reached high $G_{max\%}$ in both seed lines (**Fig. 83A-B** and **Fig. 85A-B**). However, the germination dynamics was markedly affected in the Ws-2 and Ler-0 seeds after exposure to polychromatic $UV_{200-400}$ light under simulated space vacuum (**Fig. 83A-B** and **Table 20**). These seeds germinated much slower than the control samples (78% and 165% increase in MGT, respectively), as well as the seeds that were exposed solely to simulated space vacuum (**Fig. 86A-B**). A significant increase in the MGT, which was also observed for the $T_{50\%}$ parameter (**Table 20**), was mostly due to a delayed start of germination in exposed Ws-2 (7 hours of delay) and Ler-0 (24 hours delay) seed samples (**Fig. 83A-B**). This delay in radicle emergence might be due to a longer time required for DNA repair in the embryos, prior to entering in the process of

DNA replication and subsequent cell division that are necessary for normal seedling growth. Lower germination uniformity (increase in $T_{25\text{-}75\%}$) contributed to a lesser extent to the overall slower germination in exposed Ws-2 seeds, but it had a greater contribution, together with the delayed start of germination, in overall decrease of germination speed in Ler-0 seeds (**Table 20**). Since the exposure of seeds to only simulated space vacuum did not have any adverse effect on seed germination (see discussion above), we assumed that the observed change in germination dynamics in both the Ws-2 and Ler-0 seeds were due to the effects of polychromatic $UV_{200\text{-}400}$ light.

Our results indicated that irradiated Ler-0 wild type seeds, in spite of high germinability, they had lower vigour than the Ws-2 seeds, and thus were less resistant to polychromatic $UV_{200\text{-}400}$ light. This difference is likely due to naturally occurring genetic variations, observed among different ecotypes of *Arabidopsis thaliana*, regarding the plant resistance to diverse biotic and abiotic stresses (Koornneef et al., 2004). Variations in plant response to UV radiation were also reported among *Arabidopsis* Ws, Col-0 and Ler-0 wild ecotypes (Cooley et al., 2001). We have already observed the occurrence of the ecotypic differences between the Ws-2 and Col-0 wild type lines in seed resistance to quasi-monochromatic UV-C radiation (for details see discussion above, sections **18.2** and **18.3**). We suggested that the variations in the response of these two seed lines to polychromatic $UV_{200\text{-}400}$ radiation might be due to differences in the chemical and biochemical composition of seeds and/or differences in the efficiency of detoxification and repair systems, activated after seed imbibition. Further comparative studies at molecular level (e.g. types and number of DNA lesions, expression and activity of antioxidant enzymes POD, CAT and SOD etc.), as well as further chemical studies of seed composition are necessary in order to determine the origin of ecotypic differences between Ws-2 and Ler-0 lines.

Nevertheless, previously chemical studies reported small differences in the flavonoid content of Ws-2 and Ler-0 seeds. Although these two ecotypes accumulate similar amounts of the total seed flavonids, the Ler-0 seeds accumulate less flavonols (~5.8 mg g^{-1} seeds) than the Ws-2 seeds (~7.4 mg g^{-1} seeds), particularly quercetin-3-*O*-rhamnoside (known as quercitrin) and its derivative quercetrin-di-rhamnoside, which are the two main flavonols in *Arabidopsis* seeds (Lepiniec et al., 2006; Routaboul et al., 2006). On the other hand, the Ler-0 seeds contain more proanthocyanidins (~9 mg g^{-1} seeds) in comparison to the Ws-2 seeds (~7 mg g^{-1} seeds) (Lepiniec et al., 2006; Routaboul et al., 2006). Compared to our results, these reported data might indicate the importance of flavonols, and particularly quercitrin, which accumulates in high concentration in seed coat, in a direct UV-screening protection of *Arabidopsis* seeds.

In contrast to the flavonoid-containing seeds, simultaneous exposure to polychromatic UV light and high vacuum had a dramatic impact on flavonoid-lacking *tt4-1* seeds, since the germination of exposed seeds was entirely inhibited ($G_{max\%}$ = 0%), as seen in **Fig. 83C**. In addition, the TZ test showed that all the irradiated *tt4-1* seeds that remained ungerminated, were in fact metabolically dead (**Fig. 87**). Since our results clearly indicated that a simulated space vacuum alone had no effect on the germination of the *tt4-1* seeds, it was important to examine whether the inhibition of germination was caused uniquely by polychromatic $UV_{200-400}$ light or by possible synergistic action of high vacuum and UV radiation. The same result, $G_{max\%}$ = 0%, was obtained after the exposure of the *tt4-1* seeds to polychromatic $UV_{200-400}$ light in air under atmospheric pressure (**Fig. 84**). We therefore concluded that polychromatic $UV_{200-400}$ radiation alone had a deleterious effect on the flavonoid-deficient seeds, such as to cause the accumulation of severe and unrepairable UV-induced damage that killed all irradiated seeds. Since the *tt4-1* seeds contain normal level of sinapate esters (Shirley et al., 1995), our results confirmed the importance of flavonoids as the major UV-screening compounds that efficiently protect *Arabidopsis* seeds not only from monochromatic UV-C_{254} light (see discussion above, section **18**), but also from highly energetic polychromatic solar $UV_{200-400}$ light.

The early-seedling stage

We found that 72% of the Ws-2 and 59% of the Ler-0 seeds that were exposed to polychromatic $UV_{200-400}$ radiation (1.5 x 10^5 kJm^{-2}) under simulated space vacuum germinated into normal seedlings (**Fig. 88A-B**). However, we also observed a significant increase in the percentage of abnormal seedlings in the population of irradiated Ws-2 and Ler-0 seeds (**Fig. 90A-B**). The abnormally developed Ws-2 and Ler-0 seedlings mostly exhibited short or twisted hypocotyls (**Fig. 89C**), and some of them, besides changed hypocotyl morphology, developed short roots (**Fig. 89D**). The inhibitory effect of polychromatic $UV_{200-400}$ radiation on root growth occurred even in the population of normally developed seedlings, where a significant reduction in root length was measured for both the Ws-2 (26%) and Ler-0 (60%) lines (**Fig. 91A-B**). We found that similarly to the germination stage, the Ler-0 wild type line exhibited higher sensitivity to polychromatic $UV_{200-400}$ light, compared to the Ws-0 wild type line. Furthermore, our results indicated that the morphological changes to essential seedling structures are caused by exposure to polychromatic $UV_{200-400}$ radiation, while simulated space vacuum had no effect on seedling development. Our findings are in accordance with previous studies that reported the inhibitory effects of UV radiation on hypocotyl elongation and root growth in irradiated seedlings

(Lapointe et al., 1996; Kobzar et al., 1998; Hirokazu et al., 1999; Shinkle et al., 2005; Al Khateeb and Schroeder, 2009), as well as with our studies on the effects of monochromatic UV-C_{254} light on *Arabidopsis* early-stage seedlings developed from irradiated seeds (see discussion above, section **18**). Interestingly, we found that exposure of the Ws-2 wild type seeds to polychromatic $UV_{200-400}$ radiation at a total fluence in the range of 10^5 kJm^{-2} results in less damage to early-stage seedlings (detected as a lower percentage of abnormal seedlings and less severe types of seedling damage) than in the case of exposure of the Ws-2 seeds to monochromatic UV-C_{254} light with a fluence in a similar range (compare **Fig. 72E** with **Fig. 88A**, and **Fig. 76E** with **Fig. 90A**). This phenomenon may be explained by the fact that the partial fluence at λ = 254 nm in polychromatic $UV_{200-400}$ light was 1400 times lower than the fluence of quasi-monochromatic UV-C_{254} light, which probably had potentially high damaging direct effects on DNA.

The stage of plant development

In spite of high germinability *in vitro*, the polychromatic $UV_{200-400}$ light had a strong impact on subsequent survival of in-soil grown plants, developed from exposed Ws-2 and Ler-0 seeds (**Fig. 92A-B**). Only 36% of the plants survived in the exposed Ws-2 sample, while curiously better survival was observed for Ler-0 plants (53%) (**Table 21**). This might indicate that the Ler-0 wild type, although less resistant at the germination and early-seedling developmental stages, exhibited better performance at the stage of plant development than the Ws-2 wild type. Furthermore, we found that in spite of the adverse effect on in-soil plant survival, polychromatic $UV_{200-400}$ light did not affect the reproductive output in the Ws-2 line, since all of the surviving plants developed finally into the mature plants, capable of producing the progeny (**Fig. 92D**). Nevertheless, polychromatic $UV_{200-400}$ light did reduce the percentage of fertile plants in the Ler-0 line (**Fig. 92E**). In contrast to high doses of monochromatic UV-C_{254} radiation (up to 6 x 10^5 kJm^{-2}), polychromatic $UV_{200-400}$ light (1.5 x 10^5 kJm^{-2}) did not affect vegetative plant growth in both the *Arabidopsis* wild type lines (**Fig. 92G** and **H**). In-soil experiments also confirmed that polychromatic $UV_{200-400}$ light had dramatically adverse effect on the flavonoid-deficient *tt4-1* mutant, since no germinants were observed after the irradiation to polychromatic $UV_{200-400}$ light separately or in combination with high vacuum.

Concluding remarks (8)

We demonstrated that simulated space vacuum alone, known to cause a complete desiccation, killing all vegetative bacterial cells and a considerable portion of *Bacillus* spores within several hours, had no adverse effects on *Arabidopsis* seeds even after 22 days of treatment. All *Arabidopsis* seed lines, including two wild type lines, Ws-2 and Ler-0, as well as the flavonoid-lacking mutant, *tt4-1*, exhibited a high resistance to extremely low pressure (10^{-5} Pa), expected during EXPOSE space mission. After the exposure, all seeds retained a high germinability ($G_{max\%} \approx 100\%$) and showed an excellent germination performance. In addition, all germinated vacuum-treated seeds developed into normal seedlings and further into normal mature plants with good reproductive capacity.

Our results revealed remarkably high resistance of *Arabidopsis* wild type seeds to combined effects of simulated polychromatic solar $UV_{200-400}$ radiation (1.5×10^5 kJm^{-2}) and simulated space vacuum (10^{-5} Pa), both in the range of values expected for the EXPOSE missions. Simultaneous exposure to polychromatic $UV_{200-400}$ radiation and high vacuum had no effect on germinability of the Ws-2 and Ler-0 wild type seeds ($G_{max\%}$ = 92 and 98%, respectively). Regardless of their high germination capacity, we observed a significant decline in seed vigour, which was manifested through a slower germination (increase in MGT), delayed start of germination and lower germination uniformity (increase in $T_{25-75\%}$) in both the Ws-2 and Ler-0 samples. Since the exposure of seeds to only simulated space vacuum did not have any adverse effect, we concluded that observed change in germination behaviour is due to the effect of polychromatic $UV_{200-400}$ radiation. We assumed that the delay in radicle emergence in irradiated seeds is likely due to a longer time required to cope with accumulated UV-induced molecular damage (DNA repair and *de novo* synthesis of proteins and RNAs etc.). The Ler-0 ecotype appeared more sensitive to polychromatic $UV_{200-400}$ radiation, since it exhibited more pronounced decline in the seed vigour, compared to the Ws-2 ectype. The differences in the sensitivity for these two wild types were also detected at the subsequent developmental stage, the early-seedling development. Irradiated Ler-0 seeds developed more abnormal seedlings than the Ws-2 ecotype (39% and 20%, respectively). We assumed that observed differences in the UV response between these two wild types are probably due to naturally occurring ecotypic variations (e.g. Ler-0 seeds contain 22% less flavonols, particularly quercetin-3-*O* rhamnoside and quercetin-di-rhamnoside, Routaboul et al., 2006). Damaged seedlings exhibited mostly changes in hypocotyl (short or twisted) and root growth (short primary roots). The inhibitory effect of polychromatic $UV_{200-400}$ radiation on root growth occurred even in the population of

normally developed seedlings. This might be the cause of relatively low percentage (53% Ler-0 and 36% Ws-2) of survived soil-grown plants that were developed from irradiated seeds.

In contrast to flavonoid-containing wild type seeds, simulated polychromatic solar $UV_{200-400}$ light in combination with simulated space vacuum had a dramatic effect on the flavonoid-lacking *tt4-1* seeds (Ler-0 accession), since no viable seeds were detected in irradiated sample. The same result was also obtained after the exposure of the *tt4-1* seeds only to polychromatic solar $UV_{200-400}$ light. Therefore, the deleterious effect was attributed solely to polychromatic $UV_{200-400}$ light, while the effect of high vacuum or possible synergistic action of these two parameters is here excluded. These results clearly demonstrate the importance of flavonoids in UV screening protection of plant seeds. Since the partial fluence at $\lambda = 254$ nm in simulated polychromatic solar $UV_{200-400}$ light was about 1400 times lower than for the same wavelength emitted from our quasi-monochromatic UV-C_{254} source, we concluded that flavonoids are not only good protectors against the critical UV-C_{254} wavelength, but they likely provide efficient protection all through the UV-C part of spectrum, as well as in the UV-B and UV-A wavebands that are part of polychromatic UV light.

At the germination and the early-seedling stage, we determined the scale of $UV_{200-400}$ resistance for different *Arabidopsis* genotypes as follows: Ws-2 > Ler-0 >> *tt4-1*.

However, at the stage of mature plant development we determined the following scale of $UV_{200-400}$ resistance: Ler-0 > Ws-2 >> *tt4-1*.

19.2. Effects of simulated polychromatic solar $UV_{200-400}$ radiation and simulated Mars CO_2 atmosphere*[1]

UV radiation in extraterrestrial environments is different from that encountered on the surface of present-day Earth. The UV flux on the surfaces of planetary bodies is predominantly determined by the composition of the atmosphere. Mars has a relatively thin atmosphere that has about one hundredth of the total atmospheric pressure on Earth. The Martian atmosphere is composed predominantly of CO_2 (95%) and low concentrations of N_2 (2.7%) and Ar (1.6%), with traces of O_2 (0.13%), CO (0.07%) and water vapour (0.03%) (Faure and Mensing, 2007b; Barlow, 2008). Unlike the Earth, Mars does not have a significant atmospheric ozone layer. Therefore, in addition to the UV-A (280-365 nm) part of the spectrum, the UV-B (280-315 nm) and UV-C (200-280 nm) wavebands of solar radiation reach the surface of Mars relatively unattenuated (**Fig. 14**, chapter **1**, section **3.3.1.2**) (Cockell, 2001b). Because UV radiation below 195 nm is absorbed by atmospheric CO_2, the VUV (< 200 nm) part of the solar spectrum is not of concern in the Martian surface environment (Cockell, 2001b; Cockell, 2001c). Even though Mars receives about half as much total solar radiation of Earth, the amounts of UV radiation at the Martian surface are much higher (Thomas et al., 2006). It is estimated that the biologically effective irradiance (DNA-weighted damage) on Mars is approximately 1000 times higher than on the surface of the Earth under a worst-case scenario, and it is calculated that almost 78% of this damage would be caused by the UV-C part of the spectrum (Cockell et al., 2000; Cockell, 2001b). In past years, several photobiological and dosimetric studies were undertaken under simulated Mars conditions to determine the effects of a variety of Martian environmental parameters on the growth and survival of terrestrial microorganisms. These studies aimed to estimate the possibility of existence of any past or present life on Mars, to evaluate the chances of the survival of terrestrial microbial contaminants dispersed during the course of human exploration missions on Mars, or even to determine the suitability of potential pioneering terrestrial life forms for future controlled colonization and terraforming of Mars (Schwartzkopf and Mancinelli, 1991; Mancinelli and Klovstad, 2000; Schuerger et al., 2003; Cockell et al., 2005; Thomas et al., 2006; Osman et al., 2008). The combination of parameters, characteristic for a harsh Martian environment, including the low temperature, low atmospheric pressure, low moisture, high atmospheric CO_2 and high UV flux is not experienced by any known Earth organism. Nevertheless, a variety of microorganisms are demonstrated to survive the freeze-thaw cycles from +25 to -60°C, low atmospheric pressures down to 10 mb, and levels of moisture in

[1] Mars CO_2 atmosphere* was simulated only in view of its composition (95.56% CO_2, 2.72% N_2, 1.56% Ar and 0.16% O_2), but not the pressure, since all experiments were performed at 1 atm (101.3 kPa) instead of 600 Pa.

soils of ~0.5% (Mancinelli and Klovstad, 2000, and references therein). Up to now, no terrestrial organism is known to survive exposure to sterilizing Martian UV flux . Even *Bacillus* spores, known to be among the most resistant terrestrial life forms, are completely killed within minutes of exposure to simulated Martian UV radiation (Schuerger et al., 2003; Osman et al., 2008).

In this work we demonstrated that plant seeds are particularly resistant life forms capable of surviving temperature extremes (see **Annex C**), extreme desiccation at extremely low pressure of simulated space vacuum (section **19.1.1**), as well as extremely high fluences of monochromatic UV-C_{254} (section **18.3**) and polychromatic $UV_{200-400}$ radiation (section **19.1.2**). Therefore we aimed to further examine the effects of simulated polychromatic solar $UV_{200-400}$ radiation in combination with a simulated Mars CO_2 atmosphere* on resistance of dry *Arabidopsis* seeds. However, the conditions of the simulated Mars atmosphere in our experiment differed from those present on Mars, since the total pressure of 6 mb (600 Pa) had unfortunately to be replaced by a pressure of 1 atm (~ 101.3 kPa) due to the technical problems encountered during the EVT experiments (for details see chapter **2**, sections **8.1.2.2.4** and **8.1.2.2.5**). Because we consider only the effects of the composition of CO_2 rich atmosphere, excluding possible effects of a low total atmospheric pressure, in this report, we use the term *simulated Mars CO_2 atmosphere**[12]. Previously reported data showed that the exposure to a low pressure atmosphere of 60 mb (Earth atmospheric composition) does not inhibit the germination of wheat seeds, while exposure to a CO_2 rich atmosphere (simulated Mars atmosphere), both at low and high pressure, has a significant effect on seed germination (Schwartzkopf and Mancinelli, 1991). In addition, in the present work we showed that *Arabidopsis* seeds are resistant to extremely low pressure, such as simulated space vacuum (10^{-5} Pa) (see discussion in section **19.1.1**), which is about 7 orders of magnitude lower than that of the Martian atmosphere. Therefore, we assumed that the effect of specific composition of Martian atmosphere (~ 95% CO_2) is of greater concern for our experimental model (*Arabidopsis* seeds) than the effect of low-pressure atmosphere.

19.2.1. Effects of CO_2 rich atmosphere

Several authors reviewed the plant responses to elevated atmospheric CO_2 in the context of ecological studies (Goudriaan and Unsworth, 1990; Lawlor and Mitchell, 1991; Rozema et al., 1997a). Plants respond generally positively to higher atmospheric CO_2 concentrations (Rozema et al., 1997a). The most known responses to elevated CO_2 include an increase in the rate of net photosynthesis and enhanced growth in various plant species (Rozema et al., 1997a; Ward and Strain, 1999). The germination process in seeds has been much less studied than plant growth

with respect to elevated CO_2 concentrations. Although beneficial effects on seed longevity by long-term seed storage under a pure CO_2 atmosphere have been reported in various plant species (Sayre, 1940; Barton, 1953; Harrison, 1956; Doijode, 2001), higher concentrations of CO_2 may have some effects on subsequent germination process. Here two effects should be considered, a direct action of high CO_2 concentrations on seed metabolism and, on the other hand, an effect of oxygen deprivation in seeds that are placed in atmospheres rich in CO_2. The latter also concerned our study on the effects of high vacuum on dry *Arabidopsis* seeds (see section **19.1.1**). During the germination under normal physiological conditions, O_2 is required for the respiration of imbibed seeds, while CO_2 and ethylene, which are released as the result of metabolic activity, may also interact with seed dormancy and germination (Corbineau and Côme, 1995). The effects of O_2 and CO_2 concentrations on germination are rather complex and not fully understood. Low O_2 availability during the imbibition phase reduces or even inhibits germination in most species (Hadas, 2004). On the other hand, increased concentrations of CO_2 have been shown to stimulate the germination of various seeds (reviewed by Corbineau and Côme, 1995). The effects of elevated CO_2 often interact with those of ethylene, since CO_2 enhances the production of ethylene in plants. Both gases might stimulate seed germination acting either in an additive or a synergistic manner (Corbineau and Côme, 1995). Regardless of that, several studies reported inconsistent results on the effect of elevated CO_2 on germination, ranging from the positive (Wulff and Alexander, 1985), neutral (Garbutt et al., 1990) or even negative effects (Andalo et al., 1996), depending on the plant species. It seems that only low concentrations of CO_2 (0.5-5%) can stimulate germination, while higher concentrations (above 10%) have rather inhibitory effect on seed germination (Corbineau and Côme, 1995). Therefore, in the present work, we considered necessary to better examine the effects of CO_2 rich atmosphere (96% CO_2) on *Arabidopsis* dry seeds, studying the processes of seed germination and early-seedling development. The stage of plant development, however, was not examined in this study.

The germination stage

In our experiments, dry seeds of *Arabidopsis thaliana* were first exposed to a CO_2 rich atmosphere (96% CO_2) for 21 days and then germinated under normal Earth atmosphere. Our results showed that the simulated Mars CO_2 atmosphere* (96% CO_2) did not affect germination capacity ($G_{max\%}$ = 98%) nor the germination dynamics in the Ws-2 wild type seeds (**Fig. 85D** and **Fig. 86D**, respectively).

A surprisingly different result was obtained after the treatment of the second wild type, the Ler-0 seeds. Although, the germination capacity remained unaltered and reached a high level (**Fig. 85E**), the germination speed was seriously affected after the exposure of the Ler-0 seeds to the simulated Mars CO_2 atmosphere (a two-fold increase in MGT) (**Fig. 86E**). A similar result was obtained measuring the $T_{50\%}$ parameter of germination dynamics for treated Ler-0 seeds (**Table 20**). Nevertheless, the other parameters of germination dynamics, the $T_{25\text{-}75\%}$ and the skewness of germination curve, did not differ from the control sample (**Table 20**). These results indicated that after the exposure to simulated Mars CO_2 atmosphere*, the Ler-0 seeds still retained high germination uniformity, and the overall germination process was slower mostly due to the delayed start of germination (about 8 hours) (**Fig. 83B**). Our results correlates partially with that obtained by Andalo et al. (1996), who reported that elevated atmospheric CO_2 concentrations likely reduce the seed quality in *Arabidopsis thaliana*. They demonstrated that *Arabidopsis* seeds produced under elevated CO_2 germinate slower. However, they also reported that the total germination percentage is also lower in these seeds, what was not observed in our study. On the other hand, seeds that are produced under normal atmospheric conditions, and germinated under elevated CO_2, exhibited an unaltered total germination percentage, but significantly faster germination (Andalo et al., 1996). The same authors reported significant variations in the response of seeds to elevated CO_2 in different genotypes of *Arabidopsis thaliana*, isolated from natural populations. This correlates with unexpected differences in the response of the Ws-2 and Ler-0 seeds exposed to the simulated Mars CO_2 atmosphere*. It suggested that observed differences in the CO_2-treated Ws-2 and Ler-0 seeds have likely a genetic origin (ecotypic variations). This result might be of concern for the practice of long-term seed storage under a pure CO_2 atmosphere. Since we found that sensitivity to CO_2 is not only species-specific, but also ecotype-specific, we suggest that the usage of any other inert gasous atmosphere, such as N_2, Ar or vacuum, would be more suitable for the long-term storage of seeds.

Previous studies have shown that the low partial pressure of O_2 and the high partial pressure of CO_2 in the simulated Mars atmosphere are the two major factors inhibiting the germination of wheat seeds (Schwartzkopf and Mancinelli, 1991). However, the same authors reported that treatment with simulated Mars atmosphere does not have a lethal effect on wheat seeds, since these seeds retained their germinability upon their return to a normal Earth atmosphere. In an effort to elucidate the inconsistency of the effects of CO_2 on seed germination, Yoshioka et al. (1995) found that CO_2 stimulates the germination under normal physiological conditions, but it promotes the secondary dormancy as a response to exposure of seeds to

unfavourable conditions. For instance, the same authors demonstrated the induction of secondary dormancy in seeds that were pre-exposed to CO_2 and subsequently subjected to water stress, hypoxia or an increased concentration of ABA, which is a germination-inhibitory phytohormone. Therefore, we concluded that CO_2 likely acts as an inhibitor of germination in the Ler-0 line, probably promoting the secondary dormancy in the Ler-0 seeds after the exposure to extremely hypoxic condition, such as the simulated Mars CO_2 atmosphere*. In contrast, the Ws-2 seeds appeared to be insensitive to the action of CO_2.

Furthermore, our results revealed an unexpectedly high sensitivity of dry *Arabidopsis tt4-1* seeds (Ler-0 background) to the simulated Mars CO_2 atmosphere* (**Fig. 83C**). After the exposure to CO_2 rich atmosphere, these flavonoid-lacking seeds exhibited a significant decline in their germination capacity ($G_{max\%}$ = 60%), as shown in **Fig. 85F**. In addition, these seeds germinated much slower after the exposure to high CO_2 partial pressure (137% increase in MGT) (**Fig. 86F**). Other parameters of germination dynamics in the exposed *tt4-1* seeds revealed that CO_2 did not slow down the germination of the *tt4-1* seeds only by simply delaying the start of germination (11.5 hours of delay), but also by decreasing the germination uniformity, especially in the first half of the germination process (**Table 20**). In addition to its Ler-0-based genotype, which appeared more sensitive than the Ws-2 genotype, the extreme CO_2 sensitivity of the *tt4-1* seeds might be also related to a greater seed coat permeability in this flavonoid-lacking mutant, which facilitates gas exchange between the embryo and its environment (Debeaujon et al., 2000; Debeaujon et al., 2001; Debeaujon et al., 2007). Therefore, being long-term exposed to the simulated Mars CO_2 atmosphere*, the *tt4-1* embryos were likely subjected to a much higher concentration of CO_2 than the wild type embryos. However, it remains unclear whether the high concentration of CO_2 has only an inhibitory effect on germination or whether it has also a toxic effect on *tt4-1* seeds (the effect known under the term *CO_2 narcosis*). Since the viability of CO_2-exposed *tt4-1* seeds was not examined by the TZ test, it is unknown whether the ungerminated *tt4-1* seeds were killed or just metabolically arrested due to the CO_2-induced secondary dormancy.

The early-seedling stage

In spite of the changes observed in germination dynamics of Ler-0 seeds, the subsequent early-seedling development in both, the Ws-2 and Ler-0 wild type lines, was not affected by the exposure of *Arabidopsis* seeds to high CO_2 concentration (simulated Mars CO_2 atmosphere*). Almost all treated seeds germinated into normal seedlings (**Fig. 88D-E** and **Fig. 90D-E**). It

indicated that although treated Ler-0 seeds germinated slower, these seeds did not experience a significant decline in the seed vigour after the 21-days-exposure to simulated Mars CO_2 atmosphere*. It means that the treatment with high concentrations of CO_2 had probably only an inhibitory effect on germination, rather than damaging effect on the exposed Ler-0 seeds. However, to confirm this assumption, further studies are necessary, including the determination of the level and nature of possible molecular damage in CO_2-treated seeds e.g. before imbibition (in dry exposed seeds) and after germination (in seedlings developed from exposed seeds). Furthermore, it would be also interesting to determine the activity of repair and detoxification enzymes. The treatment with germination-promoting phytohormones e.g. gibberellins (GAs) and ethylene might reveal the state of dormancy in CO_2-treated Ler-0 seeds, providing more information about assumed germination-inhibitory action of high CO_2 concentrations.

On the other hand, we found that CO_2 treatment had an effect on root growth, but only in the Ler-0 ecotype, in which normally developed seedlings in the population had in average a significantly shorter primary roots (root length reduced by 26%) (**Fig. 91E**). This result contradicts the overall belief that elevated atmospheric CO_2 stimulates root growth in plants (Del Castillo et al., 1989; Rogers et al., 1992a; Rogers et al., 1992b). Crookshanks et al. (1998) observed significant developmental changes in the roots of early-stage *Arabidopsis* seedlings, reporting an increase in root length, higher root extension rate and enhanced root branching in the seedlings that were exposed to elevated CO_2. However, these authors measured the effects of much lower CO_2 concentration (2x CO_2 Earth atmosphere that equals ~ 0.07%), compared to the simulated Mars CO_2 atmosphere* (96% CO_2) that was used in our experiments. In addition, stimulating effects of CO_2 on root growth have been found to be related to enhanced carbon transport to roots upon the exposure of aerial parts of plants to elevated CO_2 (Crookshanks et al., 1998). The metabolism and response to higher concentrations of CO_2 are likely different in plant seeds, compared to the vegetative parts of plants. For instance, Andalo et al. (1998) reported that root length and branching are reduced in *Arabidopsis* seedlings, grown from seeds that have been produced under the atmosphere with elevated CO_2. These findings are in agreement with our results on the effects of CO_2 on root shortening observed in the Ler-0 ecotype. In contrast, no effects on root growth were observed in the Ws-2 seedlings (**Fig. 91D**), confirming the occurrence of genetic variability between these two *Arabidopsis* ecotypes. Even at the stage of early-seedling development, the Ws-2 wild type line appeared more robust than the Ler-0 ecotype, being insensitive to high concentrations of CO_2.

Similarly to the germination results, the early-seedling stage revealed increased sensitivity of the flavonoid-lacking *tt4-1* mutant to the simulated Mars CO_2 atmosphere*. Besides inhibition of germination, the exposure of the *tt4-1* seeds to a high CO_2 concentration induced the development of abnormal seedlings, mostly with short or twisted hypocotyl (**Fig. 90F**). Thus, only 55% of CO_2-exposed *tt4-1* seeds grew into normal seedlings (**Fig. 88F**). Similarly to the effects in the Ler-0 background, high CO_2 concentration also caused root shortening (root length reduced by 24%) in seedlings of this flavonoid-lacking mutant (**Fig. 91F**).

19.2.2. Combined effects of polychromatic $UV_{200-400}$ light and CO_2 rich atmosphere

In this work we also examined possible combined effects of polychromatic $UV_{200-400}$ radiation and simulated Mars CO_2 atmosphere* on *Arabidopsis* seeds. These effects were studied at the two developmental stages: the stage of seed germination and the stage of early-seedling development. Relatively little is known about combined effects of CO_2 and UV radiation on plant growth and development. Few previous studies concern the ecological problems of climate change on Earth in relation to the effects of elevated Earth atmospheric CO_2 and increased solar UV radiation on terrestrial biota (reviewed by Rozema et al., 1997). Since many plants respond positively to elevated atmospheric CO_2 and negatively to enhanced UV-B radiation, most studies have reported no significant net effects on plant growth (Rozema et al., 1997a). To our knowledge, no studies on the combined effects of high concentrations of CO_2 and polychromatic UV radiation on dry plant seeds have been published yet.

The germination stage

Our results showed that simultaneous exposure to extremely energetic polychromatic $UV_{200-400}$ light (1.5×10^5 kJm^{-2}) and simulated Mars CO_2 atmosphere (96% CO_2) had no effects on germinability of the Ws-2 wild type seeds, which regardless of the exposure, reached a high $G_{max\%}$ = 97% (**Fig. 83A** and **Fig. 85D**). However, the germination dynamics in exposed Ws-2 seeds were significantly altered. These seeds germinated slower, having a relative increase of 72% in MGT (**Fig. 86D**) and a delay in germination start of about 6 hours (**Fig. 83A**). Nevertheless, comparing the shapes of the germination curves (**Fig. 83A**), the germination capacity (**Fig. 85A** and **D**) and the speed of germination (**Fig. 86A** and **D**) of the Ws-2 seeds that were irradiated under the simulated Mars CO_2 atmosphere* and those that were irradiated under

the simulated space vacuum, we concluded that these two samples share a similar germination behaviour. This result, together with the fact that neither high vacuum nor simulated Mars CO_2 atmosphere* alone affected the germination of the Ws-2 seeds, implies that the observed changes in the germination dynamics are caused by polychromatic $UV_{200-400}$ light.

On the other hand, the Ler-0 wild type seeds appeared to be much more sensitive to the combined effects of polychromatic $UV_{200-400}$ light and simulated Mars CO_2 atmosphere* than the Ws-2 wild type seeds (**Fig. 83A** and **B**). Along with our data on the effects of polychromatic $UV_{200-400}$ light under high vacuum (section **19.1.2**), and in accordance with previously reported data on ecotypic variations in *Arabidopsis* plants (Andalo et al., 1996; Torabinejad and Caldwell, 2000; Cooley et al., 2001; Koornneef et al., 2004), our results confirm the occurrence of genetic variations in seed resistance between the Ws-2 and Ler-0 ecotypes. The possible reasons for differences in the UV response of these two seed lines are discussed above. The differences between these two ecotypes in their response to polychromatic $UV_{200-400}$ light are more pronounced under the simulated Mars CO_2 atmosphere* than under simulated space vacuum. The exposed Ler-0 seeds exhibited a reduced germinability ($G_{max\%}$ = 80%), and markedly altered germination behaviour (**Fig. 83B** and **Fig. 85E**). For example, the germination process in these seeds was significantly slower, since a 4.2-fold increase (322%) in MGT was measured, relative to the control samples (**Fig. 86E**). A delay of 24 hours in germination start, as well as the lower germination uniformity ($T_{25-75\%}$), both contributed to such a significant germination slowdown of exposed Ler-0 seeds (**Fig. 83B** and **Table 20**). In addition, our results indicate that both factors, the high CO_2 concentration and the polychromatic $UV_{200-400}$ light alone had adverse effects on the germination of the Ler-0 seeds, and the combined effects of these two factors appeared even more pronounced, suggesting that they probably act in a synergistic manner (compare **Fig. 86B** and **E**). The synergistic action of simulated Martian atmosphere and simulated Martian $UV_{200-400}$ radiation was also observed by Osman et al. (2008), who studied the resistance of desiccated *Bacillus pumilus* spores and other non-spore-formining bacterial cells.

The flavonoid-deficient *tt4-1* seeds, in contrast, appeared extremely sensitive to polychromatic $UV_{200-400}$ light in combination with the simulated Mars CO_2 atmosphere*, since no germinants ($G_{max\%}$ = 0%) were detected in exposed *tt4-1* samples (**Fig. 83C** and **Fig. 85F**). In addition, the TZ test revealed that none of these ungerminated seeds remained viable (**Fig. 88**). In spite of the fact that a high concentration of CO_2 alone had a strong inhibitory effect on the germination of the *tt4-1* seeds (**Fig. 83C**), the major detrimental effects were, however, attributed to polychromatic $UV_{200-400}$ light which, regardless of being applied alone (**Fig. 84**) or in

combination with a high vacuum or simulated Mars CO_2 atmosphere* (**Fig. 83C**), killed all the irradiated *tt4-1* seeds. Similarly to our experiments with quasi-monochromatic UV-C_{254}, and in agreement with our absorption spectroscopy results (chapter **3**, section **11.4** and chapter **4**, section **14**), the results on resistance to polychromatic $UV_{200-400}$ radiation revealed the extreme UV-sensitivity of flavonoid-lacking seeds. These results demonstrate the importance of flavonoids, which act as the major UV-screening compounds in *Arabidopsis* seeds.

The early-seedling stage

Simultaneous exposure of *Arabidopsis* seeds to polychromatic $UV_{200-400}$ radiation and simulated Mars CO_2 atmosphere* had a strong impact on the subsequent development of early-stage seedlings. We observed that the percentage of normal seedlings that developed from exposed seeds dropped significantly in the Ws-2 line (56%), and even more in the Ler-0 wild type (32%), as seen in **Fig. 88D** and **E**, respectively. The effect of significant root shortening in the population of normally developed seedlings was observed in both the Ws-2 and Ler-0 samples exposed to $UV_{200-400}$ light under simulated Mars CO_2 atmosphere* (**Fig. 91D** and **E**). The abnormally developed Ws-2 and Ler-0 seedlings exhibited a variety of morphological damages (**Fig. 90D** and **E**). Damaged seedlings most frequently developed short or twisted hypocotyls alone or in combination with short primary roots (**Fig. 89C** and **D**). In addition, severely damaged seedlings were also observed, especially in the Ler-0 line, where seedlings developed retarded or even missing roots in addition to damaged hypocotyls (**Fig. 89E** and **F**). These data clearly showed that, combined together, the polychromatic $UV_{200-400}$ light and simulated Mars CO_2 atmosphere* induce more damage in the early-stage *Arabidopsis* seedlings than polychromatic $UV_{200-400}$ light in combination with high vacuum (compare **Fig. 88D-E** with **Fig. 88A-B**, as well as **Fig. 90D-E** with **Fig. 90A-B**). Similarly to the germination stage, these results indicate that a high CO_2 concentration enhances the adverse effects of highly energetic UV radiation on seedling development in both *Arabidopsis* wild type lines. These two factors might act synergistically in exposed *Arabidopsis* seeds. To our knowledge, this is the first report of possible synergistic effects of high concentrations of CO_2 and UV radiation on plant seeds and their subsequent early seedling development.

Concluding remarks (9)

In this study we considered only the effects of the gas composition (CO_2 rich atmosphere), but not the effects of a low pressure of the Martian atmosphere. Our results revealed that 21-days-exposure to only simulated Mars CO_2 atmosphere* (96% CO_2, but at 1 atm) had no effects on germination capacity and seed vigour, as well as on subsequent seedling development in the Ws-2 wild type line.

The Ler-0 wild type appeared more sensitive to high CO_2 concentrations, probably due to naturally occurring genetic variations between the Ws-2 and Ler-0 ecotype. The CO_2-treated Ler-0 seeds exhibited a high germination capacity, but altered germination behaviour. The CO_2-exposed Ler-0 seeds germinated much germinated slower due to a delayed start of germination. However, almost all CO_2-exposed Ler-0 seeds subsequently developed into normal seedlings. Therefore we assumed that high concentrations of CO_2 had probably an inhibitory effect on germination, rather than damaging effect in exposed Ler-0 seeds. Further studies on seed physiology would be necessary to confirm this hypothesis (e.g.co-treatment with germination-promoting and germination-inhibiting phytohormones, detection of ROS, measuring the activity of antioxidant enzymes etc.).

In contrast to the wild types seeds, the flavonoid-lacking *tt4-1* mutant (Ler-0 accession), showed unexpectedly high sensitivity to simulated Mars CO_2 atmosphere*, which was observed both at the germination stage and the stage of early-seedling development. Exposure to a high CO_2 concentration affected both the germination capacity and seed vigour in the *tt4-1* seeds. Only 55% of CO_2-treated *tt4-1* seeds developed into normal seedlings. One of the reasons for the increased CO_2 sensitivity of the *tt4-1* seeds might be a greater permeability of flavonoid-lacking seed coat, which enables easier penetration of CO_2 in interior of the seed.

Simultaneous exposure to simulated polychromatic solar $UV_{200-400}$ (1.5×10^5 kJm^{-2}) and simulated Mars CO_2 atmosphere* (96% CO_2, but at 1 atm) revealed a remarkably high resistance of *Arabidopsis* Ws-2 wild type seeds, which exhibited a high germination capacity ($G_{max\%}$ = 97%), even after 21 days of exposure. For comparison, under the simulated Martian atmosphere and simulated Martian polychromatic UV radiation, more than 99% of *Bacillus* spores are killed within tens of seconds to few minutes of exposure (Mancinelli and Klovstad, 2000; Schuerger et al., 2003; Osman et al., 2008). Regardless of high $G_{max\%}$, the germination behaviour in exposed Ws-2 seeds was significantly altered (slower germination, delayed start of germination and decreased germination uniformity). High similarity of germination curves between the Ws-2 sample irradiated under simulated Mars CO_2 atmosphere* and that irradiated under high vacuum,

bring us to the conclusion that observed changes in germination of exposed Ws-2 seeds were due the polychromatic $UV_{200-400}$ radiation. This conclusion is also supported by the fact that simulated Mars CO_2 atmosphere* (section **19.2.1**) or high vacuum (section **19.1.1**) applied alone had no effect on germination of the Ws-2 seeds.

The Ler-0 wild type line was more sensitive than Ws-2 line to combined effects of simulated polychromatic solar $UV_{200-400}$ and simulated Mars CO_2 atmosphere*. Acting simultaneously, these to parameters had a synergistic adverse effects, decreasing the germination capacity ($G_{max\%}$ = 72%) and lowering the seed vigour in exposed Ler-0 seeds. The exposed Ler-0 seeds showed a markedly slower germination with delayed start of germination, as well as a decreasdecline in the germination uniformity. A slower germination of irradiated Ws-2 and Ler-0 seeds correlated with higher level of accumulated unrepaired damage, manifested through significantly higher level of abnormally developed seedlings. The abnormally developed Ws-2 and Ler-0 seedlings exhibited a variety of morphological damages, ranging form the short or twisted hypocotyls in seedlings with normally developed roots up to the severely damaged seedling forms with retarded or even missing root system. The synergistic action of deleterious polychromatic $UV_{200-400}$ and simulated Mars CO_2 atmosphere* were also observed at the stage of early-seedling development. To our knowledge, this is the first report of synergistic effect of UV radiation and high CO_2 concentration on plant seeds. These results may have implication in the future photobiological and dosimetric studies, studying the chances of survival for terrestrial life on Mars (e.g. planetary protection issues, but also future terraforming and colonization issues). Here we point out that particular attention should be paid on possible synergistic effects of CO_2 and UV radiation, which might be in some cases species-specific, but also genotype- (or strain-) specific.

We demonstrated that the flavonoid-deficient *tt4-1* seeds were extremely sensitive to polychromatic $UV_{200-400}$ when irradiated under simulated Mars CO_2 atmosphere*. No viable seed were detected in irradiated samples. The effect was attributed to UV radiation, since equally deleterious effect was also obseved in *tt4-1* samples that were exposed only to polychromatic $UV_{200-400}$ radiation. This again confirmed the importance of flavonoids in UV-screening protection of seeds. We concluded that the flavonoid-lacking seeds are at least 5 orders of magnitude more sensitive to polychromatic solar $UV_{200-400}$ radiation than the wild type seeds.

At both the germination and early-seedling stage the scale of $UV_{200-400}$ resistance under the high CO_2 partial pressure was determined for different *Arabidopsis* genotypes as follows: Ws-2 > Ler-0 >>*tt4-1*.

Chapter 7

GENERAL DISCUSSION AND CONCLUSIONS

The aim of astrobiology is to extend our knowledge about the origin of life and the processes involved in evolution and distribution of life on Earth or elsewhere in the Universe, determining the physical, chemical and environmental limitation factors for survival. Despite the existence of different theories about the origin of terrestrial life (e.g. theory of abiogenesis, panspermia hypothesis etc.), many of them consider the importance of solar UV radiation in the processes that might have preceded the emergence of life and those that have likely directed the evolution of life. In spite of being the primary source of energy on the surface of Earth, solar radiation was probably a source of deleterious damage to biomolecules and cellular components during the early evolution (Cockell, 1998; Nicholson et al., 2000). Extraterrestrial environments possess quite different UV radiation regimes, both in terms of absolute flux and spectral quality, compared to that found on Earth (Cockell, 2001b). Among all parameters of space environment, UV radiation is considered as one of the most deleterious factors, limiting the chances of interplanetary transfer and dispersal of life through space (Hotchin et al., 1968; Lorenz et al., 1968; Bücker et al., 1974; Spizizen et al., 1975; Horneck et al., 1984a; Horneck et al., 1984b; Horneck, 1993; Horneck et al., 1994; Horneck, 1995). The reason for that is the occurrence of highly energetic UV-C and VUV radiation in space environment. Planetary bodies that contain atmosphere are partially protected from high fluxes of UV radiation. For instance, ozone accumulated in the Earth's atmosphere strongly absorbs the UV wavelengths shorter than 300 nm, thus shielding the terrestrial surface from highly energetic VUV, UV-C and most of UV-B wavelengths (Cockell, 1998; Cockell, 2001b; Nicholson et al., 2005). However, the atmosphere of the early Earth probably lacked a significant ozone layer. Therefore evolving on the early Earth, life had likely to cope with higher fluxes of UV-C and UV-B radiation (Cockell, 1998; Cockell, 2001a; Cockell and Raven, 2007). Mars atmosphere, which is composed mainly of carbon dioxide (CO_2), absorbs the wavelengths below 195 nm and thus shields from the VUV part of the spectrum. However, there is a considerably greater flux of UV-B radiation on the surface of Mars, in addition to UV-C wavelengths that are transmitted through the Martian atmosphere (Cockell, 2001b; Cockell, 2001c). On the other hand, the surfaces of planetary bodies that lack atmosphere (e. g. asteroids and Earth's Moon) are exposed to full spectrum of solar UV radiation (Nicholson et al., 2005).

In astrobiological studies, attention has been focused mainly on prokaryotes that show high stress resistance, including the so-called extremophiles, which flourish in environments where nothing else can survive. Some prokaryotes are highly resistant to water-stress. For instance, some cyanobacteria, such as *Chroococcidiopsis* that naturally inhabit both hot and cold deserts, can resist high desiccation (Friedmann et al., 1967; Friedmann, 1971). Spores of bacterium *Bacillus subtilis* have been shown to posses remarkably high resistance to different stress factors,

including heat, desiccation, high vacuum, chemicals, UV and ionizing radiation etc. (reviewed by Nicholson et al., 2000). The bacterium *Deinococcus radiodurans* is the most radiation-resistant microorganism known on Earth today (Levin-Zaidman et al., 2003). Meristematic black microfungi from Antarctica were reported to withstand the harsh conditions of extremely low temperature, low water availability and UV radiation (Onofri et al., 2004). Lichens, which are symbiotic associations of an alga and/or cyanobacteria and a fungus, are able to colonize habitats where conditions are too extreme to support the life of other organisms (e.g. lichens inhabit harsh Antarctica and Arctic regions, as well as tropical regions) (de Vera et al., 2004; de la Torre Noetzel et al., 2007). On the other hand, the limits of eukaryote survival are not as well known. The existence of terrestrial extremophiles has led to speculations about possible survival of organisms during interplanetary transfer and that life could be present even on other planets of the Solar system (Onofri et al., 2008).

The Earth orbit space technology has provided a new opportunity in advancing the astrobiological studies, enabling a direct exposure of terrestrial life forms and organic matter to the full spectrum of solar radiation outside the constraints of the Earth's atmosphere. In most of previous space experiments the exposure time to space environment was relatively short, ranging from few hours up to several weeks, with exception of the ERA/EURECA experiment that lasted about 11 months (see **Annex A**). To date, the maximum time that organisms have been exposed to open space environment was 6 years during the LDEF mission. *Bacillus subtilis* spores survived almost 6 years in space on board LDEF facility (NASA) when shielded against solar UV radiation (Horneck et al., 1994). However, direct exposure to the solar extraterrestrial UV radiation killed most of *Bacillus* spores. So far, lichens are the only yet studied life form capable of surviving two-week exposure to combined all parameters of space environment, including UV radiation, as tested during the BIOPAN-5 mission (Sancho et al., 2007).

Recently, the European Space Agency (ESA) has developed two EXPOSE facilities (EXPOSE-E and EXPOSE-R) that were attached to the external pallet of the International Space Station (ISS). These facilities supported long-term (about 1.5 years) photobiological and photochemical experiments that are carried out under open space conditions. Among these astrobiological experiments, the SEEDS experiments study the responses of plant seeds to extreme space conditions, notably full solar UV radiation. Prior the space flight, we performed several preliminary ground-based experiments in order to determine the resistance of *Arabidopsis* seeds to UV radiation and some other parameters of space environment. Here below are discussed some of the main conclusions that were drawn from the present study.

1. ***Due to its high absorption in the short-wavelength part of the UV spectrum, DNA is considered a particularly sensitive target to UV-induced damage. The qualitative VUV-UV absorption characteristics of DNA can slightly vary depending on the hydration status of the molecule and overall (genomic) G+C content. However, a greater influence on the UV absorption properties of DNA might be expected in the local, noncoding segments of genomic DNA, where repeated nucleotide sequences and the extreme G+C or A+T content are frequently encountered.***

DNA stores essential genetic information about the structure and function of each organism. The absorption spectrum of DNA roughly correlates with the action spectra for DNA damage and photoproduct formation (Hidea et al., 1986). We measured VUV-UV absorption spectra (λ = 125-340 nm) of DNA and its components in order to better understand the UV absorption characteristics of DNA and to predict its viability after exposure to UV light. VUV-UV absorption spectra of dry thin films of genomic DNA revealed two maxima of absorption at 264 nm (region I) and at 192 nm (region II), as well as continuously increasing absorption towards the lower end of the spectrum at 125 nm (region III). Upon hydration, a small hypsochromic shift of the absorption peak in the region I (260 nm) was observed for the same DNA sample. Since the degeneracy of genetic code allows significant variations in G+C content, we investigated whether the nucleotide content in the coding DNA regions can influence the overall UV absorption properties. We measured VUV-UV absorption spectra for synthetic, protein-encoding DNA that contained 30%, 50% and 63% G+C, while retaining the same amino acid sequence in encoded polypeptide chain. We concluded that besides a small bathochromic shift in region I, which correlated with increasing G+C content, the differences in the total G+C content in this synthetic, protein-encoding DNA had relatively small effect on the overall qualitative properties of UV absorption spectra. The VUV-UV absorption spectra of homopolymeric oligoA+T (G+C content 0%) and oligoG+C (G+C content 100%) DNA samples differed significantly from each other, as well as from that of genomic DNA. Although these extreme G+C contents do not represent in reality the nucleotide content of genomic DNA, such nucleotide sequences, known as the homopolymeric DNA tracts, do occur locally in the noncoding regions of the genomes of both prokaryotic and particularly eukaryotic organisms (Dechering et al., 1998; Shomer and Yagil, 1999). We concluded that nucleotide content in noncoding DNA regions can significantly alter the UV absorption of the local segments in genomic DNA.

2. ***Based on degree of similarity of VUV-UV absorption spectra between DNA and different studied potential, ubiquitously occurring UV screens (nucleotides, proteins, free amino acids, polyamines and tyramine), we concluded that these compounds would provide less efficient UV screening protection to genomic DNA, unless they are present in relatively high concentrations in cells. The exception are mononucleotides, particularly adenosine 5'-triphosphate (ATP), which might be better suited to protect DNA from UV-induced damage. We suggested that on the early Earth, the primitive cells might have used ATP as an ancient UV screen.***

Organisms that evolved on Earth developed different mechanisms for resisting UV radiation, including the synthesis of UV screens. We assumed that an ideal UV screen would absorb UV radiation in a manner similar to DNA. We first examined the VUV-UV properties of different organic compounds that occur in all organisms. We assumed that some of these compounds might have been present in the primitive cells on the early Earth. Comparing VUV-UV spectra (λ = 125-340 nm) of nucleotides, proteins, free amino acids, polyamines and tyramine with VUV-UV spectrum of genomic DNA, we concluded that most of these potential, ubiquitously occurring UV screens would provide relatively poor UV screening protection to DNA, unless their concentration in cell is so high that the target would be protected even at the absorption minima of screen. Such a nonspecific opacity to UV radiation would be less efficient than that afforded by a well-matched UV screen. However, among all here studied potential UV screens, we single out the free nucleotides, particularly adenosine 5'-triphosphate (ATP), which might be best suited to protect DNA from UV light throughout the DNA absorption spectrum. We suggested that during the early history of life on Earth, when organisms were likely exposed to high fluxes of energetic UV radiation, the primitive cells might have used ATP as an ancient UV screen, in addition to its primary roles in the energy transfer and building up the genetic material.

3. ***Comparing the qualitative VUV-UV absorption properties of DNA and different known specialized UV screens that occur in phylogenetically diverse groups of organisms (mycosporine-like amino acids, scytonemin, carotenoids, melanin and flavonoids), we evaluated the likely effectiveness of these molecules in shielding DNA from deleterious UV radiation. We found that among all studied substances, flavonoids (particularly glycosylated flavonols), which are plant-specific sunscreens, can be considered the ideal UV screens due to a remarkable resemblance of their VUV-UV absorption spectra with that of DNA.***

In contrast to unspecific, potential UV screens, many organisms synthesise specific chemical compounds that are highly efficient in filtration of deleterious UV wavelengths. In the present work we measured VUV-UV absorption spectra (λ = 125-340 nm) of dry thin films of different specialized UV screens. This study provides valuable spectroscopic data about the VUV-UV absorption properties of above mentioned specialized UV screens, which were previously practically unknown in the spectral region below 200 nm. Using similarity with DNA absorption spectrum as a primary criterion, we evaluated their likely effectiveness in screening deleterious UV light.

We concluded that MAAs, which are intracellular UV screens found in cyanobacteria, algae, some heteroptrophic bacteria, fungi, lichens, as well as in a variety of marine invertebrates and vertebrates, provide a relatively good screening protection against UV-B and UV-A radiation, as well as in the VUV region, but they are poor UV screens in the UV-C part of the spectrum.

Scytonemin, which is an extracellular pigment found in sheaths of many cyanobacteria, exhibits an excellent screening properties in the UV-A part of the spectrum. It likely provides a good protection to DNA in the VUV, and to the lesser extent in the UV-C part of the spectrum. However, scytonemin probably screens relatively poorly in the UV-B region. Cyanobacteria belong to an ancient phylogenetic group of phototrophic organisms that likely existed 3.5 Ga ago, when the early Earth was probably exposed to highly energetic solar UV radiation. We assumed that scytonemin, if occurred in ancient cyanobacteria, would probably not be alone sufficient to protect cells from unfiltered solar UV radiation. Ancient cyanobacteria might have used some other complementary UV screens in addition to scytonemin.

Carotenoids are synthesized by all photosynthetic organisms (including plants, algae and cyanobacteria), and in some heterotrophic bacteria and fungi. Carotenoids absorbs mainly in the visible part of the spectrum (blue light), with an extension into the UV-A. Although carotenoids would efficiently screen from VUV radiation, they would not provide good screening protection to DNA from UV-C and UV-B radiation. We suggested that carotenoids may play an important role in photoprotection, but probably acting as efficient antioxidants and free radical quenchers (indirect UV protection), rather than UV screens.

Melanins are known specialized UV screens that are widely distributed in the animal kingdom, but they could be also found in some eubacteria and fungi. The monotonous, almost linear increase in absorption throughout the visible and UV part of spectrum down to 145 nm, below which the absorption climbed steeply towards the lower end of the spectrum, revealed that melanins would provide efficient, but unspecific UV screening protection to biological material filtering out unselectively all UV wavelengths and part of visible light. This would be a

disadvantage for photosynthetic organisms and other organisms that depend on capturing sunlight.

Flavonoids are specialized UV screens found in plants. The VUV-UV absorption spectra of three here studied glycosylated flavonols (quercitrin, isoquercitrin and robinin) showed a remarkably high level of similarity with that of DNA. Complemented with proanthocyanidins (also known as condensed tannins), which are another group of catechin-containing polymeric flavonoids that are particularly rich in plant seeds, glycosylated flavonoids would screen efficiently in the VUV, UV-C, as well as the UV-B part of the spectrum. Flavonoids also strongly absorb UV-A light, possible preventing the formation of ROS that can lead to the indirect UV-induced DNA damage. We suggested that according to the UV absorption properties, flavonoids can be considered the ideal UV screens.

4. ***Plant seeds are rich sources of secondary metabolites. We confirmed that flavonoids, sinapate esters and glucosinolates are the major secondary metabolites in Arabidopsis seeds. We found that quercetin-3-O-rhamnoside (also know as quercitrin) is a dominant and remarkably abundant flavonoid in Arabidopsis seeds. Conventional UV absorption spectra in solution and VUV-UV absorption spectra in dry films revealed that flavonoids predominate the overall UV absorption spectrum of crude seed extract. We found that the majority of glucosinolates isolated from Arabidopsis seeds are poor UV absorbers, thus probably inefficient UV screens. According to UV absorption spectroscopy results, and contrary to previously reported studies, we suggested that flavonoids are better suited UV screens than sinapate esters.***

Plants produce a large variety of different secondary metabolites. Seeds accumulate relatively high amounts of secondary metabolites, particularly flavonoids. They are known to resist various harsh conditions, including biotic and abiotic stresses (Rajjou and Debeaujon, 2008). We aimed to identify and isolate the substances from *Arabidopsis* seed extract that are dominant, not only quantitatively, but also by their UV absorption features that might provide efficient UV screening protection to DNA. Our HPLC and LC-MS analyses showed that *Arabidopsis* seeds contain a large variety of chemical substances, identified and classified mainly as flavonoids, sinapate esters and glucosinolates.

Conventional UV absorption spectra in solution (λ = 200-400 nm), as well as VUV-UV absorption spectra in dry films (λ = 125-340 nm) revealed that a crude extract from *Arabidopsis* wild type seeds absorbs strongly in the UV part of the spectrum. The UV absorption characteristics of flavonoids predominated the overall UV absorption spectrum of the seed

extract. We found that quercetin-3-*O*-rhamnoside (a type of glycosylated flavonol, also know as quercitrin) is a dominant and remarkably abundant flavonoid in *Arabidopsis* seeds. Studying UV absorption spectra in solution and VUV-UV spectra in dry films, we found that glycosylated flavonols (including quercitrin) that were isolated from *Arabidopsis* seeds are well-suited UV screens, which may provide efficient screening protection to DNA in the UV-C (DNA peak I), as well as the VUV (DNA peaks II and III) part of the spectrum. Due to a high absorption in the UV-A part of the spectrum, we suggested that flavonoids may also act as efficient protectants against indirect, oxidative damage to DNA and proteins.

Besides flavonoids, were also detected smaller amounts of sinapate esters in *Arabidopsis* seed extract. Sinapate esters are known to act as efficient UV protectants in plants, and were reported to provide even better UV screening protection than flavonoids (Chapple et al., 1992; Sheahan, 1996). However, our absorption spectroscopy results led us to conclude that sinapate esters would be less suited than flavonoids in providing a direct UV screening protection to DNA, particularly in the UV-C part of the spectrum, since they showed a local absorption maximum at the wavelengths at which DNA exhibits the maximum of absorption. Nevertheless, sinapate esters might have another indirect role in the UV protection, making them more efficient protectants *in vivo* than flavonoids.

Glucosinolates, the third group of secondary metabolites isolated from *Arabidopsis* seeds, were shown to be poor UV absorbers above 250 nm. We concluded that aliphatic glucosinolates, which represent the majority of *Arabidopsis* seed glucosinolates, would provide no specific protection to DNA or other cellular targets in the UV-A, UV-B and UV-C part of spectrum.

We concluded that among different secondary metabolites isolated from plant seeds, flavonoids can be considered as the best suited UV screens. Since our UV absorption spectroscopy studies provided only preliminary estimation of UV screening efficiency, further *in vivo* experiments were necessary to confirm our hypothesis (for details see points 10. and 11.).

5. Plant seeds can be considered as a good multicellular photobiological model, particularly suitable for in vivo study of the ability of chemical substances to provide efficient UV screening protection.

The UV screens provide the first line of defence before damage occurs. Because screening compounds represent a passive method of UV protection, proving that enhanced survival in irradiated organism is only due to the presence of particular chemical substance may be a complex problem. Other physiological responses, including the active mechanisms of

photoprotection, such as the enzymatic damage repair and detoxification may also be involved. Therefore, to evaluate the UV screening efficiency *in vivo*, it is necessary to test whether the compound could provide UV protection when other physiological processes are not functioning. One of the methods is exposing the cells to UV light while they are in dry state. Whereas this method is suitable for some microbial models (e.g. spore-forming bacteria and desiccation-tolerant cyanobacteria), for the majority of multicellular organisms this approach may be problematic, since the desiccation will usually kill a whole organism (Cockell and Knowland, 1999). The exception are plant seeds, which are multicellular life forms that are extremely tolerant to desiccation thanks to the formation of intracellular glasses (Buitink and Leprince, 2004; Buitink and Leprince, 2008). The advantage of using dry seeds in photobiological studies is that they are in metabolically quiescent state. Therefore the UV resistance of plant seeds is well comparable with other model organisms used in photobiological studies e.g. *Bacillus subtilis* spores. In dry seeds, the progressive accumulation of damage occurs, and due to very low metabolic activity, there is little or no damage repair. Therefore, the efficiency in passive UV screening is one of the essential issues for survival of dry seeds. Plant seeds accumulate large amounts of UV screening compounds. They are rich sources of flavonoids, which we consider particularly efficient UV screens.

In this work we studied the UV resistance of *Arabidopsis thaliana* seeds, observed through the three different stages of plant developmental: the germination, the early seedling stage and the stage of mature plant development. Depending on the efficiency of UV screening protection and consequently, the level of accumulated damage in dry seeds, the germination is considered a decisive phase. At the germination stage, besides the germination capacity ($G_{max\%}$), we studied the dynamics of germination process, measuring the mean germination time (MGT), the median of germination ($T_{50\%}$), the germination uniformity ($T_{25\text{-}75\%}$) and the skewness of germination curve ($T_{50\%}$/MGT). We suggested that the germination capacity alone, which is observed at the end of germination process, is not sufficient to understand the physiology of seed resistance, since the germination dynamics provides additional information about the seed vigour, likely indicating the state of accumulated damage and its repair (e.g. more damage accumulated, the germination is slower due to longer time required for repair and detoxification prior the radicle emergence). In addition, comparing the resistance among different irradiated seeds samples, we found that $G_{max\%}$ parameter reveals the differences at the large scale (orders of magnitude), while by measuring the parameters of germination dynamics (e.g. MGT), we can detect fine differences in germination behaviour, measurable at the small scale (within the same order of magnitude).

In addition to the germination phase, we found that the subsequent stage of the early-seedling development is the second critical step in plant development, since it reveals whether or not the germinants are able to grow into normal seedlings with fully developed essential seedling structures: the root system, hypocotyl and cotyledons. Depending on the efficiency of repair and detoxification systems in germinating seed, the seedling damage will be more or less severe. After the exposure of *Arabidopsis* seeds to UV radiation, we found that low seed vigour was usually related to the increased number of abnormally developed seedlings, which were grouped into following five categories: (1) seedlings with short or twisted hypocotyls, but normally developed primary roots, (2) seedlings with short or twisted hypocotyls and short primary roots, (3) seedlings with short or twisted hypocotyls and retarded roots, (4) seedlings with short or twisted hypocotyls and missing roots, (5) seedling forms with missing hypocotyls, missing roots and cotyledons that are not fully developed. Categories 3, 4 and 5 we considered as severely damaged seedlings, which rarely developed further into mature plants. We concluded that the seedlings primary root system is a particularly sensitive organ, which if damaged (short, retarded or missing) will lower the chances of plant survival.

6. Dry Arabidopsis thaliana wild type seeds exhibit high resistance to extremely high fluences (up to 6 x 10^5 kJm^{-2}) of quasi-monochromatic UV-C_{254} light.

In order to predict the survivability of *Arabidopsis* seeds exposed to space conditions during 1.5 years of the EXPOSE missions, it was necessary to determine the upper limits of seed resistance to deleterious, highly energetic UV radiation. Since the action spectrum for the induction of DNA damage roughly follows the absorption spectrum of DNA, we assumed that above 200 nm the maximal biological effectiveness of DNA damage would be caused by UV-C radiation at wavelengths close to the maximum of absorption of DNA ($\lambda \approx 260$ nm). Since the light emitted from our UV-C_{254} source was not strictly monochromatic, comprising 90% of dominant UV-C_{254} radiation and the minor portion (10%) of concurrent UV-B_{312} + UV-A_{365} light, we call it the quasi-monochromatic UV-C_{254} light. As we found that the minor UV-B + UV-A portion of the incident light had no adverse effects on *Arabidopsis* wild type seeds (see point 7.), we concluded that all below described changes were due the dominant UV-C_{254} component of emitted light.

At the germination stage, we found that irradiated wild type *Arabidopsis* seeds exhibit an extremely high resistance to quasi-monochromatic UV-C_{254} light at fluence as high as 6 x 10^5 kJm^{-2} (Ws-2 ecotype) and 4.8 x 10^5 kJm^{-2} (Col-0 ecotype), showing unaltered and remarkably

high germination capacity ($G_{max\%}$ = 93-99%). However, a smaller change in germination dynamics indicated the beginning of decline in seed vigour, which was manifested through slightly slower germination and lower germination uniformity. At the early-seedling stage, we detected increased percentage of abnormal seedlings that were grown from irradiated seeds. Most of seedlings exhibited short or twisted hypocotyls, but normal or sometimes shorter roots. Some of seedlings were seriously damaged, having short or twisted hypocotyls and retarded or even missing roots. Only few germinants gave rise to the aberrant forms that had neither developed hypocotyls nor roots, and exhibiting poorly developed cotyledons. The in-soil experiments revealed that plant growth and development were affected by UV-C_{254} light. Besides decreased survival rate of mature plants (72% in the Col-0 and 53% in the Ws-2 ecotype), UV-C_{254} light had also a strong impact on vegetative growth, as well as reproductive output of plants developed from irradiated seeds. Our results demonstrated that the high germinability in UV-C_{254} irradiated seeds does not necessarily guarantee the high survival rate of mature plants, justifying the need to study not only the germination phase but also the whole process of plant development. The phenomenon of decreased plant survival rate is likely related to the lower vigour of irradiated seeds (indicating more accumulated damage), the higher rate of seedling damage, which particularly affected the root system (indicating the higher level of unrepaired damage), and the fact that the in-soil growth conditions in greenhouse are more restrictive than optimal *in vitro* conditions, used to study the germination and early-seedling development.

In spite of lower plant survival, we consider *Arabidopsis* seeds extremely resistant to UV-C_{254} light, compared to any other know terrestrial life form. *Arabidopsis* seeds are at least 6 orders of magnitude more resistant to UV-C_{254} light than *Bacillus subtilis* WT 168 spores (LD_{50} = 0.123 kJm^{-2} and LD_{90} = 0.245 kJm^{-2}, according to the present study). They are also at least 5 orders of magnitude more resistant than spores of *Bacillus pumilus* SAFR-032, an isolate obtained from an ultraclean spacecraft assembly facility, for which was reported the highest degree of spore UV-C_{254} resistance observed by any *Bacillus* spp. encountered to date (LD_{90} = 1.7 kJm^{-2}) (Link et al., 2004). *Arabidopsis* seeds are also far more resistant to UV-C_{254} light (at least 5 orders of magnitude) than radiation resistant extremophile, a bacterium *Deinococcus radiodurans* (Battista et al., 2000; Chen et al., 2000).

7. Arabidopsis thaliana wild type seeds are highly resistant to UV-B + UV-A light up to fluences of 4.3 x 10^4 kJm^{-2} and 1.2 x 10^4 kJm^{-2}, respectively, which had no effects on seed germination nor subsequent phases of the early-seedling development and the mature plant development.

Although UV-B + UV-A wavelengths represented only the minor portion (10%) of the light emitted from the UV-C_{254} source, after long-duration exposure (up to 60 days) of *Arabidopsis* seeds to incident UV light, the total fluences of the concurrent UV-B_{312} and UV-A_{365} radiation reached a very high level. Irradiated wild type *Arabidopsis* seeds showed a high resistance to UV-B + UV-A portion of the emitted light at fluences as high as UV-B = 4.3 x 10^4 kJm^{-2} and UV-A = 1.2 x 10^4 kJm^{-2} (Ws-2 ecotype) or UV-B = 3.4 x 10^4 kJm^{-2} and UV-A = 9.5 x 10^3 kJm^{-2} (Col-0 ecotype). The exposure of the Ws-2 and Col-0 wild type seeds to UV-B + UV-A radiation had no effect on germination capacity, which remained at high level ($G_{max\%}$ = 95-100%) in irradiated seeds. Similarly, there was no observed change in germination dynamics in irradiated wild type seeds. In addition, all germinated seeds subsequently developed into normal seedlings, indicating that UV-B + UV-A-induced damage ether did not occur (e.g. due to the efficient UV screening protection) or it was successfully repaired during the early phases of germination. Furthermore, we found that the exposure of the wild type seeds to UV-B + UV-A radiation had no effects on in-soil plant growth and development or reproductive capacity.

For comparison, 3 orders of magnitude lower UV-B +UV-A fluence kills 90% of *Bacillus subtilis* wild type spores (LD_{90} = 30 kJm^{-2}) (Riesenman and Nicholson, 2000; Slieman and Nicholson, 2000). The UV doses in the present study were 2-3 orders of magnitude higher than those used in previous studies on the effects of UV-B radiation on the vegetative parts of plants (Mirecki and Teramura, 1984; Murali et al., 1988; Barnes et al., 1990; Landry et al., 1995), and about 1-2 orders of magnitude higher than those used in studies on seed resistance (Musil, 1994; Musil et al., 1998; Dai and Upadhyaya, 2002). Therefore, the present study provides new data about the resistance of *Arabidopsis* seeds to high levels of UV-B + UV-A radiation. These experiments, in addition to photobiological and astrobiological context, may have ecological and agronomical implications, given the reduction of the stratospheric ozone layer and enhanced levels of UV radiation, particularly UV-B radiation, on the surface of Earth.

8. *Arabidopsis thaliana wild type seeds showed a remarkably high resistance to simulated polychromatic solar $UV_{200-400}$ (1.5×10^5 kJm^{-2}) when exposed under simulated space vacuum for 22 days. This indicated that dry Arabidopsis thaliana seeds might survive the long-term exposure to space conditions during the EXPOSE missions at the ISS.*

In space, deleterious UV radiation is encountered together with other harsh conditions. Yet, polychromatic solar UV radiation has been found to be one of the most damaging factors in space, as tested with various terrestrial biological models (Hotchin et al., 1968; Lorenz et al., 1968; Bücker et al., 1974; Spizizen et al., 1975; Horneck et al., 1984a; Horneck et al., 1984b; Horneck et al., 1994). Our results from the EVT simulation experiments showed a remarkably high resistance of *Arabidopsis* wild type seeds to simulated polychromatic solar $UV_{200-400}$ light at fluence as high as 1.5×10^5 kJm^{-2}, which corresponded to the expected total fluence of extraterrestrial solar $UV_{200-400}$ light in the EXPOSE experiments after 1.5 years of space mission outside the ISS. A special attention was paid to possible combined effects of polychromatic solar UV and extreme space vacuum, since it is known that acting together, these two factors may have a strong adverse synergistic effect (Horneck et al., 1984a; Weber and Greenberg, 1985; Dose et al., 1996; Fekete et al., 2005). Nevertheless, simultaneous exposure of dry *Arabidopsis* seeds to simulated polychromatic solar $UV_{200-400}$ radiation and simulated space vacuum (10^{-5} Pa), which corresponded to the pressure encountered outside the ISS, had no effect on germination capacity in both the Ws-2 and Ler-0 wild type seeds. This is the first report of such high level of resistance to simulated space conditions known to occur in any yet-studied life form. In spite of their high germinability ($G_{max\%}$ = 92-98%), a considerable change in germination dynamics was however observed in irradiated seeds. This indicated an important decline in seed vigour, particularly in Ler-0 seeds, which was manifested through markedly decreased germination speed, delayed start of germination and lower germination uniformity. We assumed that the delay in radicle emergence in irradiated seeds is likely due to a longer time required to cope with accumulated damage. Probably due to remaining unrepaired (or unsuccessfully reversed) damage, the percentage of abnormally developed seedlings increased in irradiated Ws-2 and Ler-0 samples. Seedlings with abnormal morphology exhibited mostly changes in growth of the hypocotyls (short or twisted) and primary roots (short roots). Only few irradiated seeds developed seriously damaged seedlings with retarded roots. We assumed that the affected root growth was the major reason of relatively low survival rate for the mature plants that were grown in soil from irradiated seeds (53% in the Ler-0 and 36% in the Ws-2 ecotype). Because we found that simulated space vacuum alone had no adverse effect on seed germination and subsequent development of early-stage seedlings and grown plant, we concluded that all here described effects are due to polychromatic $UV_{200-400}$ radiation.

Although polychromatic $UV_{200-400}$ light caused an important decrease in the final survival rate of grown plant, *Arabidopsis* seeds, however, should be considered an extremely resistant life form. For comparison, exposure of *Bacillus subtilis* spores to comparable polychromatic $UV_{200-400}$ radiation at fluences as low as 1 kJm^{-2} caused inactivation of the spores by 2 orders of magnitude (Horneck, 1993). *Arabidopsis* seeds are more than 5 orders of magnitude more resistant than *Bacillus pumilus* spores, which showed less than 10% survival after the exposure to polychromatic $UV_{200-400}$ light at 9 kJm^{-2} (Osman et al., 2008). Comparing the results from the EVT experiments that were performed in parallel to our simulation experiment, we found that *Arabidopsis* dry seeds are far more resistant to combined effects of simulated polychromatic $UV_{200-400}$ light and simulated space vacuum than the other astrobiological models. For instance, under the same experimental conditions, the isolates of Antarctic black fungi *Cryptomyces* and cryptoendolithic communities, which are considered as extremely resistant life forms particularly suitable for astrobiological studies, showed no survival (Onofri et al., 2008). Under similar simulation conditions, the lichens, such as *Xanthoria elegans*, which are used in space experiments as extremely resistant models for testing lithopanspermia theory (Sancho et al., 2007; de la Torre et al., 2010), showed about 3 orders of magnitude lower resistance to combined effects of simulated polychromatic $UV_{200-400}$ light and simulated space vacuum (de Vera et al., 2004), when compared to *Arabidopsis* dry seeds.

9. *Simultaneous exposure to simulated polychromatic solar $UV_{200-400}$ (1.5×10^5 kJm^{-2}) and simulated Mars CO_2 atmosphere* (95.6% CO_2 at 1 atm) revealed a high resistance of Arabidopsis wild type seeds even after 21 days of exposure. High concentrations of CO_2 may enhance the effects of UV radiation, suggesting that these two factors probably act in a synergistic manner.*

Mars has a thin atmosphere composed predominantly of CO_2 (~95%) at the total pressure of about 6 mb (600 Pa). Since it lacks a significant ozone layer, high fluxes of relatively unattenuated solar UV radiation, including highly energetic UV-C wavelengths reach the surface of Mars. Because in our experiments the Martian atmosphere was simulated only in view of its composition, but not the low pressure, we termed it the "simulated Mars CO_2 atmosphere*". After 21 days of exposure to polychromatic $UV_{200-400}$ light (1.5×10^5 kJm^{-2}) under the simulated Mars CO_2 atmosphere*, wild type *Arabidopsis* seeds exhibited high resistance, retaining relatively high germination capacity ($G_{max\%}$ = 97% and 80% for the Ws-2 and Ler-0 ecotypes, respectively). However, the germination dynamics was markedly altered in the exposed seeds, particularly in the Ler-0 ectype (the germination was slowed and the start of germination was considerably delayed), indicating serious decline in the seed vigour. This was consistent with

higher level of abnormally developed seedlings, which exhibited a variety of morphological changes, ranging from the short or twisted hypocotyls up to seriously damaged primary roots (retarded or even missing root system). We found that simulated polychromatic solar $UV_{200-400}$ had a stronger impact when seeds were exposed under simulated Mars CO_2 atmosphere* than under simulated space vacuum. To our knowledge, this is the first report of possible synergistic effects of high concentrations of CO_2 and UV radiation on plant seeds.

In spite of the observed effects of polychromatic solar $UV_{200-400}$ radiation and CO_2 rich atmosphere on seed germination and seedling development, we concluded that *Arabidopsis* seeds are highly resistant, when compared to the other biological models (e.g. more than 99% of *Bacillus subtilis* and *Bacillus pumilus* spores are killed within tens of seconds to few minutes of exposure to simulated Martian polychromatic UV radiation under simulated Martian atmosphere, Mancinelli and Klovstad, 2000; Schuerger et al., 2003; Osman et al., 2008). Therefore we suggested that plant seeds could be considered as a suitable eukaryotic model for the future biological exploration of Mars. For instance, in addition to the physical spectroradiometers, monolayers of dry plant seeds could be used as the passive biological UV-dosimeters in the future photobiological experiments on Mars. Previously reported biological systems, such as *Escherichia coli* vegetative cells, *Bacillus subtilis* dosimeters (DLR-biofilm) or *Chroococcidiopsis* sp. dosimeters showed relatively high sensitivity to polychromatic UV radiation (e.g. these organisms are killed within one day of UV exposure in environments that are used as terrestrial analogues for Mars) (Karentz and Lutze, 1990; Quintern et al., 1994; Rettberg and Cockell, 2004; Cockell et al., 2008). We suggest that plant seeds, as the more robust biological UV-dosimeters, which would measure the integrated biologically effective irradiance at the higher orders of magnitude scale, could be used complimentarily to above-mentioned sensitive, fine-scale biological UV-dosimeters.

10. Flavonoids and sinapate esters are the two major classes of plant UV screens that may contribute to remarkably high UV resistance of Arabidopsis seeds. Using Arabidopsis mutant seeds that were deficient in flavonoids (tt4-8 and tt4-1 mutants) and sinapate esters (fah1-2 mutant) we determined in vivo the capacity of these compounds to provide efficient UV protection. We concluded that flavonoids are capable of improving considerably the resistance of Arabidopsis seeds to quasi-monochromatic UV-C_{254}, as well as polychromatic $UV_{200-400}$ radiation.

Besides studying the responses of dry *Arabidopsis thaliana* seeds to quasi-monochromatic UV-C_{254} light and simulated polychromatic solar $UV_{200-400}$ light, in this work we aimed to

elucidate the chemical bases of such an extreme UV resistance. Flavonoids and sinapate esters are known to act in seedlings and vegetative parts of plants as efficient UV protectants, particularly in the UV-B part of spectrum (Chapple et al., 1992; Li et al., 1993; Stapleton and Walbot, 1994; Landry et al., 1995; Sheahan, 1996). Yet, little is known about their UV protection capacity in plant seeds. Even less is known about their protective efficiency in the UV-C part of spectrum. Therefore, we determined for the first time the physiological value of flavonoids and sinapate esters in protection of *Arabidopsis* seeds from quasi-monochromatic UV-C_{254} light and its UV-B + UV-A concurrent light, as well as polychromatic $UV_{200-400}$ radiation.

a) Sinapate esters

Similarly to its wild type background (Col-0), the sinapate ester-lacking seeds (*fah1-2*) showed unexpectedly high level of resistance to quasi-monochromatic UV-C_{254}, as well as to its UV-B + UV-A portion. Both lines, Col-0 and *fah1-2*, exhibited a high and unaltered germination capacity ($G_{max\%}$) even after 60 days of irradiation. Nevertheless, the germination dynamics of irradiated *fah1-2* seeds was affected by UV-B + UV-A light, and to the greater extent by the entirely transmitted quasi-monochromatic UV-C_{254} light. Comparing the differences in the relative MGT increase between irradiated *fah1-2* and Col-0 seeds, we concluded that at the germination stage, sinapate ester-lacking seeds were about 75% less resistant to UV-B + UV-A light and about 5 times less resistant to entirely transmitted quasi-monochromatic UV-C_{254} radiation than the wild type.

At the stage of mature plant, however, no effects on survival and development of in-soil grown plants were detected in the *fah1-2* mutant irradiated with UV-B + UV-A light (up to UV-B = 3.4×10^4 kJm^{-2} and UV-A = 9.5×10^3 kJm^{-2}). We concluded that at the studied UV fluence ranges, sinapate esters have a relatively small contribution in UV-B + UV-A resistance of *Arabidopsis* seeds. In contrast, quasi-monochromatic UV-C_{254} light (up to UV-C = 4.8×10^5 kJm^{-2}) had a greater impact on the final plant survival rate in irradiated *fah1-2* sample (45%) than in irradiated Col-0 sample (72%). It means that sinapate esters are either more efficient in the protection against UV-C light than in the UV-B + UV-A part of spectrum, or more likely, that the fluences of UV-B + UV-A light were not high enough to observe greater differences between the sinapate esters-lacking and wild type samples. Nevertheless, our results led us to conclude that sinapate esters do not provide the principal protection to *Arabidopsis* seeds against the UV-C radiation nor the UV-B + UV-A part of the spectrum. In addition to sinapate esters, other chemical, biochemical or structural factors are probably important in coping with UV radiation.

b) Flavonoids

Unlike all tested flavonoid-containing seeds (including the sinapate ester mutant, *fah1-2*), the flavonoid-lacking mutants, *tt4-8* and *tt4-1*, exhibited remarkably higher sensitivity to UV radiation. Quasi-monochromatic UV-C_{254} radiation and polychromatic $UV_{200-400}$ light had particularly deleterious effects on flavonoid-lacking *Arabidopsis* seeds.

At the germination stage, both germination capacity ($G_{max\%}$) and germination dynamics of irradiated *tt4-8* were seriously affected by quasi-monochromatic UV-C_{254} radiation. Only 13% of irradiated *tt4-8* seeds germinated after exposure to the maximal fluence of UV-C = 5.9 x 10^4 kJm^{-2} (139 hours of irradiation). We found that almost all ungerminated *tt4-8* seeds were metabolically dead. Since the concurrent UV-B + UV-A portion of emitted light (fluences up to UV-B = 4.2 x 10^3 kJm^{-2} and UV-A = 1.2 x 10^3 kJm^{-2}) had no effect on germinability of the flavonoid-lacking seeds, we concluded that these deleterious effects can be attributed to the dominant UV-C_{254} component of emitted light. We found that increasing fluences of UV-C_{254} light induced a progressive inhibition of germination in irradiated *tt4-8* seeds. This allowed us to establish the UV-C_{254} dose-response curve for dry flavonoid-lacking seeds and to determine the lethal UV-C_{254} doses that kill 90% and 50% of *tt4-8* seeds (LD_{90} = 6.5 x 10^4 kJm^{-2} and LD_{50} = 6.2 x 10^3 kJm^{-2}, respectively).

At the stage of plant development, we found that quasi-monochromatic UV-C_{254} radiation had an extreme inhibitory effect on plant growth and development. The survival rate of in-soil grown plants was seriously reduced (54%) after only 1 hour of irradiation (UV-C = 5.3 x 10^2 kJm^{-2}), while no survivors were detected after 5 hours of exposure (UV-C = 2.8 x 10^3 kJm^{-2}). Compared to the irradiated Ws-2 wild type seeds, these results clearly demonstrated that flavonoids are important UV screens, capable of improving the resistance of *Arabidopsis* seeds to quasi-monochromatic UV-C_{254} radiation for about 3 orders of magnitude.

Flavonoid-lacking seeds *(tt4-1* mutant) also exhibited an extremely high sensitivity to simulated polychromatic solar $UV_{200-400}$ light (1.5 x 10^5 kJm^{-2}). In contrast to wild type, which reached a high $G_{max\%}$, no flavonoid-lacking seed remained viable after the exposure to only polychromatic $UV_{200-400}$ light or in combination with simulated space vacuum or simulated Mars CO_2 atmosphere*. We concluded that the flavonoid-lacking seeds are at least 5 orders of magnitude more sensitive to simulated polychromatic solar $UV_{200-400}$ radiation than the wild type seeds. These results clearly demonstrated the importance of flavonoids in UV screening protection of plant seeds.

11. ***We found that flavonoids provide greater UV protection to Arabidopsis seeds than sinapate esters. Flavonoids are thus the major screening compounds in Arabidopsis seeds, conferring the high seed UV resistance. These in vivo results are in good agreement with our UV absorption spectroscopy results, supporting the hypothesis that flavonoids could be considered as ideal UV screens.***

Due to their high absorbance in the UV-A and UV-B part of spectrum, sinapate esters are generally considered as efficient UV screens. Earlier *in vivo* studies reported that sinapate esters are predominant and even more efficient UV protectors than flavonoids (Chapple et al., 1992; Landry et al., 1995; Sheahan, 1996). Contrary to these findings, our study clearly demonstrated that flavonoids provide greater UV protection to irradiated *Arabidopsis* seeds than sinapate esters. Comparing the responses of flavonoid-lacking seeds (*tt4-8*), sinapate ester-lacking seeds (*fah1-2*) and their respective wild type seeds, we concluded that in *Arabidopsis* seeds, flavonoids provide at least two orders of magnitude higher resistance than sinapate esters to quasi-monochromatic UV-C_{254} radiation, as well as the UV-B + UV-A portion of emitted light. These findings corroborated our results from the UV absorption spectroscopy studies (for details see point 4). The possible reason of discrepancy could be that previous studies were focused on the vegetative parts of plants (seedlings and leaves), rather than on seeds. Variations in the UV responses in different developmental stages (seeds, seedlings and plants) are likely related to the temporal and spatial differences in the types and concentrations of accumulated UV screening compounds. For instance, *Arabidopsis* seedlings contain higher amounts of sinapate esters than dry seeds (Lorenzen et al., 1996). In addition, the composition of flavonoids and sinapate esters in *Arabidopsis* seeds differs from that in the vegetative parts of plants (Chapple et al., 1992; Ruegger et al., 1999; Lepiniec et al., 2006; Routaboul et al., 2006). Further comparative quantitative studies would be necessary to determine the concentrations of the total flavonoids and sinapate esters, as well as the partial concentrations of specific compounds in the flavonoid-lacking, sinapate ester-lacking and wild type seeds, as well as the vegetative parts of seedlings and plants. It would be also interesting to study the level of UV resistance in seeds that are double mutants for both flavonoids and sinapate esters.

General conclusions

Plant seeds are adapted to survive a variety of adverse conditions on Earth, including extreme cold and heat, as well as extreme desiccation. Some seeds exhibit the exceptional longevity, remaining viable for several decades, or even millennia. Plant seeds consist of embryo, which is a preformed young plant that carries important genetic information, encapsulated within the protective seeds coat. The anatomy, chemistry and genome structure make plant seeds resistant to various harsh conditions, including UV radiation. We demonstrated that *Arabidopsis thaliana* seeds are extremely resistant to high fluences of polychromatic $UV_{200-400}$ light, UV-B_{312}+UV-A_{365} radiation, as well as UV-C_{254} radiation, which is considered as particularly deleterious due to the wavelength proximity to one of the DNA absorption maxima. To our knowledge, no other known life form is reported to resist such a high level of UV radiation. The exceptionally high UV resistance of plant seeds can be greatly attributed to flavonoids, which accumulate in high concentrations in the seed coat. Our UV absorption spectroscopy and *in vivo* studies showed that flavonoids, and particularly glycosylated flavonols (e.g. quercetin-3-*O*-rhamnoside), are the excellent UV screens, providing seeds an efficient protection against damaging UV radiation. Besides UV radiation, *Arabidopsis thaliana* seeds also showed a high resistance to the other extreme conditions that can be encountered in space (e.g. extremely high vacuum) or in extraterrestrial environments (e.g. Martian CO_2 rich atmosphere). We concluded that plant seeds can be considered as a suitable terrestrial model for photobiological and astrobiological studies that investigate the likelihood of interplanetary transfer of life. Even if viability of entire seeds would be lost during the hypothetical long-duration interplanetary journey, seeds could still contain some remaining viable cells, organelles, subcellular structures, macromolecules or small molecules, which might provide the biological or chemical basis for starting or modifying life elsewhere (for details see Tepfer and Leach, 2006).

Although the present work includes comprehensive chemical, absorption spectroscopy and plant physiology studies, it would be further interesting to study the effects of UV radiation at the molecular level, quantifying and determining the types of UV-induced DNA damage, studying the oxidative damage by measuring the accumulation of reactive oxygen species (ROS) and studying the efficiency of DNA repair and detoxification systems. Since we observed the biological endpoints of survival during only one generation cycle (M1) of *Arabidopsis thaliana* plants, grown from exposed seeds up to the stage of mature plant, we suggest that it would be also necessary to extend the study on the next generation (M2), in order to better determine the reproductive capacities and to examine the mutation frequencies in progeny.

Chapter 8
REFERENCES

Al-Shehbaz IA, O'Kane SL, Jr. (2002) Taxonomy and phylogeny of Arabidopsis (Brassicaceae): September 30, 2002. *In* The Arabidopsis Book. American Society of Plant Biologists, Rockville, MD. doi: 10.1199/tab.0001, http://www.aspb.org/publications/arabidopsis

Al Khateeb WM, Schroeder DF (2009) Overexpression of *Arabidopsis* damaged DNA binding protein 1A (DDB1A) enhances UV tolerance. Plant Molecular Biology **70:** 371-383

Allen PS, Benech-Arnold RL, Batlla D, Bradford KJ (2007) Modeling of seed dormancy. *In* K Bradford, H Nonogaki, eds, Seed development, dormancy and germination. Annual Plant Reviews, Vol 27. Blackwell Publishing, Ltd., Oxford, UK, pp 72-112

Allwood AC, Walter MR, Kamber BS, Marshall CP, Burch IW (2006) Stromatolite reef from the Early Archaean era of Australia. Nature **441:** 714-718

Alston JA (1991) Seeds in space experiment. *In* AS Levine, ed, LDEF: 69 months in space. First post-retrieval symposium. NASA Langley Research Center, Hampton, VA, pp 1625-1629

An LZ, Liu GX, Zhang MX, Chen T, Liu YH, Feng HY, Xu SJ, Qiang WY, Wang XL (2004) Effect of enhanced UV-B radiation on polyamine content and membrane permeability in cucumber leaves. Russian Journal of Plant Physiology **51:** 658-662

Andalo C, Godelle B, Lefranc M, Mousseau M, Till-Bottraud I (1996) Elevated CO_2 decreases seed germination in *Arabidopsis thaliana*. Global Change Biology **2:** 129-135

Andalo C, Raquin C, Machon N, Godelle B, Mousseau M (1998) Direct and maternal effects of elevated CO_2 on early root growth of germinating *Arabidopsis thaliana* seedlings. Annals of Botany **81:** 405-411

Anderson M, Wilson F (2000) Growth, maintenance, and use of Arabidopsis genetic resources. *In* ZA Wilson, ed, Arabidopsis: A practical approach. Oxford University Press, Oxford, UK, pp 1-27

Aneja KR (2003) Staining methods. *In* Experiments in Microbiology, Plant Pathology and Biotechnology, Ed 4th. New Age International (P) Ltd. Publishers, New Delhi, India, pp 97-128

Anikeeva ID, Akatov YA, Vaulina EN, Kostina LN, Marenny AM, Portman AI, Rusin SV, Benton EV (1990) Radiobiological experiments with plant seeds aboard the biosatellite Kosmos 1887. International Journal of Radiation Applications and Instrumentation, Part D: Nuclear Tracks and Radiation Measurements **17:** 167-171

Anikeeva ID, Kostina LN, Vaulina EN (1983) Experiments with air-dried seeds of *Arabidopsis thaliana* (L) Heynh. and *Crepis capillaris* (L) Wallr., aboard Salyut 6. Advances in Space Research **3:** 129-133

AOSA (1983) Seed Vigor Testing Handbook. Contribution No. 32 to the Handbook on Seed Testing. Association of Official Seed Analysts (AOSA), Ithaca, NY

Arcila J, Mohapatra SC (1983) Development of tobacco seedling. 2. Morphogenesis during radicle protrusion. Tobacco Science **27:** 35-40

Armstrong GA, Hearst JE (1996) Genetics and molecular biology of carotenoid pigment biosynthesis. The FASEB Journal **10:** 228-237

Arrhenius S (1903) Die Verbreitung des Lebens im Weltenraum. Die Umschau **7:** 481-485

Awramik SM (1992) The oldest records of photosynthesis. Photosynthesis Research **33:** 75-89

Awramik SM, Schopf JW, Walter MR (1983) Filamentous fossil bacteria from the Archean of Western Australia. Precambrian Research **20:** 357-374

Baeza I, Ibáñez M, Wong C, Chávez P, Gariglio P, Oró J (1992) Possible prebiotic significance of polyamines in the condensation, protection, encapsulation, and biological properties of DNA. Origins of Life and Evolution of the Biosphere **21:** 225-242

Baglioni P, Sabbatini M, Horneck G (2007) Astrobiology experiments in low Earth orbit: Facilities, instrumentation, and results. *In* G Horneck, P Rettberg, eds, Complete Course in Astrobiology. Wiley-VCH Verlag GmbH & Co. KGaA, Weinheim, DE, pp 273-320

Bailly C (2004) Active oxygen species and antioxidants in seed biology. Seed Science Research **14:** 93-107

Bair NB, Meyer SE, Allen PS (2006) A hydrothermal after-ripening time model for seed dormancy loss in *Bromus tectorum* L. Seed Science Research **16:** 17-28

Ballaré C, Barnes PW, Kendrick RE (1991) Photomorphogenic effects of UV-B radiation on hypocotyl elongation in wild type and stable-phytochrome-defficient mutant seedlings of cucumber. Physiologia Plantarum **83:** 652-658

Barlow NG (2008) Atmospheric conditions and evolution. *In* Mars: An Introduction to its Interior, Surface and Atmosphere. Cambridge University Press, New York, NY, pp 163-186

Barnes PW, Flint SD, Caldwell MM (1990) Morphological responses of crop and weed species of different growth forms to ultraviolet-B radiation. American Journal of Botany **77:** 1354-1360

Barth CA, Dick ML (1974) Ozone and the polar hood of Mars. Icarus **22:** 205-211

Barth CA, Hord CW, Stewart AI, Lane AL, Dick ML, Anderson GP (1973) Mariner 9 ultraviolet spectrometer experiment: seasonal variation of ozone on Mars. Science **179:** 795-796

Barton LV (1953) Seed storage and viability. Contributions from Boyce Thompson Institute **17:** 87-103

Bashandy T, Taconnat L, Renou J-P, Meyer Y, Reichheld J-P (2009) Accumulation of flavonoids in an *ntra ntrb* mutant leads to tolerance to UV-C. Molecular Plant **2:** 249-258

Baskin CC, Baskin JM (2001a) Ecologically meaningful germination studies. *In* Seeds: Ecology, Biogeography, and Evolution of Dormancy and Germination. Academic Press, San Diego, CA, pp 5-26

Baskin CC, Baskin JM (2001b) A geographical perspective on germination ecology: Tropical and subtropical zones. *In* Seeds: Ecology, Biogeography, and Evolution of Dormancy and Germination. Academic Press, San Diego, CA, pp 239-330

Bass LN (1980) Seed viability during long-term storage. Horticultural Reviews **2:** 117-141

Basu RN (1995) Seed viability. *In* AS Basra, ed, Seed Quality: Basic Mechanisms and Agricultural Implications. The Food Products Press, The Haworth Press, Inc., Binghamton, NY, pp 1-44

Batlla D, Benech-Arnold RL (2006) The role of fluctuations in soil water content on the regulation of dormancy changes in buried seeds of *Polygonum aviculare* L. Seed Science Research **16:** 47-59

Battista JR, Earl AM, White O (2000) The stress responses of *Deinococcus radiodurans*. *In* G Storz, R Hengge-Aronis, eds, Bacterial Stress Responses. ASM Press, Washington, DC, pp 383-391

Baumstark-Khan C, Facius R (2002) Life under conditions of ionizing radiation. *In* G Horneck, C Baumstark-Khan, eds, Astrobiology: The Quest for the Conditions of Life. Springer-Verlag, Berlin, DE, pp 261-284

Beeckman T, De Rycke R, Viane R, Inzé D (2000) Histological study of seed coat development in *Arabidopsis thaliana*. Journal of Plant Research **113:** 139-148

Bennett RN, Mellon FA, Kroon PA (2004) Screening crucifer seeds as sources of specific intact glucosinolates using ion-pair high-performance liquid chromatography negative ion electrospray mass spectrometry. Journal of Agricultural and Food Chemistry **52:** 428-438

Benson EE (2004) Cryo-conserving algal and plant diversity: Historical perspectives and future challenges. *In* BJ Fuller, N Lane, EE Benson, eds, Life in the Frozen State. CRC Press, LLC, Boca Raton, FL, pp 299-328

Bentsink L, Koornneef M (2008) Seed dormancy and germination: December 30, 2008. *In* The Arabidopsis Book. American Society of Plant Biologists, Rockville, MD. doi: 10.1199/tab.0119, http://www.aspb.org/publications/arabidopsis

Berjak P, Pammenter NW (2000) What ultrastructure has told us about recalcitrant seeds. Revista Brasileira de Fisiologia Vegetal **12:** 22-55

Berjak P, Pammenter NW (2002) Orthodox and recalcitrant seeds. *In* JA Vozzo, ed, Tropical Tree Seed Manual. Agriculture Handbook 721. US Department of Agriculture. Forest Service, Washington, DC, pp 137-147, http://www.rngr.net/publications/ttsm

Bernal-Lugo I, Leopold AC (1992) Changes in soluble carbohydrates during seed storage. Plant Physiology **98:** 1207-1210

Bernardini JN, Sawyer J, Venkateswaran K, Nicholson WL (2003) Spore UV and acceleration resistance of endolithic *Bacillus pumilus* and *Bacillus subtilis* isolates obtained from Sonoran desert basalt: Implications for lithopanspermia. Astrobiology **3:** 709-717

Bernhard WA, Close DM (2004) DNA damage dictates the biological consequences of ionizing irradiation: The chemical pathways. *In* A Mozumder, Y Hatano, eds, Charged Particle and Photon Interactions with Matter. Chemical, Physicochemical, and Biological Consequences with Applications. Marcel Dekker, Inc., New York, NY, pp 471-489

Beruto D, Beruto M, Ciccarelli C, Debergh P (1995) Matric potential evaluations and measurements for gelled substrates. Physiologia Plantarum **94:** 151-157

Beruto M, Curir P, Debergh P (1999) Influence of agar on in vitro cultures: II. Biological performance of *Ranunculus* on media solidified with three different agar brands. In Vitro Cellular & Developmental Biology - Plant **35:** 94-101

Beutner S, Bloedorn B, Frixel S, Hernández Blanco I, Hoffmann T, Martin H-D, Mayer B, Noack P, Ruck C, Schmidt M, Schülke I, Sell S, Ernst H, Haremza S, Seybold G, Sies H, Stahl W, Walsh R (2001) Quantitative assessment of antioxidant properties of natural colorants and phytochemicals: carotenoids, flavonoids, phenols and indigoids. The role of β-carotene in antioxidant functions. Journal of the Science of Food and Agriculture **81:** 559 - 568

Bewley JD (1997) Seed germination and dormancy. Plant Cell **9:** 1055-1066

Bewley JD, Black M (1994a) Cellular events during germination and seedling growth. *In* JD Bewley, M Black, eds, Seeds: Physiology of Development and Germination, Ed 2nd. Plenum publishing corporation, New York, NY, pp 147-198

Bewley JD, Black M (1994b) Seeds: germination, structure, and composition. *In* JD Bewley, M Black, eds, Seeds: Physiology of Development and Germination, Ed 2nd. Plenum publishing corporation, New York, NY, pp 1-34

Black M, Bewley JD, Halmer P, eds (2006) The Encyclopedia of Seeds: Science, Technology and Uses. CABI Publishing, Wallingford, UK, Cambridge, MA

Black M, Corbineau F, Grzesik M, Guy P, Côme D (1996) Carbohydrate metabolism in the developing and maturing wheat embryo in relation to its desiccation tolerance. Journal of Experimental Botany **47:** 161-169

Blöchl E, Rachel R, Burggraf S, Hafenbradl D, Jannasch HW, Stetter KO (1997) *Pyrolobus fumarii,* gen. and sp. nov., represents a novel group of archaea, extending the upper temperature limit for life to 113°C. Extremophiles **1:** 14-21

Bochicchio A, Vernieri P, Puliga S, Murelli C, Vazzana C (1997) Desiccation tolerance in immature embryos of maize: sucrose, raffinose and the ABA-sucrose relation. *In* RH Ellis, M Black, AJ Murdoch, TD Hong, eds, Basic and Applied Aspects of Seed Biology. Kluwer Academic Publishers, Dordrecht, NL, London, UK, pp 13-22

Boesewinkel FD, Bouman F (1995) The seed: structure and function. *In* J Kigel, G Galili, eds, Seed Development and Germination. Marcel Dekker, Inc., New York, NY, pp 1-24

Bohm BA (1998) Extraction, purification, and identification of flavonoids. *In* Introduction to Flavonoids, Vol 2. Harwood Academic Publishers, Amsterdam, NL, pp 175-242

Bolton GW, Nester EW, Gordon MP (1986) Plant phenolic compounds induce expression of the *Agrobacterium tumefaciens* loci needed for virulence. Science **232:** 983-985

Booij-James IS, Dube SK, Jansen MAK, Edelman M, Mattoo AK (2000) Ultraviolet-B radiation impacts light-mediated turnover of the photosystem II reaction center heterodimer in Arabidopsis mutants altered in phenolic metabolism. Plant Physiology **124:** 1275-1284

Bork U, Gartenbach KE, Kranz AR (1989) Early and late damages induced by heavy charged particle irradiation in embryonic tissue of Arabidopsis seeds. Advances in Space Research **9:** 117-121

Bornman JF, Reuber S, Cen Y-P, Weissenböck G (1997) Ultraviolet radiation as a stress factor and the role of protective pigments. *In* P Lumsden, ed, Plants and UV-B Responses to Environmental Change. Cambridge University Press, Cambridge, UK, pp 157-170

Bors W, Michel C (1999) Antioxidant capacity of flavanols and gallate esters: pulse radiolysis studies. Free Radical Biology & Medicine **27:** 1413-1426

Botta O, Bada JL (2002) Extraterrestrial organic compounds in meteorites. Surveys in Geophysics **23:** 411-467

Böttcher C, von Roepenack-Lahaye E, Schmidt J, Schmotz C, Neumann S, Scheel D, Clemens S (2008) Metabolome analysis of biosynthetic mutants reveals a diversity of metabolic changes and allows identification of a large number of new compounds in Arabidopsis. Plant Physiology **147:** 2107-2120

Bouchez D, Camilleri C, Caboche M (1993) A binary vector based on Basta resistance for in planta transformation of *Arabidopsis thaliana.* Comptes Rendus de l'Académie des Sciences. Série III Sciences de la Vie **316:** 1188-1193

Boudet J, Buitink J, Hoekstra FA, Rogniaux H, Larré C, Satour P, Leprince O (2006) Comparative analysis of the heat stable proteome of radicles of *Medicago truncatula* seeds during germination identifies late embryogenesis abundant proteins associated with desiccation tolerance. Plant Physiology **140:** 1418-1436

Boyes DC, Zayed AM, Ascenzi R, McCaskill AJ, Hoffman NE, Davis KR, Görlach J (2001) Growth stage-based phenotypic analysis of Arabidopsis: A model for high throughput functional genomics in plants. Plant Cell **13:** 1499-1510

Brack A (1999) Life in the solar system. Advances in Space Research **24:** 417-433

Brack A (2006) From the origin of life on Earth to life in the Universe. *In* M Gargaud, B Barbier, H Martin, J Reisse, eds, Lectures in Astrobiology, Vol 1, Part 2: From Prebiotic Chemistry to the Origin of Life on Earth. Springer-Verlag, Berlin Heidelberg, DE, pp 1-23

Bradford K (1990) A water relations analysis of seed germination rates. Plant Physiology **94:** 840-849

Bradford KJ, Côme D, Corbineau F (2007) Quantifying the oxygen sensitivity of seed germination using a population-based threshold model. Seed Science Research **17:** 33-43

Braslavsky SE (2007) Glossary of terms used in photochemistry 3rd edition (IUPAC Recommendations 2006). Pure and Applied Chemistry **79:** 293-465

Brenac P, Horbowicz M, Downer SM, Dickerman AM, Smith ME, Obendorf RL (1997) Raffinose accumulation related to desiccation tolerance during maize (*Zea mays* L.) seed development and maturation. Journal of Plant Physiology **150:** 481-488

Brinckmann E, ed (2007) Biology in Space and Life on Earth. Effects of Spaceflight on Biological Systems. Wiley-VCH Verlag GmbH & Co. KGaA, Weinheim, DE

Britt AB (1996) DNA damage and repair in plants. Annual Review of Plant Physiology and Plant Molecular Biology **47:** 75-100

Britt AB (1999) Molecular genetics of DNA repair in higher plants. Trends in Plant Science **4:** 20-25

Brown JE, Lu TY, Stevens C, Khan VA, Lu JY, Wilson CL, Collins DJ, Wilson MA, Igwegbe ECK, Chalutz E, Droby S (2001) The effect of low dose ultraviolet light-C seed treatment on induced resistance in cabbage to black rot (*Xanthomonas campestris* pv. *campestris*). Crop Protection **20:** 873-883

Brown PD, Tokuhisa JG, Reichelt M, Gershenzon J (2003) Variation of glucosinolate accumulation among different organs and developmental stages of *Arabidopsis thaliana*. Phytochemistry **62:** 471-481

Bücker H (1984) Free flyer Biostack experiment (A0015). *In* IG Clark, WH Kinard, DJ Carter, JL Jones, eds, The Long Duration Exposure Facility (LDEF). NASA SP-473, pp 139-145

Bücker H, Baltshukat K, Facius R, Horneck G, Reitz G, Schäfer M, Schott JU, Beaujean R, Enge W, Bonting SL, Delpoux M, Planel G, Francois H, Portal G, Graul EH, Rüther W, Heinrich W, Kranz AR, Pfohl R, ., Schopper E (1984) Advanced biostack: Experiment 1ES 027 on Spacelab-1. Advances in Space Research **4:** 83-90

Bücker H, Horneck G, Wollenhaupt H, Schwager M, Taylor GR (1974) Viability of *Bacillus subtilis* spores exposed to space environment in the M-191 experiment system aboard Apollo 16. Life Sciences and Space Research **12:** 209-213

Buitink J, Hoekstra FA, Leprince O (2002) Biochemistry and biophysics of tolerance system. *In* M Black, HW Pritchard, eds, Desiccation and Survival in Plants. Drying Without Dying. CABI Publishing, Wallingford, UK, New York, NY, pp 293-318

Buitink J, Leprince O (2004) Glass formation in plant anhydrobiotes: survival in the dry state. Cryobiology **48:** 215-228

Buitink J, Leprince O (2008) Intercellular glasses and seed survival in the dry state. Comptes Rendus Biologies **331:** 788-795

Burchell MJ (2010) Why do some people reject panspermia? Journal of Cosmology **5:** 828-832

Burchell MJ, Galloway JA, Bunch AW, Brandão PF (2003) Survivability of bacteria ejected from icy surfaces after hypervelocity impact. Origins of Life and Evolution of the Biosphere **33:** 53-74

Burchell MJ, Mann JR, Bunch AW (2004) Survival of bacteria and spores under extreme shock pressures. Monthly Notices of the Royal Astronomical Society **352:** 1273-1278

Cadet J, Sage E, Douki T (2005) Ultraviolet radiation-mediated damage to cellular DNA. Mutation Research **571:** 3-17

Caldwell MM, Ballaré CL, Bornman JF, Flint SD, Björn LO, Teramura AH, Kulandaivelu G, Tevini M (2003) Terrestrial ecosystems, increased solar ultraviolet radiation and interactions with other climatic change factors. Photochemical & Photobiological Sciences **2:** 29 - 38

Caldwell MM, Björn LO, Bornman JF, Flint SD, Kulandaivelu G, Teramura AH, Tevini M (1998) Effects of increased solar ultraviolet radiation on terrestrial ecosystems. Journal of Photochemistry and Photobiology B: Biology **46:** 40-52

Campbell D, Eriksson M-J, Ōquist G, Gustafsson P, Clarke AK (1998) The cyanobacterium *Synechococcus* resists UV-B by exchanging photosystem II reaction-center D1 proteins. Proceedings of the National Academy of Sciences of the USA **95:** 364-369

Canuto VM, Levine JS, Augustsson TR, Imhoff CL (1982) UV radiation from the young Sun and oxygen and ozone levels in the prebiological palaeoatmosphere. Nature **296:** 816-820

Carlberg DM (2005) Growth of microorganisms. *In* Cleanroom Microbiology for the Non-Microbiologist, Ed 2nd. CRC Press LLC, Boca Raton, FL, pp 39-72

Caspar T, Lin T-P, Kakefuda G, Benbow L, Preiss J, Somerville C (1991) Mutants of *Arabidopsis* with altered regulation of starch degradation. Plant Physiology **95:** 1181-1188

Castenholz RW, Garcia-Pichel F (2000) Cyanobacterial responses to UV-radiation. *In* BA Whitton, M Potts, eds, The Ecology of Cyanobacteria. Their Diversity in Time and Space. Kluwer Academic Publishers, Dordrecht, NL, pp 591-611

Castle LA, Meinke DW (1993) Embryo-defective mutants as tools to study essential functions and regulatory processes in plant embryo development. Seminars in Developmental Biology **4:** 31-39

Cen Y-P, Bornman JF (1993) The effect of exposure to enhanced UV-B radiation on the penetration of monochromatic and polychromatic UV-B radiation in leaves of *Brassica napus*. Physiologia Plantarum **87:** 249-255

Césarini JP (1996) Melanins and their possible roles through biological evolution. Advances in Space Research **18:** 35-40

Chapple CC, Vogt T, Ellis BE, Somerville CR (1992) An Arabidopsis mutant defective in the general phenylpropanoid pathway. Plant Cell **4:** 1413-1424

Chargaff E, Lipshitz R, Green C, Hodes ME (1951) The composition of the desoxyribonucleic acid of salmon sperm. Journal of Biological Chemistry **192:** 223-230

Chaudhuri K, Das S, Bandyopadhyay M, Zalar A, Kollmann A, Jha S, Tepfer D (2009) Transgenic mimicry of pathogen attack stimulates growth and secondary metabolite accumulation. Transgenic Research **18:** 121-134

Chen S, Halkier BA (2000) Characterization of glucosinolate uptake by leaf protoplasts of *Brassica napus*. The Journal of Biological Chemistry **275:** 22955-22960

Chen X, Quinn AM, Wolin SL (2000) Ro ribonucleoproteins contribute to the resistance of *Deinococcus radiodurans* to ultraviolet irradiation. Genes and Development **14:** 777-782

Chilton M-D, Tepfer DA, Petit A, David C, Casse-Delbart F, Tempé J (1982) *Agrobacterium rhizogenes* inserts T-DNA into the genomes of the host plant root cells. Nature **295:** 432-434

Chon S-U, Nelson CJ, Coutts JH (2004) Osmotic and autotoxic effects of leaf extracts on germination and seedling growth of alfalfa. Agronomy Journal **96:** 1673-1679

Christiansen MN, Justus N (1963) Prevention of field deterioration of cottonseed by an impermeable seed coat. Crop Science **3:** 439-440

Christiansen MN, Moore RP, Rhyne CL (1960) Cotton seed quality preservation by a hard seed coat characteristic which restricts internal water uptake. Agronomy Journal **52:** 81-84

Chyba C, Sagan C (1992) Endogenous production, exogenous delivery and impact-shock synthesis of organic molecules: an inventory for the origins of life. Nature **355:** 125-132

Chyba CF, Hand KP (2005) ASTROBIOLOGY: The study of the living universe. Annual Review of Astronomy and Astrophysics **43:** 31-74

Clarke A (2003) Evolution and low temperatures. *In* LJ Rothschild, AM Lister, eds, Evolution on Planet Earth: The Impact of the Physical Environment. Academic Press, Elsevier, London, UK, pp 187-208

Clerkx EJM, Blankestijn-De Vries H, Ruys GJ, Groot SPC, Koornneef M (2004) Genetic differences in seed longevity of various *Arabidopsis* mutants. Physiologia Plantarum **121:** 448-461

Clingen PH, Arlett CF, Roza L, Mori T, Nikaido O, Green MHL (1995) Induction of cyclobutane pyrimidine dimers, pyrimidine(6-4)pyrimidone photoproducts, and Dewar valence isomers by natural sunlight in normal human mononuclear cells. Cancer Research **55:** 2245-2248

Cockell CS (1998) Biological effects of high ultraviolet radiation on early Earth - a theoretical evaluation. Journal of Theoretical Biology **193:** 717-729

Cockell CS (2000) The ultraviolet history of the terrestrial planets - implications for biological evolution. Planetary and Space Science **48:** 203-214

Cockell CS (2001a) A photobiological history of Earth. *In* CS Cockell, AR Blaustein, eds, Ecosystems, Evolution, and Ultraviolet Radiation. Springer-Verlag New York, Inc., New York, NY, pp 1-35

Cockell CS (2001b) Ultraviolet radiation and exobiology. *In* CS Cockell, AR Blaustein, eds, Ecosystems, Evolution, and Ultraviolet Radiation. Springer-Verlag New York, Inc., New York, NY, pp 195-217

Cockell CS (2001c) The Martian and extraterrestrial UV radiation environment. Part II: Further considerations on materials and design criteria for artificial ecosystems. Acta Astronautica **49:** 631-640

Cockell CS (2008) The interplanetary exchange of photosynthesis. Origins of Life and Evolution of Biospheres **38:** 87-104

Cockell CS, Airo A (2002) On the plausibility of a UV transparent biochemistry. Origins of Life and Evolution of the Biosphere **32:** 255-274

Cockell CS, Blaustein AR, eds (2001) Ecosystems, Evolution, and Ultraviolet Radiation. Springer-Verlag New York, Inc., New York, NY

Cockell CS, Brack A, Wynn-Williams DD, Baglioni P, Brandstätter F, Demets R, Edwards HG, Gronstal AL, Kurat G, Lee P, Osinski GR, Pearce DA, Pillinger JM, Roten CA, Sancisi-Frey S (2007) Interplanetary transfer of photosynthesis: an experimental demonstration of a selective dispersal filter in planetary island biogeography. Astrobiology **7:** 1-9

Cockell CS, Catling DC, Davis WL, Snook K, Kepner RL, Lee P, McKay CP (2000) The ultraviolet environment of Mars: biological implications, past, present and future. Icarus **146:** 343-359

Cockell CS, Knowland J (1999) Ultraviolet radiation screening compounds. Biological Reviews **74:** 311-345

Cockell CS, McKay CP, Warren-Rhodes K, Horneck G (2008) Ultraviolet radiation-induced limitation to epilithic microbial growth in arid deserts - Dosimetric experiments in the hyperarid core of the Atacama Desert. Journal of Photochemistry and Photobiology B: Biology **90:** 79-87

Cockell CS, Raven JA (2007) Ozone and life on the Archaean Earth. Philosophical Transactions of the Royal Society A **365:** 1889-1901

Cockell CS, Schuerger AC, Billi D, Friedmann EI, Panitz C (2005) Effects of simulated Martian UV flux on the cyanobacterium, *Chroococcidiopsis* sp. 029. Astrobiology **5:** 127-140

Côme D (1982) Germination. *In* P Mazliak, ed, Physiologie Végétale II. Croissance et Développement. Hermann, Paris, FR, pp 129-225

Côme D, Corbineau F, Soudain P (1991) Beneficial effects of oxygen deprivation on germination and plant development. *In* MB Jackson, DD Davies, H Lambers, eds, Plant Life Under Oxygen Deprivation. Ecology, Physiology and Biochemistry. SPB Academic Publishing, The Hague, NL, pp 69-83

Côme D, Tissaoui T (1973) Interrelated effects of imbibition, temperature and oxygen on seed germination. *In* W Heydecker, ed, Seed Ecology. Butterworths, London, UK, pp 157-168

Cone JW, Spruit CJP (1983) Imbibition conditions and seed dormancy of *Arabidopsis thaliana*. Physiologia Plantarum **59:** 416-420

Coolbear P (1995) Mechanisms of seed deterioration. *In* AS Basra, ed, Seed Quality. Basic Mechanisms and Agricultural Implications. Food Products Press, The Haworth Press, Inc., Binghamton, NY, pp 223-278

Cooley NM, Higgins JT, Holmes MG, Attridge TH (2001) Ecotypic differences in responses of *Arabidopsis thaliana* L. to elevated polychromatic UV-A and UV-B+A radiation in the natural environment: a positive correlation between UV-B+A inhibition and growth rate. Journal of Photochemistry and Photobiology B: Biology **60:** 143-150

Copeland LO, McDonald MB (2001a) Flowering processes in plants. *In* Principles of Seed Science and Technology, Ed 4th. Kluwer Academic Publishers, Norwell, MA, pp 1-16

Copeland LO, McDonald MB (2001b) Seed formation and development. *In* Principles of Seed Science and Technology, Ed 4th. Kluwer Academic Publishers, Norwell, MA, pp 17-38

Copeland LO, McDonald MB (2001c) Seed germination. *In* Principles of Seed Science and Technology, Ed 4th. Kluwer Academic Publishers, Norwell, MA, pp 72-123

Copeland LO, McDonald MB (2001d) The chemistry of seeds. *In* Principles of Seed Science and Technology, Ed 4th. Kluwer Academic Publishers, Norwell, MA, pp 39-57

Copeland LO, McDonald MB (2001e) Seed storage and deterioration. *In* Principles of Seed Science and Technology, Ed 4th. Kluwer Academic Publishers, Norwell, MA, pp 192-230

Corbineau F, Côme D (1988) Storage of recalcitrant seeds of four tropical species. Seed Science and Technology **16:** 97-103

Corbineau F, Côme D (1989) Germination and storage of recalcitrant seeds of some tropical forest tree species. *In* E Dreyer, G Aussenac, M Bonnet-Masimbert, P Dizengremel, JM Favre, JP Garrec, F Le Tacon, F Martin, eds, Annales des Sciences Forestières, Vol 46 Suppl. Elsevier/INRA, Paris, FR, pp 89s-91s

Corbineau F, Côme D (1993) The concept of dormancy in cereal seeds. *In* F Corbineau, D Côme, eds, Proceedings of the 4th International Workshop on Seeds. Basic and Applied Aspects of Seed Biology (Angers, France, July 20-24, 1992), Vol 2. ASFIS, Paris, pp 581-589

Corbineau F, Côme D (1995) Control of seed germination and dormancy by the gaseous environment. *In* J Kigel, G Galili, eds, Seed Development and Germination. Marcel Dekker, Inc., New York, NY, pp 379-424

Corbineau F, Gouble B, Lecat S, Côme D (1991) Stimulation of germination of dormant oat (*Avena sativa* L.) seeds by ethanol and other alcohols. Seed Science Research **1:** 21-28

Corbineau F, Lecat S, Côme D (1986) Dormancy of three cultivars of oat seeds (*Avena sativa* L.). Seed Science and Technology **14:** 725-735

Corbineau F, Picard MA, Fougereux J-A, Ladonne F, Côme D (2000) Effects of dehydration conditions on desiccation tolerance of developing pea seeds as related to oligosaccharide content and cell membrane properties. Seed Science Research **10:** 329-339

Córdoba-Jabonero C, Lara LM, Mancho AM, Márquez A, Rodrigo R (2003) Solar ultraviolet transfer in the Martian atmosphere: biological and geological implications. Planetary and Space Science **51:** 399-410

Cottin H, Gazeau MC, Raulin F (1999) Cometary organic chemistry: a review from observations, numerical and experimental simulations. Planetary and Space Science **47:** 1141-1162

Cox CS (1993) Roles of water molecules in bacteria and viruses. Origins of Life and Evolution of the Biosphere **23:** 29-36

Crick F (1981) Life Itself: Its Origin and Nature. Simon and Schuster, New York, NY

Crick FHC, Orgel LE (1973) Directed panspermia. Icarus **19:** 341-346

Cronin JR, Pizzarello S (1983) Amino acids in meteorites. Advances in Space Research **3:** 5-18

Crookshanks M, Taylor G, Dolan L (1998) A model system to study the effects of elevated CO_2 on the developmental physiology of roots: the use of *Arabidopsis thaliana*. Journal of Experimental Botany **49:** 593-597

Crowe JH, Hoekstra FA, Crowe LM (1992) Anhydrobiosis. Annual Review of Physiology **54:** 579-599

Crowe LM, Mouradian R, Crowe JH, Jackson SA, Womersley C (1984) Effects of carbohydrates on membrane stability at low water activities. Biochimica et Biophysica Acta **769:** 141-150

D'Auria JC, Gershenzon J (2005) The secondary metabolism of *Arabidopsis thaliana*: growing like a weed. Current Opinion in Plant Biology **8:** 308-316

Dai Q, Upadhyaya MK (2002) Seed germination and seedling growth response of selected weedy species to ultraviolet-B radiation. Weed Science **50:** 611-615

Danielsson CE (1956) Plant proteins. Annual Review of Plant Physiology **7:** 215-235

Danon A, Gallois P (1998) UV-C radiation induces apoptotic-like changes in *Arabidopsis thaliana*. FEBS Letters **437:** 131-136

Darwin C (1871) Letter to Hooker, February 1871. *In* H Hartman, JG Lawless, P Morrison, eds, Search for the Universal Ancestors. National Aeronautics and Space Administration (NASA) SP-477 (1985), Washington, DC, pp 12-13

Day TA (2001) Ultraviolet radiation and plant ecosystems. *In* CS Cockell, AR Blaustein, eds, Ecosystems, Evolution, and Ultraviolet Radiation. Springer-Verlag, New York, NY, pp 80-117

de Hoffmann E, Stroobant V (2007) Isotopic abundances. *In* Mass Spectrometry. Principles and Applications, Ed 3rd. John Wiley & Sons Ltd., Chichester, UK, pp 251-257

de la Torre Noetzel R, Sancho LG, Pintado A, Rettberg P, Rabbow E, Panitz C, Deutschmann U, Reina M, Horneck G (2007) BIOPAN experiment LICHENS on the

Foton M2 mission: Pre-flight verification tests of the *Rhizocarpon geographicum*-granite ecosystem. Advances in Space Research **40:** 1665-1671

de la Torre R, Sancho LG, Horneck G, de los Ríos A, Wierzchos J, Olsson-Francis K, Cockell CS, Rettberg P, Berger T, de Vera J-P, Ott S, Frías JM, Melendi PG, Lucas MM, Reina M, Pintado A, Demets R (2010) Survival of lichens and bacteria exposed to outer space conditions - Results of the *Lithopanspermia* experiments. Icarus **208:** 735-748

De Lara J, Fernández PS, Periago PM, Palop A (2002) Irradiation of spores of *Bacillus cereus* and *Bacillus subtilis* with electron beams. Innovative Food Science and Emerging Technologies **3:** 379-384

de Vera J-P, Horneck G, Rettberg P, Ott S (2004) The potential of the lichen symbiosis to cope with the extreme conditions of outer space II: germination capacity of lichen ascospores in response to simulated space conditions. Advances in Space Research **33:** 1236-1243

Debeaujon I, Koornneef M (2000) Gibberellin requirement for *Arabidopsis* seed germination is determined both by testa characteristics and embryonic abscisic acid. Plant Physiology **122:** 415-424

Debeaujon I, Léon-Kloosterziel KM, Koornneef M (2000) Influence of the testa on seed dormancy, germination, and longevity in Arabidopsis. Plant Physiology **122:** 403-414.

Debeaujon I, Lepiniec L, Pourcel L, Routaboul J-M (2007) Seed coat development and dormancy. *In* K Bradford, H Nonogaki, eds, Seed Development, Dormancy and Germination. Annual Plant Reviews, Vol 27. Blackwell Publishing, Ltd., Oxford, UK, pp 25-49

Debeaujon I, Nesi N, Perez P, Devic M, Grandjean O, Caboche M, Lepiniec L (2003) Proanthocyanidin-accumulating cells in *Arabidopsis* testa: regulation of differentiation and role in seed development. Plant Cell **15:** 2514-2531

Debeaujon I, Peeters AJM, Léon-Kloosterziel KM, Koornneef M (2001) The *TRANSPARENT TESTA12* gene of Arabidopsis encodes a multidrug secondary transporter-like protein required for flavonoid sequestration in vacuoles of the seed coat endothelium. Plant Cell **13:** 853-871

Dechering KJ, Cuelenaere K, Konings RNH, Leunissen JAM (1998) Distinct frequency-distributions of homopolymeric DNA tracts in different genomes. Nucleic Acids Research **26:** 4056-4062

Del Castillo D, Acock B, Reddy VR, Acock MC (1989) Elongation and branching of roots on soybean plants in carbon dioxide-enriched aerial environment. Agronomy Journal **81:** 692-695

Derkx MPM, Karssen CM (1993a) Effects of light and temperature on seed dormancy and gibberellin-stimulated germination in *Arabidopsis thaliana*: studies with gibberellin-deficient and -insensitive mutants. Physiologia Plantarum **89:** 360-368

Derkx MPM, Karssen CM (1993b) Variability in light-, gibberellin- and nitrate requirement of Arabidopsis thaliana seeds due to harvest time and conditions of dry storage. Journal of Plant Physiology **141:** 574-582

Des Marais DJ (2000) When did photosynthesis emerge on Earth? Science **289:** 1703-1705

Diffey BL (1991) Solar ultraviolet radiation effects on biological systems. Physics in Medicine and Biology **36:** 299-328

Dixon RA, Palva NL (1995) Stress-induced phenylpropanoid metabolism. Plant Cell **7:** 1085-1097

Doijode SD (2001) Seeds and seed storage. *In* Seed Storage of Horticultural Crops. Food Products Press, The Haworth Press, Inc., Binghamton, NY, pp 3-22

Dose K, Bieger-Dose A, Dillmann R, Gill M, Kerz O, Klein A, Meinert H, Nawroth T, Risi S, Stridde C (1995) ERA-experiment "Space Biochemistry". Advances in Space Research **16:** 119-129

Dose K, Bieger-Dose A, Dillmann R, Gill M, Kerz O, Klein A, Stridde C (1996) UV photobiochemistry under space conditions. Advances in Space Research **18:** 51-60

Dose K, Bieger-Dose A, Dillmann R, Kerz O, Klein A, Rolf A, Stridde C (1996) UV photobiochemistry of anhydrobiotic organisms at extremely low temperatures. Advances in Space Research **18:** 69-74

Douki T, Cadet J (2003) Formation of the spore photoproduct and other dimeric lesions between adjacent pyrimidines in UVC-irradiated dry DNA. Photochemical & Photobiological Sciences **2:** 433 - 436

Douki T, Laporte G, Cadet J (2003) Inter-strand photoproducts are produced in high yield within A-DNA exposed to UVC radiation. Nucleic Acids Research **31:** 3134-3142

Drapkin R, Sancar A, Reinberg D (1994) Where transcription meets repair. Cell **77:** 9-12

Driks A (1999) *Bacillus subtilis* spore coat. Microbiology and Molecular Biology Reviews **63:** 1-20

Drlica K, Rouviere-Yaniv J (1987) Histonelike proteins of bacteria. Microbiological Reviews **51:** 301-319

Duport C, Thomassin S, Bourel G, Schmitt P (2004) Anaerobiosis and low specific growth rates enhance hemolysin BL production by *Bacillus cereus* F4430/73. Archives of Microbiology **182:** 90-95

Dyson F (1985) Origins of life. Cambridge University Press, Cambridge, UK

Eastmond PJ, Germain V, Lange PR, Bryce JH, Smith SM, Graham IA (2000) Postgerminative growth and lipid catabolism in oilseeds lacking the glyoxylate cycle. Proceedings of the National Academy of Sciences of the USA **97:** 5669-5674

Ehrenfreund P (1999) Molecules on a space odyssey. Science **283:** 1123-1124

Ehrenfreund P, Charnley SB (2000) Organic molecules in the interstellar medium, comets, and meteorites: A voyage from dark clouds to the early Earth. Annual Review of Astronomy and Astrophysics **38:** 427-483

Ehrenfreund P, Rasmussen S, Cleaves J, Chen L (2006) Experimentally tracing the key steps in the origin of life: The aromatic world. Astrobiology **6:** 490-520

Eigen M, Lindemann BF, Tietze M, Winkler-Oswatitsch R, Dress A, von Haeseler A (1989) How old is the genetic code ? Statistical geometry of tRNA provides an answer. Science **244:** 673-679

Elfakir C, Mercier JP, Dreux M (1994) Retention of some glucosinolates in anion exchange chromatography. Part II: Qualitative study on a styrene-divinylbenzene copolymeric anion exchanger. Chromatographia **38:** 585-590

Elgar G, Vavouri T (2008) Tuning in to the signals: noncoding sequence conservation in vertebrate genomes. Trends in Genetics **24:** 344-352

Ellis RH, Roberts EH (1981) The quantification of ageing and survival in orthodox seeds. Seed Science and Technology **9:** 373-409

Falk M (1964) The ultraviolet spectra of native and denatured deoxyribonucleic acid. Journal of the American Chemical Society **86:** 1226-1228

Faria JMR, Buitink J, van Lammeren AAM, Hilhorst HWM (2005) Changes in DNA and microtubules during loss and re-establishment of desiccation tolerance in germinating *Medicago truncatula* seeds. Journal of Experimental Botany **56:** 2119-2130

Farokh P, Mahmoodzadeh H, Satari TN (2010) Response of seed germination of safflower to UV-B radiation. Research Journal of Environmental Sciences **4:** 70-74

Faure G, Mensing TM (2007a) The planets of the solar system. *In* Introduction to Planetary Science: The Geological Perspective. Springer, Dordrecht, NL, pp 23-34

Faure G, Mensing TM (2007b) Earth: Model of planetary evolution. *In* Introduction to Planetary Science: The Geological Perspective. Springer, Dordrecht, NL, pp 65-86

Fekete A, Módos K, Hegedüs M, Kovács G, Rontó G, Péter Á, Lammer H, Panitz C (2005) DNA damage under simulated extraterrestrial conditions in bacteriophage T7. Advances in Space Research **36:** 303-310

Fendrihan S, Bérces A, Lammer H, Musso M, Rontó G, Polacsek TK, Holzinger A, Kolb C, Stan-Lotter H (2009) Investigating the effects of simulated martian ultraviolet radiation on *Halococcus dombrowskii* and other extremely halophilic Archaebacteria. Astrobiology **9:** 104-112

Fenner M (1987) Seedlings. New Phytologist **106 Suppl. s1:** 35-47

Finch-Savage WE, Leubner-Metzger G (2006) Seed dormancy and the control of germination. New Phytologist **171:** 501-523

Fiscus EL, Philbeck R, Britt AB, Booker FL (1999) Growth of *Arabidopsis* flavonoid mutants under solar radiation and UV filters. Environmental and Experimental Botany **41:** 231-245

Flink I, Pettijohn DE (1975) Polyamines stabilise DNA folds. Nature **253:** 62-63

Focks N, Benning C (1998) *wrinkled1*: A novel, low-seed-oil mutant of Arabidopsis with a deficiency in the seed-specific regulation of carbohydrate metabolism. Plant Physiology **118:** 91-101

Földvári I, Fekete A, Corradi G (1982) Prospects and difficulties in the far-and vacuum-ultraviolet spectroscopy of DNA. Journal of Biochemical and Biophysical Methods **5:** 319-327

Fraser CM, Thompson MG, Shirley AM, Ralph J, Schoenherr JA, Sinlapadech T, Hall MC, Chapple C (2007) Related Arabidopsis serine carboxypeptidase-like sinapoylglucose acyltransferases display distinct but overlapping substrate specificities. Plant Physiology **144:** 1986-1999

Friedberg EC, Walker GC, Siede W (1995) DNA damage. *In* DNA repair and mutagenesis. American Society for Microbiology, Washington, DC, pp 1-58

Friedmann EI (1971) Light and scanning electron microscopy of the endolithic desert algal habitat. Phycologia **10:** 411-428

Friedmann I, Lipkin Y, Ocampo-Paus R (1967) Desert algae of the Negev (Israel). Phycologia **6:** 185-200

Frisco G, Spetea C, Giacometti GM, Vass I, Barbato R (1994) Degradation of photosystem II reaction center D1-protein induced by UVB radiation in isolated thylakoids. Identification and characterization of C- and N-terminal breakdown products. Biochimica et Biophysica Acta - Bioenergetics **1184:** 78-84

Fujiwara T, Nambara E, Yamagishi K, Goto DB, Naito S (2002) Storage proteins: September 30, 2002. *In* The Arabidopsis Book. American Society of Plant Biologists, Rockville, MD. doi: 10.1199/tab.0020, http://www.aspb.org/publications/arabidopsis/

Gallardo K, Job C, Groot SPC, Puype M, Demol H, Vandekerckhove J, Job D (2002) Proteomics of Arabidopsis seed germination. A comparative study of wild-type and gibberellin-deficient seeds. Plant Physiology **129:** 823-837

Galtier N, Lobry JR (1997) Relationships between genomic G+C content, RNA secondary structures, and optimal growth temperature in prokaryotes. Journal of Molecular Evolution **44:** 632-636

Galun E, Galun E (2001) Genetic transformation. *In* The Manufacture of Medical and Health Products by Transgenic Plants. Imperial College Press, London, UK, pp 37-82

Garbutt K, Williams WE, Bazzaz FA (1990) Analysis of the differential response of five annuals to elevated CO_2 during growth. Ecology **71:** 1185-1194

Garcia-Pichel F (1998) Solar ultraviolet and the evolutionary history of cyanobacteria. Origins of Life and Evolution of the Biosphere **28:** 321-347

Garcia-Pichel F, Castenholz RW (1993) Occurrence of UV-absorbing, mycosporine-like compounds among cyanobacterial isolates and an estimate of their screening capacity. Applied Environmental Microbiology **59:** 163-169

Garcia-Pichel F, Sherry ND, Castenholz RW (1992) Evidence for an ultraviolet sunscreen role of the extracellular pigment scytonemin in the terrestrial cyanobacterium *Chlorogloeopsis* sp. Photochemistry and Photobiology **56:** 17-23

Garcia-Pichel F, Wingard CE, Castenholz RW (1993) Evidence regarding the UV sunscreen role of a mycosporine-like compound in the cyanobacterium *Gloeocapsa* sp. Applied and Environmental Microbiology **59:** 170-176

Gartenbach KE, Pickert M, Zimmermann MW, Kranz AR (1994) Cosmic ionizing radiation effects in plant seeds after short and long duration exposure flights. Advances in Space Research **14:** 105-108

Geneve RL (1991) Patterns of adventitious root formation in English ivy. Journal of Plant Growth Regulation **10:** 215-220

Geneve RL (1998) Seed dormancy in commercial vegetable and flower species. Seed Technology **20:** 236-250

Ghosal D, Omelchenko MV, Gaidamakova EK, Matrosova VY, Vasilenko A, Venkateswaran A, Zhai M, Kostandarithes HM, Brim H, Makarova KS, Wackett LP, Fredrickson JK, Daly MJ (2005) How radiation kills cells: Survival of *Deinococcus radiodurans* and *Shewanella oneidensis* under oxidative stress. FEMS Microbiology Reviews **29:** 361-375

Gomes PJ, Ribeiro PA, Shaw D, Mason NJ, Raposo M (2009) UV degradation of deoxyribonucleic acid. Polymer Degradation and Stability **94:** 2134-2141

Gómez F, Aguilera A, Amils R (2007) Soluble ferric iron as an effective protective agent against UV radiation: Implications for early life. Icarus **191:** 352-359

Gonzales-Castañeda C, Gonzales GF (2008) Hypocotyls of *Lepidium meyenii* (maca), a plant of the Peruvian highlands, prevent ultraviolet A-, B-, and C-induced skin damage in rats. Photodermatology, Photoimmunology & Photomedicine **24:** 24-31

Goto N (1985) A mucilage polysaccharide secreted from testa of *Arabidopsis thaliana*. Arabidopsis Information Service (AIS) **22:** 1-4, http://www.arabidopsis.org/ais/aishint.html

Götz T, Windhövel U, Böger P, Sandmann G (1999) Protection of photosynthesis against ultraviolet-B radiation by carotenoids in transformants of the cyanobacterium *Synechococcus* PCC7942. Plant Physiology **120:** 599-604

Goudriaan J, Unsworth MH (1990) Implications of increasing carbon dioxide and climate change for agricultural productivity and water resources. *In* BA Kimball, NJ Rosenberg, LH Allen, Jr., eds, Impact of Carbon Dioxide, Trace Gases, and Climate Change on Global Agriculture. American Society of Agronomy, Special Publication No. 53, Madison, WI, pp 111-130

Graser G, Oldham NJ, Brown PD, Temp U, Gershenzon J (2001) The biosynthesis of benzoic acid glucosinolate esters in *Arabidopsis thaliana*. Phytochemistry **57:** 23-32

Green AES, Miller JH (1975) Measures of biologically effective radiation in the 280-340 nm region. *In* DS Nachtwey, MM Caldwell, RH Biggs, eds, Impacts of Climatic Change on the Biosphere. Climate Impact Assessment Program (CIAP) Monograph No 5, Washington, DC, pp 60-70

Greenberg BM, Wilson MI, Huang X-D, Duxbury CL, Gerhardt KE, Gensemer RW (1997) The effects of ultraviolet-B radiation on higher plants. *In* W Wang, JW Gorsuch, JS Hughes, eds, Plants for Environmental Studies. CRC Press LLC, Lewis Publishers, Boca Raton, FL, pp 1-36

Gregory P (2006) Roots and the physico-chemical environment. *In* P Gregory, ed, Plant Roots: Growth, Activity and Interaction With Soils. Blackwell Publishing Ltd., Oxford, UK, pp 131-173

Grieder PKF (2001a) Energetic solar particles and photons. *In* Cosmic Rays at Earth. Researcher's Reference Manual and Data Book. Elsevier Science B. V., Amsterdam, NL, pp 927-937

Grieder PKF (2001b) X- and gamma rays. *In* Cosmic Rays at Earth. Researcher's Reference Manual and Data Book. Elsevier Science B. V., Amsterdam, NL, pp 793-837

Grigsby DK (1984) Space-Exposed Experiment Developed for Students (SEEDS) (P0004-2). *In* LG Clark, WH Kinar, DJ Carter, Jr., JL Jones, Jr., eds, The Long Duration Exposure

Facility (LDEF). Mission 1 Experiments. National Aeronautics and Space Administration (NASA) SP-473, Washington, DC, pp 148-150

Gummerson RJ (1986) The effect of constant temperatures and osmotic potentials on the germination of sugar beet. Journal of Experimental Botany **37:** 729-741

Hadas A (2004) Seedbed preparation - The soil physical environment of germinating seeds. *In* RL Benech-Arnold, RA Sánchez, eds, Handbook of Seed Physiology: Applications to Agriculture. Food Products Press, The Haworth Press, Inc., Binghamton, NY, pp 3-50

Halkier BA, Du L (1997) The biosynthesis of glucosinolates. Trends in Plant Science **2:** 425-431

Halstead TW, Dutcher FR (1987) Plants in space. Annual Review of Plant Physiology **38:** 317-345

Hammond EC, Jr., Bridgers K, Berry FD (1996) Germination, growth rates, and electron microscope analysis of tomato seeds flown on the LDEF. Radiation Measurements **26:** 851-861

Hansen G, Chilton MD (1999) Lessons in gene transfer to plants by a gifted microbe. *In* J Hammond, P McGarvey, V Yusibov, eds, Current Topics in Microbiology and Immunology. Plant Biotechnology: New Products and Applications, Vol 240. Springer-Verlag, Berlin, Heidelberg, DE, pp 21-57

Harborne JB (1998) Phenolic compounds. *In* Phytochemical Methods: A Guide to Modern Techniques of Plant Analysis, Ed 3rd. Chapman & Hall, Thomson Science, London, UK, pp 40-106

Harborne JB, Williams CA (2000) Advances in flavonoid research since 1992. Phytochemistry **55:** 481-504

Harisha S (2006) Microbiology. *In* An Introduction to Practical Biotechnology. Laxmi Publications (P) Ltd., New Delhi, India, pp 101-244

Harrington JF (1972) Seed storage and longevity. *In* TT Kozlowski, ed, Seed Biology, Vol 3. Insects and Seed Collection Storage, Testing, and Certification. Academic Press, New York, NY, pp 145-245

Harrison BJ (1956) Seed storage. John Innes Horticultural Institution: Annual Report **46:** 15-16

Hasan SS (2008) Overview of the Sun. *In* BN Dwivedi, U Narain, eds, Physics of the Sun and its Atmosphere: Proceedings of the National Workshop on Recent Advances in Solar Physics, 7-10 November 2006, Meerut, India. World Scientific Publishing Co. Pte. Ltd., Singapore, Hackensack, London, pp 9-20

Hashimoto H (2001) Plant seeds exposed to high vacuum environment. Biological Sciences in Space **15:** 252-253

Heady HF (1957) The measurement and value of plant height in the study of herbaceous vegetation. Ecology **38:** 313-320

Herman EM, Larkins BA (1999) Protein storage bodies and vacuoles. Plant Cell **11:** 601-613

Herranz JM, Ferrandis P, Martínez-Sánchez JJ (1999) Influence of heat on seed germination of nine woody *Cistaceae* species. International Journal of Wildland Fire **9:** 173-182

Hidea K, Hayakawa Y, Ito A, Kobayashi K, Ito T (1986) Wavelength dependence of the formation of single-strand breaks and base changes in DNA by the ultraviolet radiation above 150 nm. Photochemistry and Photobiology **44:** 379-383

Hilhorst HWM (2007) Definitions and hypotheses of seed dormancy. *In* K Bradford, H Nonogaki, eds, Seed Development, Dormancy and Germination. Annual Plant Reviews, Vol 27. Blackwell Publishing, Ltd., Oxford, UK, pp 50-71

Hinojosa-Rebollar E, Rangel-Mandujano A, Ortigoza-Ferado J, Mesta-Howard AM, Hernandez-Rodriguez C (1993) Synthesis and partial characterization of a melanin-like pigment of *Bacillus subtilis*. Revista Latinoamericana de Microbiologia **35:** 399-406

Hirokazu M, Tomoko N, Rie N (1999) The effect of UV irradiation on plants. Japanese Journal of Biological Education **39:** 122-128

Hochachka PW, Guppy M (1987) Anhydrobiotes. *In* Metabolic Arrest and the Control of Biological Time. Harvard University Press, Cambridge, MA, pp 146-165

Hollósy F (2002) Effects of ultraviolet radiation on plant cells. Micron **33:** 179-197

Holton TA, Cornish EC (1995) Genetics and biochemistry of anthocyanin biosynthesis. Plant Cell **7:** 1071-1083

Hoover RB (2007) Microfossils of cyanobacteria in carbonaceous meteorites. *In* RB Hoover, GV Levin, AY Rozanov, PCW Davies, eds, Instruments, Methods, and Missions for Astrobiology X, Vol 6694. Proceedings of SPIE, p 669408

Hopkins WG, Hüner NPA (2004a) Allocation, translocation, and partitioning of photoassimilates. *In* Introduction to Plant Physiology, Ed 3rd. John Wiley & Sons, Inc., Danvers, MA, USA, pp 123-144

Hopkins WG, Hüner NPA (2004b) Cells, tissues, and organs: The architecture of plants. *In* Introduction to Plant Physiology, Ed 3rd. John Wiley & Sons, Inc., Danvers, MA, USA, pp 1-28

Hopkins WG, Hüner NPA (2004c) Secondary plant metabolites. *In* Introduction to Plant Physiology, Ed 3rd. John Wiley & Sons, Inc., Danvers, MA, USA, pp 493-513

Horneck G (1992) Radiobiological experiments in space: A review. Nuclear Tracks and Radiation Measurements **20:** 185-205

Horneck G (1993) Responses of *Bacillus subtilis* spores to space environment: results from experiments in space. Origins of Life and Evolution of the Biosphere **23:** 37-52.

Horneck G (1995) Exobiology, the study of the origin, evolution and distribution of life within the context of cosmic evolution: A review. Planetary and Space Science **43:** 189-217

Horneck G (1999) European activities in exobiology: results and perspective. Advances in Space Research **23:** 381-386

Horneck G, Brack A (1992) Study of the origin, evolution and distribution of life with emphasis on exobiology experiments in Earth orbit. Advances in Space Biology and Medecine **2:** 229-262

Horneck G, Bücker H, Dose K, Martens KD, Mennigmann HD, Reitz G, Requardt H, Weber P (1984a) Photobiology in space: an experiment on Spacelab I. Origins of Life and Evolution of the Biosphere **14:** 825-832

Horneck G, Bücker H, Reitz G (1994) Long-term survival of bacterial spores in space. Advances in Space Research **14:** 41-45

Horneck G, Bücker H, Reitz G, Requardt H, Dose K, Martens KD, Mennigmann HD, Weber P (1984b) Microorganisms in the space environment. Science **225:** 226-228

Horneck G, Eschweiler U, Reitz G, Wehner J, Willimek R, Strauch K (1995) Biological responses to space: results of the experiment "Exobiological Unit" of ERA on EURECA I. Advances in Space Research **16:** 105-118

Horneck G, Reitz G, Schuber M, Kochan H, Mohlmann D, Richter L, Seidlitz H (2000) A ground-based program for exobiological experiments on the International Space Station. Planetary and Space Science **48:** 507-513

Horneck G, Rettberg P, Baumstark-Khan C, Rink H, Kozubek S, Schafer M, Schmitz C (1996) DNA repair in microgravity : studies on bacteria and mammalian cells in the experiments REPAIR and KINETICS. Journal of Biotechnology **47:** 99-112

Horneck G, Rettberg P, Rabbow E, Strauch W, Seckmeyer, Facius R, Reitz G, Strauch K, Schott J (1996) Biological dosimetry of solar radiation for different simulated ozone column thicknesses. Journal of Photochemistry and Photobiology. B: Biology **32:** 189-196

Horneck G, Rettberg P, Reitz G, Wehner J, Eschweiler U, Strauch K, Panitz C, Starke V, Baumstark-Khan C (2001) Protection of bacterial spores in space, a contribution to the discussion on Panspermia. Origigins of Life and Evolution of the Biosphere **31:** 527-547.

Horneck G, Rettberg P, Reitz G, Wehner J, Eschweiler U, Strauch K, Panitz C, Starke V, Baumstark-Khan C (2001) Protection of bacterial spores in space, a contribution to the discussion on panspermia. Origins of Life and Evolution of the Biosphere **31:** 527-547

Horneck G, Stöffler D, Eschweiler U, Hornemann U (2001) Bacterial spores survive simulated meteorite impact. Icarus **149:** 285-290

Horneck G, Stöffler D, Ott S, Hornemann U, Cockell CS, Moeller R, Meyer C, de Vera J-P, Fritz J, Schade S, Artemieva NA (2008) Microbial rock inhabitants survive hypervelocity impacts on Mars-like host planets: First phase of lithopanspermia experimentally tested. Astrobiology **8:** 17-44

Horsburgh MJ, Thackray PD, Moir A (2001) Transcriptional responses during outgrowth of *Bacillus subtilis* endospores. Microbiology **2001:** 2933–2941

Hotchin J, Lorenz P, Hemenway CL (1968) The survival of terrestrial microorganisms in space at orbital altitudes during *Gemini* satellite experiments. Life Sciences and Space Research **6:** 108-114

Hoyle F, Wickramasinghe NC (1999) Comets – a vehicle for panspermia. Astrophysics and Space Science **268:** 333-341

Inagaki T, Hamm RN, Arakawa ET, Painter LR (1974) Optical and dielectric properties of DNA in the extreme ultraviolet. The Journal of Chemical Physics **61:** 4246-4250

Ingber D (1999) How cells (might) sense microgravity. The Journal of the Federation of American Societies for Experimental Biology **13:** S3-S15

Iriti M, Guarnieri S, Faoro F (2007) Responsiveness of *Lycopersicon pimpinellifolium* to acute UV-C exposure: histo-cytochemistry of the injury and DNA damage. Acta Biochimica Polonica **54:** 273-280

ISTA (1995) Handbook of vigour test methods. The International Seed Testing Association (ISTA), Zurich, Switzerland

ISTA (1999) International Rules for Seed Testing, Rules 1999. The International Seed Testing Association (ISTA), Seed Science and Technology 27 (Supplement), Zurich, Switzerland

Ito A, Ito T (1986) Absorption spectra of deoxyribose, ribosephosphate, ATP and DNA by direct transmission measurements in the vacuum-UV (150-190 nm) and far-UV (190-260 nm) regions using synchrotron radiation as a light source. Photochemistry and Photobiology **44:** 355-358

IUPAC (1997) Compendium of chemical terminology. *In* AD NcNaught, A Wilkinson, eds, Ed 2nd (the "Gold Book"). XML on-line corrected version http://goldbook.iupac.org (2006-) created by Nic, M., Jirat, J., Kosata, B.; updates compiled by Jenkins A. Blackwell Scientific Publications, Oxford, UK

Izydorczyk M, Cui SW, Wang Q (2005) Polysaccharide gums: Structures, functional properties, and applications. *In* SW Cui, ed, Food Carbohydrates: Chemistry, Physical Properties, and Applications. Taylor & Francis, Boca Raton, London, New York, Singapore, pp 263-308

Jagger J (1985) Solar-UV actions on living cells. Praeger Scientific, New York, NY, USA

Jenkins ME, Harlow GR, Liu Z, Shotwell MA, Ma J, Mount DW (1995) Radiation-sensitive mutants of *Arabidopsis thaliana*. Genetics **140:** 725-732

Jones LW, Kok B (1966) Photoinhibition of chloroplast reactions. I. Kinetics and action spectra. Plant Physiology **41:** 1037-1043

Jönsson KI, Rabbow E, Schill RO, Harms-Ringdahl M, Rettberg P (2008) Tardigrades survive exposure to space in low Earth orbit. Current Biology **18:** R729-R731

Jordan BR (1996) The effects of ultraviolet-B radiation on plants: a molecular perspective. *In* JA Callow, ed, Advances in Botanical Research, Vol 22. Academic Press, San Diego, USA, pp 97-162

Jürgens G (1994) Pattern formation in the embryo. *In* EM Meyerowitz, CR Somerville, eds, Arabidopsis. Cold Spring Harbor Laboratory Press, New York, USA, pp 253-296

Kantar F, Pilbeam CJ, Hebblethwaite PD (1996) Effect of tannin content of faba bean (Vicia faba) seed on seed vigour, germination and field emergence. Annals of Applied Biology **128:** 85-93

Karentz D, Lutze LH (1990) Evaluation of biologically harmful ultraviolet radiation in Antarctica with a biological dosimeter designed for aquatic environments. Limnology and Oeanography **35:** 549-561

Kasting JF (1987) Theoretical constraints on oxygen and carbon dioxide concentrations in the precambrian atmosphere. Precambrian Research **34:** 205-229

Kasting JF (1993) Earth's early atmosphere. Science **259:** 920-926

Kasting JF, Zahnle KJ, Pinto JP, Young AT (1989) Sulfur, ultraviolet radiation and the early evolution of life. Origins of Life and Evolution of the Biosphere **19:** 95-108

Ke B (2001a) Light-harvesting pigment molecules. *In* Photosynthesis: Photochemistry and Photobiophysics. Kluwer Academic Publishers, Dordrecht, NL, pp 6-13

Ke B (2001b) Role of carotenoids in photosynthesis. *In* Photosynthesis: Photochemistry and Photobiophysics. Kluwer Academic Publishers, Dordrecht, NL, pp 229-250

Kerhoas L, Aouak D, Cingoz A, Routaboul J-M, Lepiniec L, Einhorn J, Birlirakis N (2006) Structural characterization of the major flavonoid glycosides from *Arabidopsis thaliana* seeds. Journal of Agricultural and Food Chemistry **54:** 6603-6612

Kielbassa C, Roza L, Epe B (1997) Wavelength dependence of oxidative DNA damage induced by UV and visible light. Carcinogenesis **18:** 811-816

Kivilaan A, Bandurski RS (1981) The one-hundred-year period for Dr. Beal's seed viability experiment. Ammerican Journal of Botany **68:** 1290-1292

Kjemtrup S, Boyes DC, Christensen C, McCaskill AJ, Hylton M, Davis K (2003) Growth Stage-Based Phenotypic Profiling of Plants. *In* E Grotewold, ed, Plant Functional Genomics: Methods and Protocols. Humana Press, Inc., Totowa, NJ, pp 427-441

Klecker B (1996) Energetic particle environment in near-Earth orbit. Advances in Space Research **17:** 37-45

Kliebenstein DJ (2004) Secondary metabolites and plant/ environment interactions: A view through *Arabidopsis thaliana* tinged glasses. Plant Cell and Environment **27:** 675-684

Kliebenstein DJ, Kroymann J, Brown PD, Figuth A, Pedersen D, Gershenzon J, Mitchell-Olds T (2001) Genetic control of natural variation in Arabidopsis glucosinolate accumulation. Plant Physiology **126:** 811-825

Kobayashi K, Kaneko T, Saito T, Oshima T (1998) Amino acids formation in gas mixtures by high energy particle irradiation. Origins of Life and Evolution of the Biosphere **28:** 155-165

Kobzar EF, Kreslavski VD, Muzafarov EN (1998) Photomorphogenetic responses to UV radiation and short-term red light in lettuce seedlings. Plant Growth Regulation **26:** 73-76

Koes RE, Quattrocchio F, Mol JNM (1994) The flavanoid biosynthetic pathway in plants : function and evolution. BioEssays **16:** 123-132

Koike J, Oshima T, Koike KA, Taguchi H, Tanaka R, Nishimura K, Miyaji M (1992) Survival rates of some terrestrial microorganisms under simulated space conditions. Advances in Space Research **12:** 271-274

Koller-Lampert K, Kranz AR (1982) Studies on biological effects of heavy ionizing particles in *Arabidopsis*. Arabidopsis Information Service (AIS) **19:** 73-78, http://www.arabidopsis.org/ais/aishint.html

Koller-Lampert K, Kranz AR (1983) Heavy ion experiments with *Arabidopsis* seeds. Arabidopsis Information Service (AIS) **20:** 27-33, http://www.arabidopsis.org/ais/aishint.html

Koornneef M (1990) Mutations affecting the testa color in *Arabidopsis*. Arabidopsis Information Service (AIS) **27:** 1-4

Koornneef M, Alonso-Blanco C, Vreugdenhil D (2004) Naturally occurring genetic variation in *Arabidopsis thaliana*. Annual Review of Plant Biology **55:** 141-172

Koornneef M, Dellaert LW, van der Veen JH (1982) EMS- and radiation-induced mutation frequencies at individual loci in *Arabidopsis thaliana* (L.) Heynh. Mutation Research **93:** 109-123

Koornneef M, Karssen CM (1994) Seed dormancy and germination. *In* EM Meyerowitz, CR Somerville, eds, Arabidopsis. Cold Spring Harbor Laboratory Press, New York, USA, pp 313-334

Kootstra A (1994) Protection from UV-B-induced DNA damage by flavonoids. Plant Molecular Biology **26:** 771-774

Kopp J, Beaujean R, Reitz G, Enge W (1999) HZE dosimetry in space using plastic track detectors. Radiation Measurements **31:** 573-578

Kowalski W (2009) Ultraviolet radiometry. *In* Ultraviolet Germicidal Irradiation Handbook: UVGI for Air and Surface Disinfection. Springer-Verlag, Berlin, Heidelberg, Germany, pp 313-336

Kozlowska H, Rotkiewicz DA, Zadernowski R, Sosulski FW (1983) Phenolic acids in rapeseed and mustard. Journal of the American Oil Chemists Society **60:** 1119-1123

Kranz AR, Bork U, Bûcker H, Reitz G (1990) Biological damage induced by ionizing cosmic rays in dry *Arabidopsis* seeds. Nuclear Tracks and Radiation Measurements **17:** 155-165

Kreuzer-Martin HW, Lott MJ, Dorigan J, Ehleringer JR (2003) Microbe forensics: Oxygen and hydrogen stable isotope ratios in *Bacillus subtilis* cells and spores. Proceedings of the National Academy of Sciences of the United States of America **100:** 815-819

Krinsky NI (1979) Carotenoid protection against oxidation. Pure and Applied Chemistry **51:** 649-660

Krueger FR, Kissel J (1987) The chemical composition of the dust of comet P/Halley as measured by "Puma" on board Vega-1. Naturwissenschaften **74:** 312-316

Kumagai J, Katoh H, Kumada T, Tanaka A, Tano S, Miyazaki T (2000) Strong resistance of *Arabidopsis thaliana* and *Raphanus sativus* seeds for ionizing radiation as studied by ESR, ENDOR, ESE spectroscopy and germination measurement: Effect of long-lived and super-long-lived radicals. Radiation Physics and Chemistry **57:** 75-83

Kunz BA, Dando PK, Grice DM, Mohr PG, Schenk PM, Cahill DM (2008) UV-induced DNA damage promotes resistance to the biotrophic pathogen *Hyaloperonospora parasitica* in Arabidopsis. Plant Physiology **148:** 1021-1031

Lagoja IM, Herdewijn P (2005) A potential prebiotic route to adenine from hypoxanthine. Chemistry & Biodiversity **2:** 923-927

Lambert N, Yarwood JN (1992) Engineering legume seed storage proteins. *In* PR Shewry, S Gutteridge, eds, Plant Protein Engineering. Cambridge University Press, Cambridge, UK, pp 167-187

Lambrix V, Reichelt M, Mitchell-Olds T, Kliebenstein DJ, Gershenzon J (2001) The Arabidopsis epithiospecifier protein promotes the hydrolysis of glucosinolates to nitriles and influences *Trichoplusia ni* herbivory. The Plant Cell **13:** 2793-2807

Landry LG, Chapple CCS, Last RL (1995) Arabidopsis mutants lacking phenolic sunscreens exhibit enhanced ultraviolet-B injury and oxidative damage. Plant Physiology **109:** 1159-1166

Lapointe G, Mori T, Evans DH (1996) Tobacco plants expressing T4 endonuclease V show enhanced sensitivity to ultraviolet light and DNA alkylating agents. Mutation Research **351:** 19-31

Larcher W (2003) Water relations. *In* Physiological Plant Ecology: Ecophysiology and Stress Physiology of Functional Groups, Ed 4th. Springer-Verlag, Berlin, Heidelberg, New York, pp 231-296

Larkum AWD, Kühl M (2005) Chlorophyll d: the puzzle resolved. Trends in Plant Science **10:** 355-357

Larsen SU, Bibby BM (2004) Use of germination curves to describe variation in germination characteristics in three turfgrass species. Crop Science **44:** 891-899

Lawlor DW, Mitchell RAC (1991) The effects of increasing CO_2 on crop photosynthesis and productivity: a review of field studies. Plant, Cell and Environment **14:** 807-818

Le Gall G, Metzdorff SB, Pedersen J, Bennett RN, Colquhoun IJ (2005) Metabolite profiling of *Arabidopsis thaliana* (L.) plants transformed with an antisense chalcone synthase gene. Metabolomics **1:** 181-198

Leach S, Smith IW, Cockell CS (2006) Introduction: Conditions for the emergence of life on the early Earth. Philosophical Transactions of the Royal Society B: Biological Sciences **361:** 1675-1679

Lean JL (2008) The Sun-Earth system: Our home in space. *In* BN Dwivedi, U Narain, eds, Physics of the Sun and its Atmosphere. Proceedings of the National Workshop on Recent Advances in Solar Physics, 7-10 November 2006, Meerut, India. World Scientific Publishing Co. Pte. Ltd, Singapore, Hackensack, London, pp 267-283

Lee HS (2000) HPLC analysis of phenolic compounds. *In* LML Nollet, ed, Food analysis by HPLC, Ed 2nd. Marcel Dekker, Inc., New York, USA, pp 775-824

Lehto HJ (2007) From the Big Bang to the molecules of life. *In* G Horneck, P Rettberg, eds, Complete Course in Astrobiology. Wiley-VCH Verlag GmbH & Co. KGaA, Weinheim, DE, pp 23-54

Lenoir C, Corbineau F, Côme D (1986) Barley (*Hordeum vulgare*) seed dormancy as related to glumella characteristics. Physiologia Plantarum **68:** 301-307

Léon-Kloosterziel KM, Keijzer CJ, Koornneef M (1994) A seed shape mutant of *Arabidopsis* that is affected in integument development. The Plant Cell **6:** 385-392

Lepiniec L, Debeaujon I, Routaboul J-M, Baudry A, Pourcel L, Nesi N, Caboche M (2006) Genetics and biochemistry of seed flavonoids. Annual Review of Plant Biology **57:** 405-430

Leprince O, Bochart R, Deltour R (1990) Changes in starch and soluble sugars in relation to the acquisition of desiccation tolerance during maturation of *Brassica campestris* seed. Plant, Cell and Environment **13:** 539-546

Leprince O, Hendry GAF, McKersie BD (1993) The mechanisms of desiccation tolerance in developing seeds. Seed Science Research **3:** 231-246

Lercari B, Sodi F, Lipucci di Paola M (1990) Photomorphogenic responses to UV radiation: Involvement of phytochrome and UV photoreceptors in the control of hypocotyl elongation in *Lycopersicon esculentum*. Physiologia Plantarum **79:** 668-672

Levin-Zaidman S, Englander J, Shimoni E, Sharma AK, Minton KW, Minsky A (2003) Ringlike structure of the *Deinococcus radiodurans* genome: a key to radioresistance? Science **299:** 254-256

Levinson HS, Hyatt MT (1970) Activation energy for glucose-induced germination of *Bacillus megaterium* spores. Journal of Bacteriology **103:** 269-270

Levinson HS, Sevag MG (1953) Stimulation of germination and respiration of the spores of *Bacillus megaterium* by manganese and monovalent anions. Journal of General Physiology **36:** 617-629

Lewis DG, Johnson WC, Jr. (1974) Circular dichroism of DNA in the vacuum ultraviolet. Journal of Molecular Biology **86:** 91-96

Li J, Ou-Lee T-M, Raba R, Amundson RG, Last RL (1993) Arabidopsis flavonoid mutants are hypersensitive to UV-B irradiation. The Plant Cell **5:** 171-179

Lichtenthaler HK, Buschmann C (2001) Chlorophylls and carotenoids: measurement and characterization by UV-VIS spectroscopy. Current Protocols in Food Analytical Chemistry**:** F4.3.1-F4.3.8

Lieberman M (1979) Biosynthesis and action of ethylene. Annual Review of Plant Physiology **30:** 533-591

Lindberg C, Horneck G (1991) Action spectra for survival and spore photoproduct formation of *Bacillus subtilis* irradiated with short-wavelength (200-300 nm) UV at atmospheric pressure and in vacuo. Journal of Photochemistry and Photobiology: B Biology **11:** 69-80

Linden K (2003) Dose measurement methods. *In* Disinfection Efficiency and Dose Measurement of Polychromatic UV Light. IWA Publishing, London, UK, pp 21-26

Ling G (2004) What determines the normal water content of a living cell? Physiological Chemistry and Physics & Medical NMR **36:** 1-19

Link BM, Durst SJ, Zhou W, Stanović B (2003) Seed-to-seed growth of *Arabidopsis thaliana* on the International Space Station. Advances in Space Research **31:** 2237-2243

Link L, Sawyer J, Venkateswaran K, Nicholson W (2004) Extreme spore UV resistance of *Bacillus pumilus* isolates obtained from an ultraclean spacecraft assembly facility. Microbial Ecology **47:** 159-163

Liu Y, Cockell CS, Wang G, Hu C, Chen L, De Philippis R (2008) Control of lunar and martian dust-experimental insights from artificial and natural cyanobacterial and algal crusts in the desert of inner Mongolia, China. Astrobiology **8:** 75-86

Lois R, Buchanan BB (1994) Severe sensitivity to ultraviolet radiation in an *Arabidopsis* mutant deficient in flavonoid accumulation. Planta **194:** 1432-2048

Lorenz P, Orlob GB, Hemenway CL (1969) Survival of micro-organisms in space. Origins of Life and Evolution of the Biosphere **1:** 491-500

Lorenz PR, Henmenway CL, Hotchin J (1968) The biological effectiveness of solar electromagnetic radiation in space. Life Sciences and Space Research **6:** 100-107

Lorenzen M, Racicot V, Strack D, Chapple C (1996) Sinapic acid ester metabolism in wild type and a sinapoylglucose-accumulating mutant of Arabidopsis. Plant Physiology **112:** 1625-1630

Luceri C, Giovanelli L, Pitozzi V, Toti S, Castagnini C, Routaboul J-M, Lepiniec L, Larrosa M, Dolara P (2008) Liver and colon DNA oxidative damage gene expression profiles of rats fed *Arabidopsis thaliana* mutant seeds containing contrasted flavonoids. Food and Chemical Toxicology **46:** 1213-1220

Ludwig MZ (2002) Functional evolution of noncoding DNA. Current Opinion in Genetics & Development **12:** 634-639

Luo J, Fuell C, Parr A, Hill L, Bailey P, Elliott K, Fairhurst SA, Martin C, Michael AJ (2009) A novel polyamine acyltransferase responsable for the accumulation of spermidine conjugates in *Arabidopsis* seed. The Plant Cell **21:** 318-333

Maher KA, Stevenson DJ (1988) Impact frustration of the origin of life. Nature **331:** 612-614

Mancinelli RL, Klovstad M (2000) Martian soil and UV radiation: microbial viability assessment on spacecraft surfaces. Planetary and Space Science **48:** 1093-1097

Mancinelli RL, White MR, Rothschild LJ (1998) BIOPAN-survival I: Exposure of the osmophiles *Synechococcus SP*. (Nageli) and *Haloarcula SP*. to the space environment. Advances in Space Research **22:** 327-334

Mansfield SG, Briarty LG (1992) Cotyledon cell development in *Arabidopsis thaliana* during reserve deposition. Canadian Journal of Botany **70:** 151-164

Marbach I, Mayer AM (1974) Permeability of seed coats to water as related to drying conditions and metabolism of phenolics. Plant Physiology **54:** 817-820

Marcano V, Benitez P, Palacios-Pru E (2006) UV-screening strategies of a lower eukaryote grown in hydrocarbon media. Origins of Life and Evolution of Biospheres **36:** 65-84

Margulis L, Walker JCG, Rambler M (1976) Reassessment of roles of oxygen and ultraviolet light in Precambrian evolution. Nature **264:** 620-624

Martin-Tanguy J (1985) The occurrence and possible function of hydroxycinnamoyl acid amides in plants. Plant Growth Regulation **3:** 381-399

Martin-Tanguy J (2001) Metabolism and function of polyamines in plants : recent development (new approaches). Plant Growth Regulation **34:** 135-148

Martin-Tanguy J, Burtin D, Tepfer D (1991) Importance des amines libres et conjuguées dans le developpement des végétaux. Approche moléculaire et utilisation d'inhibiteurs de la biosynthèse des polyamines. *In* J-P Moulinoux, V Quemener, eds, Les Polyamines. Aspects chimiques, rôles biologiques et applications médicales. Médecine-Sciences, Flammarion, Rennes, FR, pp 123-133

Maurel M-C, Vergne J, Drahi B, Decout J-L (1996) Implications of adenine in primitive catalysts and exobiology. Proceedings of the 6th European symposium on life sciences research in space, 16-20 June 1996, Trondheim, Norway. European Space Agency (ESA SP-390), Noordwijk, NL

Maurette M, Brack A, Kurat G, Perreau M, Engrand C (1995) Were micrometeorites a source of prebiotic molecules on the early Earth? Advances in Space Research **15:** 113-126

Mautner MN (2004) Seeding the Universe With Life: Securing Our Cosmological Future. Legacy Books, Christchurch, NZ

Mayne RY, Harper GA, Franz Jr. AO, Lee LS, Goldblatt LA (1969) Retardation of the elaboration of aflatoxin in cottonseed by impermeability of the seedcoats. Crop Science **9:** 147-150

McDonald MS (2003) Light and pigments. *In* Photobiology of Higher Plants. John Wiley & Sons Ltd, Chichester, UK, pp 1-32

McIntyre MP, Eilers HP, Mairs JW (1991) Physical Geography, Ed 5th. John Wiley & Sons, Inc., New York, NY, USA

McKay DS, Gibson EK, Jr., Thomas-Keprta KL, Vali H, Romanek CS, Clemett SJ, Chillier XDF, Maechling CR, Zare RN (1996) Search for past life on Mars: possible relic biogenic activity in Martian meteorite ALH84001. Science **273:** 924-930

McKinlay AF, Diffey BL (1987) A reference action spectrum for ultraviolet induced erythema in human skin. CIE Journal **6:** 17-22

Mei M, Qiu Y, He Y, Bücker H, Yang CH (1994) Mutational effects of space flight on *Zea mays* seeds. Advances in Space Research **14:** 33-39

Meinke DW (1994) Seed development in *Arabidopsis thaliana*. *In* EM Meyerowitz, CR Somerville, eds, Arabidopsis. Cold Spring Harbor Laboratory Press, New York, USA, pp 253-296

Melosh HJ (1985) Ejection of rock fragments from planetary bodies. Geology **13:** 144-148

Melosh HJ (1988) The rocky road to panspermia. Nature **332:** 687-688

Meredith P, Powell BJ, Riesz J, Nighswander-Rempel SP, Pederson MR, Moore EG (2006) Towards structure-property-function relationships for eumelanin. Soft Matter **2:** 37-44

Mileikowsky C, Cucinotta F, Wilson J, Gladman B, Horneck G, Lindegren L, Melosh J, Rickmann H, Valtonen M, Zheng JQ (2000) Natural transfer of viable microbes in space: 1. From Mars to Earth and Earth to Mars. Icarus **145:** 391-427

Miller AL (1996) Antioxidant flavonoids: structure, function and clinical usage. Alternative Medicine Review **1:** 103-111

Miller ES, Mackinney G, Zscheile Jr. FP (1935) Absorption spectra of alpha and beta carotenes and lycopene. Plant Physiology **10:** 375-381

Miller SL (1953) A production of amino acids under possible primitive Earth conditions. Science **117:** 528-529

Miller SL, Urey HC (1959) Organic compound synthesis on the primitive Earth: Several questions about the origin of life have been answered; but much remains to be studied. Science **130:** 245-251

Mirecki RM, Teramura AH (1984) Effects of ultraviolet-B irradiance on soybean. Plant Physiology **74:** 475-480

Mitchell DL, Jen J, Cleaver JE (1992) Sequence specificity of cyclobutane pyrimidine dimers in DNA treated with solar (ultraviolet B) radiation. Nucleic Acids Research **20:** 225-229

Moeller R, Douki T, Cadet J, Stackebrandt E, Nicholson WL, Rettberg P, Reitz G, Horneck G (2007a) UV-radiation-induced formation of DNA bipyrimidine photoproducts in *Bacillus subtilis* endospores and their repair during germination. International Microbiology **10:** 39-46

Moeller R, Horneck G, Facius R, Stackebrandt E (2005) Role of pigmentation in protecting *Bacillus* sp. endospores against environmental UV radiation. FEMS Microbiology Ecology **51:** 231-236

Moeller R, Stackebrandt E, Reitz G, Berger T, Rettberg P, Doherty AJ, Horneck G, Nicholson WL (2007b) Role of DNA repair by nonhomologous-end joining in *Bacillus subtilis* spore resistance to extreme dryness, mono- and polychromatic UV, and ionizing radiation. Journal of Bacteriology **189:** 3306-3311

Mohamed-Yasseen Y, Barringer SA, Splittstoesser WE, Costanza S (1994) The role of seed coats in seed viability. Botanical Review **60:** 426-439

Mojzsis SJ, Arrhenius G, McKeegan KD, Harrison TM, Nutman AP, Friend CRL (1996) Evidence for life on Earth before 3,800 million years ago. Nature **384:** 55-59

Mojzsis SJ, Harrison TM, Pidgeon RT (2001) Oxygen-isotope evidence from ancient zircons for liquid water at the Earth's surface 4,300 Myr ago. Nature **409:** 178-181

Monk JD, Beuchat LR, Doyle MP (1995) Irradiation inactivation of food-borne microorganisms. Journal of Food Protection **58:** 197-208

Montesinos MC, Ubeda A, Terencio MC, Paya M, Alcaraz MJ (1995) Antioxidant profile of mono- and dihydroxylated flavone derivatives in free radical generating systems. Der Zeitschrift für Naturforschung **50c:** 552-560

Moreno MA (1988) Microorganism transport from Earth to Mars. Nature **336:** 209

Müller K, Tintelnot S, Leubner-Metzger G (2006) Endosperm-limited Brassicaceae seed germination: Abscisic acid inhibits embryo-induced endosperm weakening of *Lepidium sativum* (cress) and endopserm rupture of cress and *Arabidopsis thaliana*. Plant and Cell Physiology **47:** 864-877

Murali NS, Teramura AH, Randall SK (1988) Response differences between two soybean cultivars with contrasting UV-B radiation sensitivities. Photochemistry and Photobiology **48:** 653-657

Murphy TM (1997) Resistance of plants to the effects of ultraviolet radiation. *In* AS Basra, RK Basra, eds, Mechanisms of environmental stress resistance in plants. Harwood Academic Publishers, Amsterdam, NL, pp 152-190

Musgrave ME (2002) Seeds in space. Seed Science Research **12:** 1-16

Musil CF (1994) Ultraviolet-B irradiation of seeds affects photochemical and reproductive performance of the arid-environment ephemeral *Dimorphotheca pluvialis* Environmental and Experimental Botany **34:** 371-378

Musil CF, Newton RJ, Farrant JM (1998) Ultraviolet irradiation effects on serotinous *Leucadendron laureolum* seeds: altered seed physiology and ultrastructure, and seedling performance. Plant Ecology **139:** 25-34

Narayanasamy P (2006) Principles and practice of postharvest disease menagement *In* Postharvest pathogens and disease management. John-Wiley & Sons, Inc., New Yersey, USA, pp 253-283

Nelson GA (2003) Fundamental space radiobiology. Gravitational and Space Biology Bulletin **16:** 29-36

Nicholson W, Setlow P (1990) Sporulation, germination and outgrowth. *In* C Harwood, S Cutting, eds, Molecular Biological Methods for Bacillus. John Wiley and Sons, Inc., Chichester, UK, pp 391-450

Nicholson WL, Fajardo-Cavazos P, Rebeil R, Slieman TA, Riesenman PJ, Law JF, Xue Y (2002) Bacterial endospores and their significance in stress resistance. Antonie van Leeuwenhoek **81:** 27-32

Nicholson WL, Galeano B (2003) UV resistance of *Bacillus anthracis* spores revisited: validation of *Bacillus subtilis* spores as UV surrogates for spores of *B. anthracis* Sterne. Applied and Environmental Microbiology **69:** 1327-1330

Nicholson WL, Munakata N, Horneck G, Melosh HJ, Setlow P (2000) Resistance of *Bacillus* endospores to extreme terrestrial and extraterrestrial environments. Microbiology and Molecular Biology Reviews **64:** 548-572

Nicholson WL, Schuerger AC, Setlow P (2005) The solar UV environment and bacterial spore UV resistance: considerations for Earth-to-Mars transport by natural processes and human space flight. Mutation Research **571:** 249-264

Nicolet M (1989) Solar spectral irradiances with their diversity between 120 and 900 nm. Planetary and Space Science **37:** 1249-1289

Nishizawa-Yokoi A, Yabuta Y, Shigeoka S (2008) The contribution of carbohydrates including raffinose family oligosaccharides and sugar alcohols to protection of plant cells from oxidative damage. Plant Signaling & Behaviour **3:** 1016-1018

Nonogaki H, Chen F, Bradford KJ (2007) Mechanisms and genes involved in germination *sensu stricto*. *In* KJ Bradford, H Nonogaki, eds, Seed Development, Dormancy and Germination: Annual Plant Reviews, Vol 27. Blackwell Publishing, Ltd., Oxford, UK, pp 264-304

NRC - National Research Council (US). Ad hoc Panel on the Biological Impacts of Ultraviolet Radiation (1973) Protection of organisms from ultraviolet radiation by shielding and avoidance. *In* Biological Impacts of Increased Intensities of Solar Ultraviolet Radiation. The National Academy of Sciences, The National Academy of Engineering, Washington, DC, USA, pp 24-26

NRC - National Research Council (US). Committee on the Evaluation of Radiation Shielding for Space (2008) Managinig Space Radiation Risk in the New Era of Space Exploration. The National Academies Press, Washington DC, USA, http://books.nap.edu/openbook.php?record_id=12045

Obe G, Johannes C, Schulte-Frohlinde D (1992) Review: DNA double-strand breaks induced by sparsely ionizing radiation and endonucleases as critical lesions for cell death, chromosomal aberrations, mutations and oncogenic transformation. Mutagenesis **7:** 3-12

Ogawa M (1971) Absorption cross sections of O_2 and CO_2 continua in the Schumann and far-UV regions. Journal of Chemical Physics **54:** 2550-2556

Ogawa M, Okita TW (2000) Seed storage proteins from the 1700s to the present. *In* S-D Kung, S-F Yang, eds, Discoveries in Plant Biology, Vol 3. World Scientific Publishing Co. Pte. Ltd., Singapore, pp 239-254

Ohto M, Stone SL, Harada JJ (2007) Genetic control of seed development and seed mass. *In* K Bradford, H Nonogaki, eds, Seed Development, Dormancy and Germination. Annual Plant Reviews, Vol 27. Blackwell Publishing, Ltd., Oxford, UK, pp 25-49

Olson JM, Pierson BK (1986) Photosynthesis 3.5 thousand million years ago. Photosynthesis Research **9:** 251-259

Onofri S, Barreca D, Selbmann L, Isola D, Rabbow E, Horneck G, de Vera J-PP, Hatton J, Zucconi L (2008) Resistance of Antarctic black fungi and cryptoendolithic communities to simulated space and Martian conditions. Studies in Microbiology **61:** 99-109

Onofri S, Selbmann L, Zucconi L, Pagano S (2004) Antarctic microfungi as models for exobiology. Planetary and Space Science **52:** 229-237

Oparin AI (1924) Proiskhozhdenie Zhizny (in Russian). Moskovski Rabochii, Moscow

Öpik H, Rolfe S (2005) Reproductive development. *In* The Physiology of Flowering Plants, Ed 4th. Cambridge University Press, Cambridge, UK, pp 270-317

Orgel LE (2004) Prebiotic adenine revisited: eutectics and photochemistry. Origins of Life and Evolution of the Biosphere **34:** 361-369

Oró J (1960) Synthesis of adenine from ammonium cyanide. Biochemical and Biophysical Research Communications **2:** 407-412

Oró J (1961) Mechanisms of synthesis of adenine from hydrogen cyanide under possible primitive Earth conditions. Nature **191:** 1193-1194

Oró J, Kimball AP (1961) Synthesis of purines under possible primitive earth conditions. I. Adenine from hydrogen cyanide. Archives of Biochemistry and Biophysics **94:** 217-227

Osborne TB (1924) The vegetable proteins, Ed 2nd. Longmans, Green and Co., London, UK

Osman S, Peeters Z, La Duc MT, Mancinelli R, Ehrenfreund P, Venkateswaran K (2008) Effects of shadowing on survival of bacteria under conditions simulating the Martian atmosphere and UV radiation. Applied and Environmental Microbiology **74:** 959-970

Owens DK, Alerding AB, Crosby KC, Bandara AB, Westwood JH, Winkel BSJ (2008) Functional analysis of predicted flavonol synthase gene family in *Arabidopsis*. Plant Physiology **147:** 1046-1061

Pammenter NW, Berjak P, Farrant JM, Smith MT, Ross G (1994) Why do stored hydrated recalcitrant seeds die? Seed Science Research **4:** 187-191

Parr AJ, Bolwell GP (2000) Phenols in the plant and in man. The potential for possible nutritional enhancement of the diet by modifying the phenols content or profile. Journal of the Science of Food and Agriculture **80:** 985-1012

Patton DA, Meinke DW (1990) Ultrastrusture of arrested embryos from lethal mutants of *Arabidopsis thaliana*. American Journal of Botany **77:** 653-661

Penfield S, Meissner RC, Shoue DA, Carpita NC, Bevan MW (2001) *MYB61* is required for mucilage deposition and extrusion in the *Arabidopsis* seed coat. The Plant Cell **13:** 2777-2791

Penfield S, Rylott EL, Gliday AD, Graham S, Larson TR, Graham IA (2004) Reserve mobilization in the *Arabidopsis* endosperm fuels hypocotyl elongation in the dark, is independent of abscisic acid, and requires PHOSPHOENOLPYRUVATE CARBOXYKINASE1. The Plant Cell **16:** 2705-2718

Perino C, Côme D (1991) Physiological and metabolic study of the germination phases in apple embryo. Seed Science and Technology **19:** 1-14

Peterbauer T, Richter A (2001) Biochemistry and physiology of raffinose family oligosaccharides and galactosyl cyclitols in seeds. Seed Science Research **11:** 185-197

Pezzella A, Napolitano A, d'Ischia M, Prota G, Seraglia R, Traldi P (1997) Identification of partially degraded oligomers of 5,6-dihidroxyindole-2-carboxylic acid in *Sepia* melanin by matrix-assisted laser desorption/ionization mass spectrometry. Rapid Communications in Mass Spectrometry **11:** 368-372

Pierson BK, Mitchell HK, Ruff-Roberts AL (1993) *Chloroflexus aurantiacus* and ultraviolet radiation: implications for archean shallow-water stromatolites. Origins of Life and Evolution of the Biosphere **23:** 243-260

Pokorny J, Reblova Z (1995) Sinapines and other phenolics of Brassicaceae seeds. Potravinářské vědy **13:** 155-168

Ponder M, Vishnivetskaya T, McGrath J, Tiedje J (2004) Microbial life in permafrost: Extended times in extreme conditions. *In* BJ Fuller, N Lane, EE Benson, eds, Life in the Frozen State. CRC Press LLC, Boca Raton, FL, USA, pp 151-170

Potts M (1999) Mechanisms of desiccation tolerance in cyanobacteria. European Journal of Phycology **34:** 319-328

Pourcel L, Routaboul J-M, Cheynier V, Lepiniec L, Debeaujon I (2000) Flavonoid oxidation in plants: from biochemical properties to physiological functions. Trends in Plant Science **12:** 29-36

Pourcel L, Routaboul JM, Kerhoas L, Caboche M, Lepiniec L, Debeaujon I (2005) TRANSPARENT TESTA10 encodes a laccase-like enzyme involved in oxidative polymerization of flavonoids in *Arabidopsis* seed coat. The Plant Cell **17:** 2966-2980

Powell AA (1989) The importance of genetically determined seed coat characteristics to seed quality in grain legumes. Annals of Botany **63:** 169-175

Preuss SB, Britt AB (2003) A DNA-damage-induced cell cycle checkpoint in *Arabidopsis*. Genetics **164:** 323-334

Proteau PJ, Gerwick WH, Garcia-Pichel F, Castenholz R (1993) The structure of scytonemin, an ultraviolet sunscreen pigment from the sheaths of cyanobacteria. Experientia **49:** 825-829

Qi X, Qi J, Wu Y (2007) RootLM: a simple color image analysis program for length measurement of primary roots in *Arabidopsis*. Plant Root **1:** 10-16

Qin H, Xue J, He F, Lai J, Zhang W, Wang J, Yan S, Zhao W, Gu H, Wang Y (2005) Biological effect of the seeds of *Arabidopsis thaliana* irradiated by MeV protons. Radiation Effects and Defects in Solids **160:** 131-136

Qin HL, Wang YG, Xue JM, Miao Q, Ma L, Mei T, Zhang WM, Guo W, Wang JY, Gu HY (2007) Biological effects of protons targeted to different ranges in *Arabidopsis* seeds. International Journal of Radiation Biology **83:** 301-308

Quintern LE, Puskeppeleit M, Rainer P, Weber S, El Naggar S, Eschweiler U, Horneck G (1994) Continuous dosimetry of the biologically harmful UV-radiation in Antarctica with the biofilm technique. Journal of Photochemistry and Photobiology B: Biology **22:** 59-66

Rabbow E (2007a) Preflight verification and test programme for EXPOSE-EUTEF EVT-E1. *In*. Report No RES-PI/SH/06.340, DLR, Institute of Aerospace Medicine, Cologne, Germany, pp 1-12

Rabbow E (2007b) Preflight verification and test programme for EXPOSE-EUTEF EVT-E2. *In*. Report No RES-PI/SH/06.340, DLR, Institute of Aerospace Medicine, Cologne, Germany, pp 1-12

Rabbow E (2009) EXPOSE-E mission overview. *In* EXPOSE-IWG-ESTEC Meeting. ESTEC, Noordwijk, NL

Rabbow E, Horneck G, Rettberg P, Schott J-U, Panitz C, L'Afflitto A, von Heise-Rotenburg R, Willnecker R, Baglioni P, Hatton J, Dettmann J, Demets R, Reitz G (2009) EXPOSE, an astrobiological exposure facility on the International Space Station - from proposal to flight. Origins of Life and Evolution of Biospheres **39:** 581-598

Rajjou L, Debeaujon I (2008) Seed longevity: Survival and maintenance of high germination ability of dry seeds. Comptes Rendus Biologies **331:** 796-805

Ranal MA, de Santana DG (2006) How and why to measure the germination process? Revista Brasileira de Botânica **29:** 1-11

Rao DLN, Gill HS (1993) Nitrogen fixation, biomass production, and nutrient uptake by annual sesbania species in an alkaline soil. Biol Fert Soils **15:** 73-78

Rao MV, Paliyath G, Ormrod DP (1996) Ultraviolet-B- and ozone-induced biochemical changes in antioxidant enzymes of Arabidopsis thaliana. Plant Physiology **110:** 125-136

Ravanat J-L, Douki T, Cadet J (2001) Direct and indirect effects of UV radiation on DNA and its components. Journal of Photochemistry and Photobiology B: Biology **63:** 88-102

Reifenrath K, Müller C (2007) Species-specific and leaf-age dependent effects of ultraviolet radiation on two Brassicaceae. Phytochemistry **68:** 875-885

Reitz G, Horneck G, Facius R, Schafer M (1995) Results of space experiments. Radiation and Environmental Biophysics **34:** 139-144

Renger G, Volker M, Eckert HJ, Fromme R, Hohm-Veit S, Graber P (1989) On the mechanism of photosystem II deterioration by UV-B irradiation. Photochemistry and Photobiology **49:** 97-105

Rettberg P, Cockell CS (2004) Biological UV dosmetry using the DLR-biofilm. Photochemistry and Photobiology Science **3:** 781-787

Rettberg P, Eschweiler U, Strauch K, Reitz G, Horneck G, Wanke H, Brack A, Barbier B (2002) Survival of microorganisms in space protected by meteorite material: results of the experiment 'EXOBIOLOGIE' of the PERSEUS mission. Advances in Space Research **30:** 1539-1545

Reuber S, Bornman JF, Weissenböck G (1996) A flavonoid mutant of barley (*Hordeum vulgare* L.) exhibits increased sensitivity to UV-B radiation in the primary leaf. Plant, Cell and Environment **19:** 593-601

Rice-Evans CA, Miller NJ, Papanga G (1997) Antioxidant properties of phenolic compounds. Trends in Plant Science **2:** 152-159

Riesenman PJ, Nicholson WL (2000) Role of the spore coat layers in *Bacillus subtilis* spore resistance to hydrogen peroxide, artificial UV-C, UV-B, and solar UV radiation. Applied and Environmental Microbiology **66:** 620-626

Riley PA (1997) Melanin. The International Journal of Biochemistry & Cell Biology **29:** 1235-1239

Rivero-Lepinckas L, Crist D, Scholl R (2006) Growth of plants and preservation of seeds. *In* J Salinas, JJ Sanchez-Serrano, eds, Arabidopsis protocols, Ed 2nd Vol 323. Humana Press, Totowa, NJ, USA, pp 3-12

Roberts EH (1973) Predicting the storage life of seeds. Seed Science and Technology **1:** 499-514

Rogers HH, Petterson CM, McCrimmon JN, Cure JD (1992a) Response of plant roots to elevated atmospheric carbon dioxide. Plant, Cell and Environment **15:** 749-752

Rogers HH, Prior AA, O'Neill E (1992b) Cotton root and rhizosphere responses to free-air CO_2 enrichment Critical Review in Plant Sciences **11:** 251-263

Rothschild LJ (1990) Earth analogs for Martian life. Microbes in evaporites a new model system for life on Mars. Icarus **88:** 246-260

Rothschild LJ, Giver LJ, White MR, Mancinelli RL (1994) Metabolic activity of microorganisms in evaporites. Journal of Phycology **30:** 431-438

Rothschild LJ, Mancinelli RL (2001) Life in extreme environments. Nature **409:** 1092-1101

Routaboul J-M, Kerhoas L, Debeaujon I, Pourcel L, Caboche M, Einhorn J, Lepiniec L (2006) Flavonoid diversity and biosynthesis in seed of *Arabidopsis thaliana*. Planta **224:** 96-107

Roy D, Najafian K, von Ragué Schleyer P (2007) Chemical evolution: The mechanism of the formation of adenine under prebiotic conditions. Proceedings of the National Academy of Sciences of the USA **104:** 17272-17277

Rozema J (2000) Effects of solar UV-B radiation on terrestrial biota. *In* RE Hester, RM Harrison, eds, Causes and environmental implications of increased UV-B radiation. Issues in environmental science and technology, Vol 14. The Royal Society of Chemistry, Cambridge, UK, pp 85-106

Rozema J, Lenssen GM, van de Staaij J, Tosserams M, Broekman RA (1997a) Effects of UV-B radiation on terrestrial plants and ecosystems: interaction with CO_2 enrichment. Plant Ecology **128:** 183-191

Rozema J, van de Staaij J, Björn LO, Caldwell M (1997b) UV-B as an environmental factor in plant life: stress and regulation. Trends in Ecology & Evolution **12:** 22-28

Rozema J, van Geel B, Björn LO, Lean JL, Madronich S (2002) Toward solving the UV puzzle. Science **296:** 1621-1622

Ruegger M, Chapple C (2001) Mutations that reduce sinapoylmalate accumulation in *Arabidopsis thaliana* define loci with diverse roles in phenylpropanoid metabolism. Genetics **159:** 1741-1749

Ruegger M, Meyer K, Cusumano JC, Chapple C (1999) Regulation of ferulate-5-hydoxylase expression in Arabidopsis in the context of sinapate ester biosynthesis. Plant Physiology **119:** 101-110

Ryan KG, Swinny EE, Markham KR, Winefield C (2002) Flavonoid gene expression and UV photoprotection in transgenic and mutant *Petunia* leaves. Phytochemistry **59:** 23-32

Ryan KG, Swinny EE, Winefield C, Markham KR (2001) Flavonoids and UV photoprotection in *Arabidopsis* mutants. Zeitschrift für Naturforschung **56c:** 745-754

Sagan C (1973) Ultraviolet radiation selection pressure on the earliest organisms. Journal of Theoretical Biology **39:** 195-200

Sagan C (1974) The origin of life in a cosmic context. Origins of Life and Evolution of the Biosphere **5:** 497-505

Sagan C, Chyba C (1997) The early faint Sun paradox: Organic shielding of ultraviolet-labile greenhouse gases. Science **276:** 1217-1221

Salaita L, Kar RK, Majee M, Downie AB (2005) Identification and characterization of mutants capable of rapid seed germination at 10 {degrees}C from activation-tagged lines of Arabidopsis thaliana. Journal of Experimental Botany **56:** 2059-2069

Sallon S, Solowey E, Cohen Y, Korchinsky R, Egli M, Woodhatch I, Simchoni O, Kislev M (2008) Germination, genetics, and growth of an ancient date seed. Science **320:** 1464

Sancho LG, de la Torre R, Horneck G, Ascaso C, de Los Rios A, Pintado A, Wierzchos J, Schuster M (2007) Lichens survive in space: results from the 2005 LICHENS experiment. Astrobiology **7:** 443-454

Sancho LG, De la Torre R, Pintado A (2008) Lichens, new and promising material from experiments in astrobiology. Fungal Biology Reviews **22:** 103-109

Saraf S, Ashawat MS, Saraf S (2007) Flavonoids: A nutritional protection against oxidative and UV induced cellular damages. Pharmacognosy Reviews **1:** 30-40

Sastry DVSSR, Upadhyaya HD, Gowda CLL (2007) Survival of groundnut seeds under different storage conditions. e-Journal of the SAT Agricultural Research | http://ejournal.icrisat.org **5:** 1-3

Sayre JD (1940) Storage tests with seed corn. The Ohio Journal of Science **XL:** 181-185

Schaeffer AB, Fulton MD (1933) A simpified method of staining endospores. Science **77:** 194-194

Schaeffer P, Millet J, Aubert JP (1965) Catabolic repression of bacterial sporulation. Proceedings of the National Academy of Science U S A **54:** 704-711

Schijlen EG, Ric de Vos CH, van Tunen AJ, Bovy AG (2004) Modification of flavonoid biosynthesis in crop plants. Phytochemistry **65:** 2631-2648

Schmidt L (2000) Seed testing. *In* Guide to Handling of Tropical and Subtropical Forest Seed. DANIDA Forest Seed Centre, Humlebaek, DK, pp 1-22, http://www.sl.life.ku.dk/publikationer/udgivelser/dfsc/dfscbook21.aspx

Schmitt-Kopplin P, Gabelica Z, Gougeon RD, Fekete A, Kanawti B, Harir M, Gabefuegi I, Eckel G, Hertkorn N (1010) High molecular diversity of extraterrestrial organic matter in Murchison meteorite revealed 40 years after its fall. Proceedings of the National Academy of Sciences of the USA **107:** 2763-2768

Scholl R, Rivero-Lepinckas L, Crist D (1998) Growth of plants and preservation of seeds. *In* JM Martinez-Zapater, J Salinas, eds, Arabidopsis protocols. Methods in molecular biology, Vol 82. Humana Press, Springer-Verlag, New York, USA, pp 1-13

Schopf JW (1993) Microfossils of the early Archean apex chert: New evidence of the antiquity of life. Science **260:** 640-646

Schopf JW (1994) Disparate rates, differing fates: Tempo and mode of evolution changed from the Precambrian to the phanerozoic. Proceedings of the National Academy of Sciences of the USA **91:** 6735-6742

Schopf JW, Packer BM (1987) Early Archean (3.3 billion to 3.5 billion years old) microfossils from Warrawoona Group, Australia. Science **237:** 70-73

Schuerger AC, Mancinelli R, Kem RG, Rothschild LJ, McKay CP (2003) Survival of endospores of *Bacillus subtilis* on spacecraft surfaces under simulated martian environments: implications for the forward contamination of Mars. Icarus **165:** 253-276

Schwartzkopf SH, Mancinelli RL (1991) Germination and growth of wheat in simulated Martian atmospheres. Acta Astronaut **25:** 245-247

Scott BR (2005) Stochastic thresholds: A novel explanation of nonlinear dose-response relationships for stochastic radiobiological effects. Dose Response **3:** 547-567

Secker J, Wesson PS, Lepock JR (1996) Astrophysical and biological constraints on radiopanspermia. Journal of the Royal Astronomical Society of Canada **90:** 184-192

Sessions A (2005) T-DNA mutagenesis: From tagging to insertion sequence databases. *In* D Leister, ed, Plant Functional Genomics The Haworth Press, Inc., Bringhamton, NY, USA, pp 23-36

Setlow B, Atluri S, Kitchel R, Koziol-Dube K, Setlow P (2006) Role of dipicolinic acid in resistance and stability of spores of *Bacillus subtilis* with or without DNA-protective alpha/beta-type small acid-soluble proteins. Journal of Bacteriology **188:** 3740-3747

Setlow P (1995) Mechanisms for the prevention of damage to DNA in spores of *Bacillus* species. Annual Review of Microbiology **49:** 29-54

Setlow RB (1974) The wavelengths in sunlight effective in producing skin cancer: a theoretical analysis. Proceedings of the National Academy of Science USA **71:** 3363-3366

Sheahan JJ (1996) Sinapate esters provide greater UV-B attenuation than flavonoids in Arabidopsis thaliana (Brassicaceae). American Journal of Botany **83:** 679-686

Shen-Miller J, Shope JW, Harbottle G, Cao R, Ouyang S, Zhou KS, Southon JR, Liu GH (2002) Long living Lotus : germination and soil y-irradiation of centuries-old fruits, and

cultivation, growth, and phenotypic abnormalities of offspring. American Journal of Botany **89:** 236-247

Shewry PR, Napier JA, Tatham AS (1995) Seed storage proteins: structures and biosynthesis. The Plant Cell **7:** 945-956

Shick JM, Dunlap WC (2002) Mycosporine-like amino acids and related gadusols: Biosynthesis, accumulation, and UV-protective functions in aquatic organisms. Annual Review of Physiology **64:** 223-262

Shinkle JR, Derickson DL, Barnes PW (2005) Comparative photobiology of growth responses to two UV-B wavebands and UV-C in dim-red-light- and white-light-grown cucumber (*Cucumis safivus*) seedlings: Physiological evidence for photoreactivation. Photochemistry and Photobiology **81:** 1069-1074

Shirley BW, Kubasek WL, Storz G, Bruggemann E, Koornneef M, Ausubel FM, Goodman HM (1995) Analysis of Arabidopsis mutants deficient in flavonoid biosynthesis. Plant Journal **8:** 659-671

Shomer B, Yagil G (1999) Long W tracts are over-represented in the *Escherichia coli* and *Haemophilus influenzae* genomes. Nucleic Acids Research **27:** 491-4500

Sinha RP, Häder D-P (2002) UV-induced DNA damage and repair: a review. Photochemical & Photobiological Sciences **1:** 225 - 236

Sinha RP, Klisch M, Groniger A, Häder D-P (1998) Ultraviolet-absorbing/screening substances in cyanobacteria, phytoplankton and macroalgae. Journal of Photochemistry and Photobiology B: Biology **47:** 83-94

Slieman TA, Nicholson WL (2000) Artificial and solar UV radiation induces strand breaks and cyclobutane pyrimidine dimers in *Bacillus subtilis* spore DNA. Applied and Environmental Microbiology **66:** 199-205

Slieman TA, Nicholson WL (2001) Role of dipicolinic acid in survival of Bacillus subtilis spores exposed to artificial and solar UV radiation. Applied and Environmental Microbiology **67:** 1274-1279

Sliney DH (2007) Radiometric quantities and units used in photobiology and photochemistry: Recommendations of the Commission Internationale de l'Eclairage (International Commission on Illumination). Photochemistry and Photobiology **83:** 425-432

Smith MAL, Spomer LA (1995) Vessels, gels, liquid media, and support systems. *In* J Aitken-Christie, T Kozai, MAL Smith, eds, Automation and environmental control in plant tissue culture. Kluwer academic publishers, Dordrecht, NL, pp 371-404

Smith R (2000) Encyclopedia of the Solar System. Salem Press, Chicago, IL, USA

Smith TA (1985) Polyamines. Annual Review of Plant Physiology **36:** 117-143

Sontag W, Weigezahn KF (1975) Absorption of DNA in the region of vacuum-uv (3-25 eV). Radiation and Environmental Biophysics **12:** 169-174

Spizizen J, Isherwood JE, Taylor GR (1975) Effects of solar ultraviolet radiations on *Bacillus subtilis* spores and T7 bacteriophage. Life Sciences and Space Research **13:** 143-149

Stapleton AE (1992) Ultraviolet radiation and plants: Burning questions. The Plant Cell **4:** 1353-1358

Stapleton AE, Walbot V (1994) Flavonoids can protect maize DNA from the induction of ultraviolet radiation damage. Plant Physiology **105:** 881-889

Stefova M, Stafilov T, Kulevanova S (2004) HPLC analysis of flavonoids. *In* J Cazes, ed, Encyclopedia of Chromatography. Marcel Dekker, New York, NY, USA, pp 113-119

Steiner AM, Ruckenbauer P (1995) Germination of 110-year-old cereal and weed seeds, the Vienna sample of 1877. Verification of effective ultra-dry storage at ambient temperature. Seed Science Research **5:** 195-199

Steinmetz V, Wellmann E (1986) The role of solar UV-B in growth regulation of cress *Lepidium sativum* seedlings. Photochemistry and Photobiology **43**

Stoks PG, Schwartz AW (1981) Nitrogen-heterocyclic compounds in meteorites: significance and mechanisms of formation Geochimica et Cosmochimica Acta **45:** 563-569

Strack D, Dahlbender B, Grotjahn L, Wrayt V (1984) 1,2-Disinapolylglucose accumulated in cotyledons of dark grown *Raphanus sativus* seedlings Photochemistry **23:** 657-659

Strack D, Sharma V (1985) Vacuolar localization of the enzymatic synthesis of hydroxycinnamic acid esters of malic acid in protoplasts from *Raphanus sativus* leaves. Physiologia Plantarum **65:** 45-50

Sueoka N (1962) On the genetic basis of variation and heterogeneity of DNA base composition. Proceedings of the National Academy of Sciences of the USA **48:** 582-592

Sun Q, Wang J-H, Sun B-Q (2007) Advances on seed vigor physiological and genetic mechanisms. Agricultural Sciences in China **6:** 1060-1066

Sutherland JC (2002) Biological effects of polychromatic light. Photochemistry and Photobiology **76:** 164-170

Tabor CW, Tabor H (1984) Polyamines. Annual Review of Biochemistry **53:** 749-790

Taji T, Ohsumi C, Iuchi S, Seki M, Kasuga M, Kobayashi M, Yamaguchi-Shinozaki K, Shinozaki K (2002) Important roles of drought- and cold-inducible genes for galactinol synthase in stress tolerance in *Arabidopsis thaliana*. The Plant Journal **29:** 417-426

Tauer CG (1979) Seed tree, vacuum, and temperature effects on eastern cottonwood seed viability during extended storage. Forest Science **25:** 112-114

Tepfer D (1983) The biology of genetic transformation of higher plants by Agrobacterium rhizogenes. *In* A Puhler, ed, Molecular Genetics of the Bacteria Plant Interaction. Springer Verlag, Berlin, D, pp 248-258

Tepfer D (1984) Transformation of several species of higher plants by *Agrobacterium rhizogenes:* sexual transmission of the transformed genotype and phenotype. Cell **37:** 959-967

Tepfer D (1995) *Agrobacterium rhizogenes* mediated transformation: transformed roots to transformed plants. *In* I Potrykus, G Spangenberg, eds, Gene Transfer to Plants. Springer-Verlag, Berlin, pp 45-52

Tepfer D (2008) The origin of life, panspermia and a proposal to seed the Universe. Plant Science **175:** 756-760

Tepfer D, Leach S (2006) Plant seeds as model vectors for the transfer of life through space. Astrophysics and Space Science **306:** 69-75

Teramura AH (1983) Effects of ultraviolet-B radiation on the growth and yield of crop plants. Physiologia Plantarum **58:** 415-427

Tevini M, Teramura AH (1989) UV-B effects on terrestrial plants. Photochemistry and Photobiology **50:** 479-487

Tevini M, Thoma U, Iwanzik W (1983) Effects of enhanced UV-B radiation on germination, seedling growth, leaf anatomy and pigments of some crop plants. Zeitschrift für Pflanzenphysiologie **109:** 435-448

Thanos CA, Georghiou K (1988) Ecophysiology of fire-stimulated seed germination in *Cistus incanus* ssp. *creticus* (L.) Heywood and *C. salvifolius* L. Plant, Cell and Environment **11:** 841-849

Thomas DJ, Boling J, Boston PJ, Campbell KA, McSpadden T, McWilliams L, Todd P (2006) Extremophiles for ecopoiesis: Desirable traits for and survivability of pioneer Martian organisms. Gravitational and Space Biology **19:** 91-103

Thuillier G, Floyd L, Woods TN, Cebula R, Hilsenrath E, Hersé M, Labs D (2004) Solar irradiance reference spectra. *In* J Pap, P Fox, C Frohlich, HS Hudson, J Kuhn, J McCormack, G North, W Sprigg, ST Wu, eds, Solar Variability and its Effect on the Earth's Atmosphere and Climate System, AGU Monograph Series. American Geophysical Union (AGU), Washington, DC, USA, p 141

Tiunaitienė N, Rančelienė V, Šlekytė K, Cieminis K (2002) Photoreactivation of the chromosomal damage induced by UVC in Crepis capillaris cells. Biologija **3:** 27-29

Toole EH, Hendricks SB, Borthwick HA, Toole VK (1956) Physiology of seed germination. Annual Review of Plant Physiology **7:** 299-324

Torabinejad J, Caldwell MM (2000) Inheritance of UV-B tolerance in seven ecotypes of Arabidopsis thaliana L. Heynh. and their F_1 hybrids. The Journal of Heredity **91:** 228-233

Torres M, Frutos G, Duran JM (1991) Sunflower seed deterioration from exposure to U. V.-C. radiation. Environmental and Experimental Botany **31:** 201-207

Tosserams M, Bolink E, Rozema J (1997) The effect of enhanced ultraviolet-B radiation on germination and seedling development of plant species occurring in a dune grassland ecosystem. Plant Ecology **128:** 139-147

Treutter D (2006) Significance of flavonoids in plant resistance: a review. Environmental Chemistry Letters **4:** 147-157

Tuteja N, Singh MB, Misra MK, Bhalla PL, Tuteja R (2001) Molecular mechanisms of DNA damage and repair: progress in plants. Critical Reviews in Biochemistry and Molecular Biology **36:** 337-397

Usoskin IG, Mursula K, Kananen H, Kovaltsov GA (2001) Dependence of cosmic rays on solar activity for odd and even solar cycles. Advances in Space Research **27:** 571-576

van Gerwen SJC, Rombouts FM, van't Riet K, Zwietering MH (1999) A data analysis of the irradiation parameter D_{10} for bacteria and spores under various conditions. Journal of Food Protection **62:** 1024-1032

Vaulina EN, Anikeeva ID, Kostina LN (1984) Radiosensibility of higher plant seeds after space flight. Advances in Space Research **4:** 103-107

Veit M, Pauli GF (1999) Major flavonoids from Arabidopsis thaliana leaves. Journal of Natural Products **62:** 1301-1303

Vergne J, Dumas L, Décout J-L, Maurel M-C (2000) Possible prebiotic catalysts formed from adenine and aldehyde. Planetary and Space Science **48:** 1139-1142

Vertucci CW, Farrant JM (1995) Acquisition and loss of desiccation tolerance. *In* J Kigel, G Galili, eds, Seed development and germination. Marcel Dekker, Inc., New York, NY, USA, pp 237-272

Vierstra RD, John TR, Poff KL (1982) Kaempferol 3-o-galactoside, 7-o-rhamnoside is the major green fluorescing compound in the epidermis of *Vicia faba*. Plant Physiology **69:** 522-525

von Roepenack-Lahaye E, Degenkolb T, Zerjeski M, Franz M, Roth U, Wessjohann L, Schmidt J, Scheel D, Clemens S (2004) Profiling of Arabidopsis secondary metabolites by capillary liquid chomatography coupled to electrospray ionization quadrupole time-of-flight mass spectrometry. Plant Physiology **134:** 548-559

Wahid A, Gelani S, Ashraf M, Foolad MR (2007) Heat tolerance in plants: An overview. Environmental and Experimental Botany **61:** 199-223

Wakamatsu K, Ito S (2002) Advanced chemical methods in melanin determination. Pigment Cell Research **15:** 174-183

Walbot V, Last RL, Hays J, Hoffman J, Lim L, Stapleton A, Landry L (1997) An Arabidopsis photolyase mutant is hypersensitive to ultraviolet-B radiation. Proceedings of the National Academy of Sciences of the USA **94:** 328-332.

Walker JCG (1985) Carbon dioxide on the early earth. Origins of Life and Evolution of the Biosphere **16:** 117-127

Walters C, Farrant JM, Pammenter NW, Berjak P (2002) Desiccation stress and damage. *In* M Black, HW Pritchard, eds, Desiccation and survival in plants: Drying without dying. CABI Publishing, New York, NY, USA, pp 263-292

Walters C, Wheeler JM, Grotenhuis JM (2005) Longevity of seeds stored in gene bank: species characteristics. Seed Science Research **15:** 1-20

Ward JK, Strain BR (1999) Elevated CO_2 studies: past, present and future. Tree Physiology **19:** 211-220

Warren PH (1994) Lunar and Martian meteorite delivery services. Icarus **111:** 338-363

Warton MJ (1955) The use of the tetrazolium test for determining the viability of seeds of the genus Brassica. Proceedings of International Seed Testing Association **20:** 81-88

Weber H, Borisjuk L, Heim U, Buchner P, Wobus U (1995) Seed coat-associated invertases of fava bean control both unloading and storage functions: cloning of cDNAs and cell type-specific expression. The Plant Cell **7:** 1835-1846

Weber H, Borisjuk L, Wobus U (1996) Controlling seed development and seed size in *Vicia faba*: a role for seed coat-associated invertases and carbohydrate state. The Plant Journal **10:** 823-834

Weber H, Borisjuk L, Wobus U (1997) Sugar import and metabolism during seed development. Trends in Plant Science **2:** 169-174

Weber P, Greenberg JM (1985) Can spores survive in interstellar space? Nature **316:** 403-407

Wehmeyer N, Vierling E (2000) The expression of small heat shock proteins in seeds responds to descrete developmental signals and suggests a general protective role in desiccation tolerance. Plant Physiology **122:** 1099-1108

Weisshaar B, Jenkins GI (1998) Phenylpropanoid biosynthesis and its regulation. Current Opinion in Plant Biology **1:** 251-257

West MAL, Harada JJ (1993) Embryogenesis in higher plants: An overview. The Plant Cell **5:** 1361-1369

Westall F (2005) Life on the early Earth: A sedimentary view. Science **308:** 366 - 367

Westall F, de Ronde CEJ, Southam G, Grassineau N, Colas M, Cockell C, Lammer H (2006) Implications of a 3.472-3.333 Gyr-old subaerial microbial mat from the Barbeton greenstone belt, South Africa for the UV environmental conditions on the early Earth. Philosophical Transactions of the Royal Society B: Biological Sciences **361:** 1857-1875

Western TL, Skinner DJ, Haughn GW (2000) Differentiation of mucilage secretory cells of the *Arabidopsis* seed coat. Plant Physiology **122:** 345-356

Wharton DA (2002) Life without water. *In* Life at the limits: organisms in extreme environments. Cambridge University Press, Cambridge, UK, pp 92-128

Wharton MJ (1955) The use of the tetrazolium test for determining the viability of seeds of the genus Brassica. Proceedings of International Seed Testing Association **20:** 81-88

Wickramasinghe C (2004) The universe: a cryogenic habitat for microbial life. Cryobiology **48:** 113-125

Wickramasinghe C (2010) The astrobiological case for our cosmic ancestry. International Journal of Astrobiology**:** 119-129

Wilde SA, Valley JW, Peck WH, Graham CM (2001) Evidence from detrital zircons for the existence of continental crust and oceans on the Earth 4.4 Gyr ago. Nature **409:** 175-178

Willats WGT, McCartney L, Knox JP (2001) In-situ analysis of pectic polysaccharides in seed mucilage and at the root surface of *Arabidopsis thaliana*. Planta **213:** 37-44

Winkel-Shirley B (1998) Flavonoids in seeds and grains: physiological function, agronomic importance and the genetics of biosynthesis. Plant Physiology **8:** 415-422

Winkel-Shirley B (2001) Flavonoid biosynthesis. A colorful model for genetics, biochemistry, cell biology, and biotechnology. Plant Physiology **126:** 485-493

Wulff RD, Alexander HM (1985) Intraspecific variation in the response to CO_2 enrichment in seeds and seedlings of *Plantago lanceolata*. Oecologia **66:** 458-460

Wynn-Williams DD, Edwards HGM (2002) Environmental UV radiation: biological strategies for protection and avoidance. *In* G Horneck, C Baumstark-Khan, eds, Astrobiology: The Quest for the Conditions of Life. Springer-Verlag, Berlin, Heidelberg, New York, pp 245-260

Xenopoulos MA, Schindler DW (2001) Physical factors determining ultraviolet radiation flux into ecosystems. *In* CS Cockell, AR Blaustein, eds, Ecosystems, Evolution, and Ultraviolet Radiation. Springer-Verlag, New York, Berlin, Heidelberg, pp 36-62

Xiong F, Kopecky J, Nedbal L (1999) The occurrence of UV-B absorbing mycosporine-like amino acids in freshwater and terrestrial microalgae (Chlorophyta) Aquatic Botany **63:** 37-49

Yamaguchi S, Smith MW, Brown RGS, Kamiya Y, Sun T (1998) Phytochrome regulation and differential expression of gibberellin 3 β–hydroxylase genes in germinating Arabidopsis seeds. The Plant Cell **10:** 2115-2126

Yeh YM, Chiu KY, Chen CL, Sung JM (2005) Partial vacuum extends the longevity of primed bitter ground seeds by enhancing their anti-oxidative activities during storage. Scientia Horticulturae **104:** 101-112

Yeung EC, Meinke DW (1993) Embryogenesis in angiosperms: Development of the suspensor. The Plant Cell **5:** 1371-1381

Yoshioka T, Ota H, Segawa K, Takeda Y, Esashi Y (1995) Contrasted effecs of CO_2 on the regulation of dormancy and germination in *Xanthium pennsylvanicum* and *Setaria faberi* seeds. Annals of Botany **76:** 625-630

Zahnle KJ, Walker JCG (1982) The evolution of solar ultraviolet luminosity. Reviews of geophysics and space physics **20:** 280-292

Zalar A (2004) Résistance des graines d'Arabidopsis aux UV et à d'autres conditions néfastes dans l'espace. Diplôme d'études supérieures de sciences (DES). Université Pierre et Marie Curie - Paris 6, Paris

Zalar A, Tepfer D, Hoffmann SV, Kenney JM, Leach S (2007a) Directed exospermia: I. Biological modes of resistance to UV light are implied through absorption spectroscopy of DNA and potential UV screens. International Journal of Astrobiology **6:** 229-240

Zalar A, Tepfer D, Hoffmann SV, Kollmann A, Leach S (2007b) Directed exospermia: II. VUV-UV spectroscopy of specialized UV screens, including plant flavonoids, suggests using metabolic engineering to improve survival in space. International Journal of Astrobiology **6:** 291-301

Zalar A, Tepfer D, Hoffmann SV, Kollmann A, Leach S (2007c) VUV-UV absorption spectroscopy of DNA and UV screens suggests strategies for UV resistance during evolution and space travel. *In* RB Hoover, GV Levin, AY Rozanov, PCW Davies, eds, Instruments, Methods, and Missions for Astrobiology X, Vol 6694. Proceedings of SPIE, p 66940U

Zimmermann MW, Gartenbach KE, Kranz AR, Baican B, Schopper E, Heilmann C, Reitz G (1996) Recent results of comparative radiobiological experiments with short and long term expositions of *Arabidopsis* seed embryos. Advances in Space Research **18:** 205-213

Zimmermann MW, Gertenbach KE, Kranz AR (1994) First radiobiological results of LDEF-1 experiment A0015 with *Arabidopsis* seed embryos and *Sordaria* fungus spores. Advances in Space Research **14:** 47-51

Zscheile FP, White Jr JW, Beadle BW, Roach JR (1942) The preparation and absorption spectra of five pure carotenoid pigments. Plant Physiology **17:** 331-346

Chapter 9
PUBLISHED ARTICLES

Article 1

Zalar A, Tepfer D, Hoffmann S V, Kenney J and Leach S (2007a) Directed exospermia: I. Biological modes of resistance to UV light are implied through absorption spectroscopy of DNA and potential UV screens. *International Journal of Astrobiology*, 6(3): 229-240

International Journal of Astrobiology 6 (3): 229–240 (2007) Printed in the United Kingdom
doi:10.1017/S1473550407003771 First published online 11 June 2007

Directed exospermia: I. Biological modes of resistance to UV light are implied through absorption spectroscopy of DNA and potential UV screens

Andreja Zalar[1], David Tepfer[1], Søren V. Hoffmann[2], John M. Kenney[3] and Sydney Leach[4]

[1]*Institut National de la Recherche Agronomique, Versailles 78026, France*
e-mail: tepfer@versailles.inra.fr
[2]*Institute for Storage Ring Facilities, University of Aarhus, Aarhus 8000, Denmark*
[3]*Department of Physics, East Carolina University, Greenville, NC 27858-4353, USA*
[4]*LERMA, UMR 8112-CNRS, Observatoire de Paris-Meudon, 92195 Meudon, France*

Abstract: Panspermia, the dissemination of life through space, would require resistance to the conditions found in space, including UV light. All known life forms depend on DNA to store information. In an effort to understand the liabilities of DNA to UV light and modes of DNA protection in terrestrial life forms, we established UV–VUV (125–340 nm) absorption spectra for dry DNA and its polymerized components and mononucleotides, as well as for a selection of potential UV screens ubiquitous in all organisms, including proteins, selected amino acids and amines (polyamines and tyramine). Montmorillonite clay was included as a potential abiotic UV screen. Among the potential screens tested, adenosine triphosphate (ATP) appeared to be particularly attractive, because its UV absorption spectrum was similar to that of DNA. We suggest that the use of ATP in UV protection could have pre-dated its current role in energy transfer. Spectroscopy also showed that UV absorption varied according to nucleotide content, suggesting that base pair usage could be a factor in adaptation to given UV environments and the availability of UV screens.

Received 12 January 2007, accepted 17 April 2007

Key words: ATP, base pair ratio, DNA photo lesions, origin of life, panspermia, plant seed, UV resistance, UV screen, VUV–UV absorption spectroscopy.

Introduction

Panspermia requires that life survive travel through space. Man has explored Earth's moon, and most of the unmanned craft sent to planets and beyond have been contaminated by microorganisms. Exospermia, the dissemination of Earth's life through space (Tepfer & Leach 2006), is thus clear, but the capacity of life to thrive in a remote environment has not been demonstrated. No other Earth-like environment is known in the Solar System, and exoplanets are only just being discovered. Conditions on these exoplanets are likely to be inhospitable or extremely deleterious to life as we know it.

The origin of life on Earth is unknown, but fossilized bacteria are found in rocks from 3.43 Gy ago, suggesting that complex life either evolved in the first gigayear of Earth's existence or was imported. The first case, spontaneous generation, could have occurred through incremental steps, starting with simple chemistry. The second case, the introduction of life from outside the Earth or introspermia (Tepfer & Leach 2006), requires that life resist conditions in space. Destructive UV light is a potential liability in both cases.

Theories of the origin of life are difficult to test, but we can use terrestrial models to study how organisms currently resist UV radiation, and we can hopefully improve this resistance. The environment on Earth and the chemistry of prebiotic life 4 Gy ago are not known with certitude (Leach *et al.* 2006). Thus, attempts to spontaneously generate life must be made under assumed conditions of simulation. On the other hand, the plausibility of panspermia can be tested by examining the ability of contemporary terrestrial life to withstand space travel. However, proof that life came to Earth via panspermia (introspermia) will require finding life elsewhere (on Mars, for instance) and showing that it uses DNA and the same genetic code as terrestrial life forms. Unfortunately, contamination (as a result of Man's space exploration) potentially complicates the search for extra-terrestrial life.

On Earth, life survives in extreme conditions, e.g. close to undersea fumaroles and in the desiccated Atacama desert. The mechanisms whereby extremophiles adapt to these environments are as diverse as the occupied niches, but they all serve, either directly or indirectly, to protect the biological information encoded in DNA. Some of the mechanisms for

conserving the genome are starting to be understood. For instance, *Deinococcus radiodurans* survives desiccation and radiation by rebuilding a functional genome from the fragments produced during stress, using a novel genome reconstruction strategy (Zahradka *et al.* 2006). In photosynthetic organisms, damage from UV radiation can be attenuated by UV shields that filter out deleterious UV radiation, but still transmit the wavelengths required to fix CO_2.

In exoenvironments, UV radiation would be a major danger for organisms dependent on light to fix carbon. Solar irradiance diminishes between 300 and 130 nm, but since photon energy increases and DNA absorbs in this range, short-wave Solar UV radiation remains a liability for unprotected organisms. On Earth, present-day organisms are shielded from these wavelengths by stratospheric ozone, but before the accumulation of atmospheric oxygen, as a result of photosynthesis, life probably had to cope with the full spectrum of Solar UV radiation. We reasoned that by examining UV shields in present-day organisms, it might be possible to understand how life could have adapted to conditions on primitive Earth, and eventually how to better prepare it for survival in exohabitats.

A UV shield should absorb incident photons and dissipate their energy, if possible without molecular damage. Physical distance between the shield and sensitive targets, such as DNA, would thus help cope with the energy absorbed. Extracellular coats or sheaths are well known in the microbial world, and plant seeds are surrounded by a seed coat. Chromosomal DNA is localized in the interior, as far as possible from incident light and other deleterious components of the environment, and is surrounded by cellular substances that help protect against UV. We assume here that an ideal UV shield for DNA would absorb UV radiation in a similar manner as DNA. We thus evaluate the potential suitability of UV shields according to the degree of similarity between their VUV–UV absorption spectrum and that of DNA. This approach allows us to propose concepts that can be experimentally verified.

In this and the following paper (Zalar *et al.* 2007), we measure VUV–UV spectra of thin films of potential and demonstrated UV shields, using synchrotron light between 125 and 340 nm, extending the energy range of existing spectra that were generally not known below 200 nm. We begin by examining absorption by DNA and its components, and then we establish absorption curves for potential universal UV screens, i.e. those found in all forms of life. (The accompanying paper (Zalar *et al.* 2007) is devoted to demonstrating UV screens in specific prokaryotic and eukaryotic organisms.) The structures of the substances examined here are given in Fig. 1.

Results

VUV–UV absorption by DNA and its components

DNA. In the dry salmon sperm DNA sample, absorption maxima (Fig. 2; see also Fig. 9) were observed at 264 nm (region I) and 192 nm (region II), with absorbance climbing to 125 nm at the lower end of the spectrum (region III). In the hydrated sample, the peak at 264 nm was shifted to 260 nm, and the peak at 192 nm was obscured by absorbance by the solvent (Fig. 2). These peak behaviours are similar to those observed in comparing the heavy-water solution spectra of native DNA and DNA denatured by heat (Falk 1964).

Oligonucleotides (*polymerized*). All oligonucleotides (homopolymers of 20 nucleotides) showed major absorption peaks grouped in three regions: 255–286 nm (region I), 159–220 nm (region II) and in a third region (III) of absorbance, increasing to the highest observed value at 125 nm, the shortest wavelength measured (Fig. 3; see also Fig. 9). The oligonucleotides showed more spectral features than DNA, with three peaks or shoulders detected for oligoT, five for oligoA and four for oligoG. The purines (A, G) thus showed more features than the pyrimidines (C, T), as expected from their more complex structures. A peak or shoulder was observed at 208 nm in all but oligoC, where a peak was seen instead at 220 nm and an inflection around 200 nm. The two purines had peaks at 255–257 nm, while the pyrimidines had peaks at 268 (oligoT) and 278 nm (oligoC).

The broad salmon sperm DNA peaks at 192 and 264 nm are thus resolvable into oligonucleotide spectral families, with the peak interval greater in the pyrimidines than in the purines. As noted above, in the purines, the region I peak occurred at 255 nm for oligoG and at 257 nm for oligoA, with shoulders at 286 and 271 nm, respectively. In oligoC, the region I peak occurred at 278 nm, but in oligoT it was found at 268 nm. In addition, the oligoG spectrum showed a strong shoulder at 286 nm. Thus, in DNA sequences rich in GC base pairs, absorption by region I should shift to longer wavelengths. A similar analysis for the region II family (150–230 nm) showed that absorption by the AT pair should occur at shorter wavelengths, compared with the GC pair, but this difference should be less dramatic than for region I.

These observations suggest that the overall absorption spectrum of DNA depends on its state of hydration and the relative frequencies of the GC versus the AT base pairs. DNA sequences composed uniquely of AT will absorb more at the short wavelengths, and those made up of GC more at the longer wavelengths.

Nucleotide monomers (*unpolymerized*). The unpolymerized monomers that make up DNA could also serve as UV filters. These include the four bases alone and their ribose derivatives: nucleosides (without the phosphate) or nucleotides (with the phosphate). A potential advantage of these small molecule UV screens would be their ability to diffuse or be transported through cellular compartments of the organism.

We therefore determined absorption spectra for the four monomer nucleotides (Fig. 4; see also Fig. 9), and compared them with our spectra for polymerized (oligo)A/G/C/T, as well as with the published spectra of thin films of the unpolymerized A/G/C/T nucleobases, measured by Yamada & Fukutome (1968) and also by Isaacson (1972) (Table 1). Our

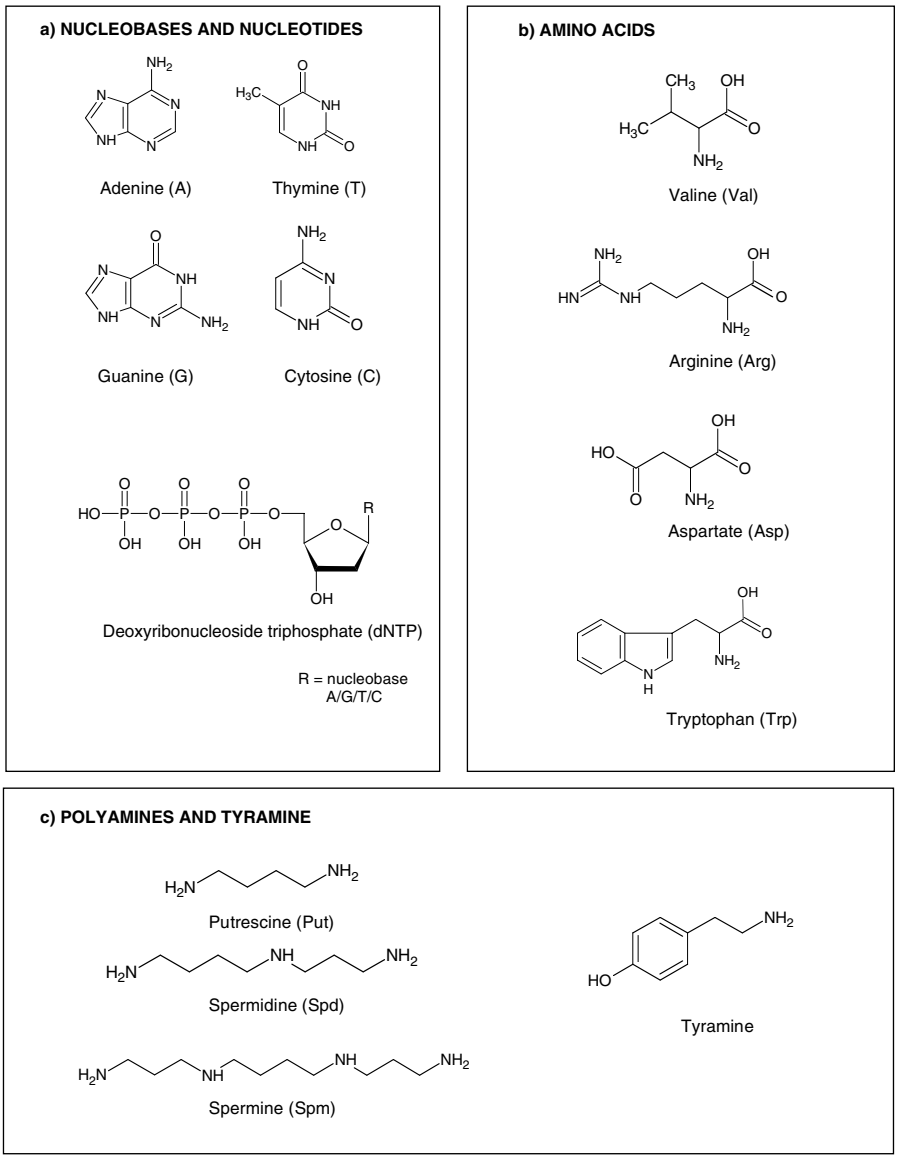

Fig. 1. Chemical structures of molecules used in VUV–UV absorption spectroscopy, including DNA, proteins (and their subunits) and potential UV screens: (a) A/G/T/C nucleobases (adenine/guanine/thymine/cytosine) and nucleotides (deoxyribonucleoside triphosphates, dNTPs); (b) amino acids (valine, Val; arginine, Arg; aspartate, Asp; tryptophan, Trp); (c) naturally occurring polyamines (putrescine, Put; spermidine, Spd; spermine, Spm) and the aromatic amine, tyramine.

peak wavelength assignments generally agreed with previous reports. In addition, the spectra for polymerized A, T and G were similar, in numbers of bands and peak wavelengths, to those of the monomers (see Fig. 9).

We can conclude for A, T and G that interaction between bases of the same type in an oligonucleotide is relatively small, beacuse polymerization has little effect on the absorption spectrum in the region we measured. Thus, the accumulation in a cell of these mononucleotides could contribute to protecting DNA against UV radiation. (The remarkable similarity between monoA and DNA absorption curves is discussed later.)

In contrast to A, T and G, the peaks in the cytidine nucleotide sample changed with polymerization, with the region I peak shifting to higher wavelengths and the region II peak shifting to lower wavelengths (Fig. 4; see also Fig. 9). A peak at 182 nm in oligoC was absent in the monomer. In water, the cytosine peak wavelengths in the 190–300 nm region are more dependent on pH than the corresponding peaks for A, G and T (Voet *et al.* 1963), and absorption spectra for monoC appear to vary for different samples and as a result of ageing (Yamada & Fukutome 1968).

UV absorption by proteins and their components

The amino acid sequence determines protein structure as well as overall charge. Basic proteins (e.g. histones) bind DNA electrostatically. Depending on their amino acid sequence, proteins have the potential to insert into membranes via

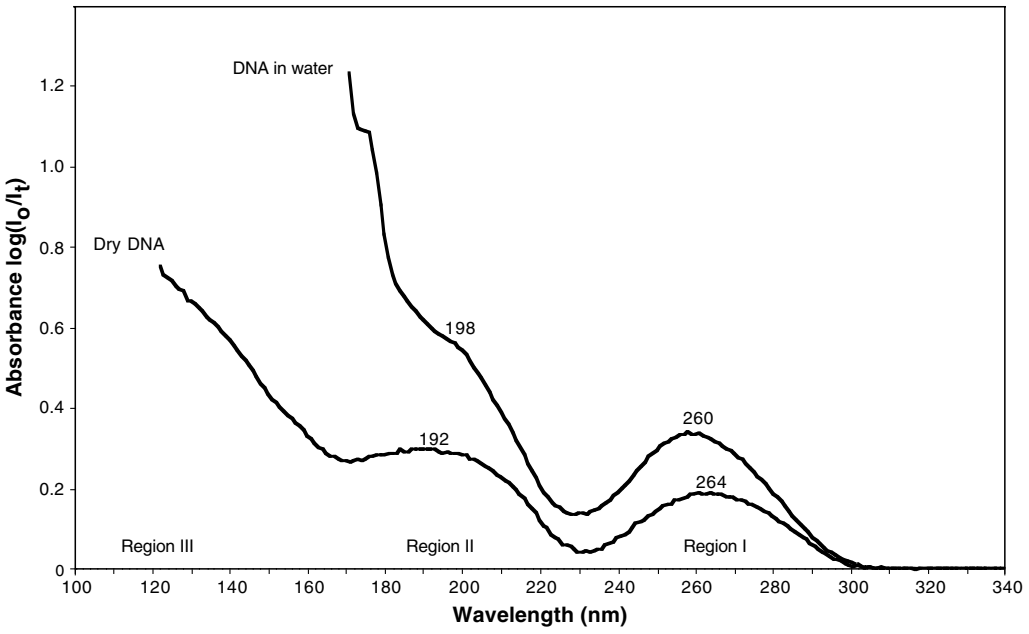

Fig. 2. VUV–UV absorption by hydrated and dry salmon sperm DNA.

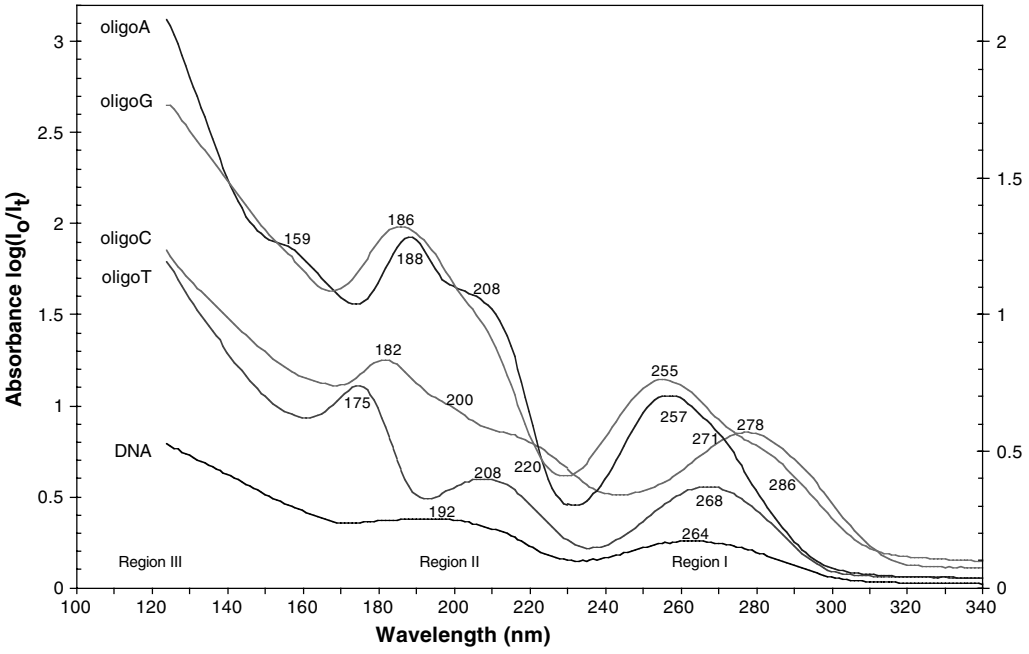

Fig. 3. VUV–UV absorption by polymerized oligonucleotides (A, T, G and C) with dry DNA as a reference.

hydrophobic residues, adhere to membrane phospholipids through electrostatic interactions or bind specifically to diverse structures or molecules (e.g. consider the interactions between antigens and antibodies, enzymes and substrates and receptors and their ligands).

We examined the UV absorption spectrum of histones, which are positively charged DNA-binding proteins found in eukaryotic cells. Absorption peaks (Fig. 5; see also Fig. 9) were observed at 170 and 192 nm, and a continuous increase in absorbance occurred below 150 nm. Although there was relatively little absorption above about 230 nm, higher protein concentration showed the characteristic protein absorbance peak at 280 nm (Fig. 5, inset). Histones do not appear to be ideal UV protectors for DNA absorption region I. An identical spectrum was obtained for bovine serum albumin (results not shown), a small globular protein of 585 amino acids.

Amino acids can be classified according to their side groups. For absorption spectroscopy, we chose one from each of two of the four standard classes. In order to better assess the influence of the aromatic ring in tryptophan, an additional two from the 'neutral and hydrophobic' class were

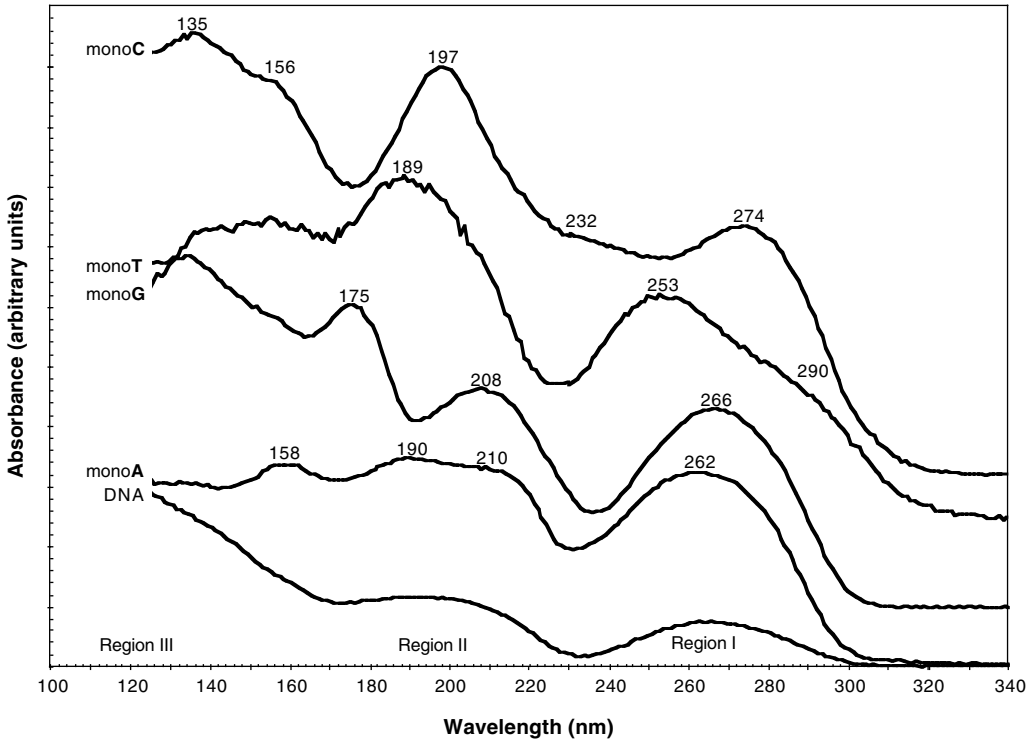

Fig. 4. VUV–UV absorption by mononucleotides (A, T, G and C) with dry DNA as a reference. Absorbance values are adjusted to make the curves understandable.

selected. (Another criterion in the choice of particular samples was the ability of amino acids to make thin films that produced a minimum of scattering.) The amino acids were: arginine (basic), tryptophan (neutral and hydrophobic), valine (neutral and hydrophobic) and aspartic acid (acidic). Their spectra (Fig. 6; see also Fig. 9) showed that potential protection of DNA absorption regions II and III in the DNA curve is a common feature, but that UV screening for region I is only seen with the aromatic amino acid, tryptophan, where a broad, complex peak at 287 nm was recorded, with a shoulder at 272 nm, reminiscent of the vibrational structure in benzenoid spectra in this region.

UV absorption by polyamines and tyramine

Polyamines are small polycationic molecules, found in all living organisms. They are essential for optimal growth and development in eukaryotic and prokaryotic cells (Martin-Tanguy *et al*. 1990). As they are positively charged at cellular pH, they interact with negatively charged molecules, such as DNA (Basu *et al*. 1990; Pohjanpelto & Holtta 1996), membrane phospholipids (Schuber *et al*. 1983; Beigbeder *et al*. 1995; Tassoni *et al*. 1996) and some proteins (Apelbaum *et al*. 1988). Putrescine (Put), spermine (Spm) and spermidine (Spd) are the major polyamines found in most cells, where they are present in high concentrations. In addition to the aliphatic polyamines (Put, Spm and Spd), aromatic amines, such as tyramine (Tyr), naturally occur in prokaryotic and eukaryotic organisms.

Polyamines can be found not only as free molecular bases, but also conjugated to small molecules or bound to proteins. In plants, polyamines and aromatic amines are usually conjugated with phenolic acids such as hydroxycinnamic acids, e.g., t-cinnamic, caffeic, ferulic and p-coumaric acids (Martin-Tanguy 1985, 1997; Martin-Tanguy *et al*. 1991). Polyamines are known in the laboratory to interact strongly with DNA, to stabilize condensed DNA conformations (Flink & Pettijohn 1975) and thus to protect DNA from degradation. In nature they are important in the regulation of growth, but they are not considered to be hormones, because of their elevated cellular concentrations. They accumulate in response to stress, possibly as a way of storing nitrogen produced by the breakdown of proteins. In plants, polyamines and their conjugates are implicated in growth, development and the regulation of flowering and responses to biotic and abiotic stress (Martin-Tanguy 1985, 1997, 2001; Martin-Tanguy *et al*. 1991; Tepfer & Martin-Tanguy 1991). Polyamine accumulation in plants was induced by UV-B (An *et al*. 2004) and by UV-C radiation (Campos *et al*. 1991).

The UV absorption spectra (Fig. 7; see also Fig. 9) for spermidine, putrescine, spermine and tyramine showed a peak in the 170 nm region, with continued absorbance to 123 nm. Tyramine gave peaks at 198 nm, at 221 nm and twin peaks in the region of 282 nm with a shoulder at 267 nm. Tyramine would thus protect DNA in both DNA absorption regions I and II.

UV absorption by clay

Inorganic materials, such as clay, which has been proposed as a catalyst in prebiotic chemistry (Bernal 1951; Ferris *et al*. 1996; Rode 1999), are obvious candidates for protecting

Table 1. *Comparison of peak wavelengths of monomer and polymerized A/G/C/T (our measurements) with those of unpolymerized A/G/C/T nucleobases measured by Yamada & Fukutome (1968) and by Isaacson (1972)*

Adenine peaks (nm)				Guanine peaks (nm)		
	MonoA				MonoG	
OligoA				OligoG		
(a)	(a)	(b)	(c)	(a)	(a)	(b)
271	262	269–272	273	286	290	282–289
257				255	253	246–251
208	210	210	212	206	(200)	198–200
188	190	182	191	186	189	185
159	158	160	161			

Cytosine peaks (nm)			Thymine peaks (nm)			
	MonoC			MonoT		
OligoC			OligoT			
(a)	(a)	(b)	(a)	(a)	(b)	(c)
278	274	271	268	266	265–270	266
220	232		208	208	211	209
200	197	199–203	175	175	176	175
182				135	144	141
162 (inflection)	156	161				
	135	150				

(a) Present paper; (b) Yamada & Fukutome (1968); (c) Isaacson (1972).

DNA and the organisms that contain it. Adsorption of DNA on soil components, particularly on clays, protects DNA against degradation by nucleases (Romanowski *et al.* 1991; Paget *et al.* 1992; Gallori *et al.* 1994; Lorenz & Wackernagel 1994; Demaneche *et al.* 2001) and DNA adsorbed on clay minerals, such as montmorillonite and kaolinite, is partially protected against UV light and X-rays (Ciaravella *et al.* 2004; Scappini *et al.* 2004). We therefore examined montmorillonite clay as a possible UV screen. The absorption spectrum of clay showed peaks at 141, 184 and 247 nm, with strongly increasing absorbance below 135 nm (Fig. 8; see also Fig. 9). Although the features are not as distinct as in other substances analysed, clay absorbed throughout the absorption spectral region of DNA, but the observed peaks were blue-shifted by about 10–20 nm with respect to dry salmon sperm DNA. These montmorillonite clay peaks could be the result of organic contamination.

Discussion

DNA conserves the information that defines life on Earth. Terrestrial life on primitive Earth or in future space travel must cope with the full spectrum of Solar UV. We therefore examined UV absorption by DNA and by a few of the possible chemical screens that could protect DNA, based on the working assumption that the DNA and UV screen absorption curves should match as closely as possible. We considered molecules common to essentially all forms of life: DNA, DNA subunits, proteins, amino acids, polyamines and tyramine. In addition, we examined a clay as a possible abiotic DNA protector.

Absorption spectra of DNA

Peak wavelengths and intensity ratios vary in published DNA absorption spectra. This could be due to differences in the source of the DNA and how it was prepared. Our salmon sperm DNA sample was extracted with organic solvents to remove proteins and small molecules. Salmon sperm DNA belongs to the AT rich class, having a GC content of 41.2% (Chargaff *et al.* 1951). Spectra in the dry and hydrated states were compared (Fig. 2), using a DNA film dried onto a MgF_2 window and the same DNA dissolved in water. DNA in films is no longer in the B state, but in a distorted configuration in which the complementary pairing and the parallel stacking of the DNA bases is reduced, but the double helical strands remain entwined (Falk *et al.* 1963; Falk 1964).

Table 2, where we compare our results with already published DNA absorption spectra (Inagaki *et al.* 1974; Sontag & Weibezahn 1975; Ito & Ito 1986), gives relative absorption intensities of DNA films at selected wavelengths, with respect to the intensity of the 260 nm band. The DNA samples of Inagaki *et al.* (1974) and those of Sontag & Weibezahn (1975) were from calf thymus, but the DNA sample of Ito & Ito (1986) was specified only as 'highly polymerized DNA'. Our relative intensities agree with those of Sontag & Weibezahn, who used lamp radiation sources. The relative intensities of Ito & Ito, who used a synchrotron radiation source, have higher values, and those of Inagaki *et al.* have lower values. The DNA films of Sontag & Weibezahn and Inagaki *et al.* were on metal mesh screens, whereas those of Ito & Ito were on CaF_2 plates.

The intensity measurements of Inagaki *et al.* were indirectly determined, partly based on a Kramers–Kronig analysis of the index of refraction of the films. They are thus subject to defects in this treatment. The higher relative intensities recorded by Ito & Ito might be due to greater scattering or to the DNA sample's unreported origin. Although the absorption spectra of the DNA films reported in Table 2 are quite similar, apart from the relative intensity differences mentioned above, they exhibit small differences in peak wavelengths, as might be expected from the different DNA source materials and sample preparations.

Effects of nucleotide composition on UV absorption

Absorption spectra of the polymerized nucleotides (homopolymers) that compose DNA suggest that absorption region I would shift to longer wavelengths in DNA composed uniquely of G and C nucleotides, compared with DNA made up of A and T. Furthermore, DNA in the dry state shows a small red-shift for region I (Fig. 2). Relative GC content varies in different organisms (Marmur & Doty 1962), e.g. between 31% (*Clostridium perfigens*) and 72% (*Micrococcus lysodeikticus*); see Lewis & Johnson (1974). The potential for G use is clear in the genetic code, where in many cases an alternative codon can contribute a supplementary G

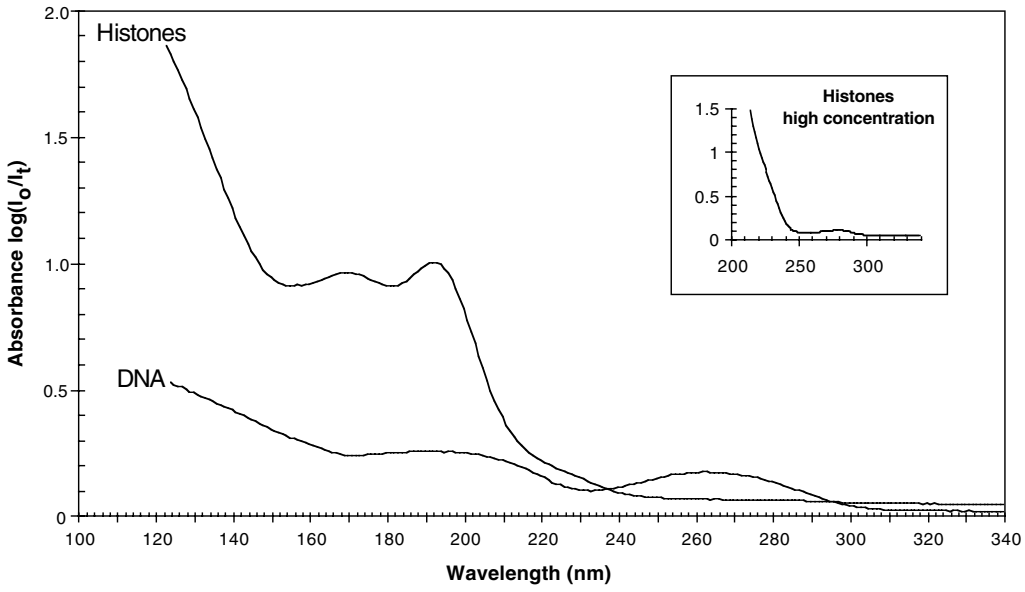

Fig. 5. VUV–UV absorption by histone protein with dry DNA as a reference. Inset gives a higher concentration to show the peak at 280 nm.

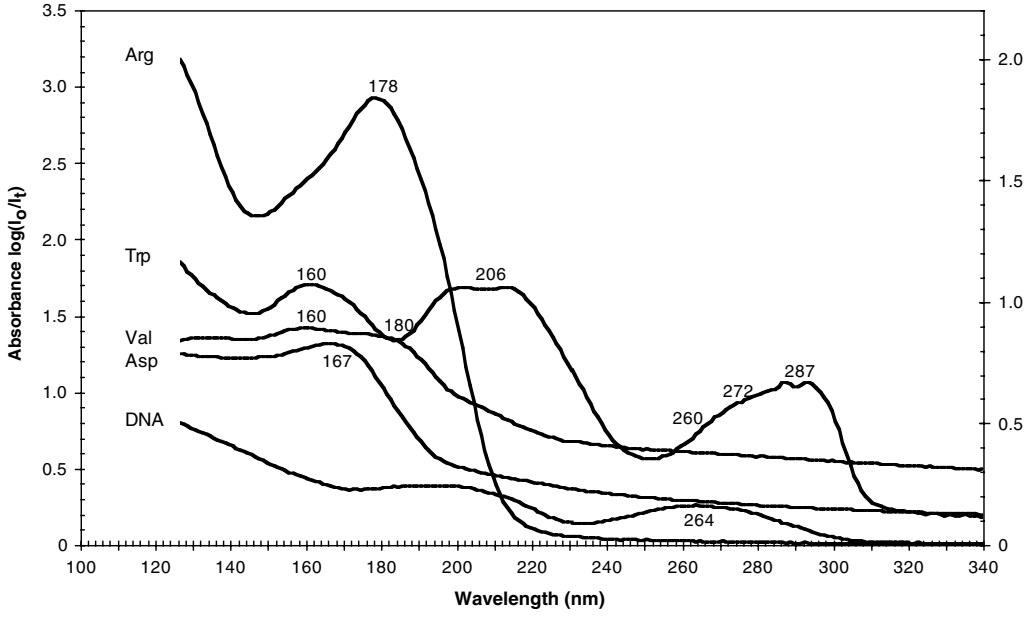

Fig. 6. VUV–UV absorption by amino acids: arginine (Arg), tryptophan (Trp), valine (Val) and aspartic acid (Asp). Dry DNA is included as a reference.

to the sequence, without changing the protein sequence. We calculate that a hypothetical gene, encoding a protein incorporating one of each of the 20 amino acids, can vary in GC content by more than twofold, without changing the amino acid sequence. (The minimum GC content was 30%; the maximum was 63%.) In theory, nucleotide content (including non-coding sequences) could thus evolve or be engineered to alter the overall absorption characteristics of the genome, but this hypothesis needs to be verified experimentally.

Three hydrogen bonds in the GC pair, as opposed to two in the AT pair, make the double helix of nucleic acids more stable at high temperatures (Galtier & Lobry 1997). According to our observations, the red-shift potentially conferred by a sequence rich in G and C should also confer better UV protection by proteins (see below section on proteins and aminoacids as UV screens). In addition, lowering the frequency of the AT pair would reduce the chances of dimerization of adjacent thymines, which are involved in the majority of the mutagenic photo lesions caused by UV radiation.

The existence and degree of a hypothetical red-shift associated with high GC can be determined by studying UV absorption by synthetic DNA sequences that vary in GC content, and the sensitivity of these hybrids to specific UV wavelengths can be measured *in vitro*. The ecological

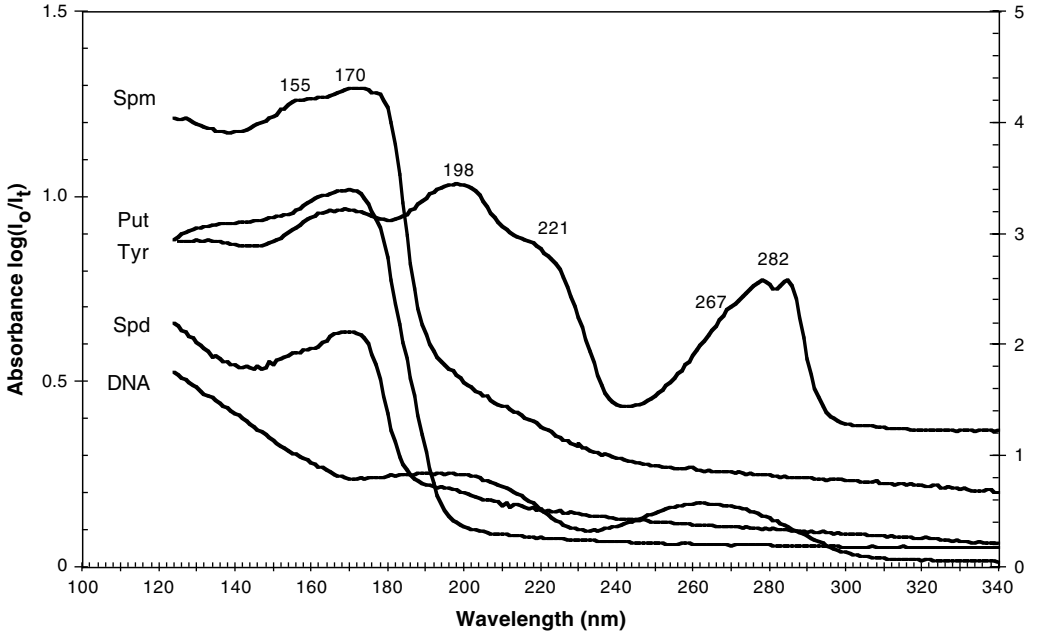

Fig. 7. VUV–UV absorption by amines: spermine (Spm), putrescine (Put), tyramine (Tyr) and spermidine (Spd). Dry DNA is included as a reference.

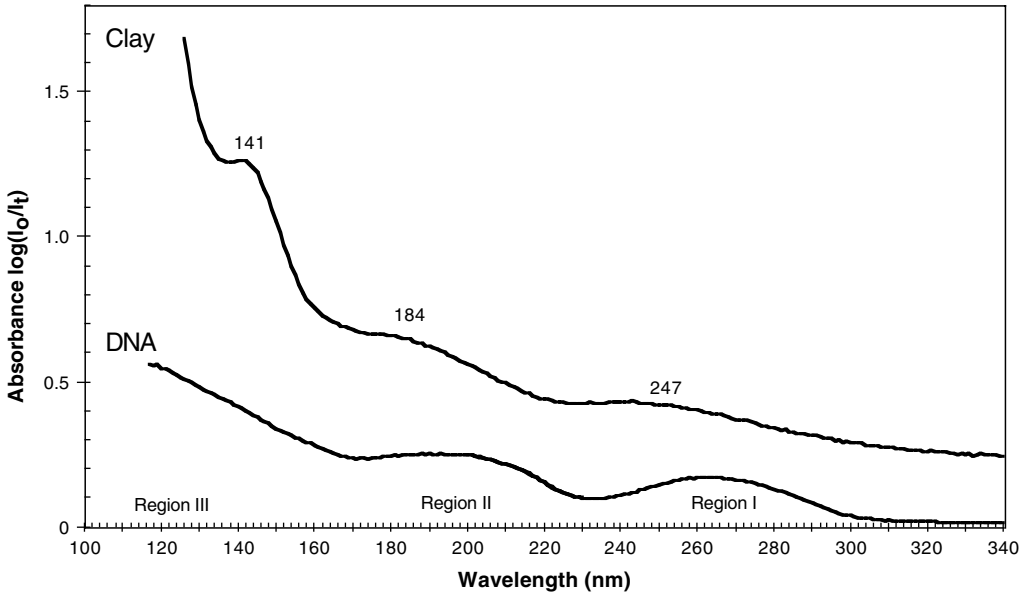

Fig. 8. VUV–UV absorption by montmorillonite clay, with dry DNA as a reference.

pertinence of altered GC content could be assessed using a gene encoding a genetic marker, such as an antibiotic resistance, that has been altered to contain more GC base pairs, while encoding the same protein. The biological robustness of this altered sequence could be tested by exposing the gene to UV radiation *in vitro* (with and without UV screens), then testing its integrity *in vivo*, by introducing it into bacteria challenged by the antibiotic. It should thus be possible to experimentally evaluate the adaptive significance of changes in the absorption spectrum of a target nucleic acid.

In addition to the above spectroscopic properties, chemical, thermodynamic and conformational attributes could be influenced by overall base composition or interactions between neighbouring bases (DNA sequence). Hydrodynamic (e.g. viscosity) and visible light-scattering properties of DNA probably depend more on gross polynucleotide structure and molecular weight, than on base composition or sequence. These characteristics could nevertheless influence genome survival, and they should be taken into account in studies of DNA stability using synthetic DNA.

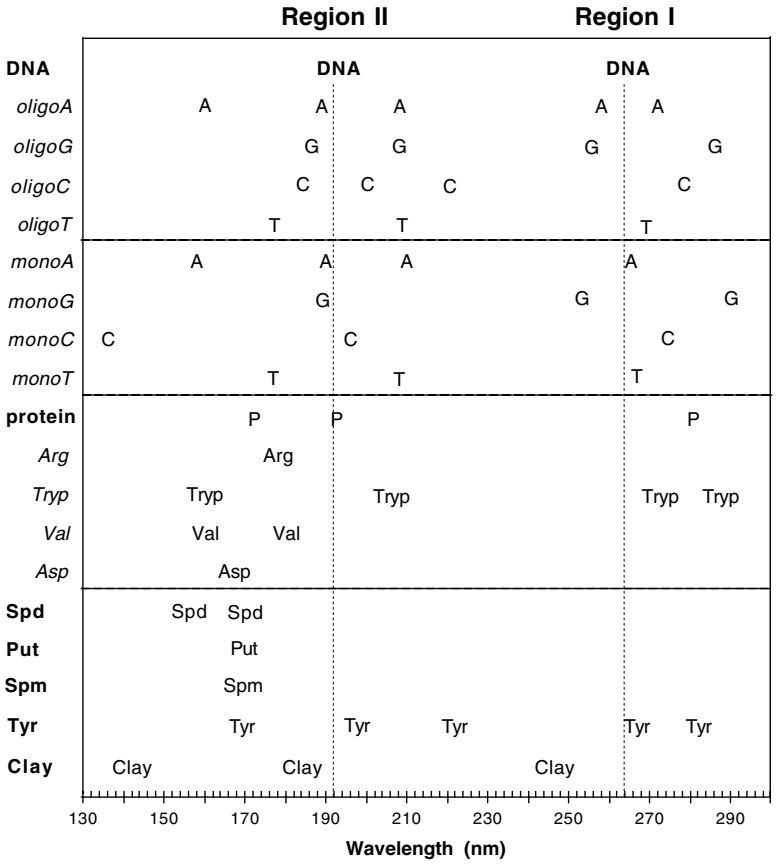

Fig. 9. A summary of results from Figs 2–8, giving the location of the major peaks for each substance analysed.

Table 2. *Comparison of the relative absorption of DNA films at selected wavelengths, relative to the 260 nm absorption peak*

DNA source (and reference)	Absorption at selected wavelengths			
	260 nm	190 nm	160 nm	150 nm
Salmon sperm DNA (present paper)	1	1.48	1.62	1.98
Calf thymus DNA (a)	1	1.47	1.52	1.91
Unspecified DNA (b)	1	1.86	1.98	2.18
Calf thymus DNA (c)	1	1.23	1.18	1.36

(a) Sontag & Weibezahn (1975); (b) Ito & Ito (1986); (c) Inagaki *et al.* (1974).

ATP as a UV screen

A simple life form could consist of DNA and molecules it encodes, which would replicate the DNA and protect it from UV radiation. The simplest UV screen for DNA would thus be nucleotide monomers, an RNA or a protein that has the same absorption spectrum as DNA. An overview of the absorption curves (Fig. 9) suggests that dry salmon sperm DNA is best protected by nucleic acids and their components, while free amines, histone protein and selected amino acids are less attractive UV screens.

Among the DNA components, the absorption spectrum of adenine mononucleotide best matches that of DNA, with absorption peaks corresponding closely to those of DNA (Fig. 4; see also Fig. 9). Adenine mononucleotide is the DNA form of ATP, which is the primary energy currency in contemporary cells. The two forms have identical spectra (unpublished results). The intracellular ATP steady state pool is about 1 mM in mammalian cells (Wang *et al.* 1997), which would provide a 30% attenuation at 260 nm for a tissue thickness of 100 μm. UV protection would be further increased in thicker tissues or if cells are adapted to accumulating higher ATP concentrations. Organisms living before the formation of our oxygen-rich atmosphere were likely exposed to high UVC and VUV, and they could have used adenine mononucleotide or ATP as an element of their UV resistance phenotype. In primitive cells, this attribute might have preceded the use of ATP in energy transfer. Thus, an answer to the question of why ATP is the energy currency of the cell might be that it was essential to accumulate high concentrations of ATP to protect the genome against UV light.

Proteins and amino acids as UV screens

DNA protection by proteins is less obvious, because DNA has an absorption peak at around 260 nm and protein has a peak around 280 nm (Fig. 5; see also Fig. 9). They both absorb around 200 nm (region II), and continue absorbing

through the VUV, but there is no obvious way for a protein to efficiently protect DNA at 260 nm (region I), unless the concentration of the screen is so high that the target is protected even at absorption minima. We assume that such a non-specific, generalized opacity to UV radiation would be less efficient than that afforded by a well-matched UV screen, such as ATP.

An examination of four amino acids, representative of the 20 that make up proteins, showed that protection of region I in DNA could be produced by the aromatic amino acid, tryptophan (region I at 272–287 nm), which carries a ring system that is rich in π electrons and reminiscent of the double ring structure found in the purines. We conclude that a DNA sequence with high GC content (which would shift region I to higher wavelengths), encoding a protein carrying aromatic amino acids, such as tryptophan, would be protected for both regions I and II. This hypothesis can be tested experimentally, by designing and expressing such a protein. Similar protein engineering might be used to improve UV protection *in vivo* in exoenvironments. For instance, storage proteins in seeds might be altered to better serve as UV screens. Proteins rich in aromatic amino acids are found in the *Bacillus subtilis* spore coat, where they are thought to play a part in UV resistance (Driks 1999; Riesenman & Nicholson 2000).

Polyamines and tyramine as UV screens

Aside from nucleic acid and protein precursors, organisms produce a variety of small metabolites through enzymatic pathways encoded in multiple genes. As the genes and regulatory systems responsible for these pathways are becoming known, they are recognized as candidates for metabolic engineering. Small metabolites constitute possible UV screening material that could diffuse within the cell and be transported across membranes.

The polyamines are an example of small diffusable molecules known to stabilize DNA and for which the molecular genetics are known, but according to their absorption spectra, they would protect regions II and III, but not region I (Figs 6 and 8). However, the aromatic amine, tyramine, carries a benzene ring, and given its UV absorption spectrum, should protect both DNA regions I and II. Tyramine is positively charged at physiological pH, so it will bind electrostatically to DNA. In plants, tyramine conjugation to hydroxycinnamic acids, which also carry a benzene ring, is induced by UV light, and hydroxycinnamic acids conjugate with polyamines, possibly improving their DNA protective capacities. Caffeic, ferulic and t-cinnamic acid have a peak around 290 nm (our unpublished results), but this could change after conjugation. Engineering of these biosynthesis pathways is possible, and as regulatory circuits are discovered that control batteries of genes, these pathways should become easier to manipulate.

Small molecules, including secondary metabolites, such as polyphenols (see the accompanying paper (Zalar *et al.* 2007)), could thus act as UV screens. Some of them, such as the polyamines, have DNA binding and DNA protecting properties. In contemporary organisms, the biosynthesis of such metabolites requires complex enzymatic reactions, but similar compounds might have been present in the prebiotic environment (Bernstein 2006). Any UV screen that also binds DNA carries the risk that the absorbed energy is transferred to the DNA, causing photosensitization rather than protection. The need to have spatial distance between the screen and the target DNA could have contributed to the evolution of cells surrounded by phospholipid bilayers, and eventually to the formation of cell walls and spore or seed coats.

The binding and UV protective characteristics of small molecules can be tested experimentally *in vitro* (e.g. using synthetic DNA sequences) and *in vivo* (e.g. by manipulating enzymatic pathways through metabolic engineering). It should thus be possible to test the predictive validity of our assumption that an ideal UV screen would have an absorption pattern similar to that of the target. Genetic engineering can also direct enzymes into selected cellular compartments or into specific tissues. For instance, a seed storage protein could be made richer in tryptophan, and the resistance of the resulting seeds assessed under space conditions.

Astrobiological considerations

The theory that life is universal (panspermia) was restated by Arrhenius at the beginning of the last century. It has since been championed by (among others) Wickramasinghe and Hoyle (Hoyle & Wickramasinghe 1986; Wickramasinghe & Wickramasinghe 2003; Wickramasinghe 2004) and by Crick and Orgel (Crick & Orgel 1973; Crick 1981). The former thought of life as intrinsic to matter and carried by comets; the latter proposed that extra-Solar System intelligences intentionally disseminated life through the universe (directed panspermia).

In exploring the Solar System and beyond, man is clearly engaged in Crick and Orgel's directed panspermia. To consciously direct it, we will need to adapt life to survival in space. The UV absorption spectra presented here suggest that DNA sequences could be altered to adapt the genome's absorption spectrum to a given UV environment or to given UV screens. UV screen synthesis could be encoded in the DNA as proteins or as enzymes that produce small molecules derived from metabolic processes. Our survey of some obvious candidates singled out adenine mononucleotide as a promising small molecule. It is theoretically possible to design a simple organism starting with the DNA sequence. Features, such as UV screens, could be built in that would make for enhanced survival in space. Similar genetic methods could be used to improve existing organisms for space travel and for possible loss of atmospheric UV protection on Earth.

Methods

Absorption spectra

Absorption spectra were recorded at the UV1 beamline at the synchrotron radiation source ASTRID (Institute for Storage Ring Facilities, University of Aarhus in Denmark). Monochromatized light was passed from the beamline

through a LiF window into a vacuum chamber capable of containing up to four MgF_2 discs. The light exited the chamber via a MgF_2 window and was detected with a UV–VUV sensitive photomultiplier tube (PMT). The discs could be placed in the beam one at a time, and the transmitted light was measured from 125 to 340 nm in 1 nm steps. Typically, three discs with dried samples were placed in the chamber and a fourth disc was kept blank. More details of how to avoid absorption of VUV light in the gap between the exit window and the PMT, and on how to avoid higher-order radiation contaminating the spectrum are described elsewhere (Eden *et al*. 2006).

Spectra are based on transmission measurements. They have scattering components in addition to absorption. Scattering due to imperfections in the MgF_2 windows was removed by computing the ratio between the transmission of the window plus the sample and that of the blank window. Absorption was thus determined as $A = \log(I_0/I_t)$ where I_0 and I_t are the measured intensity of transmitted light through the blank disc and the sample disc, respectively. Scattering was assumed to be similar for each sample, based on the reproducibility of selected spectra. In published spectra (125–400 nm) of thin films of the five nucleobases (Yamada & Fukutome 1968), scattering was estimated to be 10–30 % of the optical density at the shortest wavelengths.

Preparation of samples

Samples were air-dried onto MgF_2 windows (diameter, 23 mm). Spectroscopy using dry samples under vacuum avoided solvent absorbance, which is usually observed in absorption measurements below 200 nm (Foldvari *et al*. 1981), and approximated conditions expected in dormant spores or seeds. Sterile, ultrapure water ($R > 10$ MΩ Cm) was made with the Milli-Q apparatus (Millipore).

Salmon sperm DNA (Sigma-Aldrich, France) was extracted twice with a mixture of phenol (saturated with H_2O) and chloroform in a 1:1 ratio, in order to remove proteins. After centrifugation, the aqueous phase was extracted three times with chloroform to remove phenol, then precipitated with two volumes of ethanol in the presence of ammonium acetate. The DNA was spooled and washed with ethanol (70 %) to remove salts and the remaining traces of organic solvents. The DNA was dried and resuspended in H_2O. To facilitate pipetting, viscosity was reduced by passage through a 22-gauge needle.

Oligonucleotides (Genosys-Sigma, France) of adenine (oligoA), thymine (oligoT) and cytosine (oligoC) were purchased in the dry state as 20-mers. Oligonucleotide solutions were prepared in H_2O (pH 7.5). 200 µl of oligoA/T/G/C (100 µM each) were air-dried on MgF_2 windows. About 0.1 mg (dry weight) of each sample was deposited on each MgF_2 window.

Monomer nucleotides (monoA/T/G/C) in the form of deoxyribonucleoside triphosphates (Promega, France) were prepared as 1 mM solutions in water (pH 7.5). 750 µl of dATP and dGTP and 500 µl of dTTP and dCTP were dried onto MgF_2 windows, giving films consisting of 0.45 mg of dATP and dGTP and 0.3 mg of dTTP and dCTP.

Samples of unfractioned whole histone from calf thymus, type II-A (Sigma-Aldrich, France), were prepared in water (pH 7.5). 500 µl samples at 0.3 and 1 mg ml^{-1} were air-dried on MgF_2 windows. The dry histone samples consisted of 0.15 and 0.5 mg (high histone concentration) per MgF_2 window.

L-Arginine (Arg), L-Aspartic acid (Asp), L-Valine (Val) and L-Tryptophan (Trp) (Sigma-Aldrich, France) were dissolved in water (pH 7.5). Samples, consisting of 400 µl of Arg (2 mg ml^{-1}), 500 µl of Asp (2 mg ml^{-1}), 1 ml of Val (2.6 mg ml^{-1}) and 400 µl of Trp (0.5 mg ml^{-1}) were air-dried on MgF_2 windows. The final mass per MgF_2 window was 0.8 mg of Arg, 1 mg of Asp, 2.6 mg of Val and 0.2 mg of Trp.

Spermine (Sigma-Aldrich, France), spermidine (Sigma-Aldrich, France) and putrescine (Fluka, France), were freshly prepared in water (pH 7.5). The solutions of 1 ml of spermine (1.1 mg ml^{-1}), 500 µl of spermidine (3 mg ml^{-1}) and 500 µl of putrescine (15 mg ml^{-1}) were air-dried, so that final quantities were 1.1, 1.5 and 7.5 mg per MgF_2 window, respectively. Tyramine (Sigma-Aldrich, France) was prepared as 0.3 mg ml^{-1} solution in 100 % methanol, and 500 µl of this solution was dried on the MgF_2 window. The solid film contained 0.15 mg of tyramine per MgF_2 window.

The clay mineral (Na-montmorillonite/SWy-1, from Crook Country, Wyoming, USA, from the clay minerals repository, University of Missouri, Columbia, USA) was kindly provided by R. Prost. Clay particles were suspended in water, followed by centrifugation at 3000G for 5 min, which caused visible layering. The upper band of particles in the pellet was removed with a spatula and the process was repeated five times. A 500 µl sample (0.5 mg ml^{-1}) of Na-montmorillonite/SWy-1 was air-dried on a MgF_2 window.

Acknowledgements

Financial support was provided by the Centre National d'Etudes Spatiales and the University of Aarhus (EC Integrated Activity on Synchrotron and Free Electron Laser Science, contract number R113-CT-2004-50608). R. Prost generously provided the clay sample.

References

An, L.Z., Liu, G.X., Zhang, M.X., Chen, T., Liu, Y.H., Feng, H.Y., Xu, S.J., Qiang, W.Y. & Wang, X.L. (2004). *Russian J. Plant Physiol*. **51**, 658–652.

Apelbaum, A., Canellakis, Z.N., Applewhite, P.B., Kaur-Sawhney, R. & Galston, A.W. (1988). *Plant Physiol*. **88**, 996–998.

Basu, H.S., Schwietert, H.C., Feuerstein, B.G. & Marton, L.J. (1990). *Biochemical J*. **269**, 329–334.

Beigbeder, A., Vavadakis, M., Navakoudis, E. & Kotzabasis, K. (1995). *J. Photochem. Photobiol. B: Biol*. **28**, 235–242.

Bernal, J.D. (1951). *The Physical Basis of Life*, p. 80. Routledge and Kegan Paul, London.

Bernstein, M. (2006). *Phil. Trans. R. Soc. London B: Biol. Sci*. **361**, 1689–1702.

Campos, J.L., Figueras, X., Boronat, A., Pinot, M.T. & Tiburcio, A.F. (1991). *Lecture Course on Polyamines as Regulators of Plant*

Development, eds Galston, G.W. & Tiburcio, C.F., pp. 78–80. Fundation Juan March.
Chargaff, E., Lipshitz, R., Green, C. & Hodes, M.E. (1951). *J. Biol. Chem.* **192**, 223–230.
Ciaravella, A., Scappini, F., Franchi, M., Cecchi-Pestellini, C., Barbera, M., Candia, R., Gallori, E. & Micela, G. (2004). *Int. J. Astrobiol.* **3**, 31–35.
Crick, F. (1981). *Life Itself*. Simon and Schuster, New York.
Crick, F.H.C. & Orgel, L.E. (1973). *Icarus* **19**, 341–346.
Demaneche, S., Bertolla, F., Buret, F., Nalin, R., Sailland, A., Auriol, P., Vogel, T.M. & Simonet, P. (2001). *Appl. Environ. Microbiol.* **67**, 3440–3444.
Driks, A. (1999). *Microbiol. Mol. Biol. Rev.* **63**, 1–20.
Eden, S., Limão-Vieira, P., Hoffmann, S.V. & Mason, N.J. (2006). *Chem. Phys.* **323**, 313–333.
Falk, M. (1964). *J. Amer. Chem. Soc.* **86**, 1226–1228.
Falk, M., Hartman, K.A. & Lord, R.C. (1963). *J. Amer. Chem. Soc.* **85**, 391–394.
Ferris, J.P., Hill, A.R. Jr., Liu, R. & Orgel, L.E. (1996). *Nature* **381**, 59–61.
Flink, I. & Pettijohn, D.E. (1975). *Nature* **253**, 62–63.
Foldvari, I., Fekete, A. & Corradi, G. (1981). *J. Biochem. Biophys. Meth.* **5**, 319–327.
Gallori, E., Bazzicalupo, M., Dal Canto, L., Fani, R., Nannipieri, P., Vettori, C. & Stotzky, G. (1994). *FEMS Microbiol. Ecol.* **15**, 119–126.
Galtier, N. & Lobry, J.R. (1997). *J. Mol. Evolution* **44**, 632–636.
Hoyle, F. & Wickramasinghe, N.C. (1986). *Nature* **322**, 509–511.
Inagaki, T., Hamm, R., Arakawa, E. & Painter, L. (1974). *J. Chem. Phys.* **61**, 4246–4250.
Isaacson, M. (1972). *J. Chem. Phys.* **56**, 1803–1812.
Ito, A. & Ito, T. (1986). *Photochem. Photobiol.* **44**, 355–358.
Leach, S., Smith, I.W. & Cockell, C.S. (2006). *Phil. Trans. R. Soc. London B* **361**, 1675–1679.
Lewis, D.G. & Johnson, W.C. Jr. (1974). *J. Mol. Biol.* **86**, 91–96.
Lorenz, M.G. & Wackernagel, W. (1994). *Microbiol. Rev.* **58**, 563–602.
Marmur, J. & Doty, P. (1962). *J. Mol. Biol.* **5**, 109–118.
Martin-Tanguy, J. (1985). *Plant Growth Regulation* **3**, 381–399.
Martin-Tanguy, J. (1997). *Physiologia Plantarum* **100**, 675–688.
Martin-Tanguy, J. (2001). *Plant Growth Regulation* **34**, 135–148.
Martin-Tanguy, J., Tepfer, D. & Burtin, D. (1991). *Plant Sci.* **80**, 131–144.
Martin-Tanguy, J., Tepfer, D., Paynot, M., Burtin, D., Heisler, L. & Martin, C. (1990). *Plant Physiol.* **92**, 912–918.
Paget, E., Jocteur-Monrozier, L. & Simonet, P. (1992). *FEMS Microbiol. Lett.* **97**, 31–39.
Pohjanpelto, P. & Holtta, E. (1996). *The EMBO Journal* **15**, 1193–1200.
Riesenman, P.J. & Nicholson, W.L. (2000). *Appl. Environ. Microbiol.* **66**, 620–626.
Rode, B.M. (1999). *Peptides* **20**, 773–786.
Romanowski, G., Lorenz, M.G. & Wackernagel, W. (1991). *Appl. Environ. Microbiol.* **57**, 1057–1061.
Scappini, F., Casadei, F., Zamboni, R., Franchi, M., Gallori, E. & Monti, S. (2004). *Int. J. Astrobiol.* **3**, 17–19.
Schuber, F., Hong, K., Duzgunes, N. & Papahadjopoulos, D. (1983). *Biochemistry* **22**, 6134–6140.
Sontag, W. & Weibezahn, K.F. (1975). *Radiation Environ. Biophys.* **12**, 169–174.
Tassoni, A., Antognoni, F. & Bagni, N. (1996). *Plant Physiol.* **110**, 817–824.
Tepfer, D. & Leach, S. (2006). *Astrophys. Space Sci.* **306**, 69–75.
Tepfer, D. & Martin-Tanguy, J. (1991). *Rice Biotech. Quart.* **6**, 43–44.
Voet, D., Gratzer, W.B., Cox, R.A. & Doty, P. (1963). *Biopolymers* **1**, 193–208.
Wang, R.H., Tao, L., Trumbore, M.W. & Berger, S.L. (1997). *J. Biol. Chem.* **272**, 26 405–26 412.
Wickramasinghe, C. (2004). *Cryobiology* **48**, 113–125.
Wickramasinghe, N.C. & Wickramasinghe, J.T. (2003). *Astrophys. Space Sci.* **286**, 453–459.
Yamada, T. & Fukutome, H. (1968). *Biopolymers* **6**, 43–54.
Zahradka, K., Slade, D., Bailone, A., Sommer, S., Averbeck, D., Petranovic, M., Lindner, A.B. & Radman, M. (2006). *Nature* **443**, 569–573.
Zalar, A., Tepfer, D., Hoffmann, S. V., Kollmann, A. & Leach, S. (2007). *Int. J. Astrobiol.*, in press.

Article 2

Zalar A, Tepfer D, Hoffmann S V, Kollmann A and Leach S (2007b) Directed exospermia: II. VUV-UV spectroscopy of specialized UV screens, including plant flavonoids, suggests using metabolic engineering to improve survival in space. *International Journal of Astrobiology*, 6(4): 291-301

International Journal of Astrobiology, Page 1 of 11 Printed in the United Kingdom
doi:10.1017/S1473550407003849

Directed exospermia: II. VUV-UV spectroscopy of specialized UV screens, including plant flavonoids, suggests using metabolic engineering to improve survival in space

Andreja Zalar[1], David Tepfer[1], Søren V. Hoffmann[2], Albert Kollmann[1] and Sydney Leach[3]

[1]*Institut National de la Recherche Agronomique, Versailles 78026, France*
e-mail:tepfer@versailles.inra.fr
[2]*Institute for Storage Ring Facilities, University of Aarhus, Aarhus 8000, Denmark*
[3]*LERMA, UMR 8112-CNRS, Observatoire de Paris-Meudon, 92195 Meudon, France*

Abstract: We used synchrotron light to determine VUV-UV absorption spectra (125–340 nm) of thin films of substances associated with UV resistance in specific groups of organisms or across limited phylogenetic boundaries: scytonemin, mycosporine-like amino acids, dipicolinic acid, β-carotene, melanin and flavonoids (quercitrin, isoquercitrin, robinin and catechin). The objective was to extend known UV absorption spectra into the vacuum UV, and to evaluate the likely effectiveness of these molecules in shielding DNA from the unfiltered solar UV found in space, using similarity with DNA absorption spectra as the primary criterion. The spectroscopy indicated that plant flavonoids would be ideal UV screens in space. We suggest that flavonoids represent primitive UV screens, and offer explanations (including horizontal gene transfer) for their presence in plants. We also discuss the possibility of improving UV resistance by increasing flavonoid accumulation through metabolic engineering, in the hope of better adapting life for space travel, i.e. for its dissemination away from the Earth (exospermia). Finally, we propose using plant seeds as exospermia vehicles for sending life (including artificial life) into space.

Received 15 February 2007, accepted 18 May 2007

Key words: β-carotene, dipicolinic acid, flavonoids, melanin, mycosporine-like amino acids, panspermia, scytonemin, seed, UV resistance, VUV-UV absorption spectroscopy.

Introduction

The spectrum of solar UV emission is generally divided into the UVA (315–400 nm), the UVB (280–315 nm), the UVC (200–280 nm) and the VUV (<200 nm). Biological energy on today's Earth is mostly derived from photosynthesis. Currently, ozone blocks UV light below 300 nm but, in the distant past, primitive photosynthetic organisms probably had to cope with more energetic wavelengths in order to benefit from the light required to fix atmospheric carbon compounds. Since contemporary bacterial spores are killed after a short exposure to unfiltered solar UV in space (Horneck *et al*. 2001), we need to explain how organisms adapted to UV liability on primitive Earth, in the absence of atmospheric oxygen and ozone.

Possibilities include a protective organic haze (Westall *et al*. 2006), displacement within microbial mats (Bebout & Garcia-Pichel 1995) and accumulation of UV screens, e.g. scytonemin in cyanobacteria (Garcia-Pichel *et al*. 1992), that protect throughout the UV, but do not interfere with photosynthesis. Biological molecules of all sorts absorb UV light. They are thus potential UV screens, as well as targets for photodestruction. In the accompanying paper (Zalar *et al*. 2007), we used synchrotron light to examine UV absorption between 125 and 340 nm for a few of the potential UV screens that are ubiquitous in the cells of all organisms. DNA was considered to be the principal target. In this paper we apply the same approach to known UV screens from a variety of organisms.

DNA absorbs in three regions: I (with a peak at 260–264 nm), II (with a peak at 192 nm) and III (below 125 nm). Dehydration shifts the peak in region I to longer wavelengths (from 260 to 264 nm), and this peak could also shift to longer wavelengths with increased frequency of the guanine–cytosine (GC) base pair, which is also considered to be more stable than the adenine–thymine (AT) base pair (see the accompanying paper). Solar emission declines to essentially zero at 125 nm; thus absorption peaks

corresponding to regions I and II would be the major source of UV liability.

We present here thin-film VUV-UV absorption spectra for known UV screens: scytonemin, mycosporin-like amino acids, dipicolinic acid, β-carotene, melanin and flavonoids (quercitrin, isoquercitrin, robinin and catechin). They are evaluated according to the degree of spectral similarity between the screen and the target DNA. The results are discussed with reference to the origin and evolution of life and the possibility of dispersal of life via directed exospermia.

Methods

The flavonoids analysed in this study were: quercitrin (quercitin-3-*O*-rhamnoside), isoquercitrin (quercetin-3-β-D-glucoside), robinin (kaempferol-3-*O*-robinoside-7-*O*-rhamnoside) and (+)-catechin (+)-3,3′,4′,5,7-pentahydroxyflavan). Standard solutions (3 mg ml^{-1}) of quercitrin (Sigma-Aldrich, France), isoquercitrin (Fluka, France) and catechin (Extrasynthese, France) were prepared in 100% (v/v) methanol, while robinin (Extrasynthese, France) was prepared as an aqueous solution (1 mg ml^{-1}). Dipicolinic acid (DPA, 2,6-pyridinedicarboxylic acid) was purchased from Sigma-Aldrich, France. A standard solution (4 mg ml^{-1}) of DPA was prepared in 100% (v/v) methanol. The calcium chelate of DPA (Ca-DPA) was made by mixing (1:1) equimolar volumes of the DPA standard solution and aqueous solution of $CaCl_2$ (2.4×10^{-2} M). Melanin (Sigma-Aldrich, France) was purchased as synthetic melanin, made by the oxidation of tyrosine with hydrogen peroxide. A standard solution (1 mg ml^{-1}) of melanin was prepared in 1 N NH_4OH. A standard solution (1 mg ml^{-1}) of β-carotene (Extrasynthese, France) was prepared in 100% ethyl acetate and stored at −20 °C, protected from light. Chlorophyll *a* and *b* (from spinach) were purchased from Fluca (France). Stock solutions (0.5 mg ml^{-1}) were prepared in absolute ethanol.

Scytonemin was extracted from UVA induced cells of the cyanobacterium, *Chroococcidiopsis* CCMEE 5056, kindly provided by R. Castenholtz. The UV induced and control (non-induced) cells of *Chroococcidiopsis* were collected by centrifugation and pellets were kept frozen in the dark. Thawed cells were oven dried at 50 °C for 1 h, then homogenized in 3 ml acetone (100% v/v) by sonication (VibraCell, Sonics & Materials, Danbury CT), while cooling on ice and protected from light. The resulting suspension was kept at 4 °C for 20 h in the dark. The extracts were centrifuged and about 3 ml of yellow supernatant, containing scytonemin, were collected and stored at −20 °C. The scytonemin was further purified by high-performance liquid chromatography (HPLC). The acetone from the crude extracts was removed by evaporation under a stream of nitrogen and dry residues were dissolved in 100% (v/v) acetonitrile. The separation of the compounds by HPLC was performed on a Waters 600 multisolvent delivery system, using a Kromasil C18 column (250×4.6 mm^2 i.d., 5 μm particle size, Alltech, France). The mobile phase comprised the mixture of solvent A (pure water) and solvent B (acetonitrile: methanol: tetrahydrofuran, 75:15:10, v/v/v) at a flow rate of 1 ml ml^{-1} and a linear gradient of solvents A:B (70:30, v/v) from 0 to 10 min, changing to 0:100 (v/v) after 20 min and ending with the initial conditions A:B (70:30 v/v) for 10 min. The chromatographic and spectral data were acquired with a Waters 990 photodiode array detector set at 388 nm and HPLC fractions were collected.

The scytonemin fraction was identified by its characteristic UV absorption spectrum (Proteau *et al.* 1993; Sinha & Hader 2002). Purified scytonemin was dried under a stream of nitrogen, quantified and dissolved in 100% (v/v) ethyl acetate, yielding 0.5 mg ml^{-1}. The presence of scytonemin in the prepared sample and its purity were further confirmed by mass spectrometry (see below).

Liquid chromatography–mass spectroscopy (LC-MS) was performed using an Alliance 2695 (Waters, USA) reverse phase HPLC system coupled to a Quattro LC mass spectrometer (MicroMassCo, Manchester, UK) with an electrospray ionization interface. Data acquisition and analyses were performed by MassLynx software. Chromatography was carried out on a C18 Uptisphere column (150×2 mm^2, i.d., 5 μm particle size; Interchrom, France), connected to a Waters 2487 UV detector set at 252 nm and 386 nm. The mobile phase, at a flow rate of 0.15 ml min^{-1}, contained the mixture of two solvents, acetonitrile and water, both acidified with 0.5% (v/v) acetic acid. The gradient profile comprised initial conditions (acetonitrile:water, 2:98 v/v) for 5 min, linear gradient up to 100:0 v/v acetonitrile:water for 25 min and a rinsing step (acetonitrile:water, 100:0 v/v) for 10 min. Prior the LC-MS analysis, the solvent ethyl acetate was removed from the scytonemin sample by evaporation under a stream of nitrogen and replaced by acetonitrile, as a more suitable solvent for liquid chromatography. The 5 μl aliquot of the 10 times diluted scytonemin fraction was injected and data were acquired for both positive and negative ionization modes.

LC-MS results showed that the HPLC fraction of the cyanobacteria extract, further used for absorption analysis, contained high amounts of well-purified scytonemin. Strong signals of $[M+H]^+$ ion at mass-to-change ratio (m/z) 545 in positive mode and $[M+H]^-$ ion at m/z 543 in negative mode were observed, confirming the presence of scytonemin (molecular weight 544). Moreover, the ion at m/z 273 was observed in the positive mode, resulting from the fragmentation of the scytonemin molecule into two symmetric halves. Beside the common form of scytonemin, which was dominant (93%) in the sample, small amounts (7%) of the reduced form were also observed, confirming a previous report (Squier *et al.* 2004). A reduced form of scytonemin was commonly found in the anoxic layers of microbial mats (Garcia-Pichel & Castenholz 1991; Proteau *et al.* 1993).

Two mycosporine-like amino acid samples, MAA-6 and MAA-9, isolated from the marine red algae, *Corallina officinalis*, and prepared in 0.2% (v/v) acetic acid, were kindly provided by the group of D.-P. Häder. Conventional (LC-MS) and tandem mass spectrometry (LC-MS-MS) were performed in order to determine the type of mycosporine-like acid

present in the MAA-6 and MAA-9 samples (Whitehead & Hedges 2003). The LC-MS system is described above.

10 µl aliquots of 10 times diluted MAA-6 and MAA-9 samples were eluted on an Uptisphere C18 column (150×2 mm^2, i.d., 5 µm particle size; Interchrom, France) with a mobile phase that was composed of solvent A (acetonitrile:water, 95:5, v/v, 0.2% acetic acid) and solvent B (water:acetonitrile, 95:5, v/v, 0.2% acetic acid) at a flow rate of 0.15 ml min^{-1}. The gradient profile comprised initial conditions (A:B, 0:100 v/v) for 5 min, linear gradient up to 100:0 v/v, A:B for 50 min and a rinsing step (A:B, 100:0 v/v) for 5 min. Absorption was measured continuously at 290 nm and 259 nm.

Mass spectra showed that the MAA-9 sample contained porphyra-334 (molecular weight 346), forming a $[M+H]^+$ ion at m/z 347 and a $[M+H]^-$ ion at m/z 345 in positive and in negative modes, respectively. Besides porphyra-334, as a major component, small amounts of shinorine (molecular weight 332) and palythinol (molecular weight 302) were detected. Shinorine and palythinol gave the signal only in positive mode, forming $[M+H]^+$ ions at m/z 333 and 303, respectively. Traces of unidentified molecules that gave the $[M+H]^+$ ions at m/z 163, 205, 223, 255 and 279 were also detected, and they were thought to be impurities.

Fraction MAA-6 contained the same impurities found in fraction MAA-9. The MAA palythine (molecular weight 244) that formed a $[M+H]^+$ ion at m/z 245 in positive mode was also detected, but in small amounts in the MAA-6 sample. The presence of porphyra-334 in MAA-9, and palythine in MAA-6 was further confirmed by tandem LC-MS-MS, comparing the characteristic fragmentation patterns with those previously reported (Whitehead & Hedges 2003). Although MAA-6 and MAA-9 contained trace amounts of impurities, their absorption spectra, which were obtained by conventional spectrophotometry in solution (the results are not presented), showed $\lambda_{max} = 320$ nm for MAA-6 and $\lambda_{max} = 334$ nm for MAA-9, which are characteristic absorption maxima for porphyra-334 and palythine, respectively (Takano *et al.* 1978, 1979; Sinha *et al.* 1998).

The VUV-UV absorption spectra, in the 125–340 nm region, were obtained using the UV1 beamline (Eden *et al.* 2006) at the Synchrotron Radiation source ASTRID, Institute for Storage Ring Facilities, University of Aarhus, Denmark. The resulting spectra were based on the measurements of UV light transmitted through the sample, which was dried onto a MgF_2 window (diameter 23 mm). The installation and the measurement technique are described in detail in the accompanying paper (Zalar *et al.* 2007). Recorded spectra were the result of absorption and scattering. For the sake of simplicity and the small contribution of scattering to the optical density, the obtained spectra in this study are called absorption spectra. The scattering problems of dry films are discussed in the accompanying paper. Since most of the samples were prepared in organic solvents that absorb UV light below 200 nm, the absorption spectra were measured in a vacuum, with the samples prepared as thin, solid films.

Dry films of the melanin and flavonoid samples (quercitrin, isoquercitrin, robinin and catechin) were produced by air-drying 500 µl of each diluted standard solution (0.1 mg ml^{-1}) on the surface of a MgF_2 window. Two dilutions of the β-carotene standard solution, 0.5 mg ml^{-1} (high concentration) and 0.125 mg ml^{-1}, were prepared in ethyl acetate, with 300 µl and 250 µl dried on a MgF_2 window, respectively. The solution of Ca-DPA chelate was diluted in 50% (v/v) methanol and 500 µl of a 0.4 mg ml^{-1} solution was air-dried on a MgF_2 window. The MAA-6 and MAA-9 samples, containing mycosporine-like amino acids (MAAs), were prepared in 0.2% acetic acid. 500 µl of each (MAA-6 and MAA-9) were dried on MgF_2 windows. The solid film of scytonemin was prepared by drying 900 µl of the sample solution, which contained purified scytonemin (0.5 mg ml^{-1}), in ethyl acetate, onto MgF_2 windows.

In order to exclude the background absorption by the remaining traces of solvents in the dry samples, 500 µl of water (pH 7), 0.2% (v/v) acetic acid, 1 N NH_4OH, 100% (v/v) methanol, 100% (v/v) ethyl acetate and a solution of $CaCl_2$ (1.2×10^{-2} M) in 50% methanol were dried onto MgF_2 windows and the absorption was measured. No absorption or a weak absorption signal was detected for all tested solvents.

Results

UV absorption by scytonemin and mycosporine-like amino acids

Following exposure to UVA, scytonemin accumulates as a yellow pigment in sheathed cyanobacteria (Garcia-Pichel *et al.* 1992). Scytonemin (see Fig. 1) consists of four benzene rings and four five-member rings (Proteau *et al.* 1993). The published UV absorption spectrum for scytonemin in solution (Proteau *et al.* 1993; Sinha *et al.* 1998) shows peaks at 212, 252, 278, 300 and 386 nm, with the major peaks at 252 and 386 nm. We used HPLC to purify scytonemin from UVA-induced cyanobacteria, kindly provided by R. Castenholtz. Conventional solution UV spectroscopy (not shown) confirmed peaks at 211, 253, 298 and 388 nm, with major peaks at 253 and 388 nm. Our far-UV spectrum of thin films showed peaks at 195 and 253 nm, and below 195 nm, absorbance climbed strongly to 125 nm, the end of the spectrum (Fig. 2).

The MAAs (Fig. 1) are diverse structures that include a six-carbon ring (cyclohexenone or cyclohexenimine), conjugated with the nitrogen of an amino acid or its imino alcohol (Nakamura *et al.* 1982; Sinha *et al.* 1999; Shick & Dunlap 2002). Their absorption maxima range from 310 to 360 nm (Nakamura *et al.* 1982). MAAs accumulate in response to UV exposure in certain cyanobacteria and algae (Garcia-Pichel *et al.* 1993; Sinha & Hader 2002). MAAs have also been found in heterotrophic bacteria, fungi, lichens and in a variety of marine invertebrates and vertebrates (Shick & Dunlap 2002). VUV-UV absorption spectra (Fig. 2) were qualitatively similar for two mycosporine-like amino acids, palithyne (MAA-6) and porphyra-334 (MAA-9), generously provided by the group of D.-P. Häder. MAA-6 showed absorbance at

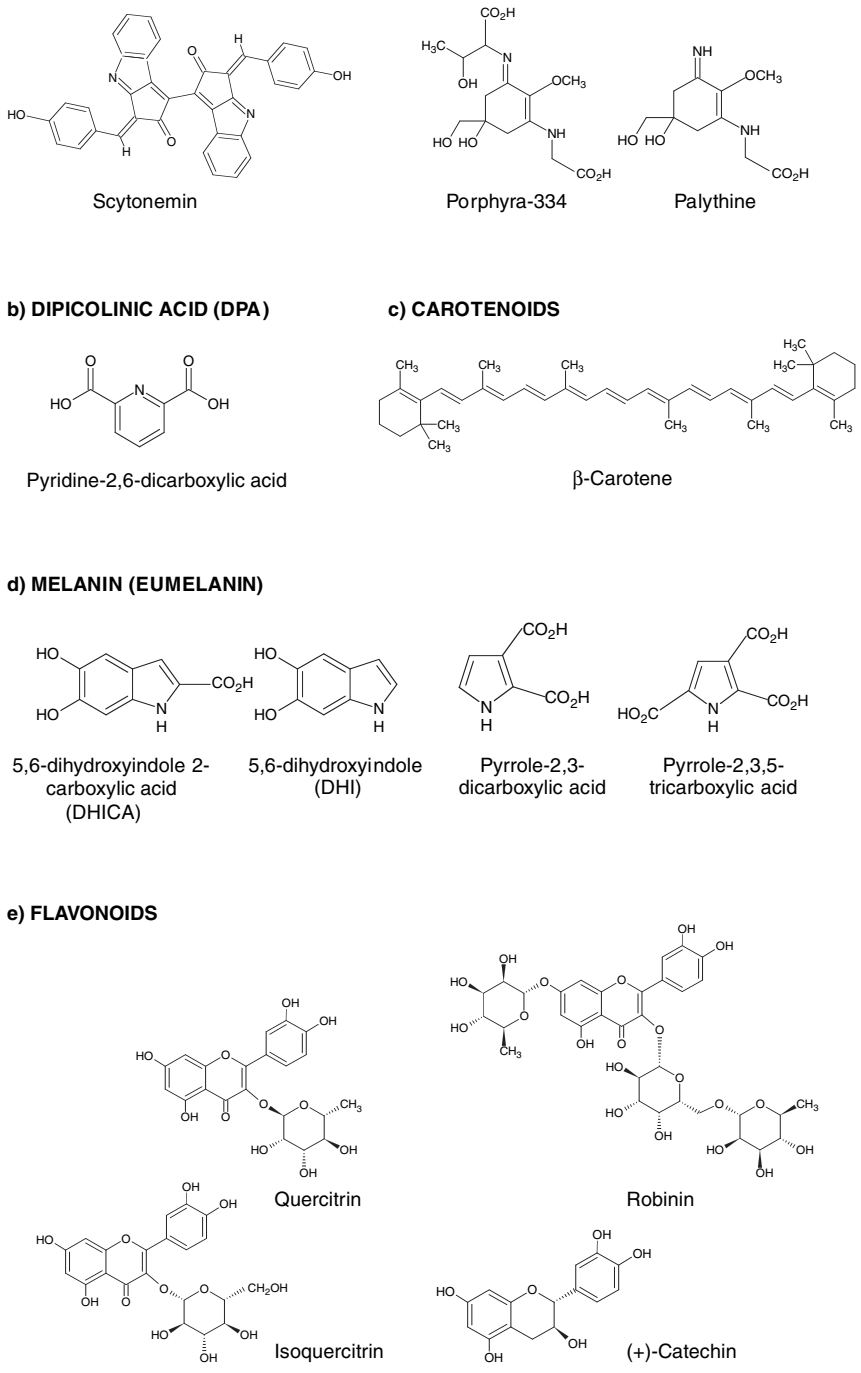

Fig. 1. Chemical structures of the UV screens, used in VUV-UV absorption spectroscopy: (a) scytonemin and MAAs – porphyra-334 and palythine; (b) DPA; (c) β-carotene; (d) subunits of melanin (eumelanin) – 5,6-dihydroxyindole 2-carboxylic acid (DHICA), 5,6-dihydroxyindole (DHI), pyrrole-2,3-dicarboxylic acid and pyrrole-2,3,5-tricarboxylic acid; (e) flavonoids – quercitrin, isoquercitrin, robinin and (+)-catechin.

164 and 195 nm (with a weak peak at 300 nm), while MAA-9 absorbed at 164, 192 and 340 nm. Published solution spectra show strong absorbance in the UVB (Sinha *et al.* 1998).

UV absorption by dipicolinic acid

DPA (2,6-pyridinedicarboxylic acid) is located in the *Bacillus subtilis* spore core as a 1:1 chelate with divalent cations, predominantly Ca^{2+} (Murrell 1967; Setlow *et al.* 2006). It comprises about 10% of the dry weight of the spores (Murrell 1967; Setlow 1994; Paidhungat *et al.* 2001; Slieman & Nicholson 2001). DPA is a substituted six member ring, carrying a single nitrogen in the ring (Setlow *et al.* 2006) (Fig. 1). The calcium chelate (Ca-DPA) was used for spectroscopy. DPA protects spores from wet heat,

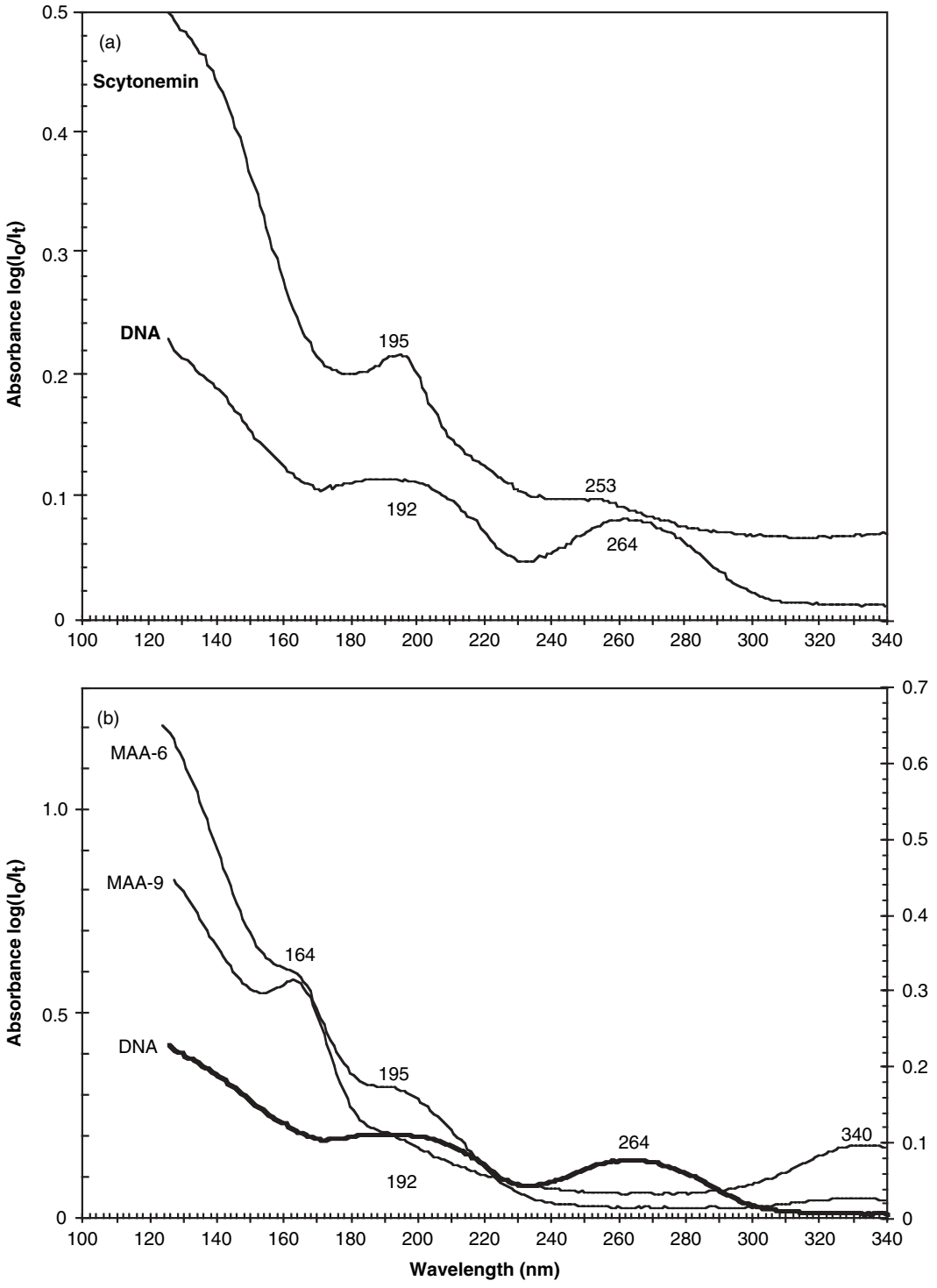

Fig. 2. VUV-UV absorbance spectrum of (a) scytonemin (0.45 mg per sample) and (b) two mycosporine-like amino acids, MAA-6 (containing palythine and impurities – see the Methods section) and MAA-9 (essentially containing porphyra-334). The DNA spectrum is included for reference.

probably by reducing water content (Setlow *et al.* 2006). DPA can act either as a UV protector (Berg & Grecz 1970; Grecz *et al.* 1973; Slieman & Nicholson 2001) or as a UV photosensitizer (Germaine & Murrell 1973; Lindsay & Murrell 1983; Setlow & Setlow 1993), promoting formation of spore photo product in damaged DNA (Douki *et al.* 2005; Setlow *et al.* 2006). We chose DPA (Ca-DPA) for VUV-UV spectroscopic studies, because of the high amounts of Ca-DPA present in the spores, the low content of water in the spore core (25–55%) and the complex role of DPA in the photochemistry of spore DNA (Douki *et al.* 2005).

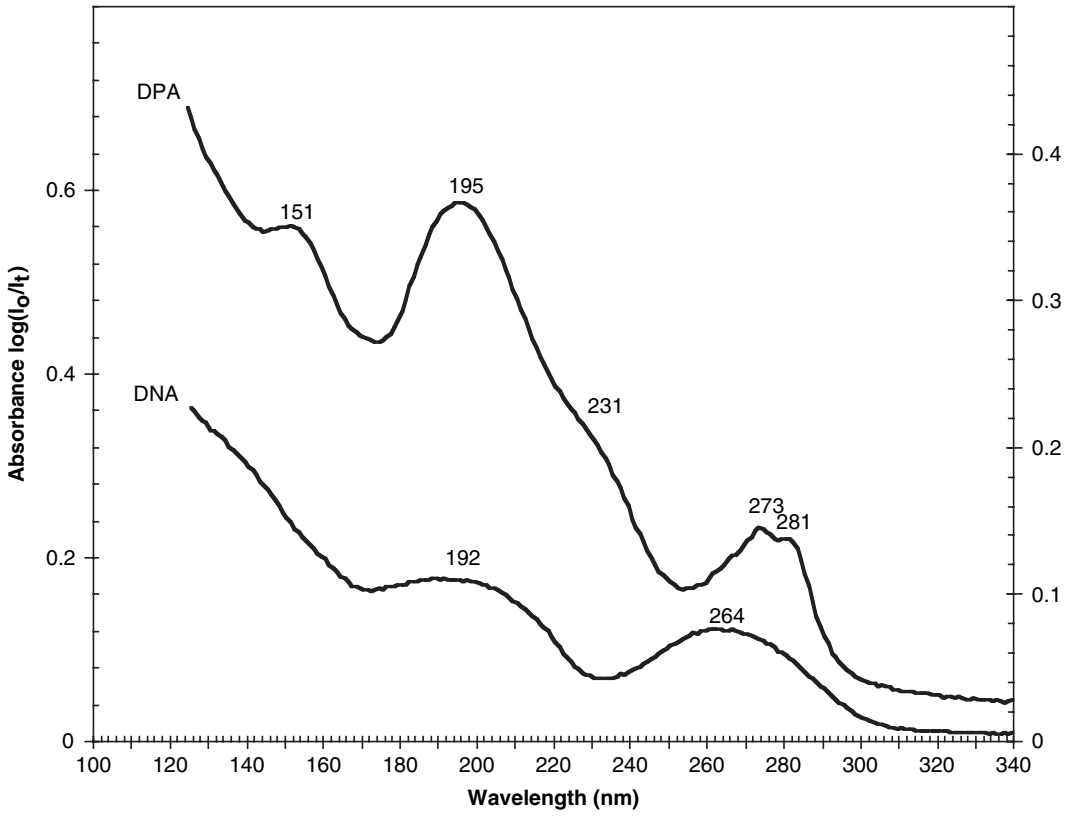

Fig. 3. VUV-UV absorption spectrum of DPA, analysed as a chelate with calcium (Ca-DPA) (0.2 mg per sample). The DNA spectrum is included for reference.

The UV absorbance spectrum of DPA thin films showed peaks at 151, 195, 231, 273 and 281 nm (Fig. 3). It should thus protect DNA in region II, but not in region I, unless region I absorption were shifted to longer wavelengths, e.g. due to a high content of GC, see the accompanying paper (Zalar *et al.* 2007). Additional absorption in the UVB and UVA was not seen, and this was confirmed using conventional solution spectrophotometry (unpublished results).

UV absorption by β-carotene and melanin

Carotenoids are isoprenoid compounds, found in many photosynthetic organisms and in some non-photosynthetic bacteria (Armstrong 1994; Duc le *et al.* 2006). They accumulate following UV stress, and are generally considered to protect against UV by acting as antioxidants. β-carotene consists of two six-carbon rings at opposite ends of a polyene chain (Fig. 1). This structure suggested an appropriate UV screen for DNA in the UVC region. The absorption spectrum showed peaks at 195 and 277 nm (Fig. 4). β-carotene should thus protect DNA region II, but would afford less protection for DNA region I, unless absorption by region I is shifted to higher wavelengths owing to high GC content, see the accompanying paper (Zalar *et al.* 2007).

Melanin pigments are widely distributed in the animal and plant kingdoms, and they are found in some bacteria (Hinojosa-Rebollar *et al.* 1993). Besides photoprotection as their primary biological function, melanins have chemoprotective roles as free radical scavengers and antioxidants (Riley 1997). There are two types of animal melanins, eumelanin (black-brown) and pheomelanin (yellow-reddish). The precise structure of natural melanin is not known, because of its poor solubility and its association with proteins and lipids. Melanin is thus considered to be a highly irregular heteropolymer, containing indoles and other intermediate products derived from the oxidation of tyrosine (Pezzella *et al.* 1997; Riley 1997). It has been suggested that eumelanins form nano-aggregates that contain a mixture of smaller oligomers (Clancy *et al.* 2000), composed of 5,6-dihydroxyindole 2-carboxylic acid (DHICA) and 5,6-dihydroxyindole (DHI) derivatives linked with pyrrole units (Wakamatsu & Ito 2002). The chemical structures of the main building units of melanin are presented in Fig. 1.

Our absorption spectrum (Fig. 4) of a dry film of melanin showed uniform absorption in the studied spectral region, with an exponential increase of absorbance towards lower wavelengths and two small peaks at 161 and 186 nm. Melanin should thus provide non-specific UV protection over a wide range of wavelengths. A characteristic broad band absorption of melanins in the UV and visible part of the spectrum with an exponential increase of absorbance in the UV was previously reported (Meredith & Riesz 2004). The monotonic absorption profile with no specific features can be explained by the complexity of the melanin structure. Rather than a single chromophore, melanins appear to be composed of groups of similar species, giving a smooth, featureless exponential curve (Meredith *et al.* 2006).

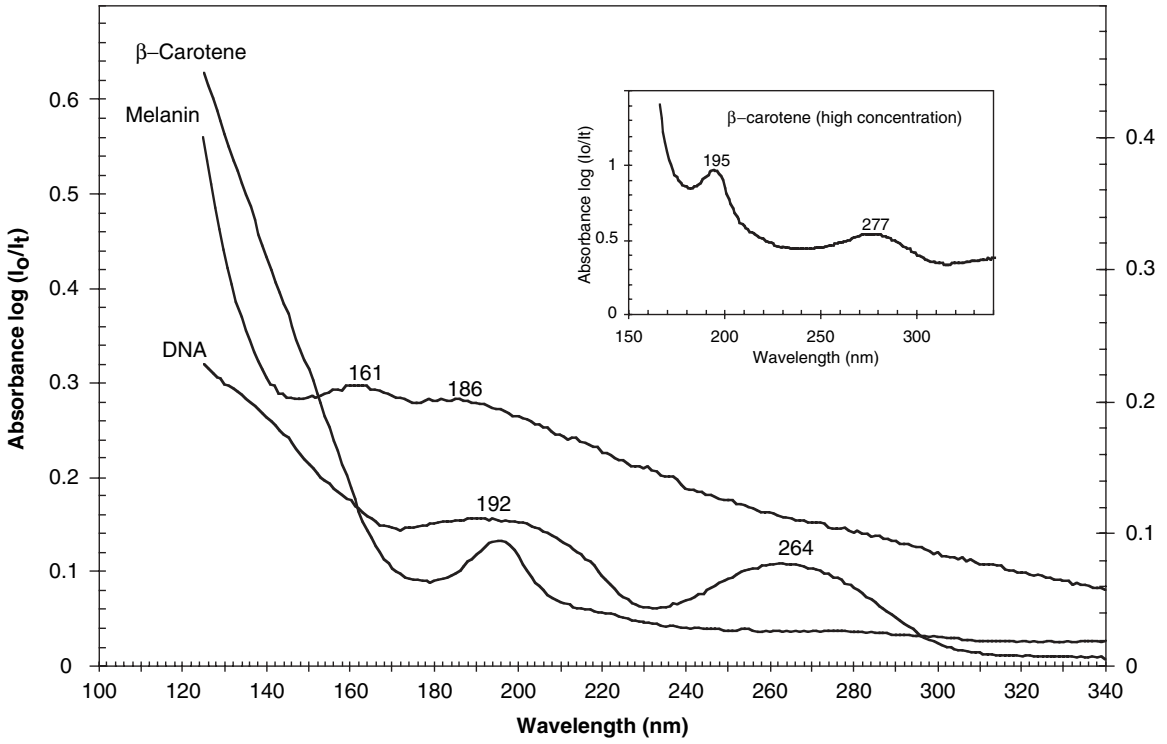

Fig. 4. VUV-UV absorption spectra of β-carotene (0.03 mg per sample) and melanin (0.05 mg per sample). The primary axis gives absorbance for β-carotene and the secondary for melanin and DNA. A spectrum with β-carotene at higher concentration (0.15 mg per sample) is included to show the peak at 277 nm. The DNA spectrum is included for reference.

UV absorption by flavonoids

Flavonoids are produced from phenylalanine through the phenylpropanoid pathway (Dixon *et al*. 1998; Winkel-Shirley 2001). They are representative of the approximately 8000 polyphenols identified in plants. In seeds, flavonoids are concentrated in the seed coat, where they are thought to provide a UV shield. The basic flavonoid structure is two aromatic rings linked through an oxygenated heterocycle (Fig. 1). We determined UV absorption spectra for the major seed flavonoids, including quercitrin, isoquercitrin, robinin and catechin. The first three are conjugated with sugars, and the last is the catechin monomer that is condensed to form tannins. The spectra of catechin, quercitrin and isoquercitrin showed a broad peak at 204 nm, and the corresponding peak in robinin was at 199 nm (Fig. 5). The region I peak was at 258 nm for quercitrin and isoquercitrin, with a shoulder at 270 nm. The robinin region I peak was at 269 nm. Catechin showed a peak at 280 nm, and then absorbance was flat to 340 nm. In contrast, absorbance increased to 340 nm for quercitrin, isoquercitrin and robinin. The presence of a peak at 355 nm was confirmed by conventional solution UV spectroscopy (not shown). The absorption spectrum for condensed tannins, i.e. polymerized catechin (not shown), was similar to that of catechin. Quercitrin (quercetin-3-*O*-rhamnoside) is the dominant flavonoid found in *Arabidopsis* seeds, at a concentration of 3.6 mg g^{-1} of seeds (Routaboul *et al*. 2006). Its UV absorption curve matched that of DNA, and it also absorbed strongly in the UVA and UVB. The combination of these four flavonoids from *Arabidopsis* seeds should provide protection over the entire UV spectrum.

Absorption in the visible region

Absorption in the visible region was measured in solution (data not shown) for all the UV screens studied, and it was compared with chlorophyll *a* and *b* (measured in ethanol), which absorbed strongly at 410 nm and 660 nm (chlorophyll *a*) and 450 nm and 635 nm (chlorophyll *b*). Scytonemin (in ethyl acetate) absorbed at 388 nm, possibly causing interference with the chlorophyll *a* peak at 410 nm. β-carotene in (ethyl acetate) absorbed between 430 and 480 nm, which could partially mask absorption by chlorophyll *a* and strongly mask absorption by chlorophyll *b*. Neither scytonemin nor β-carotene showed possible masking of chlorophyll in the region between 635 nm and 660 nm. The other compounds studied did not absorb in the visible region, and thus should not interfere with photosynthesis.

Discussion

Biological protection by UV screens

We used spectroscopy to evaluate known UV screens, in the hope of learning their possible role in the origin and development of life and finding ways of protecting life during space travel, i.e. during exospermia, the dissemination of life away from Earth. UV screens accumulate in an organism after exposure to UV (Garcia-Pichel *et al*. 1992; Garcia-Pichel

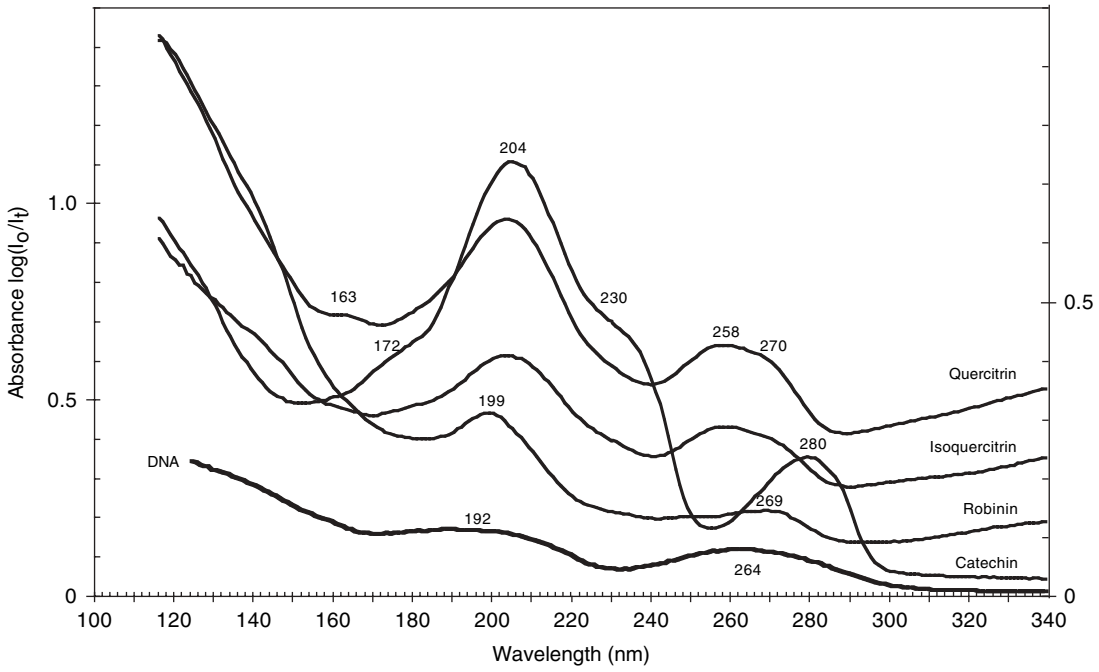

Fig. 5. VUV-UV absorption spectra of the major flavonoids found in the seeds of *Arabidopsis thaliana*: quercitrin, isoquercitrin, robinin and catechin. (All samples were at 0.05 mg per sample.) The DNA spectrum is included for reference.

& Castenholz 1993; Garcia-Pichel *et al.* 1993; Cockell & Knowland 1999; Castenholz & Garcia-Pichel 2000). They absorb UV energy and dissipate it towards relatively insensitive targets. DNA is the prime example of a sensitive target, but other substances vital to life (or that become deleterious after absorbing UV) could also be targets, e.g. proteins and lipids. Free radicals, produced by UV at wavelengths where DNA does not absorb, can later attack DNA. An ideal UV screen would therefore not just protect DNA, but also a variety of substances that absorb at other wavelengths.

Not surprisingly, UV screens (such as carotenoids and flavonoids) are often also free radical scavengers (Everett *et al.* 1995). A given molecule can thus be recruited by evolution for more than one function, and it can be difficult to evaluate the importance of such functions – in this case, the relative contribution of free radical scavenging and physical screening of UV.

UV absorbance by organic molecules is largely due to conjugated double bonds, either in chains or in rings. All of the UV screens examined absorbed in the vicinity of DNA absorption regions I and II (Fig. 6), mostly due to aromatic rings of various sorts. For example, the flavonoids, e.g. quercitrin and robinin, have absorption peaks at 204 and 199 nm, respectively, and the quercitrin peak is broad, giving good coverage to DNA region II at 192 nm (Figs 5 and 6). The melanin peak at 186 nm is part of a generally increasing absorbance, and should thus also protect DNA region II (Figs 4 and 6). β-carotene, DPA, MAA-9 (porphyra-334), MAA-6 (palythine) and scytonemin showed peaks at 195 nm, protecting DNA region II (Figs 2–4 and 6), although the MAA-9 peak was weak (Fig. 2).

In contrast to this generalized absorbance corresponding to region II, clear protection for DNA region I (264 nm) was less common (Figs 6 and 7). Scytonemin absorbed at 253 nm, DPA absorbed at 273–281 nm and β-carotene at 277 nm (Figs 2–4, 6 and 7). While scytonemin and DPA could clearly protect DNA in this region, their peaks were displaced by 10 nm below and above that of DNA.

On the other hand, absorption close to DNA region I was clearer in quercitrin, isoquercitrin and robinin, which also absorbed in the UVB (Figs 5 and 6). The fourth flavonoid, catechin, showed a peak at 280 nm, and no absorption in the UVB (Fig. 5). Thus, the first three flavonoids had absorption spectra remarkably similar to that of DNA, with additional absorption in the UVB, while catechin absorbed more like a protein.

We conclude that flavonoids would protect DNA from incident UV throughout the DNA absorption spectrum, and that they would protect other molecules by absorbing in the UVB. They are known free radical scavengers and metal chelators. Their accumulation in plants is stimulated in response to UV, and mutants of *Arabidopsis* lacking flavonoids show increased sensitivity to UV (Li *et al.* 1993). In seeds, flavonoids are concentrated in the seed coat, which serves to protect the embryo and nutrient reserves until germination is induced. The concentration of a flavonoid UV shield in the seed coat would distance the screen from the target DNA carried in the embryo, facilitating transfer of the energy absorbed without harm to the chromosomal DNA.

A comparison of absorption spectra for flavonoids and scytonemin revealed an interesting paradox (Figs 2, 5 and 6). Quercitrin, isoquercitrin and robinin are better mimics of the DNA spectrum than is scytonemin, which protects DNA

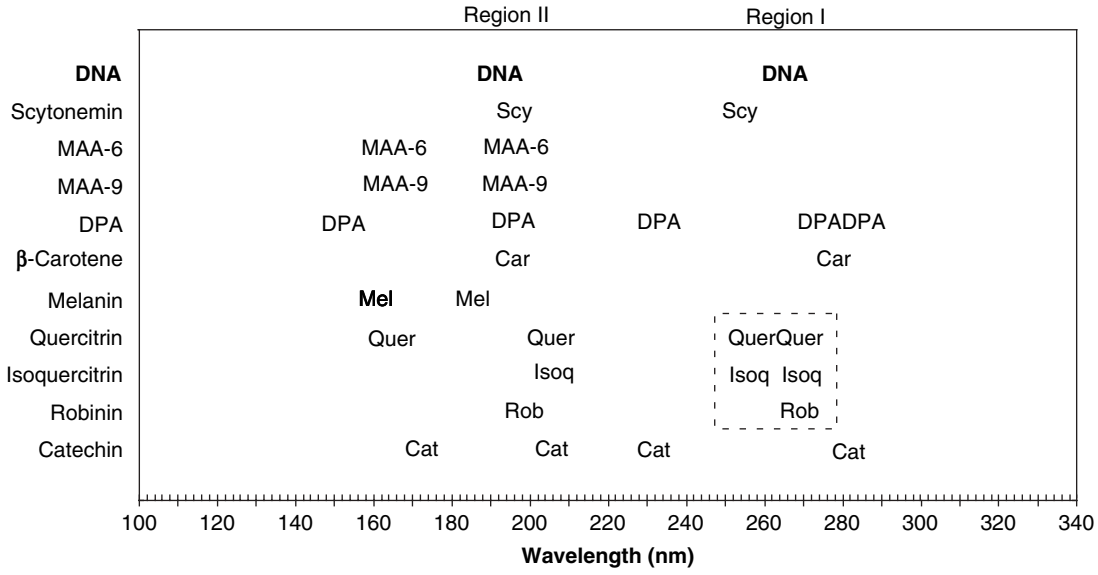

Fig. 6. A summary of results from Figs 2–5, giving the location of the major peaks for each substance analysed. The box indicates the three flavonoids having peaks corresponding to DNA region I absorbance. The DNA peaks are included for reference.

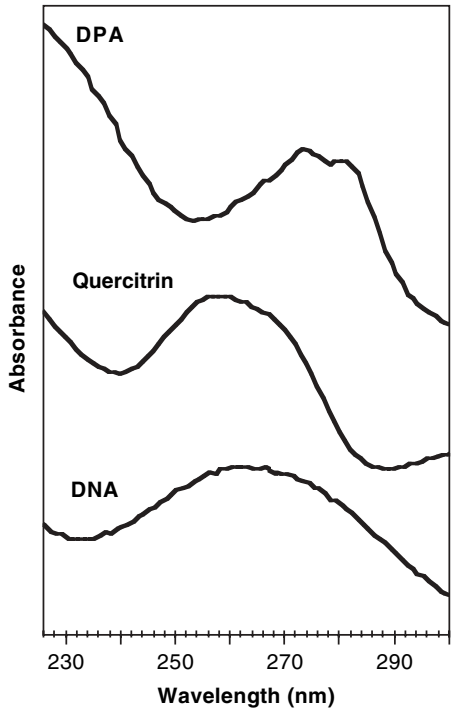

Fig. 7. Alignment of the region I peaks for DPA, quercitrin and DNA. (Absorbance values are adjusted to show positions of the peaks.)

region II and affords protection in the UVB, but the nearest scytonemin peak to DNA region I (264 nm) was at 253 nm. In contrast, quercitrin, isoquercitrin and robinin showed absorption at 258–270 nm, which should better protect DNA region I. Paradoxically, scytonemin should represent more ancient pigments (Garcia-Pichel & Castenholz 1991; Garcia-Pichel *et al.* 1991), yet it seems better adapted to protecting DNA from the UVA and UVB present in today's environment, than from the UVA, UVB and UVC thought to have been a liability on early Earth.

There are several possible explanations for this discrepancy. One concerns the validity of the criterion used for predicting protection (the degree of similarity between the target and the screen absorption spectra), but some of these predictions based on this criterion can be tested experimentally. Another explanation is that plants have retained the ancestral genes encoding primitive UV screens. Plant chloroplasts are considered to be ancient cyanobacteria, acquired through endosymbiosis. The bulk of the chloroplast genome has found its way into the host cell's nucleus, through horizontal gene transfer facilitated by endosymbiosis (Martin *et al.* 2002). It is thus conceivable that genes encoding flavonoids (or their ancestral forms) were transferred to the host plant genome following endosymbiosis and retained even after oxygen build-up in the atmosphere made their UVC filtering no longer vital. They remain important for plants, where they have acquired new functions, e.g. mediating plant–microorganism interactions (Firmin *et al.* 1986), and they continue to screen against UVA and UVB. Over time, these genes could have been lost in modern, free-living cyanobacteria.

A third explanation is that the ancestral vehicle that may have brought life to Earth was something like a plant seed, carrying multiple life forms, which started the three domains of life. In this scenario, the ability to make UV screens, such as flavonoids, would have been advantageous before life's arrival on Earth and during the build-up of an oxygen atmosphere. The accumulation of UV screens, such as flavonoids, might be an essential characteristic of DNA-based life. We discuss this reversal of the usual scenario for the origin of life in more detail elsewhere (Tepfer & Leach 2006), and restrict ourselves here to the transfer of life through space.

The transfer of life through space

Introspermia, the introduction of life onto Earth, is an attractive way to account for the origin of the life forms we know, but it is difficult to prove after the fact. In contrast, exospermia, the exportation of life from Earth, is proven by Man's recent space explorations. Exospermia is reminiscent of the 'directed panspermia', proposed by Orgel and Crick as a refinement of the panspermia hypothesis. They proposed that '… organisms were deliberately transmitted to the Earth by intelligent beings on another planet' (Crick & Orgel 1973; Crick 1981). According to their theory, life has had time to originate, to evolve, to be dispersed in a primitive state and to evolve again to its present forms. Unfortunately, directed panspermia, like all theories concerning the origin of life, is hard to test. (Intelligent beings have not been found elsewhere, and science has not spontaneously generated life.) Thus, to bring things down to Earth, we can consider Man as the 'intelligent being' envisioned in directed panspermia and that Man's explorations of the Solar System constitute directed exospermia.

Our proposal evades the issue of the origin of life, and implies that, instead of worrying about where we came from, we should think about where we are going. This could involve the preparation of life for deliberate dispersal through space. In the context of the present work, UV resistance might be improved by engineering the hyperaccumulation of one or more UV screens in a spore or in a seed that is already adapted to survive harsh conditions. An ideal UV screen would protect DNA and other targets, and it could also scavenge free radicals. Flavonoids, such as quercitrin, appear to be ideal UV screens throughout the UV spectrum. In addition, catechin mimics protein absorption at 280 nm. Flavonoids are also antioxidants and chelators. The genes and enzymes responsible for flavonoid biosynthesis are well characterized in *Arabidopsis*, so they are available for improving flavonoid accumulation in plants and other organisms using metabolic engineering.

Metabolic engineering is not the only way to accumulate UV screens. Organisms rely on diet as a source of bioactive molecules. For example, carotenoids and flavonoids are acquired in humans through ingestion. An organism could thus be preloaded with UV protecting substances prior to space travel. In the case of a dormant spore or seed, the loaded molecules could remain protective indefinitely, until germination.

For agricultural use, seeds are routinely coated with substances that protect them against pathogens and provide nutrients to germinating seedlings (Taylor & Harman 1990). Thus, through coating, seeds could not only benefit from improvement in their intrinsic resistance to space conditions, but beneficial substances, such as UV screens, could be added to their exterior. Plant cells carry endosymbionts, and seeds can include both obligate and free-living microorganisms. It should be possible to load seeds with free-living bacteria such as *Deinococcus radiodurans*, which can survive radiation and desiccation by rebuilding its genome from fragments. Beneficial organisms, e.g. the obligate mycorrhizal fungi, which are necessary for plant growth on Earth, might be incorporated inside plant seeds. These are just two examples of the endoorganisms that could be loaded into plant seeds to increase the chances of survival of a life form in an exoenvironment.

The most 'intelligent' Crick and Orgel exospermia experiment would consist of creating a life form from scratch, designed to resist space travel and colonize the universe. The technology for synthesizing long DNA sequences is improving and, with increased knowledge of genomes on Earth, it should be possible to synthesize an artificial organism starting with the DNA sequence. Base pair preferences could be adjusted to produce an optimal DNA absorption spectrum (see the accompanying paper), and UV screens could be made to accumulate (e.g., the flavonoids), which would protect DNA and detoxify free radicals. This artificial life form could be included within an existing one, e.g. a plant seed, as an endoorganism.

Life's place in the Universe is a fundamental question in human culture. Is life on Earth a unique or a trivial component of the Universe? Panspermia suggests that life is not unique to Earth, but rather that life is universal. Scientific discussion of these questions is impeded by a lack of information. (Life is difficult to define, and its origin can only be imagined.) Nevertheless, some things are fairly sure. All life on Earth probably came from the same source, since life is based on DNA and uses the same genetic code. While spontaneous generation, the alternative to panspermia, has not been shown, we know that humans are sending life into space. Thus, self-dispersal, which is an essential attribute of life, it is not limited to our biosphere. Directed exospermia is a logical step for Man to take, but sending humans great distances in space is not feasible. Instead, we propose to send plant seeds (and associated endoorganisms) or biological entities based on enhanced versions of their relevant properties.

Acknowledgments

Financial support was provided by the Centre National d'Etudes Spatiales and the University of Aarhus (EC Integrated Activity on Synchrotron and Free Electron Laser Science, contract number R113-CT-2004-50608). We are indebted to Dick Castenholz (University of Oregon) for providing the UVA induced *Chroococcidiopsis* cells and to the group of D.-P. Häder (Friedrich-Alexander-Universität) for the MAA extracts. Lucien Kerhoas generously performed the mass spectrometry.

References

Armstrong, G.A. (1994). *J. Bacteriol.* **176**, 4795–4802.

Bebout, B.M. & Garcia-Pichel, F. (1995). *Appl. Environ. Microbiol.* **61**, 4215–4222.

Berg, P.E. & Grecz, N. (1970). *J. Bacteriol.* **103**, 517–519.

Castenholz, R. & Garcia-Pichel, F. (2000). *The Ecology of Cyanobacteria*, ed. Potts, M. & Whittton, B.A., pp. 591–611. Kluwer Academic Publishers, Dordrecht.

Clancy, C.M.R., Nofsinger, J.B., Hanks, R.K. & Simon, J.D. (2000). *J. Phys. Chem.* B **104**, 7871–7873.

Cockell, C.S. & Knowland, J. (1999). *Biol. Rev. Cambr. Philos. Soc.* **74**, 311–345.

Crick, F. (1981). *Life Itself*. Simon and Schuster, New York.

Crick, F.H.C. & Orgel, L.E. (1973). *Icarus* **19**, 341–346.

Dixon, R.A., Howles, P.A., Lamb, C., He, X.Z. & Reddy, J.T. (1998). *Adv. Exp. Med. Biol.* **439**, 55–66.

Douki, T., Setlow, B. & Setlow, P. (2005). *Photochem. Photobiol. Sci.* **4**, 591–597.

Duc le, H., Fraser, P.D., Tam, N.K. & Cutting, S.M. (2006). *FEMS Microbiol. Lett.* **255**, 215–224.

Eden, S., Limão-Vieira, P., Hoffmann, S.V. & Mason, N.J. (2006). *Chem. Phys.* **323**, 313–333.

Everett, S.A., Kundu, S.C., Maddix, S. & Willson, R.L. (1995). *Biochem. Soc. Trans.* **23**, 230S.

Firmin, J., Wilson, K., Rossen, L. & Johnston, A.W.B. (1986). *Nature* **324**, 90–92.

Garcia-Pichel, F. & Castenholz, R.W. (1991). *J. Phycology* **27**, 395–409.

Garcia-Pichel, F. & Castenholz, R.W. (1993). *Appl. Environ. Microbiol.* **59**, 163–169.

Garcia-Pichel, F., Sherry, N.D. & Castenholz, R.W. (1992). *Photochem. Photobiol.* **56**, 17–23.

Garcia-Pichel, F., Wingard, C.E. & Castenholz, R.W. (1993). *Appl. Environ. Microbiol.* **59**, 170–176.

Germaine, G.R. & Murrell, W.G. (1973). *Photochem. Photobiol.* **17**, 145–154.

Grecz, N., Tang, T. & Frank, H.A. (1973). *J. Bacteriol.* **113**, 1058–1060.

Hinojosa-Rebollar, E., Rangel-Mandujano, A., Ortigoza-Ferado, J., Mesta-Howard, A.M. & Hernandez-Rodriguez, C. (1993). *Revista Latinoamer. Microbiol.* **35**, 399–406.

Horneck, G., Rettberg, P., Reitz, G., Wehner, J., Eschweiler, U., Strauch, K., Panitz, C., Starke, V. & Baumstark-Khan, C. (2001). *Orig. Life Evol. Biosph.* **31**, 527–547.

Li, J., Ou-Lee, T.M., Raba, R., Amundson, R.G. & Last, R.L. (1993). *Plant Cell* **5**, 171–179.

Lindsay, J.A. & Murrell, W.G. (1983). *Biochem. Biophys. Res. Commun.* **113**, 618–625.

Martin, W., Rujan, T., Richly, E., Hansen, A., Cornelsen, S., Lins, T., Leister, D., Stoebe, B., Hasegawa, M. & Penny, D. (2002). *Proc. Natl. Acad. Sci. USA* **99**, 12 246–12 251.

Meredith, P., Powell, B.J., Riesz, J., Nighswander-Rempel, S.P., Pederson, M.R. & Moore, E.G. (2006). *Soft Matter* **2**, 37–44.

Meredith, P. & Riesz, J. (2004). *Photochem. Photobiol.* **79**, 211–216.

Murrell, W.G. (1967). *Adv. Microbial Physiol.* **1**, 133–251.

Nakamura, H., Kobayashi, J. & Hirata, Y. (1982). *J. Chromatography* **250**, 113–118.

Paidhungat, M., Ragkousi, K. & Setlow, P. (2001). *J. Bacteriol.* **183**, 4886–4893.

Pezzella, A., Napolitano, A., d'Ischia, M., Prota, G., Seraglia, R. & Traldi, P. (1997). *Rapid Commun. Mass Spectrom.* **11**, 368–372.

Proteau, P.J., Gerwick, W.H., Garcia-Pichel, F. & Castenholz, R. (1993). *Experientia* **49**, 825–829.

Riley, P.A. (1997). *Int. J. Biochem. Cell Biol.* **29**, 1235–1239.

Routaboul, J.-M., Kerhoas, L., Debeaujon, I., Pourcel, L., Caboche, M., Einhorn, J. & Lepiniec, L. (2006). *Planta* **224**, 96–107.

Setlow, B., Atluri, S., Kitchel, R., Koziol-Dube, K. & Setlow, P. (2006). *J. Bacteriol.* **188**, 3740–3747.

Setlow, B. & Setlow, P. (1993). *Appl. Environ. Microbiol.* **59**, 640–643.

Setlow, P. (1994). *J. Appl. Bacteriol.* **76**, 49S–60S.

Shick, J.M. & Dunlap, W.C. (2002). *Ann. Rev. Physiol.* **64**, 223–262.

Sinha, R.P. & Hader, D.P. (2002). *Adv. Space Res.* **30**, 1547–1556.

Sinha, R.P., Klisch, M., Gröniger, A. & Häder, D.-P. (1998). *J. Photochem. Photobiol. B: Biol.* **47**, 83–94.

Sinha, R.P., Klisch, M. & Hader, D.-P. (1999). *J. Photochem. Photobiol. B: Biol.* **52**, 59–64.

Slieman, T.A. & Nicholson, W.L. (2001). *Appl. Environ. Microbiol.* **67**, 1274–1279.

Squier, A.H., Hodgson, D.A. & Keely, B.J. (2004). *Organic Geochem.* **35**, 1221–1228.

Takano, S., Nakanishi, D. & Uemura, D. (1979). *Chem. Lett.* **8**, 419–420.

Takano, S., Uemura, D. & Hirata, Y. (1978). *Bot. Mar.* **23**, 65–68.

Taylor, A.G. & Harman, G.E. (1990). *Ann. Rev. Phytopathol.* **28**, 321–339.

Tepfer, D. & Leach, S. (2006). *Astrophys. Space Sci.* **306**, 69–75.

Wakamatsu, K. & Ito, S. (2002). *Pigment Cell Res.* **15**, 174–183.

Westall, F., de Ronde, C.E., Southam, G., Grassineau, N., Colas, M., Cockell, C. & Lammer, H. (2006). *Phil. Trans. R. Soc. Lond.* **361**, 1857–1875.

Whitehead, K. & Hedges, J.I. (2003). *Rapid Commun. Mass Spectrom.* **17**, 2133–2138.

Winkel-Shirley, B. (2001). *Plant Physiol.* **126**, 485–493.

Zalar, A., Tepfer, D., Hoffmann, Søren V., Kenney, J.M. & Leach, S. (2007). *Int. J. Astrobiol.* **6(3)**, 229–240.

Article 3

Zalar A, Tepfer D, Hoffmann S V, Kollmann A and Leach S (2007c) VUV-UV absorption spectroscopy of DNA and UV screens suggests strategies for UV resistance during evolution and space travel. *In* BH Richard, VL Gilbert, YR Alexei, CWD Paul, eds, Instruments, Methods, and Missions for Astrobiology X, Vol 6694. *Proceedings of SPIE*, Vol. 6694 pp 66940U (1-15)

VUV-UV absorption spectroscopy of DNA and UV screens suggests strategies for UV resistance during evolution and space travel

Andreja Zalar*[a], David Tepfer[a], Søren V. Hoffmann[b], Albert Kollmann[a], Sydney Leach[c]

[a]PESSAC, Institut National de la Recherche Agronomique (INRA), Route de St Cyr, 78026 Versailles, France
[b]Institute for Storage Ring Facilities (ISA), University of Aarhus, Ny Munkegade, 8000 Aarhus C, Denmark
[c]LERMA, Observatoire de Paris-Meudon, 5 Place Jules Janssen, 92195 Meudon, France

ABSTRACT

Early life on Earth had to cope with harsh conditions, including full spectrum solar UV. Since DNA absorbs in the highly energetic UV-C and VUV, solar irradiation was likely an obstacle to the expansion of life on Earth, until biological mechanisms evolved to cope with UV liability (including the biosynthesis of UV screens) and ozone (derived from oxygen produced by photosynthesis) accumulated in the stratosphere. In an effort to better understand the UV liability of DNA, we used synchrotron light to measure VUV-UV absorption spectra (125-340 nm) for DNA and its components (oligonucleotides and mononucleotides). We also measured VUV-UV absorption spectra for potential and known UV screens, including amino acids, proteins, amines (including polyamines), scytonemin, mycosporine-like amino acids, β-carotene, melanin and flavonoids. Among these, flavonoids seem remarkably suited to protecting DNA in the VUV-UV. Flavonoids accumulate in seed coats, where they confer resistance to monochromatic UV (254 nm) and polychromatic UV (200-400 nm). We discuss these findings in relation to the origin and evolution of life and its potential dispersal through space.

Keywords: VUV-UV absorption spectroscopy, UV screens, UV resistance, plant seeds, flavonoids, space travel, origin of life, panspermia

1. INTRODUCTION

1.1 Emerging life and solar UV light

Since ancient times people have tried to answer fundamental questions about life: "What is it?" How did it appear?" Is it universal? Defining universal life is complicated by the fact that we are only familiar with life on Earth. Nevertheless, a few of attributes of the life we know are clear: 1. Life is cellular. 2. Life self-replicates. 3. Life varies in different replica. 4. Life evolves. Determining the origin of life is even more difficult than defining it. The numerous theories proposed to explain the appearance of life on Earth generally invoke either *spontaneous generation* from prebiotic matter or *panspermia* via importation from elsewhere in the Universe. These theories are difficult to evaluate, but it is certain that life has successfully evolved and expanded on Earth for more than three billion years (Gyr), and it is reasonable to assume that all known life forms on Earth came from a single source, since the genetic code is similar in all known organisms.

Much essential information is missing, however. Our solar system was formed 4.56 Gyr ago[1], and there are suggestions that life was present on Earth as early as 3.8 Gyr ago[2]. The fossil record shows microbial life 3.43 Gyr ago[3]. Thus, life had roughly 1 Gyr to emerge and to evolve into complex cells, which seems short given the complexity of the job and the probability that conditions on early Earth were unfriendly to life. Although the environment and prebiotic chemistry on early Earth are not known with certitude[4], emerging life probably had to cope with harsh conditions, including the full spectrum of solar UV.

Solar UV emission is generally divided into four regions: the UV-A (315-400 nm), the UV-B (280-315 nm), the UV-C (200-280 nm) and the VUV (< 200 nm) (Fig 1a). The Solar UV that reaches the surface of present-day Earth is high in the UV-A, decreases sharply in the UV-B region, and it drops to nearly zero below 290 nm, thanks to absorption by

Instruments, Methods, and Missions for Astrobiology X
edited by Richard B. Hoover, Gilbert V. Levin, Alexei Y. Rozanov, Paul C. W. Davies
Proc. of SPIE Vol. 6694, 66940U, (2007) · 0277-786X/07/$18 · doi: 10.1117/12.733699

stratospheric ozone. Almost all of the oxygen in the atmosphere comes from photosynthesis. It is therefore generally accepted that the atmosphere of the prebiotic Earth was poor in oxygen, and it did not contain protective ozone. Thus, the surface of early Earth was likely exposed to highly energetic UV radiation. The evolution of oxygen-producing photosynthesis could have occurred as early as 3.5 Gyr ago[5, 6], but the oxygen level in the atmosphere probably only started to rise 2.5-2.0 Gyr ago, resulting in the slow accumulation of an ozone layer and the attenuation of intensive VUV, UV-C and UV-B light on the Earth's surface[7]. Until the formation of this ozone layer, photosynthetic organisms that used visible light in the 400-750 nm range also had to cope with short wavelength UV.

1.2 DNA as a target for UV damage

UV radiation is absorbed by and damages molecular targets as diverse as nucleic acids, proteins and lipids. Although unfiltered solar emission in the short wavelengths (VUV and the UV-C) is relatively weak (Fig 1a), this part of the spectrum is biologically damaging because of the high energies involved and because biological targets often absorb in these regions. For instance, nucleic acids (DNA and RNA) are prime targets for UV damage, due to their absorption in the UV-C and VUV (Fig. 1b). In microorganisms, the action spectrum for decline in viability follows the absorption spectrum profile of DNA[7].

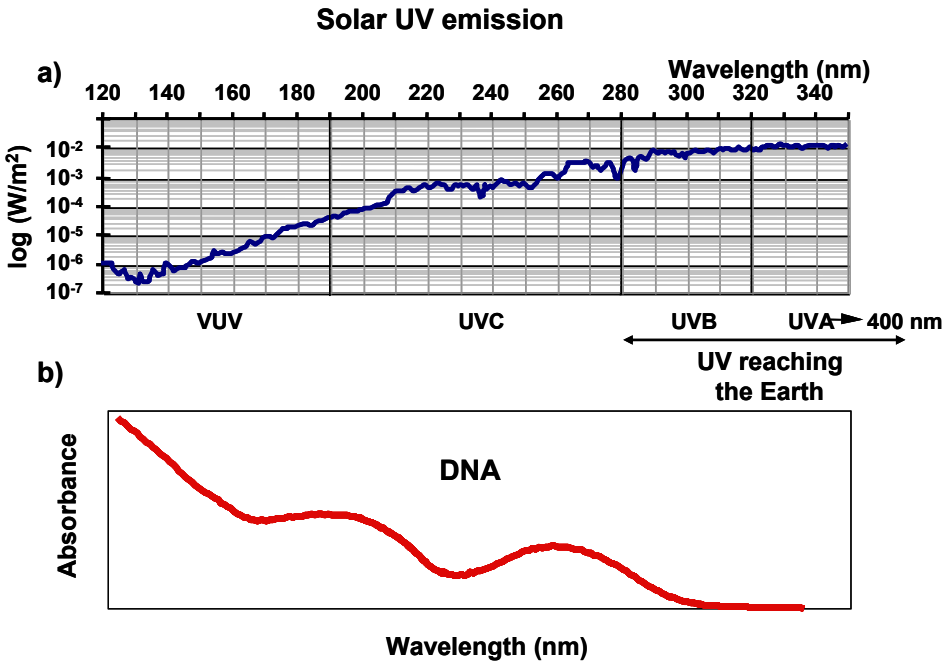

Fig. 1. (a) Solar UV emission spectrum. (b) UV absorption by DNA. (The absorption spectrum of DNA is adapted from reference[8].)

UV radiation induces a wide variety of DNA damage, including pyrimidine dimer formation, single strand breaks, double strand breaks and DNA-DNA and DNA-protein crosslinks. Damage products include cyclobutane pyrimidine dimers (CPD) and pyrimidine (6-4) pyrimidinone dimers (6-4 photoproducts) (75% and 25%, respectively).[9, 10, 11] Both types of lesions distort the DNA double helix[11]. Structural changes to DNA interfere with DNA replication and RNA transcription, leading to mutation or cell death. The most common deleterious DNA photoproduct is the CPD-type dimer that forms between two adjacent thymine residues (TT dimer). Besides these direct effects, UV can interact with other cellular compounds, leading to free radical formation, causing indirect damage to DNA.

1.3 UV screens

Organisms evolved mechanisms for resisting UV radiation, including avoidance, protection (UV screens) and repair. UV screens provide a first line of defense against UV radiation. Protection is passive—UV light is absorbed, and its energy is dissipated away from sensitive cellular targets[7]. UV screens are physical or biological[12]. Physical substrates (such as water, rocks, sand particles, salt, iron compounds and sulfur), can absorb UV light. However, most physical screens also attenuate the visible part of spectrum and thus interfere with photosynthesis. Iron compounds (particularly Fe^{3+} ions) and elemental sulfur could provide some specific UV protection and still transmit visible light[12]. Given the limitations of

physical UV screens, organisms had to develop more efficient and specific ways of coping with UV. The synthesis of biological UV screens enabled the filtering of specific UV wavelengths, without attenuating photosynthetically active radiation. Four criteria have been proposed to define biological UV screens[13]: (i) a compound must absorb the biologically damaging radiation, (ii) screening activity must be demonstrated *in vivo* (iii), biosynthesis should be inducible by the relevant radiation and (iv) the pigment should biologically protect from the filtered radiation. We propose that some ubiquitous biological substances could also serve as constitutive UV screens, without meeting all of these criteria.

Due to its absorption spectrum and biological importance, DNA is a particularly sensitive target. Its protection by UV screens can be achieved at several levels, depending on the structural and chemical complexity of the cell (Fig. 2). In the simplest case, DNA is concentrated in the interior, as far as possible from the incident light, and it is surrounded by UV-absorbing molecules that are *ubiquitous* in all cells, such as proteins (histones in eukaryotes and histone-like proteins in bacteria) and polyamines (and their conjugates), which can stabilize DNA, forming compact structures that are less susceptible to damage. These ubiquitous putative screens do not meet all of the conditions proposed[13], but they have absorption properties that indicate a potential for some constitutive protection. Another level of protection, which does meet the proposed criteria[13], is achieved by the induced accumulation of *specialized* UV screens that are efficient and specific UV absorbers. Many organic compounds incorporate a π-electron system (*e.g.* in the conjugated bonds of aromatic and cyclic structures), and thus provide efficient screening of UV at some of the wavelengths absorbed by DNA (see below). Some of these can accumulate to high concentrations in response to UV. The protection of the cell or tissue can be further achieved by peripheral structures, such as cell walls and capsules, in which specialized UV screens accumulate. Physical distance between the shield and the target is advantageous, because it reduces the risk that energy absorbed by the screen is transferred to the target DNA. UV can trigger the production of specialized screens, such as scytonemin and flavonoids (see below), which accumulate in peripheral structures and tissues, *e.g.* extracellular coats and sheaths in microorganisms and seed coats in plant seeds.

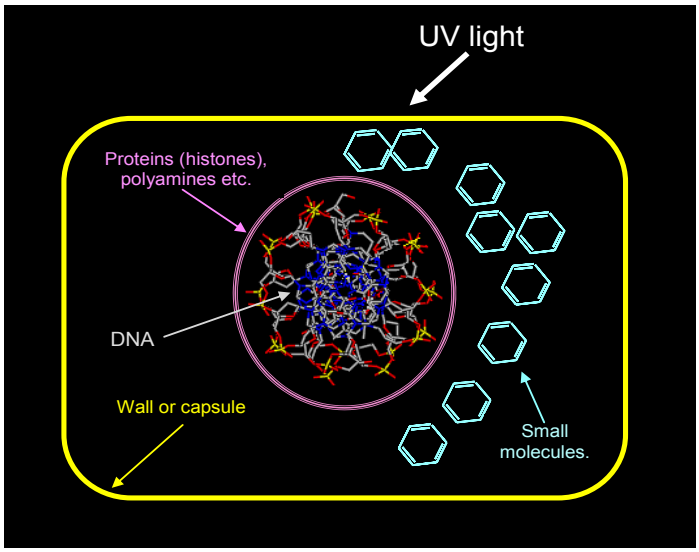

Fig. 2. UV protection in a hypothetical cell. Ubiquitous molecules with multiple functions, *e.g.* proteins and polyamines, provide constitutive protection. Another level of protection is induced by exposure to UV light, and consists of the accumulation of specialized UV screens, small molecules that are efficient UV absorbers. The cell is further protected by peripheral structures, *e.g.* capsules or cell walls, where these specialized UV screens can accumulate, distancing the screen from the target.

The screening effect should be maximal at the wavelengths of maximal absorption and negligible where the compound does not significantly absorb[14]. The search for UV screens is complicated by the propensity of evolution for finding multiple uses for a given substance. For instance, a UV screen can also protect against free radicals or have functions unrelated to stress. In order to simplify and enlarge the search for UV screens, we have worked with the hypothesis that absorbance by the screen should match absorbance of the target. This approximate approach to identifying UV screens brings diverse molecules into consideration, but provides only a preliminary identification of compounds that might be

used to protect life from UV. Nevertheless, it enlarges the search to include substances that might have been important on early Earth or in the Universe, where the atmospheric protection that life currently enjoys on Earth is lacking.

2. METHODOLOGY

The VUV-UV absorption spectroscopy measurements were carried out at the ultraviolet beamline (UV1) of the ASTRID (electron) storage ring facility (Fig. 3.), at the Institute for Storage Ring Facilities (ISA), University of Aarhus, Denmark. Technical details about UV1 setup are given elsewhere[15]. Synchrotron radiation was the light source for measuring absorption spectra (125-340 nm) in thin films, dried onto MgF_2 discs, held in a sample holder (Fig. 4b) that was placed vertically in the vacuum chamber of the UV1 absorption spectroscopy installation (Fig. 4a). In each experiment, one MgF_2 window was kept blank and used as a reference, while three MgF_2 windows carried dried samples. The position of the sample holder was adjusted so that only one sample at a time was placed perpendicularly into the beam. Monochromatized light from the beamline passed thought a LiF window into the vacuum chamber containing the samples. Transmitted light exited the sample chamber through a MgF_2 window and it was detected by VUV-UV sensitive photomultiplier tube (PMT). For wavelength scans below 200 nm, helium was flushed through the small gap between the photomultiplier tube and the exit window, to prevent any absorption by air from contributing to the spectrum. The resulting spectra were based on transmission measurements. Absorption was calculated as $A=\log (I_o/I_t)$, where I_o represents the intensity of the light transmitted through the reference (blank window) and I_t is the intensity of the light transmitted through the sample. Although recorded spectra were the result of absorption and scattering, for the sake of simplicity and because of the small contribution of scattering[16], all spectra are called absorption spectra.

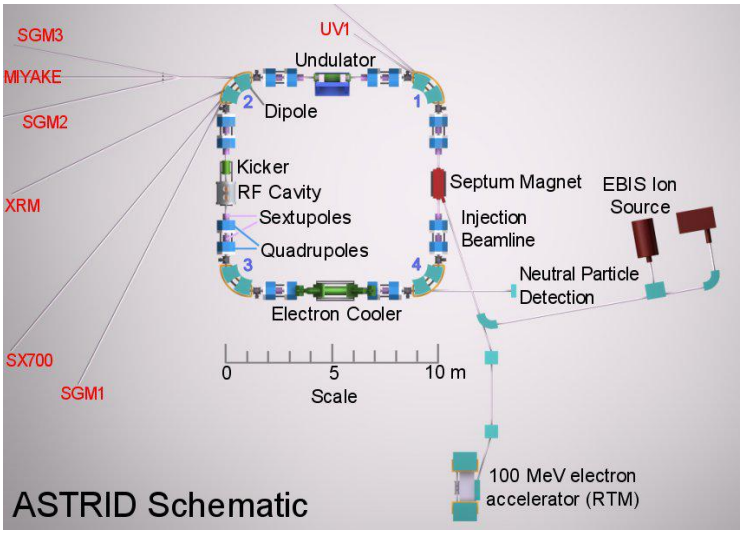

Fig. 3. Schematic representation of the ASTRID ring storage facility at the ISA, University of Aarhus. (Layout of ASTRID taken from http://www.isa.au.dk/facilities/astrid/astrid.html).

Samples were prepared for spectroscopy as thin, dry films in order to avoid background absorption from solvents, because most of the solvents used absorb strongly below 200 nm. Since all spectroscopic measurements were performed in a high vacuum, all samples (including DNA) were in a dehydrated state. Films were prepared by drying substances onto MgF_2 windows. Films of salmon sperm DNA, synthesized oligonucleotides and mononucleotides (including ATP) were prepared as described elsewhere[8]. The samples of complementary 20-mer homonucleotides ($oligoA_{20}$ +$oligoT_{20}$ and $oligoG_{20}$ +$oligoC_{20}$) were obtained by mixing (1:1) equimolar volumes of $oligoA_{20}$ with $oligoT_{20}$ and $oligoG_{20}$ with $oligoC_{20}$. All homonucleotides (Genosys-Sigma, France) were prepared as 100 μM solutions in water (pH 7.5). Synthetic 60-mer oligonucleotides (Fig. 5) with different G+C content (30%, 50% and 63%), purchased from Genosys-Sigma, France, were designed to encode the same protein, including one of each of the 20 amino acids. In order to mimic the contribution of both DNA strands, we prepared equimolar (25 μM) mixtures of sense + antisense strands. Samples of potential and ubiquitous UV screens included proteins (histones from calf thymus and bovine serum albumin), amino acids (L-arginine, L-valine, L-aspartic acid and L-tryptophan), polyamines (putrescine, spermine, spermidine) and the

aromatic amine, tyramine. (Details of the preparation of these samples are given elsewhere[8]). Dry films of the following known UV screens were prepared: scytonemin, mycosporine-like amino acids (MAAs), β-carotene, synthetic melanin (made by oxidation of tyrosine with hydrogen peroxide) and flavonoids (quercitrin isoquercitrin, robinin and catechin)[16]. Scytonemin was extracted from UV-A induced cells of the cyanobacterium, *Chroococcidiopsis* (provided by R. Castenholz), purified by HPLC and analyzed by LC-MS[16]. The two MAA samples (a gift from D.-P. Häder) were isolated from the marine red alga, *Corallina officinalis,* and shown by us, using LC-MS, to contain porphyra-334 and palythine[16]. Chlorophylls a and b from spinach (Fluka, France) were prepared as described elsewhere[16].

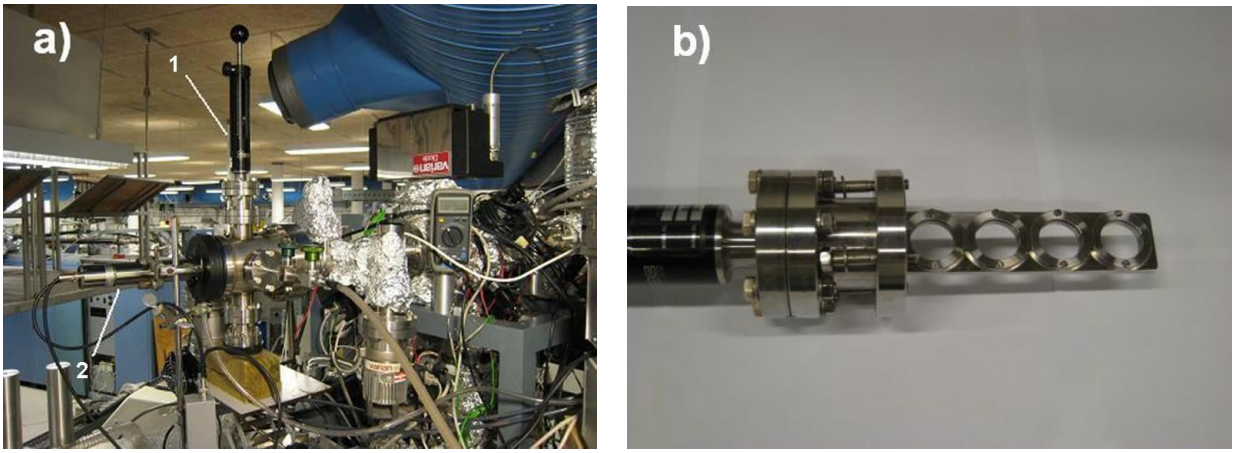

Fig. 4. a) VUV-UV absorption spectroscopy installation at the UV1. (1) shows the sample holder, containing samples placed vertically into the vacuum chamber. The UV beam passes horizontally through the sample, and transmitted light is detected by a VUV-UV sensitive photomultiplier tube (2). b) Detail of the sample holder, which carries four samples dried onto MgF_2 discs.

30% G+C

Sense (+)	5' ATGTTTTGGCAAAGAGCTAATGATGTATGTAAACATGGTATATTACCAACTTATGAATCT 3'
Antisense (-)	3' TACAAAACCGTTTCTCGATTACTACATACATTTGTACCATATAATGGTTGAATACTTAGA 5'
Peptide	H_2N-Met-Phe-Trp-Gln-Arg-Ala-Asn-Asp-Val-Cys-Lys-His-Gly-Ile-Leu-Pro-Thr-Tyr-Glu-Ser-COOH

50% G+C

Sense (+)	5' ATGTTCTGGCAGCGAGCTAATGACGTATGTAAGCATGGAATCCTCCCTACCTACGAGTCG 3'
Antisense (-)	3' TACAAGACCGTCGCTCGATTACTGCATACATTCGTACCTTAGGAGGGATGGATGCTCAGC 5'
Peptide	H_2N-Met-Phe-Trp-Gln-Arg-Ala-Asn-Asp-Val-Cys-Lys-His-Gly-Ile-Leu-Pro-Thr-Tyr-Glu-Ser-COOH

63% G+C

Sense (+)	5' ATGTTCTGGCAGCGGGCGAACGACGTCTGCAAGCACGGGATCCTGCCGACCTACGAGTCC 3'
Antisense (-)	3' TACAAGACCGTCGCCCGCTTGCTGCAGACGTTCGTGCCCTAGGACGGCTGGATGCTCAGG 5'
Peptide	H_2N-Met-Phe-Trp-Gln-Arg-Ala-Asn-Asp-Val-Cys-Lys-His-Gly-Ile-Leu-Pro-Thr-Tyr-Glu-Ser-COOH

Fig. 5. Synthetic 60-mer oligonucleotides with different G+C content (30%, 50% and 63%), represented by coding sense (+) strand and the complementary antisense (-) strand. These oligonucleotides have different nucleotide composition and sequence, but encoding the same peptide, which contain one of each of 20 amino acids (amino acid sequence is presented under each oligonucleotide pair).

3. RESULTS AND DISCUSSION

3.1 The VUV-UV absorption properties of DNA (influence of nucleotide content and sequence)

The DNA polymer is composed of monomer units (mononucleotides), which differ in their nucleobases: adenine (A), guanine (G), thymine (T) and cytosine (C). The absorption spectrum of DNA correlates with the action spectra for DNA damage and photoproduct formation[17]. Absorption by DNA (and thus susceptibility to UV) could depend on overall base composition and nucleotide sequence. Using synchrotron light, absorption can be measured from 125 to 340 nm, including the VUV-UV part of spectrum encountered in space. Dry salmon sperm DNA (genomic DNA) showed absorption maxima at 264 nm (region I), at 192 nm (region II) and continuously increasing absorption toward 125 nm (region III)[8] .

Polymerized homonucleotides (short tracts of single-stranded DNA), containing 20 identical nucleotides (oligoA_{20}, oligoT_{20}, oligoC_{20} and oligoG_{20}) showed differences in their absorption spectra, but absorption peaks could be grouped into three regions, corresponding to the absorption peaks observed in the genomic DNA: 286-255 nm (region I), 220-159 nm (region II) and below 159 nm (region III). In all four oligonucleotides, region III exhibited continuously increasing absorbance toward the low wavelength end of the spectrum, but these oligonucleotides differ in characteristics in regions I and II. The oligoA spectrum included a prominent peak at 257 nm in region I, while region II consisted of a shoulder at 208 nm, a peak at 188 nm and a small peak at 159 nm. With oligoG, a broad peak was observed, a shoulder at 286 nm and a maximum at 255 nm (region I), while region II consisted of a dominant peak at 186 nm. The oligoT spectrum included three well-resolved peaks: one at 268 nm (region I) and two peaks at 208 and 175 nm (region II). With oligoC, a peak at 278 nm (region I) was recorded, while region II consisted of a small peak at 220 nm, an inflection at 200 nm and a peak at 182 nm (spectra are presented elsewhere[8]). Purine base oligonucleotides (oligoA and oligoG) had greater peak intervals between region I and region II, compared to pyrimidine base oligonucleotides (oligoT and oligoC). The homonucleotides showed more spectral features (peaks and shoulders) than the genomic DNA, including differences in the number and positions of the absorption peaks. A particularly interesting difference was a bathochromic shift in region I for oligoC (a peak at 278 nm) and for oligoG (a broad peak with a strong shoulder at 286 nm), compared to genomic DNA. These observations suggested that DNA sequences rich in G+C nucleotides, might have the absorption maximum in region I shifted toward 280 nm[8].

In order to examine the influence of G+C content on overall UV absorption by DNA, we measured the absorption of equimolar mixtures of two complementary homonucleotides (oligoA_{20} + oligoT_{20} and oligoG_{20} + oligoC_{20}) (Fig. 6). These single-stranded DNA samples consisted of two complementary strands of homopolymeric DNA (dA:dT or dG:dC), representing the two extreme G+C contents (100 and 0%, respectively). Differences between oligoA+T and oligoG+C spectra were observed, and both spectra differed from that of genomic DNA (salmon sperm DNA, which belongs to the A+T rich class, having a G+C content of 41.2 %)[18]. Like genomic DNA, oligoG+C absorbed in regions I, II and III. In region I, oligoG+C showed complex absorbance between 240 and 315 nm, as a broad peak, which represents at least two fused absorption peaks. In contrast, oligoG+C absorbed as a single peak (185 nm) in region II. The pattern of oligoA+T absorbance was reversed, with a single peak at 263 nm in region I and complexity in region II, which was spread out between 155-208 nm, with three peaks (155, 177 and 208 nm). The oligoA+T absorption maximum (263 nm) in region I coincided with peak I in salmon sperm DNA (264 nm), reflecting the A+T rich composition of this genomic DNA, however the two samples differed in region II, probably due to the influence of the G and C bases, present in the genomic DNA. This conjecture is consistent with the occurrence of a single peak for oligoG+C in region II. However, this peak showed a hypsochromic shift of about 7 nm, compared to the peak of genomic DNA.

The genetic code uses all four nucleotides to encode the 20 amino acids. However, extreme nucleotide contents, known as homopolymeric DNA tracts, do occur locally in noncoding regions of the genomes of both eukaryotic and prokaryotic organisms. Moreover, long poly(dA:dT) tracts, reaching a size well above 25 base pairs, appear at high frequencies in some eukaryotes, enriching genomes for A and T nucleotides[19]. Other eucaryotic genomes are enriched in dG:dC tracts, while others are depleted in these tracts[19]. In prokaryotes, homopolymeric tracts occur, but less frequently[19]. The formation of the different UV photoproducts in free DNA depends on wavelength and DNA sequence[20]. For instance, sequences rich in adjacent thymines are prone to the formation of thymine dimers (TT), the most frequent type of UV damage. Other pyrimidine dimers (CT, TC and CC) could be also formed, although at lower frequencies. Adjacent GC bases favor the formation of the 6-4 photoproduct, which is produced 10 times less often than the pyrimidine dimers.

In region I, the oligoG+C homopolymer absorbance (Fig. 6) between 240 and 315 nm suggests that DNA containing poly(G:C) tracts might be damaged by a wider range of UV wavelengths than DNA containing A:T tracts, where absorbance stops at 300 nm. The major photoproduct would be the CC type of pyrimidine dimer. This is in agreement with a previous study[20], where an increase in the formation of CC dimers, relative to TT dimers, was demonstrated in DNA after irradiation with UV-B light. It was further observed that the frequency of TT dimers, relative to the other dimers that contain cytosine (CT, TC and CC), was greater after exposure to UV-C[20]. In addition, the induction of specific photoproducts is influenced by the DNA sequence around potential sites of UV induced lesions[20]. It would thus seem likely that DNA sequences would evolve as a function of environmental UV and the available UV screens.

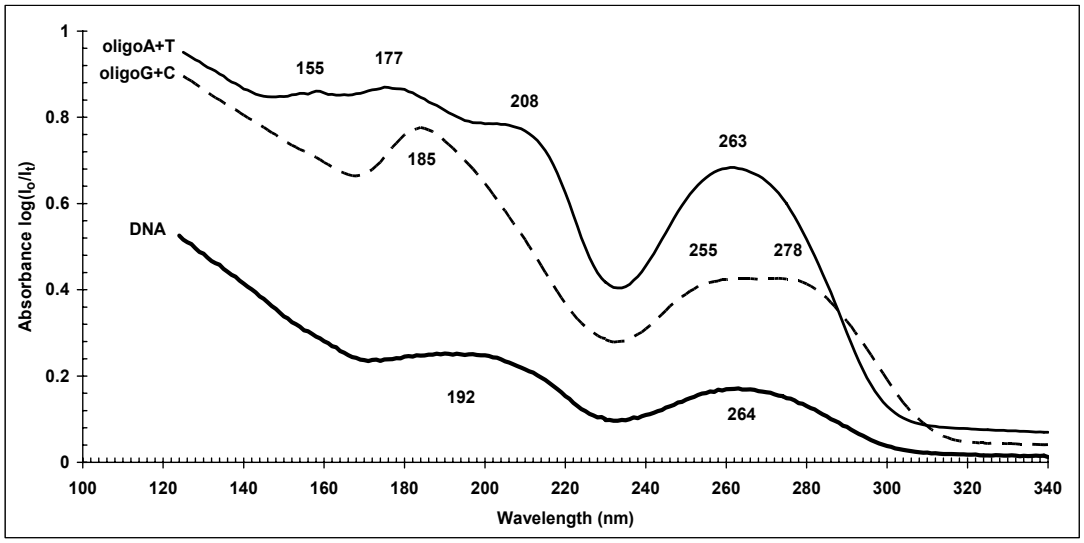

Fig. 6. VUV-UV absorption spectra of equimolar mixtures of complementary homonucleotides, each containing 20 identical nucleotides, oligoA_{20} + oligoT_{20} (oligoA+T) and oligoG_{20} +oligoC_{20} (oligoG+C) with salmon sperm DNA as a reference. (The absorption spectrum of dry DNA is taken from reference[8].)

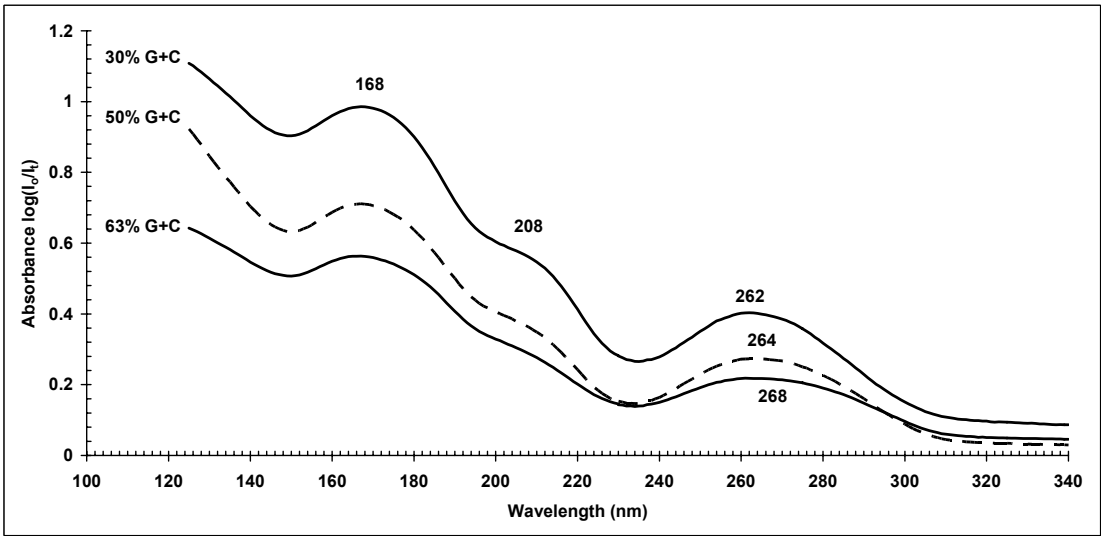

Fig. 7. VUV-UV absorption spectra of equimolar mixtures of single stranded (sense + antisense strand), synthetic oligonucleotides with 30%, 50%, 63% G+C content. The oligonucleotides are made of 60 nucleotides, having different nucleotide compositions and sequences, while encoding the same polypeptide, containing one of each of 20 amino acids.

In an attempt to further understand the relationship between base pair frequencies and absorption, we measured absorption in equimolar mixtures of single stranded (sense and antisense strands), synthetic oligonucleotides having 30%, 50% or 63% G+C content. The degeneracy of the genetic code enabled us to design 60-mer oligonucleotides with different nucleotide compositions and sequences, while encoding the same polypeptide, containing one of each of the 20 amino acids. In nature, the G+C content varies from approximately 25% to 75%[21]. Although no major differences in the absorption spectra of the different oligonucleotides were observed (Fig. 7), in region I a bathochromic shift was correlated with increasing G+C content. Thus, peak I absorption maxima increased in wavelength according to G+C content (262 nm at 30%, 264 at 50% and 268 nm at 63%). At 63% G+C, peak I was also broader. For all three oligonucleotides, region II was composed of a dominant peak at 168 nm and a shoulder at 208 nm, which was stronger with 30% G+C, weak with 50% G+C and still weaker with 63% G+C content. In the genomic DNA (salmon sperm DNA), the shoulder in region II was absent, and we observed a single, broad peak at 192 nm, probably due to extensive polymer length and nucleotide diversity. These changes correlated with G+C content might be too small to affect susceptibility to VUV-UV. Nevertheless, local sequence and G+C content, *e.g.* in noncoding, homopolymeric tracts, could influence the wavelength-dependant response to UV radiation. Overall (genomic) G+C content might have less effect.

3.2 The VUV-UV absorption properties of putative and known UV screening compounds

3.2.1. Ubiquitous, putative UV screens

Nucleotides, the monomer units of nucleic acids (DNA and RNA), play important roles in energy metabolism and cell signaling processes, in addition to their use in information storage and retrieval. Free mononucleotides are therefore abundant in cells. Adenosine 5'-triphosphate (ATP), which is necessary for intracellular energy transfer (the energy "currency" in all known living organisms), accumulates to millimolar concentrations. It is produced during photosynthesis, glycolysis and cellular respiration, and the energy stored in ATP is subsequently used in metabolic reactions. Absorption spectroscopy of mononucleotides (monophosphates and triphosphates)[8] revealed peaks in region I (135 – 232 nm) and in region II (253 – 290 nm). Among the four nucleotides, ATP had the absorption curve that best matched absorption by salmon sperm DNA, showing a peak at 261 nm (region I) and poorly resolved peaks at 159, 192 and 210 nm (region II). We therefore suggested that primitive cells might have used ATP as a UV screen, before or at the same time it was used in intracellular energy transfer[8].

Proteins are macromolecules, composed of amino acid monomers. They have catalytic, structural, mechanical and regulatory functions. Although proteins are themselves a target for UV, some proteins might directly protect DNA by altering DNA tertiary structure or by absorbing UV light. For example, histones are small, positively charged DNA-binding proteins, abundant in all eukaryotic cells. Assembled into nucleosomes, they serve in the packing of large eukaryotic genomes into compact structures that fit into nuclei. Compact DNA structures are less exposed to damaging agents. In bacteria, a DNA-packing function is attributed to proteins, termed histone-like proteins[22].

We used VUV-UV spectroscopy to examine the possibility that proteins could serve as UV screens. VUV-UV absorption spectra of histones showed the characteristic protein peak at 280 nm, but this peak was seen only in highly concentrated samples, and it was weak compared to the peaks at 192 and 170 nm (spectra presented in reference[8]). Below 150 nm, a steep increase in absorption was observed. A similar absorption curve was recorded for BSA (bovine serum protein), which is a small, neutral protein that is not known to bind DNA. We concluded that although proteins could provide UV screening protection to DNA in the VUV part of spectrum (DNA peak II), they would provide poor protection for DNA peak I (264 nm).

Nevertheless, proteins with their characteristic peak at 280 nm, might protect DNA peak I, if the DNA is rich in G+C, which can shift peak I toward higher wavelengths (see above). We therefore examinated the influence of selected amino acids on UV absorption of proteins by measuring the VUV-UV absorption spectra of selected amino acids. Valine (neutral and hydrophobic), arginine (basic) and aspartic acid (acidic) had absorption maxima in the VUV, with little absorbance above 210 nm. In contrast, tryptophan (neutral, hydrophobic and representative of the aromatic amino acids) showed a broad and complex peak at 287 nm, with a shoulder at 272 nm. At lower wavelengths, tryptophan absorbed as one broad peak, composed of fused peaks with local maxima at 214 and 200 nm, plus one well-resolved peak at 160 nm (detailed spectra are published elsewhere[8]). Aromatic amino acids (tryptophan, phenylalanine and tyrosine) would thus increase absorption in the region close to 280 nm. Therefore, proteins rich in aromatic acids could provide UV protection for DNA, particularly in DNA segments with high G+C content.

Polyamines are small organic molecules, containing two or more primary amino groups. They are ubiquitous in all prokaryotic and eukaryotic cells, and they play important roles in the regulation of cell growth and differentiation. The major cellular polyamines are putrescine, spermidine and spermine[23, 24, 25]. At physiological pH, polyamines are cationic molecules that interact with negatively charged nucleic acids, proteins and phospholipids[25]. They bind DNA *in vitro*, neutralizing negative charges on the phosphate groups. Polyamines thus enable folding of DNA, and they stabilize condensed DNA[23, 26]. Polyamines accumulate in cells as a result of abiotic and biotic stresses[24, 25]. In plants, their synthesis is induced by UV-B[27] and UV-C radiation[25]. Like histones, polyamines could protect DNA by stabilizing and compacting it. We therefore examined the UV screening potential of polyamines.

Putrescine, spermidine and spermine absorbed only in the VUV, with a steep increase in absorption at 200 nm and continuously high absorption through the VUV[8]. Thus, polyamines could act as UV screens only in the VUV part of the spectrum, protecting DNA in regions II and III. However, in addition to these aliphatic amines, we measured the absorption of tyramine, an aromatic amine that occurs in prokaryotic and eukaryotic organisms. Beside strong absorption in the VUV, with peaks at 170 nm and 198 nm and a shoulder at 221, tyramine absorbed strongly at 282 nm, with a shoulder at 267 nm (see published spectra[8]). We concluded that tyramine could serve as a UV screen, protecting DNA in all three regions. Beside their free forms, tyramine and polyamines occur in plants as conjugates with hydroxycinnamic acid and its derivatives[25, 28]. These organic acids carry an aromatic ring, which is an efficient absorber in the VUV and UV-C regions[8], thus improving the potential UV screening capacities of the conjugated forms of polyamines, particularly in region I.

3.2.2. Specialized UV screens

Scytonemin is a yellow-brown, lipid-soluble, extracellular pigment, found in cyanobacterial sheaths[12, 29, 30]. Cyanobacteria belong to an ancient phylogenic group of phototrophic organisms. Their microfossils date as far back as, at least, 2.5 Gyr ago. They are the only known phototrophic prokaryotes capable of carrying out plant-like photosynthesis[31]. Since cyanobacteria require visible light as a source of energy, we can assume that their ancestors had to cope with UV radiation on primitive Earth. UV screening compounds, such as scytonemin, help present day cyanobacteria to deal with the current UV environment. Synthesis of scytonemin is induced by UV-A, and scytonemin accumulates at concentrations up to 5% of the cellular dry weight[29]. Scytonemin is dimeric, made up of indolic and phenolic subunits. The reported absorption spectrum of scytonemin in solution shows strong absorption in the UV-A, with a maximum at 386 nm. However, significant absorbance was observed in the UV-B (peak at 300 nm) and in the UV-C (peaks at 278 and 252 nm[30]). Our absorption study[16] of scytonemin in thin films extended these spectra into the VUV-UV, showing a relatively small peak at 253 nm and a well-resolved peak at 195 nm. Comparing this to the DNA spectrum, we concluded that scytonemin would provide efficient protection to the DNA in regions III and region II (peak at 192 nm), but the DNA peak at 264 nm (region I) would remain unprotected, unless it were shifted to longer wavelengths.

Photosynthesis is also sensitive to UV. Photosynthetic pigments, including chlorophyll a and b, are bleached by UV light[31]. Therefore, we compared VUV-UV absorption by scytonemin and chlorophylls a and b (Fig. 8). Chlorophyll a had peaks at 295 and 193 nm, with an inflection at 250 nm, while chlorophyll b showed peaks at 308 and 258 nm, with an inflection at 228 nm and a peak at 195 nm. Both chlorophylls showed increased absorption toward the upper (340 nm) end of the spectrum and a steep increase in absorption toward the lower end (125 nm). The scytonemin UV absorption curve matched both the chlorophyll a and b curves, indicating that scytonemin would provide efficient UV protection (Fig. 8). Absorption spectra (measured in ethanol) in the visible region showed peaks at 410 and 660 nm for chlorophyll a and 450 and 655 nm for chlorophyll b (data not shown). Scytonemin, with its broad peak at 386 nm, would partially mask the chlorophyll peak at 410 nm, but harvesting of some solar energy should still be possible. This overlap could reduce the effectiveness of scytonemin.

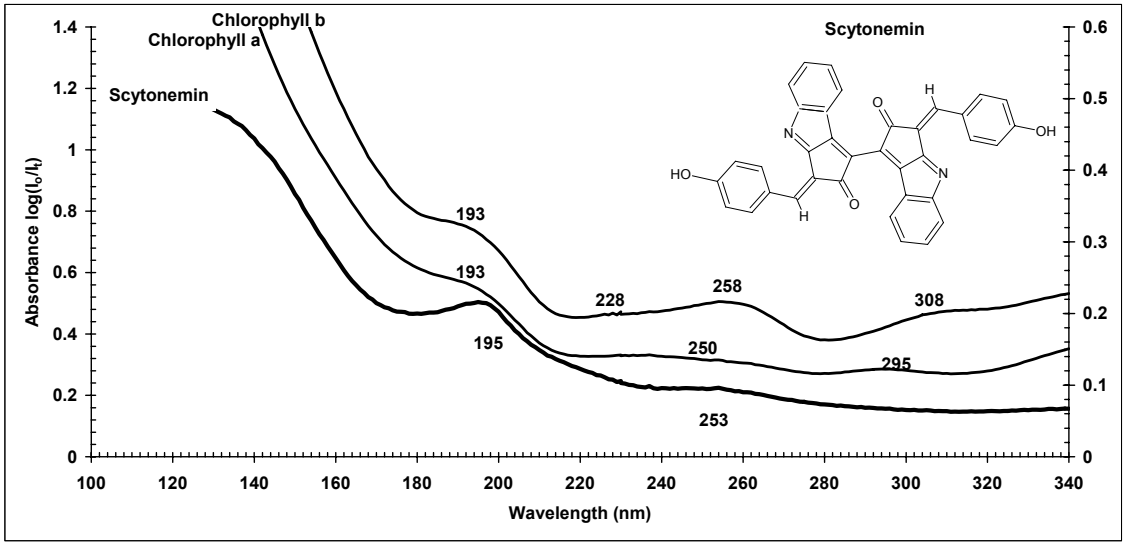

Fig. 8. VUV-UV absorption spectra for chlorophyll a and chlorophyll b, compared to the absorption spectrum for scytonemin. (The absorption spectrum of scytonemin is taken from reference [16].)

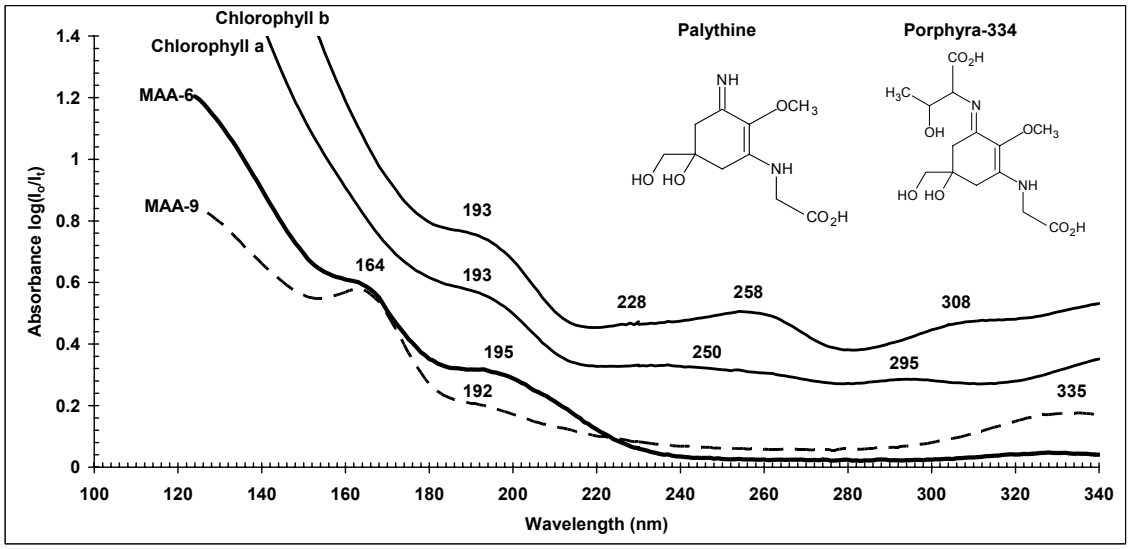

Fig. 9. VUV-UV spectra for chlorophyll a and chlorophyll b, compared to the absorption spectra of two mycosporine-like amino acid extracts: MAA-6 (containing palythine) and MAA-9 (essentially containing porphyra-334). (The absorption spectra of MAA-6 and MAA-9 are taken from reference[16].)

Mycosporine-like amino acids (MAAs) are a group of intracellular, water-soluble, colorless compounds, which are found in taxonomically diverse organisms, such as cyanobacteria, marine heterotrophic bacteria, eukaryotic algae, fungi, marine invertebrates, fish and other marine organisms[12, 29, 32]. MAAs consist of either a cyclohexenone or a cyclohexenimine ring, conjugated to the nitrogen of an amino acid or its imino alcohol. They are reported to have single absorption maxima in the range of 310-360 nm[29, 32]. The synthesis of MAAs is induced by UV-B, while visible light and UV-A have no significant impact on accumulation[33]. The MAAs occur at up to 1% of the dry weight[29]. The VUV-UV absorption spectra for two MAAs, porphyra-334 and palythine (which were isolated from the marine red alga, *Corallina officinalis*), showed qualitative similarity[16]. Porhyra-334 had a peak at 335-340 nm region, a weak peak at 192 nm and a

well-resolved peak at 164 nm, while palythine had a weak peak at 330 nm and peaks at 195 and 164 nm (spectra published elsewhere[16]). The MAAs should thus protect DNA from damage in VUV, preventing absorptions by DNA in region II and III, but the DNA peak at 264 nm (region I) would be unprotected, since MAAs showed minimal absorption between 230 and 300 nm. Therefore, MAAs would not provide sufficient protection against the full spectrum of solar UV, unless they were complemented by other UV screens, such as scytonemin. MAAs would protect chlorophylls a and b from VUV radiation, but not from UV-C (Fig. 9). Since MAAs do not absorb in the visible part of the solar spectrum, they would not interfere with photosynthesis.

Carotenoids are lipid-soluble pigments, synthesized by plants, algae and some bacteria[12]. They are terpenoids, made up of a polyene chain, terminated by rings. They are frequently associated with cellular membranes, such as chloroplast thylakoids. Their absorption maxima occur mainly in the visible part of the spectrum, with an extension into the UV-A[30]. It appears that they play an indirect role in UV protection, acting as anti-oxidants and scavengers of reactive oxygen species and other free radicals[12, 29]. A VUV-UV absorption spectrum for β-carotene showed a minor peak at 277 nm and a well-resolved peak at 195 nm, with steeply increasing absorption toward the lower wavelengths[16]. Compared to the absorption curve of DNA, that of β-carotene suggests protection of DNA only in the VUV, while the DNA peak at 264 nm would remain unprotected. Similarly, β-carotene would protect chlorophylls a and b only in the VUV region. Measurements of absorption in the visible part of the spectrum showed a complex, broad peak between 430 and 480 nm for β-carotene in ethyl acetate, which could partially mask the chlorophyll a peak at 410 nm and entirely mask the chlorophyll b peak at 450 nm (Fig. 10). Carotenoids can transfer light energy to the chlorophylls, contributing to photosynthesis as accessory pigments[34].

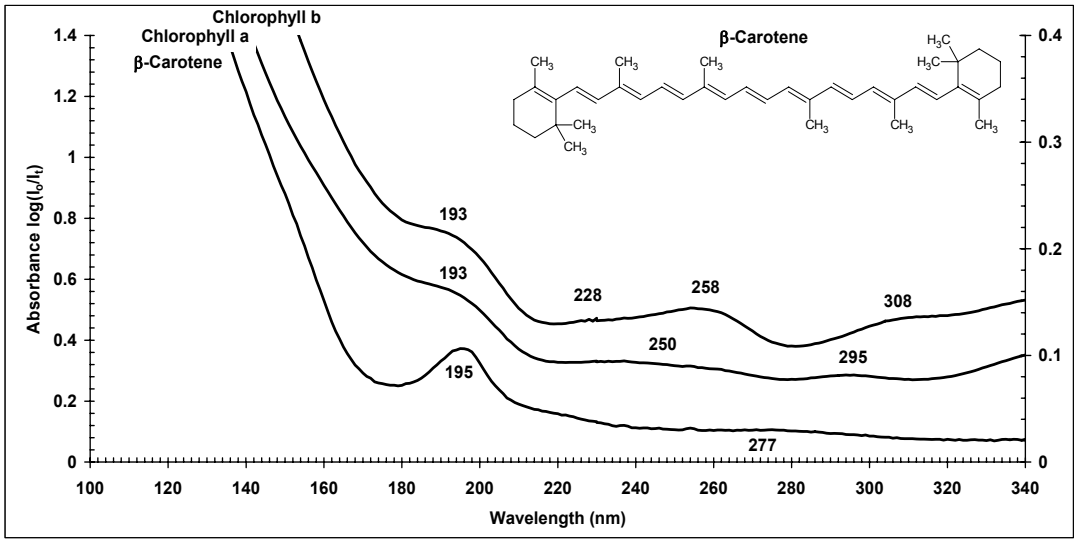

Fig. 10. VUV-UV spectra of chlorophyll a and chlorophyll b, compared to the absorption spectrum of β-carotene. (The absorption spectrum of β-carotene is adapted from reference[16].)

Melanins are found in animals, fungi, higher plants and in some bacteria[31]. There are two classes of melanins: eumelanin (brown-black) and pheomelanin (yellow-reddish)[35]. They are produced by the enzymatic oxidation of tyrosine, and they are highly irregular polymeric compounds, containing indolic subunits, known in eumelanin as 5,6-dihydroxyindole (DHI) and 5,6-dihydroxyindole-2-carboxylic acid (DHICA)[35, 36]. Melanins occur in large aggregates, frequently associated with proteins and lipids[12, 36, 37]. Although they are constitutive pigments, their synthesis and accumulation is induced in response to UV radiation. Eumelanins have strong broad band absorption in the UV and visible regions. They are efficient anti-oxidants and free radical scavengers[37]. Our VUV-UV spectra of dry films of synthetic melanin showed continuous absorption with small, unresolved peaks at 161 and 186 nm and an exponential increase of absorption at wavelengths below 145 nm[16]. High complexity in their structure could explain the lack of spectral features[37]. We can conclude that melanins could provide efficient, but not specific, protection to DNA throughout the UV and particularly VUV regions.

Flavonoids represent a large group of plant polyphenolic substances that are derived from phenylalanine and synthesized through the phenylpropanoid metabolic pathway[38, 39]. Flavonoids are characterized by a three-ring structure, the flavan ring, which contains two aromatic rings linked through a heterocyclic pyrone ring. Various types of flavonoids are created by substitutions to the flavone ring, including hydroxyl groups, methyl groups, oxygen and sugars. Their synthesis is induced by UV-A and UV-B radiation[12, 38]. Flavonoids accumulate in cell vacuoles and walls[12, 39]. They are involved in a wide range of biological functions, including signaling between plants and soil bacteria, and they play important roles in mechanisms of resistance to biotic and abiotic stress[38]. Flavonoids occur in relatively high concentrations in seeds, where they accumulate in seed coats. Quercitrin (quercetin-3-*O*-rhamnoside), the dominant flavonoid in *Arabidopsis* seeds, reaches a concentration of 3.6 mg g^{-1} of seeds[40].

Flavonoids are efficient UV screens in the UV-A and UV-B[12, 38, 39]; they also have protective functions as antioxidants and free radical scavengers[12, 39]. VUV-UV spectra of glycosilated flavonoids (quercetrin, isoquercitrin and robinin) show remarkable similarity to DNA spectra[16]. Quercitrin and isoquercitrin showed prominent and broad peaks with a maximum at 204 nm, while robinin had a maximum at 199 nm. They would thus protect DNA peak II. In addition, all three glycosilated flavonoids would efficiently protect DNA peak I, since quercitrin and isoquercitrin showed broad peaks at 258 nm and a shoulder at 270 nm, while robinin had a broad peak at 269 nm. We observed that absorption by all three flavonoids increased toward the high wavelength end of the spectrum (340 nm), and a peak at 355 nm was confirmed by conventional solution spectroscopy (unpublished data). We concluded that glycosilated flavonoids would act as ideal UV screens, providing protection throughout the VUV-UV.

We also measured the absorption of catechin, which is the aglycone monomer of the condensed tannins. The VUV-UV absorption spectrum[16] showed a strong, broad peak at 204 nm and a shoulder at 230 nm, indicating that catechin would screen UV in region II. Since we observed a minimum of absorption at 256 nm and a peak at 280 nm, we concluded that catechin would not be an efficient UV screen for DNA, but it could provide UV protection to proteins. In addition, conventional solution spectroscopy and spectroscopy of dry films revealed that catechin does not absorb wavelengths above 300 nm (unpublished results). Catechin and tannins (polymers of catechin), known to be antioxidants and free radical scavengers, could play important roles in coping with UV, because they are generally found in combination with other flavonoids.

Flavonoids could protect chlorophyll pigments against UV damage. Comparing VUV-UV spectra for flavonoids and those for chlorophylls a and b (Fig. 11), it would seem that glycosilated flavonoids would protect both chlorophylls a and b in the VUV and UV-C, but they would provide weaker protection in UV-B. Catechin would be less suited to protect chlorophylls a and b, except in the region close to the VUV. Since the flavonoids we studied do not absorb visible light, they should not interfere with photosynthesis.

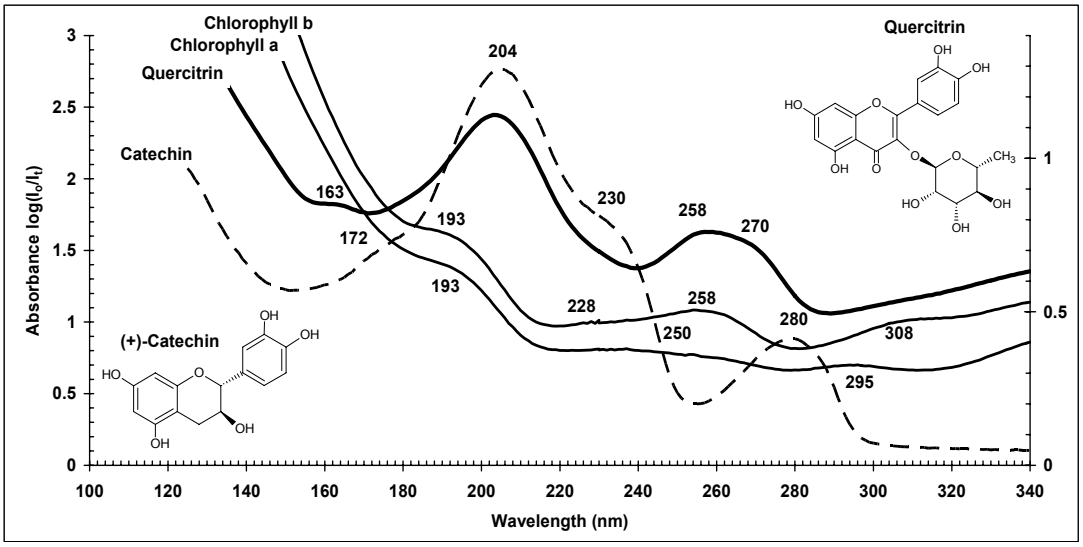

Fig. 11. VUV-UV absorption spectra for chlorophyll a and chlorophyll b, compared to the absorption spectra of two flavonoids, quercitrin (glycosilated flavonoid) and catechin (aglycone flavonoid), both found in seeds. (The absorption spectra of quercitrin and catechin are adapted from reference[17].)

4. CONCLUSION AND PERSPECTIVES

The surface of early Earth was likely exposed to a high flux of short wavelength solar UV until photosynthesis produced enough oxygen for a significant ozone layer to form. Organisms evolved various mechanisms to resist UV, including the synthesis of screens that absorb incident UV light and dissipate it away from potential cellular targets, such as DNA. We used synchrotron radiation to determine the UV absorption spectra of DNAs with different G+C contents, and we measured the absorption spectra of putative and known UV-screens, isolated from phylogenetically distinct groups of organisms. These spectra, which included the VUV, the UV-C, the UV-B and part of the UV-A, allowed us to compare the potential of these natural substances to protect DNA.

Since most solvents absorb UV light below 200 nm, absorption spectra were determined under vacuum, and the samples were prepared as thin dry films. Synchrotron light allowed us to extend spectra down to 125 nm in the VUV region. (Absorption had generally not been studied below 200 nm.) These VUV-UV absorption spectra revealed that differences in total G+C content in synthetic, protein encoding DNA had small effects on the absorption spectra, while the extreme G+C content of synthetic homopolymeric DNA tracts, known to occur in genomic DNA, had more of an influence. Thus we propose that local nucleotide sequence and G+C content might alter UV absorption in noncoding regions of genomic DNA, where sequences are often repeated. Adaptation of DNA sequences to particular UV environments and UV screens could be a function of this noncoding "junk" DNA in higher organisms (which represents 80-90% of the human genome). Genomes could thus be designed with altered UV absorbing characteristics due to the inclusion of repeated sequences. This hypothesis can be tested using synthetic DNA fragments.

Comparing the VUV-UV spectra of DNA and the spectra of substances that we considered putative UV screens, we found that DNA would be best protected by free nucleotides, particularly by adenosine 5'-triphosphate (ATP), present in high concentrations in cells. Thus, in primitive cells, beside its role in energy transfer and its role as a precursor in the synthesis of nucleic acids, ATP might have functioned as a UV screen. Among previously defined, specialized UV screens, we single out flavonoids, because their VUV-UV absorption spectra closely resemble that of DNA. Flavonoids could be ideal UV screens for DNA, but this attribute is no longer required on Earth, thanks to the ozone layer. Flavonoids might represent a relic from early evolution, prior to the full oxygenesis of the atmosphere. If this is true, how did they get into higher plants? We suggest that they came from the endosymbiotic organisms that were the precursors to current chloroplasts[16]. Whatever the origin of the flavonoids, perturbation of the ozone layer, *e.g.* as a result of Man's activities, would require reinforcement of UV protection, particularly for plants, which provide biological energy through photosynthesis. Flavonoid accumulation could be engineered into a variety of organisms to make them more resistant to short wavelength UV and dispersal through space.

In addition to their spectroscopic properties, the UV protective role of flavonoids was demonstrated in experiments *in vivo*, using *Arabidopsis thaliana* seeds (manuscript in preparation) [41]. In plant seeds, flavonoids accumulate in the seed coat, protecting the embryo and its genomic DNA from damaging UV radiation. Germination of wild type *Arabidopsis* seeds was not reduced after exposure to the monochromatic UV-C light (254 nm) at doses up to 2.28×10^5 kJ/m^2. In contrast, germination of a mutant that is deficient in flavonoids was inhibited by UV (254 nm), at the doses 100 times lower than those applied to wild type seeds. Similarly, experiments where *Arabidopsis* seeds were exposed to polychromatic UV (200-400 nm) at total doses up to 3×10^3 kJ/m^2, showed that mutant seeds were particularly sensitive, compared to wild type seeds. Removal of the seed coat from both mutant and wild type embryos increased their sensitivity to UV (254 nm). Exposure of mutant seeds to UV (254 nm), filtered through dry layers of different flavonoids, showed that flavonoids can improve the resistance of mutant seeds to UV (manuscript in preparation)[41].

The remarkable resistance of plant seeds to stress, including high doses of UV, makes them valuable terrestrial models for studying the possibility of transfer of life through space[42]. In order to further evaluate the resistance of seeds to the full spectrum of solar light, we are currently preparing long exposure experiments in space. Seeds and dry layers of purified UV screens will be exposed to the space environment for 18 months. These experiments are part of the EXPOSE photobiology/exobiology research project, supported by the European Space Agency (ESA), and they will take place on the exterior of the International Space Station (ISS), beginning in late 2007. Better knowledge of how terrestrial life deals with UV will hopefully contribute to identifying protective agents that can be manipulated through genetic engineering to better protect organisms from solar UV, both on Earth and in space. The ability of dormant forms of life to withstand UV light and other conditions in space supports the concept of panspermia, which requires that life be dispersed through space.

ACKNOWLEDGMENTS

Financial support was provided by the Centre National d'Etudes Spatiales (CNES) and the University of Aarhus (EC Integrated Activity on Synchrotron and Free electron Laser Science, contract number R113-CT-2004-50608). We warmly thank Nykola C. Jones for her efficient help in the storage ring experiments. We are grateful to Richard W. Castenholz for providing the UV-A induced *Chroococcidiopsis* cyanobacteria cells as a source of scytonemin and D.-P. Häder for providing us MAA extracts. We kindly thank Lucien Kerhoas for the mass spectrometry analysis.

REFERENCES

1. Y. Amelin, A. N. Krot, I. D. Hutcheon and A. A. Ulyanov, "Lead isotopic ages of chondrules and calcium-aluminum-rich inclusions," *Science* **297** (5587), 1678-1683 (2002)
2. S. J. Mojzsis, G. Arrhenius, K. D. McKeegan, T. M. Harrison, A. P. Nutman and C. R. L. Friend, "Evidence for life on Earth before 3,800 million years ago," *Nature* **384**, 55-59 (1996)
3. A. C. Allwood, M. R. Walter, B. S. Kamber, C. P. Marshall and I. W. Burch, "Stromatolite reef from the early Archaean era of Australia," *Nature* **441**, 714-718 (2006)
4. S. Leach, I. W. M. Smith and C. S. Cockell, "Introduction: conditions for the emergence of life on the early Earth," *Phil. Trans. R. Soc. London B* **361**, 1675-1679 (2006)
5. R. E. Summons, L. L. Jahnke, J. M. Hope and G. A. Logan, "2-Methylhopanoids as biomarkers for cyanobacterial oxygenic photosynthesis," *Nature* **400**, 554-557 (1999)
6. D. J. Des Marais, "When did photosynthesis emerge on Earth?," *Science* **289**(5485), 1703-1705 (2000)
7. C. S. Cockell, "Biological effects of high ultraviolet radiation on early Earth – a theoretical evaluation," *J. Theor. Biol.* **193**, 717-729 (1998)
8. A. Zalar, D. Tepfer, S. V. Hoffmann, J. M. Kenney and S. Leach, "Directed exospermia: I. Biological modes of resistance to UV light are implied through absorption spectroscopy of DNA and potential UV screens," *Int. J. Astrobiol.* **6**(3), 229-240 (2007)
9. A. B. Britt, "DNA damage and repair in plants," *Annu. Rev. Plant Physiol. Plant Mol. Biol.* **47**, 75-100 (1996)
10. N. Tuteja, M. B. Singh, M. K. Misra, P. L. Bhalla and R. Tuteja, "Molecular mechanisms of DNA damage and repair: Progress in plants," *Crit. Rev. Biochem. Mol. Biol.* **36**(4), 337-397 (2001)
11. R. P. Sinha and D.-P. Häder, "UV-induced DNA damage and repair: a review," *Photochem. Photobiol. Sci.* **1**, 225-236 (2002)
12. C. S. Cockell and J. Knowland, "Ultraviolet radiation screening compounds," *Biol. Rev*. **74**, 311-345 (1999)
13. Y Gauslaa and E. M. Ustvedt, "Is parietin a UV-B or a blue-light screening pigment in the lichen *Xanthoria parietina*?," *Photochem. Photobiol. Sci*. **2**, 424-432 (2003)
14. F. Garcia-Pichel, C. E. Wingard and R. W. Castenholz, "Evidence regarding the UV sunscreen role of mycosporine-like compound in the cyanobacterium *Gleocapsa sp*.," *Appl. Environ. Microbiol.* **59**(1), 170-176 (1993)
15. S. Eden, P. Limão-Vieira, S. V. Hoffmann and N. J. Mason, "VUV photoabsorption in CF_3X (X = Cl, Br, I) fluoro-alkanes," *Chem. Phys.* **323**, 313-333 (2006)
16. A. Zalar, D. Tepfer, S. V. Hoffmann, A. Kollmann and S. Leach, "Directed exospermia: II. VUV-UV spectroscopy of specialized UV screens, including plant flavonoids, suggests using metabolic engineering to improve survival in space," *Int. J. Astrobiol.* In press (2007)
17. K. Hieda, Y. Hayakawa, A. Ito, K. Kobayashi and T. Ito, "Wavelength dependence of the formation of single-strand breaks and base changes in DNA by the ultraviolet radiation above 150 nm," *Photochem. Photobiol.* **44**(3), 379-383 (1986)
18. E. Chargaff, R. Lipshitz, C. Green and M. E. Hodes, "The composition of the desoxyribonucleic acid of salmon sperm," *J. Biol. Chem.* **192**, 223-230 (1951)
19. K. J. Dechering, K. Cuelenaere, R. N. H. Konings and J. A. M. Leunissen, "Distinct frequency-distributions of homopolymeric DNA tracts in different genomes," *Nucl. Acids. Res.* **26**(17), 4056-4062 (1998)
20. D. L. Mitchell, J. Jen and J. E. Cleaver, "Sequence specificity of cyclobutane pyrimidine dimers in DNA treated with solar (ultraviolet B) radiation," *Nucl. Acids Res.* **20**(2), 225-229 (1992)
21. N. Sueoka, "On the genetic basis of variation and heterogeneity of DNA base composition," *Proc. Natl. Acad. Sci. USA* **48**(4), 582-592 (1962)
22. K. Drlica and J. Rouviere-Yaniv, "Histonlike proteins of bacteria," *Microbiol. Rev.* **51**(3), 301-319 (1987)

23. C. W. Tabor and H. Tabor, "Polyamines," *Ann. Rev. Biochem.* **53**, 749-790 (1984)
24. T. A. Smith, "Polyamines," *Ann. Rev. Plant Physiol.* **36**, 117-143 (1985)
25. J. Martin-Tanguy, "Metabolism and function of polyamines in plants: recent development (new approaches)," *Plant Growth Regul.* **34**, 135-148 (2001)
26. I. Flink and D. E. Pettijohn, "Polyamines stabilise DNA folds," *Nature* **253**, 62-63 (1975)
27. L. Z. An, G. X. Liu, M. X. Zhang, T. Chen, Y. H. Liu, H. Y. Feng, S. J. Xu, W. Y. Qiang and X. L. Wang, "Effect of enhanced UV-B radiation on polyamine content and membrane permeability in cucumber leaves," *Russian J. Plant Physiol.* **51**(5), 658-662 (2004)
28. J. Martin-Tanguy, "The occurence and possible function of hydroxycinnamoyl acid amides in plants," *Plant Growth Regul.* **3**, 381-399 (1985)
29. R.W. Castenholz and F. Garcia-Pichel, *The Ecology of Cyanobacteria*, 591-611, Kluwer Academic Publishers, Dordrecht, 2000
30. P. J. Proteau, W. H. Gerwick, F. Garcia-Pichel and R. Castenholz, "The structure of scytonemin, an ultraviolet sunscreen pigment from the sheaths of cyanobacteria," *Experientia* **49**, 825-829 (1993)
31. F. Garcia-Pichel, "Solar ultraviolet and the evolutionary history of cyanobacteria," *Orig. Life Evol. Biosphere* **28**, 321-347 (1998)
32. J. M. Shick and W. C. Dunlap, "Mycosporine-like amino acids and related gadusols: Biosynthesis, accumulation, and UV-protective functions in aquatic organisms," *Annu. Rev. Physiol.* **64**, 223-262 (2002)
33. R. P. Sinha, M. Klisch, E. W. Helbling and D.-P. Häder, "Induction of mycosporine-like amino acids (MAAs) in cyanobacteria by solar ultraviolet-B radiation," *J. Photochem. Photobiol. B: Biol.* **60**, 129-135 (2001)
34. B. Ke, Photosynthesis: Photochemistry and Photobiophysics, 229-250, Kluwer Academic Publishers, Dordrecht, 2001
35. K. Wakamatsu and S. Ito, "Advanced chemical methods in melanin determination," *Pigment Cell Res.* **15**, 174-183 (2002)
36. A. Pezzella, A. Napolitano, M. d'Ischia, G. Prota, R. Seraglia and P. Traldi, "Identification of partially degraded oligomers of 5,6-dihidroxyindole-2-caboxylic acid in *Sepia* melanin by matrix-assisted laser desorption/ionization mass spectrometry," *Rapid Comun. Mass Spectrom.* **11**, 368-372 (1997)
37. P. Meredith, B. J. Powell, J. Riesz, S. Nighswander-Rempel, M. R. Pederson and E. Moore, "Towards structure-property-function relationships for eumelanin," *Soft Matter* **2**(1), 37-44 (2006)
38. R. A. Dixon and N. L. Paiva, "Stress-induced phenylpropanoid metabolism," *The Plant Cell* **7**, 1085-1097 (1995)
39. A. J. Parr and G. P. Bolwell, "Phenols in the plant and in man. The potential for possible nutritional enhancement of the diet by modifying the phenols content or profile," *J. Sci. Food Agric.* **80**, 985-1012 (2000)
40. J-M. Routaboul, L. Kerhoas, I. Debeaujon, L. Pourcel, M. Caboche, J. Einhorn and L. Lepiniec, "Flavonoid diversity and biosynthesis in seed of *Arabidopsis thaliana*," *Planta* **224**(1), 96-107 (2006)
41. A. Zalar, "Résistace des graines *d'Arabidopsis* aux UV et à d'autres conditions néfastes dans l'espace," Diplôme d'études supérieures de sciences, Université Pierre et Marie Curie Paris 6 (2004)
42. D. Tepfer and S. Leach, "Plant seeds as model vectors for the transfer of life through space," *Astrophys. Space Sci.* **306**, 69-75 (2006)

Article 4

Chaudhuri K, Das S, Bandyopadhyay M, Zalar A, Kollmann A, Jha S and Tepfer D (2009) Transgenic mimicry of pathogen attack stimulates growth and secondary metabolite accumulation, *Transgenic Research* 18(1): 121-134

Transgenic Res (2009) 18:121–134
DOI 10.1007/s11248-008-9201-8

ORIGINAL PAPER

Transgenic mimicry of pathogen attack stimulates growth and secondary metabolite accumulation

Kuntal Chaudhuri · Sudripta Das · Moumita Bandyopadhyay · Andreja Zalar · Albert Kollmann · Sumita Jha · David Tepfer

Received: 18 January 2008 / Accepted: 24 June 2008 / Published online: 31 July 2008

Abstract Plant secondary metabolites, including pharmaceuticals, flavorings and aromas, are often produced in response to stress. We used chemical inducers of the pathogen defense response (jasmonic acid, salicylate, killed fungi, oligosaccharides and the fungal elicitor protein, cryptogein) to increase metabolite and biomass production in transformed root cultures of the medicinal plant, *Withania somnifera*, and the weed, *Convolvulus sepium*. In an effort to genetically mimic the observed effects of cryptogein, we employed *Agrobacterium rhizogenes* to insert a synthetic gene encoding cryptogein into the roots of *C. sepium*, *W. somnifera* and *Tylophora tanakae*. This genetic transformation was associated with stimulation in both secondary metabolite production and growth in the first two species, and in growth in the third. In whole plants of *Convolvulus arvensis* and *Arabidopsis thaliana*, transformation with the cryptogein gene led, respectively, to increases in the calystegines and certain flavonoids. A similar transgenic mimicry of pathogen attack was previously employed to stimulate resistance to the pathogen and abiotic stress. In the present study of biochemical phenotype, we show that transgenic mimicry is correlated with increased secondary metabolite production in transformed root cultures and whole plants. We propose that natural transformation with genes encoding the production of microbial elicitors could influence interactions between plants and other organisms.

Keywords Cryptogein · Flavonoids · *Withania* · *Tylophora* · *Convolvulus* · *Calystegia*

K. Chaudhuri · S. Das · M. Bandyopadhyay · S. Jha
Department of Botany, University of Calcutta, 35 Ballygunge Circular Road, Calcutta 700019, India

Present Address:
K. Chaudhuri
Department of Botany, Vivekananda College, 269 Diamond Harbour Road, Calcutta 700063, India

Present Address:
S. Das
Department of Biotechnology, Tea Research Association, Tocklai, Jorhat 785008, Assam, India

A. Zalar · A. Kollmann · D. Tepfer (✉)
Biologie de la Rhizosphère, Institut National de la Recherche Agronomique, Versailles Cedex 78026, France
e-mail: tepfer@versailles.inra.fr

Introduction

Plant secondary metabolites are the origin of many, if not most, of our pharmaceuticals, flavorings and aromas. Plants have a privilaged access to energy through photosynthesis; they can thus afford to synthesize a wide spectrum of exotic chemicals to aid their survival. Plant secondary metabolites are essential to functions ranging from allelopathy to resistance to UV light and biological aggression. Given the opportunistic nature of evolution, it is not

surprising that a single substance serves in several functions. For instance, the calystegines are nutritional mediators of plant/bacteria interactions (Tepfer et al. 1988), and they are potent glycosidase inhibitors (Molyneux et al. 1993), implicated in allelopathy directed at other plants and probably at animals, as well. Flavonoids are antioxidants, phytoalexins and UV protectors (Li et al. 1993; Harborne and Williams 2000; Pietta 2000). Thanks to the chemical and functional diversity of plant secondary metabolites, a given medicinal plant can be used for treating a variety of animal ailments, and plants form the basis of our pharmacopia.

Many medicinal plants are poorly adapted to mass cultivation, and the active ingredients they produce are too complex to synthesize in large quantities. Therefore, natural populations are under pressure from human harvesting (Shinwari and Gilani 2003; Olsen 2005). Genetic methods can be applied to increase the production of a given metabolite or a group of related compounds, e.g. via traditional breeding and screening (Buter et al. 1998; Long et al. 2006), through the expression of genes encoding key enzymes (Holmberg 1997; Dueckershoff et al. 2005; Tian and Dixon 2006; Inui et al. 2007; Liu et al. 2007) or through functional genomics (Goossens et al. 2003), but despite these successes, metabolic engineering of the relevant biosynthetic pathways is often hampered by a lack of knowledge of the enzymes and genes involved. Indirect approaches to improving metabolite production have thus been explored, including treating whole plants and in vitro cultures of organs or cells with inducers of plant defense responses, since the reaction to both biotic and abiotic stress can include increased accumulation of secondary metabolites (Lin and Wu 2002; Ye et al. 2004; Matthews et al. 2005; Wolucka et al. 2005; Zhao et al. 2005; Zobayed et al. 2005; Shi et al. 2007; Zhang and Fevereiro 2007).

Another indirect genetic approach has yielded increases in secondary metabolite production in a variety of species. Genetic transformation by the Ri TL-DNA of *Agrobacterium rhizogenes* produces roots that can be cultured in vitro (Tepfer and Tempé 1981; Tepfer 1984), which often show high accumulation of secondary metabolites (Flores et al. 1987; Jung and Tepfer 1987; Guillon et al. 2006). Furthermore, plants regenerated from transformed roots have profuse root systems, and they are easy to root by cutting (Tepfer 1983a, b, 1984). They could be used to improve secondary metabolite (or protein) production via plants grown in hydroponics or aeroponics. The morphological and physiological changes caused by the Ri T-DNA are similar in many dicot species (Tepfer 1984, 1989); thus, Ri T-DNA might be used to improve secondary metabolite production in multiple species, without knowledge of the underlying enzymology and genetics. In the following paper, we employ this transformation by *A. rhizogenes* in combination with another indirect genetic approach, which relies on transformation by a gene encoding a fungal elicitor.

β-cryptogein (Crypt) is a sterol scavenging protein secreted by the oomycite, *Phytophthora cryptogea* (Ricci et al. 1989; Boissy et al. 1996; Mikes et al. 1997). It elicits a defense response in tobacco through interaction with a receptor, followed by signal transduction, which leads to the expression of a transcription factor (Lecourieux et al. 2002; Guo et al. 2004; Kasparovsky et al. 2004; Lochman et al. 2005; Ren et al. 2006), which in turn is thought to be responsible for a generalized stress response. Knowledge of the amino acid sequence of the Crypt protein (Ricci et al. 1989) allowed the synthesis of a *crypt* gene, whose expression in *Escherichia coli* led to the production of Crypt protein that induced (in tobacco) the necrosis associated with the defense response (O'Donohue et al. 1995). Genetic transformation of tobacco with this synthetic gene, under the control of the 35S CaMV promoter, rendered two independent lines of tobacco plants resistant to *P. parasitica* var. *nicotianae* (Tepfer et al. 1998). Resistance was transmitted to progeny via meiosis, and it was higher in hemizygotes than in homozygotes. A lysine to valine mutation (K13V) at amino acid position 13 was also associated with resistance in hemizygotes in two lines. Presence of the Crypt protein was shown by immunoblot.

A similar transformation of tobacco was made using a natural *crypt* gene cloned from *Phytophthora cryptogea*, controlled by the promoter from the plant gene *hsr203J*, which is induced by pathogen attack (Keller et al. 1999). A resistance response was reported, although in a single transformed line, and transmission of the transformed phenotype through meiosis was not shown. However, resistance was detected against three other fungal pathogens. In a third rendition of this experiment (Jiang et al. 2002,

2004), a mutated *crypt* gene (K13V) was controlled by a rice phenylalanine ammonia-lyase promoter. Resistance was reported in transgenic tobacco to *Phytophthora parasitica*, *Alternaria alternata* and *Pseudomonas syringae*. In addition, transgenic plants were tolerant to salt.

In all, three different promoters were used, and the coding sequence was introduced in synthetic, natural and mutated forms. Resistance was observed in tobacco, using five pathogens and one abiotic stress. Thus, the principle of transgenetic mimicry of pathogen attack, leading to a generalized stress response, is established for the *crypt* gene in tobacco; however, the biological basis for the resistance is not known. Physiological correlates have been examined, including production of reactive oxygen species and the role of nitric oxide (Foissner et al. 2000; Lamotte et al. 2004; Planchet et al. 2006; Ashtamker et al. 2007). Crypt (as well as other elicitors) induced a transcription factor (OPBP1), probably responsible for the activation of multiple genes involved in stress responses, including genes involved in resistance to fungal pathogens (Guo et al. 2004). There was thus ample reason to expect the expression of *crypt* to lead to increased accumulation of some secondary metabolites.

In an effort to predict the effects of the *crypt* gene, before using it in transformation, we treated transformed root cultures (carrying just Ri T-DNA) with the cryptogein protein (Crypt), as well as with known chemical elicitors and a killed strain of *P. parasitica* var. *nicotianae*, which makes no known protein elicitor for tobacco. Effects on root growth and accumulation of withanoferin A in *W. somnifera* and calystegines in *C. sepium* were recorded. Withaferin A is steroidal lactone that resembles the ginsenosides in structure and medicinal use. Calystegines are potent glucosidase inhibitors and nutritional mediators in plant-bacteria interactions (Tepfer et al. 1988a; Goldmann et al. 1993; Molyneux et al. 1993).

In a test of the hypothesis that the gene encoding cryptogein (*crypt*) could also increase metabolite production via production of the Crypt protein *in planta*, the synthetic gene was introduced into the roots of *W. somnifera*, *C. sepium* and *Tylophora tanakae*, also transformed by *A. rhizogenes*. The roots in these experiments were transformed by *A. rhizogenes* to facilitate growth in vitro and to measure possible gain in metabolite production from elicitation by genetic mimicry in combination with transformation by Ri T-DNA.

The *crypt* gene was also transformed into whole plants. Morning glory (*Convolvulus arvensis*), was co-transformed with *crpt* and Ri T-DNA, and *A. thaliana* was transformed by *crypt* without Ri T-DNA. Calystegins were measured in *C. arvensis*, and *A. thaliana* served as a model for the production of flavonoids. In all cases, increases in growth and secondary metabolite accumulation were associated with the presence of the *crypt* gene.

Materials and methods

Plant materials

C. sepium and *C. arvensis* and were collected near the INRA, Versailles, campus. *W. somnifera* was from the tissue culture collection at the University of Calcutta, India. Seeds of *T. tanakae* were obtained from F. Abe.

Tissue culture and transformation

Methods for obtaining and culturing transformed roots are described elsewhere (Tepfer 1984; Chaudhuri et al. 2005; Bandyopadhyay et al. 2007). Briefly, surface-sterilized shoots (internodes and petioles) and leaves were infected with *A. rhizogenes* strains LBA9402 or A4, with or without the synthetic *crypt* gene (O'Donohue et al. 1995), under the control of the CaMV promoter (Tepfer et al. 1998). Roots induced at the site of inoculation were decontaminated by growth through Murashige and Skoog medium (Murashige and Skoog 1962) with 3% (w/v) sucrose (Sigma, USA) and one-fifth of the standard N-salts, solidified with 0.8% (w/v) agar (Sigma, USA). Transformed root cultures were subcultured every 4 weeks. For growth and metabolite extraction and analysis (see below), about 0.2 g fresh weight (FW) roots were grown in 100 ml liquid medium in 250 ml culture flasks on a rotary shaker at 100 rpm in the dark. Roots were cultured up to 13 days (*W. somnifera* and *C. sepium*) or 21 days (*T. tanakae*). Each root line was cultured in triplicate and the experiments were repeated at least once. The transgenic plants that spontaneously regenerated from transformed *C. arvensis* roots were cultured on agar

medium in culture tubes for 4–7 days, in a growth chamber (20°C, 16-h photoperiod, TFL 110 fluorescent Philips tubes, 65 µmol m^{-2} s^{-1}). Arabidopsis plants were transformed by the floral dip method (Desfeux et al. 2000) with *A. tumefaciens* strains carrying only the *nptII* gene (*nptII* control) or with both the *nptII* and *crypt* genes. One set of plants was not inoculated to serve as a negative (wild type) control. Plants were transferred to the greenhouse for seed production (see below). Seeds were collected, sterilized and germinated in vitro (Desfeux et al. 2000) on Arabidopsis-agar medium (Bechtold et al. 1993) in the presence of 50 mg l^{-1} kanamycin (Sigma, USA); kanamycin-resistant plants were transferred to the greenhouse.

Plant cultivation

Plants were grown in the greenhouse in the spring and summer in a mixture of peat, sand and vermiculite and watered three times per week with a nutrient solution (Coïc and Lesaint 1973). When necessary, day length was extended to 16 h using artificial light. Transgenic lines of *C. arvensis* were grown from stem cuttings of primary regenerants for 3 months before metabolite extraction and analysis (see below). Kanamycin-resistant Arabidopsis plants were checked for the presence of transgenes (see below), and their seeds were collected for flavonoid analysis.

DNA isolation and PCR analysis

Total DNA was extracted from transformed roots and transgenic plants (leaf tissue) according published methods (Dellaporta et al. 1983). The different transformed genotypes were verified by polymerase chain reaction (PCR) analysis for *rolC* (for the TL-DNA), *nptII* and *crypt*. Plasmid DNA from appropriate *Agrobacterium* strains (see above) was used as a positive control, and DNA isolated from the leaves of wild-type plants served as a negative control. Oligonucleotide primers for the *rolC* gene were 5′-TAACATGGCTGAAGACGACC and 5′-AAACTTG CACTCGCCATGCC (Slightom et al. 1986). The amplified product had the expected size of 534 bp. Samples were denatured at 95°C for 5 min, followed by 30 amplification cycles of 1 min at 94°C (denaturization), 1 min at 53°C (annealing) and 1.5 min at 72°C (extension), with a final extension step at 72°C for 5 min. The primers for *nptII* were 5′-GAACAA GATGGATTGCACGC and 5′-GAAGGCGATAGA AGGCGATGC (de Vries and Wackernagel 1998). The conditions were: 1 cycle at 94°C for 5 min; 40 cycles at 94°C for 1 min, 54°C for 2 min and 72°C for 4 min; 1 cycle of 72°C 12 min. Amplification resulted in a 412 bp amplified product. The primers for *crypt* were 5′-CCATGTCGACCTACAAGGAA-GAGCACTTGT and 5′-TCCGGTCGACATGGCT TGCACTGCTAC (O'Donohue et al. 1995). An initial 1 min step at 95°C was followed by 35 cycles (1 min at 95°C, 1 min at 55°C, and 1 min at 72°C) and a final 5 min step at 72°C. The amplified product had the expected size of 329 bp. In each case, the PCR mixture consisted of 200 ng DNA, 12.5 pmol of each primer, 200 mM of dNTPs, 1.5 U Taq polymerase (Invitrogen, USA) and buffer supplied by the manufacturer in a total volume of 25 µl. The PCR products were analyzed by electrophoresis on a 2% (w/v) agarose gel with a 1 kbp DNA ladder (Promega, USA).

Elicitor treatment

Purified β-cryptogein protein, a gift from M. O'Donohue and J.-C. Pernollet, was produced using *Pichia pastoris* (O'Donohue et al. 1996). Jasmonic acid (Sigma, USA) and salicylic acid (Sigma, USA) were dissolved in ethanol as filter-sterilized, 0.1 M stock solutions. α-1,4-oligogalacturonides from partial digestion of polygalacturonic acid with endopolygalacturonase from *Aspergillus niger* (Spiro et al. 1993) were provided by A. Aziz. They were dissolved in liquid medium to a concentration of 0.5 mg ml^{-1} and filtered-sterilized. *P. parasitica* var. *nicotianae* (strain INRA A183) was cultured on malt-agar medium. Agar plugs were cut out after 5–7 days and dissolved in liquid medium. The fungus was heat-killed by autoclaving, and the medium, with the cell-debris, was filter sterilized. Cryptogein protein (O'Donohue et al. 1996) was dissolved in water (0.1 mg ml^{-1}) and filter sterilized. Elicitors were added to 6-day-old (log phase) liquid cultures of *W. somnifera* and *C. sepium*, transformed with *A. rhizogenes* LBA9402. Jasmonate, salicylate and oligogalacturonides were added to the culture medium at a final concentration of 0.3 mM. One volume of fungal extract and 0.05 volumes of cryptogein protein stock were added to culture medium. When

necessary, controls received ethanol. Roots were harvested for growth studies and metabolite extraction and analysis (see below) after 48 h (5 days), 96 h (10 days) and 168 h (13 days) of elicitor treatment. Samples were in triplicates, and each experiment was repeated at least once.

Study of root growth

The initial FW was recorded at inoculation time, and roots were harvested over time. They were removed from the medium, washed with deionised water, blotted dry and weighed to determine the final FW. Growth was calculated as (Final FW − Initial FW)/Initial FW. Growth was also measured on a dry weight basis (DW), after desiccation for 16 h at 55°C.

Metabolite extraction and analysis

For the analysis of tylophorine and withanolides, roots were oven-dried at 55°C, powdered and extracted for HPLC as described previously (Chaudhuri et al. 2005; Bandyopadhyay et al. 2007). Calystegines in roots and root-regenerated shoots were extracted from 100 mg (FW) with 0.02 N HCl. The extracted samples were subjected to high voltage paper electrophoresis at 2,500 V for 20 min on 3 M chromatography paper (Whatman, USA) and visualized with silver staining (Tepfer et al. 1988a). Spots were analyzed by a Fluorchem 8000 Imaging system (Alpha Innotech Corporation, USA), coupled with a Multimage Light Cabinet II with automatic enhancer and detector. Calystegines were quantified using a standard curve, based on pure calystegine B2, which was linear between 1 and 10 µg. Flavonoids were extracted from 100 mg (FW) T1-seeds of Arabidopsis with 75% (v/v) methanol (in water), defattened with cyclohexane, eluted with methanol through a C-18 cartridge, dried under a stream of liquid nitrogen and redissolved in 15% (v/v) acetonitrile (in water). HPLC was performed on a Waters 990 system (Milford, USA), equipped with a Waters photodiode array detector and a Waters 600 multisolvent delivery system. Separation was with a Varian C-18 90A (reverse phase) column (150 × 4.6 mm, 5 µm particle size), and gradient elution was in 10–100% acetonitrile over 20 min at a flow rate of 1.0 ml min^{-1}. Quercitrine was detected at a retention time of 19.4 min, determined by spiking with a standard compound (Sigma, USA). Comparisons were made on the basis of peak areas at 230 nm absorption. The flavonoid content of the HPLC peaks was determined by mass spectroscopy (Routaboul et al. 2006).

Statistical analysis

Experiments were set up in a randomized design; sampling was in triplicate. Data were subjected to analysis of variance (ANOVA).

Results

Chemical elicitation in transformed roots

Transformed roots were induced on sterilized leaves of *W. somnifera* and on stem segments of *C. sepium*, using the LBA9402 strain of *A. rhizogenes* (pRi 1855), carrying only Ri T-DNA. Sterile root lines (representing independent transformation events) were derived and used to test the effects of known chemical inducers (including the cryptogein protein) on growth and secondary metabolite accumulation.

In *C. sepium* roots, all elicitors stimulated growth, except the killed *Phytophtora* cells (Fig. 1a). In *Withania* roots, both the killed *Phytophthora* cells and salcylate had no effect on growth (Fig. 1b). Among the elicitors tested in both species, the Crypt protein was the most growth stimulating, particularly in *Withania*, where it was associated with a 211% increase in growth.

The Crypt protein also stimulated calystegine content in *C. sepium* (336%), but it did not increase withanolide content in *W. somnifera* (Fig. 1c, d). Nevertheless, oligogalacturonides and jasmonate did stimulate withanolide accumulation. Despite the limited effects of the Crypt protein on secondary metabolite production, the promotion of growth in the two species and calystegine content in *C. sepium* were sufficiently encouraging to warrant transformation with the *crypt* gene, since the stimulation of biomass accumulation in vitro can, by itself, increase overall metabolite production.

In order to test the effects of the gene (*crypt*) that encodes the Crypt protein, we made use of the synthetic *crypt* gene in the pBin19 transformation vector (Bevan 1984), under the control of the 35S

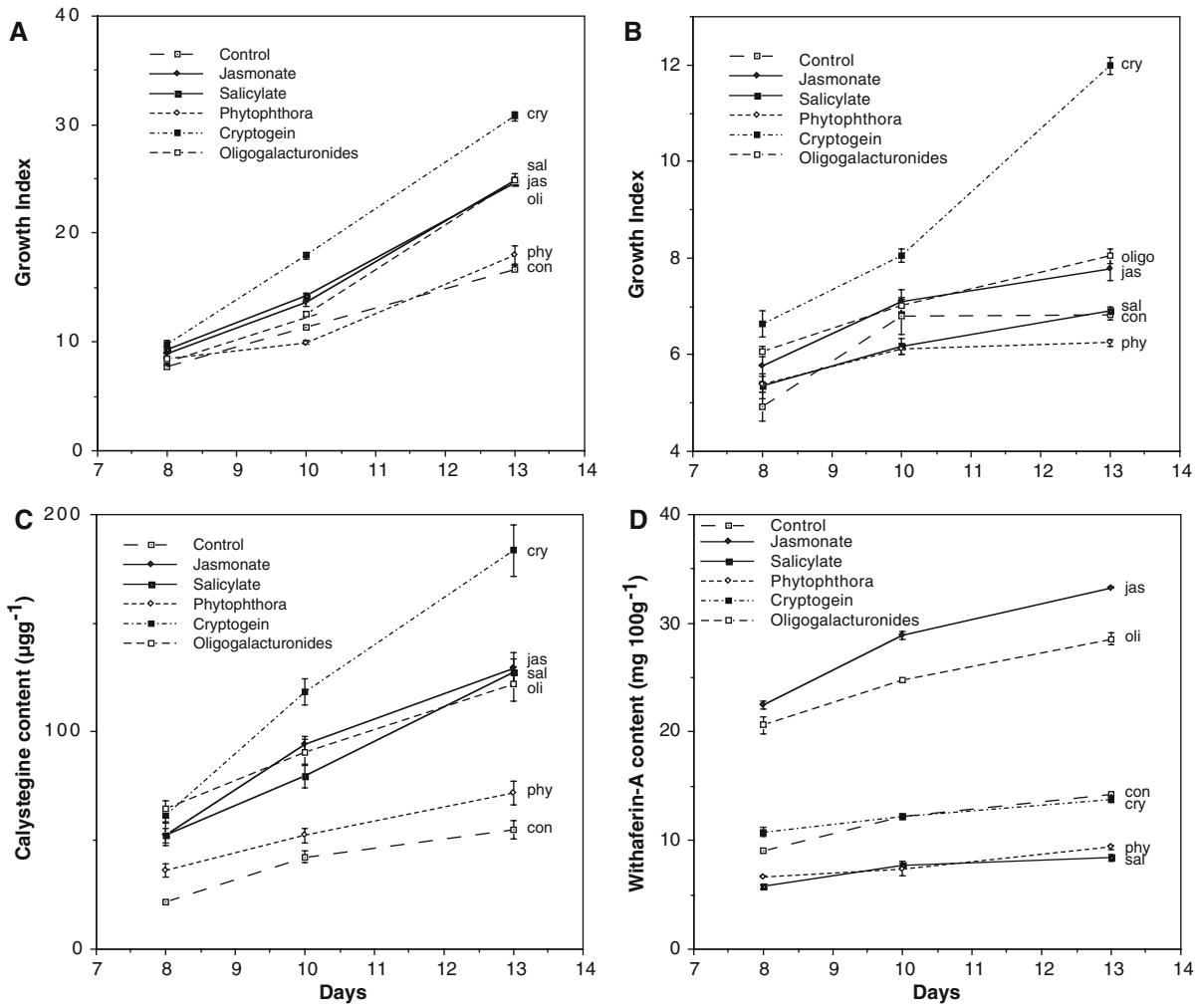

Fig. 1 Effects of chemical elicitors on transformed root growth and secondary metabolite production. Transformed root cultures, carrying just Ri T-DNA of *C. sepium* (**a**, **c**) and *W. somnifera* (**b**, **d**) were treated with known elicitors of defense responses: purified *β*-cryptogein protein (cry), jasmonic acid (jas), salicylic acid (sal) and α-1,4-oligogalacturonides (oli). An autoclaved and filtered culture of *P. parasitica* var. *nicotianae* (phy) was also tested, as well as no treatment (con). The effects were measured on growth (**a**, **b**) and secondary metabolite production (**c**, **d**). Calystegines were assayed in *C. sepium* and withaferin A was quantified in *W. somnifera*. Determinations were in triplicate; error bars represent standard deviations

CaMV promoter, which was previously shown to be associated with resistance to *Phytophthora* in tobacco (Tepfer et al. 1998). Transformed root lines were produced from single roots on different explants to insure that each line represented a distinct transformation event. The accumulation of secondary metabolites was measured in each root line over time. Controls consisted of root lines transformed by wild type *A. rhizogenes*. Transformation by *crypt* was demonstrated by PCR. In *W. somnifera*, three lines did not contain *crypt*, although they were produced using *A. rhizogenes* carrying the *crypt* construct. These lines, in which the binary vector T-DNA was not transferred, served as supplementary controls, since they carried only the Ri T-DNA.

Genetic elicitation using transformed roots

The presence of the *crypt* gene in transformed root lines was associated with a stimulation of root growth and secondary metabolite accumulation in both *C. sepium* and *W. somnifera* (Fig. 2). After 13 days

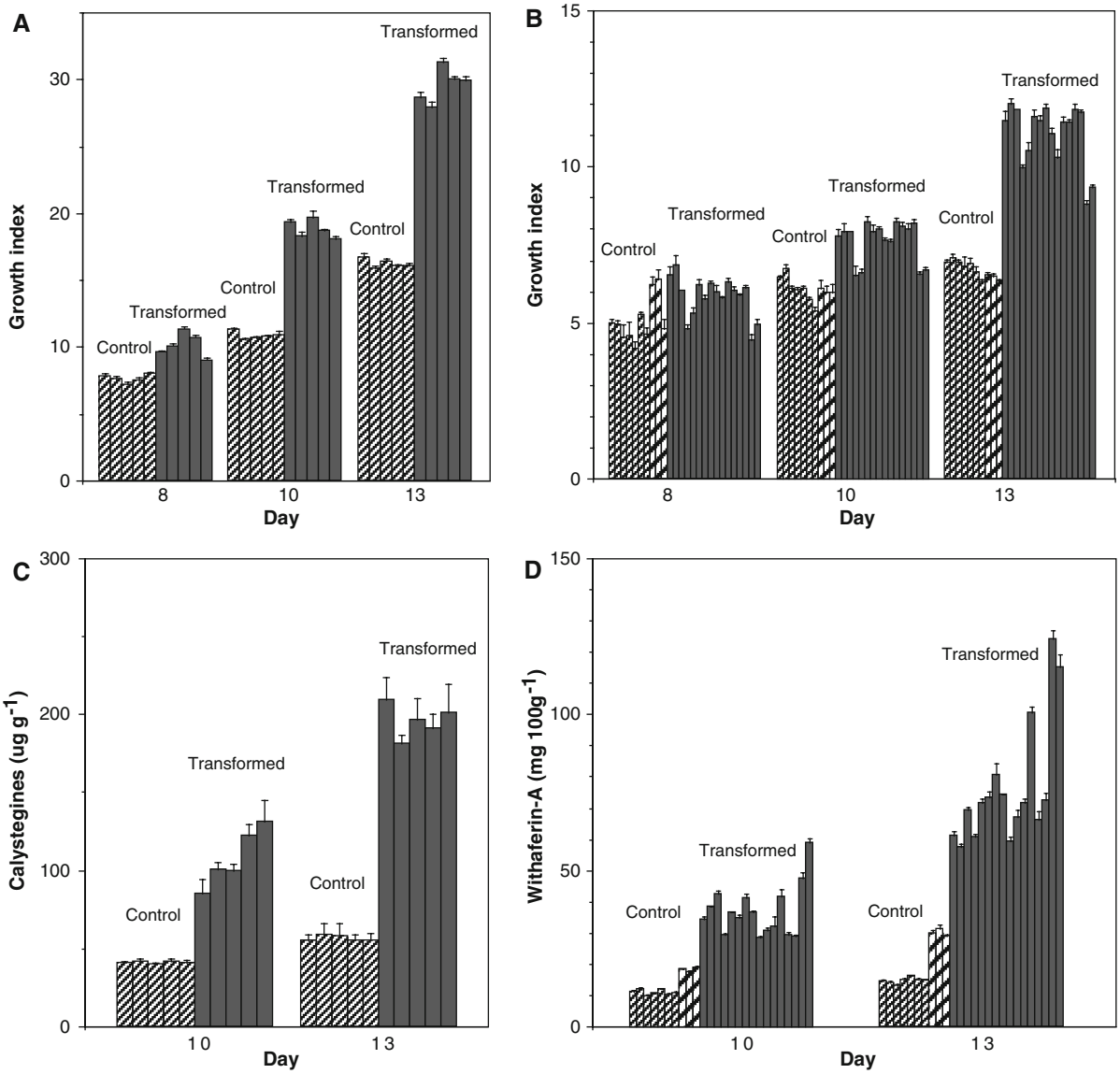

Fig. 2 Effects of genetic transformation with the *crypt* gene on growth and secondary metabolite production. The *crypt* gene was introduced into *C. sepium* (**a**, **c**) and *W. somnifera* (**b**, **d**) using *A. rhizogenes*. Growth (**a**, **b**) and secondary metabolite accumulation (**c**, **d**) were recorded over time. Bars represent individual root clones from independent transformation events: dark hatching, roots containing *crypt* and Ri T-DNA; medium density hatching, roots containing just Ri T-DNA produced by wild type *A. rhizogenes*; light hatching, roots produced by *A. rhizogenes* carrying the *crypt* gene construct, but which did not receive the *crypt* gene from the pBin19 binary vector

of culture, root growth increased by at least 50% and secondary metabolite production by as much as 8-fold in exceptional root clones (Fig. 2d). These results were taken as support for the hypothesis that genetic (endogenous) expression of the Cry protein can mimic the effects of exogenous treatment on growth and secondary metabolite accumulation. In order to validate and extend this finding, we introduced the *crypt* gene into three other species: *C. arvensis* (a morning glory that regenerates from roots), *Tylophora* (an Indian medicinal plant) and *Arabidopsis* (a model for flavonoid production).

Tylophora root clones were established in liquid culture, as for other species. Their growth was studied by incubating 200 mg of roots (in triplicates) in 100 ml N/5 liquid medium in 250 ml flasks, for

21 days in the dark at 100 rpm. Root lines were analyzed after 3 months in culture. One-way ANOVA analysis showed a significantly ($P \leq 0.05$) greater growth and biomass productivity in root clones carrying *crypt*, compared to control clones (Fig. 3). These *crypt* clones grew and accumulated biomass (FW and DW) about 1.5-fold faster than the corresponding control clones. The difference in growth was evident in both DW and FW measurements. Thus, the stimulation of growth observed in *Withania* and *Calystegia* was repeated in *Tylophora*.

Tylophorine content in root lines carrying *crypt* was not significantly increased, compared to the controls. Thus, tylophorine production (a function of growth and metabolite content) in liquid culture by these *crypt* clones would be significantly improved. After 6 months in liquid culture, the differences in growth between the controls and the lines containing *crypt* were no longer detected (results not shown.) We conclude that the *crypt* gene has the potential to stimulate tylophorine production, but to a lesser extent than the other metabolites studied in other species, and that this stimulation is unstable.

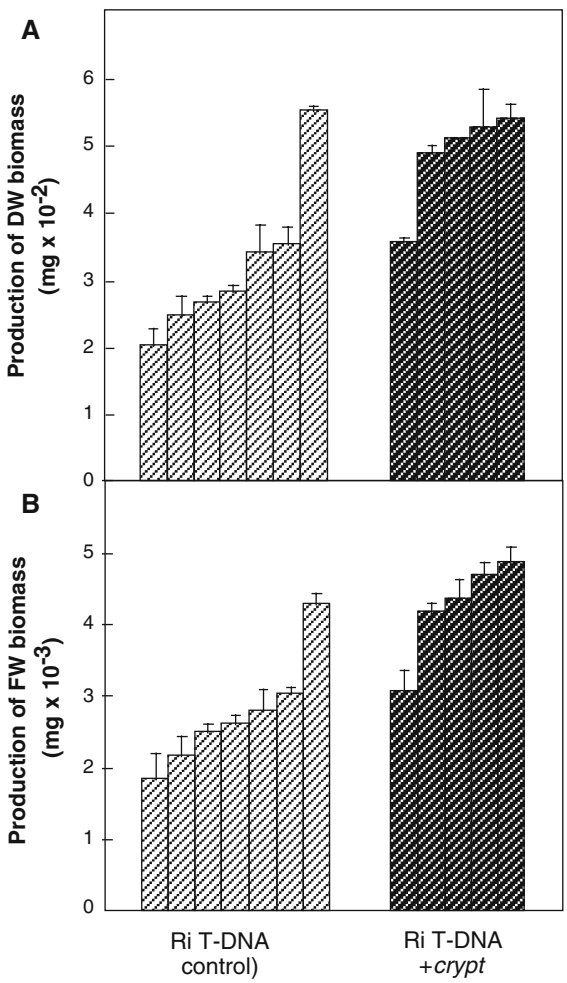

Fig. 3 Effects of *crypt* on growth of transformed *Tylophora* roots. Growth was significantly stimulated in root clones carrying both *crypt* and Ri T-DNA, independently of water content. (**a**) DW; (**b**) FW. Each bar represents an independently transformed line

Genetic elicitation using transformed plants

The effects of the *crypt* gene in whole plants was first studied in *Convolvulus arvensis*, a close relative of *C. sepium*, which regenerates directly from its roots. When the *crypt* gene was present in *C. arvensis* plants, calystegine content in the roots of *C. arvensis* plants carrying the *crypt* gene increased by 35% ($P \leq 0.05$) (Fig. 4). In the shoots, mean calystegine content increased by 42% ($P \leq 0.05$). Thus the stimulation in calystegine content, previously observed for root cultures of *C. sepium*, was repeated in whole transgenic plants of *C. arvensis*. (Changes in growth and development were not observed). We concluded that the initial metabolite accumulation results from *Withania* and *C. sepium* were validated in whole plants of *C. arvensis*.

The above experiments relied on *A. rhizogenes* for transformation, because we were interested in measuring a possible gain in secondary metabolites, due to co-transformation by Ri T-DNA plus the *crypt* gene, particularly in transformed root cultures. In Arabidopsis, we transformed without Ri T-DNA, using Agrobacterium *tumefaciens* and a standard floral dip transformation method, because transformation with the genetic marker alone (*nptII*) in Arabidopsis generates considerable genetic and phenotypic variability (Fig. 5), and we did not want to combine this with the previously described variation associated with Ri T-DNA (Tepfer 1984).

Since flavonoids accumulate in seeds and (particularly) in seed coats, whole seed flavonoids from controls and transformants were extracted and separated by HPLC, and the two major flavonoid peaks were examined by mass spectrometry to identify their components (Table 1). Peak I contained quercitrin almost exclusively, while peak II contained three flavonoid derivatives (Table 1) and traces of two

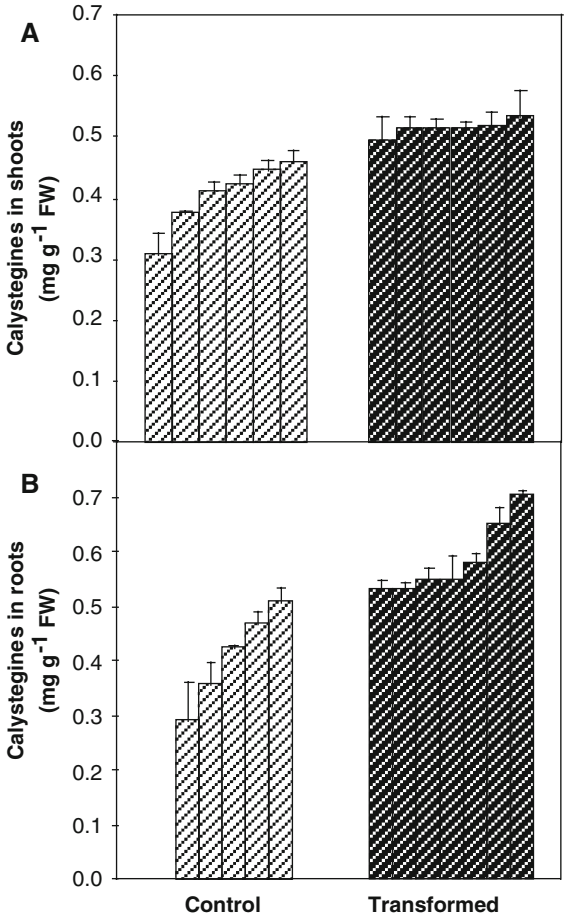

Fig. 4 Effects of the *crypt* gene on calystegine content in *C. arvensisi* shoots and roots. Transformation by *crypt* and Ri T-DNA resulted in increased calystegine accumulation in whole plants, both in shoots (**a**) and roots (**b**). Each bar represents an independently transformed line

others (not shown). HPLC was then routinely used to measure possible effects of the *crypt* construct on these seed flavonoids.

Flavonoids varied among individual transformants in both the controls, carrying *nptII*, and in plants carrying the *crypt* gene. Similar variability was not seen in the wild type control. Thus, transformation alone with the *nptII* gene altered the content of seed flavonoids in individual transformants, and it complicated detection of differences due to *crypt*.

Flavonoid peak I, composed of quercitrin (quercetin-3-*O*-rhamnoside) did not statistically increase in the lines transformed by the crypt gene, but the chances of finding high-producing lines in this population were increased (see Discussion).

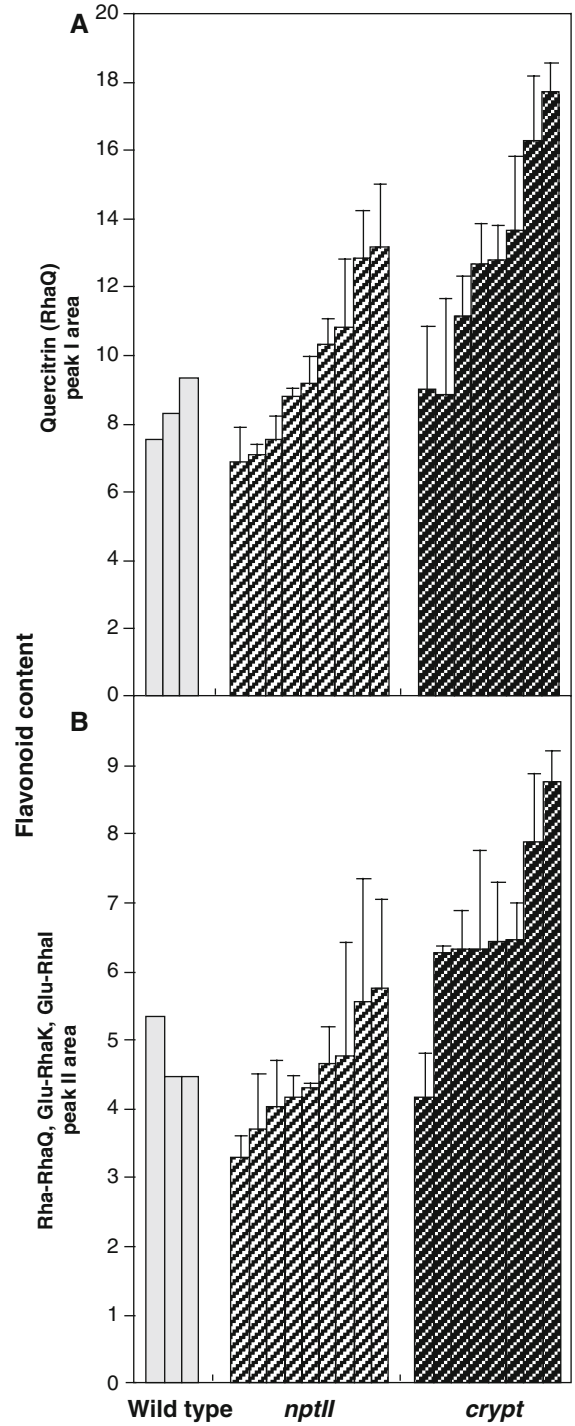

Fig. 5 Flavonoids in the seeds of T1 generation transgenic Arabidopsis plants. Arabidopsis was transformed with the *crypt* gene, using *A. tumefaciens*. Flavonoids were analyzed using HPLC. The results for two peaks are shown (**a**, peak I; **b**, peak II). The *crypt* gene was not associated with a significant increase in peak I, but it was for peak II (see Table 1 for peak compositions)

Table 1 Flavonoid content of HPLC peaks

Flavonoid peak (HPLC)	Common name	Chemical abbreviation	Chemical name	Molecular weight	Retention time
Peak I	quercitrin	RhaQ	Quercetin-3-*O*-rhamnoside	448	19.4
Peak II		Glu-RhaI	Isorhamnetin-hexoside-rhamnoside	624	15.6
		Rha-RhaQ	Quercetin-di-rhamnoside	594	15.3
		Glu-RhaK	Kaempferol-3-*O*-glucoside-7-*O*-rhanoside	594	15.2

Flavonoid peak II, containing three flavonoid derivatives, increased by about 40% ($P = 0.005$), relative to the *nptII* transformants, which were not significantly different ($P = 0.59$) from the wild type control. (Changes in growth and development were not observed). We conclude that transformation with the cryptogein gene can stimulate the accumulation of certain (but not all) flavonoids in Arabidopsis seeds.

Discussion

These findings validate the hypothesis that transgenetic mimicry of fungal attack can lead to increased secondary metabolite production. To better focus on testing transgenetic elicitation in multiple species, we limited the analysis to phenotypic changes, deferring verification of underlying biochemical and genetic changes to future studies. We assumed that, as for other elicitors (Zhao et al. 2005), the synthesis of the Crypt protein in plant tissues initiates a signal transduction cascade that results in the induction of one or more transcription factors, responsible for a generalized defense response. Inducible expression and secretion of *crypt* could be used to verify this assumption. The CaMV promoter used here is considered to be constitutive, but no signal peptide was attached to the *crypt* coding sequence, and we have no information about the fate of the Crypt protein after synthesis, although the protein encoded by this construct was detected in transgenic tobacco plants (Tepfer et al. 1998). Cryptogein has sterol scavenging activates, and it could be toxic for the plant cell. Thus, high-producing transformants were likely counterselected after transformation. How the protein, produced on the inside of the cell, can act with the receptor, presumed to be on the outside, is not known, although leakage, e.g. through cell injury, was proposed (Tepfer et al. 1998). Despite these uncertainties, the phenomen of secondary metabolite and root growth stimulation seems clear, and it is reproducible, albeit to varying degrees, in different plant species producing different secondary metabolites.

In all species examined, root transformation by the *crypt* gene was correlated with increased biomass accumulation in vitro. FW and DW accumulations were similar (Fig. 3, other data not shown), thus increases in biomass were not due to increases in water content. Since metabolite production is a function of concentration and biomass accumulation, the effect of *crypt* on growth could significantly contribute to the production of metabolites in transformed root cultures, even if increases in metabolite content are modest. Other chemical inducers of plant defenses also stimulated root growth; thus, increased root growth might be a generalized reaction to stress. It is logical that pathogen attack leading to necrosis in one part of a root system would be compensated by increased growth in other parts of the root system—i.e. that a general defense response would stimulate the growth of the surviving root system.

Increases in metabolite content in transformed root cultures were recorded in all but one (*Tylophora*) of the five species tested. For a given species, levels of stimulation varied among clones, but results were reproducible within a given clone, indicating that the chemical measurements were accurate. Clonal variation was expected, due to diverse factors, including insertion site and transgene copy number. Clonal variation did not prevent finding that the root lines containing *crypt* contained statistically more secondary metabolites than the controls. Variation can, in itself, contribute to obtaining high-producing clones. The lack of a stable increase in *Tylophora* could be due to the high stimulation of tylophorines in roots transformed by the Ri T-DNA alone (Chaudhuri et al.

2005). We presume that maximum metabolite accumulation is limited by carbon availability and toxicity.

Statistically significant stimulation of calystegine production was observed in *C. arvensis* leaves and roots (increases of 30% and 40%, respectively). Calystegins are allelopathic glycosidase inhibitors that likely poison the plants that produce them, probably limiting the amount that these plants can produce. They are tropane derivatives (Goldmann et al. 1990) that served here as a convenient model to determine whether an exotic tropane alkaloid pathway can be stimulated by transformation with the *crypt* gene. In nature, their allopathic properties are likely used in defense against microbial pathogens and in competition among plant species (Goldmann et al. 1996). They also serve as nutritional mediators in interactions with *Rhizobium meliloti* (*Sinorhizobium meliloti*) Tepfer et al. (1988a, b). Changes in calystegine production might thus alter rhizosphere population dynamics.

A. rhizogenes was used for transformation (except in *Arabidopsis*); thus, Ri T-DNA was co-introduced with the *crypt* gene. The phenotypic expression of the Ri T-DNA was optimized by screening for rapid root growth in vitro. In contrast to the other species, *Arabidopsis* was transformed by *A. tumefaciens*. Transformation of *Arabidopsis* with Ri T-DNA plus *crypt* (via floral dip using *A. rhizogenes*) might further improve flavonoid production. It would be appropriate to test the effects of *crypt* on other substances known to accumulate in response to pathogen attack in *Arabidopsis*, including polyamines and other polyphenols, such as camalexin (Glawischnig 2007).

In the case of quercitrin (peak I), the population of clones transformed by *crypt* was not significantly different from the controls transformed by *nptII*. Nevertheless, transformation by *crypt* increased the chances of obtaining high-producing lines. If a 50% increase in quercitrin content is used to define a high-producing line, than the population of crypt lines included five out of eight (63%) high producers, whereas the population transformed by *nptII* alone included two out of nine (22%) high producers. The highest producing line transformed by *crypt* showed a stimulation of 111%, and the highest producing line transformed by *nptII* alone showed a stimulation of 57%. Thus, even in the absence of a statistically significant difference between the two populations, the chances of obtaining high quercitrin production were increased when the *crypt* gene was present.

Flavonoid peak II contained three flavonoid derivatives. The lines containing *crypt* showed a statistically significant, 39% stimulation in peak II, compared to the control lines carrying just *nptII*, which was not statistically different from the wild type controls. The best producing line contained 85% more flavonoids than the control. The ranking of the lines was the same for both peaks I and II. Increases in flavonoids were not observed for a third flavonoid peak (not shown). The effects of *crypt* on flavonoid accumulation in *Arabidopsis* seeds would seem to be limited to certain substances, possibly due to a redistribution of carbon in the phenylpropanoid pathway.

The metabolites stimulated by *crypt* represent a variety of natural products, produced by widely different species, perhaps reflecting the wide host specificity of *Phytophthora* species (Erwin and Ribeiro 1966). The metabolites included diverse structures: calystegines A and B (tropane derivatives), withaferin A (a steroidal lactone), and a group of flavonol glycosides. Although tylopohorine B (a phenanthroindolizidine alkaloid) was not increased, the ability of the *crypt* gene to stimulate the accumulation of substances of varying chemical nature suggests that the production of certain medicines, aromas and colours might be improved without understanding the underlying biochemistry and genetics. The increases recorded here varied from a few tens of a percent to several fold, but even small, significant increases suggest that improvement might be possible by using, for instance, inducible and tissue-specific promoters. A general method for improving the production of key metabolites could have economic applications in the pharmaceutical and food industries and at the same time provide a scientific tool for studying the biology and function of secondary metabolites.

We previously showed in tobacco that the *crypt* construct conferred resistance to *Phytophthora*, and we suggested that natural genetic transformation by a gene such as *crypt* could play a role in evolution (Tepfer et al. 1998). Here, we extend the analysis of the phenotypic changes associated with *crypt* to secondary metabolites and to five new species. Secondary metabolites serve multiple functions,

ranging from attractants to allelopathic poisons. Changes in chemical phenotype could therefore have wide-ranging effects on fitness. *A. rhizogenes* is capable of inducing transformed roots in a variety of plant species, and in many of these species, shoots regenerate spontaneously from roots, propagating the transformed genotype and phenotype through meiosis (Tepfer 1983a, b, 1984; Tepfer et al. 1989). In nature, enhanced secondary metabolite production could be acquired via genetic transformation with an *A. rhizogenes*, carrying a T-DNA encoding a defense response eliciter. Artificial transformation by the *crypt* gene thus illustrates how natural transfer to plants of a single gene from the soil metagenome could have important repercussions in relationships between plants and other organisms.

Acknowledgements We thank Lucien Kerhoas for the LC-MS and Brigitte Message for general technical support. Aziz Aziz generously provided the oligogalacturonides, and Michael O'Donohue and Jean-Claude Pernollet donated the purified cryptogein protein. Seeds of *T. tanakae* and purified tylophorine were a kind gift from Fumiko Abe. This research was made possible by the Centre Franco-Indien pour la Promotion de la Recherche Avancée (Project 2503-2).

References

Ashtamker C, Kiss V, Sagi M, Davydov O, Fluhr R (2007) Diverse subcellular locations of cryptogein-induced ROS production in tobacco BY-2 cells. Plant Physiol 143(4):1817–1826

Bandyopadhyay M, Jha S, Tepfer D (2007) Changes in morphological phenotypes and withanolide composition of Ri-transformed roots of *Withania somnifera*. Plant Cell Rep 26:599–609. doi:10.1007/s00299-006-0260-0

Bechtold N, Ellis J, Pelletier G (1993) In planta Agrobacterium mediated gene transfer by infiltration of adult *Arabidopsis thaliana* plants. C R Acad Sci 316(3):1194–1199

Bevan M (1984) Binary *Agrobacterium* vectors for plant transformation. Nucleic Acids Res 12:8711–8721. doi:10.1093/nar/12.22.8711

Boissy G, de La Fortelle E, Kahn R, Huet JC, Bricogne G, Pernollet JC et al (1996) Crystal structure of a fungal elicitor secreted by *Phytophthora cryptogea*, a member of a novel class of plant necrotic proteins. Structure 4:1429–1439. doi:10.1016/S0969-2126(96)00150-5

Buter B, Orlacchio C, Soldati A, Berger K (1998) Significance of genetic and environmental aspects in the field cultivation of *Hypericum perforatum*. Planta Med 64:431–437. doi:10.1055/s-2006-957475

Chaudhuri KN, Ghosh B, Tepfer D, Jha S (2005) Genetic transformation of *Tylophora indica* with Agrobacterium rhizogenes A4: growth and tylophorine productivity in different transformed root clones. Plant Cell Rep 24:25–35. doi:10.1007/s00299-004-0904-x

Coïc Y, Lesaint C (1973) La nutrition minérale en horticulture avancée. Rev Hortic Paris 2816:29–34

Dellaporta S, Wood J, Hicks J (1983) A plant DNA minipreparation: version II. Plant Mol Biol Rep 1:19–21. doi:10.1007/BF02712670

Desfeux C, Clough S, Bent A (2000) Female reproductive tissues are the primary target of *Agrobacterium*-mediated transformation by the Arabidopsis floral-dip method. Plant Physiol 123:895–904. doi:10.1104/pp. 123.3.895

Dueckershoff K, Unger M, Frank A, Gillam EM, Guengerich FP, Warzecha H (2005) Modified nicotine metabolism in transgenic tobacco plants expressing the human cytochrome P450 2A6 cDNA. FEBS Lett 579:2480–2484. doi:10.1016/j.febslet.2005.02.082

Erwin DC, Ribeiro OK (1966) Phytophthora diseases worldwide. American Phytopathological Society Press, St. Paul

Flores H, Hoy M, Pickard J (1987) Secondary metabolites from root cultures. Trends Biotechnol 5:64–69. doi:10.1016/S0167-7799(87)80013-6

Foissner I, Wendehenne D, Langebartels C, Durner J (2000) In vivo imaging of an elicitor-induced nitric oxide burst in tobacco. Plant J 23:817–824. doi:10.1046/j.1365-313X.2000.00835.x

Glawischnig E (2007) Camalexin. Phytochemistry 68:401–406. doi:10.1016/j.phytochem.2006.12.005

Goldmann A, Milat ML, Ducrot PH, Lallemand JY, Maille M, Lepingle A et al (1990) Tropane derivatives from *Calystegia sepium*. Phytochemistry 29:2125–2127. doi:10.1016/0031-9422(90)83019-W

Goldmann C, Message B, Lecoeur L, Delarue M, Maille M, Tepfer D (1993) Metabolic signals in the rhizosphere: catabolism of calystegins and betaines by *Rhizobium meliloti*. In: van Beek T, Breteler H (eds) Phytochemistry and agriculture. Oxford University Press, Oxford

Goldmann A, Message B, Tepfer D, Molyneux R, Duclos O, Boyer F-D et al (1996) Biological activities of the nortropane alkaloid, calystegine B2, and analogs: structure–function relationships. J Nat Prod 59:1137–1142. doi:10.1021/np960409v

Goossens A, Hakkinen ST, Laakso I, Seppanen-Laakso T, Biondi S, De Sutter V et al (2003) A functional genomics approach toward the understanding of secondary metabolism in plant cells. Proc Natl Acad Sci USA 100:8595–8600. doi:10.1073/pnas.1032967100

Guillon S, Tremouillaux-Guiller J, Pati PK, Rideau M, Gantet P (2006) Hairy root research: recent scenario and exciting prospects. Curr Opin Plant Biol 9:341–346. doi:10.1016/j.pbi.2006.03.008

Guo ZJ, Chen XJ, Wu XL, Ling JQ, Xu P (2004) Overexpression of the AP2/EREBP transcription factor OPBP1 enhances disease resistance and salt tolerance in tobacco. Plant Mol Biol 55:607–618. doi:10.1007/s11103-004-1521-3

Harborne JB, Williams CA (2000) Advances in flavonoid research since 1992. Phytochemistry 55:481–504. doi:10.1016/S0031-9422(00)00235-1

Holmberg N (1997) Stragedies for the production of secondary metabolites by pri-transformed regenerants. Plant Tissue Cult Biotechnol 3:128–137

Inui T, Tamura K, Fujii N, Morishige T, Sato F (2007) Overexpression of *Coptis japonica* norcoclaurine 6-O-methyltransferase overcomes the rate-limiting step in Benzylisoquinoline alkaloid biosynthesis in cultured *Eschscholzia californica*. Plant Cell Physiol 48:252–262. doi:10.1093/pcp/pcl062

Jiang DH, Chen XJ, Wu KL, Guo ZJ (2002) Site-directed mutagenesis of cryptogein gene (CryK13V) and generation of transgenic tobacco plants with nonspecific disease resistance. J Plant Physiol Mol Biol 28:399–406

Jiang D, Chen X, Wu K, Guo Z (2004) Expression of cryptogein in tobacco plants exhibits enhanced disease resistance and tolerance to salt stress. Chin Sci Bull 49:803–809

Jung G, Tepfer D (1987) Use of genetic transformation by the Ri T-DNA of *Agrobacterium rhizogenes* to stimulate biomass and tropane alkaloid production in *Atropa belladonna* and *Calystegia sepium* roots. Plant Sci 50:145–151. doi:10.1016/0168-9452(87)90151-8

Kasparovsky T, Blein J-P, Mikes V (2004) Ergosterol elicits oxidative burst in tobacco cells via phospholipase A2 and protein kinase C signal pathway. Plant Physiol Biochem 42:429–435. doi:10.1016/j.plaphy.2004.04.003

Keller H, Pamboukdjian N, Ponchet M, Poupet A, Delon R, Verrier J et al (1999) Pathogen-induced elicitin production in transgenic tobacco generates a hypersensitive response and nonspecific disease resistance. Plant Cell 11:223–236

Lamotte O, Gould K, Lecourieux D, Sequeira-Legrand A, Lebrun-Garcia A, Durner J et al (2004) Analysis of nitric oxide signaling functions in tobacco cells challenged by the elicitor cryptogein. Plant Physiol 135:516–529. doi:10.1104/pp.104.038968

Lecourieux D, Mazars C, Pauly N, Ranjeva R, Pugin A (2002) Analysis and effects of cytosolic free calcium increases in response to elicitors in *Nicotiana plumbaginifolia* cells. Plant Cell 14:2627–2641. doi:10.1105/tpc.005579

Li J, Ou-Lee TM, Raba R, Amundson RG, Last RL (1993) Arabidopsis flavonoid mutants are hypersensitive to UV-B irradiation. Plant Cell 5:171–179

Lin L, Wu J (2002) Enhancement of shikonin production in single- and two-phase suspension cultures of Lithospermum erythrorhizon cells using low-energy ultrasound. Biotechnol Bioeng 78:81–88. doi:10.1002/bit.10180

Liu R, Hu Y, Li J, Lin Z (2007) Production of soybean isoflavone genistein in non-legume plants via genetically modified secondary metabolism pathway. Metab Eng 9:1–7. doi:10.1016/j.ymben.2006.08.003

Lochman J, Kasparovsky T, Damborsky J, Osman H, Marais A, Chaloupkova R et al (2005) Construction of cryptogein mutants, a proteinaceous elicitor from Phytophthora, with altered abilities to induce a defense reaction in tobacco cells. Biochemistry 44:6565–6572. doi:10.1021/bi0502285

Long M, Millar DJ, Kimura Y, Donovan G, Rees J, Fraser PD et al (2006) Metabolite profiling of carotenoid and phenolic pathways in mutant and transgenic lines of tomato: identification of a high antioxidant fruit line. Phytochemistry 67:1750–1757. doi:10.1016/j.phytochem.2006.02.022

Matthews D, Jones H, Gans P, Coates S, Smith LM (2005) Toxic secondary metabolite production in genetically modified potatoes in response to stress. J Agric Food Chem 53:7766–7776. doi:10.1021/jf050589r

Mikes V, Milat M-L, Ponchet M, Ricci P, Blein J-P (1997) The fungal elicitor cryptogein is a sterol carrier protein. FEBS Lett 416:190–192. doi:10.1016/S0014-5793(97)01193-9

Molyneux R, Pan Y, Goldmann A, Tepfer D, Elbein A (1993) Calystegins, a novel class of alkaloid glycosidase inhibitors. Arch Biochem Biophys 304:81–88. doi:10.1006/abbi.1993.1324

Murashige T, Skoog F (1962) A revised medium for rapid growth and bio assays with tobacco tissue cultures. Physiol Plant 15:473–497. doi:10.1111/j.1399-3054.1962.tb08052.x

O'Donohue M, Gousseau H, Huet J-C, Tepfer D, Pernollet J-C (1995) Chemical synthesis, expression and mutagenesis of a gene encoding β-cryptogein, an elicitin produced by *Phytophthora cryptogea*. Plant Mol Biol 27:577–586. doi:10.1007/BF00019323

O'Donohue MJ, Boissy G, Huet J-C, Nespoulous C, Brunie S, Pernollet J-C (1996) Overexpression in *Phichia pastoris* and crystallization of an elicitor protein secreted by the phytopathogenic fungus, *Phytopthora cryptogea*. Protein Expr Purif 8:254–261. doi:10.1006/prep.1996.0098

Olsen CS (2005) Valuation of commercial central Himalayan medicinal plants. Ambio 34:607–610. doi:10.1639/0044-7447(2005)034[0607:VOCCHM]2.0.CO;2

Pietta PG (2000) Flavonoids as antioxidants. J Nat Prod 63:1035–1042. doi:10.1021/np9904509

Planchet E, Sonoda M, Zeier J, Kaiser WM (2006) Nitric oxide (NO) as an intermediate in the cryptogein-induced hypersensitive response—a critical re-evaluation. Plant Cell Environ 29:59–69. doi:10.1111/j.1365-3040.2005.01400.x

Ren D, Yang KY, Li GJ, Liu Y, Zhang S (2006) Activation of Ntf4, a tobacco MAPK, during plant defense response and its involvement in hypersensitive response-like cell death. Plant Physiol 141(4):1482–1493

Ricci P, Bonnnet P, Huet JC, Sallantin M, Beauvais-Cante F, Bruneteau M et al (1989) Structure and activity of proteins from pathogenic fungi *Phytophthora* eliciting necrosis and acquired resistance in tobacco. Eur J Biochem 183:555–563. doi:10.1111/j.1432-1033.1989.tb21084.x

Routaboul J-M, Kerhoas L, Debeaujon I, Pourcel L, Caboche M, Einhorn J et al (2006) Flavonoid diversity and biosynthesis in seed of *Arabidopsis thaliana*. Planta 224:96–107. doi:10.1007/s00425-005-0197-5

Shi M, Kwok KW, Wu JY (2007) Enhancement of tanshinone production in Salvia miltiorrhiza Bunge (red or Chinese sage) hairy-root culture by hyperosmotic stress and yeast elicitor. Biotechnol Appl Biochem 46:191–196. doi:10.1042/BA20060147

Shinwari ZK, Gilani SS (2003) Sustainable harvest of medicinal plants at Bulashbar Nullah, Astore (Northern Pakistan). J Ethnopharmacol 84:289–298. doi:10.1016/S0378-8741(02)00333-1

Slightom J, Durand-Tardif M, Jouanin L, Tepfer D (1986) Nucleotide sequence analysis of TL-DNA of *Agrobacterium rhizogenes* agropine type plasmid. J Biol Chem 261:108–121

Spiro MD, Kates KA, Koller AL, O'Neill MA, Albersheim P, Darvill AG (1993) Purification and characterization of biologically active 1,4-linked α-D-oligogalacturonides

after partial digestion of polygalacturonic acid with endopolygalacturonase. Carbohydr Res 247:9–20. doi:10.1016/0008-6215(93)84237-Z

Tepfer D (1983a) The biology of genetic transformation of higher plants by *Agrobacterium rhizogenes*. In: Puhler A (ed) Molecular genetics of the bacteria plant interaction. Springer Verlag, Berlin

Tepfer D (1983b) The potential uses of *Agrobacterium rhizogenes* in the genetic engineering of higher plants: nature got there first. In: Lurquin P, Kleinhofs A (eds) Genetic engineering in eukaryotes. Plenum Press, New York

Tepfer D (1984) Transformation of several species of higher plants by *Agrobacterium rhizogenes*: sexual transmission of the transformed genotype and phenotype. Cell 37:959–967. doi:10.1016/0092-8674(84)90430-6

Tepfer D (1989) Ri T-DNA from *Agrobacterium rhizogenes:* a source of genes having applications in rhizosphere biology and plant development, ecology, and evolution. In: Kosuge T, Nester E (eds) Plant–microbe interactions. McGraw Hill, New York

Tepfer D, Tempé J (1981) Production d'agropine par des racines formées sous l'action d'*Agrobacterium rhizogenes*, souche A4. C R Acad Sci 292:153–156

Tepfer D, Goldmann A, Fleury V, Maille M, Message B, Pamboukdjian N et al (1988a) Calystegins, nutritional mediators in plant-microbe interactions. In: Palacios R, Verma D (eds) Molecular genetics of plant–microbe interactions. APS Press, St Paul

Tepfer D, Goldmann A, Pamboukdjian N, Maille M, Lépingle A, Chevalier D et al (1988b) A plasmid of *Rhizobium meliloti* 41 encodes catabolism of two compounds from root exudate of *Calystegia sepium*. J Bacteriol 170:1153–1161

Tepfer D, Metzger L, Prost R (1989) Use of roots transformed by *Agrobacterium rhizogenes* in rhizosphere research: applications in studies of cadmium assimilation from sewage sludges. Plant Mol Biol 13:295–302. doi:10.1007/BF00025317

Tepfer D, Boutteaux C, Vigon C, Aymes S, Perez V, O'Donohue MJ, Huet J-C, Pernollet J-C (1998) Phytophtora resistance through production of a fungal protein elicitor (B-cryptogein) in tobacco. Mol Plant Microbe Interact 11(1):64–67

Tian L, Dixon RA (2006) Engineering isoflavone metabolism with an artificial bifunctional enzyme. Planta 224:496–507. doi:10.1007/s00425-006-0233-0

de Vries J, Wackernagel W (1998) Detection of *nptII* (kanamycin resistance) genes in genomes of transgenic plants by marker-rescue transformation. Mol Gen Genet 257:606–613. doi:10.1007/s004380050688

Wolucka BA, Goossens A, Inze D (2005) Methyl jasmonate stimulates the de novo biosynthesis of vitamin C in plant cell suspensions. J Exp Bot 56:2527–2538. doi:10.1093/jxb/eri246

Ye H, Huang LL, Chen SD, Zhong JJ (2004) Pulsed electric field stimulates plant secondary metabolism in suspension cultures of *Taxus chinensis*. Biotechnol Bioeng 88:788–795. doi:10.1002/bit.20266

Zhang C, Fevereiro PS (2007) The effect of heat shock on paclitaxel production in *Taxus yunnanensis* cell suspension cultures: role of abscisic acid pretreatment. Biotechnol Bioeng 96:506–514. doi:10.1002/bit.21122

Zhao J, Davis LC, Verpoorte R (2005) Elicitor signal transduction leading to production of plant secondary metabolites. Biotechnol Adv 23:283–333. doi:10.1016/j.biotechadv.2005.01.003

Zobayed SM, Afreen F, Kozai T (2005) Temperature stress can alter the photosynthetic efficiency and secondary metabolite concentrations in St. John's wort. Plant Physiol Biochem 43:977–984. doi:10.1016/j.plaphy.2005.07.013

ANNEXES

ANNEX A:

History of the major space experiments testing responses of organisms to parameters of space environment

Table A-1. Some of the major space experiments performed to test the survivability of different terrestrial model organisms in harsh space environment.

Year	Mission	Duration	Experiment	Exposure conditions	Model system (organism)		Study	Reference
1972	Apollo 16/ 17	1.3 hours	Biostack I/ II	Space vacuum Solar UV radiation Cosmic rays	*Bacillus subtilis* spores	Bacteria	Short-term survival in space	Bücker et al. (1974) Horneck (1993)
1983	Spacelab 1 (SL-1)	10 days	Microorganisms and biomolecules in hard space environment (1ES 029)	Space vacuum Solar UV radiation Cosmic rays	*Bacillus subtilis* spores	Bacteria	Inactivation Mutation UV-induced DNA damage	Horneck et al. (1984a) Horneck et al. (1984b) Horneck (1993)
			Advanced Biostack (1ES 027)	Cosmic rays	*Bacillus subtilis* spores	Bacteria	Radiobiological studies	Bücker et al. (1984) Zimmermann et al. (1996) Gartehbach et al. (1994)
					Sordaria fimicola spores	Fungi		
					Arabidopsis thaliana seeds	Plants		
					Artemia salina cyst	Animals (Crustacea)		
1984-1990	LDEF	2107 days (~6 years)	Exostack	Space vacuum Solar UV radiation Cosmic rays	*Bacillus subtilis* spores	Bacteria	Long-term survival in space	Horneck (1993) Horneck et al. (1994)
			Free-Flyer Biostack (A0015)	Cosmic rays	*Bacillus subtilis* spores	Bacteria	Radiobiological studies	Bücker (1984) Bücker (1984) Zimmermann et al. (1994) Zimmermann et al (1996) Gartehbach et al. (1994) Mei et al. (1994)
					Arabidopsis thaliana seeds	Plants		
					Zea mays seeds			
					Oryza sativa seeds			
					Nicotiana tabaccum seeds			
					Sordaria fimicola spores	Fungi		
					Artemia salina cyst	Animals (Crustacea)		
			SEEDS	Space vacuum Cosmic rays	*Plant seeds* (106 plant species), including *Lycopersicon esculentum* seeds	Plants	Students experiment: Long-term survival of plant seeds in space	Alston (1991) Grigsby (1984) Hammond (1996)
1987	BIOKOSMOS 8/ Kosmos 1887	13 days	Biorack	Cosmic rays	*Arabidopsis thaliana* seeds	Plants	Radiobiological studies	Kranz et al. (1990) Zimmermann et al. (1996)
			Exobloc II	Space vacuum Solar UV radiation Cosmic rays	*Arabidopsis thaliana* seeds	Plants	Radiobiological studies	Anikeeva et al. (1990)
					Crepis capillaris seeds			
1989	BIOKOSMOS 9 / Kosmos 2044	13.8 days	Biorack	Cosmic rays	*Arabidopsis thaliana* seeds	Plants	Radiobiological studies	Zimmermann et al. (1996)

Table A-1. Some of the major space experiments performed to test the survivability of different terrestrial model organisms in harsh space environment (continued from previous page).

Year	Mission	Duration	Experiment	Exposure conditions	Model organism		Study	Reference
1992-1993	EURECA/ ERA	336 days	Exobiological Unit (ER 161)	Space vacuum Solar UV radiation Cosmic rays	Plasmid DNA *Bacillus subtilis* spores *Deinococcus radiodurans* cells *Aspergillus sp.*conidia *Saccharomyces cerevisiae* cells	Bacteria Fungi	Long-term effects of solar UV and/or vacuum	Horneck et al. (1995) Dose et al. (1995)
				Cosmic rays	*Arabidopsis thaliana* seeds	Plants	Radiobiological studies	Zimmermann et al. (1996)
1993	Spacelab D2	10 days		Space vacuum Solar UV radiation Cosmic rays	*Bacillus subtilis* spores	Bacteria	Action spectra Role of ozone layer	Horneck et al. (1996)
				Cosmic rays	*Arabidopsis thaliana* seeds	Plants	Radiobiological studies	Zimmermann et al. (1996)
1994-2007	BIOPAN-1-6/ Foton	10-15 days		Space vacuum Solar UV radiation Cosmic rays	*Bacillus subtilis* spores *Holoarcula sp.*cells *Synechococcus sp.* cells *Rhizocarpon geographicum* *Xantoria ellegans* *Richterius coronifer* *Milnesium tardigradum*	Bacteria Archaea (osmophilc) Cyanobacteria (osmophilic) Lichens Animals (Tardigrades)	Short-term survival in space Protection of microorganisms by clay, salt crystals, pigments etc.	Horneck et al. (2001) Mancinelli et al. (1998) Sancho et al. (2007) Jönsson et al. (2008)
1999	PERSEUS/ MIR station	98 days	EXOBIOLOGIE	Space vacuum Solar UV radiation Cosmic rays	*Bacillus subtilis* spores	Bacteria	Survival of bacterial spores embedded in real and artificial meteorite material	Rettberg et al. (2002)
2005-2007	STONE-5-6/ Foton		Lithopanspermia/ Stone	re-entry velocity 7.5 km/s	*Bacillus subtilis* spores *Chroococcidiopsis sp.*cells *Rhizocarpon geographicum*	Bacteria Cyanobacteria Lichens	Effects on physicochemical and physical properties of rocks, and endolithic microbial communities upon their re-entry	Cockell et al. (2007) de la Torre (2010)

ANNEX B:

Technical drawings of sample facilities from EXPOSE-E and EXPOSE-R space projects

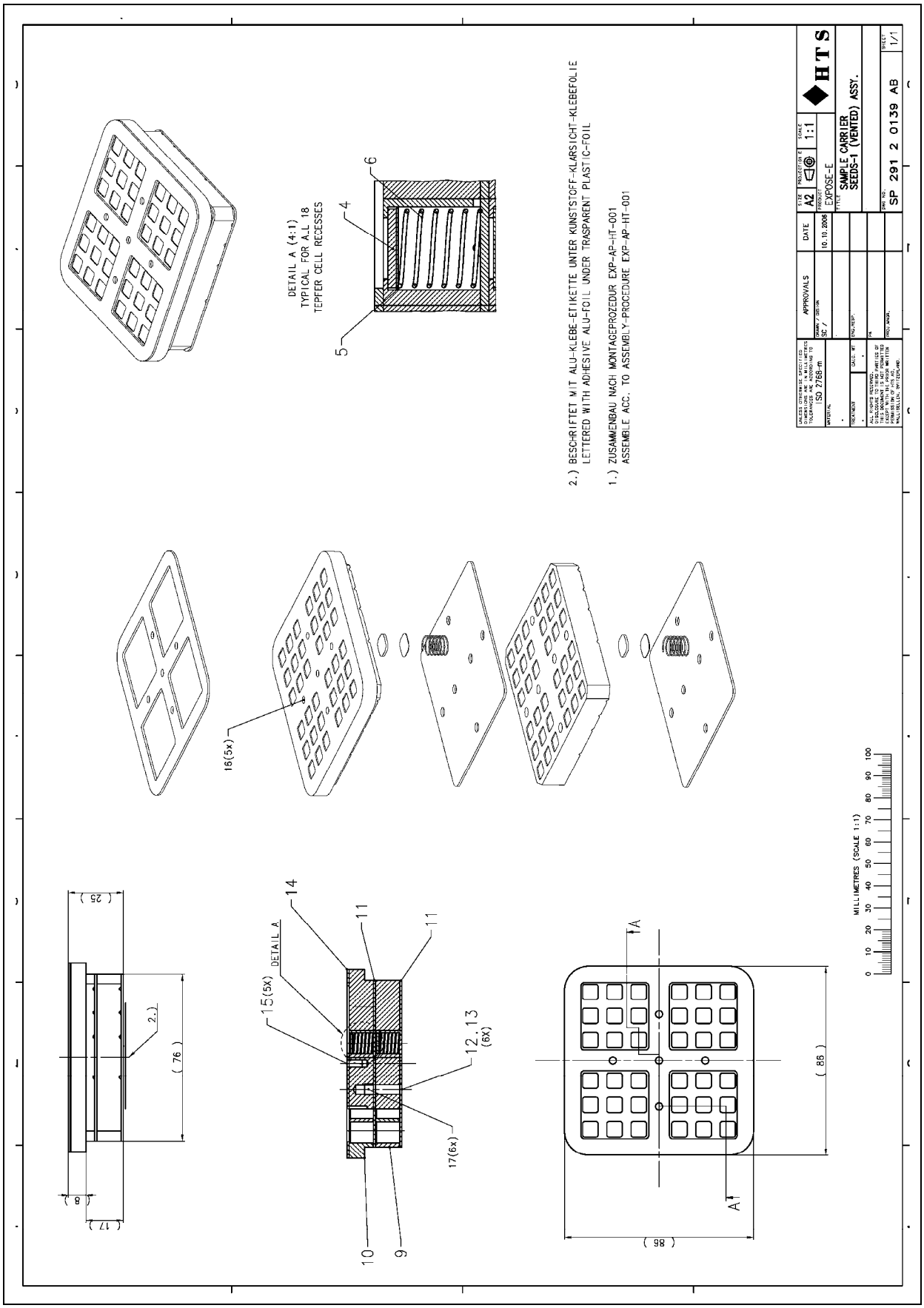

Fig. B-1. Technical drawing of EXPOSE-E/ SEEDS sample carriers (Credit HTS AG., Wallisellen, CH).

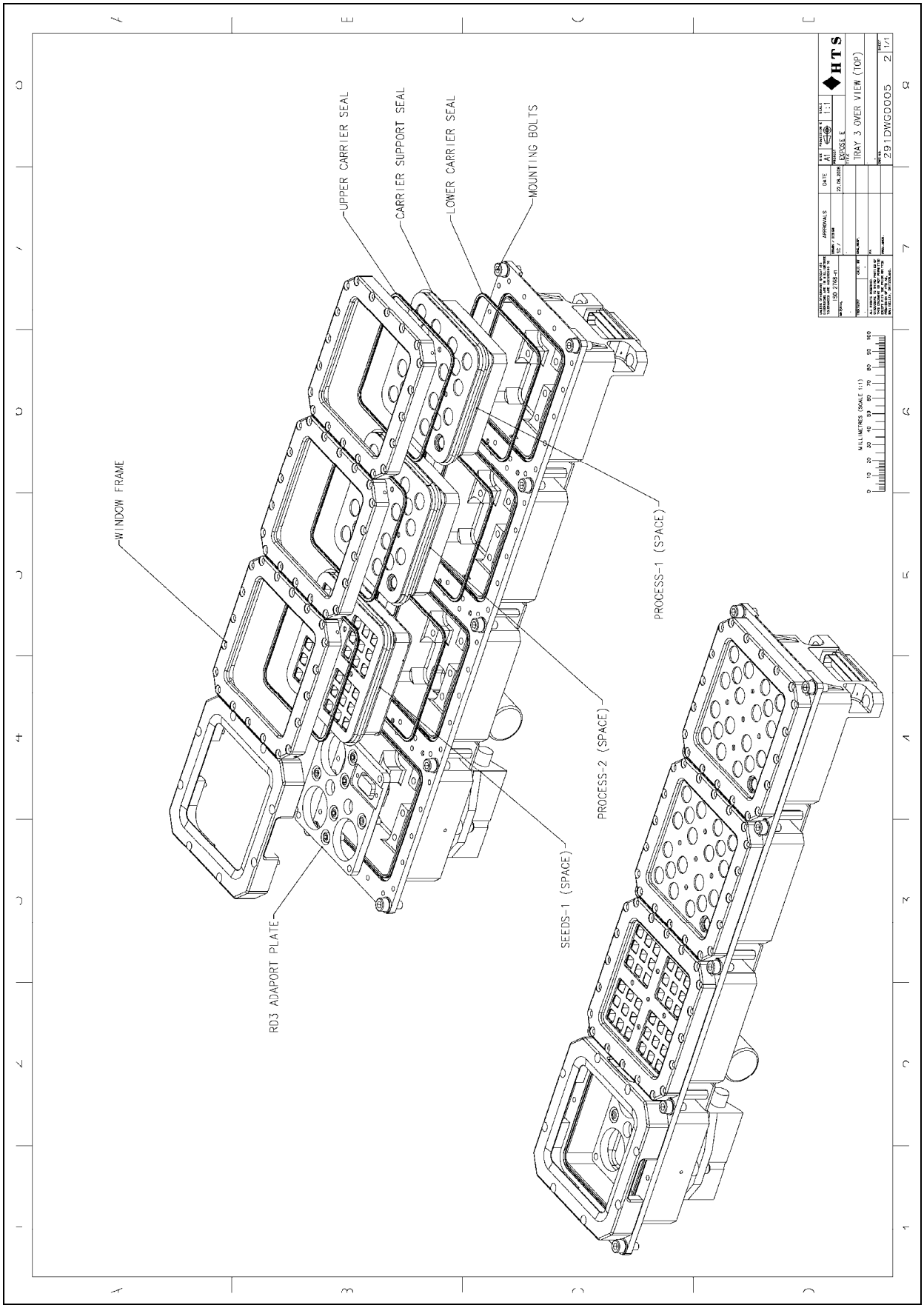

Fig. B-2. Technical drawing of EXPOSE-E tray 3 with integrated R3D instrument, SEEDS and PROCESS sample carriers (Credit HTS AG., Wallisellen, CH).

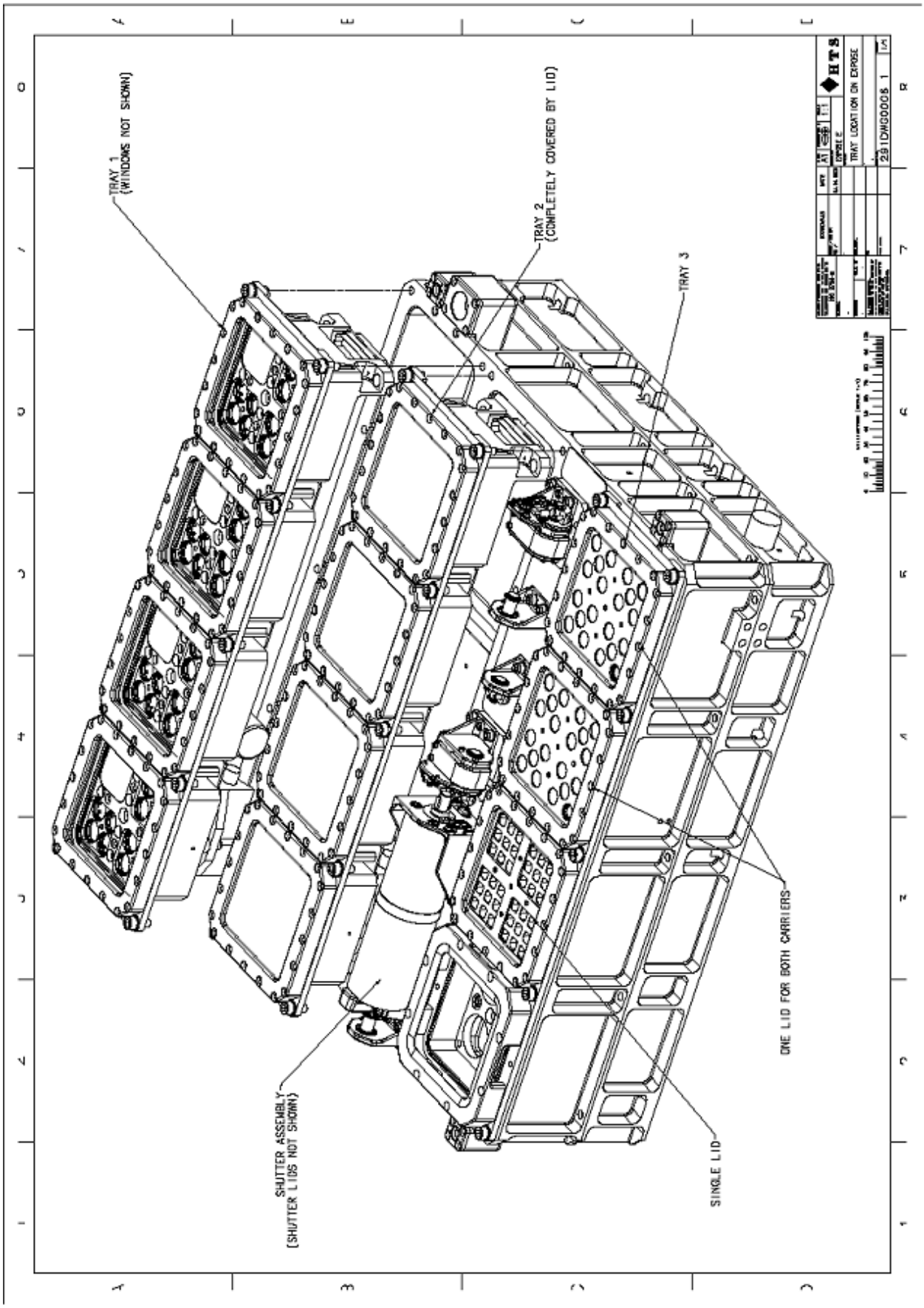

Fig. B-3. Technical drawing of EXPOSE-E facility with integrated three trays carrying different sample carriers (Credit HTS AG., Wallisellen, CH).

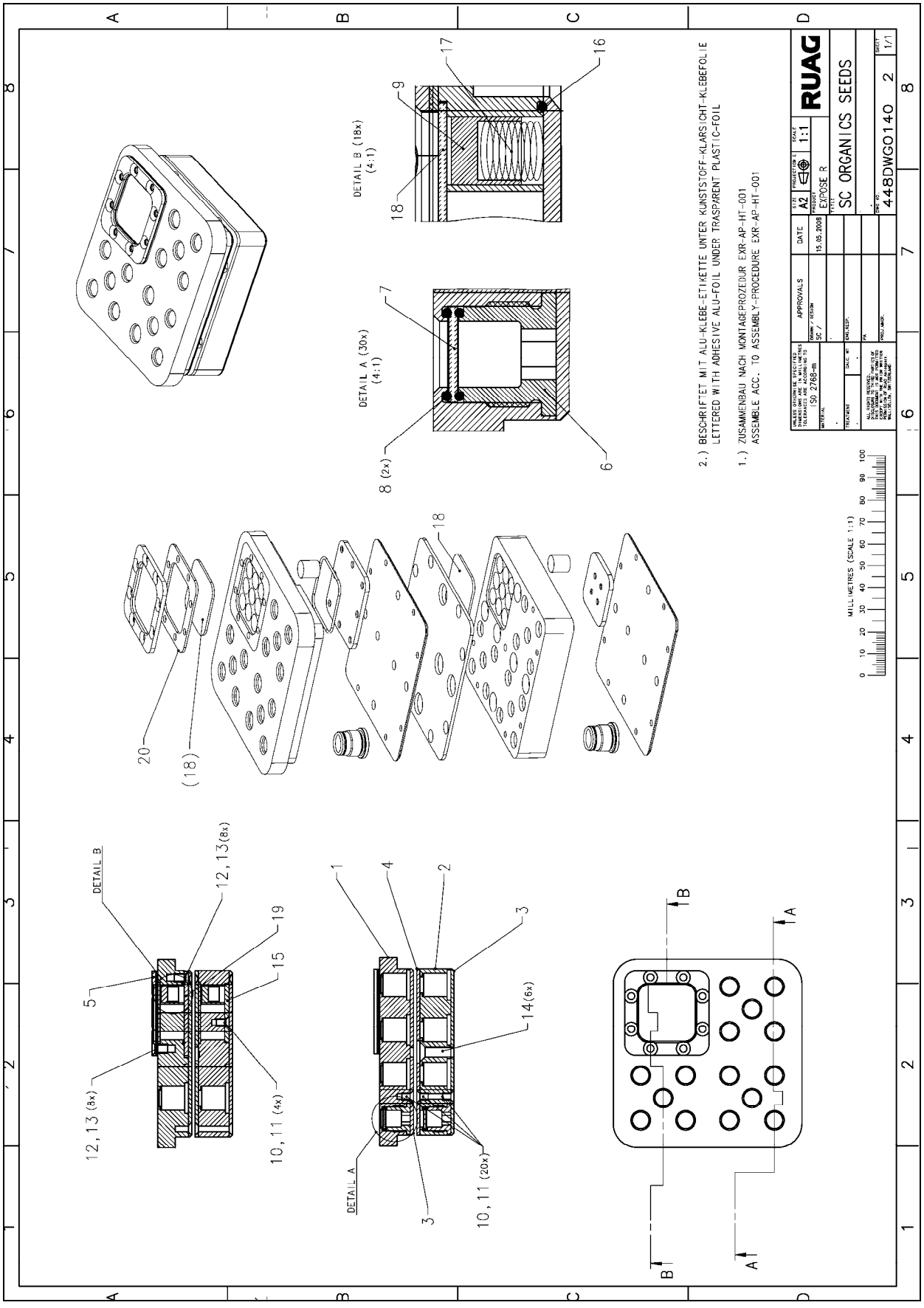

Fig. B-4. Technical drawing of ORGANIC/ SEEDS carrier for EXPOSE-R mission (Credit HTS AG., Wallisellen, CH).

ANNEX C:

Resistance of *Arabidopsis* seeds to other parameters of the space environment

In addition to full spectrum UV radiation, other physical parameters, such as ultra high vacuum, microgravity, temperature extremes and ionizing radiation, may influence the survival of organisms in the environment of space. Because of the large amount of the results obtained in the EXPOSE pre-flight simulation experiments, other space parameters, besides UV radiation and high vacuum that were investigated in details and discussed here above, were not in the focus of the present work. However, the effects of some of these simulated space parameters on *Arabidopsis* seeds were examined in our recent studies and the results will be presented in our forthcoming publications. Our unpublished results are summarized here below.

Microgravity

Low gravitational force (10^{-6}g) is experienced in the interplanetary space. At low Earth orbit (LEO) altitudes (between 200 and 600 km above the surface of the Earth), where gravitational field is about 90% of the strength at the Earth's surface, the microgravity ranges from 10^{-3} to 10^{-6}g (Horneck et al., 2000; Nicholson et al., 2000). The ISS is orbiting in LEO, approximately 400 km above the Earth's surface. Several space experiments studied the effects of microgravity on the seed storage, the germination, as well as the plant growth and development (reviewed in Halstead and Dutcher, 1987; Musgrave, 2002). Most of these studies confirmed that the microgravity does not affect the germination performed during the space flight, but the effects on plant growth are less clear (Halstead and Dutcher, 1987). However, Link et al. (2003) succeeded to grow *Arabidopsis thaliana* plants from seed-to-seed inside the ISS. They reported that *Arabidopsis* seeds successfully germinated and the plants grew and developed well, completing their full life cycle in microgravity environment. According to Vaulina et al. (1984) and Anikeeva et al. (1983), the microgravity does not have any significant effect on the plant seeds after relatively short-duration space flight. Therefore we reasoned that the microgravity is of no major concern for our SEEDS experiments at the ISS, and in our work we did not seek to further examine the effects of this space parameter.

Temperature extremes

In the interplanetary space, the extremely low temperatures of 4 K (-269°C) may be experienced (Horneck et al., 2000). However, in the Earth orbit, the values are higher, since the temperature of a body in space depends on its position with respect to the Sun, its surface, mass, size, albedo etc. Nevertheless, due to periodical shading from the Sun, the Earth orbiting object

can be exposed to both extremely high and extremely low temperatures (Nicholson et al., 2000). The ISS orbits the Earth within period of 90 min, being exposed to the Sun for about 60 min and shaded by the Earth for about 30 min. The extreme temperatures may be expected at the level of the ISS, ranging from -120°C to +120°C (Baglioni et al., 2007). However, during the EXPOSE-EuTEF mission at the ISS, less extreme temperatures are measured, ranging from about -15°C to about +60°C (Rabbow, 2009).

In general, the plant seeds withstand the low temperatures, even at sub-zero level. Desiccated seeds may be successfully stored for extended periods when frozen at -20°C (Doijode, 2001). Sometimes, the cryogenic conditions at -196°C (77 K) are used for ultra long-term storage of seeds, enabling successful germplasm preservation (Benson, 2004). Our preliminary results showed that almost all *Arabidopsis* seeds, both flavonoid-containing (Ws-2) and flavonoid-deficient (*tt4-8*) seeds, as well as tobacco seeds survived the treatment at extremely low temperature (about -196°C) during more than 3 months storage in liquid nitrogen, without addition of any cryoprotector. The germination capacity ($G_{max\%}$) in all treated samples was about 100%, although seeds germinated slightly slower than the control samples (our unpublished data).

High temperatures, on the other hand, may cause more damaging effects, inducing severe cellular injuries and eventually the cell death due to protein denaturation and aggregation, increased fluidity of membrane lipids, loss of membrane integrity etc. Heat stress is also related to an increased accumulation of toxic compounds and reactive oxygen species (ROS) in plant cells (Wahid et al., 2007). Seeds of some plant species are well adapted to withstand extremely high temperatures e. g. seeds of *Cistus* and *Halimium* species, grown in habitats prone to fire, are not only resistant to temperatures up to 150°C, but the seed germination is fire-stimulated (Thanos and Georghiou, 1988; Herranz et al., 1999). Our experiments revealed the extreme resistance of *Arabidopsis* seeds to very high temperatures (unpublished data). Wild type Ws-2 seeds survived dry-heating at 100°C, even after 6 hours of treatment, reaching 88% germination. Surprisingly, even at 120°C, the Ws-2 seeds survived 1-hour treatment, although reaching significantly lower $G_{max\%}$ (28%). Interestingly, the flavonoid-lacking seeds appeared less resistant to high temperature than wild type seeds, since only 10% of the *tt4-8* seeds survived 6-hours treatment at 100°C (our unpublished data). This phenomenon might be related to the increased permeability of the seed coats in the *tt4-8* seeds, which probably allows faster water loss, as well as faster overheating. On the other hand, this finding might provide an additional evidence of the role of flavonoids in the heat stress protection of plant seeds. Phenolic

compounds, including flavonoids, have been found to accumulate in the plant cells that were exposed to the heat stress (Wahid et al., 2007). Since the heat stress, in addition to tissue dehydration, induces the oxidative damage in exposed cells (Wahid et al., 2007), flavonoids might have an important protective role as efficient antioxidants and free radical scavengers.

Therefore, from our preliminary results we concluded that plant seeds, similarly to *Bacillus* spores, are markedly resistant life forms that withstand both extremely low and extremely high temperatures. Although the effects of ultra low temperatures (< 10K) that might be experienced in interplanetary space has not yet been investigated on seed resistance, this parameter of space environment is likely not limiting factor for hypothetical journey through space. The average surface temperatures on the terrestrial planets of our solar system range from -33°C on Mars to +167°C on Mercury (with the exception of anomalously high temperature of -464°C on Venus)(Faure and Mensing, 2007a). Our results indicated that some plant seeds might survive the temperature regimes on the planetary bodies, such as Mars (average surface temperature from -140°C to +20°C). However, the combined effects of temperature extremes and other parameters of space environment should be also considered. Laboratory experiments showed that extremely low temperatures (< 80 K) decrease the damaging effects of UV radiation when these two parameters are applied in the combination (Weber and Greenberg, 1985; Dose et al., 1996). Besides, fluctuations between low and high temperature extremes might be also an important factor for the survival. Although measured temperature ranges during the EXPOSE-EuTEF and EXPOSE-R missions at the ISS are well within the limits for the survival of *Arabidopsis* and tobacco seeds, the results from these space experiments and accompanied ground-based simulation experiments will reveal whether the fluctuations in temperature during 90-min cycle affect the viability of plant seeds. In addition, these experiments will provide more information about possible combined effects of temperature extremes and other parameters of the space environment.

Ionizing radiation

The hazard of the exposure to high doses of ionizing radiation is one of the major concerns in the space environment. The ionizing radiation that is encountered in space has a heterogeneous nature, being composed of both the particulate components (e. g. accelerated protons, electrons, α-particles etc.) and the electromagnetic radiation (e. g. X- and γ-rays). Different ionizing components of such complex radiation field in our solar system are of galactic (GCR) and solar origin (SCR). Cosmic radiation is composed predominantly of protons (about

90%) and smaller amounts of α-particles. Although contributing only about 1% to cosmic radiation flux, heavier nuclei (Z>2), known as the HZE particles, have a strong deleterious effect on biological systems (Horneck, 1992; Reitz et al., 1995; Nelson, 2003; NRC`, 2008). In addition, all the objects in LEO, which is characteristic for the Space Shuttle or Space Station scenario, are exposed to increased radiation from particles (mostly protons) that are geomagnetically trapped in the Earth's Van Allen radiation belts (Baumstark-Khan and Facius, 2002; Baglioni et al., 2007). Therefore, the living systems in LEO environment are exposed to high doses of cosmic radiation, ranging from 400 - 10 000 Gy/year (for shielding of 0.15 g/cm^2), while low doses of ≤ 0.1 Gy/year are estimated in the interplanetary space (Horneck et al., 2000; Baglioni et al., 2007).Besides particulate radiation, the highly energetic electromagnetic radiation, the X-rays (1-100 keV) and the γ-rays (>100 keV) contribute, although only to a smaller extent, to ionizing radiation fields in our solar system (Baumstark-Khan and Facius, 2002). Due to such large variety of radiations in space, which act jointly and each might induce different mechanisms for damage and the repair, the effects of each component of space radiation field should be analysed separately as far as possible.

The main biological effect of ionizing radiation is the generation of free radicals, notably the hydroxyl radical, which together with the direct effects of ionizing radiation, induce severe and hardly reparable damages to DNA, such as single- and double-strand DNA breaks (Obe et al., 1992; Britt, 1996; Baumstark-Khan and Facius, 2002). The ionizing radiation is lethal for humans at doses above 10 Gy, and doses as low as 0.2 Gy are related to higher incidence of some types of the cancer. Microorganisms are more resistant to ionizing radiation than mammalian cells, where X- and γ-rays and found to show similar inactivation levels in the vegetative bacterial cells, as well as the bacterial spores (De Lara et al., 2002). However, vegetative cells of bacteria are more sensitive to ionizing radiation, with the D_{10} (dose of ionizing radiation that reduces the survival to 10%) usually lower than 1 kGy, while bacterial spores, including *Bacillus subtilis* spores, exhibit high radiation resistance, with the D_{10} in the range 1-4 kGy (Monk et al., 1995; van Gerwen et al., 1999; De Lara et al., 2002; Ghosal et al., 2005). The most radiation resistant bacterium known is *Deinococcus radiodurans*, since it was demonstrated that its vegetative cells resist extremely high doses, with the D_{10} values are usually in the range above 10 kGy (De Lara et al., 2002; Ghosal et al., 2005).

Plant seeds were shown to be highly resistant to ionizing radiation. Kumagai et al. (2000) reported that more than 90% of *Arabidopsis thaliana* and *Rhaphanus sativus* seeds germinated after the exposure to γ-radiation or electron beam irradiation at doses up to 1 kGy, although high

doses of 10 kGy inhibited the germination.. Besides high resistance to ionizing electromagnetic radiation, plant seeds withstand the exposure to highly energetic particle irradiation, such as accelerated protons and heavy charged particles (HZE). The ground-based simulation experiments with *Arabidopsis* seeds that were exposed to accelerated heavy ions, with the particle fluence of 10^5 - 10^8 particles/cm^2, revealed that the damaging effects of HZE irradiation depend on the atomic number (charge), particle fluence and energy carried by the particle (Koller-Lampert and Kranz, 1982; 1983; Bork et al., 1989). Depending on the kind and energy of the HZE particle, the range of particle fluence above 10^6 particles/cm^2 is found to be critical for the survival of *Arabidopsis* seedlings developed from irradiated seeds (Koller-Lampert and Kranz, 1983).

Several radiobiological experiments that have been performed directly in space studied the effects of cosmic ionizing radiation on dry *Arabidopsis* seeds during the short-term (IML-1, D2, SL-1, BION8, 9 and 10) and long-term space missions (ERA-1 and LDEF) (reviewed in Zimmermann et al., 1996). These experiments were performed in LEO, either inside or outside the spacecrafts at different altitudes (215-508 km) and inclinations (28.5-82.3°), where the seed samples received the doses ranging from 47 up to 1130 μGy/day. The post-flight experiments revealed that irradiated *Arabidopsis* seeds retained a high germination capacity and high level of plant survival (more than 70%) even after almost 6 months of exposure to ionizing radiation during LDEF mission (maximal absorbed dose 3.4 Gy, HZE fluence ~ 6.5 x 10^6 particles/cm^2, LET > 10 keV/μm) (Zimmermann et al., 1996). Similarly, Anikeeva et al. (1990) reported a high level (about 90%) of germination capacity of seeds and survival rate of *Arabidopsis thaliana* and *Crepis capillaris* plants after the 13-day-exposure to the open space environment, including ionizing radiation at doses of 15-36 Gy. Nevertheless, increased level of mutability and higher frequencies of chromosome aberrations, as well as decreased plant fertility were observed in seeds exposed to ionizing radiation of space (Anikeeva et al., 1990; Kranz et al., 1990; Zimmermann et al., 1996)

Despite the fact that the HZE particles are likely one of the most biologically effective species of ionizing space radiation due to the high penetration and their extremely dense pattern of energy deposition into the matter, and for the same reason they have been in the focus of many radiobiological studies, the HZE particles have very low contribution in the total flux of particulate radiation in space. Therefore, the hit by the HZE particle in space is likely a relatively rare event, especially for the biological objects of the small size. In contrast, much less attention has been paid to the biological effects of accelerate protons, which in spite of their low-LET

(linear energy transfer), represent a predominant component of ionizing radiation in space, particularly in LEO environment (more than 90%). Therefore, we reasoned that before exposing the seeds to space environment during EXPOSE missions, it would be necessary to investigate in details the effects of accelerated proton particles on *Arabidopsis* seeds using ground-based simulation facilities, a 5 MeV van de Graff accelerator at the University of Aarhus, Denmark (our unpublished data). Dry seeds were irradiated with 2 MeV proton beam with high fluences of protons ranging from 2.8 x 10^{10} up to 6 x 10^{14} particles/cm^2. The stopping power (18.1 keV/μm) and theoretical range (76.92 μm) of 2 MeV protons in water medium was calculated using SRIM/ TRIM code (Ziegler et al., version SRIM-2008.04, htp://www.SRIM.com). For the estimated C_{25}:H_{49}:O_{24}:N_2 ratio and the average mass density of 1.1 g/cm3 for *Arabidopsis* seeds (Qin et al., 2007), we calculated that 2 MeV protons penetrate into the seeds at the range of 71.50 μm. Since the dimension of *Arabidopsis* seeds is about 300-500 μm, and the seed coat thickness is about 20-μm, with single-cell layer of endosperm underneath (Debeaujon et al., 2000; Al-Shehbaz and O'Kane, 2002; Qin et al., 2005; Qin et al., 2007), we estimated that 2 MeV protons will be stopped within the seeds, deposing the energy into the embryo.

Our preliminary results revealed high resistance of *Arabidopsis* seeds to proton radiation. The irradiated *Arabidopsis* wild-type seeds (Ws-2) retained high germination capacity (above 90%) after the exposure to accelerated protons with the fluences as high as 9.3 x 10^{13} particles/cm^2. However, unexpected decrease of $G_{max\%}$ (64%) occurred at intermediate fluence of 1.3 x 10^{12} particles/cm^2. Similar result was also obtained with flavonoid-lacking *tt4-8* seeds. This unusual non-linear trend of the fluence-response curve, with intermediate peak at 1.3 x 10^{12} particles/cm^2 was also observed for the MGT parameter of germination dynamics. Similar phenomenon of so called “saddle shaped” fluence-response curve, with the maximal effectiveness at exactly the same intermediate fluence of proton particles, was also reported for imbibed and dry *Arabidopsis* Col-0 seeds that were irradiated with 1 MeV and 2.6 MeV, as well as for some other biological and macromolecular models (Qin et al., 2005; Qin et al., 2007). Although the mechanism is not clear, the non-linear behaviour of proton fluence-response curve is probably related to low-LET radiation, which might induce specific activation and deactivation of different repair systems that co-exist in the cells. Being exposed to increasing fluences of proton radiation, different targets might be specifically damaged and the protective systems might reach specific dose thresholds resulting in the repair mechanism switch. Similar concept was theoretically discussed by Scott (2005).

At the high proton fluences of 1.0 x 10^{14} and 6.0 x 10^{14} particles/cm^2, the germination capacity of *Arabidopsis* Ws-2 seeds seriously decreased at about 57% and 35%, respectively. At the same fluence range, flavonoid-lacking *tt4-8* seeds appeared less resistant, exhibiting lower $G_{max\%}$ values (our unpublished data). This might indicate that flavonoids are also the important protectors against ionizing radiation due to their known efficiency in scavenging of free radicals. Furthermore, our results revealed that irradiation of *Arabidopsis* seeds with 2 MeV proton beam affected subsequent development of seedlings and plants, where higher frequencies of aberrant seedling forms and lower percentages of fertile plants were observed.